ACQUIRED HEART DISEASE IN CHILDREN: PATHOGENESIS, DIAGNOSIS AND MANAGEMENT

EDITED BY: Fangqi Gong, Fu Lijun, Xupei Huang and Hongfang Jin

PUBLISHED IN: Frontiers in Pediatrics and Frontiers in Cardiovascular Medicine

frontiers Research Topics

frontiers

ISSN 1664-8714
ISBN 978-2-88971-327-1
DOI 10.3389/978-2-88971-327-1

About Frontiers

Frontiers is more than just an open-access publisher of scholarly articles: it is a pioneering approach to the world of academia, radically improving the way scholarly research is managed. The grand vision of Frontiers is a world where all people have an equal opportunity to seek, share and generate knowledge. Frontiers provides immediate and permanent online open access to all its publications, but this alone is not enough to realize our grand goals.

Frontiers Journal Series

The Frontiers Journal Series is a multi-tier and interdisciplinary set of open-access, online journals, promising a paradigm shift from the current review, selection and dissemination processes in academic publishing. All Frontiers journals are driven by researchers for researchers; therefore, they constitute a service to the scholarly community. At the same time, the Frontiers Journal Series operates on a revolutionary invention, the tiered publishing system, initially addressing specific communities of scholars, and gradually climbing up to broader public understanding, thus serving the interests of the lay society, too.

Dedication to Quality

Each Frontiers article is a landmark of the highest quality, thanks to genuinely collaborative interactions between authors and review editors, who include some of the world's best academicians. Research must be certified by peers before entering a stream of knowledge that may eventually reach the public - and shape society; therefore, Frontiers only applies the most rigorous and unbiased reviews.
Frontiers revolutionizes research publishing by freely delivering the most outstanding research, evaluated with no bias from both the academic and social point of view. By applying the most advanced information technologies, Frontiers is catapulting scholarly publishing into a new generation.

What are Frontiers Research Topics?

Frontiers Research Topics are very popular trademarks of the Frontiers Journals Series: they are collections of at least ten articles, all centered on a particular subject. With their unique mix of varied contributions from Original Research to Review Articles, Frontiers Research Topics unify the most influential researchers, the latest key findings and historical advances in a hot research area! Find out more on how to host your own Frontiers Research Topic or contribute to one as an author by contacting the Frontiers Editorial Office: frontiersin.org/about/contact

ACQUIRED HEART DISEASE IN CHILDREN: PATHOGENESIS, DIAGNOSIS AND MANAGEMENT

Topic Editors:
Fangqi Gong, Zhejiang University, China
Fu Lijun, Shanghai Children's Medical Center, China
Xupei Huang, Florida Atlantic University, United States
Hongfang Jin, Peking University First Hospital, China

Citation: Gong, F., Lijun, F., Huang, X., Jin, H., eds. (2021). Acquired Heart Disease in Children: Pathogenesis, Diagnosis and Management. Lausanne: Frontiers Media SA. doi: 10.3389/978-2-88971-327-1

Table of Contents

frontiers in Pediatrics

EDITORIAL
published: 15 July 2021
doi: 10.3389/fped.2021.725670

Editorial: Acquired Heart Disease in Children: Pathogenesis, Diagnosis and Management

Ying Liao[1], *Hongfang Jin*[1]*, *Xupei Huang*[2], *Fangqi Gong*[3] and *Lijun Fu*[4]

[1] Department of Pediatrics, Peking University First Hospital, Beijing, China, [2] Department of Biomedical Science, Charles E. Schmidt College of Medicine, Florida Atlantic University, Boca Raton, FL, United States, [3] Department of Cardiology, National Clinical Research Center for Child Health, Children's Hospital, Zhejiang University School of Medicine, Hangzhou, China, [4] Department of Cardiology, Shanghai Children's Medical Center, Shanghai Jiao Tong University School of Medicine, Shanghai, China

Keywords: myocarditis, pericarditis, cardiomyopathy, pathogenesis, management

Editorial on the Research Topic

Acquired Heart Disease in Children: Pathogenesis, Diagnosis and Management

Myocarditis, pericarditis, and cardiomyopathy are important acquired heart diseases during childhood. Under the Research Topic "Acquired Heart Disease in Children: Pathogenesis, Diagnosis and Management," totally seven literatures focused on the above diseases and shed light on the pathogenesis, diagnosis and treatment of the diseases, attracting large numbers of readers, and stimulating their thinking in the future studies on these diseases.

OPEN ACCESS

Edited and reviewed by:
Ruth Heying,
University Hospital Leuven, Belgium

***Correspondence:**
Hongfang Jin
jinhongfang51@126.com

Specialty section:
This article was submitted to Pediatric Cardiology, a section of the journal Frontiers in Pediatrics

Received: *15 June 2021*
Accepted: *24 June 2021*
Published: *15 July 2021*

Citation:
Liao Y, Jin H, Huang X, Gong F and Fu L (2021) Editorial: Acquired Heart Disease in Children: Pathogenesis, Diagnosis and Management. Front. Pediatr. 9:725670. doi: 10.3389/fped.2021.725670

MYOCARDITIS

The diagnosis and treatment of myocarditis, especially acute fulminant myocarditis (AFM), in pediatric population are challenging. Three articles in this Topic reported the research advance in pediatric AFM, although it is unclear why children with AFM manifest such critical symptoms and rapid progression, abnormal immune response triggered by certain pathogens in susceptible individuals may be considered as possible mechanisms (1). To investigate the potential pathogenesis of AFM, Liu et al. analyzed the profiles of long non-coding RNAs (lncRNAs) and mRNA in the leukocytes of pediatric patients with AFM as well as controls using microarrays and found that the expressions of lncRNAs and mRNAs were distinctly different between the two groups of the subjects. Further analysis on the potential biological function and the molecular interactions of these differentially expressed genes revealed that immune processes such as T cell activation and several signaling pathways related to immune activation may take part in the pathogenic process of AFM. Furthermore, the study showed that most differentially expressed lncRNAs were related to the target genes that were adjacent to them. Although the functional prediction still needs to be verified, these results may provide important clues on the immune mechanisms for AFM. Early diagnosis and appropriate evaluation for patients' condition are pivotal aspects in the management of pediatric AFM. Lv et al. reviewed 20 pediatric patients with AFM and summarized their clinical features. Particular attention was paid to the value of cardiovascular magnetic resonance (CMR) in the diagnosis as well as follow-up of AFM in this study. Abnormal findings of CMR, mainly including high signal in T2-weighted image and late gadolinium enhancement, were determined in 80% of the cases. Another study from Zhu et al. retrospectively analyzed the alert

symptoms and other manifestations of 23 pediatric patients with AFM. The above two studies showed that extracardiac symptoms were the most common initial manifestations of their patients with AFM, which was also consistent with the previous studies (2). Therefore, it is suggested that hypoperfusion signs with abdominal pain, vomiting, dizziness, or/and convulsions may be the alert of AFM in children. Besides, treatment for children with AFM included intravenous immunoglobulin (IVIG), glucocorticoids and the supportive therapies such as continuous renal replacement therapy, extracorporeal membrane oxygenation, and temporary pacemakers according to the two studies.

Although it is believed that the pathogenesis of myocarditis may involve abnormal immune reaction to the pathogen, the present views on immunosuppressive therapy with steroids or immunomodulatory therapy with IVIG for treating myocarditis in children are still controversial (3, 4). To evaluate the therapeutic response to corticosteroids and IVIG in pediatric myocarditis, Li et al. conducted a meta-analysis on the topic. The results supported that IVIG was effective in enhancing the impaired left ventricular ejection fraction (LVEF) as well as survival for children with myocarditis; while corticosteroids didn't show an efficacy advantage over the conservative treatment. The authors also called for large sample size, randomized controlled trials because of the limited numbers of associated studies on the topic.

PERICARDITIS

Recurrence pericarditis (RP) stands for the recurrence of acute pericarditis after a recorded first course with a symptom-free interval of at least 4–6 weeks (5). Tombetti et al. reviewed the present advances in etiology, pathogenesis, diagnosis, management, and prognosis of RP in children and adolescents. Tuberculosis is still the commonest cause of RP worldwide, while 70% of children with RP were attributed to an idiopathic origin in developed countries. It was recommended that the genetic factors should be paid great attention in children with RP when certain warning signals existed. As for the prognosis, deaths related to idiopathic RP were rare, and frequent recurrence, cardiac tamponade, pericardial constriction, and myocardial involvement were the most concerned conditions. They also summarized some risk factors of the recurrence and complications, which were helpful for clinical practice. Anti-IL1 therapy was highlighted in the management of RP based on an accurate diagnosis and a reasonable treatment algorithm.

CARDIOMYOPATHY

According to the latest scientific statement from the American Heart Association (AHA) on classification of cardiomyopathy in children, the morphofunctional phenotype is still the primary hierarchy in the diagnostic system, including dilated, hypertrophic, restrictive, non-compaction, and arrhythmogenic cardiomyopathies (6). In this Research Topic, Guo et al. evaluated a series of drug-related receptors in pediatric patients suffering from dilated cardiomyopathy (DCM). It is highly valuable that they analyzed the drug-related receptors on left ventricular tissue from children with idiopathic DCM who underwent heart transplantations, from the controls (heart donors) and from adult DCM. As a result, the difference in distributions of drug-related receptors on heart tissue provided significant clues to make a specific medication regimen for pediatric patients. Another article from Bai et al. focused on the genetic mechanisms for non-compaction of ventricular myocardium (NVM). They discovered a *de novo MTUS1* mutation from a rare family with NVM and found that the mutation can reduce the stability of microtubules and increase the polarity of cell through the Rac1/Cdc42 signaling pathway in *in vitro* studies. However, the role of this mutation in *MTUS1* gene in the pathogenesis of NVM still merits further studies.

In summary, the articles from this Research Topic showed the latest advances in the above acquired heart diseases in children. The discoveries would not only deepen the understanding of the mechanisms, but also bring important improvement to clinical practice. However, there are still a lot of issues in this field, such as the pathogenesis of pediatric myocarditis, cardiomyopathy as well as pericarditis, and the biomarker-based individualized therapy for different categories of cardiomyopathies, need further investigation.

AUTHOR CONTRIBUTIONS

HJ organized the Research Topic and revised the editorial. YL wrote the draft of this editorial. XH, FG, and LF reviewed the Research Topic articles and revised the manuscript. All authors listed have made a substantial, direct and intellectual contribution to the work, and approved it for publication.

REFERENCES

1. Maisch B. Cardio-immunology of myocarditis: Focus on immune mechanisms and treatment options. *Front Cardiovasc Med.* (2019) 6:48. doi: 10.3389/fcvm.2019.00048
2. Matsuura H, Ichida F, Saji T, Ogawa S, Waki K, Kaneko M, et al. Clinical features of acute and fulminant myocarditis in children- 2nd nationwide survey by Japanese Society of Pediatric Cardiology and Cardiac Surgery. *Circ J.* (2016) 80:2362–8. doi: 10.1253/circj.CJ-16-0234
3. Fung RCM, Hon KL, Leung AKC. Acute myocarditis in children: An overview of treatment and recent patents. *Recent Pat Inflamm Allergy Drug Discov.* (2020) 14:106–16. doi: 10.2174/1872213X14666200204103714
4. Ammirati E, Frigerio M, Adler ED, Basso C, Birnie DH, Brambatti M, et al. Management of acute myocarditis and chronic inflammatory cardiomyopathy: an expert consensus document. *Circ Heart Fail.* (2020) 13:e007405. doi: 10.1161/CIRCHEARTFAILURE.120.007405
5. Adler Y, Charron P. The 2015. ESC Guidelines on the diagnosis and management of pericardial diseases. *Eur Heart J.* (2015) 36:2873–4. doi: 10.1093/eurheartj/ehv479
6. Lipshultz SE, Law YM, Asante-Korang A, Austin ED, Dipchand AI, Everitt MD, et al. Cardiomyopathy in children: Classification

and diagnosis: a scientific statement from the American Heart Association. *Circulation.* (2019) 140:e9–68. doi: 10.1161/CIR.0000000000000682

Conflict of Interest: The authors declare that the research was conducted in the absence of any commercial or financial relationships that could be construed as a potential conflict of interest.

frontiers in Pediatrics

CASE REPORT
published: 05 June 2019
doi: 10.3389/fped.2019.00219

Chronic Active Epstein-Barr Virus Infection With Systemic Vasculitis and Pulmonary Arterial Hypertension in a Child

Hongjun Ba[1†], Lingling Xu[2†], Huimin Peng[1], Yuese Lin[1], Xuandi Li[1], Huishen Wang[1] and Youzhen Qin[1]*

[1] Department of Pediatric Cardiology, Heart Center, The First Affiliated Hospital, Sun Yat-sen University, Guangzhou, China,
[2] Department of Pediatrics, The First Affiliated Hospital, Sun Yat-sen University, Guangzhou, China

OPEN ACCESS

Edited by:
Fu Lijun,
Shanghai Children's Medical Center, China

Reviewed by:
Hanmin Liu,
West China Second University Hospital of Sichuan University, China
Ruifeng Zhang,
Sir Run Run Shaw Hospital, China

***Correspondence:**
Youzhen Qin
qyouzhen@163.com

[†] These authors have contributed equally to this work

Specialty section:
This article was submitted to Pediatric Cardiology, a section of the journal Frontiers in Pediatrics

Received: 08 February 2019
Accepted: 15 May 2019
Published: 05 June 2019

Citation:
Ba H, Xu L, Peng H, Lin Y, Li X, Wang H and Qin Y (2019) Chronic Active Epstein-Barr Virus Infection With Systemic Vasculitis and Pulmonary Arterial Hypertension in a Child. Front. Pediatr. 7:219. doi: 10.3389/fped.2019.00219

Introduction: A chronic active Epstein–Barr virus (EBV) infection (CAEBV), which is characterized by persistent "infectious mononucleosis-like" symptoms, can lead to cardiovascular complications, including coronary artery aneurysms. No published studies have reported an occurrence of chronic EB virus infection in conjunction with systemic vasculitis and pulmonary hypertension.

Case Presentation: Herein, we present a case of a 9-year-old boy with CAEBV, associated with pulmonary arterial hypertension (PAH) and systemic vasculitis. Recurrent skin ulcers were a major early clinical manifestation in this case. The histopathological examination of a dermal biopsy sample from the lesions revealed vasculitis, and the *in-situ* hybridization test was positive for EBV-encoded small RNA.

Results: The patient was administered immunosuppressants (prednisolone and cyclophosphamide) and targeted drugs (sildenafil and bosentan) to control the pulmonary pressure. This combination therapy decreased the systolic pulmonary arterial pressure to 40 mm Hg (on echocardiography), and the N-terminal pro b-type natriuretic peptide level also reduced to 62.3 pg/ml. After discontinuation of prednisone, the child developed shortness of breath, edema, and oliguria. He was again started on prednisone, with an addition of thalidomide. Sildenafil was replaced by riociguat, due to the side effect of penile erection. The patient is being followed up every 2 months at the clinic. The most recent follow-up visit was 2 weeks before this report was written, during which, the child was observed to have no rash, shortness of breath, edema, and other symptoms. Written informed consent was obtained from the parents for the publication of this case report.

Conclusion: A CAEBV should be considered among the differential diagnoses while managing a pediatric patient with secondary PAH and systemic vasculitis. However, elucidation of its potential pathophysiological mechanisms requires further study.

Keywords: chronic active Epstein–Barr virus infection, coronary artery aneurysm, pulmonary arterial hypertension, vasculitis, cardiac insufficiency

BACKGROUND

Chronic active Epstein–Barr virus (EBV) infection (CAEBV) was first reported in 1978 (1). It is now considered to be an EBV-related T-cell, natural killer (NK)-cell, or B-cell type of lymphoproliferative disorder or lymphoma. The pathogenesis of the infection is still unclear and is suggested to have a correlation with an abnormal proliferation of EBV-infected cells. Its "infectious mononucleosis-like," non-specific, common clinical symptoms include malaise, fatigue, headache, sore throat, nausea, abdominal pain, myalgia, and fever, which may be of an acute-onset or prolonged (for >1 week). A clinical presentation in the form of skin lesions or pulmonary arterial hypertension (PAH) is very rare. No previous reports in the existing literature have highlighted cases of chronic EB virus infection occurring in conjunction with systemic vasculitis and pulmonary hypertension. Here, we report a rare case of a pediatric patient with CAEBV, presenting with PAH and systemic vasculitis.

CASE PRESENTATION

We describe the case of a child, who first presented to us at 8 years of age, with a complaint of recurrent calf ulcers for >3 years. The histopathological examination of a skin biopsy sample from the lesion showed vasculitis, and an *in-situ* hybridization test was positive for EBV-encoded small RNA (EBER) (**Figure 1**). The EBV load in the plasma was at a level of 4.53×10^6 copies/L, the EBV viral capsid antigen-immunoglobulin (Ig) G was positive, and the level of serum IgE was also significantly high. The patient had no obvious manifestations of pulmonary hypertension. An echocardiography revealed an enlargement of the aortic sinus along with pulmonary arterial hypertension (PASP = 54 mmHg). A further cardiac computed tomography (CT) examination was recommended; however, the family refused this.

Based on these findings, the treating dermatologist diagnosed the child with EB virus-related lymphoblastic proliferative disease at the time. The therapeutic regimen included a small dose of prednisone (10 mg qd), thymic peptide (30 mg qid), anti-allergic, and antiviral (valaciclovir 0.5 g bid) drugs. Two months after this treatment, the child's rash disappeared, resulting in the healing of ulcers.

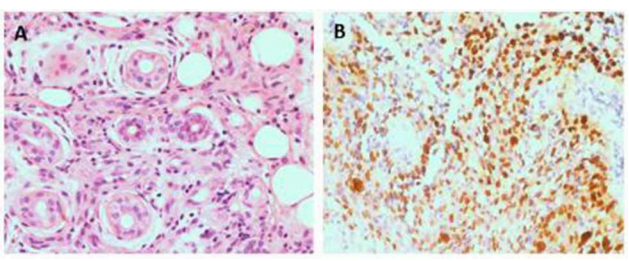

FIGURE 1 | Pathological analysis of skin ulcer shows a perivascular lymphocytic infiltrate and fibrinoid necrosis of small vascular wall(HE 400x) **(A)**. The lymphoma cells are positive for EBER(400x) **(B)**.

Abbreviations: EBV, Epstein–Barr virus; CAEBV, Chronic active Epstein–Barr virus infection; PAH, Pulmonary arterial hypertension; EBER, EBV-encoded small RNA; Ig, Immunoglobulin; NT-proBNP, N-terminal pro b-type natriuretic peptide; PAP, Pulmonary arterial pressure; CT, Computed tomography.

One year later, at the age of 9 years, the child was again brought to the hospital with complaints of edema and easy fatiguability on ambulation. On physical examination, significant findings including systemic edema, hepatomegaly, and a pronounced second heart sound. Laboratory results showed elevated levels of both erythrocyte sedimentation rate (70 mm/h; normal reference range: 0–30 mm/h) and N-terminal pro b-type natriuretic peptide (NT-proBNP) (1,381 pg/ml; normal reference range: 0–84 pg/ml). On echocardiography, the estimated systolic pulmonary arterial pressure (PAP; evaluated on the basis of the tricuspid regurgitation velocity), was 60 mmHg, suggestive of PAH (**Figure 2**). Bilateral coronary aneurysms were also detected. A general CT scan of the aorta revealed dilatation of the aortic sinus. The bilateral pulmonary and coronary arteries were also found to be dilated (**Figure 3**), while the abdominal aortic stem and the distal section of the superior mesenteric artery showed minor dilatation. An electrocardiogram revealed ST-segment and T-wave changes. There were no other findings suggestive of connective tissue disease, and a contrast-enhanced abdominal CT scan did not show the presence of an intrahepatic shunt. The child's family refused a right heart catheterization procedure. Therefore, the patient was diagnosed with (1) CAEBV; (2) PAH; (3) cardiac insufficiency (Class III); and (4) systemic vasculitis and managed conservatively. He was administered immunosuppressants (prednisolone 25 mg qd), the targeted pulmonary pressure-reducing drugs (sildenafil 25 mg bid and bosentan 31.25 mg bid) and antiplatelet therapy (clopidogrel 50 mg qd). The patient was also administered cyclophosphamide 4 times pulse therapy once every 2 weeks, with a cumulative 4-g dose of the drug. This combination therapy resulted in a decrease in his systolic PAP to 40 mmHg on echocardiography, and a reduction of NT-proBNP level to 62.3 pg/ml.

At 9 months after last vist, once the prednisone administration was discontinued, the child developed shortness of breath, edema, and oliguria. The child was once again administered prednisone (5 mg qd) along with thalidomide (25 mg bid).

Three months later, due to the side effect of penile erection, sildenafil was replaced by riociguat (0.5 mg bid), another drug that targets pulmonary pressure.

The patient is being followed up regularly at every 2-month intervals at our rheumatic immunology and cardiovascular pediatric clinic. The most recent follow-up visit was 2 weeks before this report was written, during which, the child was observed to have no rash, shortness of breath, edema, and other symptoms. Echocardiography revealed mild pulmonary arterial hypertension (PASP = 39 mmHg). Current treatments include prednisone (5 mg qod), thalidomide (25 mg bid),bosentan (31.25 mg bid), riociguat (0.5 mg bid), and clopidogrel (50 mg qd). Written informed consent was obtained from the parents for the publication of this case report.

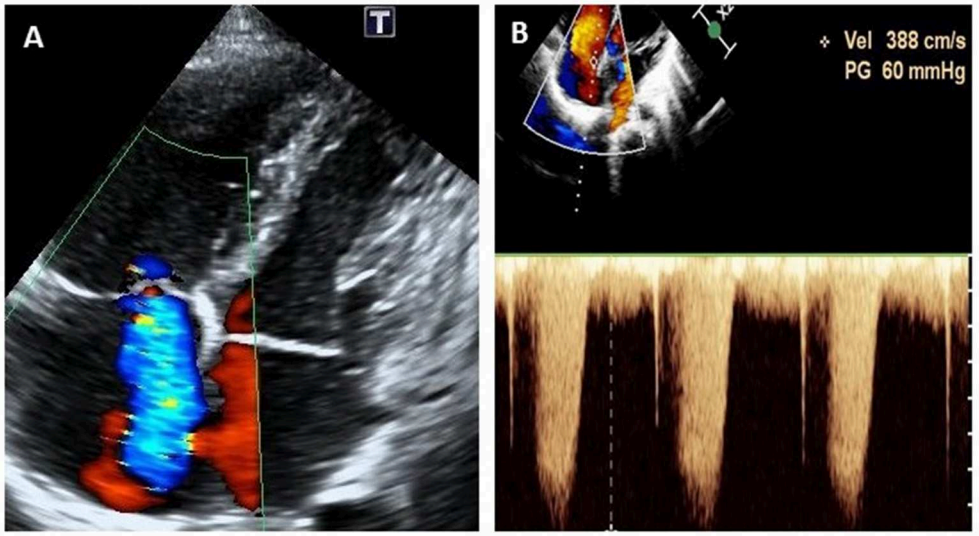

FIGURE 2 | Echocardiogram (apical four-chamber view) at the onset of pulmonary arterial hypertension at 9 years of age, showing severe tricuspid regurgitation **(A)** and continuous wave doppler estimation of tricuspid reflux velocity 3.88 m/s, PG = 60 mmHg **(B)**.

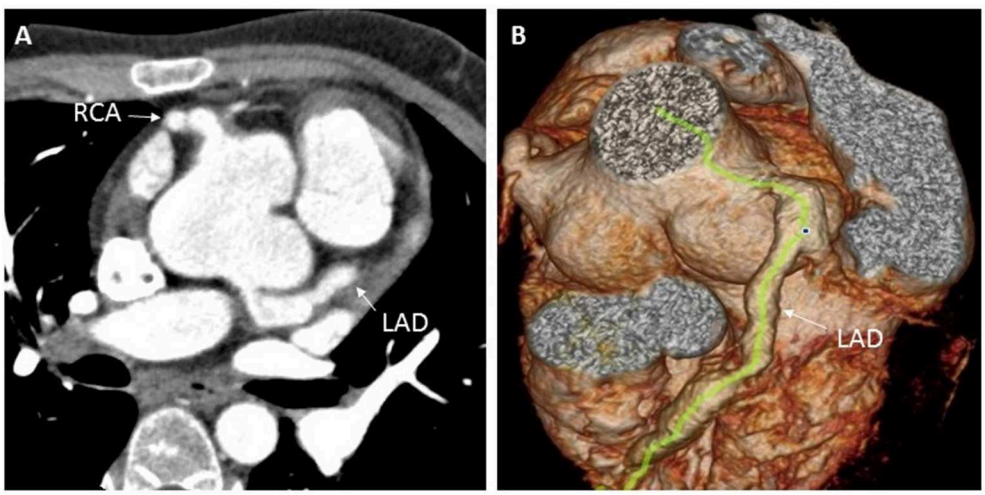

FIGURE 3 | Enhanced coronary CT examination showing left and right coronary artery aneurysms **(A)**, and three-dimensional CT reconstruction of the aorta showing dilation of the aortic root and the left anterior descending coronary artery **(B)**. CT, computed tomography; LAD, left anterior descending; RCA, right coronary artery.

DISCUSSION

Although no typical symptoms and signs of EBV infection were observed in this patient, the child had experienced recurring skin damage over many years. The histopathological assessment of the dermal biopsy sample showed vascular inflammation, and the *in-situ* hybridization test of the damaged tissue suggested the presence of EBV infection, during the initial assessment. Since then, the plasma EBV- deoxyribonucleic acid load may have continued to increase, causing the many vasculitic changes in the patient's major arteries, which were eventually detected during the second visit. Following an exclusion of the currently known, commoner autoimmune disorders, malignancies, and immunodeficiency diseases, we evaluated whether the patient was fulfilling the diagnostic criteria for CAEBV (2).

CAEBV can usually involve multiple organ systems and present with diverse clinical signs. The main clinical manifestations include continuous or intermittent fever, hepatomegaly, splenomegaly, abnormal liver function, thrombocytopenia, anemia, and lymphadenopathy. Previous reports indicate that the occurrence of skin damage due to CAEBV is rare in children but not in adults. The differential diagnosis for CAEBV-induced skin rash includes measles, mosquito bites, allergic reaction, acne blisters, vaccine-induced blistering disease, and nasal K/T lymphocytic lymphoma (3). Kimura et al. reported that about 32.9% of the 82 patients

with EBV infection in their study were allergic to mosquito bites, 25.6% had rashes, and 9.8% had a blistering disease (4). Therefore, for patients with recurring skin damage showing an unsatisfactory response to conventional treatment, it is necessary to be aware of the possibility of EBV infection. The pathophysiological mechanism of EBV-induced skin damage remains unclear. The histopathological examination of the damaged skin revealed a large number of infiltrating lymphocytes and neutrophils, and the *in-situ* hybridization test was positive for EBER, suggesting that it may be related to an abnormal proliferation and replication of the virus within the EBV-infected cells. Our findings suggest that resolving the dermal pathophysiology of EBV infections can lead to an early diagnosis and treatment of the disease.

The child showed systemic vasculitis during the illness, associated with coronary artery aneurysms and severe PAH. Cardiovascular complications are characteristic of CAEBV. Two different studies have respectively, documented that ∼9.8 and 17.9% of patients with CAEBV developed complications involving the circulatory system (5, 6). Most cases present with coronary artery aneurysms or myocarditis (7). PAH associated with CAEBV is rare, and there has been only previously one reported case in the pediatric age-group (8). Unlike our case, the patient was an 11-year-old boy with PAH and junctional ectopic tachycardia, who did not suffer from any other major symptoms attributable to CAEBV. Hashimoto et al. reported the first case of CAEBV-associated PAH in a 45-year old man in 2011 (9). In this adult patient, PAH with heart failure and liver dysfunction manifested in the initial part of the illness, prior to the diagnosis of CAEBV. The patient also did not have any major symptoms attributable to CAEBV. There have been reported cases of CAEBV occurring in combination with mild pulmonary hypertension (10), but these patients also have associated severe liver dysfunction and portal hypertension. The authors speculated that pulmonary arterial hypertension may be related to severe hepatic functional impairment and subsequent portal hypertension. Our patient had significant systemic vasculitis, however, there was no associated liver dysfunction or portal hypertension. Therefore, we theorized that the PAH in our patient might be a consequence of the systemic vasculitis.

The pathophysiology of the development of PAH in CAEBV is unclear. It may be related to lymphocytic infiltration and the resultant damage to the pulmonary vascular endothelium caused by EBV infection or may occur secondary to the vascular damage caused by inflammatory reactions induced by EBV infection (11, 12). The current treatment strategies for CAEBV with pulmonary hypertension consist of targeted antihypertensive therapy, combined with immunosuppressants. Our patient had endothelial dysfunction due to vasculitis, and the targeted pulmonary pressure-reducing drugs mainly reduced the pulmonary pressure by supporting endothelial function. It has been reported that stem cell transplantation can effectively control the disease, but the treatment involves serious risks (13). At present, our patient is being followed up regularly. However, we are not optimistic about his long-term prognosis.

To the best of our knowledge, this is the first reported case of systemic vasculitis and PAH associated with CAEBV in a pediatric patient. This case report shows that a CAEBV should be considered within the differential diagnoses while managing a pediatric patient with secondary PAH and systemic vasculitis. And when the patient shows shortness of breath, edema, and other clinical manifestations of cardiac insufficiency, the PAH should be considered and given immunosuppressants combined with the targeted pulmonary pressure-reducing drugs. It must be emphasized that immunosuppressants are the main drugs and need for long-term treatment.

ETHICS STATEMENT

Written informed consent was obtained from the parents for the publication of this case report.

AUTHOR CONTRIBUTIONS

All authors listed have made a substantial, direct and intellectual contribution to the work, and approved it for publication.

REFERENCES

1. Virelizier JL, Lenoir G, Griscelli C. Persistent Epstein-Barr virus infection in a child with hypergammaglobulinaemia and immunoblastic proliferation associated with a selective defect in immune interferon secretion. *Lancet*. (1978) 2:231–4. doi: 10.1016/S0140-6736(78)91744-0
2. Kimura H, Hoshino Y, Kanegane H, Tsuge I, Okamura T, Kawa K, et al. Clinical and virologic characteristics of chronic active Epstein-Barr virus infection. *Blood*. (2001) 98:280–6. doi: 10.1182/blood.V98.2.280
3. Gru AA, Jaffe ES. Cutaneous EBV-related lymphoproliferative disorders. *Semin Diagn Pathol*. (2017) 34:60–75. doi: 10.1053/j.semdp.2016.11.003
4. Kimura H, Morishima T, Kanegane H, Ohga S, Hoshino Y, Maeda A, et al. Japanese association for research on epstein-barr V and related D. Prognostic factors for chronic active Epstein-Barr virus infection. *J Infect Dis*. (2003) 187:527–33. doi: 10.1086/367988
5. Lu G, Xie ZD, Zhao SY, Ye LJ, Wu RH, Liu CY, et al. Clinical analysis and follow-up study of chronic active Epstein-Barr virus infection in 53 pediatric cases. *Chin Med J*. (2009) :122:262–6. doi: 10.3760/cma.j.issn.0366-6999.2009.03.005
6. Ishihara S, Okada S, Wakiguchi H, Kurashige T, Morishima T, Kawa-Ha K. Chronic active Epstein-Barr virus infection in children in Japan. *Acta Paediatr*. (1995) 84:1271–5. doi: 10.1111/j.1651-2227.1995.tb13547.x
7. Muneuchi J, Ohga S, Ishimura M, Ikeda K, Yamaguchi K, Nomura A, et al. Cardiovascular complications associated with chronic active Epstein-Barr virus infection. *Pediatr Cardiol*. (2009) 30:274–81. doi: 10.1007/s00246-008-9343-8
8. Fukuda Y, Momoi N, Akaihata M, Nagasawa K, Mitomo M, Aoyagi Y, et al. Pulmonary arterial hypertension associated with chronic active Epstein-Barr virus infection. *Pediatr Int*. (2015) 57:731–4. doi: 10.1111/ped.12578
9. Hashimoto T, Sakata Y, Fukushima K, Maeda T, Arita Y, Shioyama W, et al. Pulmonary arterial hypertension associated with chronic active Epstein-Barr virus infection. *Intern Med*. (2011) 50:119–24. doi: 10.2169/internalmedicine.50.4143
10. Song HM, Wu XY, Wang W, Xing Y, Li F, Qiu JJ, et al. Clinical characteristics and follow-up of 12 cases with severe chronic active

Epstein-Barr virus infection. *Zhonghua Er Ke Za Zhi*. (2009) 47:682–6. doi: 10.3760/cma.j.issn.0578-1310.2009.09.012

11. Fujiwara M, Shimozono H, Ono H, Fujita N, Nishimura S, Ueda K, et al. Polyclonal proliferation of lymphocytes containing the epstein-barr virus genome in a patient dying of myocarditis in chronic active Epstein-Barr virus infection. *J Pediatr Hematol Oncol*. (2003) 25:85–8. doi: 10.1097/00043426-200301000-00018
12. Kanno H, Watabe D, Shimizu N, Sawai T. Adhesion of Epstein-Barr virus-positive natural killer cell lines to cultured endothelial cells stimulated with inflammatory cytokines. *Clin Exp Immunol*. (2008) 151:519–27. doi: 10.1111/j.1365-2249.2007.03584.x
13. Gotoh K, Ito Y, Shibata-Watanabe Y, Kawada J, Takahashi Y, Yagasaki H, et al. Clinical and virological characteristics of 15 patients with chronic active Epstein-Barr virus infection treated with hematopoietic stem cell transplantation. *Clin Infect Dis.* (2008) 46:1525–34. doi: 10.1086/587671

Conflict of Interest Statement: The authors declare that the research was conducted in the absence of any commercial or financial relationships that could be construed as a potential conflict of interest.

frontiers in Pediatrics

CASE REPORT
published: 06 June 2019
doi: 10.3389/fped.2019.00221

Extracorporeal Membrane Oxygenation Support for Cardiac Dysfunction Due to Kawasaki Disease Shock Syndrome

*Han Zhang†, Lijian Xie† and Tingting Xiao**

Department of Cardiology, Shanghai Children's Hospital, Shanghai Jiaotong University, Shanghai, China

Background: Kawasaki disease (KD) is usually characterized as an inflammatory vasculitis during early childhood, which predominantly involves medium-sized arteries and is treated with intravenous γ-globulin (IVIG) and oral aspirin. KD with hemodynamic instability, characterized by systolic blood pressure decreasing by more than 20% below the normal range, is defined as Kawasaki disease shock syndrome (KDSS). The pathogenesis of KDSS is still not comprehensively understood. Life-threatening cardiogenic shock can occur during the acute phase of KDSS, while the mechanism of cardiac dysfunction due to KDSS is still controversial, and such cases are rarely reported. Here, we present the application of veno-arterial (VA) extracorporeal membrane oxygenation (ECMO) for cardiac function support of a child with KDSS. By doing so, it will be a reminder that KDSS can cause severe cardiac dysfunction, and we should stay vigilant at the early stage of the disease to distinguish KDSS from toxic septic shock in the first place and initiate the appropriate treatment at the right moment, in order to prevent such patients from having irreversible outcomes.

Keywords: Kawasaki disease, Kawasaki disease shock syndrome, extracorporeal membrane oxygenation, cardiogenic shock, intravenous γ-globulin resistance

OPEN ACCESS

Edited by:
Fu Lijun,
Shanghai Children's Medical Center, China

Reviewed by:
Fang Liu,
Fudan University, China
Zhong-Dong Du,
Capital Medical University, China

****Correspondence:***
Tingting Xiao
ttxiao2017@163.com

†These authors share first authorship

Specialty section:
This article was submitted to Pediatric Cardiology, a section of the journal Frontiers in Pediatrics

Received: *03 March 2019*
Accepted: *16 May 2019*
Published: *06 June 2019*

Citation:
Zhang H, Xie L and Xiao T (2019) Extracorporeal Membrane Oxygenation Support for Cardiac Dysfunction Due to Kawasaki Disease Shock Syndrome. Front. Pediatr. 7:221. doi: 10.3389/fped.2019.00221

INTRODUCTION

Kawasaki disease (KD) is an inflammation related to vasculitis and mostly involving medium-sized arteries (1). The incidence of Kawasaki disease shock syndrome (KDSS) among patients with KD ranges from 1.9 to 7.0 (2–5). Children with KDSS require hemodynamic support and intensive medical care (6). The diagnosis of KDSS can be easily ignored, which can sometimes lead to irreversible consequences (7). In industrialized countries, KD is the leading cause of acquired heart disease during early childhood, and may result in long-term, potentially severe cardiovascular sequelae (8). Patients who clinically present with high degree of fever, rash, conjunctivitis, and severe cardiac and other organ dysfunction, mimicking toxic septic shock syndrome, lead to a diagnosis of KDSS (9). Use of extracorporeal life support for cardiac failure should be considered for patients with evidence of inadequate end organ perfusion and oxygen delivery resulting from inadequate systemic cardiac output: (a) Hypotension despite maximum doses of two inotropic or vasopressor medications. (b) Low cardiac output with evidence of end organ mal-perfusion despite medical support as described above: persistent oliguria, diminished peripheral pulses. (c) Low cardiac output with mixed venous or superior caval central venous (for single ventricle patients)

oxygen saturation <50% despite maximal medical support. (d) Low cardiac output with persistent lactate >4.0 and persistent upward trend despite optimization of volume status and maximal medical management (10). The case we reported here describes the successful deployment of veno-arterial (VA) extracorporeal membrane oxygenation (ECMO) under such circumstance.

CASE PRESENTATION

A 4-year-old girl (weight, 18 kg) with no medical history presented with 3 days of fever, 2 days of rash, and conjunctivitis. Physical examination revealed bilateral cervical lymphadenopathy and swelling of limb extremities. Chest and cardiac examination results were unremarkable. Laboratory test showed that the white blood cell (WBC) count was 12.50 $\times$ 10^9/L, neutrophils ratio (NE%) was 70.8%, platelet count (PLT) was 121 $\times$ 10^9/L, and C-reactive protein (CRP) was 127 mg/L. Erythrocyte sedimentation rate (ESR) was 90 mm. Serum albumin (ALB) and sodium were 38.17 g/L and 129 mmol/L, respectively. Troponin I was 0.07. Brain natriuretic peptide (BNP) was 147.03 pg/ml. Echocardiography on day 1 was normal (shortening fraction: 35%; ejection fraction: 66%). Diameters of the left and right coronary arteries were 0.24 and 0.20 cm (*Z* score, 2.0). Hence, she was suspected of having KD, and on day 2 of admission, before we could treat her with IVIG, she showed signs of shock, including increase in heart speed, cool extremities, oliguria, tachypnea, and hypotension (70/33 mmHg) requiring mechanical ventilation. She was immediately transferred to the intensive care unit. Electrocardiography (ECG) showed sinus tachycardia with alternation of T wave on leads II, III, and avF (**Figure 1a**). Chest X-ray showed bilateral lung field exudation and cardiomegaly. Arterial blood gas showed a lactate of 4.9 mmol/L. The urine output of the patient was <0.5 ml/kg/h. She urgently received continuous renal replacement therapy (CRRT) in CVVHDF mode and therapy for septic shock. Echocardiography showed a depression of systolic function (EF 35%) with dilation of left ventricular end diastolic dimension (LVDd 3.7 cm) and severe tricuspid valve regurgitation (TR; **Figures 1b,c**). Cardiac index (CI) was 1.7 L/min/m^2. Despite 0.6 μg/kg/min of both epinephrine and norepinephrine, her blood pressure couldn't be maintained (range, 57–69/31–40 mmHg). BNP was >15,000.00 pg/ml, and troponin I was 0.55. Laboratory findings and clinical features concluded the diagnosis of cardiogenic shock resulting from KDSS. Four hours later, she was placed onto central VA ECMO via neck cannulation.

A 15-Fr cannula (Medtronic or Edward's Lifesciences, Irvine, CA, USA) was placed in the right atrium and a 12-Fr cannula (Medtronic or Edward's Lifesciences, Irvine, CA, USA) was placed in the right common carotid aorta (**Figure 2a**). The fraction of inspiration O_2 (FiO_2) was 1.0, blood flow was 0.8 L/min, and gas sweep flow was 1.0 L/min. Treatment with 2 days of IVIG (1 g/kg per day) and 5 days of intravenous methylprednisolone (2 mg/kg per day) were initiated right away. A mean blood pressure level of 50–60 mmHg was maintained by the initial flows of ECMO, and the serum lactate was normalized within 8 h. After 2 days of IVIG, her body temperature still

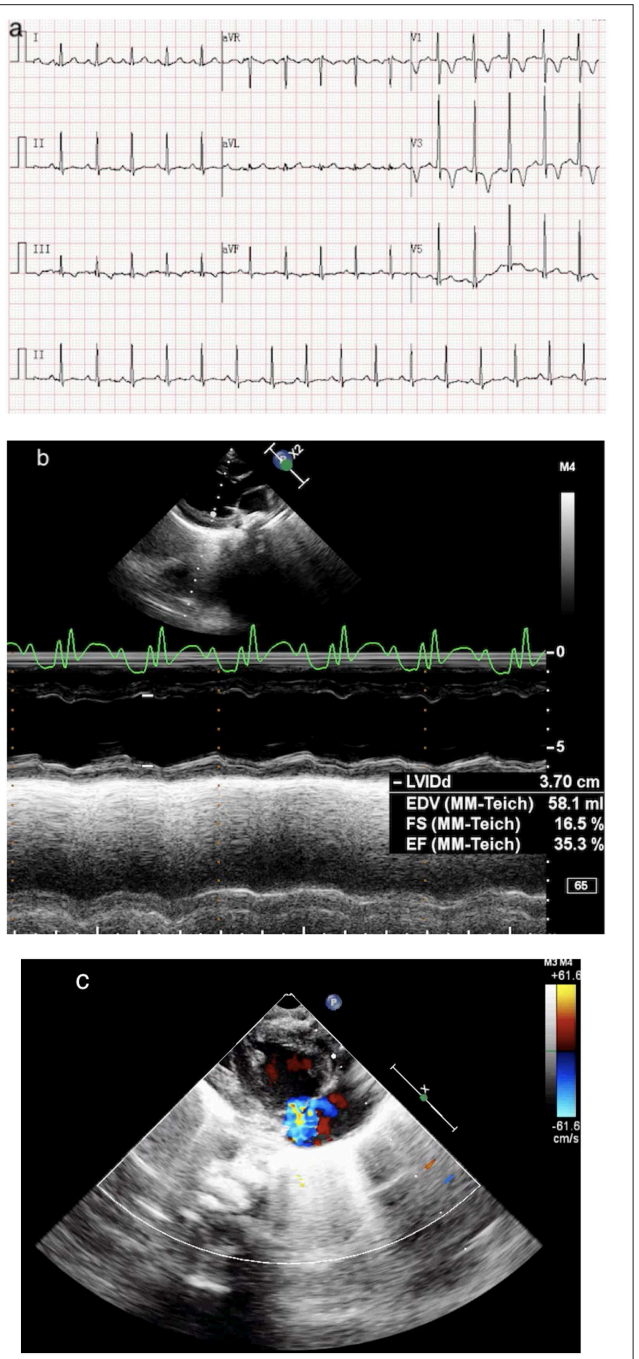

FIGURE 1 | (a) ECG shows sinus tachycardia with lowering and inverted T wave on leads II, III, and avF. **(b)** Echo shows a dilated, poorly functioning left ventricle (EF 35%). **(c)** Echo shows a severe TR.

fluctuated, and she was considered to be IVIG-resistant; she received plasma exchange (PE) for 6 h to reduce the inflammatory and immune reaction. Aspirin was maintained for 3 days at a dose of 30 mg/kg, and then at a dose of 5 mg/kg since. Fever settled on day 6.

The cardiac function of the patient recovered promptly on ECMO, and blood flow was reduced to 0.18 L/min and gas

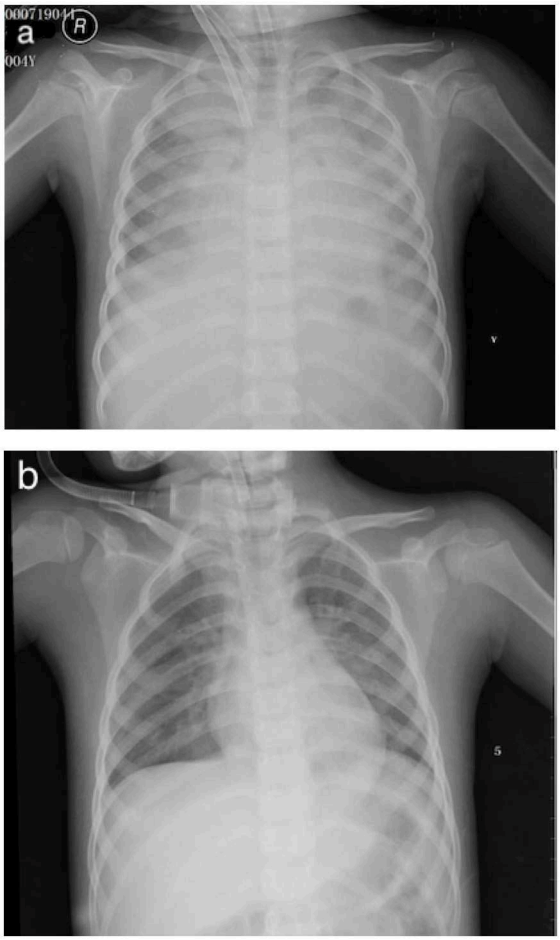

FIGURE 2 | (a) V-A ECMO via neck cannulation with a 15-Fr cannula in the right atrium and a 12-Fr cannula in the right common carotid aorta. **(b)** Chest X-ray post-ECMO.

sweep flow was 0.3 L/min after 76 h, which meets the standard of separation of ECMO. **Figure 2b** showed the X-ray post-ECMO. The patient's vital signs tended to be stable during ECMO, with proper blood pressure, adequate urine output, and resolution of heart failure (EF 46% at day 2 ECMO and EF 54% at day 3 ECMO). Bilateral blood culture detected no infections spreading through the bloodstream. **Table 1** shows laboratory findings pre- and post-ECMO. On day 9, the mechanical ventilation was separated and she was discharged on day 22. Follow-up within 3 months demonstrated that the cardiac and vascular functions were in the normal range (EF 65%, coronary arteries; *Z* score, 2.0).

TABLE 1 | Laboratory findings pre- and post-ECMO.

Day of admission	1	2*	3	4	5#	6
WBC ($\times 10^9$/L)	12.50	17.05	30.75	13.91	23.51	22.80
N (%)	70.8	81.2	82.5	84.2	89.6	77.8
PLT ($\times 10^9$/L)	121	118	210	112	112	116
AST (mmol/L)	54	50	74	591	2,720	633
ALT (mmol/L)	38	52	50	251	1,060	640
CRP (mg/L)	127	>180	>170	117	107	47
Albumin (g/L)	38.17	27.12	31.76	39.13	38.31	42.53
Sodium (mmol/L)	129	129	132	135	139	141
BNP (pg/ml)	147.03	>15,000.00	>15,000.00	>15,000.00	11,446.35	7,723.41
Troponin I	0.07	0.55	1.08	0.57	0.33	0.15

**ECMO was initiated. #ECMO was separated.*

DISCUSSION

KD is usually regarded as a type of systematic inflammatory vasculitis, of which coronary artery lesions (CALs) are the most common cardiovascular complications (2). Occasionally, life-threatening cardiac complications may occur during the acute phase of KD or even later as a consequence of myocardial involvement (9). KD is diagnosed according to the American Heart Association (AHA) guidelines (11). Acute cardiac dysfunction was observed at nearly 20% of KD cases, which is considered to be related to the higher incidence of coronary artery dilatation (9).

KDSS is a manifestation of KD that is uncommonly seen, defined as systolic hypotension or signs of poor perfusion (12). Capillary leakage caused by vasculitis and cytokine dysregulation due to inflammatory syndrome may be responsible for KDSS, although the actual cause is still unclear (13). Recently, one case of a KD patient was reported with suspected systemic capillary leak syndrome (SCLS) (3). As in our case, the patient could have experienced plasma extravasation due to such capillary leakage, and myocardial destruction may be linked to the elevated BNP and troponin I level. In a recent study, researchers suggested that acute LV dysfunction and mitral regurgitation (MR) are associated with inflammation-related laboratory findings, such as decreased ALB and elevated ESR (14). Cardiac abnormalities without coronary artery involvement and CALs in acute KD may develop from a common pathological mechanism relating to systemic inflammation (14). Qiu et al. (2) spoke highly of the specificity of cardiac injury markers compared to inflammatory indicators in KD patients complicated with cardiac dysfunction and thus concluded that the blood pressure of such patients who show signs of accelerated heart rate, diminished urine output, and cool extremities should be closely monitored and that more attention should be paid to their echocardiography and laboratory findings. Among patients with KDSS, the lower serum albumin, sodium, and potassium concentrations may be related to protein leakage caused by vascular inflammation (2). In addition, Schuster et al. (15) suggested that the presence of a low level of serum sodium is associated with the presence of shock. Further studies are necessary to assess whether the presence of moderate/severe hyponatremia may be used to predict KDSS. KDSS is often associated with more severe laboratory markers of inflammation and higher risk of coronary arterial dilation (11). In recent studies, the profound inflammation may be associated with a higher incidence of CALs in KDSS patients compared with KD patients without KDSS (4), while there were opposite results in other series (16). In our case, there were no positive coronary artery findings through the whole stage of her hospitalization, even during follow-up. Further investigation of the mechanism of

TABLE 2 | Clinical features in ELSO data comparing our case.

ELSO Data (Cardiac/ECPR) for Kawasaki disease: 1999–2017			Our reported case
	Median	Range	
Age (days)	248	51–4,625	1,645
Weight (kg)	8	5–50	18
Ventilation time prior to ECMO (h)	22	2–201	5
Blood flow 4 h (ml/kg/min)	85.5	46–156	50
Blood flow 24 h (ml/kg/min)	95	39–155	55

KDSS cardiac dysfunction might be helpful for us to understand the consequences of KD in the long run (14).

Manifestation of KDSS can be similar with clinical features of toxic shock syndrome, when hypotension was most commonly observed (17). The profound cardiac failure led to shock, which was difficult for us to distinguish from toxic septic shock at the beginning. As in our case, the profound shock manifested on day four of the illness, before the patient could meet the diagnostic criteria of complete KD. The high degree of the inflammatory indexes led us to the diagnosis of toxic septic shock. The echocardiography finding in toxic septic shock patients at early stage is mostly hyperdynamic systolic function of LV without myocardial dysfunction (18). This finding in toxic septic shock may suggest a compensating reaction to physiological shock, rather than a direct myocardial involvement (18). As a result, emergency bedside echocardiography and Uscom were used to detect ejection fraction and CI, which were helpful for us to distinguish cardiogenic shock caused by KDSS from septic shock.

Given the diagnosis of the shock in our case, we used V-A ECMO via neck cannulation. We searched through the Extracorporeal Life Support Organization (ELSO) Registry database. ECMO applications for 23 KD patients were reported from 1999 to 2017. Among those, 9 were supported for respiratory indication, while the other 14 underwent ECMO support for indications of cardiac or ECMO CPR (ECPR) (9, 19). In the accessible literature, we found that VA ECMO cardiac or ECPR support for KD cases was scarcely reported. Although ELSO is the authority in terms of ECMO use worldwide, it may be incomplete. There may still be other cases of VA ECMO support for KD that were not reported. **Table 2** compares the mean clinical features of patients from the ELSO database and our case, which shows that the ECMO flows we used were similar to that used in such population.

Taddio et al. (4) reported that a reduced ejection fraction was frequently seen in KDSS patients. Most cardiovascular complications recovered rapidly during the sub-acute or convalescent phase, and no patient presented persistent CALs. Some researchers have concluded that the prompt LV function resolution was associated with the modulation of immune-mediated processes (14). As in our case, we detected such cardiac abnormalities without CALs, including acute LV systolic dysfunction and severe TR, which were transient under VA ECMO support. The situation in our case was similar to prior studies (14). At the acute stage of KDSS, it may be misdiagnosed as toxic septic shock and be treated with inappropriate fluid resuscitation, hence worsening cardiac function or delaying IVIG treatment. As in our case, the cardiogenic shock occurred on day 4 of fever, before the patient met the diagnostic criteria of complete KD and also earlier than we usually initiate IVIG treatment as we deal with KD patients without KDSS. According to the AHA guidelines, such patients should be treated with high-dose IVIG (2 g/kg given as a single intravenous infusion) within 10 days of illness onset but as soon as possible after diagnosis (11). As in our case, the IVIG was not given in one large dose, which may be responsible for the rapid deterioration of the patients' situation. To sum up, it is vital to increase the knowledge of KDSS early recognition. Further studies on the correct use of IVIG for KDSS might help reveal the approach of preventing such patients from having irreversible outcomes.

CONCLUDING REMARKS

KDSS can cause life-threatening cardiac dysfunction, potentially complicated by coronary artery involvement. Clinicians should pay closer attention to KDSS, and IVIG should be initiated as a single intravenous infusion as soon as possible in such patients. Emergency bedside echocardiography and Uscom may serve as sensitive methods for early differentiation between KDSS and toxic septic shock. Although rarely reported, VA ECMO is useful as a lifesaving procedure for cardiac support in such cases.

DATA AVAILABILITY

All datasets generated for this study are included in the manuscript and/or the supplementary files.

ETHICS STATEMENT

This study was carried out in accordance with the recommendations of International Ethical Guidelines for Health-related Research Involving Humans, Council for International Organizations of Medical Sciences (CIOMS) with written informed consent from all subjects. All subjects gave written informed consent in accordance with the Declaration of Helsinki. The protocol was approved by the Institutional Review Board of Shanghai Children's Hospital.

AUTHOR CONTRIBUTIONS

HZ and LX prepared the entire manuscript. TX contributed to the conception of the case and revised the manuscript. HZ organized the database. All authors are responsible for manuscript revision and approved the submission of the case.

FUNDING

This work was supported by the Research Fund for Shanghai Healthy Committee (grant number: 201540099),

Shanghai Jiaotong University Medical Technology Crossing Project (YG2016ZD05), Shanghai Jiaotong University Medical Technology Crossing Project (YG2016QN41). No benefits in any form have been or will be received from a commercial organization directly or indirectly.

REFERENCES

1. Mandal S, Pande A, Mandal D, Sarkar A, Kahali D, Panja M. Various coronary artery complications of Kawasaki disease: series of 5 cases and review of literature. *J. Cardiovasc. Dis. Res.* (2012) 3:231e5. doi: 10.4103/0975-3583.98900
2. Qiu H, Li C, He Y, Weng F, Shi H, Pan L, et al. Association between left ventricular ejection fraction and Kawasaki disease shock syndrome. *Cardiol Young.* (2019) 29:178–84. doi: 10.1017/S1047951118002056
3. Chen PS, Chi H, Huang FY, Peng CC, Chen MR, Chiu NC. Clinical manifestations of Kawasaki disease shock syndrome: a case–control study. *J Microbiol Immunol Infect.* (2015) 48:43–50. doi: 10.1016/j.jmii.2013.06.005
4. Taddio A, Rossi ED, Monasta L, Pastore S, Tommasini A, Lepore L, et al. Describing Kawasaki shock syndrome: results from a retrospective study and literature review. *Clin Rheumatol.* (2017) 36:223–8. doi: 10.1007/s10067-016-3316-8
5. Lin MT, Fu CM, Huang SK, Wu MH. Population-based study of Kawasaki disease shock syndrome in Taiwan. *Pediatr Infect Dis J.* (2013) 32:1384–6. doi: 10.1097/INF.0b013e31829efae6
6. Yim D, Ramsay J, Kothari D, Burgner D. Coronary artery dilatation in toxic shock-like syndrome: the Kawasaki disease shock syndrome. *Pediatr Cardiol.* (2010) 31:1232–5. doi: 10.1007/s00246-010-9771-0
7. Ma L, Zhang YY, Yu HG. Clinical manifestations of Kawasaki disease shock syndrome. *Clin Pediatr.* (2018) 57:428–35. doi: 10.1177/0009922817729483
8. Phuong LK, Curtis N, Gowdie P, Akikusa J, Burgner D. Treatment options for resistant Kawasaki disease. *Paediatr Drugs.* (2018) 20:59–80. doi: 10.1007/s40272-017-0269-6
9. Best D, Millar J, Kornilov I, Sinelnikov Y, Chiletti R, Rycus P, et al. Extracorporeal membrane oxygenation for Kawasaki disease: two cases reports and the Extracorporeal Life Support Organization experience 1999–2015. *Perfusion.* (2017) 32:609–12. doi: 10.1177/0267659117701564
10. Extracorporeal Life Support Organization ECLS Guidelines. *Guidelines for Pediatric Cardiac Failure*. (2018). Available online at: https://www.elso.org/Portals/0/IGD/Archive/FileManager/ELSO_Reformatted_2018.02.23.pdf.
11. McCrindle BW, Rowley AH, Newburger JW, Burns JC, Bolger AF, Gewitz M, et al. Diagnosis, treatment, and long-term management of Kawasaki disease: a scientific statement for health professionals from the American Heart Association. *Circulation.* (2017) 135:927–99. doi: 10.1161/CIR.0000000000000484
12. Dominguez SR, Friedman K, Seewald R, Anderson MS, Willis L, Glodé MP. Kawasaki disease in a pediatric intensive care unit: a case–control study. *Pediatrics.* (2008) 122:786–90. doi: 10.1542/peds.2008-1275
13. Wang W, Zhu WH, Qi YQ, Fu SL, Gong FQ. Cardiogenic shock: do not forget the possibility of Kawasaki disease. *Turk J Pediatr.* (2012) 54:86–9.
14. Printz B, Sleeper L, Newburger J, Minich L, Bradley T, Cohen M, et al. Noncoronary cardiac abnormalities are associated with coronary artery dilation and with laboratory inflammatory markers in acute Kawasaki disease. *J Am Coll Cardiol.* (2011) 57:86–92. doi: 10.1016/j.jacc.2010.08.619
15. Schuster JE, Palac HL, Innocentini N, Rowley AH, Young LT, Shulman ST. Hyponatremia is a feature of Kawasaki disease shock syndrome: a case–control study. *J Pediatr Infect Dis Soc.* (2017) 6:386–8. doi: 10.1093/jpids/piw081
16. Gordon JB, Kahn AM, Burns JC. When children with Kawasaki disease grow up: myocardial and vascular complications in adulthood. *J Am Coll Cardiol.* (2009) 54:1911–20. doi: 10.1016/j.jacc.2009.04.102
17. Gamez-Gonzalez LB, Moribe-Quintero I, Cisneros-Castolo M, Varela-Ortiz J, Muñoz-Ramírez M, Garrido-García M, et al. Kawasaki disease shock syndrome: unique and severe subtype of Kawasaki disease. *Pediatr Int.* (2018) 60:781–90. doi: 10.1111/ped.13614
18. Lin YJ, Cheng MC, Lo MH, Chien SJ. Early differentiation of Kawasaki disease shock syndrome and toxic shock syndrome in a pediatric intensive care unit. *Pediatr Infect Dis J.* (2015) 34:1163–7. doi: 10.1097/INF.0000000000000852
19. *Extracorporeal Life Support Organization: ECLS Registry Report International Summary*. (2017). Available online at: https://www.elso.org/Registry/Statistics.aspx (accessed August 15, 2017).

Conflict of Interest Statement: The authors declare that the research was conducted in the absence of any commercial or financial relationships that could be construed as a potential conflict of interest.

frontiers in Pediatrics

ORIGINAL RESEARCH
published: 27 June 2019
doi: 10.3389/fped.2019.00261

Long-Term Outcomes of Children and Adolescents With Postural Tachycardia Syndrome After Conventional Treatment

Chunyan Tao[1], Wenxin Lu[1], Jing Lin[1], Hongxia Li[1], Xueying Li[2], Chaoshu Tang[3], Junbao Du[1,4] and Hongfang Jin[1]**

[1] Department of Pediatrics, Peking University First Hospital, Beijing, China, [2] Department of Medical Statistics, Peking University First Hospital, Beijing, China, [3] Department of Physiology and Pathophysiology, Peking University Health Science Center, Beijing, China, [4] Key Laboratory of Molecular Cardiovascular Science, The Ministry of Education, Beijing, China

OPEN ACCESS

Edited by:
Giovanni Biglino,
University of Bristol, United Kingdom

Reviewed by:
Amy C. Arnold,
Pennsylvania State University, United States
Yogen Singh,
Cambridge University Hospitals NHS Foundation Trust, United Kingdom

***Correspondence:**
Junbao Du
junbaodu1@126.com
Hongfang Jin
jinhongfang51@126.com

Specialty section:
This article was submitted to Pediatric Cardiology, a section of the journal Frontiers in Pediatrics

Received: 25 February 2019
Accepted: 07 June 2019
Published: 27 June 2019

Citation:
Tao C, Lu W, Lin J, Li H, Li X, Tang C, Du J and Jin H (2019) Long-Term Outcomes of Children and Adolescents With Postural Tachycardia Syndrome After Conventional Treatment. Front. Pediatr. 7:261. doi: 10.3389/fped.2019.00261

Objectives: To explore the long-term outcomes of children and adolescents with postural tachycardia syndrome receiving conventional interventions.

Materials and Methods: A total of 121 patients were recruited, but 6 (5.0%) of them were lost at follow-up. The detailed clinical data were collected, and the reoccurrence and frequency of orthostatic intolerance symptoms were evaluated with a mean followed-up period of 18.7 months (range, 14–74 months). The Kaplan-Meier curve was used to show the cumulative symptom-free rate of patients over time. Factors influencing the long-term outcomes were examined using the Cox's proportional hazards models.

Results: The cumulative symptom-free rate was gradually increased over time. It was 48.4% at the 1-year follow-up and increased to 85.6% at the 6-year follow-up. The duration of symptoms before treatment and the maximum upright heart rate in standing-up test were identified as independent indicators for the long-term outcomes. Each 1-month prolongation in the duration of symptoms before treatment was associated with a 1.2% decrease in the cumulative symptom-free rate. However, each 1-bpm increase in the maximum upright heart rate in standing-up test was associated with a 2.1% increase in the cumulative symptom-free rate.

Conclusions: The long-term outcomes of postural tachycardia syndrome patients who received conventional interventions are benign and the cumulative symptom-free rate was gradually increased over time. The prolonged duration of symptoms before treatment and the reduced maximum upright heart rate in standing-up test are the independent risk indicators.

Keywords: postural tachycardia syndrome, conventional interventions, long-term outcomes, children, adolescents

INTRODUCTION

Postural tachycardia syndrome (POTS) is an important form of orthostatic intolerance (OI) and is a constellation of symptoms including lightheadedness, chest discomfort, blurred vision, palpitations, and even syncope, which are elicited by excessive upright tachycardia and relieved by recumbence (1).

POTS in adolescents was firstly described by Bou-Holaigah et al. and it occurs at an estimated rate of 6.8% (2, 3). It negatively affects their physical and psychological health and impairs their quality of life (4, 5). Therefore, the investigation of the treatment for POTS has attracted great interest of clinical scientists. Up to now, multiple therapeutic methods have been introduced to deal with POTS in children and adolescents (6), among which conventional interventions are irreplaceable for their simplicity and for no obvious adverse effects (7, 8). There have been several studies on the therapeutic efficacy of conventional interventions in pediatric POTS patients (9–14). However, their long-term outcomes have never been reported, which limits pediatricians to predict the prognosis of this disease.

Therefore, this study focuses on the long-term outcomes and the associated factors of pediatric POTS patients receiving conventional treatment.

MATERIALS AND METHODS

We enrolled 121 patients [54 males and 67 females, median age 12.0 (10.0, 13.0) years] with a diagnosis of POTS and treated with conventional interventions at the Department of Pediatrics of Peking University First Hospital from July 2012 to July 2017. One hundred and fifteen patients completed our follow-up by telephone or clinic visits, but the remaining six patients (5.0%) were lost. This research was authorized by the Ethics Committee of Peking University First Hospital and all guardians of included patients gave written informed consent in accordance with the percepts expressed in the Declaration of Helsinki.

Mean corpuscular hemoglobin concentration and platelet were from blood routine test. Blood was drawn by venipuncture after at least 4 h fast and collected in a tube containing ethylene diamine tetraacetic acid. It was tested immediately at the Medical Laboratory of Peking University First Hospital (XE-5000, SYSMEX Corporation, Kobe, Japan) (13).

A urine collection kit for each patient was prepared in advance. A 24 h urine sample was collected and females were asked to take the 24 h urine samples during non-menstrual days. The 24 h urinary sodium excretion was determined using the ion-selective electrode method (Cobas 6000, Roche, Switerland). Twenty-four hours urinary sodium excretion = the concentration of sodium × the total urine volume (15).

Drugs influencing autonomic nervous function were avoided for at least 3 days before standing-up test. The testing environment was quiet, warm and dimly lit. Heart rate and blood pressure were recorded after 10–20 min of supine rest. Then, the patient was asked to stand for another 10 min, with simultaneously monitoring of heart rate and blood pressure (Dash 2000, General Electric, Schenectady, New York). The test was terminated ahead if the patient could not persist in finishing it. ΔHR = the maximum heart rate during standing—the baseline heart rate during supine (16).

Criteria of POTS in children and adolescents consisted of the following: (1) the presence of predisposing factors such as prolonged standing, rapid postural changes or exposure to emotional stress; (2) suffering from OI symptoms; (3) a positive response during standing-up test [normal heart rate in the supine position and an increment of heart rate $\geq$ 40 bpm or a maximum heart rate $\geq$ 130 bpm (in children aged 6–12 years) or $\geq$ 125 bpm (in adolescents aged 13–18 years) in standing-up test, without a decrease in blood pressure $\geq$20/10 mmHg]; and (4) the exclusion of other diseases that may likely cause OI symptoms (16).

The symptom scores of POTS were determined by the presence of typical symptoms (dizziness, headache, syncope, blurred vision, palpitation, chest discomfort, nausea, tremors, and sweating). Each symptom was counted based on its frequency (0 score, no symptom; 1 score, each symptom occurring once per month; 2 scores, 2–4 times per month; 3 scores, 2–7 times per week; 4 scores, more than once per day) and the total scores were calculated by summing all of the scores of each symptom (17).

Conventional interventions were used for each patient once diagnosed with POTS. Details of conventional interventions were listed as follows: (1) health education: informing patients and their guardians of possible causes, and teaching them how to avoid triggers and to protect themselves when experiencing OI symptoms; (2) supplement of water and salt: one bag of oral rehydration saline (Anjian Pharma Company, Xi'an, China) per day, containing 0.650 g sodium chloride, 0.725 g sodium citrate, 0.375 g potassium chloride and 3.375 g anhydrous glucose; (3) orthostatic training: asking patients to stand against a wall with the feet 15 cm away from the wall for a gradually increasing duration from 3 to 30 min, 2–3 times a day, depending on their orthostatic tolerance (11, 18). None of the patients continued implementing these interventions during the long-term follow-up. However, two of them got metoprolol or midodrine hydrochloride treatment for recurrent OI symptoms and they were regarded as censored subjects at the beginning of the introduction of the abovementioned new interventions. Designated doctors conducted the follow-up tasks by telephone or clinic visits in October 2018, with a mean follow-up duration of 18.7 months (range, 14–74 months). The main content of follow-up contained the reoccurrence and frequency of OI symptoms.

SPSS version 21.0 (IBM, Armonk, New York) was used for all data analyses. The normality of continuous data was examined by the Shapiro-Wilk test and continuous data with normal distribution are presented as mean ± standard deviation, otherwise as median (P_{25}, P_{75}). Bivariate correlations for continuous variables were tested using Pearson's correlation coefficient. Categorical variables are summarized as numbers (percentages). No reoccurrence of OI symptoms during follow-up was defined "event." The Kaplan-Meier curve was used to show the trend of cumulative symptom-free rate of patients

Abbreviations: POTS, Postural tachycardia syndrome; OI, Orthostatic intolerance.

TABLE 1 | Baseline demographic and clinical characteristics of the study participants.

Characteristics	Values
Participants (*n*)	115
Age (years)	12.0 (10.0, 13.0)
Gender (n, male/female)	50/65
Body mass index (kg/m^2)	17.4 (16.1, 19.8)
Duration of symptoms before treatment (months)	10.5 (2.0, 36.0)
MEDICAL HISTORY	
Predisposing factors (n, yes/no)	77/38
Syncope (n, yes/no)	61/54
Symptom scores before treatment (points)	4 (3, 7)
PERSONAL HISTORY	
Motion sickness (n, yes/no)	16/99
Allergic diseases (n, yes/no)	29/86
Family history about OI (n, yes/no)	29/86
CHARACTERISTICS IN STANDING-UP TEST	
Supine heart rate (bpm)	74 ± 11
Maximum upright heart rate (bpm)	121 ± 14
Changes of heart rate (bpm)	46 (40, 53)
ITEMS OF BLOOD ROUTINE TEST	
Mean corpuscular hemoglobin concentration (g/L)	347 (339, 354)
Platelet (*10^9/L)	257 (229, 298)
24 h urinary sodium excretion (mmol/24 h)	102 (73, 135)
Duration of treatment (months)	3.5 (3, 5)

OI, orthostatic intolerance. Continuous data with normal distribution are presented as mean ± standard deviation, otherwise as median (P_{25}, P_{75}) and categorical variables are summarized as numbers.

over time. The prognostic significance of baseline demographics, clinical characteristics, personal history, family history about OI, characteristics during standing-up test, blood routine test parameters and 24 h urinary sodium excretion with respect to long-term outcomes was examined using the Cox's proportional hazards models. Parameters with a p-value <0.1 in univariate model were introduced in the multivariate model by a stepwise method. All p-values were 2-sided and a p-value <0.05 was considered statistically significant.

RESULTS

A total of 121 pediatric POTS patients receiving conventional treatment were enrolled in this research, but 6 of them were lost at follow-up (5.0%). Among the 115 followed-up cases [50 males and 65 females, median age 12.0 (10.0, 13.0) years], 77 cases (67.0%) were accompanied with predisposing factors (prolonged standing as the most common one, then postural changes) and 61 cases (53.0%) suffered from syncopal events. A varied period of treatment, 3.5 (3, 5) months, was mainly because of the difference in the time of re-visiting our clinics and the more details are presented in **Table 1**.

In **Figure 1**, the number of patients with OI symptoms was gradually decreased over time, with a range of duration from 14 to 74 months to demonstrate the patients' outcomes at varied follow-up time. The cumulative symptom-free rates at 1, 2, 3, 4, 5, and 6 years after the beginning of follow-up were 48.4, 59.8, 73.0, 82.0, 85.6 and 85.6%, respectively.

Parameters with a $p < 0.1$ in the Cox univariate analysis (the duration of symptoms before treatment, the supine heart rate and the maximum heart rate in standing-up test, **Table 2**) were introduced in the multivariate analysis. However, given the strong collinearity between the supine heart rate and the maximum heart rate in standing-up test ($r = 0.711$, 95% CI, 0.620–0.795, $p < 0.001$) and the maximum heart rate used as one of the diagnostic criteria for POTS in standing-up test (16), only the maximum upright heart rate and the duration of symptoms before treatment were included eventually. The multivariate model showed that both of them were independent indicators for the long-term outcomes of the study patients ($p < 0.05$, **Table 3**). For each 1-month prolongation in the duration of symptoms before treatment, a decrease of 1.2% in the cumulative symptom-free rate was detected. However, for each 1-bpm acceleration in the maximum upright heart rate during standing-up test, an increase of 2.1% was detected.

DISCUSSION

In this research, we found that the cumulative symptom-free rate was gradually increasing during follow-up period. The duration of symptoms before treatment and the maximum upright heart rate in standing-up test were independent indicators for the long-term outcomes of pediatric POTS patients after conventional treatment, the former being a risk factor with its prolongation and the latter being a protective factor with its acceleration.

POTS is a hot topic in pediatrics, not only for its relatively high prevalence but also for its impact on the quality of life (19). We found that although most patients had benign outcomes, some of them still sustained OI symptoms for such a long term that it would be of help to reduce their psychological burden if clinicians could predict the prognosis and its influencing factors in advance. Kimpinski et al. conducted a prospective study to demonstrate favorite clinical outcomes at the 1-year follow-up, however, their therapeutic regimens were miscellaneous (20).

Prolonged duration of symptoms before treatment was identified as a risk factor for the prognosis of POTS patients receiving conventional interventions. Namely, the earlier such treatment was carried out, the better the prognosis would be. Unfortunately, in a large pediatric sample-sized study, Boris et al. observed that most of the participants visited doctors after suffering from OI symptoms for about 2 years (21), implying that the patients and their guardians might overlook such symptoms and more importantly, the physicians might lack the awareness of POTS and make misdiagnosis sometimes (22). Our results provided physicians with the evidence to encourage patients to visit doctors as early as possible and emphasized the importance of recognizing POTS.

When changing from supine to upright, gravity produces a rapid and large downward shift from thorax into vessels of the lower body. Simultaneously, the endogenous integrated

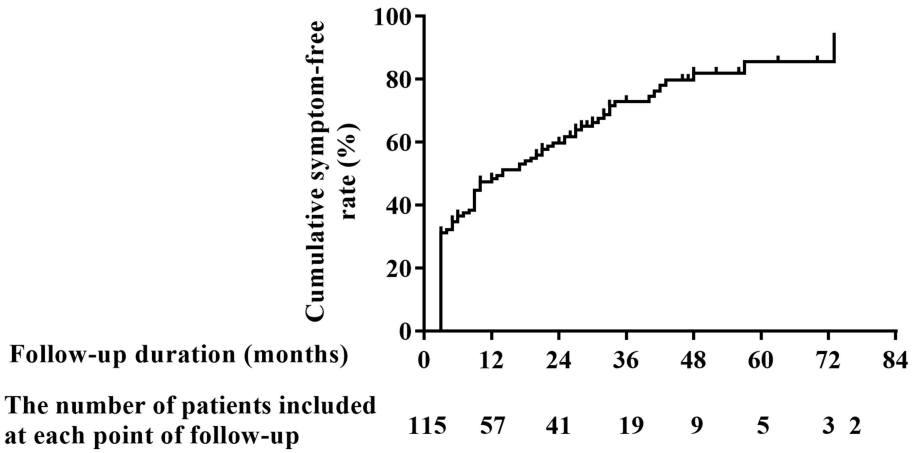

FIGURE 1 | Cumulative symptom-free rate of POTS patients receiving conventional interventions during long-term follow-up. POTS, postural tachycardia syndrome.

TABLE 2 | Results of univariate Cox's proportional hazard model regression.

Characteristics	B	SE	Wald	*p*-value	HR (95% CI)
Age (years)	−0.067	0.045	2.164	0.141	0.936 (0.856–1.022)
Gender (male vs. female)	−0.181	0.221	0.674	0.412	0.834 (0.541–1.286)
Body mass index (kg/m^2)	−0.033	0.043	0.582	0.445	0.968 (0.890–1.052)
Duration of symptoms before treatment (months)	−0.009	0.005	3.481	0.062	0.991 (0.982–1.000)
MEDICAL HISTORY					
Predisposing factors (yes vs. no)	−0.160	0.234	0.465	0.495	0.852 (0.539–1.349)
Syncope (yes vs. no)	−0.028	0.22	0.016	0.900	0.973 (0.632–1.498)
Symptom scores before treatment (points)	−0.001	0.028	0.001	0.978	0.999 (0.946–1.055)
PERSONAL HISTORY					
Motion sickness (yes vs. no)	0.387	0.317	1.488	0.223	1.472 (0.791–2.739)
Allergic diseases (yes vs. no)	−0.198	0.25	0.625	0.429	0.821 (0.503–1.340)
Family history about OI (yes vs. no)	0.11	0.253	0.191	0.662	1.117 (0.681–1.832)
CHARACTERISTICS IN STANDING–UP TEST					
Supine heart rate (bpm)	0.025	0.011	5.703	0.017	1.026 (1.005–1.047)
Maximum upright heart rate (bpm)	0.014	0.008	3.153	0.076	1.014 (0.999–1.030)
Changes of heart rate (bpm)	−0.001	0.011	0.004	0.952	0.999 (0.977–1.022)
ITEMS OF BLOOD ROUTINE TEST					
Mean corpuscular hemoglobin concentration (g/L)	0.011	0.009	1.437	0.231	1.011 (0.993–1.029)
Platelet (*10^9/L)	0.002	0.002	0.757	0.384	1.002 (0.998–1.006)
24 h urinary sodium excretion (mmol/24 h)	−0.001	0.002	0.218	0.641	0.999 (0.995–1.003)
Duration of treatment (months)	−0.001	0.106	<0.001	0.989	0.999 (0.812–1.228)

OI, orthostatic intolerance.

mechanisms are activated to compensate the reduced venous return. Any abnormality in the regulated progress might result in postural tachycardia (23). Our team previously found that the maximum upright heart rate in standing-up test $\geq$ 123 bpm could predict a favorable outcome after oral rehydration saline therapy in pediatric POTS patients (10). Tachycardia would be more obvious when reduced blood volume and impaired muscle sympathetic nerve activity occur concurrently in POTS patients, both of which are identified as common mechanisms for POTS (24, 25). Supplement of water and salt and orthostatic training could not only increase blood volume but also improve muscle sympathetic nerve activity (10, 26, 27). Under such condition, conventional treatment might improve patients' well-being significantly. It was observed in this study that the cumulative symptom-free rate would increase by 2.1% if there was a 1-bpm acceleration in the maximum upright heart rate in standing-up test. However, body mass index, mean corpuscular hemoglobin concentration, 24 h urinary sodium excretion and platelet, reported to have correlations with blood volume or autonomic nervous function (9, 10, 12, 28), were not

TABLE 3 | Results of multivariate Cox's proportional hazard model regression.

Characteristics	B	SE	Wald	*p*-value	HR (95% CI)
Duration of symptoms before treatment (months)	−0.012	0.005	5.652	0.017	0.988 (0.979–0.998)
Maximum upright heart rate in standing-up test (bpm)	0.021	0.009	5.661	0.017	1.021 (1.004–1.039)

independent indicators for the long-term outcomes for their unrepresentativeness of both blood volume and autonomic nervous function. Additionally, allergic diseases, common comorbidities in pediatric POTS patients (29, 30), and inheritance were not testified as independent factors.

Exactly, some limitations existed in the present study: (1) there is no control group in the present study. We could not tell the differences among patients receiving conventional interventions, pharmacological therapies and nothing; (2) there is a possibility of bias for the retrospective study design; (3) the study have the limitation of generalizability to other study populations for the characteristics, such as the similar gender ratio of the subjects in our study; and (4) the hazard ratios of the duration of symptoms before treatment and the maximum upright heart rate in the standing-up test were close to one.

To interpret the results of this study cautiously, the data showed that the cumulative symptom-free rate of POTS patients receiving conventional treatment would increase gradually over time and implementing conventional interventions to POTS patients with obvious tachycardia as early as possible might be of great help in improving their long-term outcomes.

DATA AVAILABILITY

The raw data supporting the conclusions of this manuscript will be made available by the authors, without undue reservation, to any qualified researcher.

ETHICS STATEMENT

This research was authorized by the Ethics Committee of Peking University First Hospital and all guardians of included patients gave written informed consent in accordance with the percepts expressed in the Declaration of Helsinki.

AUTHOR CONTRIBUTIONS

CyT had primary responsibility for the protocol development, patient enrollment, data collecting, preliminary data analysis, and writing the manuscript. WL, JL, and HL assisted with data collecting and preliminary data analysis. XL gave important advice on study design and revised data analysis. CsT gave important advice on the subject and revised the manuscript. JD and HJ supervised the design and execution of the study, checked the data analysis, contributed to the writing of the manuscript, and had a final approval of the manuscript submitted. All authors have read and approved the final manuscript and assumed full responsibility for its contents.

ACKNOWLEDGMENTS

The authors thank the children and their parents who participated in this study. This study was supported by Science and Technology Program of Beijing (Z171100001017253), Peking University Clinical Scientist Program (BMU2019LCKXJ001, Beijing, China) and the Fundamental Research Funds for the Central Universities.

REFERENCES

1. Jones PK, Shaw BH, Raj SR. Clinical challenges in the diagnosis and management of postural tachycardia syndrome. *Pract Neurol.* (2016) 16:431–8. doi: 10.1136/practneurol-2016-001405
2. Bou-Holaigah I, Rowe PC, Kan J, Calkins H. The relationship between neurally mediated hypotension and the chronic fatigue syndrome. *JAMA*. (1995) 274:961–7. doi: 10.1001/jama.274.12.961
3. Lin J, Han Z, Li X, Ochs T, Zhao J, Zhang X, et al. Risk factors for postural tachycardia syndrome in children and adolescents. *PLoS ONE.* (2014) 9:e113625. doi: 10.1371/journal.pone.0113625
4. Benrud-Larson LM, Dewar MS, Sandroni P, Rummans TA, Haythornthwaite JA, Low PA. Quality of life in patients with postural tachycardia syndrome. *Mayo Clin Proc.* (2002) 77:531–7. doi: 10.4065/77.6.531
5. Raj V, Haman KL, Raj SR, Byrne D, Blakely RD, Biaggioni I, et al. Psychiatric profile and attention deficits in postural tachycardia syndrome. *J Neurol Neurosurg Psychiatr.* (2009) 80:339–44. doi: 10.1136/jnnp.2008.144360
6. Johnson JN, Mack KJ, Kuntz NL, Brands CK, Porter CJ, Fischer PR. Postural orthostatic tachycardia syndrome: a clinical review. *Pediatr Neurol.* (2010) 42:77–85. doi: 10.1016/j.pediatrneurol.2009.07.002
7. Thieben MJ, Sandroni P, Sletten DM, Benrud-Larson LM, Fealey RD, Vernino S, et al. Postural orthostatic tachycardia syndrome: the Mayo clinic experience. *Mayo Clin Proc.* (2007) 82:308–13. doi: 10.4065/82.3.308
8. Ruzieh M, Grubb BP. Orthostatic intolerance and postural tachycardia syndrome: new insights into pathophysiology and treatment. *Herzschrittmacherther Elektrophysiol.* (2018) 29:183–6. doi: 10.1007/s00399-018-0563-1
9. Zhang Q, Liao Y, Tang C, Du J, Jin H. Twenty-four-hour urinary sodium excretion and postural orthostatic tachycardia syndrome. *J Pediatr.* (2012) 161:281–4. doi: 10.1016/j.jpeds.2012.01.054
10. Lin J, Liu P, Wang Y, Li H, Li X, Zhao J, et al. Evaluation of the changes in heart rate during head-up test predicting the efficacy of oral rehydration salts on postural tachycardia syndrome in children. *Chin J Pediatr.* (2015) 53:25–9. doi: 10.3760/cma.j.issn.0578-1310.2015.01.005
11. Li H, Liao Y, Wang Y, Liu P, Sun C, Chen Y, et al. Baroreflex sensitivity predicts short-term outcome of postural tachycardia syndrome in children. *PLoS ONE.* (2016) 11:e0167525. doi: 10.1371/journal.pone.0167525
12. Li H, Wang Y, Liu P, Chen Y, Feng X, Tang C, et al. Body mass index (BMI) is associated with the therapeutic response to oral rehydration solution in children with postural tachycardia syndrome. *Pediatr Cardiol.* (2016) 37:1313–8. doi: 10.1007/s00246-016-1436-1

13. Lu W, Yan H, Wu S, Xu W, Jin H, Du J. Hemocytometric measures predict the efficacy of oral rehydration for children with postural tachycardia syndrome. *J Pediatr.* (2017) 187:220–4. doi: 10.1016/j.jpeds.2017.04.034
14. Lu W, Yan H, Wu S, Chen S, Xu W, Jin H, et al. Electrocardiography-derived predictors for therapeutic response to treatment in children with postural tachycardia syndrome. *J Pediatr.* (2016) 176:128–33. doi: 10.1016/j.jpeds.2016.05.030
15. Chen SL, Dahl C, Meyer HE, Madar AA. Estimation of salt intake assessed by 24-hour urinary sodium excretion among Somali adults in Oslo, Norway. *Nutrients.* (2018) 10:E900. doi: 10.3390/nu10070900
16. Wang C, Li Y, Liao Y, Tian H, Huang M, Dong X, et al. Chinese Pediatric Cardiology Society (CPCS) guideline for diagnosis and treatment of syncope in children and adolescents. *Sci Bull.* (2018) 63:1558–64. doi: 10.1016/j.scib.2018.09.019
17. Tao C, Chen S, Li H, Wang Y, Wang Y, Liu P, et al. Value of immediate heart rate alteration from supine to upright in differential diagnosis between vasovagal syncope and postural tachycardia syndrome in children. *Front Pediatr.* (2018) 6:343. doi: 10.3389/fped.2018.00343
18. Tao C, Li X, Tang C, Jin H, Du J. Acceleration index predicts efficacy of orthostatic training on vasovagal syncope in children. *J Pediatr.* (2018) 207:54–8. doi: 10.1016/j.jpeds.2018.10.063
19. Pederson CL, Brook JB. Health-related quality of life and suicide risk in postural tachycardia syndrome. *Clin Auton Res.* (2017) 27:75–81. doi: 10.1007/s10286-017-0399-5
20. Kimpinski K, Figueroa JJ, Singer W, Sletten DM, Iodice V, Sandroni P, et al. A prospective, 1-year follow-up study of postural tachycardia syndrome. *Mayo Clin Proc.* (2012) 87:746–52. doi: 10.1016/j.mayocp.2012.02.020
21. Boris JR, Bernadzikowski T. Demographics of a large paediatric postural orthostatic tachycardia syndrome program. *Cardiol Young.* (2018) 28:668–74. doi: 10.1017/S1047951117002888
22. Stiles LE, Cinnamon J, Balan I. The patient perspective: what postural orthostatic tachycardia syndrome patients want physicians to know. *Auton Neurosci.* (2018) 215:121–5. doi: 10.1016/j.autneu.2018.06.002
23. Arnold AC, Ng J, Raj SR. Postural tachycardia syndrome-diagnosis, physiology, and prognosis. *Auton Neurosci.* (2018) 215:3–11. doi: 10.1016/j.autneu.2018.02.005
24. Medow MS, Stewart JM. The postural tachycardia syndrome. *Cardiol Rev.* (2007) 15:67–75. doi: 10.1097/01.crd.0000233768.68421.40
25. Lin J, Jin H, Du J. Assessment of therapeutic biomarkers in the treatment of children with postural tachycardia syndrome and vasovagal syncope. *Cardiol Young.* (2014) 24:792–6. doi: 10.1017/S1047951114000316
26. Endo Y, Yamauchi K, Tsutsui Y, Ishihara Z, Yamazaki F, Sagawa S, et al. Changes in blood pressure and muscle sympathetic nerve activity during water drinking in humans. *Jpn J Physiol.* (2002) 52:421–7. doi: 10.2170/jjphysiol.52.421
27. Tan MP, Newton JL, Chadwick TJ, Gray JC, Nath S, Parry SW. Home orthostatic training in vasovagal syncope modifies autonomic tone: results of a randomized, placebo-controlled pilot study. *Europace.* (2010) 12:240–6. doi: 10.1093/europace/eup368
28. Ozdemir O, Soylu M, Alyan O, Geyik B, Demir AD, Aras D, et al. Association between mean platelet volume and autonomic nervous system functions: Increased mean platelet volume reflects sympathetic overactivity. *Exp Clin Cardiol.* (2004) 9:243–7. doi: 10.1111/j.1542-474X.2004.94575.x
29. Liao Y, Zhang Q, Li H, Wang Y, Liu P, Du J, et al. Co-morbidity of vasovagal syncope and postural tachycardia syndrome with allergic diseases in children. *J Peking Univ Health Sci.* (2017) 49:783–8. doi: 10.3969/j.issn.1671-167X.2017.05.007
30. Penny HA, Aziz I, Ferrar M, Atkinson J, Hoggard N, Hadjivassiliou M, et al. Is there a relationship between gluten sensitivity and postural tachycardia syndrome? *Eur J Gastroenterol Hepatol.* (2016) 28:1383–7. doi: 10.1097/MEG.0000000000000740

Conflict of Interest Statement: The authors declare that the research was conducted in the absence of any commercial or financial relationships that could be construed as a potential conflict of interest.

frontiers in Pediatrics

ORIGINAL RESEARCH
published: 28 June 2019
doi: 10.3389/fped.2019.00237

MiR-222-3p in Platelets Serves as a Distinguishing Marker for Early Recognition of Kawasaki Disease

*Bo Wang[1], Li-nong Wang[1], Fang-fang Cheng[1], Hai-tao Lv[1], Ling Sun[1], Dong-kai Wei[2], Yu Pu[2], Jie Wu[2], Yuan-yuan Hou[2], Bin Wen[2], Xia-ping Xu[2] and Wen-hua Yan[1]**

[1] Internal Medicine-Cardiovascular Department, Children's Hospital of Soochow University, Suzhou, China, [2] QIAGEN (Suzhou) Translational Medicine Co., Ltd., Suzhou, China

Kawasaki disease (KD) is an acute vasculitis, which leads to 20% of sufferers developing coronary artery aneurysm in children if not appropriately treated. Therefore, the early diagnosis of KD is essential for alleviating the risk of developing heart disease. MicroRNAs (miRNAs) are a large class of small non-coding RNAs which post-transcriptionally regulate gene expression and have been shown to play critical roles in numerous biological processes and diseases. In this study, we used high-throughput miRNA sequencing and found dozens of miRNAs are highly expressed in platelets. By comparing the miRNA expression profile of platelets of acute KD patients and other febrile patients, miR-222-3p is validated to be significantly upregulated in platelets of acute KD patients. Furthermore, KEGG pathway analysis shows that targets of miR-222-3p are enriched in immune-related signaling pathways. Our study uncovers the potential of miR-222-3p in platelets as biomarker for early diagnosis of Kawasaki disease.

Keywords: Kawasaki disease, other febrile illness, miRNAs, platelets, miR-222-3p

OPEN ACCESS

Edited by:
Xupei Huang, Florida Atlantic University, United States

Reviewed by:
Keiichi Hirono, University of Toyama, Japan
Hong–Ren Yu, Chang Gung Memorial Hospital, Taiwan

***Correspondence:**
Wen-hua Yan
whyan328@sina.com

Specialty section:
This article was submitted to Pediatric Cardiology, a section of the journal Frontiers in Pediatrics

Received: *14 February 2019*
Accepted: *24 May 2019*
Published: *28 June 2019*

Citation:
Wang B, Wang L, Cheng F, Lv H, Sun L, Wei D, Pu Y, Wu J, Hou Y, Wen B, Xu X and Yan W (2019) MiR-222-3p in Platelets Serves as a Distinguishing Marker for Early Recognition of Kawasaki Disease. Front. Pediatr. 7:237. doi: 10.3389/fped.2019.00237

INTRODUCTION

Kawasaki disease (KD) is also known as mucocutaneous lymph node syndrome (1), which is a systemic vasculitis and its etiology remains obscure. Asian children and those younger than 5 years are more prone to be afflicted with Kawasaki disease (2). Approximately 15–25% cases of Kawasaki disease children may develop coronary artery abnormalities if not treated appropriately (3). It turns out to be the leading cause of pediatric acquired heart disease and increases the risk of myocardial infarction (4).

According to previous studies, intravenous immunoglobulin (IVIG) and aspirin can significantly reduce the incidence of coronary artery lesions (CALs) to ∼5% if treated in the first 10 days of KD (5, 6). However, the diagnosis of KD can be very challenging. Kawasaki disease is presented by prolonged fever for at least 5 days and coupled with at least four of the following clinical criteria: (1) bilateral non-exudative conjunctival injection; (2) changes in the mucosa of the oropharynx, including injected pharynx, dry fissured lips and strawberry tongue; (3) polymorphous exanthema; (4) changes of the peripheral extremities such as indurative oedema or erythema of hands and feet in the acute phase, and later membranous desquamation starting around the nail bed; (5) cervical lymphadenopathy >1.5 cm usually unilateral (7–11). Children with inadequate diagnostic criteria are classified as incomplete KD or atypical KD patients (8, 12), who are easily misdiagnosed and their treatment may be subsequently delayed, which greatly increases the risk of CALs. Thus, the identification of reliable biomarkers may facilitate early diagnosis and effective treatment of KD.

Some attempts have been made to identify protein biomarkers for KD. A study indicated that fibrinogen-related plasma protein (fibrinogen, alpha-1-antitrypsin, clusterin, and CD5L) levels are highly elevated during acute KD (13), among which plasma clusterin, also known as apolipoprotein J, has been recognized as a prognostic biomarker for CAL sequelae in KD (14). Besides, N-terminal pro-BNP (NTpro-BNP) was found to be elevated in the acute phase of KD (13, 15) and possess diagnostic utility and predictive value (16, 17). Kim et al. reported serum cardiac troponin I (cTnI) and creatinine kinase (CK)-MB as two biomarkers, occurring at higher level in KD patients in comparison to age-matched, non-KD control patients (18). Furthermore, nitric oxide synthases (iNOS) in neutrophils have also been identified as a promising biomarker, and have been found at higher expression levels during acute KD (19). Another important finding is that CXCL10 (IP-10) levels were significantly increased in KD patients, and there was IP-10 receptor CXCR3 activation in T cells of the acute KD cohort (20), providing insight into the use of cytokines as biomarkers for KD (21). Moreover, Yayoi et al. proved the potential of LRG1 as a biomarker to facilitate KD diagnosis by mass spectrometry (MS) (22).

Although various biomarkers have been reported, the consistency between different studies remains challenged. Besides, the low sensitivity to quantify low-abundant proteins and antibody-based detection limits the utility of protein biomarkers (23). Therefore, much easier detected and more delicate biomarkers are necessary.

Recent studies on cancer have revealed the potential importance of platelets in biomarker assessment from blood samples (24). Circulating platelets were reported to crosstalk with various cells such as leukocyte, endothelial cell et al. and molecules like ATP, thus serving as active media of intracellular communication. Furthermore, the transcriptome of platelets is swift altered responding to extracellular queues (25). Apart from mRNAs, platelet transcriptome contains various non-coding RNAs, including microRNAs and circular RNAs. These non-coding RNAs involve in multifarious biological processes, including vascular homeostasis, inflammation and contribute to platelet function (14).

To date, whether these non-coding RNAs, especially miRNAs in platelets have the potential as diagnostic biomarkers is still not clear. MicroRNAs (miRNAs) are a class of small RNA transcripts ranging from 18 to 25 nucleotides which post-transcriptionally regulate gene expression through destabilizing mRNA and/or translation inhibition. Previous studies have demonstrated that miRNAs play critical roles in numerous biological processes and diseases such as tumorigenesis (26–30), immune responses (31–34), differentiation (35–39), and apoptosis (40, 41). Furthermore, miRNA profiles are specific to various physiological and pathological conditions (42). Additionally, miRNA profiling has been shown to be more accurate than mRNA expression profiling in characterizing the difference of multiple human cancers (43), which postulates the possibility of platelets miRNAs as predictive biomarkers (44). In the current study, we investigated the potential of platelet miRNAs as biomarker for early diagnosis of Kawasaki disease and identified miR-222-3p as a distinguishing marker.

METHODS

Platelets Isolation

This study was carried out in accordance with the principles of the Basel Declaration and recommendations of guidelines for good clinical practice (GCP). The protocol (No.2018LW001) was approved by Children's Hospital of Soochow University ethics committee. Peripheral blood from KD patients and other febrile controls was obtained at initial diagnosis from Children's Hospital of Soochow University, Suzhou. Platelets were isolated from plasma at room temperature. In brief, a total of 1 ml peripheral whole blood was collected from the patients, anticoagulated with EDTA in purple-cap BD Vacutainers. The blood was centrifuged at 120 g for 20 min to collect platelet-rich plasma. The platelet-rich plasma was further centrifuged at 360 g for 20 min, after which the platelet pellet was washed twice in PBS (Gibco). The isolated platelet pellets were snap-frozen at −80°C for future use.

RNA Isolation

The mirVana^{TM} miRNA isolation kit (P/N: AM1560, Applied Biosystems) was chosen for the isolation of platelet miRNAs, and used according to the manufacturer's instructions with some modifications. Briefly, the platelet pellet was lysed and vortexed to obtain a homogenous lysate. A tenth volume of miRNA homogenate additive was added to the lysate and the sample was mixed rigorously by vortex before incubation on ice for 10 min. The mix was purified with acid-phenol: chloroform, followed by filter through solid-phase cartridge. The flow-through was discarded and the column was subjected to washing steps. 100μl of nuclease-free water, preheated to 95°C, was used to elute platelet miRNA and centrifuged at 11,000 g for 45 s. The RNA was quantified with Nanodrop spectrophotometer (ND1000). RNA sample quality was evaluated by Agilent 2100 Bioanalyzer (Agilent Technologies).

Small RNA Library Construction and Sequencing

All small RNA libraries were prepared using NEBNext Multiplex Small RNA Library Prep Set (NEW ENGLAND Biolabs). Briefly, 100 ng of total RNA was prepared from each sample to ligate diluted 3' SR adaptor directly. Subsequently excessed 3′ SR adaptors were hybridized with SR RT primer to prevent adaptor-dimer formation, followed by ligation of 5′ SR adaptor with T4 RNA ligase and reverse transcription to generate single-strand cDNA. To enrich the products for sequencing, 15-cycle PCR amplification was performed on the first cDNA strands using Illumina compatible multiplexed primer sets. The resulting library was subjected to size selection and purification with 10% PAGE gel (Solarbio). The concentration and quality of each small RNA library was examined by Qubit 2.0 (Invitrogen) and DNA High Sensitivity Chip (Agilent). High quality libraries with size between 150 and 160bp were pooled in equimolar concentration and sequenced for SE50 on Hiseq 2500 (Illumina).

Quantitative Real-Time PCR (qRT-PCR) Validation of miRNAs

The cDNA was synthesized in a 25 μl volume containing 50 ng total RNA, 5 μl 5 × PAP/RT buffer, 1 μl RTase mix and 1 μl 2.5 U/μl Poly A Polymerase included in the All-in-One™ miRNA First-Strand cDNA Synthesis kit (GeneCopoeia). RT reactions were incubated at 37°C for 1 h, followed by 85°C for 5 min to inactivate reverse transcriptase mix and placed on ice. The resultant cDNAs were diluted to 1 ng/μl before use. MiRNA qPCR primers were designed based on mature miRNA sequences from miRBase v20. For has-miR-222-3p the primer sequence is AGCTACATCTGGCTACTGGGTAA and for C.elegans miR-39-3p the primer sequence is: TCACCGGGTGTAAATCAGCTTGAA. Quantitative real-time PCR reactions were conducted on the 7500 Real-Time PCR system (Applied Biosystems) using the All-in-OneTM miRNA qRT-PCR Detection kit (GeneCopoeia).

Bioinformatics

MiRNA sequencing reads were matched to the miRBase miRNA hairpin precursors by mapper.pl provided by miRDeep2, after trimming the adapter sequence with fastx_clipper from fastx toolkit. CPM was obtained with the raw read count of each miRNA normalizing to library size of corresponding sample. R 3.5.1 was used for the generation of venn diagram, heatmap and violin plot. Python 3.5.5 was used to build random forest classifier model and generate receiver operating characteristic (ROC) curve and histogram.

RESULTS

Sets of miRNAs Are Differentially Expressed in Platelets of Kawasaki Disease and Other Febrile Patients

To identify candidate miRNAs differentiating Kawasaki disease (KD) and other febrile illness (OFI), we enrolled 32 pediatric patients, including 16 children diagnosed with KD and 16 diagnosed with pneumonia, Bronchitis et al. which were grouped into OFI (**Supplementary Table 1**). Patients included in KD and OFI were matched for age and prolonged fever time (**Supplementary Figure 1**). Total RNA was extracted from platelets after elaborating isolation of platelets from whole blood. The platelet RNA was subjected to small RNA sequencing library construction and sequenced. Count per million (CPM) was used for expression level quantification. MiRNAs with CPM higher than 100 in at least half samples were considered expressed for further analysis (**Supplementary Table 2**).

The most abundant microRNAs in platelets of KD patients are members of the let-7 microRNA family, which represented 42.84% of the platelet microRNA content (**Figure 1A**), consistent with previous identified miRNA profile in human platelets (45–47). The data pertaining to the 10 most abundant platelet microRNA families are compiled (**Supplementary Table 3**) and show that individual microRNAs, such as miR-21-5p, miR-30a/d-5p, miR-92a-3p, miR-103a-3p, miR-148a-3p, miR-26a-5p, miR-222-3p, and miR-151a-3p also accounted for an important proportion of human platelet microRNAs. 123 and 121 miRNAs were detected in platelets of OFI and KD patients, respectively, and the majority of miRNAs (78.1%) were both expressed in different disease states (**Figure 1B**), including key miRNAs in innate immune responses such as miR-146a and miR-155 (48). Among the expressed miRNAs in either KD or OFI patients' platelets, volcano plot showed that 35 miRNAs were differentially regulated with average CPM change for more than 2 folds and p-value < 0.01 (**Figures 1C,D**). 12 miRNAs were upregulated in KD patients' platelets while 23 miRNAs were downregulated.

MiR-222-3p Is Identified as a Distinguishing Marker in KD and OFI Patients

We reasoned that these differentially expressed miRNAs may largely contribute to the distinguished bio-signatures of KD and OFI patients, and thus may play important roles in the early diagnosis of Kawasaki disease. A random forest classifier (RFC) model was built with a training set containing 22 samples (11 KD and 11 OFI) using differentially expressed 35 miRNAs as features. Parameters were optimized by Bayesian Optimization (49) and used to train the model. Furthermore, we examined the generalization ability of the model by interrogating the remaining 10 samples (5 KD and 5 OFI). The receiver operating characteristic (ROC) curve was generated by comparing the predicted result with true sample class and the area under curve (AUC) reached 0.94 (**Figure 2A**), which suggested the high quality of this model in distinguishing KD from OFI samples. These data showed that the differentially expressed platelet miRNAs hold great potential in distinguishing KD patients from other febrile illness patients. To determine the most important miRNA in differentiating KD and OFI patients, the relative rank (i.e., depth) of miRNAs was used as decision node in the RFC model. As a result, miR-222-3p was shown as the miRNA feature with greatest importance (**Figure 2B**). MiR-222-3p shares identical seed sequence "GCUACAU" with miR-221-3p, both of which belong to miR-221 family of miRNAs, are highly expressed in platelets of KD patients (**Figure 1A**), which denotes it as a potent distinguishing marker in KD and OFI.

MiR-222-3p Is Validated to Be Upregulated in Platelets of KD Patients

With the high throughput miRNA sequencing data, we found that miR-222-3p expression was significantly upregulated in KD patients comparing with OFI patients (**Figure 2C**). Quantitative real time PCR (qRT-PCR) was performed to validate the expression change of miR-222-3p in KD patients. Due to the limited amount of platelet RNA available from patients, we only performed qPCR on 6 samples with platelet RNA remained (3 KD and 3 OFI). With C.elegans miR-39-3p as exogenous miRNA normalization control as suggested by Nicholas et al. (47), miR-222-3p was upregulated for 2.41 fold (**Figure 2D**), which was consistent with the small RNA sequencing data. These data demonstrate that miR-222-3p is upregulated in platelets of KD

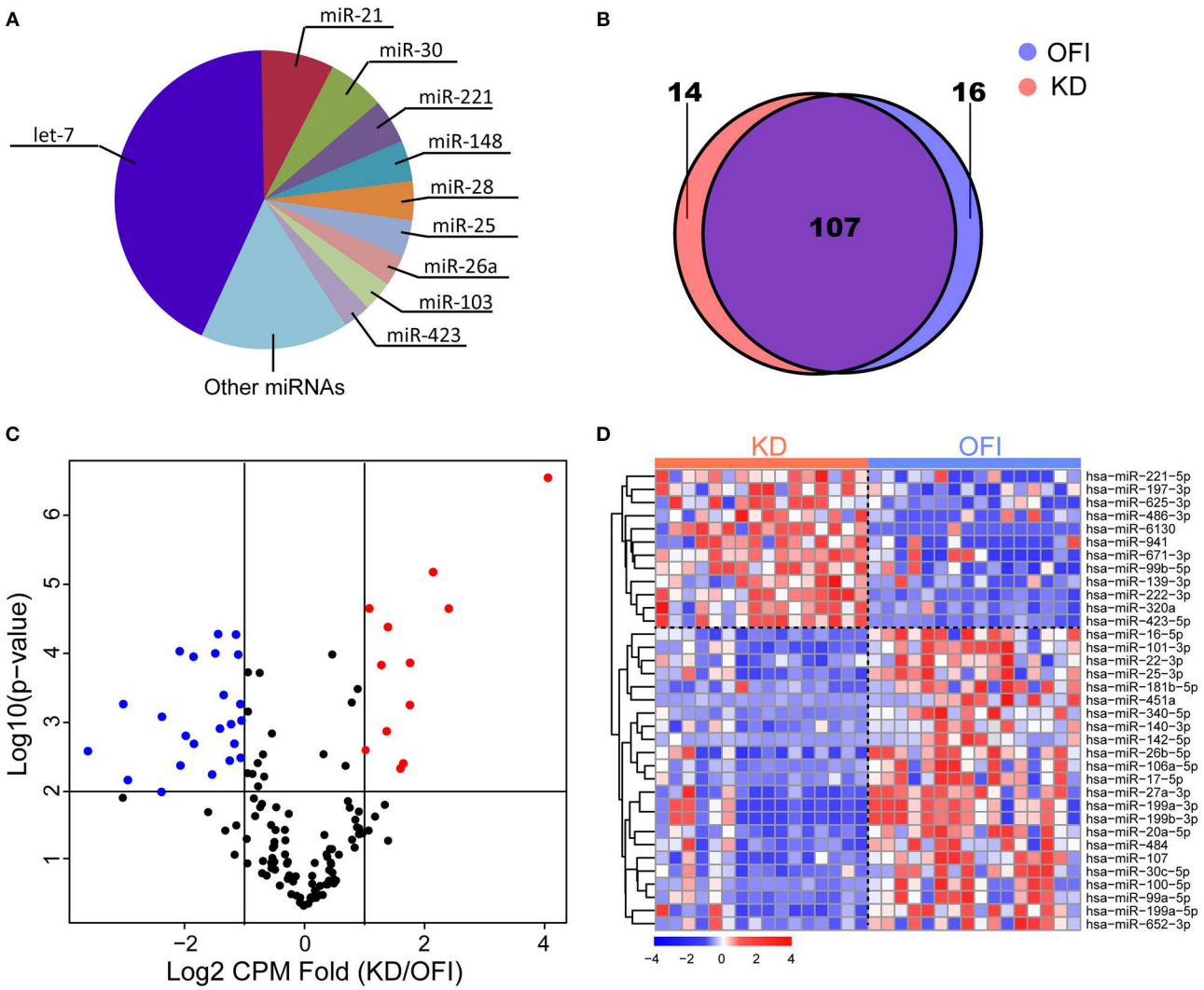

FIGURE 1 | MiRNA expression profile of platelets of Kawasaki disease and other febrile patients. **(A)** Ten most abundant miRNA families expressed in platelets of KD samples. **(B)** Patients with KD or OFI share majority of expressed miRNAs in platelets. **(C)** Volcano plot of expressed miRNAs. **(D)** Heatmap of 35 miRNAs differentially expressed in KD compared with other febrile patients.

patients, which may act as a potential biomarker for the diagnosis of Kawasaki disease.

KEGG Pathway Enrichment of Predicted Target Genes of miR-222-3p

To further understand the biological significance of the upregulation of miR-222-3p in platelets of KD patients, we conducted KEGG pathway enrichment analysis of predicted miR-222-3p target genes. Three target prediction tools were chosen to identify authentic target genes of miR-222-3p, including TargetScan (50), miRanda (51) and MirTarget2 (52). A total of 165 common target genes of hsa-miR-222-3p were identified by comparing three sets of predicted target genes (**Figure 3A**). DAVID (53) was used for KEGG pathway enrichment analysis and the top 10 pathways were listed (**Figure 3B**). Surprisingly, the predicted target genes of miR-222-3p were most enriched in the T cell receptor signaling pathway, as well as B cell receptor signaling pathway, suggesting the involvement of platelet miRNAs in immune dysfunction. Consistently, KD is characterized with down-regulation of T cell receptor and B cell receptor signaling pathways by several studies (54–56).

DISCUSSION

Due to the long-lasting and detrimental coronary effects that Kawasaki disease may cause (11), accurate early diagnosis is necessitated for early recognition of the disease. To our knowledge, this is the first study showing potential of implementing platelet miRNAs in clinical practice for the diagnosis of Kawasaki disease. Here we show that human platelets express dozens of miRNAs, including miRNA families reported previously, such as let-7, miR-21, miR-25, miR-203 et al. (45). We

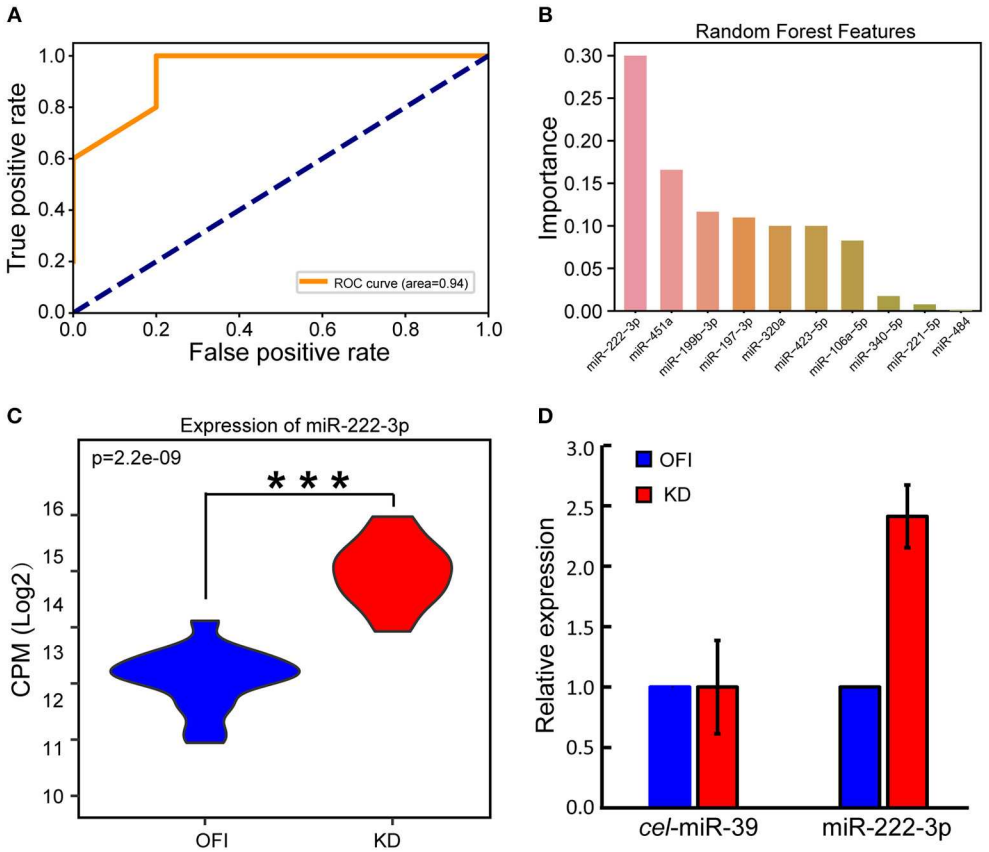

FIGURE 2 | MiR-222-3p was identified as a distinguishing marker in KD and OFI samples. **(A)** Receiver operating characteristic (ROC) curve of RFC model on test set. **(B)** Relative rank of miRNAs used as decision node in the RFC model. **(C)** CPM distribution of miR-222-3p by small RNA sequencing. **(D)** qRT-PCR validation of miR-222-3p expression. C.elegans miR-39-3p was used as control. ***$P < 0.001$.

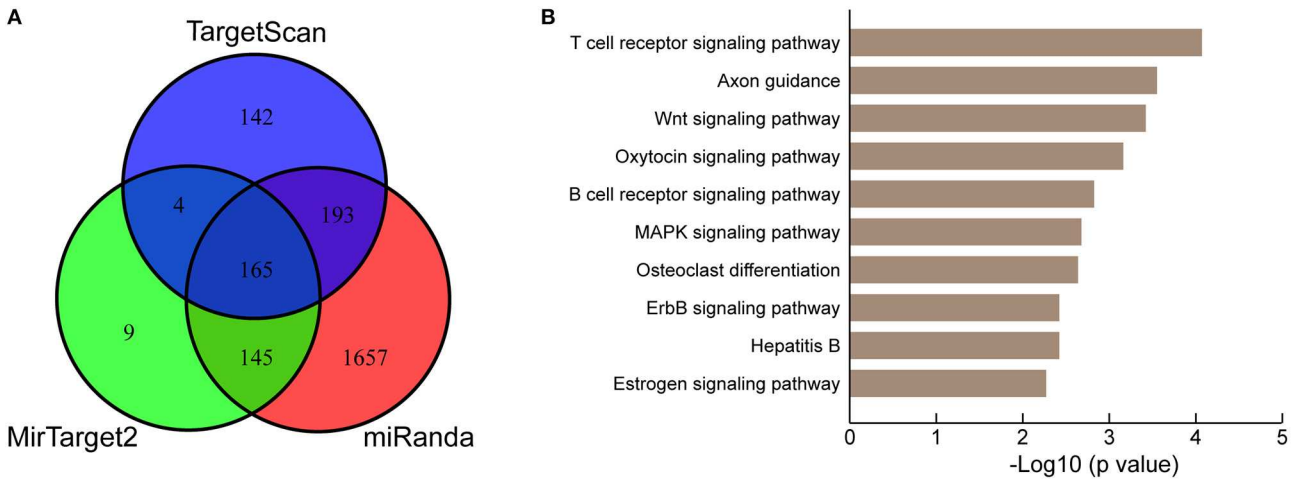

FIGURE 3 | KEGG pathway analysis of miR-222-3p predicted targets. **(A)** Three miRNA target prediction tools are used for identifying authentic targets of miR-222-3p. **(B)** KEGG pathways enriched by common miR-222-3p predicted targets.

further identify 35 miRNAs differentially expressed in platelets of KD patients and other febrile patients, among which miR-222-3p was validated to be upregulated in KD platelets. KEGG pathway analysis revealed that the targets of miR-222-3p were enriched in T-cell receptor pathway, indicating the crosstalk of miRNA between immune pathways. Further interactome

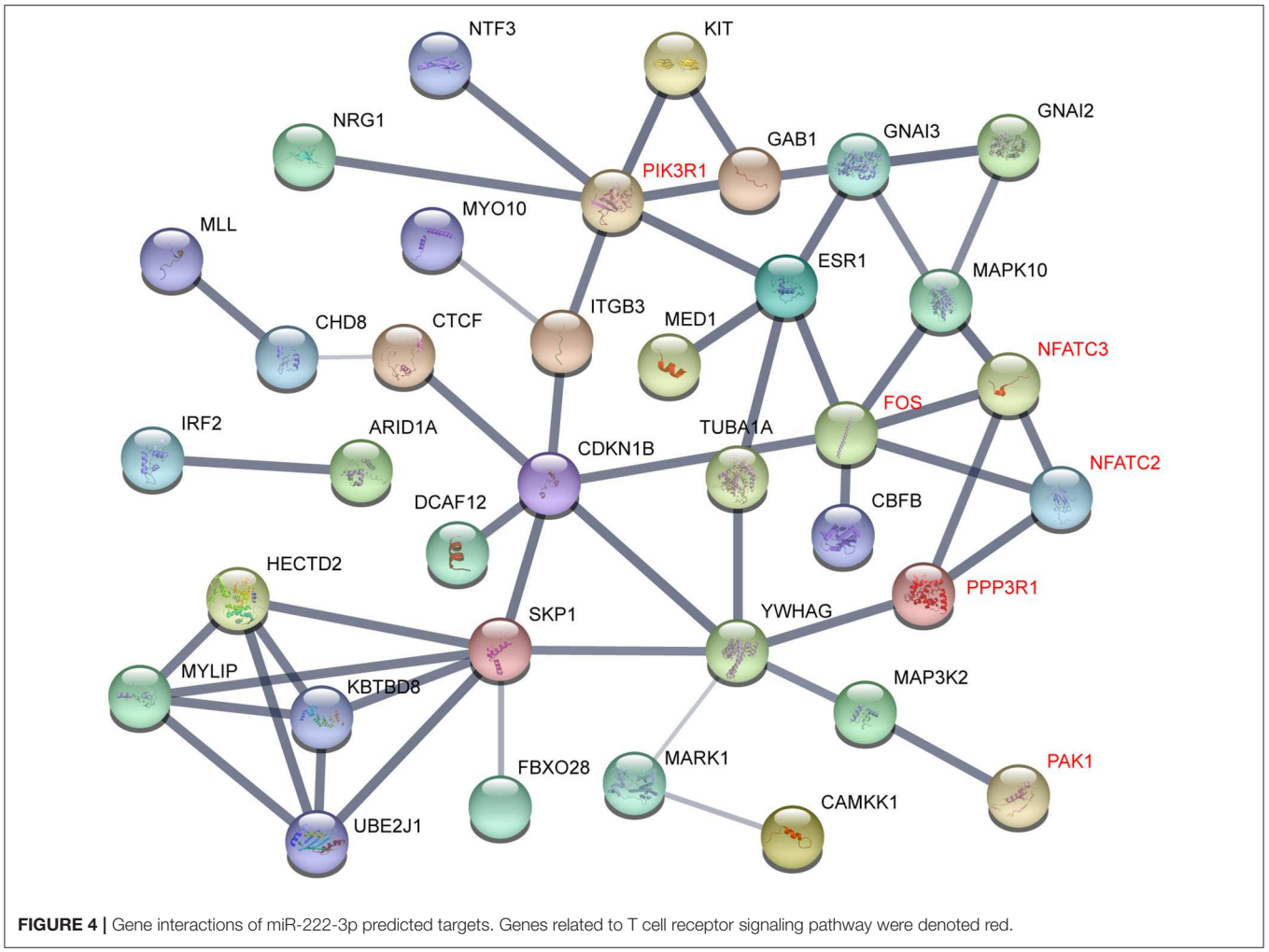

FIGURE 4 | Gene interactions of miR-222-3p predicted targets. Genes related to T cell receptor signaling pathway were denoted red.

analysis suggested that the predicted target genes of miR-222-3p constituted a network of signaling pathways.

A few studies have been focusing on miRNA biomarkers for Kawasaki disease. Jia et al. reported that two pairs of serum exosomal miRNAs, including miR-1246/miR-4436b-5p, and miR-197-3p/miR-671-5p, distinguish KD patients from healthy individuals and those with viral infection as candidate diagnostic biomarkers (57). Another study uncovered seven miRNAs were significantly upregulated (hsa-let-7b-5p, hsa-miR-223-3p, hsa-miR-4485, hsa-miR-4644, hsa-miR-4800-5p, hsa-miR-6510-5p, and hsa-miR-765) and three were significantly downregulated (hsa-miR-33b-3p, hsa-miR-4443, and hsa-miR-4515) in plasma of acute KD compared with the healthy controls (58). A similar study claimed that miR-200c and miR-371-5p were elevated in serum in children with Kawasaki disease (59). In our study, hsa-let-7b-5p and hsa-miR-223-3p were slightly downregulated, while miR-200c, miR-197-3p and miR-671-5p was upregulated in KD for 2.09, 2.09 and 2.43 fold, respectively, and the rest of the above mentioned miRNAs were detected in neither KD nor OFI platelet samples. The discrepancy lies in the different background of starting material, indicating specific miRNA expression profile in exosome, plasma and platelets.

There were 35 miRNAs differentially expressed for more than 2 fold, among which miR-222-3p was the top miRNA with highest expression. Previous study revealed that serum miR-221/222 level was significantly elevated in patients with coronary artery disease, suggesting they might be potential diagnostic biomarkers (60). Another important finding is that pathway significance analysis of blood lymphocyte-specific gene markers revealed that T cell receptor signaling pathway is down-regulated in KD, compared to febrile controls (55). Intriguingly, the overlapped miR-222-3p predicted targets were enriched in the T cell receptor signaling pathway and the B cell receptor signaling pathway. Thus, the upregulation of miR-222-3p in KD platelets may partially explain the downregulation due to the crosstalk between platelets and leukocytes. However, more delicate validations are imperative of whether these target genes are indeed regulated by miR-222-3p. These data indicated the involvement of platelet miRNAs in regulation of essential signaling pathways in immune response, which is worthy of further mechanistic investigations.

To understand the interactome of predicted targets of miR-222-3p, the total 165 targets overlapped by the three prediction tools were used to construct the interaction network

with STRING (61). The core sub-network was shown with default settings (**Figure 4**). The genes involved in T and B cell receptor signaling pathway were denoted red, including PIK3R1, FOS, NFATC2, NFATC3, PPP3R1, and PAK1. These genes also interacted with many other factors involved in various signaling pathways, resulting in a network influenced by miR-222-3p.

This study brings the possibility of miR-222-3p as potential diagnostic biomarker for Kawasaki disease. MiR-222 has been reported to participate in the pathogenesis of many inflammatory diseases, including rheumatoid arthritis, atherosclerosis and obesity-related inflammation (62, 63). Comparing to the miRNAs merely enriched by bioinformatics, miR-222-3p was more biological. Besides, even in the KD group, miR-222-3p was lower in those suffering with coronary artery lesion (**Supplementary Figure 3**), indicating the potential of using miR-222-3p as predictor of CAL. Future work shall be focused on application of this miRNA in clinical diagnosis of KD, such as developing easily handled *in vitro* diagnostic kits and exploring combinatory diagnostic miRNA sets. Besides, it turns out that the KD group patients are prone to have high CRP levels and platelet count at initial diagnosis (**Supplementary Figure 2**), which has been reported as inflammatory biomarkers for Kawasaki disease (64). Incorporating clinical manifestations such as CRP and/or platelet count with miRNAs as combinatory biomarkers to facilitate diagnosis is worthy of further investigation.

HUMAN SUBJECTS/INFORMED CONSENT STATEMENT

All procedures followed were in accordance with the ethical standards of the responsible committee on human experimentation (institutional and national) and with the Helsinki Declaration of 1975, as revised in 2000. Informed consent was obtained from all patients for being included in the study.

ANIMAL STUDIES

No animal studies were carried out by the authors for this article.

DATA AVAILABILITY

The normalized CPM of miRNAs expressed in the clinical samples are listed in **Supplementary Figure 2**. The original miRNA sequencing data can be available upon request.

ETHICS STATEMENT

This study was carried out in accordance with the recommendations of guidelines for good clinical practice (GCP) with written informed consent from all subjects. All subjects gave written informed consent in accordance with the Declaration of Helsinki. The protocol was approved by the Children's Hospital of Soochow University ethics committee.

AUTHOR CONTRIBUTIONS

WY and DW conceived and planned the study and wrote the paper. JW, BWa, and YH performed the experiments with the help from other authors. YP performed bioinformatics analysis for data from small RNA sequencing experiments. All authors participated in data analysis and figure preparation.

FUNDING

Our work is supported by the National Natural Science Foundation of China (grant Nos. 81600391, 81700439, and 81800437).

ACKNOWLEDGMENTS

We thank Qianwen Wang for clinical sample collection and our group members for helpful discussion.

SUPPLEMENTARY MATERIAL

The Supplementary Material for this article can be found online at: https://www.frontiersin.org/articles/10.3389/fped.2019.00237/full#supplementary-material

Supplementary Figure 1 | Patients included in KD and OFI are matched for age and illness day. **(a)** Comparison of age of patients enrolled in each group. **(b)** Comparison of duration of fever before sample collection.

Supplementary Figure 2 | Detailed comparison of clinical lab data between KD and OFI samples. WBC, white blood cell; AST, aspartate aminotransferase; CRP, C-reaction protein; PLT, platelet count (at initial diagnosis). Each point represents one sample. $^{*}P < 0.05$; $^{**}P < 0.01$.

Supplementary Figure 3 | MiR-222-3p expression within KD group differentiated with coronary artery lesion. Each point represents one sample.

Supplementary Table 1 | Clinical manifestations of samples enrolled in this study.

Supplementary Table 2 | CPM of expressed miRNAs.

Supplementary Table 3 | Ten most abundant platelet microRNA families expressed in KD samples.

REFERENCES

1. Billoo AG, Lone SW, Siddiqui S, Atiq H. Incomplete Kawaski disease: are we missing it? *J Pak Med Assoc.* (2009) 59:42–3.
2. Kawasaki T, Kosaki F, Okawa S, Shigematsu I, Yanagawa H. A new infantile acute febrile mucocutaneous lymph node syndrome (MLNS) prevailing in Japan. *Pediatrics.* (1974) 54:271–6.
3. Rawat A, Singh S. Biomarkers for diagnosis of Kawasaki disease. *Indian Pediatr.* (2015) 52:473–4. doi: 10.1007/s13312-015-0658-2
4. Kuo HC, Yang KD, Chang WC, Ger LP, Hsieh KS. Kawasaki disease: an update on diagnosis and treatment. *Pediatr Neonatol.* (2012) 53:4–11. doi: 10.1016/j.pedneo.2011.11.003
5. Newburger JW, Takahashi M, Beiser AS, Burns JC, Bastian J, Chung KJ, et al. A single intravenous infusion of gamma globulin as compared with four infusions in the treatment of acute Kawasaki syndrome. *N Engl J Med.* (1991) 324:1633–9. doi: 10.1056/NEJM199106063242305
6. Wilder MS, Palinkas LA, Kao AS, Bastian JF, Turner CL, Burns JC. Delayed diagnosis by physicians contributes to the development of coronary artery

aneurysms in children with Kawasaki syndrome. *Pediatr Infect Dis J.* (2007) 26:256–60. doi: 10.1097/01.inf.0000256783.57041.66
7. Rowley AH, Gonzalez-Crussi F, Gidding SS, Duffy CE, Shulman ST. Incomplete Kawasaki disease with coronary artery involvement. *Prog Clin Biol Res.* (1987) 250:357–65. doi: 10.1016/S0022-3476(87)80503-6
8. Newburger JW, Takahashi M, Gerber MA, Gewitz MH, Tani LY, Burns JC, et al. Diagnosis, treatment, and long-term management of Kawasaki disease: a statement for health professionals from the Committee on Rheumatic Fever, Endocarditis, and Kawasaki Disease, Council on Cardiovascular Disease in the Young, American Heart Association. *Pediatrics.* (2004) 114:1708–33. doi: 10.1542/peds.2004-2182
9. Principi N, Rigante D, Esposito S. The role of infection in Kawasaki syndrome. *J Infect.* (2013) 67:1–10. doi: 10.1016/j.jinf.2013.04.004
10. Yim D, Curtis N, Cheung M, Burgner D. An update on Kawasaki disease II: clinical features, diagnosis, treatment and outcomes. *J Paediatr Child Health.* (2013) 49:614–23. doi: 10.1111/jpc.12221
11. Harnden A, Takahashi M, Burgner D. Kawasaki disease. *BMJ.* (2009) 338:b1514. doi: 10.1136/bmj.b1514
12. Sittiwangkul R, Pongprot Y, Silvilairat S, Makonkaewkeyoon K. Clinical spectrum of incomplete Kawasaki disease in Thailand. *Paediatr Int Child Health.* (2013) 33:176–80. doi: 10.1179/2046905513Y.0000000062
13. Yu HR, Kuo HC, Sheen JM, Wang L, Lin IC, Wang CL, et al. A unique plasma proteomic profiling with imbalanced fibrinogen cascade in patients with Kawasaki disease. *Pediatr Allergy Immunol.* (2009) 20:699–707. doi: 10.1111/j.1399-3038.2008.00844.x
14. Yu HR, Kuo HC, Huang EY, Liang CD, Hwang KP, Lin IC, et al. Plasma clusterin levels in predicting the occurrence of coronary artery lesions in patients with Kawasaki disease. *Pediatr Cardiol.* (2010) 31:1151–6. doi: 10.1007/s00246-010-9769-7
15. McNeal-Davidson A, Fournier A, Spigelblatt L, Saint-Cyr C, Mir TS, Nir A, et al. Value of amino-terminal pro B-natriuretic peptide in diagnosing Kawasaki disease. *Pediatr Int.* (2012) 54:627–33. doi: 10.1111/j.1442-200X.2012.03609.x
16. Dahdah N, Siles A, Fournier A, Cousineau J, Delvin E, Saint-Cyr C, et al. Natriuretic peptide as an adjunctive diagnostic test in the acute phase of Kawasaki disease. *Pediatr Cardiol.* (2009) 30:810–7. doi: 10.1007/s00246-009-9441-2
17. Kawamura T, Wago M, Kawaguchi H, Tahara M, Yuge M. Plasma brain natriuretic peptide concentrations in patients with Kawasaki disease. *Pediatr Int.* (2000) 42:241–8. doi: 10.1046/j.1442-200x.2000.01225.x
18. Kim M, Kim K. Elevation of cardiac troponin I in the acute stage of Kawasaki disease. *Pediatr Cardiol.* (1999) 20:184–8. doi: 10.1007/s002469900437
19. Yu X, Hirono KI, Ichida F, Uese K, Rui C, Watanabe S, et al. Enhanced iNOS expression in leukocytes and circulating endothelial cells is associated with the progression of coronary artery lesions in acute Kawasaki disease. *Pediatr Res.* (2004) 55:688–94. doi: 10.1203/01.PDR.0000113464.93042.A4
20. Ko TM, Kuo HC, Chang JS, Chen SP, Liu YM, Chen HW, et al. CXCL10/IP-10 is a biomarker and mediator for Kawasaki disease. *Circ Res.* (2015) 116:876–83. doi: 10.1161/CIRCRESAHA.116.305834
21. Parthasarathy P, Agarwal A, Chawla K, Tofighi T, Mondal TK. Upcoming biomarkers for the diagnosis of Kawasaki disease: a review. *Clin Biochem.* (2015) 48:1188–94. doi: 10.1016/j.clinbiochem.2015.02.013
22. Kimura Y, Yanagimachi M, Ino Y, Aketagawa M, Matsuo M, Okayama A, et al. Identification of candidate diagnostic serum biomarkers for Kawasaki disease using proteomic analysis. *Sci Rep.* (2017) 7:43732. doi: 10.1038/srep43732
23. Zhang G, Wang T, He Q. How to discover new proteins-translatome profiling. *Sci China Life Sci.* (2014) 57:358–60. doi: 10.1007/s11427-014-4618-1
24. Sabrkhany S, Kuijpers MJ, Verheul HM, Griffioen AW, Egbrink MG. Platelets: an unexploited data source in biomarker research. *Lancet Haematol.* (2015) 2:e512–3. doi: 10.1016/S2352-3026(15)00225-2
25. Best MG, Vancura A, Wurdinger T. Platelet RNA as a circulating biomarker trove for cancer diagnostics. *J Thromb Haemost.* (2017) 15:1295–306. doi: 10.1111/jth.13720
26. Husemann Y, Geigl JB, Schubert F, Musiani P, Meyer M, Burghart E, et al. Systemic spread is an early step in breast cancer. *Cancer Cell.* (2008) 13:58–68. doi: 10.1016/j.ccr.2007.12.003
27. Liu X, Sempere LF, Ouyang H, Memoli VA, Andrew AS, Luo Y, et al. MicroRNA-31 functions as an oncogenic microRNA in mouse and human lung cancer cells by repressing specific tumor suppressors. *J Clin Invest.* (2010) 120:1298–309. doi: 10.1172/JCI39566
28. Sarver AL, Li L, Subramanian S. MicroRNA miR-183 functions as an oncogene by targeting the transcription factor EGR1 and promoting tumor cell migration. *Cancer Res.* (2010) 70:9570–80. doi: 10.1158/0008-5472.CAN-10-2074
29. Fang L, Deng Z, Shatseva T, Yang J, Peng C, Du WW, et al. MicroRNA miR-93 promotes tumor growth and angiogenesis by targeting integrin-beta8. *Oncogene.* (2011) 30:806–21. doi: 10.1038/onc.2010.465
30. Diosdado B, van de Wiel MA, Terhaar Sive Droste JS, Mongera S, Postma C, Meijerink, WJ, et al. MiR-17-92 cluster is associated with 13q gain and c-myc expression during colorectal adenoma to adenocarcinoma progression. *Br J Cancer.* (2009) 101:707–14. doi: 10.1038/sj.bjc.6605037
31. Taganov KD, Boldin MP, Chang KJ, Baltimore D. NF-kappaB-dependent induction of microRNA miR-146, an inhibitor targeted to signaling proteins of innate immune responses. *Proc Natl Acad Sci USA.* (2006) 103:12481–6. doi: 10.1073/pnas.0605298103
32. Perry MM, Moschos SA, Williams AE, Shepherd NJ, Larner-Svensson HM, Lindsay MA. Rapid changes in microRNA-146a expression negatively regulate the IL-1beta-induced inflammatory response in human lung alveolar epithelial cells. *J Immunol.* (2008) 180:5689–98. doi: 10.4049/jimmunol.180.8.5689
33. Moschos SA, Williams AE, Perry MM, Birrell MA, Belvisi MG, Lindsay MA. Expression profiling in vivo demonstrates rapid changes in lung microRNA levels following lipopolysaccharide-induced inflammation but not in the anti-inflammatory action of glucocorticoids. *BMC Genomics.* (2007) 8:240. doi: 10.1186/1471-2164-8-240
34. Lu TX, Munitz A, Rothenberg ME. MicroRNA-21 is up-regulated in allergic airway inflammation and regulates IL-12p35 expression. *J Immunol.* (2009) 182:4994–5002. doi: 10.4049/jimmunol.0803560
35. Gu KL, Zhang Q, Yan Y, Li TT, Duan FF, Hao J, et al. Pluripotency-associated miR-290/302 family of microRNAs promote the dismantling of naive pluripotency. *Cell Res.* (2016) 26:350–66. doi: 10.1038/cr.2016.2
36. Wang Y, Melton C, Li YP, Shenoy A, Zhang XX, Subramanyam D, et al. miR-294/miR-302 promotes proliferation, suppresses G1-S restriction point, and inhibits ESC differentiation through separable mechanisms. *Cell Rep.* (2013) 4:99–109. doi: 10.1016/j.celrep.2013.05.027
37. Ma Y, Yao N, Liu G, Dong L, Liu Y, Zhang M, et al. Functional screen reveals essential roles of miR-27a/24 in differentiation of embryonic stem cells. *EMBO J.* (2015) 34:361–78. doi: 10.15252/embj.201489957
38. Xu N, Papagiannakopoulos T, Pan G, Thomson JA, Kosik KS. MicroRNA-145 regulates OCT4, SOX2, and KLF4 and represses pluripotency in human embryonic stem cells. *Cell.* (2009) 137:647–58. doi: 10.1016/j.cell.2009.02.038
39. Tay Y, Zhang J, Thomson AM, Lim B, Rigoutsos I. MicroRNAs to Nanog, Oct4 and Sox2 coding regions modulate embryonic stem cell differentiation. *Nature.* (2008) 455:1124–8. doi: 10.1038/nature07299
40. Zheng GX, Ravi A, Calabrese JM, Medeiros LA, Kirak O, Dennis LM, et al. A latent pro-survival function for the mir-290-295 cluster in mouse embryonic stem cells. *PLoS Genet.* (2011) 7:e1002054. doi: 10.1371/journal.pgen.1002054
41. Yuan K, Ai WB, Wan LY, Tan X, Wu JF. The miR-290-295 cluster as multi-faceted players in mouse embryonic stem cells. *Cell Biosci.* (2017) 7:38. doi: 10.1186/s13578-017-0166-2
42. O'Connell RM, Rao DS, Chaudhuri AA, Baltimore D. Physiological and pathological roles for microRNAs in the immune system. *Nat Rev Immunol.* (2010) 10:111–22. doi: 10.1038/nri2708
43. Lu M, Zhang Q, Deng M, Miao J, Guo Y, Gao W, et al. An analysis of human microRNA and disease associations. *PLoS ONE.* (2008) 3:e3420. doi: 10.1371/journal.pone.0003420
44. Bijak M, Dzieciol M, Rywaniak J, Saluk J, Zielinska M. Platelets miRNA as a prediction marker of thrombotic episodes. *Dis Markers.* (2016) 2016:2872507. doi: 10.1155/2016/2872507
45. Ple H, Landry P, Benham A, Coarfa C, Gunaratne PH, Provost P. The repertoire and features of human platelet microRNAs. *PLoS ONE.* (2012) 7:e50746. doi: 10.1371/journal.pone.0050746
46. Pontes TB, Moreira-Nunes Cde F, Maues JH, Lamarao LM, de Lemos JA, Montenegro RC, et al. The miRNA profile of platelets stored in a blood bank and its relation to cellular damage from storage. *PLoS ONE.* (2015) 10:e0129399. doi: 10.1371/journal.pone.0129399

47. Sunderland N, Skroblin P, Barwari T, Huntley RP, Lu R, Joshi A, et al. MicroRNA biomarkers and platelet reactivity: the clot thickens. *Circ Res.* (2017) 120:418–35. doi: 10.1161/CIRCRESAHA.116.309303
48. Roy S, Sen CK. MiRNA in innate immune responses: novel players in wound inflammation. *Physiol Genomics.* (2011) 43:557–65. doi: 10.1152/physiolgenomics.00160.2010
49. Snoek J, Larochelle H, Adams RP. Practical bayesian optimization of machine learning algorithms. In: *NIPS'12 Proceedings of the 25th International Conference on Neural Information Processing Systems*. Advances in neural information processing systems. Lake Tahoe, NV (2012). p. 2951–2959.
50. Lewis BP, Burge CB, Bartel DP. Conserved seed pairing, often flanked by adenosines, indicates that thousands of human genes are microRNA targets. *Cell.* (2005) 120:15–20. doi: 10.1016/j.cell.2004.12.035
51. Betel D, Koppal A, Agius P, Sander C, Leslie C. Comprehensive modeling of microRNA targets predicts functional non-conserved and non-canonical sites. *Genome Biol.* (2010) 11:R90. doi: 10.1186/gb-2010-11-8-r90
52. Wang X, El Naqa IM. Prediction of both conserved and nonconserved microRNA targets in animals. *Bioinformatics.* (2008) 24:325–32. doi: 10.1093/bioinformatics/btm595
53. Huang da W, Sherman BT, Lempicki RA. Systematic and integrative analysis of large gene lists using DAVID bioinformatics resources. *Nat Protoc.* (2009) 4:44–57. doi: 10.1038/nprot.2008.211
54. Ikeda K, Yamaguchi K, Tanaka T, Mizuno Y, Hijikata A, Ohara O, et al. Unique activation status of peripheral blood mononuclear cells at acute phase of Kawasaki disease. *Clin Exp Immunol.* (2010) 160:246–55. doi: 10.1111/j.1365-2249.2009.04073.x
55. Ling XB, Lau K, Kanegaye JT, Pan Z, Peng S, Ji J, et al. A diagnostic algorithm combining clinical and molecular data distinguishes Kawasaki disease from other febrile illnesses. *BMC Med.* (2011) 9:130. doi: 10.1186/1741-7015-9-130
56. Hoang LT, Shimizu C, Ling L, Naim AN, Khor CC, Tremoulet AH, et al. Global gene expression profiling identifies new therapeutic targets in acute Kawasaki disease. *Genome Med.* (2014) 6:541. doi: 10.1186/s13073-014-0102-6
57. Jia HL, Liu CW, Zhang L, Xu WJ, Gao XJ, Bai J, et al. Sets of serum exosomal microRNAs as candidate diagnostic biomarkers for Kawasaki disease. *Sci Rep.* (2017) 7:44706. doi: 10.1038/srep44706
58. Chen Y, Ding YY, Ren Y, Cao L, Xu QQ, Sun L, et al. Identification of differentially expressed microRNAs in acute Kawasaki disease. *Mol Med Rep.* (2018) 17:932–8. doi: 10.3892/mmr.2017.8016
59. Yun KW, Lee JY, Yun SW, Lim IS, Choi ES. Elevated serum level of microRNA (miRNA)-200c and miRNA-371-5p in children with Kawasaki disease. *Pediatr Cardiol.* (2014) 35:745–52. doi: 10.1007/s00246-013-0846-6
60. Minami Y, Satoh M, Maesawa C, Takahashi Y, Tabuchi T, Itoh T, et al. Effect of atorvastatin on microRNA 221 / 222 expression in endothelial progenitor cells obtained from patients with coronary artery disease. *Eur J Clin Invest.* (2009) 39:359–67. doi: 10.1111/j.1365-2362.2009.02110.x
61. Szklarczyk D, Morris JH, Cook H, Kuhn M, Wyder S, Simonovic M, et al. The STRING database in 2017: quality-controlled protein-protein association networks, made broadly accessible. *Nucleic Acids Res.* (2017) 45:D362–8. doi: 10.1093/nar/gkw937
62. Song J, Ouyang Y, Che J, Li X, Zhao Y, Yang K, et al. Potential Value of miR-221/222 as diagnostic, prognostic, and therapeutic biomarkers for diseases. *Front Immunol.* (2017) 8:56. doi: 10.3389/fimmu.2017.00056
63. Ortega FJ, Moreno M, Mercader JM, Moreno-Navarrete JM, Fuentes-Batllevell N, Sabater M, et al. Inflammation triggers specific microRNA profiles in human adipocytes and macrophages and in their supernatants. *Clin Epigenetics.* (2015) 7:49. doi: 10.1186/s13148-015-0083-3
64. Simonini G, Masi L, Giani T, Piscitelli E, Cimaz R, Vierucci S, et al. Osteoprotegerin serum levels in Kawasaki disease: an additional potential marker in predicting children with coronary artery involvement. *J Rheumatol.* (2005) 32:2233–8.

Conflict of Interest Statement: DW, YP, JW, YH, BWe, and XX were employed by company QIAGEN (Suzhou) Translational Medicine Co.

The remaining authors declare that the research was conducted in the absence of any commercial or financial relationships that could be construed as a potential conflict of interest.

frontiers in Pediatrics

ORIGINAL RESEARCH
published: 02 July 2019
doi: 10.3389/fped.2019.00247

A *de novo* Mutation in the *MTUS1* Gene Decreases the Risk of Non-compaction of Ventricular Myocardium via the Rac1/Cdc42 Pathway

Xuehan Bai[1,2†], *Yuanlin Zhou*[3†], *Na Ouyang*[1,2], *Lingjuan Liu*[1,2], *Xupei Huang*[4], *Jie Tian*[1,2] *and Tiewei Lv*[1,2*]

[1] Department of Cardiology, Children's Hospital of Chongqing Medical University, Chongqing, China, [2] China International Science and Technology Cooperation Base of Child Development and Critical Disorders, Chongqing Key Laboratory of Pediatrics, Ministry of Education Key Laboratory of Child Development and Disorders, Chongqing, China, [3] Chengdu Women's and Children's Central Hospital, Chengdu, China, [4] Department of Biomedical Science, Charlie E. Schmidt College of Medicine, Florida Atlantic University, Boca Raton, FL, United States

OPEN ACCESS

Edited by:
Antonio Francesco Corno, University of Leicester, United Kingdom

Reviewed by:
Junbao Du, Peking University First Hospital, China
Shiwei Yang, Children's Hospital of Nanjing Medical University, China

***Correspondence:**
Tiewei Lv
ltw200145@163.com

[†]These authors have contributed equally to this work

Specialty section:
This article was submitted to Pediatric Cardiology, a section of the journal Frontiers in Pediatrics

Received: 12 January 2019
Accepted: 30 May 2019
Published: 02 July 2019

Citation:
Bai X, Zhou Y, Ouyang N, Liu L, Huang X, Tian J and Lv T (2019) A de novo Mutation in the MTUS1 Gene Decreases the Risk of Non-compaction of Ventricular Myocardium via the Rac1/Cdc42 Pathway. Front. Pediatr. 7:247. doi: 10.3389/fped.2019.00247

Background: The *MTUS1* gene encodes a microtubule-associated protein involved in multiple processes including cell polarity and microtubule balance during myocardial development.

Aims: To investigate the association between a *de novo* c. 2617A->C mutation in *MTUS1* (NM_001001924.2) and non-compaction of ventricular myocardium (NVM) and explore the potential mechanisms.

Methods: A *de novo* mutation in *MTUS1* was identified for a familial pedigree with NVM. Lentiviral vectors containing *MTUS1* wild type or the mutation *MTUS1* were constructed and co-infected into HEK-293 cells. *MTUS1*, Rac1/Cdc42, α-tubulin, α/β-tubulin, polarity protein (PAR6), and the morphology of daughter cells were measured by real-time PCR, Western blot, and immunofluorescence assays, respectively.

Results: The lentiviral vectors were constructed successfully. Immunofluorescence assays revealed the fluorescence intensity of α-tubulin to be decreased and α/β-tubulin to be increased in the mutation *MTUS1* group. The fluorescence intensity of PAR6 was higher and morphology of the daughter cells in the mutation group was different from the wild type group. The phosphorylation of Rac1/Cdc42 in the mutation group was significantly lower than in the wild type group.

Conclusions: A *de novo* mutation in *MTUS1* decreased the stability of microtubules and increased cell polarity via the Rac1/Cdc42 pathway, which may partly elucidate the mechanism underlying cellular protection in NVM.

Keywords: non-compaction of ventricular myocardium, MTUS1, microtubule, cell polarity, Rac1/Cdc42

INTRODUCTION

Non-compaction of ventricular myocardium (NVM) is a structural abnormality of the left ventricular myocardium that is accompanied by severe clinical symptoms and a poor prognosis with no currently available effective prevention and therapeutic methods (1–4). NVM is diagnosed based on the ratio of the thickness of the non-compact endocardial layer to the thickness of the compact epicardial layer being >2.0 on echocardiograph (5). In the majority of patients, NVM is associated with genetic disease, particularly neuromuscular disorders and chromosomal defect (6, 7). The polarity of myocardial cells was recently reported to play an important role in the development of NVM (8, 9). However, the underlying molecular mechanisms regulating cell polarity during early cardiac development and trabecular formation remain poorly understood.

Polarity is one of the basic processes that occur in living organisms (10). Cell polarity is the result of asymmetrical organization of cell membrane proteins and cell contents and can influence cell fate and specialized functions, such as migration, development, and proliferation (11). Cell polarity is controlled by Rho GTPase family members, the Par polarity complex, and cytoskeleton (12). Microtubules are a component of the cytoskeleton, found in eukaryotic cells, and formed by the polymerization of a dimer of two globular proteins, α, and β tubulin. These tubular polymers of tubulin are highly dynamic and stabilize the cell structure, transport intracellular substances, and mediate cell movement. The Rho GTPase family consists of six subfamilies: Rho, Rac, Cdc42, Rnd, RhoBTB, and RhoT/Miro (13). The Rho GTPase family mediates the formation of the Par polarity complex, which causes cell polarity. The PAR proteins PAR3, PAR6, and aPKC localize to the anterior cortex, where PAR1 and PAR2 localize to the posterior pole and have essential functions in the first asymmetric division (14). Polar proteins are transported to the cell membrane through microtubule dynamic balance, thus forming polar protein complexes (15). In cardiac development, disruption of the cell polarity complex by targeted gene mutations results in aberrant mitotic spindles, loss of polarized cardiomyocyte division, and loss of normal myocardial trabeculation (9).

Microtubule-associated tumor suppressor 1 (MTUS1) encodes the microtubule-associated protein ATIP3, which cooperates with type-2 angiotensin II receptor (AGTR2) to inhibit extracellular signal-regulated kinase 2 (ERK2) activation and cell proliferation, which are closely related to cell division and migration (16, 17). A recently published study showed that MTUS1 knock-out mice developed spontaneous heart hypertrophy (18), suggesting that MTUS1 may affect cardiovascular system development.

However, the specific mechanisms underlying these processes have not yet been elucidated. Our team discovered a *de novo* mutation in *MTUS1*, c. 2617A->C (rs187103704), in a rare NVM family, that is likely associated with the mechanism underlying NVM. Therefore, the aim of this study was to investigate the association between a *de novo* mutation in *MTUS1* with NVM and to explore the potential mechanisms underlying this association. The current findings may help understand the genetic basis of NVM development, provide a theoretical basis for genetic counseling, prenatal diagnosis, and early intervention, and facilitate the development of new strategies for personalized medicine.

Abbreviations: NVM, non-compaction of ventricular myocardium; MTUS1, Microtubule-associated tumor suppressor 1; AGTR2, type-2 angiotensin II receptor; ERK2, extracellular signal-regulated kinase 2; WES, whole exome sequencing; ANOVA, one-way analysis of variance; RHD, rheumatic heart disease.

MATERIALS AND METHODS

Subjects

A rare NVM family pedigree was discovered at the Children's Hospital of Chongqing Medical University. Blood samples were collected from the propositus and her family (sister, mother and aunt) for DNA extraction and whole exome sequencing (WES) (Deyi Oriental Translational Medicine Research Center, China). The original WES data were analyzed to confirm the biological relationships between the daughters, their mother and their aunt. First, the mutations identified by WES were selected by bioinformatics analysis and then functional predictions were made by making comparisons using Genebank, including the UCSC Genome Browser (http://genome.ucsc.edu/), GENECARDS (https://www.genecards.org/), the NCBI database (https://www.ncbi.nlm.nih.gov/), UNIPROT (https://www.uniprot.org/), and STRING (https://string-db.org/). Then the well-conserved mutations that caused amino acid polarity changes in important functional domains were screened as possibly pathogenic for NVM. The mutations were then identified by Sanger sequencing, with the Chromas software used for data analysis.

Cell Culture and Transfections

HEK-293 cells, a classic cell line used in cell biology and gene research, were maintained at 37°C in a humidified atmosphere with 5% CO_2 in Dulbecco's Modified Eagle Medium (Hyclone) containing 4.5 g/l glucose, 10% fetal bovine serum (Hyclone), and 100 mg/ml penicillin/streptomycin (19). Plasmosin (55 μl; InvivoGen, ant-mpt) was added to 550 ml complete medium to avoid mycoplasma contamination. *MTUS1* has multiple different isoforms with distinct functions. ATIP3 isoform (encoded by *MTUS1* gene), which expresses most in heart, has been studied most extensively. This isoform is known to play an important role in microtubule functions. We avoided selecting truncations or short isoforms which contain the mutant site of *MTUS1*, and we chose full length genes to construct lentiviruses, in order to avoid that the mutation site may affect the function of different functional domains through interaction. Lentiviruses containing GFP and FLAG-tags were completed by Genechem (China). To co-transfect with lentiviruses, HEK-293 cells were plated at a density of 2×10^5 cells/5 ml in T25 culture flasks. Media were replaced with fresh media daily. Once the cells reached a density of about 40–50%, they were co-transfected with mutation variant, wild type, and vector lentiviruses at an MOI of 5. A total of 12 h after

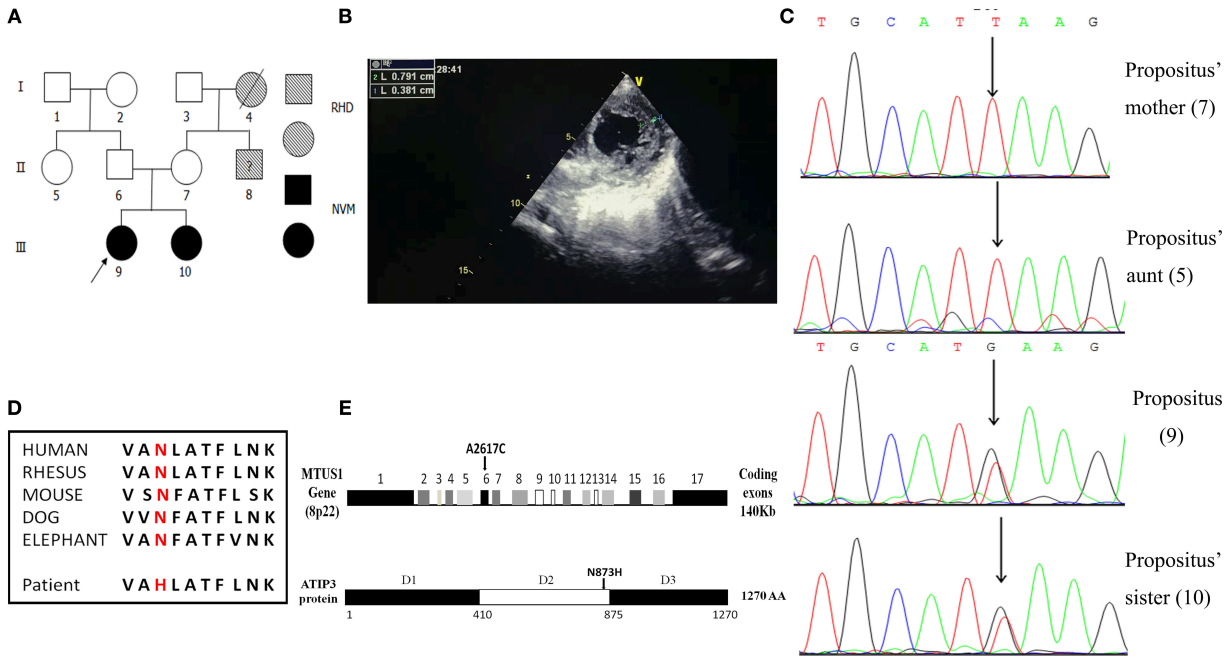

FIGURE 1 | Familial pedigrees of NVM and information of the *de novo* mutation of *MTUS1* c. 2617A->C. **(A)** Pedigree showing individuals with non-compaction of ventricular myocardium (NVM) and Rheumatic Heart Disease (RHD). The arrow shows the index patient with NVM carrying the *MTUS1* mutation (c. 2617A->C). Squares, men; circles, women; black figures, individuals with NVM; oblique line figures, individuals with RHD; oblique line figures with a black question mark in the middle, suspicious RHD patient. **(B)** The echocardiographic image showing that the ratio of the thickness of the non-compact endocardial layer to the thickness of the compact epicardial layer was >2.0 (0.791/0.381). **(C)** Backward sequencing chromatogram of propositus and her family (sister, mother, and aunt). Parts of the nucleotide sequence are given below. The mutation site is pointed by an arrow (the position means c. 2617A->C). **(D)** Evolutionary conservation of c. 2617A->C mutation in all species. **(E)** Schematic representation of the structural organization shows human *MTUS1* gene and ATIP3 (encoded by *MTUS1* gene) protein regions. The *de novo* mutation of *MTUS1* c. 2617A->C located in exon 6. Position of the mutant amino-acid sequence was in D2. D1: domain 1, D2: domain 2, D3: domain 3.

transfection, lentivirus-containing medium was replaced with fresh medium.

MTUS1 Expression Based on Real-Time PCR

At 24 h post-transfection, total RNA was extracted from HEK-293 cells using a TRIzol Reagent kit (Ambion) per the manufacturer's instructions and quantified by spectrophotometry at 260 nm. The mRNA was reversely transcribed using the Prime Script RT reagent kit containing gDNA Eraser (Takara, NO: RR047A) as described (20). The primers used for amplification were as follows: MTUS1, GAGCTGAGCACTTACAGCAACAA (forward) and TTCAACTGCATTAAGAGCTGTAA (reverse); and β-actin, CTCTTCCAGCCTTCCTTCCT (forward) and AGCACTGTGTTGGCGTACAG (reverse). The mRNA levels were normalized using β-actin as a housekeeping gene. Each experiment was repeated at least three times.

Immunofluorescence Staining for Tubulin and PAR6

Cells plated on coverslips that were 30–40% confluent were fixed in an ice-cold 4% formaldehyde solution for 20 min prior to incubating for 15 min at room temperature with 0.05% Triton-X100 (21). The slides were then blocked with normal goat serum for 30 min. Slides were washed three times for at least 3 min each time after each incubation and then incubated overnight at 4°C with mouse anti-α-tubulin antibodies (Santa Cruz, USA, sc-5286, 1:50), rabbit anti-α/β-tubulin antibodies (Cell signaling, USA, Cat:2148,1:50), or rabbit anti-PAR6 antibodies (Abcam, USA, ab49776, 1:200). After washing three times the following day, cells were incubated for 60 min at room temperature with either Cy-3-conjugated anti-mouse antibodies or Cy-3-conjugated anti-rabbit antibodies (Seville, wuhan, 1:250) and then washed three times. The cell nuclei were identified by staining with DAPI (Roche, 10236276001, 5 μg/ml) for 15 min at room temperature. Coverslips were mounted on glass slides using DAPI Fluoromount-GTM (YEASEN, 36308ES11, Shanghai) and examined by confocal microscopy. Image analysis was performed using NIH and Image J software. Each experiment was repeated at least three times.

Western Blot Analysis of Rac1/Cdc42

Protein was extracted from cells in exponential growth. Total cellular protein was extracted on ice using 1× lysis buffer (KeyGEN BioTECH, NO: KGP250) supplemented with protease inhibitor (Roche, Switzerland) and phosphatase inhibitor (Roche, Switzerland). The entire protein extraction was performed strictly on ice. Protein concentrations were measured with the Coomassie (Bradford) Protein Assay (KeyGEN BioTECH,

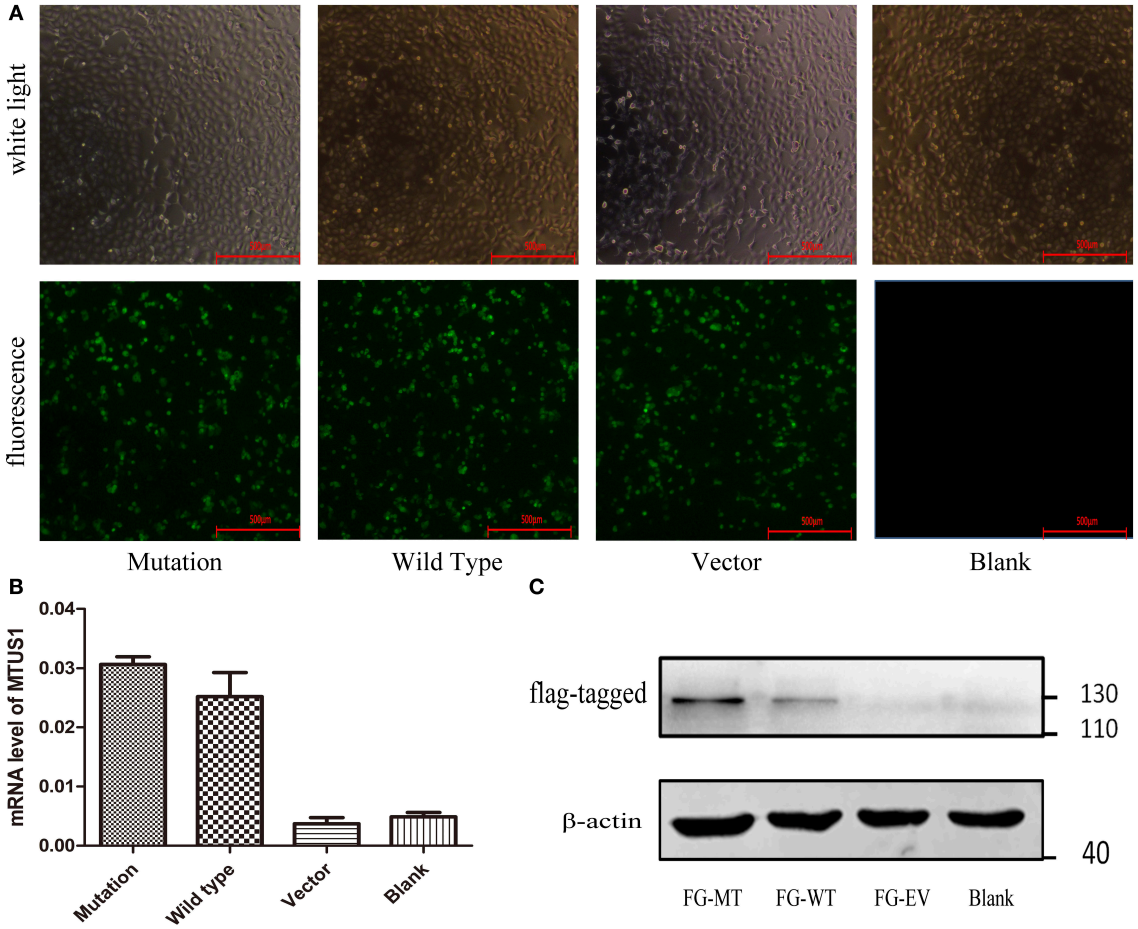

FIGURE 2 | Lentiviral vector validation and transfection. **(A)** Co-transfect with lentiviruses containing GFP (c. 2617A->C mutation, wild type, vector, respectively), 48 h after transfection, cell state and transfection efficiency of each group were observed under ordinary microscope and fluorescence microscope. **(B)** After 48 h transfection, the *MTUS1* mRNA level expression was increased in the mutation and wild type group. **(C)** When GFP fluorescence occurs in mutation, wild type and vector group, the expression of flag-MTUS1 protein was detected to verify successful overexpression in HEK293 cells. FG-MT: flag-c. 2617A->C mutation, FG-WT: flag-wild type, FG-EV: flag-vector, Scale bar = 500 μm.

China). Total protein, 150 μg per lane, was separated on 12% SDS-PAGE gels. The SDS-PAGE gels and PVDF membranes were cut into corresponding sizes according to the molecular weights of the target proteins. Proteins were then transferred onto 0.22-μm PVDF membranes. Non-specific bands were blocked with Tris-buffered saline and Tween 20 (TBST) containing 5% bovine serum albumen for 1.5 h at room temperature. Then the membranes were incubated with specific primary antibodies at 4°C overnight. The next day, the PVDF membranes were incubated with the corresponding secondary antibodies at room temperature for 1.5 h (19, 20). Proteins bound to the 0.22-μm PDVF membranes were detected using primary antibodies against β-actin (4A Biotech, China, 1:1000), Rac1/Cdc42 (Cell signaling, 4651, USA, 1:1000), phospho-Rac1/Cdc42 (Ser71) (Cell signaling, 2461, USA, 1:500), or OctA-Probe (FLAG-tagged proteins; Santa Cruz, sc-166384, 1:500). Secondary antibodies were goat anti-mouse IgG (Millipore, GGHL-90P, 1:10000) or goat anti-rabbit IgG (Millipore,GGHL-15P,1:10000). Each experiment was repeated at least five times.

Statistical Data Analysis

Statistical analysis was performed in SPSS version 20. At least three grids were prepared for each experimental condition examined in this study. Results are expressed as mean ± standard deviation. Differences among groups were analyzed by one-way analysis of variance (ANOVA). All *P*-values were two sided. $P < 0.05$ was considered statistically significant.

RESULTS

Gene Sequencing Outcomes in Patients in Pedigree With NVM

In a rare patient with an NVM family pedigree, the propositus and her elder sister (**Figure 1A**) were definitively diagnosed with NVM based on clinical manifestations, echocardiography, and related examinations. **Figure 1B** shows the echocardiography analysis result of the propositus, which indicates that the ratio of the thickness of the non-compact endocardial layer to the thickness of the compact epicardial layer was 2.076

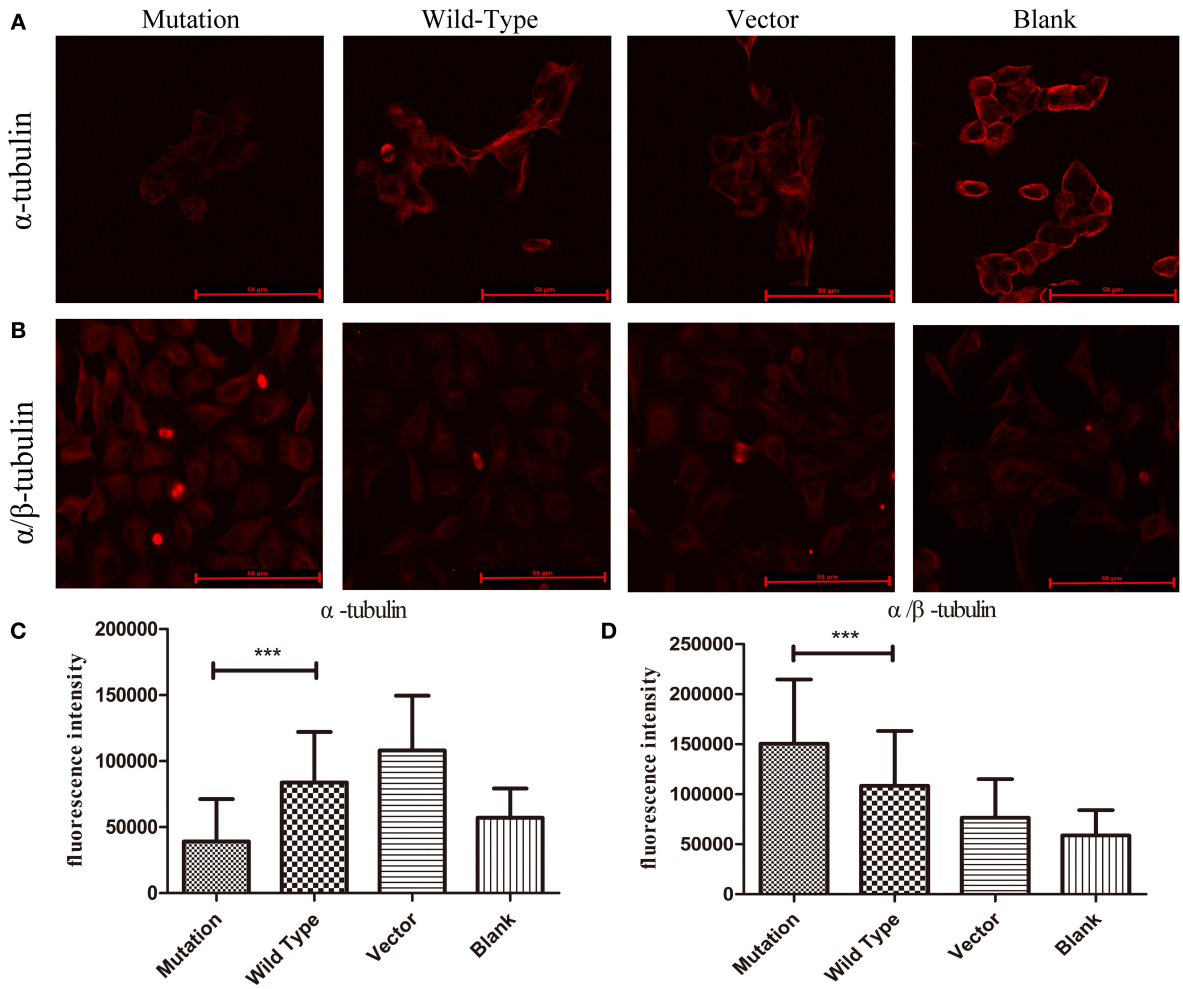

FIGURE 3 | The stability of microtubules in HEK293 cells by immunofluorescence. **(A)** Images showing α-tubulin expression in four groups. The expression of α-tubulin in c. 2617A->C mutation group was significantly decreased than wild type group. **(B)** Images showing α/β-tubulin expression in four groups. Increased expression levels of α/β-tubulin in c.2617A->C mutation group were observed compared with wild type group. **(C)** Quantification of fluorescence intensity measurements of α-tubulin in four groups under the conditions described in **(A)**. **(D)** The quantification of fluorescence intensity of α/β-tubulin in four groups under the conditions described in **(B)**. ***$P < 0.001$; scale bar = 50 μm. Error bars show mean ± standard deviation in **(C,D)**.

(0.791/0.381). Interestingly, their parents had normal clinical phenotypes. DNA samples from the two sisters and their mother and aunt were screened by WES and 32 mutation sites in 18 genes were selected for bioinformatics analysis and functional predictions. Other potential functional variants are shown in **Supplementary Materials**.

By Sanger sequencing analysis of the *MTUS1* gene in the two sisters, a heterozygous single nucleotide exchange at the position c. 2617A->C was identified (**Figure 1C**). In addition, we found that the c. 2617A->C mutation site was highly conserved among different species. The mutation changed the amino acid polarity from the hydrophobic Asn to the hydrophilic His at position 873 (N873H), leading to replacement of neutral amino-acids (amide side chains) by basic residues (**Figure 1D**). In schematic representation of the human *MTUS1* gene, the site of c. 2617A->C mutation located in exon 6, and in structural organization of ATIP3 protein (encoded by *MTUS1* gene), the position of the mutant amino-acid sequence was in D2 (**Figure 1E**), which decorates and stabilizes microtubules (22). It indicated that the mutant localized to an important functional domain. This mutation was present in the two sisters affected by NVM but absent from their mother and aunt. It means that a correlation between the NVM phenotype and the c. 2617A->C mutation was discovered in this NVM family. In a nutshell, the c. 2617A->C mutation in *MTUS1* is a *de novo* mutation and may be pathogenic for NVM.

Lentiviral Vector Validation and Transfection

For HEK-293 cells, 48 h post-transfection, GFP and FLAG tag expressions by the lentiviral vector were measured based on fluorescence staining (**Figure 2A**) and western blot (**Figure 2C**). Meanwhile, *MTUS1* mRNA levels were increased based on real-time PCR (**Figure 2B**) in the mutation and wild type

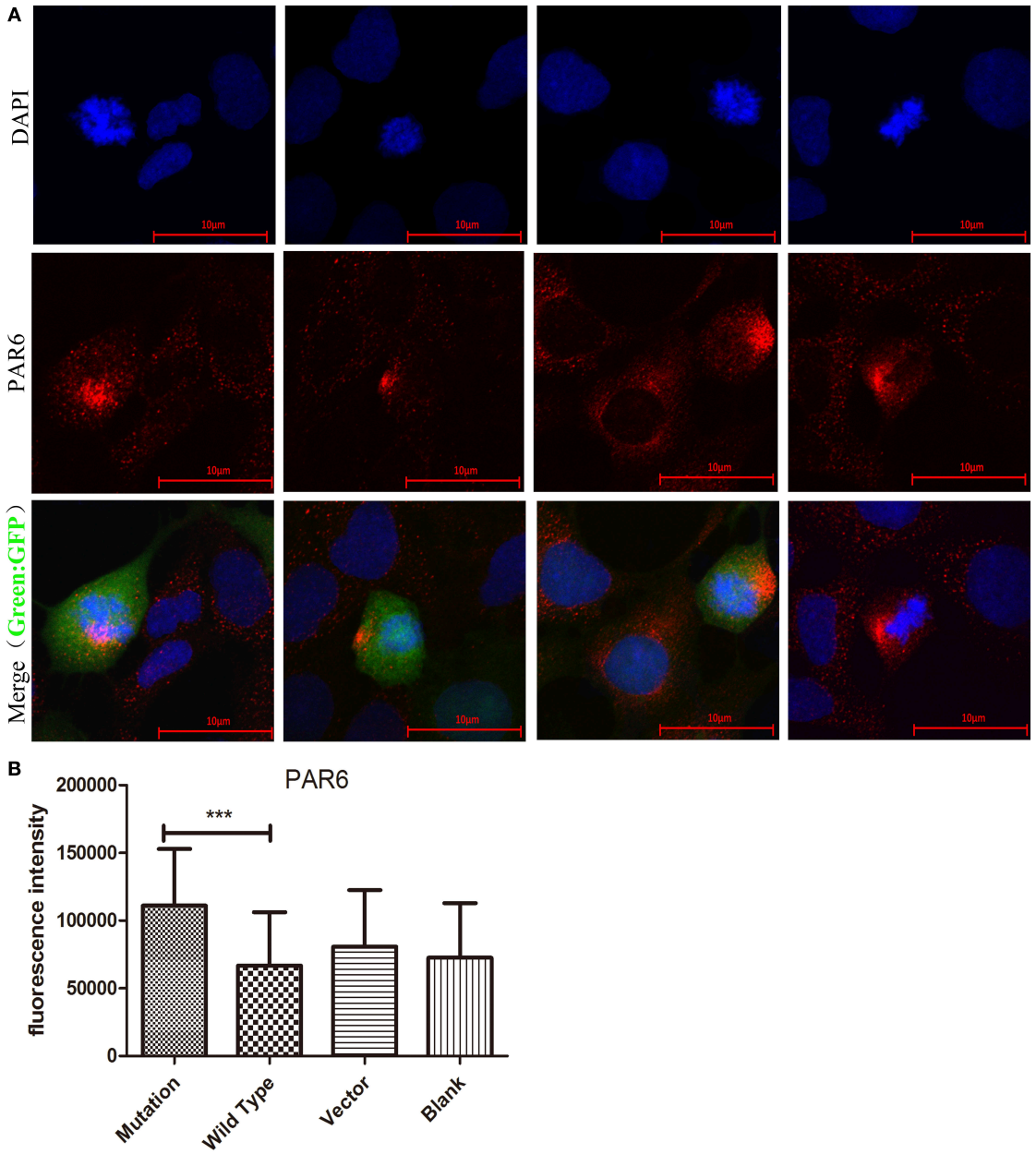

FIGURE 4 | The c. 2617 A->C mutation increased PAR6 protein expression. **(A)** Images showing PAR6 protein (red) expression and location in four groups in cell division. Nuclei were stained by DAPI (blue). In Merged images, the location of PAR6 protein in c.2617A->C mutation group was abnormal, more partial to the side of daughter cells, compared with wild type group. **(B)** Quantification of fluorescence intensity of PAR6 in four groups under the conditions described in A. ***$P < 0.001$, Scale bar =10 μm. Error bars show mean ± standard deviation.

groups compared to the vector and blank groups. These results indicated transfection of the c. 2617A->C mutation *MTUS1* gene was successful.

The c. 2617A->C Mutation Decreased α-tubulin Expression and Increased α/β-tubulin Expression

The protein α-tubulin is a globular tubulin that serves as a subunit of microtubules to assess microtubule stability in this study. α/β-tubulin, the heterodimers have roles in the transportation functions of microtubule (21), which were examined to assess PAR protein transportation when *MTUS1* contained the c.2617A->C mutation. The fluorescence intensity of α-tubulin was found to be decreased in the c.2617A->C mutation group compared to the wild type group ($P < 0.001$, **Figures 3A**,**C**). Conversely, the fluorescence intensity of α/β-tubulin in the c. 2617A->C mutation group was significantly higher than in the wild type group ($P < 0.001$, **Figures 3B**,**D**).

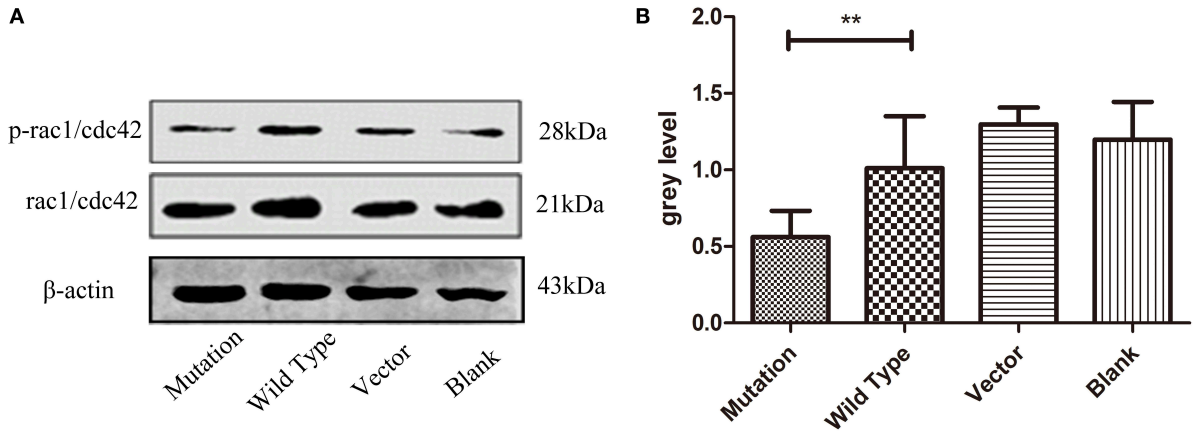

FIGURE 5 | The c. 2617 A->C mutation regulated PAR6 protein expression in association with Rac1/Cdc42 signaling. **(A)** Western blotting analysis of phosphorylated Rac1/Cdc42 protein in four groups. Total Rac1/cdc42 is shown as a loading control. In cell division, the expression level of phosphorylated Rac1/Cdc42 was decreased in c. 2617A->C mutation than that in wild type group. **(B)** Quantification of western blot measurements of p-Rac1/Cdc42 level (total Rac1/Cdc42 as control) in four groups under the conditions described in A. $^{**}P < 0.01$; Error bars show mean ± standard deviation in **(B)**.

The c. 2617A->C Mutation Increased PAR6 Protein Expression

PAR6, which acts as a polarity protein, is transported by microtubule heterodimers to one side of the cell membrane and forms polar PAR6-PAR3-aPKC complexes that affect cell polarity (23). The expression and location of PAR6 were analyzed in cells transfected with different recombinant lentiviruses to determine whether the c. 2617A->C mutation influences PAR6 protein. Our study showed that the fluorescence intensity of PAR6 protein was significantly increased in the c. 2617A->C mutation group compared to the wild type group ($P < 0.001$, **Figure 4B**), Interestingly, we found that the location of PAR6 protein in the mutation group was abnormal, where it was more partial to the side of daughter cells, compared to the wild type and blank groups (**Figure 4A**).

The c. 2617A->C Mutation Regulated PAR6 Protein Expression in Association With Rac1/Cdc42 Signaling

Rac1/Cdc42, the subfamily members of the Rho GTPase family, affect cell polarity, migration, and differentiation (24). Some studies have reported that Rac1/Cdc42 signaling plays a crucial role in adjusting the formation of PAR6-PAR3-aPKC complexes (25). Phosphorylated Rac1/Cdc42 inhibits GTP binding to Rac1/Cdc42, thereby weakening the downstream signal transduction pathway (26). Our study revealed that PAR6 protein levels were subject to Rac1/Cdc42 phosphorylation levels. Western blot analysis confirmed significantly lower phosphorylated Rac1/Cdc42 protein expression in the mutation group compared to the wild type and blank groups ($P = 0.003$, $P < 0.01$, **Figures 5A,B**). These findings indicate that PAR6 protein expression in the mutation group was regulated by the phosphorylation level of Rac1/Cdc42.

High Expression of PAR6 Protein in the c. 2617A->C Mutation-Carrying Cells Altered the Morphology of Daughter Cells

Cellular polarity cannot be established in the absence of the polarity protein complex. Disruption of the polarity protein complex results in aberrant mitotic spindle alignment and the loss of polarization of cells during cell division (27). Furthermore, changing the polarity of cells can lead to abnormal cell morphology and spindle localization (28). To further investigate the effect of increased expression of PAR6 protein in the mutation group on daughter cell morphology, we stained HEK-293 cells in each group for α-tubulin. We then examined the difference in the stained area in daughter cells and the distance between the spindle and cytoplasmic membrane in the daughter cells during cell division by immunofluorescence with confocal microscopy. The area in the daughter cells staining positive for α-tubulin in the mutation group was significantly larger than in the other groups ($P < 0.001$, **Figures 6A,C**). The distance between the spindle and cytoplasmic membrane of the daughter cells in the mutation group was significantly larger than in the wild type group ($P < 0.01$, **Figures 4A,B**). These results indicate that the c. 2617A->C mutation changed the morphology of the daughter cells after cell division by affecting the polarity of the cells.

DISCUSSION

NVM is a rare congenital cardiomyopathy resulting from an arrest in normal endomyocardial embryogenesis. The characteristic echocardiographic findings of NVM consist of multiple, prominent myocardial trabeculations, and deep intertrabecular recesses communicating with the left ventricular cavity (29, 30). The genetic causes and pathogenic mechanisms underlying this disease are largely unknown (31), though it has been described as an inherited cardiomyopathy with both familial

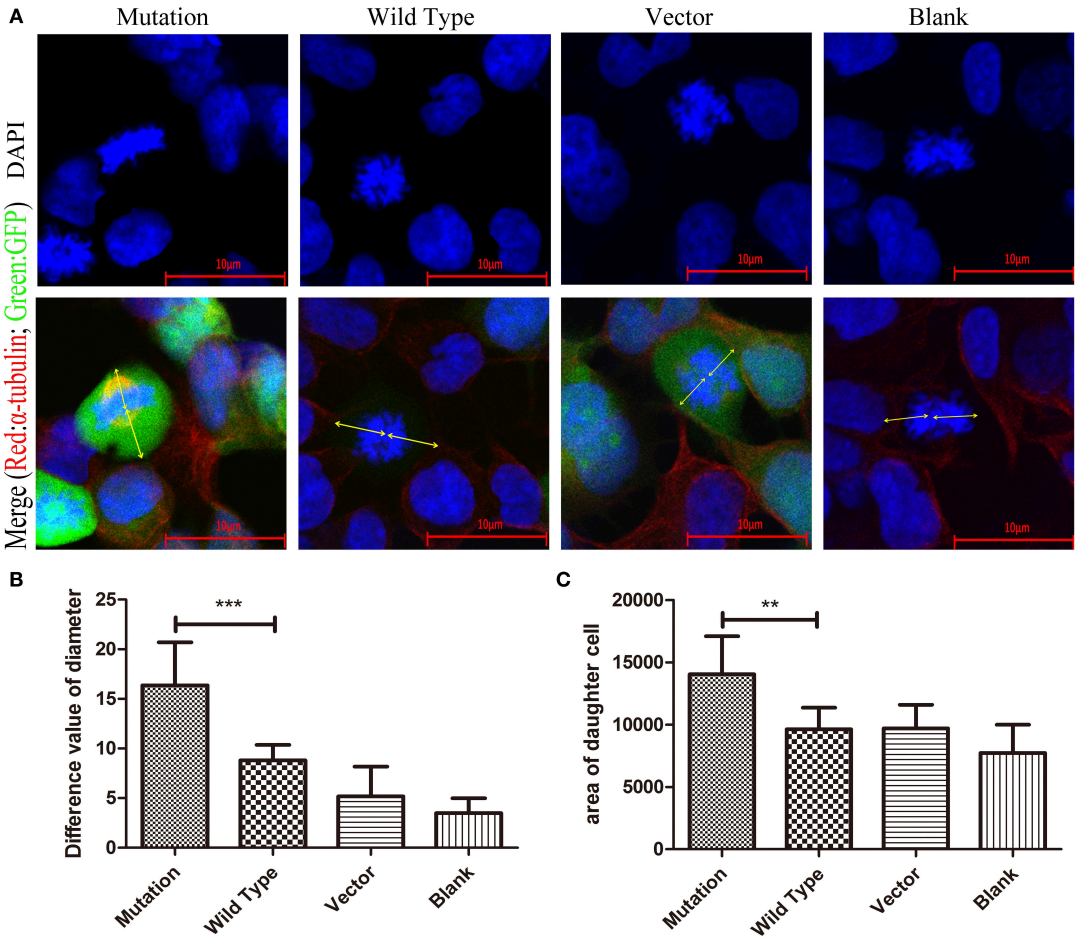

FIGURE 6 | The morphology of daughter cells in HEK293 cells transfected with c. 2617A->C mutation. **(A)** In the merge images, the arrows (yellow) represent the distance from the spindle to the daughter cell membrane respectively at the stage of cell division. **(B)** Quantification of the distance from the spindle to the daughter cell membrane respectively at the stage of cell division in four groups under the conditions described in **(A)**. **(C)** The area of daughter cells in mutation group was obviously significantly larger than other groups. Blue, DAPI; Red, α-tubulin; Green, GFP. $^{**}P < 0.01$; $^{***}P < 0.001$. Scale bar =10 μm. Error bars show mean ± standard deviation in **(B,C)**.

and sporadic forms. Since the first genetic cause of NVM was identified as mutations in the X-linked TAZ gene, an increasing number of related genes have been found, including the sarcomere-encoding genes MYH7, ACTC, TNNT2, MYBPC3, TMP1, and TNNI3, Z-line protein-encoding ZASP/LDB3 gene, sodium channel gene SCN5A, and calcium-handling genes TAZ and LMNA (4, 32, 33). However, there have been few publications reporting an association between NVM and the gene encoding microtubules.

In the present study, we demonstrated a *de novo* mutation in *MTUS1*, a gene encoding microtubule-associated protein, caused decreased expression of α-tubulin, increased expression of α/β-tubulin heterodimer and PAR6 protein, enlarged the area of the daughter cells and the distance between the spindle and cytoplasmic membrane in daughter cells, and decreased levels of phosphorylated Rac1/Cdc42. These data are consistent with our hypothesis that the *de novo* c. 2617A->C mutation in *MTUS1* decreased the stability of microtubules and increased cell polarity, which might be through the Rac1/Cdc42 pathway, thus partly elucidating the protective mechanism in NVM.

The cytoskeleton is well known to be a dynamic three-dimensional structure that fills the cytoplasm of cells and is responsible for cell movement, cytokinesis, and the organization of organelles or organelle-like structures within cells. The major components of the cytoskeleton include microfilaments, microtubules, and intermediate filament systems. As one of the components of the cytoskeleton, microtubules may cause abnormalities in cardiac compacting during embryogenesis (34). In our study, we found that the fluorescence intensities in the mutated *MTUS1* group differed from the wild type group, indicating the microtubule stability in the mutated *MTUS1* group may have been destroyed. These results suggest the mutated *MTUS1* may alter myocardial densification by affecting microtubules during cardiac development.

Cell polarity refers to the unequal distribution of some cytoplasmic components in a cell in a certain spatial order,

thus forming a concentration gradient of various intracellular components. Cellular biologic functions related to cell polarity include asymmetric cell division, migration, and proliferation. Some studies have found cardiomyocyte polarity to be disordered and cardiomyocyte morphology abnormal in heart slices from NVM model mice compared with normal heart sections, suggesting destruction of myocardial cell polarity may be involved in the occurrence of myocardial insufficiency during cardiac development (35, 36). The presence of cell polarity is inseparable from the formation of polar protein complexes and regulation of the Rho GTPase family, which are key regulatory factors associated with the cytoskeleton or microtubule stability (37, 38). The polar protein is transported from the cell cytoplasm to one side of the cell membrane by microtubule heterodimers to form the polar protein complexes that mediate polar cellular division. In the present study, we demonstrated that the *de novo* c. 2617A->C mutation in *MTUS1* increased cell polarity and concurrently decreased levels of phosphorylated Rac1/Cdc42. In addition, we found expression of polar protein PAR6, one of the members of the front-end polar protein complex, enhanced cell division, and located on the side of cell in the mutant group during cell division. These outcomes suggest that mutation of *MTUS1* increased polarity of HEK-293 cells by first lowering the phosphorylation level of Rac1/Cdc42 and then increasing expression of the polar protein PAR6, which is a downstream target gene of Rac1/Cdc42.

Biological functions related to cell polarization include asymmetric cell division and cell migration. However, cellular contents are unequally distributed when cell polarity is present (39). In this study, we found the area in daughter cells staining for α-tubulin and the distance between the spindle and cytoplasmic membrane of the daughter cells during cell division in the mutant group were obviously significantly larger than in other groups. It is suggested that the HEK-293 cells with the c. 2617A->C mutation underwent more asymmetric division than the wild type group due to changes in PAR6 protein levels. Furthermore, these results further suggest the *de novo* c. 2617A->C mutation in *MTUS1* promotes cell polarity in patients with NVM during cardiac development, increasing resistance to the disorder of adult cardiomyocytes that will occur in the development of NVM.

Although the present study was conducted in a cell culture system, the data had clinical relevance because the acquired mutation studied originated from a clinical patient. However, future studies are warranted to verify the effect of the *de novo* c. 2617A->C mutation in *MTUS1* on development of NVM and the underlying mechanism(s) using animal models and living human tissue. To date, there are no well-established animal models of NVM. Furthermore, it is prohibited to use living human tissue for ethical reasons. To overcome this challenge, we have already obtained the patient urine cells and generated induced pluripotent stem cell-derived cardiomyocytes, which carry the same genetic background as the patient (data not published). Next, to alleviate the phenotype of NVM mice model, the adeno associated virus (AAV) vectors containing mutation *MTUS1* will be injected into the pregnant mice of NVM model. Through these technologies, we will elucidate the roles of the *MTUS1* mutation in the NVM pathogenesis, as well as the underlying mechanism(s).

CONCLUSION

Taken together, the data from the present study demonstrate that the Rac1/Cdc42 pathway might be involved in the control of cell polarity by the *de novo* c. 2617A->C mutation in *MTUS1*, thus may promote densification of the myocardium and reduce the occurrence of myocardial densification arrest. Therefore, the *de novo* c. 2617A->C mutation in *MTUS1* may be protective during cardiac development and may decrease the risk of NVM. This is the first study assessing the effects of *MTUS1* gene polymorphisms on cell polarity in NVM. These findings may help understand the genetic basis of cell polarity and provide insight for developing new approaches in the pathogenesis of NVM and reducing the prevalence of NVM through early gene intervention.

ETHICS STATEMENT

This study was approved by the Institutional Review Board of Children's Hospital of Chongqing Medical University, China (Approval Notice 24/2015) and abided by the ethical principles outlined in the Declaration of Helsinki.

AUTHOR CONTRIBUTIONS

All authors contributed substantially to the conception and design of the study, and to the critical review of the manuscript. NO collected the samples and evaluated the WES result. YZ did the WES data analysis. XB completed the whole basic experiment and wrote the manuscript. LL, JT, XH, and TL reviewed the manuscript. All authors read and approved the final manuscript.

FUNDING

This work was supported by the National Natural Science Foundation of China (Grant Number: 81570218).

ACKNOWLEDGMENTS

We thank professor Weinian Shou from Indiana University School of Medicine for his guidance to our research. We also thank Beijing deyi Oriental translational medicine research center for their help with DNA extraction and whole exome sequencing for samples.

SUPPLEMENTARY MATERIAL

The Supplementary Material for this article can be found online at: https://www.frontiersin.org/articles/10.3389/fped.2019.00247/full#supplementary-material

REFERENCES

1. Elliott P, Andersson B, Arbustini E, Bilinska Z, Cecchi F, Charron P, et al. Classification of the cardiomyopathies: a position statement from the European Society Of Cardiology Working Group on Myocardial and Pericardial Diseases. *Eur Heart J*. (2008) 29:270–6. doi: 10.1093/eurheartj/ehm342
2. Anderson RH, Ho SY, Sanchez-Quintana D, Redmann K, Lunkenheimer PP. Heuristic problems in defining the three-dimensional arrangement of the ventricular myocytes. *Anat Rec A Discov Mol Cell Evol Biol*. (2006) 288:579–86. doi: 10.1002/ar.a.20330
3. Pankuweit S, Richter A, Ruppert V, Maisch B. Classification of cardiomyopathies and indication for endomyocardial biopsy revisited. *Herz*. (2009) 34:55–62. doi: 10.1007/s00059-009-3195-8
4. Luxan G, Casanova JC, Martinez-Poveda B, Prados B, D'Amato G, MacGrogan D, et al. Mutations in the NOTCH pathway regulator MIB1 cause left ventricular noncompaction cardiomyopathy. *Nat Med*. (2013) 19:193–201. doi: 10.1038/nm.3046
5. Aras D, Tufekcioglu O, Ergun K, Ozeke O, Yildiz A, Topaloglu S, et al. Clinical features of isolated ventricular noncompaction in adults long-term clinical course, echocardiographic properties, and predictors of left ventricular failure. *J Card Fail*. (2006) 12:726–33. doi: 10.1016/j.cardfail.2006.08.002
6. Hussein A, Karimianpour A, Collier P, Krasuski RA. Isolated noncompaction of the left ventricle in adults. *J Am Coll Cardiol*. (2015) 66:578–85. doi: 10.1016/j.jacc.2015.06.017
7. Towbin JA, Lorts A, Jefferies JL. Left ventricular non-compaction cardiomyopathy. *Lancet*. (2015) 386:813–25. doi: 10.1016/S0140-6736(14)61282-4
8. Zhang W, Chen H, Qu X, Chang CP, Shou W. Molecular mechanism of ventricular trabeculation/compaction and the pathogenesis of the left ventricular noncompaction cardiomyopathy (LVNC). *Am J Med Genet C Semin Med Genet*. (2013) 163C:144–56. doi: 10.1002/ajmg.c.31369
9. Passer D, van de Vrugt A, Atmanli A, Domian IJ. Atypical protein kinase C-dependent polarized cell division is required for myocardial trabeculation. *Cell Rep*. (2016) 14:1662–72. doi: 10.1016/j.celrep.2016.01.030
10. Raman R, Pinto CS, Sonawane M. Polarized organization of the cytoskeleton: regulation by cell polarity proteins. *J Mol Biol*. (2018) 430:3565–84. doi: 10.1016/j.jmb.2018.06.028
11. Bryant DM, Mostov KE. From cells to organs: building polarized tissue. *Nat Rev Mol Cell Biol*. (2008) 9:887–901. doi: 10.1038/nrm2523
12. Tepass U. The apical polarity protein network in Drosophila epithelial cells: regulation of polarity, junctions, morphogenesis, cell growth, and survival. *Annu Rev Cell Dev Biol*. (2012) 28: 655–85. doi: 10.1146/annurev-cellbio-092910-154033
13. Bustelo XR, Sauzeau V, Berenjeno IM. GTP-binding proteins of the Rho/Rac family: regulation, effectors and functions *in vivo*. *Bioessays*. (2007) 29:356–70. doi: 10.1002/bies.20558
14. Munro E, Nance J, Priess JR. Cortical flows powered by asymmetrical contraction transport PAR proteins to establish and maintain anterior-posterior polarity in the early *C. elegans* embryo. *Dev Cell*. (2004) 7:413–24. doi: 10.1016/j.devcel.2004.08.001
15. Badano JL, Katsanis N. Life without centrioles: cilia in the spotlight. *Cell*. (2006) 125:1228–30. doi: 10.1016/j.cell.2006.06.013
16. Seibold S, Rudroff C, Weber M, Galle J, Wanner C, Marx M. Identification of a new tumor suppressor gene located at chromosome 8p21.3-22. *FASEB J*. (2003) 17:1180–2. doi: 10.1096/fj.02-0934fje
17. Rodrigues-Ferreira S, Di TA, Dimitrov A, Cazaubon S, Gruel N, Colasson H, et al. 8p22 MTUS1 gene product ATIP3 is a novel anti-mitotic protein underexpressed in invasive breast carcinoma of poor prognosis. *PLoS ONE*. (2009) 4:e7239. doi: 10.1371/journal.pone.0007239
18. Zuern C, Krenacs L, Starke S, Heimrich J, Palmetshofer A, Holtmann B, et al. Microtubule associated tumor suppressor 1 deficient mice develop spontaneous heart hypertrophy and SLE-like lymphoproliferative disease. *Int J Oncol*. (2012) 40:1079–88. doi: 10.3892/ijo.2011.1311
19. Zhang W, Chen H, Wang Y, Yong W, Zhu W, Liu Y, et al. Tbx20 transcription factor is a downstream mediator for bone morphogenetic protein-10 in regulating cardiac ventricular wall development and function. *J Biol Chem*. (2011) 286:36820–9. doi: 10.1074/jbc.M111.279679
20. Wu X, Pan B, Wang Y, Liu L, Huang X, Tian J. The protective role of low-concentration alcohol in high-fructose induced adverse cardiovascular events in mice. *Biochem Biophys Res Commun*. (2018) 495:1403–10. doi: 10.1016/j.bbrc.2017.11.141
21. Boczonadi V, Gillespie R, Keenan I, Ramsbottom SA, Donald-Wilson C, Al Nazer M, et al. Scrib:Rac1 interactions are required for the morphogenesis of the ventricular myocardium. *Cardiovasc Res*. (2014) 104:103–15. doi: 10.1093/cvr/cvu193
22. Molina A, Velot L, Ghouinem L, Abdelkarim M, Bouchet BP, Luissint AC, et al. ATIP3, a novel prognostic marker of breast cancer patient survival, limits cancer cell migration and slows metastatic progression by regulating microtubule dynamics[J]. *Cancer Res*. (2013) 73:2905–15. doi: 10.1158/0008-5472.CAN-12-3565
23. Berika M, Elgayyar ME, El-Hashash AH. Asymmetric cell division of stem cells in the lung and other systems. *Front Cell Dev Biol*. (2014) 2:33. doi: 10.3389/fcell.2014.00033
24. Liu Y, Wang J, Li J, Wang R, Tharakan B, Zhang SL, et al. Deletion of Cdc42 in embryonic cardiomyocytes results in right ventricle hypoplasia. *Clin Transl Med*. (2017) 6:40. doi: 10.1186/s40169-017-0171-4
25. Etienne-Manneville S, Hall A. Rho GTPases in cell biology. *Nature*. (2002) 420:629–35. doi: 10.1038/nature01148
26. Huang Q, Shen HM, Ong CN. Emodin inhibits tumor cell migration through suppression of the phosphatidylinositol 3-kinase-Cdc42/Rac1 pathway. *Cell Mol Life Sci*. (2005) 62:1167–75. doi: 10.1007/s00018-005-5050-2
27. Gomez-Lopez S, Lerner RG, Petritsch C. Asymmetric cell division of stem and progenitor cells during homeostasis and cancer. *Cell Mol Life Sci*. (2014) 71:575–97. doi: 10.1007/s00018-013-1386-1
28. Derivery E, Seum C, Daeden A, Loubéry S, Holtzer L, Jülicher F, et al. Polarized endosome dynamics by spindle asymmetry during asymmetric cell division. *Nature*. (2015) 528:280–5. doi: 10.1038/nature16443
29. Weiford BC, Subbarao VD, Mulhern KM. Noncompaction of the ventricular myocardium. *Circulation*. (2004) 109:2965–71. doi: 10.1161/01.CIR.0000132478.60674.D0
30. Engberding R, Yelbuz TM, Breithardt G. Isolated noncompaction of the left ventricular myocardium – a review of the literature two decades after the initial case description. *Clin Res Cardiol*. (2007) 96:481–8. doi: 10.1007/s00392-007-0528-6
31. Arbustini E, Weidemann F, Hall JL. Left ventricular noncompaction: a distinct cardiomyopathy or a trait shared by different cardiac diseases. *J Am Coll Cardiol*. (2014) 64:1840–50. doi: 10.1016/j.jacc.2014.08.030
32. Pentassuglia L, Sawyer DB. ErbB/integrin signaling interactions in regulation of myocardial cell-cell and cell-matrix interactions. *Biochim Biophys Acta*. (2013) 1833:909–16. doi: 10.1016/j.bbamcr.2012.12.007
33. Field LJ, Shou W, Markham L. 2017 riley heart center symposium on cardiac development: development and repair of the ventricular wall. *Pediatr Cardiol*. (2018) 39:1067–8. doi: 10.1007/s00246-018-1942-4
34. Chen H, Zhang W, Sun X, Yoshimoto M, Chen Z, Zhu W, et al. Fkbp1a controls ventricular myocardium trabeculation and compaction by regulating endocardial Notch1 activity. *Development*. (2013) 140:1946–57. doi: 10.1242/dev.089920
35. Ajima R, Bisson JA, Helt JC, Nakaya MA, Habas R, Tessarollo L, et al. DAAM1 and DAAM2 are co-required for myocardial maturation and sarcomere assembly. *Dev Biol*. (2015) 408:126–39. doi: 10.1016/j.ydbio.2015.10.003
36. Leung C, Liu Y, Lu X, Kim M, Drysdale TA, Feng Q. Rac1 signaling is required for anterior second heart field cellular organization and cardiac outflow tract development. *J Am Heart Assoc*. (2015) 5:1. doi: 10.1161/JAHA.115.002508

37. Wu G, Huang X, Hua Y, Mu D. Roles of planar cell polarity pathways in the development of neural [correction of neutral] tube defects. *J Biomed Sci*. (2011) 18:66. doi: 10.1186/1423-0127-18-66
38. Gönczy P. Mechanisms of asymmetric cell division: flies and worms pave the way. *Nat Rev Mol Cell Biol.* (2008) 9:355–66. doi: 10.1038/nrm2388
39. El-Hashash AH, Warburton D. Cell polarity and spindle orientation in the distal epithelium of embryonic lung. *Dev Dyn.* (2011) 240:441–5. doi: 10.1002/dvdy.22551

Conflict of Interest Statement: The authors declare that the research was conducted in the absence of any commercial or financial relationships that could be construed as a potential conflict of interest.

frontiers in Pediatrics

ORIGINAL RESEARCH
published: 09 July 2019
doi: 10.3389/fped.2019.00280

Catheter Ablation of Ventricular Arrhythmias Originating From the Pulmonary Sinus Cusp in Pediatric Patients: A Single-Center Retrospective Study

Tian Liu[1†], Dongpo Liang[1†], Zili Liao[2], Zhiwei Zhang[1], Shushui Wang[1] and Shaoying Zeng[1]*

[1] Guangdong Provincial Key Laboratory of South China Structural Heart Disease, Department of Pediatric Cardiology, Guangdong Cardiovascular Institute, Guangdong Provincial People's Hospital, Guangdong Academy of Medical Sciences, Guangzhou, China, [2] Guangdong Provincial Key Laboratory of South China Structural Heart Disease, Department of Cardiology, Guangdong Cardiovascular Institute, Guangdong General Hospital, Guangdong Academy of Medical Sciences, Guangzhou, China

OPEN ACCESS

Edited by:
Fu Lijun,
Shanghai Children's Medical Center, China

Reviewed by:
Li Xiaomei,
Tsinghua University, China
Fen Li,
Shanghai Children's Medical Center, China

***Correspondence:**
Shaoying Zeng
shaoyingzeng123@126.com

[†] These authors have contributed equally to this work

Specialty section:
This article was submitted to Pediatric Cardiology, a section of the journal Frontiers in Pediatrics

Received: 12 February 2019
Accepted: 21 June 2019
Published: 09 July 2019

Citation:
Liu T, Liang D, Liao Z, Zhang Z, Wang S and Zeng S (2019) Catheter Ablation of Ventricular Arrhythmias Originating From the Pulmonary Sinus Cusp in Pediatric Patients: A Single-Center Retrospective Study. Front. Pediatr. 7:280. doi: 10.3389/fped.2019.00280

Objective: There are few reports of ventricular arrhythmias (VAs) originating from the pulmonary sinus cusp (PSC) in pediatric patients. Thus, we investigated the ablation of PSC-VAs in pediatric patients.

Study Design: Clinical, echocardiographic, and ablation data were reviewed in 10 consecutive symptomatic children who underwent successful ablation of VAs of PSC origin at our center between March 2014 and June 2018.

Results: The 10 patients' weights ranged from 29 to 63.5 kg, and all had structurally normal hearts and VAs with left bundle branch block (LBBB) morphologies and inferior axes. The initial ablation was performed in the right ventricular outflow tract (RVOT) or the aortic sinus cusp, which failed to terminate the VAs in nine patients. The successful ablation site was in the right cusp (RC) in seven patients, the anterior cusp in two patients, and the left cusp (LC) in one patient. The earliest potential recorded at the PSC ablation site preceded the onset of the QRS complex during VAs by 29.4 ± 4.9 ms.

Conclusions: VAs with a LBBB morphologies and inferior axes may originate within the PSC of children. Ablation was effective and safe for the eradication of VAs originating from the PSCs in children. Due to the particularity of ablations in pediatric patients, mapping of PSCs should be considered when ablation fails in the RVOT.

Keywords: ventricular arrhythmia, radiofrequency catheter ablation, pulmonary sinus cusp, pediatric patient, ventricular tachycardia, premature ventricular contractions

INTRODUCTION

Ventricular arrhythmias (VAs) are prevalent in pediatric patients and most occur without underlying heart disease. Idiopathic ventricular tachycardia (VT) or premature ventricular contractions (PVCs) with left bundle branch block (LBBB) morphologies and inferior axes in pediatric patients, most commonly originate from the right ventricular outflow tract (RVOT) (1).

Radiofrequency catheter ablation (RFCA) has been increasingly used in the treatment of such arrhythmias; however, their high recurrence rate adversely impacts prognosis. Ablation of VAs from the pulmonary sinus cusp (PSC) has recently been reported in adult patients at our center (2), but not in pediatric populations. In this study, we investigated the catheter ablation of outflow tract ventricular arrhythmias, as well as focusing on the ECG characteristics, mapping, and ablation of VAs arising from the PSC in pediatric patients.

PATIENTS AND METHODS

Study Population

Between March 2014 and June 2018, 43 consecutive symptomatic children (28 males, mean age 10.1 ± 2.9 years, mean weight 37.3 ± 13.6 years) with frequent VAs were referred to our department for catheter ablation. All patients had structurally normal hearts. The ECG recorded during the VAs showed LBBB morphologies and inferior axes in all patients. All children had rhythm-correlated symptoms due to frequent PVCs or VTs. Successful ablations were achieved in 40 patients, including 29 in RVOT (72.5%), one in the right aortic sinus cusp (2.5%), and 10 in the PSC (25.0%). Among the remaining three patients, ablation was unsuccessful in two, while ablation could not be performed in the third due to the pain caused by the procedure.

Prior to electrophysiological examination, all patients underwent non-invasive cardiac evaluations, including reviews of family histories, physical examinations, 12-lead electrocardiograms (ECG), 24-h Holter ECGs, and transthoracic echocardiography. All patients had a normal ECG during sinus rhythm, and no structural abnormalities were apparent upon physical examination. The indications for catheter ablation included symptomatic VAs and ineffective treatments with antiarrhythmic drugs. The exclusion of VAs was due to transient reversible causes, such as acute myocarditis or drug toxicity. The cardiac dimensions of children were in accordance with their ages, heights, body weights, and body surface areas. Cardiac dilatation was defined as an echocardiography-measured cardiac cavity size beyond one standard deviation. The hospital ethics committee approved the study, and all patients' guardians provided written informed consent before procedures were performed.

Electrophysiological Analyses

All antiarrhythmic drugs were withdrawn for a duration of at least five half-lives. Catheters were inserted through the right femoral vein into the right atrium, right ventricle, and PA using fluoroscopic guidance. If the clinical arrhythmia failed to occur spontaneously and was not provoked by the administration of intravenous isoproterenol infusion, programmed ventricular stimulation, and incremental burst pacing were performed at two basic drive cycle lengths with < 2 extra stimuli to a minimum coupling interval of 230 ms. During the procedure, intravenous heparin was delivered as a 100 IU/kg bolus dose and again every hour thereafter to maintain an activated clotting time between 250 and 300 s.

Mapping and RFCA

After the baseline study, a steerable 7.5-F catheter with a 3.5-mm irrigated-tip electrode with 2-5-2 mm inter-electrode spacing (NaviStar ThermoCool, Biosense Webster, Diamond Bar, California), was used for 3-dimensional electroanatomical mapping and ablation. The catheter was advanced, via the 8.5-F SL1 long sheath and introduced through the right femoral vein into the right ventricle. Point-by-point mapping was used to create anatomic maps, and activation mapping was performed during spontaneous/induced VT or PVCs to identify the origin of the VAs. Pace mapping was also used during the electrophysiological study to capture the ventricular myocardium at the site of the earliest activation. The pacing morphology was compared with the spontaneous arrhythmia. A good pace map was defined as a paced QRS morphology that matched the clinical VAs in $\geq$10 of 12 leads. The suitable ablation target site was defined as the site where the best pace mapping and/or the earliest activation time could be obtained during the VT or PVCs.

In 10 patients, the successful ablation sites were in the PSC. According to QRS morphologies during VAs, initial mapping was performed in the RVOT in nine patients, and in the aortic sinus cusp in one patient. When ablation failed, or suitable ablation sites were not found in the RVOT or aortic sinus cusp, mapping within the PSC was performed. Detailed mapping within the PSC was performed using a reversed U curve of the ablation catheter. The SL1 long sheath was used to advance into the right ventricle to permit a reversed U curve in the PA, which could enhance stability of the catheter. Furthermore, the long sheath helped clockwise or counterclockwise catheter rotation to access the three individual PSCs (2).

The irrigated radiofrequency current was delivered in power-controlled mode, with a preselected temperature of 40–43°C, a radiofrequency energy of 25–30 W, and a flow rate of 17–20 ml/min. If arrhythmias were eliminated, or decreased in frequency by radiofrequency within the initial 15 s, the radiofrequency energy applications were maintained for 60–90 s. Following elimination of the VAs by radiofrequency delivery, the catheter position was evaluated and confirmed by repeat pulmonary arteriograms, right ventriculography, or coronary angiography. However, intracardiac echocardiography was not used to evaluate catheter position. After successful ablation, intravenous isoproterenol infusion was administered, and programmed stimulation was performed to confirm the elimination of clinical arrhythmias. Transthoracic echocardiography was performed to assess pericardial effusion during the procedure.

Successful RFCAs were determined by three criteria: (1) the absence of spontaneous or induced clinical VAs upon completion of the procedure; (2) the absence of VTs or PVCs during 24-h ECG monitoring with the patient not administered antiarrhythmic drugs; and (3) no recurrence of VTs or PVCs in the absence of antiarrhythmic drugs for at least 1 year following

the procedure. Transthoracic echocardiography was performed before hospital discharge for all pediatric patients.

Follow-up

Following ablation, all children received 3–5 mg/kg per day of aspirin for 3 months, but no antiarrhythmic drugs. The follow-up consisted of examinations at an outpatient clinic. Patients were assessed at 1, 3, and 6 months after the procedure, and yearly thereafter. A 12-lead ECG was performed at each visit, while transthoracic echocardiography and 24-h Holter ECG were performed at the 3, 6-month, and annual follow-up visits.

Statistical Analysis

Data were presented using counts (%) for categorical variables and means ± standard deviations (SD) for normally-distributed continuous variables. The parameters in different groups were compared using the Student's unpaired *t*-test. A two-tailed *p*-value <0.05 was considered statistically significant. Data analyses were performed using SPSS 19.0 (SPSS Inc., USA).

RESULTS

The characteristics of the 40 pediatric patients, with successful ablations, are given in **Table 1**. Patient symptoms consisted of dizziness, palpitations, chest distress, or exercise intolerance upon the presentation of VAs. None of the patients experienced syncope at the presentation of VAs. Prior to ablation, all patients received medical therapy, where 30 (75%) were managed with one antiarrhythmic drug, and 10 (25%) were administered more than two consecutive or concomitant antiarrhythmic drugs. The drugs consisted of oral amiodarone, metoprolol, and propafenone. Medical therapy was ineffective in all patients. In 29 patients, the successful ablation sites were in the RVOT (at the posteroseptal region in 12, midseptal region in three, anteroseptal region in eight, the anterior free wall in three, and the posterior free wall in three).

The 10 patients with VAs from the PSC (mean age, 11.3 ± 2.1 years) group included six males and four females, with a mean weight of 43.1 ± 10.9 (range, 29–63.5) kilograms. During electrophysiological analyses, Clinical arrhythmias occurred spontaneously or were provoked by the administration of intravenous isoproterenol infusion in seven patients, while clinical PVCs were induced by programmed ventricular stimulation and burst pacing in three of the 10 patients. A previous ablation had been performed successfully in one patient. The site of termination of the PVC was in the RVOT; however, VAs with the same morphologies recurred during follow-up examinations after the patient's first ablation. A repeat procedure was performed 4 months later.

The initial ablation was performed in the left aortic sinus cusp in one patient, in the RVOT in eight patients, and in the PSC in one patient (**Table 2**). The initial ablation in the left aortic sinus cusp failed to decrease the VAs in one patient. In the left aortic sinus cusp, the recorded local ventricular activation preceded the QRS onset during VAs by 15 ms, and a good pace map was obtained. In the RVOT, the site was at the posteroseptal region in two patients, at the midseptal region in one patient, at the anteroseptal region in one patient, and at the anterior free wall in four patients. Local ventricular activation recorded at the initial ablation site preceded the QRS onset during the VAs by 20.3 ± 5.2 ms, and a good pace map was obtained at those sites in five patients.

Ablation in the RVOT resulted in transient suppression in seven patients, with a minor change in the QRS morphology of the PVCs in two patients, and termination in one patient. Mapping within the PSC was subsequently performed in those children.

Two ventricular activation components, including near-field and far-field activation, were recorded at the earliest site in all patients during sinus rhythm, and its relationship was reversed during VAs. When the earliest ventricular activation was identified within the PSC on the bipolar recording, simultaneous activation in the unipolar recording demonstrated the QS morphology. The sharp potential recorded at the PSC ablation site preceded the onset of the QRS complex during VAs by 29.4 ± 4.9 ms, which was significantly greater than the earliest activation time recorded in the RVOT and aortic sinus cusp (p <0.05). Pace mapping was performed at the site of the earliest ventricular

TABLE 1 | Characteristics of pediatric patients with successful ablation.

Characteristic	PSC group (n = 10)	RVOT group (n = 29)	ASC group (n = 1)
Age (years)	11.3 ± 2.1	9.4 ± 2.9	12
Male	6 (60)	20 (69.0)	1 (100)
Weight	43.1 ± 10.9	34.3 ± 13.8	32
Age at VAs onset (years)	10.2 ± 1.6	8.2 ± 3.6	10
CLINICAL VAs			
Only PVCs	8 (80)	24 (82.8)	1 (100)
PVCs and non-sustained VT	2 (20)	5 (17.2)	0
MEDICAL THERAPY			
One single antiarrhythmic drug	6 (60)	23 (79.3)	1 (100)
More than two antiarrhythmic drug	4 (40)	6 (20.7)	0
PVCs burden on 24-h Holter electrocardiogram(%)	32 ± 7.7	32.4 ± 11.4	46.5
ECHOCARDIOGRAM			
Normal cardiac cavity size	10 (100)	29 (100)	1 (100)
Left ventricular ejection fraction (%)	71.3 ± 7.5	70.0 ± 6.4	61

Values are given as no. (%) or means ± SD. PSC, pulmonary sinus cusp; RVOT, right ventricular outflow tract; ASC, aortic sinus cusp; Vas, ventricular arrhythmias; PVCs, premature ventricular contractions; VT, ventricular tachycardia.

TABLE 2 | The initial ablation site and the successful ablation site in 10 patients.

Patient	1	2	3	4	5	6	7	8	9	10
The initial ablation site	RVOT	RVOT	ASC	RVOT	RVOT	RVOT	RC	RVOT	RVOT	RVOT
The successful ablation sit	RC	AC	AC	RC	RC	RC	RC	LC	RC	RC

RVOT, right ventricular outflow tract; ASC, aortic sinus cusp; RC, right cusp; AC, anterior cusp; LC, left cusp.

activation in all patients, with good pace maps obtained in seven patients (64%). VAs originated from the right cusp (RC) in seven patients (70%) (**Figure 2**), the anterior cusp (AC) in two patients (20%) (**Figure 3**), and the left cusp (LC) in one patient (10%) (**Figure 1**; **Table 2**). Fluoroscopy was used in all patients and the mean fluoroscopy time was 10.2 ± 6.4 min. The mean procedure duration was 131.3 ± 27.5 min.

The ECG recorded during the VAs revealed a LBBB morphology and inferior axis in all patients (**Figures 1**–**3**). The QRS duration was 126.3 ± 17.3 ms in lead V1. Among patients with structurally normal hearts, the precordial transition lead was often observed at V3 and V4, occurring from V3 in three VAs, from V4 in six VAs, and from V5 in one VA. There was a notch on the R-wave in the inferior leads in six patients. A QS-wave was present in avR and avL in all patients.

No complications occurred during ablation. At a mean follow-up of 2.7 years (1–4.5 years), all patients in the study were alive. All patients were free of antiarrhythmic drugs and free of VAs, with no arrhythmia recurrence. Echocardiographic examinations showed left ventricular function was normal in all patients.

DISCUSSION

The main finding of this 10-patient study was that VAs with LBBB morphologies and inferior axes may have originated within the PSC in children. Ablation was effective and safe for the eradication of VAs originating from the PSC in children. Because of the particularity of ablation in pediatric patients, mapping in PSCs should be considered when ablation fails in the RVOT. In all patients, two ventricular activation components were recorded at the successful ablation site within the PSC.

PVCs are most commonly seen in healthy children. When the PVCs are isolated, they rarely need treatment (3). In studies of adults with structurally normal hearts, frequent VAs can increase the risk of left ventricular dysfunction, and are associated with PVC-induced cardiomyopathy when the burden of PVCs is at least 10% (generally 20–30%) (4, 5). Some studies in children have reached similar conclusions (6, 7). When frequent PVCs have correlated symptoms, or when VAs reduce the left ventricular function, or have hemodynamic compromise, VAs should be treated using drug therapy or ablation (3, 8) in children. All participants in this study had rhythm-correlated symptoms due to VAs, and medical therapy was ineffective.

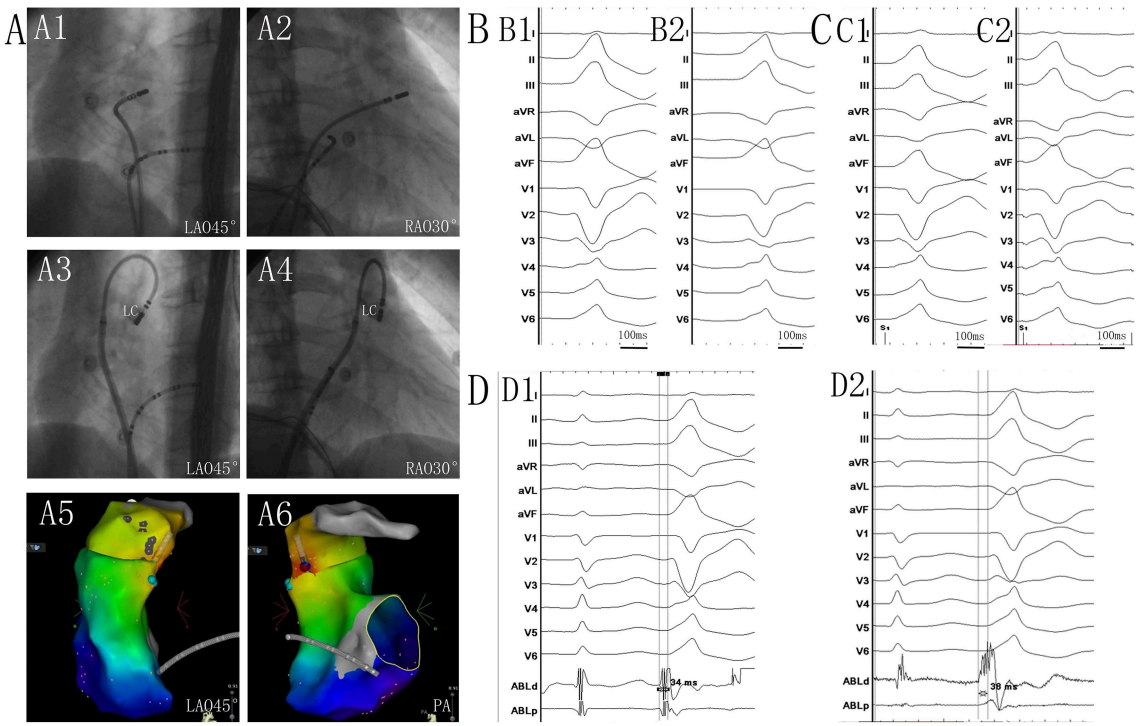

FIGURE 1 | (A1) Left anterior oblique (LAO) 45° and **(A2)** right anterior oblique (RAO) 30° views showing the position of the ablation catheter at the site of the anteroseptal region of the right ventricular outflow tract (RVOT). **(A3)** LAO 45° and **(A4)** RAO 30° views showing the position of the successful ablation site within the left cusp (LC). **(A5)** LAO 45° and **(A6)** posteroanterior view showing the anatomic CARTO map of the right ventricle and pulmonary artery (PA). The blue tag represents the earlier activation site in the RVOT anteroseptal region. The red tag represents the earliest site in the LC. **(B1)** Twelve-lead ECG recordings during spontaneous PVC. **(B2)** QRS morphological changes after ablation in the RVOT. Twelve-lead ECG recordings during pacing at the sites of the RVOT anteroseptal region **(C1)**, and at the LC **(C2)**. QRS morphology during pacing in the LC matched that of the spontaneous PVC, and was similar to that of the spontaneous PVC when pacing at the RVOT. **(D1)** The potential preceded the QRS complex by 34 ms during the PVC recording from the catheter at the site of the earlier activation in the RVOT anteroseptal region. **(D2)** The potential preceded the QRS complex by 38 ms during the PVC recording at the site of the earliest activation in the LC. Near- and far-field activations were recorded during sinus rhythm, and its relationship was reversed during PVC.

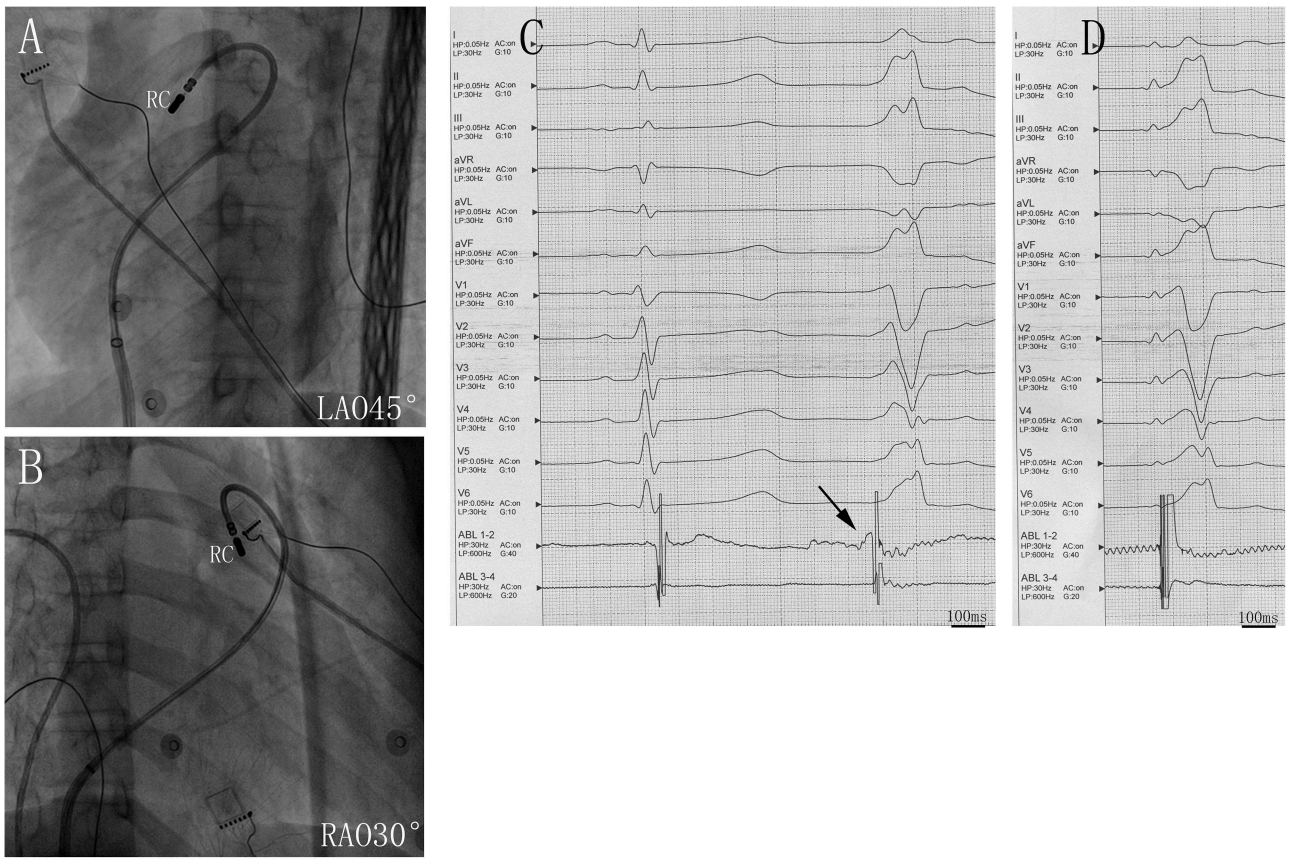

FIGURE 2 | Successful ablation site within the right cusp (RC) in **(A)** left anterior oblique (LAO) 45° and **(B)** right anterior oblique (RAO) 30° views. **(C)** Twelve-lead ECG and ablation catheter (ABL 1-2) recordings during spontaneous PVCs. The potential preceded the QRS complex at the earliest activation site in the RC. **(D)** Twelve-lead ECG recordings during pacing at RC sites with QRS morphologies matching that of spontaneous PVC. Abbreviations are the same as in **Figure 1**.

In adult patients, although VAs can originate from almost any site in the ventricle, they are most commonly located in the RVOT and other sites, including the left ventricular outflow tract, the mitral and tricuspid annuli, the PA, and the aortic sinus cusp. Similar electrophysiological findings have been reported in pediatric patients (9).

Myocardial extensions into the great arteries above the semilunar cusps—or intercuspal—are likely to be secondary to incomplete myocardial regression, and may provide the substrate for PVCs. In previous studies, ventricular myocardial extensions into the PA—beyond the ventriculo-arterial junction—were relatively common, with a prevalence of 17–74% (10, 11). Using direct intracardiac echocardiography visualization, Liu et al. confirmed that 46% of RVOT-VA foci were localized in the PA (median 8.2 mm above PV), indicating that those arrhythmias should be reclassified as pulmonary arterial arrhythmias. Myocardial extensions may provide a substrate for PVCs, since some individuals with myocardial extensions do not experience VAs (12).

Ablation at and around the ventriculo-arterial junction is being increasingly practiced. Some studies demonstrating that the site of origin for outflow tract VAs may be truly intramural, and the ablation strategy chosen is based on proximity and safety (13). Thus, wherever ablation occurs, including in the RVOT, the left ventricular outflow tract, the aorta, or the PSC, it would provide a safe site for ablation. When arrhythmias cannot be eliminated after ablation in the RVOT, subsequent mapping and ablation should be performed in the PA, the aorta, or the PSC. Ablation in PSC would provide a new alternative methodology for the elimination of VAs. Liao et al. reported that in 11% of adults, idiopathic outflow tract-like VAs treated by RFCA could arise from PSCs and be successfully ablated within the PSC (2). Additionally, Zhang et al. reported that ablation within the PSCs effectively eliminated 90% of unselected idiopathic RVOT-type VAs (14). To date, there are no published data on the characteristics and ablation of VAs originating from the PSC in pediatric patients. In this study, we found that in 25% of pediatric patients, idiopathic outflow tract-like Vas, treated by RFCA, were effectively ablated within the PSC.

Activation originating from the PSC is followed by conduction through a pathway to the RVOT. Similar to the interruption of conduction in an accessory atrioventricular pathway, the interruption of conduction either at the beginning or exit of the PSC in the RVOT may abolish VAs (15). Zhang et al.

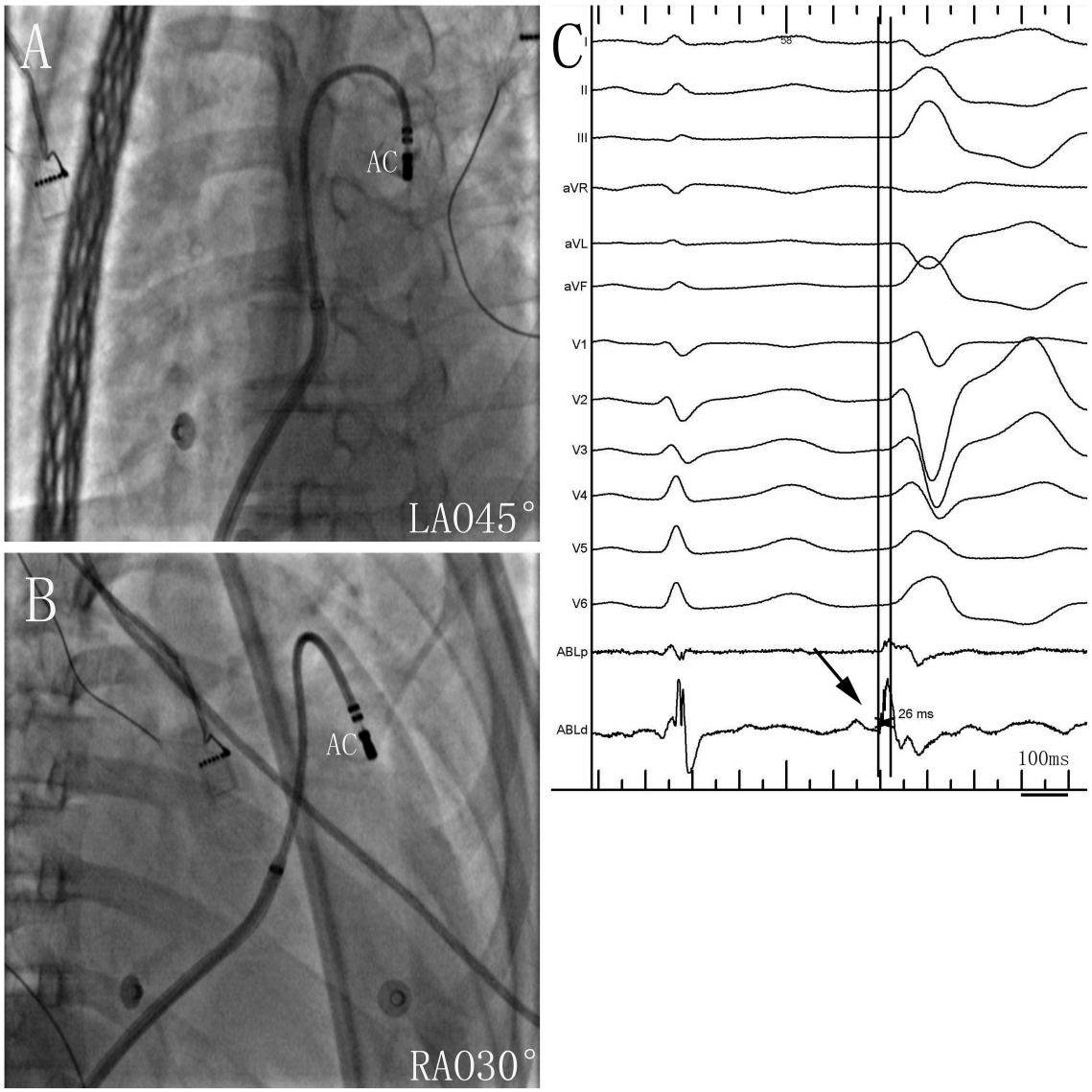

FIGURE 3 | Successful ablation site within the anterior cusp (AC) in **(A)** left anterior oblique (LAO) 45° and **(B)** right anterior oblique (RAO) 30° views. **(C)** Twelve-lead ECG and ablation catheter (ABL d) recordings during spontaneous PVCs. The potential preceded the QRS complex by 26 ms at the earliest activation site in the AC. Abbreviations are the same as in **Figure 1**.

hypothesized that PSC-VAs could be eliminated in the RVOT in some patients when the RVOT exit site was narrow. However, when the exit site is broad or there is an alternative pathway, insufficient ablation may alter the activation impulse and change the QRS morphologies of the PVCs (14, 15). In the present study, the initial ablation was performed in the RVOT in eight patients, resulting in a small change in the QRS morphologies of the PVCs in two patients. Furthermore, the myocardial extensions always had a narrow and thin distal end at the PSC, which may have benefited successful ablations. In this study, consolidating ablation was performed in the PSC after ablation in the RVOT in one patient. All VAs were successfully ablated within the PSC, and in all patients, two ventricular activation components were recorded at the successful ablation site. The sharp potential recorded at the successful ablation site preceded the onset of the QRS by 29.4 ± 4.9 ms, during VAs. The sharp potential was recorded late during sinus rhythm before ablation, and disappeared after ablation. However, most of the local electrograms at the earliest activation sites in the RVOT exhibited a single component. The discrete potential recorded within the PSCs during the VAs and sinus rhythm was characteristic of PSC-VAs. The latter phenomenon was consistent with a report by Liao et al. (2).

The ECG characteristics of the VAs were difficult to distinguish between VAs of RVOT and PSC origins. In our experience, mapping and ablation in the RVOT should be the

first consideration in children, as the catheter may injure the valve when approaching the PSC through the pulmonary valve. Mapping in the PSC or left ventricular outflow tract should be considered when ablation fails, or suitable ablation sites are not found in the RVOT. When performing ablation in the RVOT or the PSC, attention must also be paid to the damage caused to the left main coronary artery (16). Mapping and ablation in the PSC was facilitated in our patients by using a reversed U curve ablation catheter that was supported by a long sheath. The weight of the smallest child undergoing ablation within the PSC was 29 kg, and there is limited experience with ablation in the PSCs of smaller children. We suggest that mapping and ablation at the PSC should be performed cautiously in children, and only be performed at experienced and skilled cardiac electrophysiology centers.

The ECG characteristics of VAs originating from PSCs have rarely been reported. In our research of children with structurally normal hearts, the ECG recorded during VAs showed LBBB morphologies and inferior axes with the transitional zone often observed at V3 and V4. Additionally, a notch on the R-wave in the inferior leads was observed in some patients, similar to that reported in adults by Liao et al. (2). These authors also reported smaller R-wave amplitudes in the inferior leads, with longer QRS durations, and larger R-waves in lead I in RC-Vas, compared to that of the AC-VAs and LC-VAs. However, the smaller number of cases in our study precluded comparisons of ECG characteristics between VAs originating from the PSCs in children.

LIMITATIONS

The present study was limited by its single center, retrospective design with small sample size. Those limitations also precluded comparisons of ECG characteristics between PSC-Vas. However, most pediatric studies reported thus far have smaller sample sizes.

In this study of a pediatric population, the vast majority of VAs originating within the PSC exhibited LBBB morphologies, with inferior axes. Ablation was effective and safe for the eradication of VAs originating from the PSC in children. This study established a foundation for ablation in PSCs in children at cardiac electrophysiology centers. Because of the particularity of ablation in pediatric patients, mapping in the PSC should be considered when ablation fails in the RVOT. Additionally, mapping and ablation at the PSC should be performed cautiously in children.

DATA AVAILABILITY

All datasets generated for this study are included in the manuscript and/or the supplementary files.

ETHICS STATEMENT

This study was carried out in accordance with the recommendations of Guangdong provincial peoples hospital ethics committee with written informed consent from all subjects. All subjects gave written informed consent in accordance with the Declaration of Helsinki. The protocol was approved by the Guangdong provincial peoples hospital ethics committee.

AUTHOR CONTRIBUTIONS

SZ has obtained the approval of all other co-authors to submit the manuscript to your journal. All the authors have contribution to the manuscript.

ACKNOWLEDGMENTS

This work was supported by the National Key Research and Development Program (No. 2018YFC1002600) and the Guangdong Project of Science and Technology (Nos. 2017A070701013, 2017B090904034, and 2017B030314109).

REFERENCES

1. Pfammatter JP, Paul T. Idiopathic ventricular tachycardia in infancy and childhood: a multicenter study on clinical profile and outcome. Working group on dysrhythmias and electrophysiology of the association for european pediatric cardiology. *J Am Coll Cardiol*. (1999) 33:2067–72. doi: 10.1016/S0735-1097(99)00105-9
2. Liao Z, Zhan X, Wu S, Xue Y, Fang X, Liao H, et al. Idiopathic ventricular arrhythmias originating from the pulmonary sinus cusp: prevalence, electrocardiographic/electrophysiological characteristics, and catheter ablation. *J Am Coll Cardiol*. (2015) 66:2633–44. doi: 10.1016/j.jacc.2015.09.094
3. Crosson JE, Callans DJ, Bradley DJ, Dubin A, Epstein M, Etheridge S, et al. PACES/HRS expert consensus statement on the evaluation and management of ventricular arrhythmias in the child with a structurally normal heart. *Heart Rhythm*. (2014) 11:e55–78. doi: 10.1016/j.hrthm.2014.05.010
4. Baman TS, Lange DC, Ilg KJ, Gupta SK, Liu TY, Alguire C, et al. Relationship between burden of premature ventricular complexes and left ventricular function. *Heart Rhythm*. (2010) 7:865–9. doi: 10.1016/j.hrthm.2010.03.036
5. Ban JE, Park HC, Park JS, Nagamoto Y, Choi JI, Lim HE, et al. Electrocardiographic and electrophysiological characteristics of premature ventricular complexes associated with left ventricular dysfunction in patients without structural heart disease. *Europace*. (2013) 15:735–41. doi: 10.1093/europace/eus371
6. Beaufort-Krol GC, Dijkstra SS, Bink-Boelkens MT. Natural history of ventricular premature contractions in children with a structurally normal heart: does origin matter? *Europace*. (2008) 10:998–1003. doi: 10.1093/europace/eun121
7. West L, Beerman L, Arora G. Ventricular ectopy in children without known heart disease. *J Pediatr*. (2015) 166:338–42. doi: 10.1016/j.jpeds.2014.10.051
8. Philip SJ, Kanter RJ, Abrams D, Asirvatham S, Bar-Cohen Y, Blaufox AD, et al. PACES/HRS expert consensus statement on the use of catheter ablation in children and patients with congenital heart disease: developed in partnership with the Pediatric and Congenital Electrophysiology Society (PACES) and the Heart Rhythm Society (HRS). Endorsed by the governing bodies of PACES, HRS, the American Academy of Pediatrics (AAP), the American Heart Association (AHA), and the Association for European Pediatric and Congenital Cardiology (AEPC). *Heart Rhythm*. (2016) 13:e251–89. doi: 10.1016/j.hrthm.2016.02.009
9. Fukuhara J, Sumitomo N, Nakamura T, Ichikawa R, Matsumura M, Abe O, et al. Electrophysiological characteristics of idiopathic ventricular tachycardia in children. *Circ J*. (2011) 75:672–6. doi: 10.1253/circj.CJ-10-0339

10. Hasdemir C, Aktas S, Govsa F, Aktas EO, Kocak A, Bozkaya YT, et al. Demonstration of ventricular myocardial extensions into the pulmonary artery and aorta beyond the ventriculo-arterial junction. *Pacing Clin Electrophysiol*. (2007) 30:534–9. doi: 10.1111/j.1540-8159.2007.00704.x
11. Gami AS, Noheria A, Lachman N, Edwards WD, Friedman PA, Talreja D, et al. Anatomical correlates relevant to ablation above the semilunar valves for the cardiac electrophysiologist: a study of 603 hearts. *J Interv Card Electrophysiol*. (2011) 30:5–15. doi: 10.1007/s10840-010-9523-3
12. Liu CF, Cheung JW, Thomas G, Ip JE, Markowitz SM, Lerman BB. Ubiquitous myocardial extensions into the pulmonary artery demonstrated by integrated intracardiac echocardiography and electroanatomic mapping: changing the paradigm of idiopathic right ventricular outflow tract arrhythmias. *Circ Arrhythm Electrophysiol*. (2014) 7:691–700. doi: 10.1161/CIRCEP.113.001347
13. Hutchinson MD, Garcia FC. An organized approach to the localization, mapping, and ablation of outflow tract ventricular arrhythmias. *J Cardiovasc Electrophysiol*. (2013) 24:1189–97. doi: 10.1111/jce.12237
14. Zhang J, Tang C, Zhang Y, Su X. Pulmonary sinus cusp mapping and ablation: a new concept and approach for idiopathic right ventricular outflow tract arrhythmias. *Heart Rhythm*. (2018) 15:38–45. doi: 10.1016/j.hrthm.2017.08.007
15. Timmermans C, Rodriguez LM, Crijns HJ, Moorman AF, Wellens HJ. Idiopathic left bundle-branch block-shaped ventricular tachycardia may originate above the pulmonary valve. *Circulation*. (2003) 108:1960–7. doi: 10.1161/01.CIR.0000095026.19339.BB
16. Walsh KA, Fahy GJ. Anatomy of the left main coronary artery of particular relevance to ablation of left atrial and outflow tract arrhythmias. *Heart Rhythm*. (2014) 11:2231–8. doi: 10.1016/j.hrthm.2014.08.006

Conflict of Interest Statement: The authors declare that the research was conducted in the absence of any commercial or financial relationships that could be construed as a potential conflict of interest.

frontiers in Pediatrics

ORIGINAL RESEARCH
published: 09 July 2019
doi: 10.3389/fped.2019.00281

Simultaneous Semi-Mechanistic Population Pharmacokinetic Modeling Analysis of Enalapril and Enalaprilat Serum and Urine Concentrations From Child Appropriate Orodispersible Minitablets

Muhammad Faisal[1], Willi Cawello[1], Bjoern B. Burckhardt[1], Jan de Hoon[2], Stephanie Laer[1] and LENA Consortium*

[1] Institute of Clinical Pharmacy and Pharmacotherapy, Heinrich-Heine-University Düsseldorf, Düsseldorf, Germany, [2] Center for Clinical Pharmacology, University Hospitals Leuven/KU Leuven, Leuven, Belgium

OPEN ACCESS

Edited by:
Hongfang Jin,
Peking University First Hospital, China

Reviewed by:
Wei Zhao,
Shandong University, China
Zhiping Li,
Children's Hospital, Fudan University, China

***Correspondence:**
Muhammad Faisal
muhammad.faisal@HHU.de

Specialty section:
This article was submitted to Pediatric Cardiology, a section of the journal Frontiers in Pediatrics

Received: *01 May 2019*
Accepted: *24 June 2019*
Published: *09 July 2019*

Citation:
Faisal M, Cawello W, Burckhardt BB, de Hoon J, Laer S and LENA Consortium (2019) Simultaneous Semi-Mechanistic Population Pharmacokinetic Modeling Analysis of Enalapril and Enalaprilat Serum and Urine Concentrations From Child Appropriate Orodispersible Minitablets. Front. Pediatr. 7:281. doi: 10.3389/fped.2019.00281

Enalapril is recommended as the first line of therapy and is proven to improve survival rates for treatment of Pediatric Heart Failure; however, an approved drug and child appropriate dosage formulation is still absent. The present analysis was conducted to perform a detailed model informed population pharmacokinetic analysis of prodrug enalapril and its active metabolite enalaprilat in serum and urine. Further, a model informed dosage form population-pharmacokinetic analysis was conducted to evaluate differences in pharmacokinetics of enalapril and its active metabolite enalaprilat when prodrug was administered to 24 healthy adults in a crossover, two periods, two treatments, phase I clinical trial using child-appropriate orodispersible mini-tablets (ODMT) and reference (Renitec®) dosage formulation. A simultaneous semi-mechanistic population-pharmacokinetic model was developed using NONMEM software, which predicted full profile serum and urine concentrations of enalapril and enalaprilat. First-order conditional estimation with interaction was used for parameter estimation. Transit compartments added using Erlang distribution method to predicted enalapril absorption and enalaprilat formation phases. Normalized body weight was identified as covariate related to enalapril volume of distribution. Visual predictive check (VPC) plots and conducted bootstrap analysis validated the model. The data from the two formulations were pooled for population-pharmacokinetic analysis and covariate effect of the formulation was found on mean transit time (MTT1) of enalapril absorption. In addition, data of each formulation were modeled separately and the estimated parameters of each individual administered both formulations were correlated using paired samples Wilcoxon rank test ($p < 0.05$ = significant) which also showed only a significant difference ($p = 0.03$) in MTT1 i.e., 5 min early appearance of enalapril from ODMT compared to reference tablets. No difference in the pharmacokinetics of active enalaprilat

was found from the ODMT compared to the reference formulation. The population pharmacokinetic analysis provided detailed information about the pharmacokinetics of enalapril and enalaprilat, which showed that the ODMT formulation might have similar pharmacodynamic response compared to the reference formulation.

Keywords: enalapril, enalaprilat, heart failure, population pharmacokinetics modeling analysis, NONMEM, orodispersible mini-tablets, child appropriate dosage forms

INTRODUCTION

Despite the major success of the US Food and Drug Authority (FDA) and the European Medicine Agency (EMA) legislative and incentive initiatives toward pediatric drug development, the treatment of congestive heart failure in pediatrics (CHF) still lacks an approved drug and dosage formulation (1, 2). Lack of approved dosage forms leads to manipulation, modification, and extemporaneous administration of drugs (3, 4). These sub-optimal practices can result in compromised safety and efficacy and emphasize the need to develop a child appropriate dosage formulations (5, 6).

Enalapril has been recommended for the treatment of adult heart failure (7) and has been shown to prolong the survival rates in CHF patients (8). Around 60% of the administered oral dose of the drug is absorbed through the gastrointestinal tract. Enalapril is an inactive prodrug which is biotransformed in the liver by the carboxylesterases I (CES I) enzyme into an active angiotensin-converting enzyme inhibitor (ACE-I) enalaprilat (9, 10). Enalapril and enalaprilat are eliminated through the renal route without further metabolism. Around 60% of the administered dose is recovered in urine as enalapril and enalaprilat (11). At present, no other route of elimination has been reported for the enalapril and enalaprilat.

The ethical constraints in conducting pediatric clinical trials have restricted detail biopharmaceutical analysis of drugs and dosage formulations in children. Despite the physiological, biochemical, and pathological differences with pediatrics (12–14), healthy adult volunteers are usually hired and a non-compartmental analysis is conducted to assess the bioavailability and bioequivalence of drugs administered using child-appropriate dosage formulations (15).

One such initiative was taken by European commission to develop a child appropriate dosage formulation of enalapril for the treatment of CHF (16). A non-compartment analysis has been conducted to compare bioavailability and bioequivalence of enalapril administered using child-appropriate orodispersible mini-tablets (ODMT) with reference (Renitec®) tablet formulation (16). In addition, a model-dependent pharmacokinetic analysis has been conducted using least square minimization method of parameter estimation, which provided additional pharmacokinetics information including the same rate constant of absorption but an early appearance of enalapril from ODMT formulation compared to reference tablet formulation (8). Early drug absorption of active parent drugs from ODMTs may be useful in achieving an early pharmacodynamic response of some drugs especially those BCS Class I drugs which have a concentration-dependent pharmacodynamic response (17). However, for the inactive drugs like enalapril having a metabolite concentration-dependent pharmacodynamic response, the pharmacodynamic effect is expected to be dependent on the biotransformation rate and appearance time of metabolite in serum (18).

Therefore, the present analysis was conducted in which the data from the ODMT and reference formulation were pooled and the simultaneous semi-mechanistic population pharmacokinetic model was developed to predict the serum and urine concentrations and pharmacokinetics of the inactive prodrug enalapril. Simultaneously, the concentrations and pharmacokinetics of enalaprilat i.e., biotransformation of the prodrug from administered formulations to active metabolite and its disposition were predicted. The covariate effect of formulation on each population pharmacokinetic model estimated parameter was assessed. In addition to that, the data sets of each formulation were modeled separately and the estimated individual pharmacokinetic parameters of the drug and metabolite from the two formulations were statistically compared to account any pharmacokinetic differences.

The population pharmacokinetic modeling analysis was performed to obtain further deep evaluation and any differences in the pharmacokinetics of enalapril and bio-transformed active ACE inhibitor enalaprilat from the two formulations. This shall provide deeper insights regarding the expected pharmacodynamic effects of enalaprilat from the developed child appropriate ODMT formulation compared to the reference formulation.

METHOD

Study Design

The dataset for the simultaneous serum and urine population pharmacokinetic modeling analysis consisted of full time vs. serum and urine concentration profiles of enalapril and its active metabolite enalaprilat. The dataset was obtained from a two-phase, two treatment, crossover, phase I clinical trial, which was the part of LENA project (labeling of enalapril from neonate to adolescence, European Union Seventh Framework Program (FP7/2007-2013) under the grant agreement no 602295). The independent Ethics Committee of the University Hospitals KU Leuven approved the trial protocol and the study was conducted in accordance with the International Council on Harmonization (ICH) tripartite Guideline on Good Clinical Practices (19). The design of the clinical study has been publically outlined (16). In this study, 10 mg single extravascular dose of enalapril maleate was administered in two different periods to 24 healthy adult volunteers to compare the pharmacokinetics of drug and metabolite from the two formulations. Reference

treatment consisted of two 5 mg strength of enalapril maleate market authorized conventional tablet formulation (Renitec®) administered with 240 ml of water. The ODMTs consisted of 10 child appropriate mini-tablets of 1 mg strength administered simultaneously with 240 ml of water. Serum samples were collected at the time intervals of 0.17, 0.33, 0.5, 0.75, 1, 1.25, 1.5, 2, 2.5, 3, 3.5, 4, 4.5, 5, 6, 8, 10, 12, 24, 48 h after dose administration. Enalapril and enalaprilat urine samples were collected at the time intervals of, 0–2, 2–4, 4–8, 8–12, 12–24, 24–36, 36–48 h after the dose administration. The urine concentrations were converted into the cumulative amount of the drug and metabolite excreted in urine after each time interval. The data sets of drug and metabolite concentrations were merged into a single data set for a simultaneous population pharmacokinetic modeling analysis.

Information related to biometric covariates including age, weight, height, sex, and total body water was available to evaluate their relationship with model parameters (**Table 2**). The total body water parameter was estimated for male and female subjects by Equations 1 and 2 (20).

Total body water for male subjects was calculated by using Equation 1;

$$\textbf{Total}\ \text{body water}\ V\mathbf{d}\ (\mathbf{L}) = 0.3625 * \text{Body Weight}\ (\text{kg}) + 0.2239 * \text{Height}\ (\text{cm}) - 0.1387 * \text{Age}\ (\text{yr}) - 14.47 \quad (1)$$

Total body water for female subjects was calculated by using Equation 2;

$$\textbf{Total body water}\ V\mathbf{d}\ (\mathbf{L}) = 0.2363 * \text{Body Weight}\ (\text{kg}) + 0.1962 * \text{Height}\ (\text{cm}) - 0.0272 * \text{Age}\ (\text{yr}) - 10.26 \quad (2)$$

Bioanalysis of Serum and Urine Samples

For a reliable determination of unknown samples, 50-μL serum or 100-μL urine were necessary for the simultaneous determination of enalapril and enalaprilat. In-house solid-phase extraction protocols were applied to purify serum and urine samples before liquid chromatography coupled to tandem mass spectrometric analysis. While a simple protocol was sufficient for serum samples (MAX 96-well plate), the known high intra and inter-subject variability of urine samples could only be sufficiently controlled by a two-step cleaning approach applying WAX followed by MCX solid phase extraction. The eluates were evaporated to dryness under a gentle stream of nitrogen. The established protocols enabled process efficiencies of the urinary solid-phase extraction between 87.2 to 106.8% (enalapril) and 64.1 to 90.2% (enalaprilat) (put a reference from literature here/see below). The serum process efficiency ranged between 65 to 93% for enalapril and 95 to 119% for enalaprilat.

Chromatographic separation and detection for both biological matrices were performed on a modular Shimadzu HPLC 10 coupled with AB Sciex API 2000 mass spectrometer. The ion transitions were the mass-to-charge ratio (m/z) 377.3 to 234.2 m/z for enalapril, 349.3 to 206.1 m/z for enalaprilat, and 425.3 to 351.2 m/z for benazepril (IS). The data acquisition and processing were carried out with Analyst 1.5.1 (Applied Biosystems/MDS SCIEX, Concord, Canada) with IntelliQuan® as an integration algorithm without smoothing.

Concerning the determination in serum, the fully validated bioanalytical method was characterized by a small sample volume of 50-μL serum encompassing a calibration range from 0.195 to 200 ng/mL for enalapril and 0.180 to 188 ng/mL for enalaprilat. Obtained mean accuracy values ranged from 91.6 to 108.4% of the nominal concentrations for enalapril and from 88.0 to 106.4% for enalaprilat. The time-different intermediate precision for the drug substance enalapril varied between 5.0 and 9.5% across all concentration levels and was subsequently well within the guideline limits of ±15% (±20% at LLOQ). The same applies to enalaprilat (4.3 to 13.4%). The relative matrix effect (expressed as CV) in enalapril samples at a low concentration (0.39 ng/mL [enalapril] and 0.35 ng/mL [enalaprilat]) was 5.49% for enalapril and 12.56% for enalaprilat. At the ULOQ, a coefficient of variation of 1.87% for enalapril and 8.96% for enalaprilat was evaluated for all seven different human sources.

The calibration curves of the urine method were constructed in the range of 11.6–1,2000 ng/mL for enalapril and 8.8–9,000 ng/mL for enalaprilat. The mean relative error across all *four* quality control levels ranged from −2.0 to 4.3% for enalapril and from −0.7 to 1.8% for enalaprilat. Intra-run and inter-run precision were 2.4–6.1 and 3.9–7.9% for enalapril as well as 3.1–9.4% and 4.7–12.7% regarding enalaprilat. The obtained variation coefficient of the IS-normalized matrix effects was 4.04 and 8.97% for enalapril and enalaprilat at the lower limit of quantification. At the upper limit of quantification, the CV was determined as 1.22% for enalapril and 1.21% for enalaprilat.

All unknown samples were quantified using freshly prepared calibration curves by plotting the concentration ratio of enalapril/enalaprilat to IS against the peak area of enalapril/enalaprilat to IS. Enalapril and enalaprilat were obtained as European Pharmacopeia Reference Standard. Study samples measured below the LLOQ were not included in the population pharmacokinetic modeling analysis (21).

Population Pharmacokinetic Modeling Strategy

1) A simultaneous semi-mechanistic population pharmacokinetic model was developed to predict the pooled data of serum and urine concentrations of enalapril and its active metabolite enalaprilat representing the ODMTs and the reference formulations. Covariate analysis was conducted to test the effect of formulation on estimated model par ameters.
2) In addition to this, the data of ODMT and reference formulations were modeled separately and the individual model estimated pharmacokinetic parameters were statistically correlated to account any difference in the pharmacokinetics of drug and metabolite from the two formulations.

Population Pharmacokinetic Model Structure

Population pharmacokinetic model was developed using a non-linear mixed effect modeling software NONMEM version 7.4.0 (ICON, Development Solutions, Elliot City, MD, USA)

(22). The ADVAN 6 sub-routine was used to define the system of differential equations whereby each compartment was connected by constants of first-order rate transfer. The one and two-compartment models were tested for enalapril. The one, two and three-compartment models were tested to predict enalaprilat concentrations in the combined model. Selection of the appropriate model was based on visual inspection of the goodness of fit plots (23), successful convergence, acceptable relative standard error values, a significant drop in the objective function value and no boundary problems. Maximum likelihood approach using first-order conditional estimate with interaction (FOCE+I) was used for parameter estimation.

After the analysis of goodness of fit plots, objective function value, and the estimated relative standard errors, the one-compartment model disposition parameters were selected for the population pharmacokinetic modeling of enalapril. Previous studies have reported that around 60% of the total administered enalapril is absorbed from the gastrointestinal tract (24, 25). Therefore, the bioavailability (F1) parameter was estimated to account the total amount of drug absorbed in central circulation. As per our current knowledge in the literature (25), we assumed that the enalapril and enalaprilat are only eliminated through urine and the drug is only metabolized to enalaprilat, which is not further metabolized. The assumption is supported by the reported value of the total amount of dose recovered in urine as enalapril and enalaprilat which is equal to the total amount of drug absorbed from the gastrointestinal tract (11). As we have serum and urine data for the drug and metabolite, the system becomes quantifiable and F1 parameter becomes identifiable and was estimated in the model. The estimated value of F1 parameter was 60% and was in line to already published value of 60% of drug absorption given in the literature (24, 25). To predict the lower concentrations at the delayed absorption phase of enalapril, a lag time model and system of transit compartments were used and analyzed (26). Transit compartments were added in a stepwise approach using erlang distribution method where the optimum number of transit compartments were estimated by adding one transit at a time until there was no further drop in the objective function value of 3.8 or more was observed (27, 28). The mean transit time parameter (MTT1) was estimated and rate transfer through transit compartments was calculated using the expression MTT1 = N+1/KTR, where N is the optimal number of transit compartments and KTR is the rate transfer through these transits (27). The rate constant of absorption (KA) was the transfer rate of the drug from the last transit into enalapril central compartment. To account the renal and metabolic elimination pathways, the elimination of enalapril from serum was estimated using rate constants of enalapril elimination through urine (KREN) and eliminated through enalaprilat formation (KM). The volume of distribution of enalapril in the central circulation (VC) and highly perfused tissues was estimated.

The two-compartment model parameters estimated for the modeling of enalaprilat concentrations were rate constant of enalaprilat formation (KM), volume of distribution of enalaprilat in central circulation (VM), rate constants of intercompartmental distribution (KQ1 and KQ2), rate constant of elimination (KME) and mean transit time of enalaprilat formation (MTT2). Transit compartments were added using erlang distribution method to predict the lower concentrations enalaprilat formation phase. All the model parameters of enalapril and enalaprilat were identifiable. The blueprints of the combined model are given in **Figure 1**.

Between-subject variability of parameters was modeled using exponential error model described as Equation 3.

$$\boldsymbol{Pi} = TVp \ * \exp(\mathrm{ETA}i) \tag{3}$$

Where **Pi** was the individual parameter estimate, **TVp** was the typical mean estimated value of the parameter of the population and **ETAi** was the individual random effect for each parameter per individual. The distribution of ETA in population was assumed to be following a normal distribution with mean zero and variance equals omega square (29).

Combined additive plus proportional residual error was introduced separately for serum concentrations and separate proportional error was introduced for urine concentrations of enalapril and enalaprilat, respectively, to account unexplained variability between the observed and predicted concentrations. Residual variability was defined using Equations 4 and 5.

$$\boldsymbol{Ci} = Cp \ * (1 + \varepsilon i1) + \varepsilon i2 \tag{4}$$

$$\boldsymbol{Ci} = Cp \ * (1 + \varepsilon i1) \tag{5}$$

Where $\mathbf{C}_\mathrm{p}$ was the predicted concentrations, $\boldsymbol{\varepsilon}\mathbf{i}$ represented the distribution of residuals between enalapril observed and model-predicted concentrations added by both proportional $\boldsymbol{\varepsilon}\mathbf{i1}$ and additive terms $\boldsymbol{\varepsilon}\mathbf{i2}$. The distribution of residual variability was assumed to be normally distributed with mean zero and variance sigma squared.

Covariate Modeling Analysis

To build a full population pharmacokinetic model, a stepwise approach was used to evaluate the effect of estimated parameters on biometric covariates. The effect of normalized body weight added on the parameter estimates was evaluated using Equation 6 (30).

$$\boldsymbol{TV} = \theta_{TV} * \left(\frac{WT_{ind}}{WT_{ref}}\right)^{\theta} \tag{6}$$

Where **TV** indicates the typical population value of the model estimates, $\boldsymbol{\theta}_\mathrm{TV}$ indicates the typical value of the model estimates for an individual; $\mathbf{WT}_\mathrm{ind}$ indicates body weight of individual subject and $\mathbf{WT}_\mathrm{ref}$ indicates weight normalized by the mean body weight of the present study. The parameter $\boldsymbol{\theta}$ was tested with a fixed value of 1 for the volume of distribution and 0.75 for clearance. The inclusion of covariate was subjected to a significant drop in the objective function of more than 3.8.

For the pooled data analysis, the exponential relationship was incorporated using Equation 7 to evaluate the covariate effect of formulation on all model-estimated parameters.

$$\boldsymbol{TV} = \theta X * \theta 12^{FORM} * \exp^{\eta} \tag{7}$$

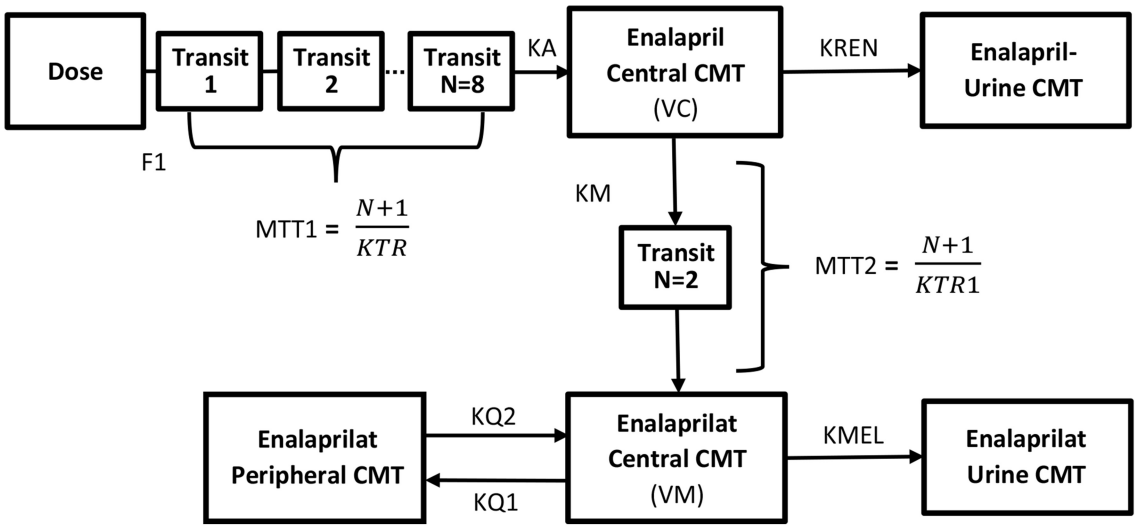

FIGURE 1 | Blueprints of the semi-mechanistic population pharmacokinetic model of enalapril and enalaprilat in serum and urine after the administration of 10 mg of enalapril maleate using reference and ODMT formulations. The system of transit compartments with drug passing through by rate constant **(KTR)** was used to describe the absorption phase of enalapril, whereas the parameter **(F1)** subtracted the amount of drug metabolized pre-systemically in the gastrointestinal tract. The parameter **(KA)** describes the rate constant of absorption of the enalapril into the central compartment and instantaneously distribute to highly perfused tissues with a volume of distribution equals **(VC)**. The biphasic elimination of the drug i.e., bio-transformed to enalaprilat and eliminated via urine is described by the parameters **(KM)** and **(KREN)** from the central compartment. The formed metabolite transits through the delay compartments by mean residence time **(MTT2)** into the central compartment and distributing in the central **(VM)** and to the peripheral compartments **(KQ1 and KQ2)**. The elimination of enalaprilat takes place through the urine compartment **(KMEL)**.

Where TV represents typical population value of model parameters, θ_X represents the mean population value of the model parameters, θ_{12} represents a fixed effect parameter to give a proportional increase or decrease in parameter value with ODMT (FORM = 1) or reference formulation (FORM = 0), and η represents interindividual variability.

Model Evaluation

The goodness of fit plots were used for the evaluation of model performance. For the evaluation of individual *post-hoc* estimation with FOCE+I method of parameter estimation method, conditional weighted residuals were estimated and visual plots given in **Figure 2** were analyzed. Visual predictive check (VPC) plots and the non-parametric bootstrap method were used for model validation. For VPC plots, the final model was used to perform 1000 Monte Carlo simulations (31). The precision of the estimated model parameters was evaluated using a non-parametric bootstrap method using Perl-speaks-NONMEM (PsN) (32) by calculating the confidence interval (CI) of the estimated model parameters. The subjects of the original dataset were randomly resampled to create 200 datasets and the new dataset was modeled using the final model. From the bootstrap analysis, the 2.5th, 50th, and 97.5th percentiles were simulated. **Table 1** summarizes the results of the bootstrap analysis with 95th percent CI values of each parameter.

Due to the long run time of model, a faster than bootstrap method i.e., Sampling importance-resampling (SIR) method was also used to evaluate parameter uncertainty. SIR was performed by running 20,000 final samples and a resample size of 2,000. From SIR method, 95th, CI values were estimated for parameter uncertainty test (33, 34).

For the evaluation of the stability of estimated parameters of the model, initial fixed and random effect parameter values were changed stepwise by 10 percent and the population-estimated parameters along with the objective function value were assessed for any change.

Correlation of Reference and Child Appropriate Dosage Forms

The covariate effect of formulation on estimated model parameters of the pooled data was assessed using Equation 7. In addition to this, the estimated individual pharmacokinetic parameters of enalapril and enalaprilat of each subject administered ODMTs and reference formulations in two-phase crossover trial were statistically correlated using a paired sample Wilcoxon rank test using an R program with a significant level of $p < 0.05$. The rate constants of enalapril and enalaprilat renal elimination were converted to their respective clearance values to correlate the clearances of drug and metabolite following the administration of both formulations.

RESULTS

The dataset of enalapril and the active metabolite enalaprilat consisted of 24 healthy subjects with 2,208 serum and urine

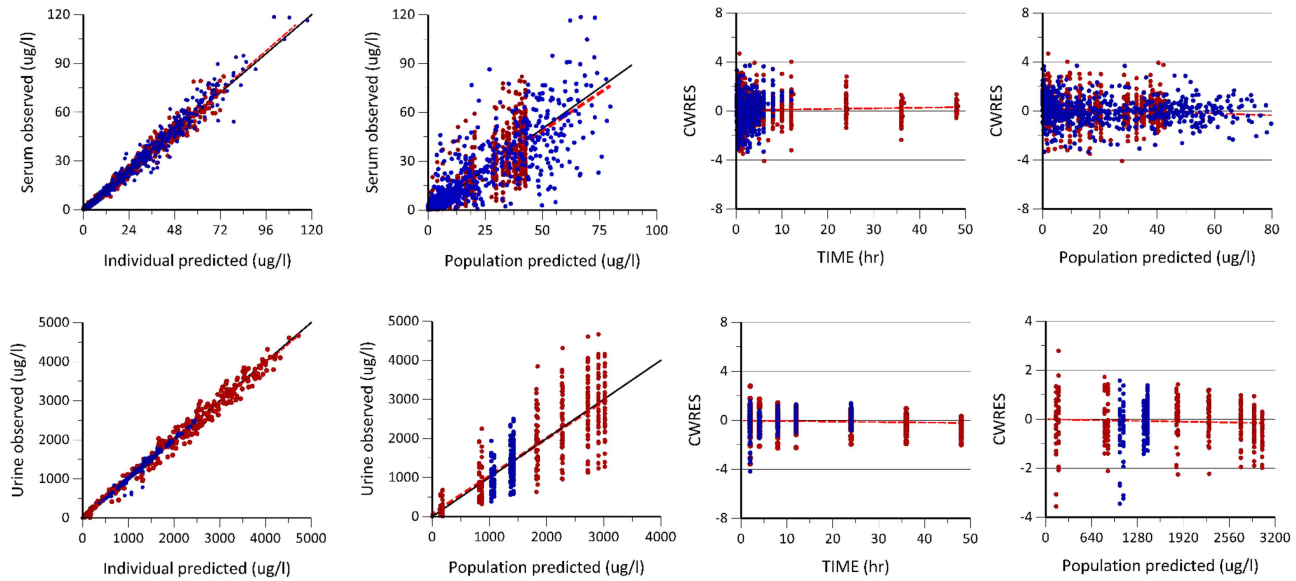

FIGURE 2 | Goodness of fit plots including the observed vs. individual and population predicted plots, conditional weighted residuals (CWRES) vs. population predicted (PRED) and time plots of enalapril and enalaprilat in serum and urine generated after the population pharmacokinetic modeling of pooled data of two formulations. The first row shows the predictive performance of the model for enalapril and enalaprilat in serum. The second row shows the predictive performance of enalapril and enalaprilat in urine, respectively. The blue dots represent enalapril concentrations, whereas the red dots represent the enalaprilat concentrations in serum and urine, respectively.

concentrations. Patients' demographics are summarized in **Table 2**. After the extravascular administration, the C_{max} of enalapril was achieved in almost 1 h and time vs. serum concentration of enalapril showed a mono-exponential decay. The drug is eliminated in almost 10 h from the serum. Biotransformed enalaprilat achieved C_{max} in around 3 to 4 h and showed a bi-phasic exponential decay.

Model Evaluation Results

The **Table 1** summarizes the final population pharmacokinetic model parameter estimates, relative standard errors (RES), SIR and 95th% Bootstrap confidence interval values of the pooled data of the two formulations. For the formulations modeled separately, the typical population and diagnostic parameters along with diagnostic plots are given in **Supplementary Material**. The RES, SIR, and bootstrap confidence intervals for all parameters were narrow and had the same median values as estimated by the model. This shows that parameters were precisely estimated. The goodness of fit plots given in **Figure 2** shows that the model performed well in predicting the serum and urine concentrations of enalapril and enalaprilat. Eta shrinkage values for most of the parameters were lower than 20 percent and hence the individual model predicted concentration vs. the observed serum and urine concentration plots of enalapril and enalaprilat given in **Figure 2** were informative and showed agreement between the observed and predicted concentrations (35). The VPC plots given in **Figure 3** showed no model misspecification and almost all of the serum and urine observed concentrations were within the prediction intervals.

Visual inspection of the time vs. enalapril concentration plot showed a mono-exponential phase of elimination and did not have sufficient data for the estimation of the peripheral volume of distribution. The selected one compartment model adequately predicted the time vs. enalapril serum concentrations. The two-compartment model resulted in a significant drop in the objective function but at the expense of higher relative standard errors of the estimated parameters. An optimum number of transit compartments were added using erlang distribution method to account the absorption phase of enalapril. Eight transits (transits = 8) were added for reference and pooled data analysis and 6 transits were added for the ODMT formulation (transits = 6). The absorption phase of enalapril was not adequately predicted with or without incorporating a LAG time model. The introduction of transit compartments resulted in a significant drop in the objective function compared to the lag time model. The bioavailability parameter (F1) accounted for the percent of drug absorbed while subtracting it from the drug eliminated by pre-systemic metabolism. The enalapril population mean parameter estimates along with their relative standard errors are given in **Table 1**.

The biphasic enalaprilat time vs. serum concentration profile was predicted using the two-compartment model. The one compartment model was not able to predict the second longer phase of elimination. The two-compartment model also resulted in a significant drop in the objective function value compared to the one compartment model. A lag time parameter was not able to predict the lower concentrations at the skewed formation phase of enalaprilat; therefore, two-transit compartments were added using erlang distribution method to incorporate a delay

TABLE 1 | Enalapril and enalaprilat estimated population pharmacokinetic parameters with percent relative standard errors (RES), sampling importance resampling (SIR) and bootstrap confidence interval (CI) values estimated for pooled data analysis.

Parameters	Population estimates (% RSE)	SIR 95th% CI	Bootstrap 95th% CI
	FINAL (FULL) MODEL	**FINAL MODEL**	**FINAL MODEL**
BASIC PHARMACOKINETIC MODEL PARAMETERS			
KA (1/h)	6.010 (15.0%)	4.780–7.859	4.640–8.200
VC (L)	51.10 (4.00%)	47.92–54.34	47.38–55.09
F1	0.606 (3.00%)	0.580–0.640	0.570–0.646
MTT1 (h)	0.558 (9.00%)	0.480– 0.640	0.466–0.648
KREN (1/h)	0.305 (4.00%)	0.290–0.320	0.286–0.330
KM (1/h)	0.688 (4.00%)	0.640–0.740	0.647–0.725
VM (L)	46.10 (4.00%)	42.80–49.55	42.21–49.79
KQ1 (1/h)	0.060 (4.00%)	0.056–0.064	0.056–0.064
KQ2 (1/h)	0.054 (10.0%)	0.046–0.063	0.048–0.620
KME (1/h)	0.184 (4.00%)	0.171–0.196	0.171–0.197
MTT2 (h)	0.910 (8.00%)	0.800–1.044	0.802–1.080
THETA (X)	0.730 (12.0%)		
INTERINDIVIDUAL VARIABILITY (IIV)			
IIV_KA	0.688 (31.0%)	0.474–1.132	0.362–1.005
IIV_VC	0.058 (24.0%)	0.041–0.086	0.039–0.080
IIV_F1	0.041 (22.0%)	0.030–0.060	0.023–0.067
IIV_MTT1	0.151 (22.0%)	0.114–0.220	0.097–0.192
IIV_KREN	0.058 (24.0%)	0.042–0.084	0.038–0.074
IIV_KM	0.078 (22.0%)	0.058–0.112	0.050–1.101
IIV_VM	0.069 (23.0%)	0.050–0.102	0.033–0.105
IIV_KME	0.063 (23.0%)	0.047–0.092	0.039–0.086
IIV_ MTT2	0.296 (22.0%)	0.221–0.430	0.196–0.384
RESIDUAL UNEXPLAINED VARIABILITY (RUV)			
Serum Enalapril			
Proportional error (σ2)	0.010 (8.00%)	0.008–0.011	0.006–0.013
Additive error (μg/l)	0.188 (15.0%)	0.150–0.240	0.132–0.294
Serum Enalaprilat			
Proportional error (σ2)	0.018 (9.00%)	0.015–0.020	0.010–0.026
Additive error (μg/l)	0.220 (13.0%)	0.180–0.277	0.144–0.301
Urine Enalapril			
Proportional error (σ2)	0.019 (9.00%)	0.016–0.021	0.009–0.028
Urine Enalaprilat			
Proportional error (σ2)	0.005 (11.0%)	0.004–0.006	0.002–0.009

***KA**, rate constant of enalapril absorption; **VC**, Volume of distribution of enalapril in central compartment; **F1**, bioavailability of enalapril after extravascular administration; **MTT1**, delay time for enalapril to appear in serum; **KREN**, Rate constant of enalapril elimination in urine; **KM**, rate constant of metabolite formation; **KQ1**, Rate constant of enalaprilat distribution from central to peripheral compartment; **KQ2**, Rate constant of enalaprilat distribution from peripheral to central compartment; **KME**, rate constant of enalaprilat elimination in urine; **VM**, Volume of distribution of enalaprilat in urine; **MTT2**, delay time for enalaprilat to appear in serum.*

TABLE 2 | Summary of biometric covariate values used in population pharmacokinetic analysis.

Biometric covariate	Mean	Median	Minimum	Maximum
AGE (yrs.)	28.00	24.40	22.08	47.16
Weight (kg)	69.76	67.60	51.80	95.60
Height (cm)	174.5	176.0	153.0	189.0
Body water (L)	42.06	41.31	32.86	53.70

in metabolite formation. First order rate of enalapril and enalaprilat elimination was adequate to predict the cumulative amount of drug and metabolite excreted in the urine. The structure explained in **Figure 1** constituted the serum and urine simultaneous semi-mechanistic population pharmacokinetics of enalapril and enalaprilat. Structural population parameters and random variability values have been summarized in **Table 1**. The fixed effect parameters and the random variance was precisely estimated along-with the eta-shrinkage values, lower than 25%.

The forward addition of potential covariate i.e., weight normalized on the volume of distribution of enalapril resulted in a significant drop of the objective function value by 18.2, similarly, the addition of formulation effect on mean transit time (MTT1) of enalapril further resulted in a significant drop of the objective function by 6.51. The weight normalized on the volume of distribution was tested using the backward elimination method and resulted in a significant increase in the objective function value. Therefore, both covariates were retained in the final population model.

As like the base model, the relative standard error values of the fixed and random effect parameters of the final covariate model showed a precise estimation of the parameters. The change in the typical population and random variability of the parameters of the base and full covariate models were <25 percent and show that the covariates are clinically unimportant (35).

Pharmacokinetics Comparison of ODMT and Reference Formulation

The pooled data analysis revealed that the formulation had a covariate effect on the mean transit time of enalapril absorption. Similarly, the results of the paired samples Wilcoxon rank test given in **Table 3** showed a significant difference between the mean transits times of enalapril (MTT1) when the drug was absorbed from ODMT compared to conventional tablets. The typical population mean value of MTT1 showed that the drug was absorbed around 5 min earlier from ODMT compared to the reference formulation. No other pharmacokinetic differences in the comparison of the two formulations were observed. The statistical comparison showed that the two formulations are relatively bioavailable. The pharmacokinetic comparison showed that the drug and metabolite had a similar volume of distribution and clearance from the body.

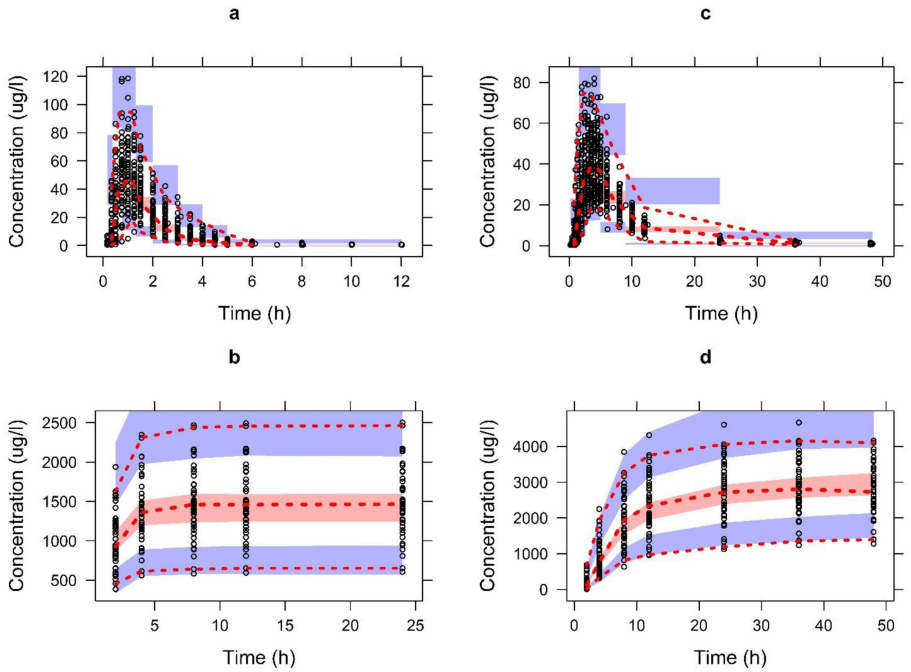

FIGURE 3 | The visual predictive check plots for the final model of enalapril in serum **(A)** and urine **(B)** and enalaprilat in serum **(C)** and urine **(D)** validating the model performance to describe the pooled observed data. Open circles represent the pooled observed data of drug and metabolite. The red dashed line represents the 2.5th, 50th, and 97.5th percentiles of the pooled observed data. The shaded areas represent the 95% CI of the 2.5th, 50th, and 97.5th percentiles of predictions.

DISCUSSION

A Validated simultaneous semi-mechanistic population pharmacokinetic model adequately predicted the full profiles of serum and urine concentrations of enalapril and enalaprilat. A covariate analysis on population pharmacokinetic model parameters of pooled data showed the effect of formulation on the estimated mean transit time of enalapril absorption from the two formulations. In addition to the pooled data analysis, the statistical comparison of individual pharmacokinetic model parameters estimated separately for ODMTs and reference formulation data revealed that enalapril administered using ODMTs absorbed 5 min earlier than the reference tablet formulation. However, no difference in the rate and onset of the formation and disposition of the active ACE-I enalaprilat was noticed. Therefore, no differences in the pharmacodynamic effects are expected from ODMTs compared to the reference formulation.

Selection of the final model was based on the successful convergence with no boundaries, goodness of fit plots, acceptable relative standard errors, and a significant drop in objective function value. Visual predictive check plots (31), bootstrap analysis (32), SIR procedure (34) validated the model. The calculated relative standard errors showed that the model parameters were estimated with acceptable precision.

The model informed pharmacokinetic estimates given in **Table 1** were in line to the already published value and showed that the population pharmacokinetic model estimated reliable pharmacokinetic parameters. For instance, the estimated fraction of enalapril absorbed was 60% and was in line with the literature value of 60% (24, 25). Similarly, the estimated values of the rate constant of absorption and delay in the appearance of enalapril in serum were 6.03 1/h and 0.56 h and were in line to the respective reported value of 6.4–12 1/h and 0.5 h (36). The value of the total rate constant of enalapril elimination through renal and metabolic route was estimated to be 0.93 1/h and was in line to the reported value of 0.94 1/h (36). The value of the rate constant of metabolite formation (KM) estimated using transit compartment model was 0.69 1/h and was in line to the reported value of 0.9 1/h estimated using the LAG time model (7). The estimated value of the rate constant of enalaprilat elimination was 0.175 1/h and was in line to the reported value of 0.14 1/h (36).

Semi-mechanistic population pharmacokinetic models have been reported in the literature to predict plasma and urine concentrations of drug and metabolite (37). A simultaneous enalapril and enalaprilat population pharmacokinetic model has not been reported in the literature. Based on the goodness of fit plots, objective function, and precision of parameters the selected one-compartment model was adequate to predict enalapril concentrations and has already been reported in the literature (8, 36). The two-compartment model used for enalapril estimated high standard errors of one or more parameters with no improvement in the goodness of fit plots and therefore was rejected (29). The one compartment model using the first order of absorption without accounting a delay in absorption did not account the absorption phase of enalapril. The LAG time model

TABLE 3 | Result of the two-sided paired Wilcoxon rank sum test to compare pharmacokinetic parameters of enalapril and enalaprilat in serum and urine after the administration of enalapril using ODMT and reference formulation.

P-value	ODMT vs. Reference formulation
KA (1/h)	0.87
VC (L)	0.85
F1	0.19
CLREN (L/h)	0.19
MTT1 (h)	0.03
KM (1/h)	0.70
VM (L)	0.13
MTT2 (h)	0.26
CLENT (L/h)	0.22

***KA**, rate constant of enalapril absorption; **VC**, Volume of distribution of enalapril in central compartment; **F1**, bioavailability of enalapril after extravascular administration; **CLREN**, Clarence of enalapril in urine; **MTT1**, delay time for enalapril to appear in serum; **KM**, rate constant of enalaprilat formation; **VM**, Volume of distribution of enalaprilat in central compartment; **MTT2**, delay time for enalaprilat to appear in serum; **CLENT**, Clarence of enalaprilat in urine.*

used to incorporate a delay in absorption did not predict the lower concentrations. A system of transit compartments was used to account the lower concentrations of the absorption phases of enalapril. The use of transit compartments also resulted in a significant drop in the objective function compared to the LAG time model. The transit compartments were added sequentially and have been used in literature to account the absorption phase of drugs (28, 38).

The selected two-compartment model for enalaprilat significantly dropped the objective function as compared to the one compartment model. The one compartment model was also not able to predict the bi-exponential elimination phase of the metabolite. The two-compartment population pharmacokinetic model with proportional residual error model has been reported in the literature to model enalaprilat concentrations, however, a combined additive plus proportional residual error model significantly dropped the objective function and was used in our final base model (7). A three-compartment model was also tested but resulted in higher standard errors with no significant change in the objective function and was rejected.

The covariate analysis of the pooled data of the two formulations found that formulations have a covariate effect on the mean transit time of enalapril in serum. The pairwise statistical comparison of model parameters estimated separately for ODMT and reference formulation data also showed a difference in mean transit time of enalapril absorption from the two formulations. Comparison of the absolute values of the mean transit time of absorption showed around 5 min early appearance of enalapril in serum from ODMTs compared to the reference formulation. The early appearance of enalapril may be due to the higher surface area of ODMTs provided for fast dissolution and disintegration rates of the developed tablets compared to the reference tablet formulation. The absorption and plasma concentration profile of an orally administered drug also depends on its transit time and absorbability in the gastrointestinal tract (39). The drug from the small-sized disintegrated and dissolved ODMTs are expected to be emptied earlier from the stomach to reach rapidly at the site of absorption in the intestine (40). This may lead to the early availability of the drug for absorption. Enalapril is a BCS class III drug and follows a permeability-limited absorption from the intestine. Therefore, an early appearance of the drug had no effect on the rate constant of enalapril absorption.

The difference in the model informed transit time of enalapril in the gastrointestinal tract and different excipients of the reference and ODMT formulations had no effect on intestinal permeation i.e., rate constant of absorption of the drug. These results support the biowaivers given by the FDA to BCS class III drugs whereby the excipients should not have an effect on bioavailability and drug permeability (41, 42). No other differences in the physiological parameters like the volume of distribution and elimination were observed for enalapril. The implication of early appearance of the drug from ODMTs can be useful for classes of drugs like analgesics or in case of an emergency clinical situation such as a hypertensive crisis or an angina attack. For instance, fast disintegrating and dissolving small sized ODMT formulation of nitroglycerin if develop requires less saliva and can be more beneficial to deliver drug sublingually for achieving early antianginal effect compared to sublingual dosage forms which require more saliva and higher disintegration time to release the drug (43). Use of ODMTs may have earlier pharmacodynamic effects, especially for the orally administered BCS class I drugs having higher solubility and permeability. However, in our case, the pro-drug enalapril is inactive and its early appearance will have no expected clinical significance because the pharmacodynamic response will depend on the pharmacokinetics of enalaprilat.

The developed population pharmacokinetic model also informed that the early appearance of drug in the serum had no effect on the onset and rate of enalaprilat biotransformation. This may be due to the same rate constant of absorption and extent of absorption of enalapril from the two formulations. In addition, the uptake of the drug from the systemic circulation into the liver by organic anion-transporting polypeptide (OATP1B1) transporters (44) and the basolateral efflux of the bio-transformed enalaprilat back into the systemic circulation by multidrug resistance-associated protein (MRP4) transporters follows a permeability-limited transport (45). The volume of distribution and clearance of enalaprilat also showed no difference between the two formulations. Due to similar enalaprilat pharmacokinetics, a similar pharmacodynamic response can be expected from the reference and ODMT formulation.

Typically a non-compartmental analysis is conducted to compare the pharmacokinetic parameters of drug including area under the curve, maximum concentration in biological fluid, and time to get the maximum concentration in biological fluid from reference and developed formulations. However, the population pharmacokinetic modeling analysis has provided deeper insights relating to the onset of absorption and metabolism. The model can further be used to perform simulations in order to predict the serum

concentrations of enalapril and enalaprilat at different dose and dosing frequencies.

CONCLUSION

The semi mechanistic population pharmacokinetic model predicted the detailed pharmacokinetics of enalapril and enalaprilat in serum and urine. The model informs that enalapril is absorbed 5 min earlier when administered using ODMT compared to the reference formulation. The model also informed no difference in the pharmacokinetics of enalaprilat bio-transformed from the administered parent drug formulations. This may lead to a similar pharmacodynamic response from ODMTs and reference formulations.

DATA AVAILABILITY

The datasets for this study will not be made publicly available because, the dataset is currently being used for further analysis and hence cannot be shared.

ETHICS STATEMENT

Approval for the trial protocol was given by the independent Ethics Committee of the University Hospitals KU Leuven and the study was conducted in accordance with the international Council on Harmonization (ICH) Tripartite Guideline on Good Clinical Practice.

AUTHOR CONTRIBUTIONS

MF, WC, and SL contributed to the idea. MF and WC develop the overall population pharmacokinetic model. MF performed population pharmacokinetic modeling analysis. BB performed bioanalysis of plasma and urine samples. MF, BB, and WC contributed to the drafting of the manuscript. WC, SL, and JdH critically checked the manuscript. All authors agreed on the contents of this manuscript.

FUNDING

The research work was a part of project LENA which is funded by a European Union Seventh Framework Program (FP7/2007-2013) under the grant agreement no 602295. The research work was also supported by a scholarship from the Higher Education Commission (HEC), Pakistan in collaboration with the German Academic Exchange Program (DAAD), Germany.

ACKNOWLEDGMENTS

We thank our colleagues from LENA consortium for conducting the bioavailability study including Dr. Anne van Hecken, Marissa Herbort, from Centre for Clinical Pharmacology, Catholic University Leuven, Belgium; Prof. Dr. Jörg Breitkreutz, Dr. Wolfgang Wiedey, from Ethicare GmbH, Germany; Dr. Ingrid Klingmann and Lucie Spatenkova, from Pharmaplex bvba, Belgium; Dr. Florian Lagler and Dr. Angelika Moder from Medizinische Privatuniversität (PMU) Salzburg, Austria and Dr. Feras Khalil, Heinrich-Heine University Düsseldorf, Germany.

SUPPLEMENTARY MATERIAL

The Supplementary Material for this article can be found online at: https://www.frontiersin.org/articles/10.3389/fped.2019.00281/full#supplementary-material

REFERENCES

1. Ponikowski P, Voors AA, Anker SD, Bueno H, Cleland JGF, Coats AJS, et al. 2016 ESC Guidelines for the diagnosis and treatment of acute and chronic heart failure. *Ear Heart J*. (2016) 37:2129–200. doi: 10.1093/eurheartj/ehw128
2. Hsu DT, Pearson GD. Heart failure in children part I: history, etiology, and pathophysiology. *Circ Hear Fail*. (2009) 2:63–70. doi: 10.1161/CIRCHEARTFAILURE.108.820217
3. Brion F, Nunn A, Rieutord A. Extemporaneous (magistral) preparation of oral medicines for children in European hospitals. *Acta Paediatr*. (2007) 92:486–90. doi: 10.1111/j.1651-2227.2003.tb00583.x
4. Lopez FL, Ernest TB, Tuleu C, Gul MO. Formulation approaches to pediatric oral drug delivery: benefits and limitations of current platforms. *Expert Opin Drug Deliv*. (2015) 12:1727–40. doi: 10.1517/17425247.2015.1060218
5. Rossano JW, Shaddy RE. Heart failure in children: etiology and treatment. *J Pediatr*. (2014) 165:228–33. doi: 10.1016/j.jpeds.2014.04.055
6. Ivanovska V, Rademaker CMA, van Dijk L, Mantel-Teeuwisse AK. Pediatric drug formulations: a review of challenges and progress. *Pediatrics*. (2014) 134:361–72. doi: 10.1542/peds.2013-3225
7. Kechagia IA, Kalantzi L, Dokoumetzidis A. Extrapolation of enalapril efficacy from adults to children using pharmacokinetic/pharmacodynamic modelling. *J Pharm Pharmacol*. (2015) 67:1537–45. doi: 10.1111/jphp.12471
8. Faisal M, Cawello W, Laer S. Model-dependent pharmacokinetic analysis of enalapril administered to healthy adult volunteers using orodispersible minitablets for use in pediatrics. *Drug Des Devel Ther*. (2019) 13:481–90. doi: 10.2147/DDDT.S188417
9. Casey Laizure S, Herring V, Hu Z, Witbrodt K, Parker RB. The role of human carboxylesterases in drug metabolism: have we overlooked their importance? *Pharmacotherapy*. (2013) 33:210–22. doi: 10.1002/phar.1194
10. Na K, Lee EY, Lee HJ, Kim KY, Lee H, Jeong SK, et al. Human plasma carboxylesterase 1, a novel serologic biomarker candidate for hepatocellular carcinoma. *Proteomics*. (2009) 9:3989–99. doi: 10.1002/pmic.200900105
11. Kubo SH, Cody RJ. Clinical pharmacokinetics of the angiotensin converting enzyme inhibitors. A review. *Clin Pharmacokinet*. (1985) 10:377–91. doi: 10.2165/00003088-198510050-00001
12. Fernandez E, Perez R, Hernandez A, Tejada P, Arteta M, Ramos JT. Factors and mechanisms for pharmacokinetic differences between pediatrie population and adults. *Pharmaceutics*. (2011) 3:53–72. doi: 10.3390/pharmaceutics3010053
13. Kearns GL, Abdel-Rahman SM, Alander SW, Blowey DL, Leeder JS, Kauffman RE. Developmental pharmacology - drug disposition, action, and therapy in infants and children. *N Eng J Med*. (2003) 349:1157–67. doi: 10.1056/NEJMra035092
14. Beggs S, Thompson A, Nash R, Tompson A, Peterson G. *17th Expert Committee on the Selection and Use of Essential Medicines Geneva. Cardiac Failure in Children*. (2009). Available online at: https://www.who.int/selection_medicines/committees/expert/17/application/paediatric/Paed_Cardiac_Failure_Review.pdf (accessed January 11, 2019).

15. Purohit VS. Biopharmaceutic planning in pediatric drug development. *AAPS J*. (2012) 14:519–22. doi: 10.1208/s12248-012-9364-3
16. ClinicalTrials.gov. *Ethicare GmbH: National Library of Medicine* (US). 30/9/2014. *Identifier NCT02252692, Relative Bioavailability Study With Enalapril in Healthy Volunteers*). Available online at: https://clinicaltrials.gov/ct2/show/NCT02252692?spons$=$Ethicare&rank$=$4 (accessed September 30, 2014).
17. Portolés A, Puerro M, Terleira A, Rodríguez A, Caturla MC, Fernández N, et al. A new high-absorption-rate paracetamol 500-mg formulation: a comparative bioavailability study in healthy volunteers. *Curr Ther Res*. (2003) 64:401–11. doi: 10.1016/S0011-393X(03)00110-3
18. Ing Lorenzini K, Daali Y, Dayer P, Desmeules J. Pharmacokinetic-pharmacodynamic modelling of opioids in healthy human volunteers. A minireview. *Basic Clin Pharmacol Toxicol*. (2012) 110:219–26. doi: 10.1111/j.1742-7843.2011.00814.x
19. *HEALTH.2013.4.2-1 -Investigator-Driven Clinical Trials for Off-Patent Medicines Using Innovative, Age-Appropriate Formulations and/or Delivery Systems*. Available online at: https://cordis.europa.eu/programme/rcn/18549_en.html (accessed August 13, 2018).
20. May TW, Brandt C, Helmer R, Bien CG, Cawello W. Comparison of lacosamide concentrations in cerebrospinal fluid and serum in patients with epilepsy. *Epilepsia*. (2015) 56:1134–40. doi: 10.1111/epi.13022
21. Burckhardt BB, Tins J, Ramusavic S, Laer S. Tailored assay for pharmacokinetic and pharmacodynamic investigations of Aliskiren and enalaprilin children: an application in serum, uirne and saliva. *J pediatr Pharmacol Ther*. (2015) 20:431–52. doi: 10.5863/1551-6776-20.6.431
22. Sheiner LB, Beal SL. Evaluation of methods for estimating population pharmacokinetic parameters. III. Monoexponential model: routine clinical pharmacokinetic data. *J Pharmacokinet Biopharm*. (1983) 11:303–19. doi: 10.1007/BF01061870
23. Nguyen THT, Mouksassi MS, Holford N, Al-Huniti N, Freedman I, Hooker AC, et al. Model evaluation of continuous data pharmacometric models: metrics and graphics. *CPT Pharmacometrics Syst Pharmacol*. (2017) 6:87–109. doi: 10.1002/psp4.12161
24. Ajayi AA, Hockings N, Reid JL. Age and the pharmacodynamics of angiotensin converting enzyme inhibitors enalapril and enalaprilat. *Br J Clin Pharmacol*. (1986) 21:349–57. doi: 10.1111/j.1365-2125.1986.tb05206.x
25. Ulm E, Hichens M, Gomez H, Till A, Hand E, Vassil T, et al. Enalapril maleate and a lysine analogue (MK-521): disposition in man. *Br J Clin Pharmacol*. (1982) 14:357–62. doi: 10.1111/j.1365-2125.1982.tb01991.x
26. Koch G, Krzyzanski W, Pérez-Ruixo JJ, Schropp J. Modeling of delays in PKPD: classical approaches and a tutorial for delay differential equations. *J Pharmacokinet Pharmacodyn*. (2014) 41:291–318. doi: 10.1007/s10928-014-9368-y
27. Vanobberghen F, Penny MA, Duthaler U, Odermatt P, Sayasone S, Keiser J, et al. Population pharmacokinetic modeling of tribendimidine metabolites in Opisthorchis viverrini-infected adults. *Antimicrob Agents Chemother*. (2016) 60:5695–704. doi: 10.1128/AAC.00655-16
28. Lindauer A, Siepmann T, Oertel R, Jung A, Ziemssen T, Jaehde U, et al. Pharmacokinetic/pharmacodynamic modelling of venlafaxine: pupillary light reflex as a test system for noradrenergic effects. *Clin Pharmacokinet*. (2008) 47:721–31. doi: 10.2165/00003088-200847110-00003
29. Owen JS, Fiedler-kelly J. *Mixed Effects Models Introduction to Population*. Hoboken, NJ: John Wiley & Sons, Inc.
30. Choi HY, Choi S, Kim YH, Lim HS. Population pharmacokinetic and pharmacodynamic modeling analysis of GCC-4401C, a novel direct factor xa inhibitor, in healthy volunteers. *CPT Pharmacometrics Syst Pharmacol*. (2016) 5:532–43. doi: 10.1002/psp4.12103
31. Bergstrand M, Hooker AC, Wallin JE, Karlsson MO. Prediction-corrected visual predictive checks for diagnosing nonlinear mixed-effects models. *AAPS J*. (2011) 13:143–51. doi: 10.1208/s12248-011-9255-z
32. Lindbom L, Pihlgren P, Jonsson N. PsN-Toolkit - a collection of computer intensive statistical methods for non-linear mixed effect modeling using NONMEM. *Comput Methods Programs Biomed*. (2005) 79:241–57. doi: 10.1016/j.cmpb.2005.04.005
33. Ashraf MW, Peltoniemi MA, Olkkola KT, Neuvonen PJ, Saari TI. Semimechanistic population pharmacokinetic model to predict the drug-drug interaction between s-ketamine and ticlopidine in healthy human volunteers. *CPT Pharmacometrics Syst Pharmacol*. (2018) 7:687–97. doi: 10.1002/psp4.12346
34. Dosne AG, Bergstrand M, Karlsson MO. An automated sampling importance resampling procedure for estimating parameter uncertainty. *J Pharmacokinet Pharmacodyn*. (2017) 44:509–20. doi: 10.1007/s10928-017-9542-0
35. Knebel W, Tammara B, Udata C, Comer G, Gastonguay MR, Meng X. Population pharmacokinetic modeling of pantoprazole in pediatric patients from birth to 16 years. *J Clin Pharmacol*. (2011) 51:333–45. doi: 10.1177/0091270010366146
36. Weisser K, Schloos J, Lehmann K, Düsing R, Vetter H, Mutschler E. Pharmacokinetics and converting enzyme inhibition after morning and evening administration of oral enalapril to healthy subjects. *Ear J Clin Pharmacol*. (1991) 40:95–9. doi: 10.1007/BF00315146
37. Abduljalil K, Frank D, Gaedigk A, Klaassen T, Tomalik-Scharte D, Jetter A, et al. Assessment of activity levels for CYP2D6*1, CYP2D6*2, and CYP2D6*41 genes by population pharmacokinetics of dextromethorphan. *Clin Pharmacol Ther*. (2010) 88:643–51. doi: 10.1038/clpt.2010.137
38. Savic RM, Jonker DM, Kerbusch T, Karlsson MO. Implementation of a transit compartment model for describing drug absorption in pharmacokinetic studies. *J Pharmacokinet Pharmacodyn*. (2007) 34:711–26. doi: 10.1007/s10928-007-9066-0
39. Kimura T, Higaki K. Gastrointestinal transit and drug absorption. *Biol Pharm Bull*. (2002) 25:149–64. doi: 10.1248/bpb.25.149
40. Centre M. Transit of pharmaceutical dosage forms through the small intestine. *Gut*. (1986) 27:886–92. doi: 10.1136/gut.27.8.886
41. Parr A, Hidalgo IJ, Bode C, Brown W, Yazdanian M, Gonzalez MA, et al. The effect of excipients on the permeability of BCS class III compounds and implications for biowaivers. *Pharm Res*. (2016) 33:167–76. doi: 10.1007/s11095-015-1773-4
42. Gajendran J, Krämer J, Shah VP, Langguth P, Polli J, Mehta M, et al. Biowaiver monographs for immediate-release solid oral dosage forms: nifedipine. *J Pharm Sci*. (2015) 104:3289–98. doi: 10.1002/jps.24560
43. Sidhu M, Boden WE, Padala SK, Cabral K, Buschmann I. Role of short-acting nitroglycerin in the management of ischemic heart disease. *Drug Des Dev Ther*. (2015) 9:4793. doi: 10.2147/DDDT.S79116
44. Liu L, Cui Y, Chung AY, Shitara Y, Sugiyama Y, Keppler D, et al. Vectorial transport of enalapril by Oatp1a1/Mrp2 and OATP1B1 and OATP1B3/MRP2 in rat and human livers. *J Pharmacol Exp Ther*. (2006) 318:395–402. doi: 10.1124/jpet.106.103390
45. Ferslew BC, Köck K, Bridges AS, Brouwer KLR. Role of multidrug resistance - associated protein 4 in the basolateral efflux of hepatically derived enalaprilat. *Drug Metab Dispos*. (2014) 42:1567–74. doi: 10.1124/dmd.114.057554

Conflict of Interest Statement: The authors declare that the research was conducted in the absence of any commercial or financial relationships that could be construed as a potential conflict of interest.

frontiers in Pediatrics

ORIGINAL RESEARCH
published: 11 July 2019
doi: 10.3389/fped.2019.00283

Long Non-coding RNA Expression Profile and Functional Analysis in Children With Acute Fulminant Myocarditis

Qingqing Liu, Yaru Kong, Bo Han, Diandong Jiang, Hailin Jia and Li Zhang*

Department of Pediatrics, Shandong Provincial Hospital Affiliated to Shandong University, Jinan, China

Long non-coding RNA (lncRNA) has been associated with human diseases. To study the role of lncRNA in the pathogenic mechanism of acute fulminant myocarditis (AFM), we used a microarray to analyze lncRNA and messenger RNA (mRNA) expression in leukocyte samples from AFM patients and normal children. In total, using a 2/0.5-fold change and $P < 0.05$ as the cutoff criteria, we found that 3,101 lncRNAs and 2,170 mRNAs were differentially expressed in AFM patients. Quantitative real-time polymerase chain reaction (RT-qPCR) analysis was used to verify the microarray data. Eight differentially expressed molecules were randomly selected, including 3 upregulated lncRNAs, 3 downregulated lncRNAs, and 2 upregulated mRNAs. Among them, 7 expression profiles were consistent with the microarray results. Gene Ontology enrichment and Kyoto encyclopedia of genes and genomes (KEGG) pathway analysis were used to investigate the biological functions of these genes. Establishment of a lncRNA-mRNA co-expression network and lncRNA target predication were performed to study the molecular interactions of these molecules. Our study is the first to use microarrays to examine the lncRNA and mRNA expression profiles associated with AFM, and the results indicate that the immune system plays an important role in AFM. These findings may provide a new perspective for the pathogenesis, diagnosis, and therapy of AFM.

Keywords: acute fulminant myocarditis, long non-coding RNAs, microarray, messenger RNA, functional analysis

OPEN ACCESS

Edited by:
Fu Lijun,
Shanghai Children's Medical Center, China

Reviewed by:
Bing He,
Wuhan University, China
Giuseppe Limongelli,
Second University of Naples, Italy

****Correspondence:***
Bo Han
hanbo35@163.com

Specialty section:
This article was submitted to Pediatric Cardiology, a section of the journal Frontiers in Pediatrics

Received: *04 April 2019*
Accepted: *25 June 2019*
Published: *11 July 2019*

Citation:
Liu Q, Kong Y, Han B, Jiang D, Jia H and Zhang L (2019) Long Non-coding RNA Expression Profile and Functional Analysis in Children With Acute Fulminant Myocarditis. Front. Pediatr. 7:283. doi: 10.3389/fped.2019.00283

INTRODUCTION

Acute fulminant myocarditis (AFM) is an inflammatory process that occurs in the myocardium and causes acute-onset heart failure (1). It is a type of myocarditis that can arise quickly, progress rapidly and lead to sudden cardiac death, with mortality rates as high as 50–70% (2). At present, many studies have aimed to determine the clinical features of AFM, including the clinical presentation, diagnosis, treatment, and outcome (3–6). However, few studies have examined the pathogenic mechanism of AFM, except for myocarditis. Previous records have confirmed the relationship between myocarditis and the immune system. On the one hand, some moieties, such as Toll-like receptors (TLRs) (7), midkine (8), and STATs (9), can activate inflammatory responses to conserve the host protective system. On the other hand, when an antigen interacts with the variable region of the T cell receptor, acquired immunity will be activated (10).

Data have shown that myocarditis is closely related to signaling pathways, such as NF-κB (11), AKT/caspase-3 (12), IL-1β (13), MAPK (14), and TLR-4/NF-κB p65 (15). However, little attention has been focused on the molecular mechanism of the immune system of AFM patients.

Long non-coding RNAs (lncRNAs) are defined as transcripts of more than 200 nucleotides that are not translated into proteins (16), including antisense, intronic, intergenic, pseudogene, and retrotransposon transcripts (16). LncRNAs participate in various developmental processes, acting as signals, decoys, guides, and scaffolds in epigenetic, transcriptional, or post-transcriptional regulation (17). At present, an increasing number of lncRNAs are emerging as having roles in cardiovascular diseases (18). Some lncRNAs are involved in cardiovascular system diseases, including atherosclerosis (19), heart failure (20), and arrhythmia (21). However, data related to myocarditis are scarce, and only two studies have focused on lncRNAs and cardiac inflammation (22, 23). We aim to provide further information on lncRNAs and AFM to examine the potential pathogenicity of lncRNAs in AFM patients. In addition, microarrays have been regarded as a useful tool in transcriptome gene expression profiling. They have been broadly used to investigate the pathobiology of diverse forms of diseases (24, 25).

To determine whether lncRNAs of peripheral leukocytes might correlate with AFM, we used a microarray to analyze the dysregulated profiles of lncRNAs and mRNAs in leukocytes of children with AFM and healthy children.

MATERIALS AND METHODS

Patients and Samples

We recruited children (aged 4 months−10 years) with AFM in this study based on the following criteria (26): sudden onset of disease, obvious initial symptoms of viral infection (especially severe fatigue and poor appetite), rapidly emerging severe hemodynamic dysfunction, serious myocardial injury, and a diffuse decrease in ventricular wall motion. The exclusion criteria included coronary heart disease, viral pneumonia, sepsis myocarditis, common acute myocarditis, AFM caused by autoimmune disease, toxic drug effects, or drug allergies. The controls consisted of healthy children.

Blood samples (3 ml) were collected into EDTA anticoagulant tubes. Leukocytes were isolated within 4 h and were immediately frozen at −80°C with 1 ml of RNeasy Total RNA Isolation Kit reagent (Qiagen, GmBH, Germany). A total of 10 children from Shandong Provincial Hospital Affiliated to Shandong University (May 2018 to February 2019) were included in this study, including 5 controls and 5 patients. The clinical characteristics of patients and controls are presented in **Tables 1**, **2**. All patients were diagnosed with AFM using cardiac magnetic resonance imaging. Three AFM samples (M1, M2, M3) and three control samples (N1, N2, N3) were used for microarray analysis.

RNA Extraction

Total RNA was extracted from isolated leukocytes using the RNeasy Total RNA Isolation Kit (Qiagen, GmBH, Germany) according to the manufacturer's protocols. The RNA integrity coefficient (RIN) was determined by an Agilent Bioanalyzer 2,100 (Agilent Technologies, Santa Clara, CA, US).

Microarray Analysis

RNA samples were used to generate biotinylated cDNA targets with the Sino Human ceRNA array V3.0 (Shanghai Sinomics Corporation, Shanghai, China) (27). Upon hybridization of the biotinylated cRNA targets, an Agilent Microarray Scanner (Agilent Technologies) was used for slide scanning. Data were extracted with Feature Extraction software 10.7 (Agilent Technologies). Raw data were normalized using the Quantile algorithm in the R package "limma." Data analysis was conducted at Sinotech Genomics Corporation according to the protocol specified by Agilent Technologies. A fold change cutoff of 2 was adopted.

qRT-PCR Validation

Quantitative real-time polymerase chain reaction (qRT-PCR) analysis with a LightCycler 480 (Roche, Shanghai, China) system was used to verify the microarray data. Extracted RNA was

TABLE 1 | Detailed information about the patients and controls.

Sample ID	Sex	Age (years)	Hs-TnT (pg/ml)	BNP (pg/ml)	LVEF (%)	LVEDD (cm)
M1	Female	9	1,028	8,577	61	4.01
M2	Male	7	7,134	8,909	20	4.66↑
M3	Male	10	1,802	7,051	46	4.11
M4	Female	7	1,105	21,835	39	4.30↑
M5	Male	0.4	3,800	>35,000	34	2.69
N1	Male	10	Normal	Normal	64	3.81
N2	Female	7	Normal	Normal	64	3.55
N3	Male	8	Normal	Normal	65	3.75
N4	Female	5	Normal	Normal	64	3.40
N5	Male	6	Normal	Normal	65	3.50

Hs-TnT, hypersensitive troponin T, normal range, 3–14 pg/ml; BNP, brain natriuretic peptide, normal range 0–450 pg/ml; LVEF, left ventricular ejection fraction, determined by echocardiography, normal value >60%; LVEDD, left ventricular end-diastolic dimension, determined by echocardiography; ↑, larger than normal.

TABLE 2 | Clinical presentations of patients.

Sample	Symptoms at onset	ECG	BP (mmHg)	Phenotypes	Assisted circulation
M1	Repeated syncope	III° AVB	92/64	Adams-Stokes syndrome	Temporary pacemaker
M2	Headache, stomachache, emesis	I° AVB	86/60	Acute cardiac insufficiency	ECMO
M3	Fever, headache, emesis, chest pain, chest distress	ST-T change	80/51	Acute heart failure	None
M4	Fever, cough, emesis, chest pain, weakness, poor general condition	III° AVB	77/53	Acute heart failure Cardiac shock	Temporary pacemaker
M5	Fever, poor appetite, poor general condition	Inverted T wave	Undetectable	Acute heart failure Cardiac shock	ECMO

ECG, electrocardiograph; AVB, atrioventricular block; BP, blood pressure at admission; ECMO, extracorporeal membrane oxygenation.

subjected to cDNA synthesis with the PrimeScriptTM RT reagent Kit (Takara, Beijing, China). qRT-PCR was conducted with TB GreenTM Premix Ex TaqTM II (Takara) as directed by the manufacturer. The relative expression levels were determined by the $2^{-\Delta\Delta Ct}$ method. Primer sequences used in the qRT-PCR analysis of lncRNA were shown in **Table 3**.

GO and KEGG Pathway Analysis

Gene Ontology (GO) analysis was performed to determine the biological significance of genes in unique or representative maps of differentially expressed genes (28). KEGG pathway analysis was used to predict the underlying biological functions of dysregulated lncRNAs in pathways (29). GO and KEGG pathway analysis were performed for annotation of genes as a whole network, and differentially expressed genes were analyzed using Fisher's exact test in the R package "cluster profiler." GO categories and pathways with P <0.05 in Fisher's exact test were selected.

Co-expression Network Analysis

We predicted the co-expression relationship between lncRNAs and mRNAs according to the dynamic changes in the gene expression signal values to investigate the relationship between lncRNAs and mRNAs. Through the co-expression network, we analyzed regulatory ability of genes and determined the core regulatory genes. The co-expression network was constructed using Cytoscape.

Cis/trans lncRNA Target Prediction

We predicted the cis and trans targets of lncRNAs. Cis target gene prediction involved identification of mRNAs genes located within 10 kb upstream or downstream of the lncRNA as the target gene of the lncRNA. Trans target gene prediction was based on the principle of complementary sequence pairing. Blast alignment was used to obtain mRNAs that were complementary with lncRNAs. Then, RNA plex software was used to calculate the thermodynamic parameters of lncRNAs that were complementary with mRNAs, and sequences with e $\leq$30 were selected.

TABLE 3 | Primer sequences used in the qRT-PCR analysis of lncRNA.

LncRNA/mRNA	Forward primer (5′-3′)	Reverse primer (5′-3′)
NONHSAT253897.1	AGTCCTCTTGCCT CCACCTTC	AGTTACCACTACTC AGCGTTTT
NONHSAT256669.1	TTAATCCGCCTAACAA CCTTGC	GCCCGTTCATCT TCCAGTTC
NR_126169.1	GATTGTTCTTGTC CACCTTTGTTT	CTCACAGCATCCT TGAATCCCT
NONHSAT234238.1	CTAAGTTATGTAA AGGGAGTGG	GACAGTAAAGAG GGCTAAGAG
NONHSAT177112.1	GGCTTGTTTGTG CTTCGTGTA	AAGGAGGAACTGTT GTTTCCATT
NONHSAT232454.1	GCTGGGTAGGGTG GTGAACGA	ATGGTGGCGGGAG CCTGTAAT
IL10	CCACGCTTTCTA GCTGTTGAG	CTCCGAGACACTG GAAGGTGA
SOS2	CTTAAATGCCGGTAT TTGCTG	CATTGGGTTATGTAGT CTTTGT

Statistical Analysis

Statistically significant differences between groups were estimated by the Mann-Whitney U test using SPSS 25.0; $P < 0.05$ was considered statistically significant.

RESULTS

Differential Expression of lncRNAs and mRNAs

Three samples each from the AFM patient and healthy control groups were analyzed using Sino Human ceRNA Array V3.0 microarray hybridization. Volcano plot analysis was used to assess variations in lncRNA and mRNA expression between these two populations (**Figures 1A,B**). Moreover, hierarchical clustering was used to distinguish AFM patients from healthy children based on gene expression data (**Figures 1C,D**). In total, using a 2/0.5-fold change and $P < 0.05$ as the cutoff criteria, 3,101 lncRNAs displayed differential expression in AFM patients,

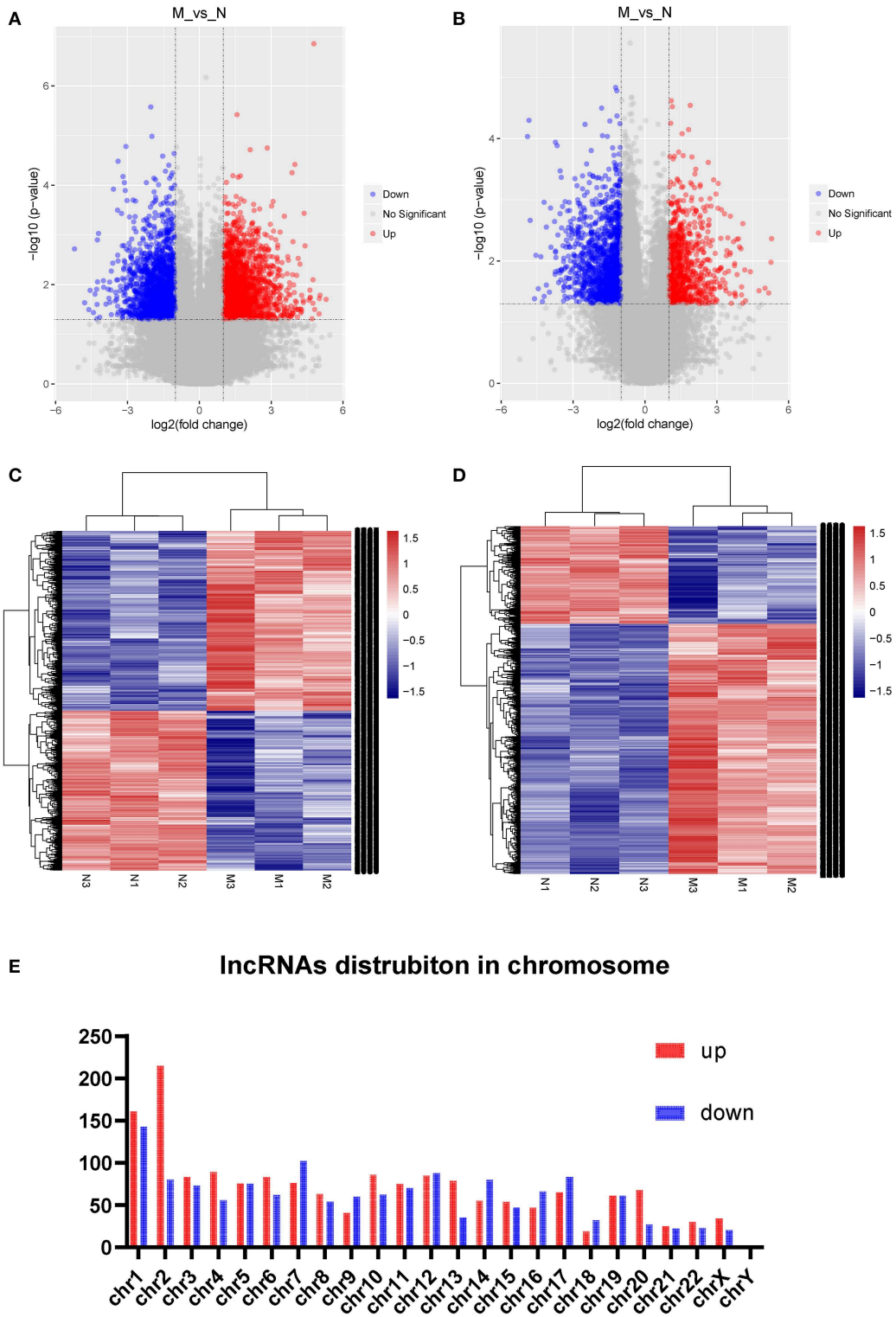

FIGURE 1 | Expression profile of lncRNAs and mRNAs in AFM patients. Volcano plots were used to distinguish differentially expressed lncRNAs **(A)** and mRNAs **(B)**. Hierarchical clustering analysis of differentially expressed lncRNAs **(C)** and mRNAs **(D)**. Distribution of dysregulated lncRNAs in human chromosomes **(E)**. Red and blue represent upregulated and downregulated expression, respectively. M indicates the experimental group; N indicates the normal group.

TABLE 4 | Top 10 upregulated and downregulated (fold change ≥2 and $P < 0.05$) lncRNAs in AFM patients.

LncRNA	Source	*P*	Fold change	Regulation	Chromosome
ENST00000604514	Ensembl	0.047661	73.91975111	up	chr7
NONHSAT072850.2	NONCODE	0.045686	72.50661902	up	chr2
NONHSAT001832.2	NONCODE	0.002136	61.61702903	up	chr1
NONHSAT241868.1	NONCODE	0.049366	60.65420759	up	chr2
XR_001741857.1	NCBI_Gnomon	0.019768	39.22838893	up	chr4
NONHSAT067896.2	NONCODE	0.016283	32.88315135	up	chr19
XR_923024.2	NCBI_Gnomon	0.019056	32.25257773	up	chr2
NONHSAT243915.1	NONCODE	0.038709	32.01786323	up	chr20
NONHSAT167476.1	NONCODE	0.031587	28.15381126	up	chr13
NONHSAT186382.1	NONCODE	0.000000141	27.51917455	up	chr2
NONHSAT173447.1	NONCODE	0.025139761	0.017186109	down	chr16
NONHSAT251804.1	NONCODE	0.00190319	0.026931659	down	chr6
NONHSAT246340.1	NONCODE	0.023122156	0.036114184	down	chr3
NONHSAT214997.1	NONCODE	0.031748829	0.040875939	down	chr7
NONHSAT186791.1	NONCODE	0.013033559	0.042375267	down	chr2
NONHSAT162427.1	NONCODE	0.036500459	0.04659379	down	chr12
NONHSAT248478.1	NONCODE	0.015468853	0.048774319	down	chr4
NONHSAT129423.2	NONCODE	0.012387715	0.051147658	Down	chr8
NR_136191.1	NCBI_BestRefSeq	0.025003999	0.051754137	Down	chr4
NONHSAT214023.1	NONCODE	0.001251946	0.052252876	Down	chr7

including 1,645 upregulated lncRNAs, and 1,456 downregulated lncRNAs. The top of 10 upregulated and downregulated lncRNAs are shown in **Table 4**. The distribution of differentially expressed lncRNAs on human chromosomes is shown in **Figure 1E**. In addition, a total of 2,170 mRNAs were dysregulated; among them, 733 were upregulated, and 1,437 were downregulated.

Validation by qRT-PCR

To confirm the microarray data, we randomly selected 3 upregulated lncRNAs (NONHSAT253897.1, NONHSAT177112.1, and NONHSAT234238.1), 3 downregulated lncRNAs (NONHSAT256669.1, NR_126169.1, and NONHSAT232454.1), and 2 mRNAs (IL10 and SOS2), for qRT-PCR analysis ($n = 10$) (**Figure 2**). The results of 5 lncRNAs (NONHSAT253897.1, NONHSAT177112.1, NONHSAT256669.1, NR_126169.1, and NONHSAT232454.1) and 2 mRNAs (IL10 and SOS2) were consistent with the microarray data. The results for NONHSAT234238.1 were inconsistent with the trend sown by the microarray data.

GO and Pathway Analysis

We performed GO analysis to determine the potential biological role of the dysregulated lncRNAs. The GO enrichment terms of the 30 top cis- (**Figure 3A**) and trans-acting lncRNAs (**Figure 3D**) were determined. The most prominent GO terms were T cell activation and T cell receptor complex for cis-acting lncRNAs and pyramidal neuron development, nuclear membrane, and transmembrane receptor protein serine/threonine kinase activity for trans-acting lncRNAs. According to the KEGG classification, the immune system and signal transduction were notable pathways. We chose the 10 top KEGG pathways (**Figures 3C,D**) within the immune system and signal transduction pathways are notable in **Supplementary Figure 1**; the notable pathways included hematopoietic cell lineage, complement and coagulation cascades, antigen processing, and presentation, T cell receptor signaling pathway, and Jak-STAT signaling pathway.

lncRNA-mRNA Co-expression Network

To predict gene function, we constructed an lncRNA-mRNA co-expression network and performed pathway analyses (**Figure 4**). We identified a total of 95 lncRNAs and 20 mRNAs in the T cell receptor and Jak-STAT signaling pathways (Pearson's coefficient >0.95). The co-expression network was composed of 115 network nodes and 186 connections. Each mRNA was associated with 1 to 17 lncRNAs, and each lncRNA was associated with 1–31 mRNAs.

Cis/trans lncRNA Target Prediction

Target prediction was performed for differentially expressed lncRNAs to investigate whether they can regulate genes and to determine the signaling pathways associated with AFM. We performed partial lncRNA target prediction in the T cell receptor and Jak-STAT signaling pathways (**Figure 5**). The principle of cis target gene prediction is that the function of the lncRNA is related to the protein-coding genes adjacent to its location. The basic principle of trans target gene prediction is that the lncRNA is a distant transcriptional activator or repressor of the target. The data showed that most lncRNAs acted in a cis manner. This information may aid in determining the functional mechanism of AFM.

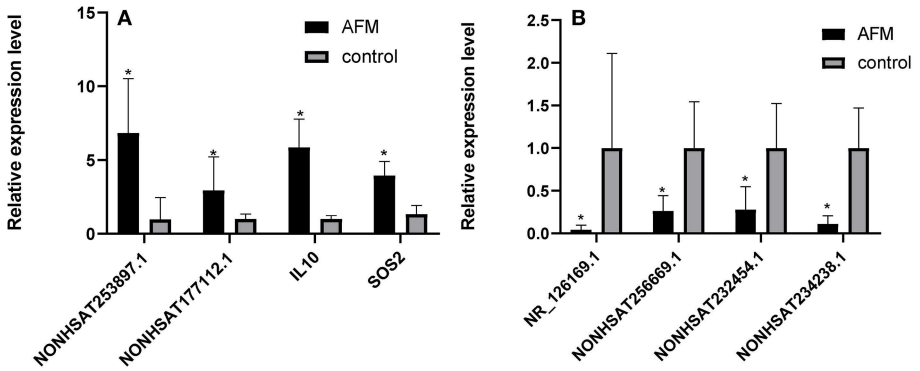

FIGURE 2 | Comparison of the relative RNA expression levels between AFM patients and normal children. The expression of 2 upregulated mRNAs **(A)** and 3 downregulated and 1 upregulated lncRNA **(B)** were validated using the $2^{-\Delta\Delta CT}$ method. The data are displayed as the mean ± SD, and samples of the two groups were compared using the Mann-Whitney U test. *$P < 0.05$; AFM acute fulminant myocarditis; lncRNAs long non-coding RNAs.

DISCUSSION

AFM is characterized by acute and severe inflammation and global myocardium injury (30). The etiology and pathophysiological mechanism of AFM are unknown because of its complexity. Moreover, most of the present research focuses on the diagnosis and treatment of AFM, and the molecular mechanism of AFM is rarely reported. Many researchers believe that AFM is closely related to the immune system, which provides a platform for the study of the pathophysiological mechanisms of AFM.

LncRNAs including antisense, intronic, intergenic, pseudogene, and retrotransposon transcripts, play a vital role in biological processes (16), acting as signals, decoys, guides and scaffolds in epigenetic, transcriptional, or post-transcriptional regulation, and these molecules are emerging as dominating regulators of gene expression in the immune system. At present, most descriptions of the function of lncRNAs include modulation of the target genomic loci in a cis or in trans manner by binding to target DNA based on recognition of specific chromatin features or as an RNA-DNA heteroduplex or RNA-DNA-DNA triplex (31). LncRNAs can also function through RNA-RNA interactions. They can act as "sponges" for miRNA (32) or act by N6-methyladenosine to modify introns to form a secondary structure (33). Many studies have focused on the roles of lncRNAs in the immune system, but only a few studies have demonstrated that lncRNAs are associated with AFM. Zhang et al. (22) studied the relationship between lncRNAs and myocardial inflammation for the first time. They suggested that lncRNA TUG1 inhibits apoptosis and the inflammatory response in lipopolysaccharide (LPS)-treated H9c2 cells by downregulating mir-29b. Zhang et al. (23) demonstrated that silencing lncRNA CHRF protects H9c2 cells against LPD-induced injury via upregulation of mir-221. These two studies discussed the relationship between lncRNA and microRNA but did not examine mRNA. However, research on the transcriptional regulation of myocarditis has mainly focused on the role of mRNAs and their translated proteins.

Our study showed differential expression profiles of lncRNAs and mRNAs in children with AFM and healthy controls. We found 1,645 upregulated lncRNAs, 1,456 downregulated lncRNAs, 733 upregulated mRNAs, and 1,437 downregulated mRNAs. To verify the accuracy of the microarray, we randomly selected 8 molecules for qRT-PCR, including 3 upregulated lncRNAs (NONHSAT253897.1, NONHSAT177112.1, and NONHSAT234238.1), 3 downregulated lncRNAs (NONHSAT256669.1, NR_126169.1, and NONHSAT232454.1), and 2 upregulated mRNAs (IL-10 and SOS2). Among them, 7 molecules showed the same upregulation or downregulation trends of lncRNAs in the AFM and healthy groups. Therefore, the results from the qPCR analysis coincided with the microarray data.

Next, we used GO and KEGG analysis to determine the potential biological functions of differentially expressed lncRNAs and mRNAs. The most notable cellular processes were immune processes, including T cell activation, immune response, T cell receptor complex, negative regulation of complement activation, T-helper 17 cell differentiation, and T cell differentiation for GO terms, and those for the KEGG pathways included the complement and coagulation cascades, antigen processing and presentation, the T cell receptor signaling pathway, the Jak-STAT signaling pathway, the TLR signaling pathway, and the MAPK signaling pathway. These data further indicate the accuracy of the microarray analysis and provide more potential biological functions of lncRNAs and mRNAs related to AFM.

Furthermore, we constructed an lncRNA-mRNA co-expression network in the T cell receptor and Jak-STAT signaling pathways to obtain additional information on lncRNAs and mRNAs. We compared differentially correlated lncRNAs and mRNAs from the leukocytes of AFM patients and healthy

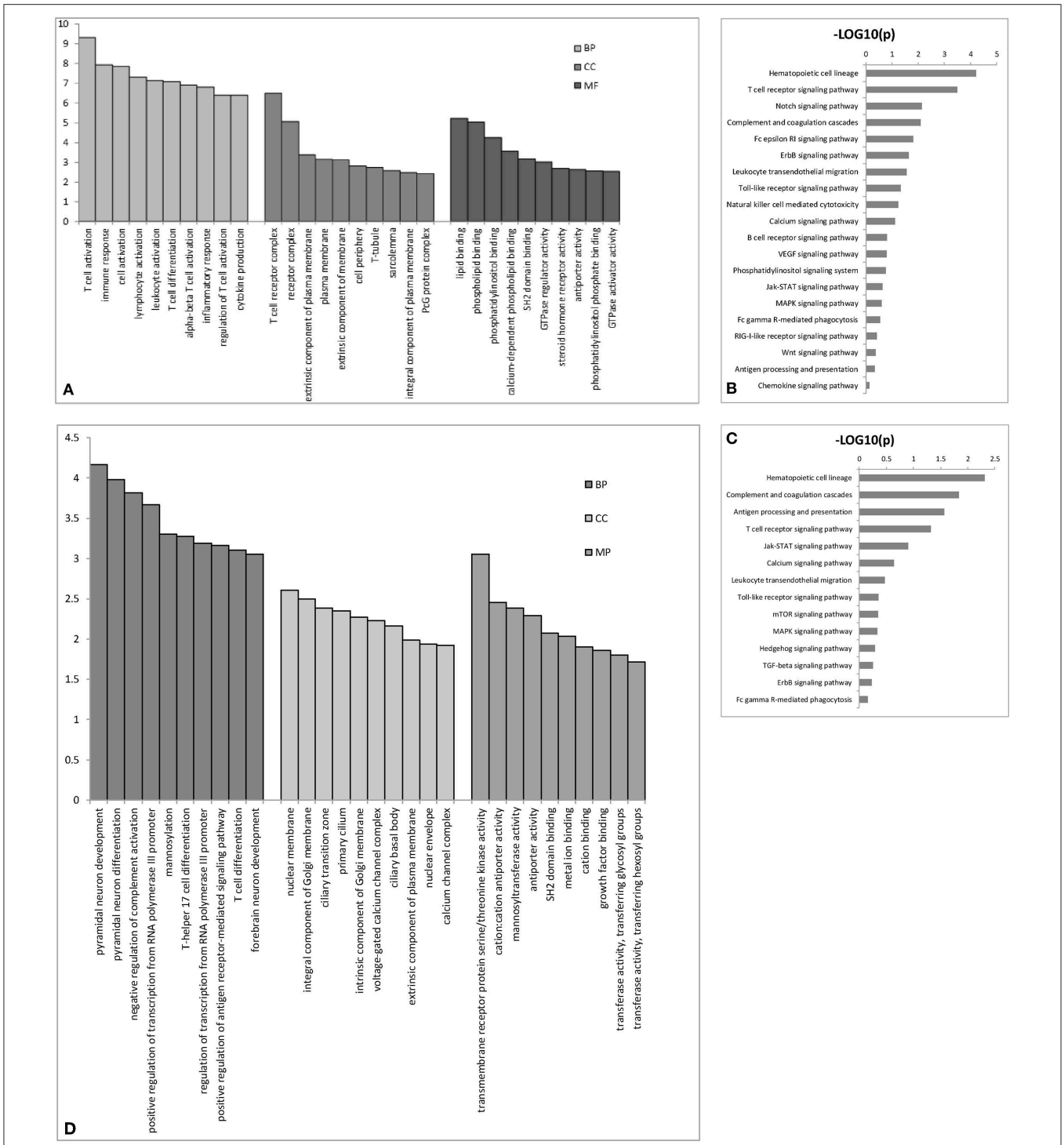

FIGURE 3 | The top 30 GO terms for cis- **(A)** or trans-acting lncRNAs **(D)**. The top 10 KEGG pathways for cis- **(B)** or trans-acting lncRNAs **(C)**. BP biological process; CC cellular component; MP molecular function.

children, which will provide a better understanding of the pathogenic mechanism of AFM.

In conclusion, the data indicate that mutual regulation between lncRNAs and mRNAs may be involved in the pathogenic process of AFM, and the results provide essential information to identify AFM.

Our study had some limitations. First, due to the low incidence of fulminant myocarditis, the sample size of the

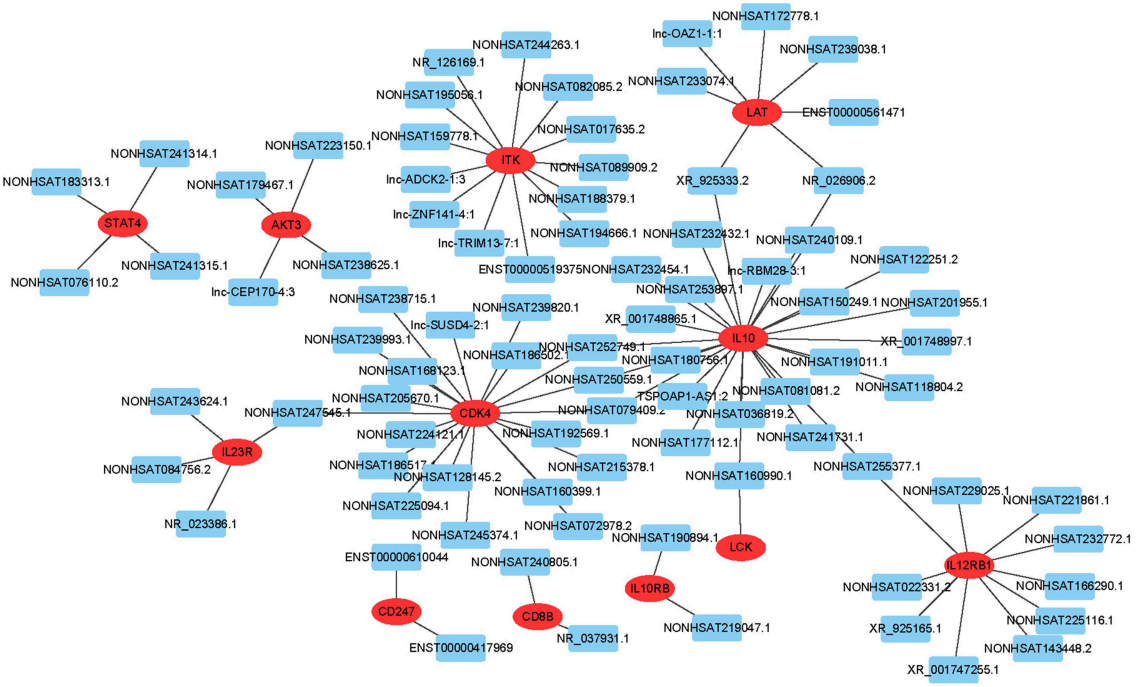

FIGURE 4 | lncRNA-mRNA network analysis of the T cell receptor and Jak-STAT signaling pathways (Pearson's coefficient > 0.95). Red ovals represent mRNAs, blue rectangles represent lncRNAs, a line represents the correlation.

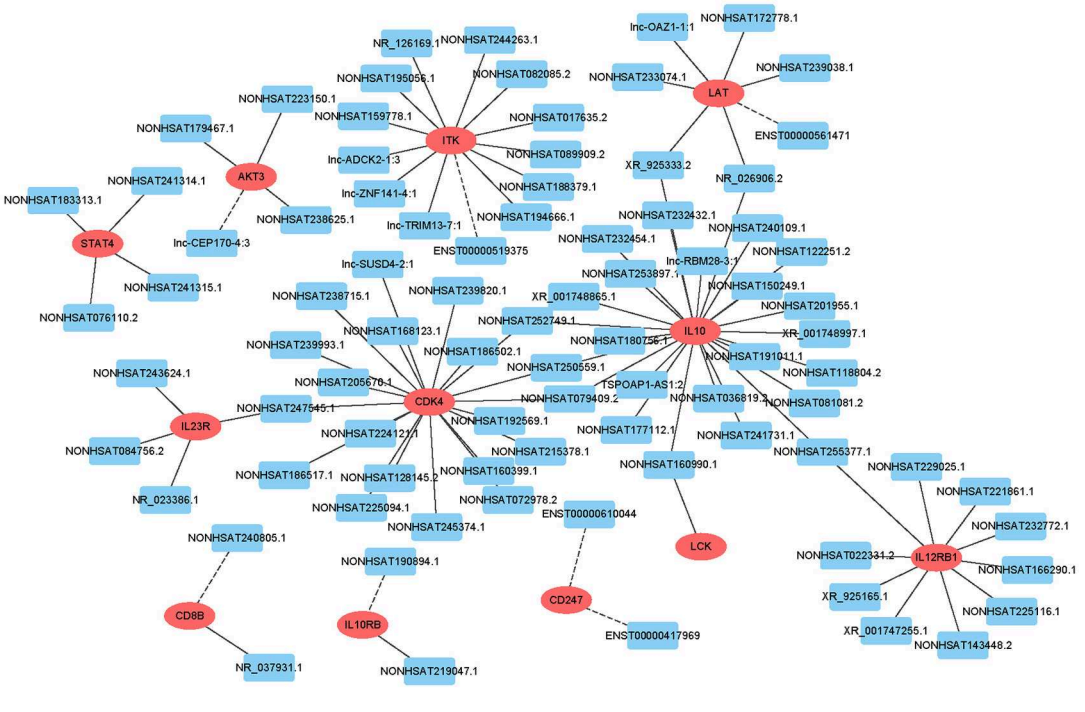

FIGURE 5 | Cis/trans lncRNA target prediction in the T cell receptor and Jak-STAT signaling pathways. Red ovals represent mRNAs, blue rectangles represent lncRNAs. The solid line indicates a trans lncRNA, and the dotted line indicates a cis lncRNA.

microarray analysis and that used to verify the results was small. Second, the subsequent functional verification needs to be further improved.

DATA AVAILABILITY

The raw data supporting the conclusions of this manuscript will be made available by the authors, without undue reservation, to any qualified researcher.

ETHICS STATEMENT

This study was conducted in accordance with the recommendations and guidelines of the Ethics Committee of Shandong Provincial Hospital Affiliated to Shandong University. All study participants and their parents gave written informed consent in accordance with the Declaration of Helsinki. The protocol was approved by the Ethics Committee of Shandong Provincial Hospital Affiliated to Shandong University.

AUTHOR CONTRIBUTIONS

QL designed the study and performed the experiments. YK, LZ, and HJ performed the experiments, analyzed the data, and wrote the manuscript. BH and DJ supervised the experiments.

FUNDING

This study was supported by the Science and Technology Development Plan of Jinan City (No. 201805020), the Taishan scholars (No. ts201511099), and National Natural Science Foundation of China (No. 8187020860).

SUPPLEMENTARY MATERIAL

The Supplementary Material for this article can be found online at: https://www.frontiersin.org/articles/10.3389/fped.2019.00283/full#supplementary-material

Supplementary Figure 1 | KEGG classification of lncRNAs in patients with AFM. Immune system and signal transduction are notable in the figure.

REFERENCES

1. Gupta S, Markham DW, Drazner MH, Mammen PP. Fulminant myocarditis. *Nat Clin Pract Cardiovasc Med*. (2008) 5:693–706. doi: 10.1038/ncpcardio1331
2. Wang D, Li S, Jiang J, Yan J, Zhao C, Wang Y, et al. Chinese society of cardiology expert consensus statement on the diagnosis and treatment of adult fulminant myocarditis. *Sci China Life Sci*. (2018) 62:187–202. doi: 10.1007/s11427-018-9385-3
3. Ammirati E, Veronese G, Cipriani M, Moroni F, Garascia A, Brambatti M, et al. Acute and fulminant myocarditis: a pragmatic clinical approach to diagnosis and treatment. *Curr Cardiol Rep*. (2018) 20:114. doi: 10.1007/s11886-018-1054-z
4. Callan PD, Baltabaeva A, Kamal M, Wong J, Lane R, Robertus JL, et al. Acute fulminant necrotizing eosinophilic myocarditis: early diagnosis and treatment. *ESC Heart Fail*. (2017) 4:660–4. doi: 10.1002/ehf2.12146
5. Wang Q, Pan W, Shen L, Wang X, Xu S, Chen R, et al. Clinical features and prognosis in Chinese patients with acute fulminant myocarditis. *Acta Cardiol*. (2012) 67:571–6. doi: 10.1080/AC.67.5.2174132
6. Xiong H, Xia B, Zhu J, Li B, Huang W. Clinical outcomes in pediatric patients hospitalized with fulminant myocarditis requiring extracorporeal membrane oxygenation: a meta-analysis. *Pediatr Cardiol*. (2017) 38:209–14. doi: 10.1007/s00246-016-1517-1
7. Marsland BJ, Nembrini C, Grun K, Reissmann R, Kurrer M, Leipner C, et al. TLR ligands act directly upon T cells to restore proliferation in the absence of protein kinase C-theta signaling and promote autoimmune myocarditis. *J Immunol*. (2007) 178:3466–73. doi: 10.4049/jimmunol.178.6.3466
8. Weckbach LT, Grabmaier U, Uhl A, Gess S, Boehm F, Zehrer A, et al. Midkine drives cardiac inflammation by promoting neutrophil trafficking and NETosis in myocarditis. *J Exp Med*. (2019) 216:350–68. doi: 10.1084/jem.20181102
9. Gonnella PA, Del Nido PJ, McGowan FX. Oral tolerization with cardiac myosin peptide. (614-629) ameliorates experimental autoimmune myocarditis: role of STAT 6 genes in BALB/CJ mice. *J Clin Immunol*. (2009) 29:434–43. doi: 10.1007/s10875-009-9290-z
10. Tavares PS, Rocon-Albuquerque R, Leite-Moreira AF. Innate immune receptor activation in viral myocarditis: pathophysiologic implications. *Rev Port Cardiol*. (2010) 29:57–78. doi: 10.1038/ki.2010.111
11. Xue YL, Zhang SX, Zheng CF, Li YF, Zhang LH, Hao YF, et al. Silencing of STAT4 protects against autoimmune myocarditis by regulating Th1/Th2 immune response via inactivation of the NF-κB pathway in rats. *Inflammation*. (2019). doi: 10.1007/s10753-019-00978-3. [Epub ahead of print].
12. Wang X, Li M, Yu Y, Liu G, Yu Y, Zou Y, et al. FTY720 alleviates coxsackievirus B3-induced myocarditis and inhibits viral replication through regulating sphingosine 1-phosphate receptors and AKT/caspase-3 pathways. *J Cell Physiol*. (2019) 234:18029–40. doi: 10.1002/jcp.28434
13. Kraft L, Erdenesukh T, Sauter M, Tschope C, Klingel K. Blocking the IL-1beta signalling pathway prevents chronic viral myocarditis and cardiac remodeling. *Basic Res Cardiol*. (2019) 114:11. doi: 10.1007/s00395-019-0719-0
14. Zheng C, Wu SM, Lian H, Lin YZ, Zhuang R, Thapa S, et al. Low-intensity pulsed ultrasound attenuates cardiac inflammation of CVB3-induced viral myocarditis via regulation of caveolin-1 and MAPK pathways. *J Cell Mol Med*. (2019) 23:1963–75. doi: 10.1111/jcmm.14098
15. Liu T, Zhang M, Niu H, Liu J, Ruilian M, Wang Y, et al. *Astragalus* polysaccharide from *Astragalus* Melittin ameliorates inflammation via suppressing the activation of TLR-4/NF-kappaB p65 signal pathway and protects mice from CVB3-induced virus myocarditis. *Int J Biol Macromol*. (2019) 126:179–86. doi: 10.1016/j.ijbiomac.2018.12.207
16. Kopp F, Mendell JT. Functional classification and experimental dissection of long non-coding RNAs. *Cell*. (2018) 172:393–407. doi: 10.1016/j.cell.2018.01.011
17. Ma H, Hao Y, Dong X, Gong Q, Chen J, Zhang J, et al. Molecular mechanisms and function prediction of long non-coding RNA. *Scient World J*. (2012) 2012:541786. doi: 10.1100/2012/541786
18. Coelho-Lima J, Spyridopoulos I. Non-coding RNA regulation of T cell biology: implications for age-associated cardiovascular diseases. *Exp Gerontol*. (2018) 109:38–46. doi: 10.1016/j.exger.2017.06.014
19. Cremer S, Michalik KM, Fischer A, Pfisterer L, Jae N, Winter C, et al. Hematopoietic deficiency of the long non-coding RNA MALAT1 promotes atherosclerosis and plaque inflammation. *Circulation*. (2018) 139:1320–34. doi: 10.1161/CIRCULATIONAHA.117.029015
20. Boeckel JN, Perret MF, Glaser SF, Seeger T, Heumuller AW, Chen W, et al. Identification and regulation of the long non-coding RNA Heat2 in heart failure. *J Mol Cell Cardiol*. (2018) 126:13–22. doi: 10.1016/j.yjmcc.2018.11.004
21. Li Z, Wang XM, Wang WZ, Du JJ, Wei JQ, Zhang Y, et al. Altered long non-coding RNA expression profile in rabbit atria with atrial fibrillation: TCONS_00075467 modulates atrial electrical remodeling by sponging

miR-328 to regulate CACNA1C. *J Mol Cell Cardiol.* (2017) 108:73–85. doi: 10.1016/j.yjmcc.2017.05.009
22. Zhang H, Li H, Ge A, Guo E, Liu S, Zhang L. Long non-coding RNA TUG1 inhibits apoptosis and inflammatory response in LPS-treated H9c2 cells by down-regulation of miR-29b. *Biomed Pharmacother*. (2018) 101:663–9. doi: 10.1016/j.biopha.2018.02.129
23. Zhang L, Wang L, Guo E, Qi Y. Silence of lncRNA CHRF protects H9c2 cells against lipopolysaccharide-induced injury via up-regulating microRNA-221. *Exp Mol Pathol*. (2019) 107:43–50. doi: 10.1016/j.yexmp.2019.01.010
24. Kierzek R, Turner DH, Kierzek E. Microarrays for identifying binding sites and probing structure of RNAs. *Nucleic Acids Res.* (2015) 43:1–12. doi: 10.1093/nar/gku1303
25. Mantione KJ, Kream RM, Kuzelova H, Ptacek R, Raboch J, Samuel JM, et al. Comparing bioinformatic gene expression profiling methods: microarray and RNA-Seq. *Med Sci Monit Basic Res*. (2014) 20:138–42. doi: 10.12659/MSMBR.892101
26. Sun D, Ding H, Zhao C, Li Y, Wang J, Yan J, et al. Value of SOFA, APACHE IV and SAPS II scoring systems in predicting short-term mortality in patients with acute myocarditis. *Oncotarget*. (2017) 8:63073–83. doi: 10.18632/oncotarget.18634
27. Zhang H, Zhu L, Bai M, Liu Y, Zhan Y, Deng T, et al. Exosomal circRNA derived from gastric tumor promotes white adipose browning by targeting the miR-133/PRDM16 pathway. *Int J Cancer*. (2018) 144:2501–15. doi: 10.1002/ijc.31977
28. Huang DW, Sherman BT, Lempicki RA. Systematic and integrative analysis of large gene lists using DAVID bioinformatics resources. *Nat Protoc*. (2009) 4:44–57. doi: 10.1038/nprot.2008.211
29. Khatri P, Sirota M, Butte AJ. Ten years of pathway analysis: current approaches and outstanding challenges. *PLoS Comput Biol.* (2012) 8:e1002375. doi: 10.1371/journal.pcbi.1002375
30. Zhang J, Hang W, Hui R, Zhao Q, Desai SS. China's treatment regimen for fulminant myocarditis is bringing wonderful achievement to the world. *Sci China Life Sci*. (2019) 62:282–4. doi: 10.1007/s11427-018-9445-2
31. Chen YG, Satpathy AT, Chang HY. Gene regulation in the immune system by long non-coding RNAs. *Nat Immunol.* (2017) 18:962–72. doi: 10.1038/ni.3771
32. Dykes IM, Emanueli C. Transcriptional and post-transcriptional gene regulation by long non-coding RNA. *Genomics Proteomics Bioinformat*. (2017) 15:177–86. doi: 10.1016/j.gpb.2016.12.005
33. Linder B, Grozhik AV, Olarerin-George AO, Meydan C, Mason CE, Jaffrey SR. Single-nucleotide-resolution mapping of m6A and m6Am throughout the transcriptome. *Nat Methods*. (2015) 12:767–72. doi: 10.1038/nmeth.3453

Conflict of Interest Statement: The authors declare that the research was conducted in the absence of any commercial or financial relationships that could be construed as a potential conflict of interest.

frontiers in Pediatrics

REVIEW
published: 23 July 2019
doi: 10.3389/fped.2019.00302

Bosentan for Treatment of Pediatric Idiopathic Pulmonary Arterial Hypertension: State-of-the-Art

Yuchen Wang[1,2], *Selena Chen*[3] *and Junbao Du*[1,4]*

[1] Department of Pediatrics, Peking University First Hospital, Beijing, China, [2] Department of Clinical Medicine, Peking University Health Science Center, Beijing, China, [3] Division of Biological Sciences, University of California, San Diego, La Jolla, CA, United States, [4] Key Laboratory of Molecular Cardiovascular Sciences, Ministry of Education, Beijing, China

Idiopathic pulmonary arterial hypertension (IPAH) is a complex disease associated with progressive deterioration. Targeted therapy for IPAH has improved in the last several decades. However, there remain many challenges to current treatment of children with IPAH, including poor prognosis and a median survival of 0.8 years. Endothelin-1 (ET-1) appears to be a key mediator in the pathogenesis of IPAH, with elevated concentrations in the plasma. Bosentan, an endothelin receptor antagonist, has been confirmed in Food and Drug Administration (FDA) to effectively treat IPAH when administered in recent studies. This review focuses on related studies and advance of bosentan in the treatment of IPAH in children.

Keywords: idiopathic pulmonary hypertension, target therapy, bosentan, pediatrics, pharmacology

OPEN ACCESS

Edited by:
Fangqi Gong,
Children's Hospital, School of Medicine, ZheJiang University, China

Reviewed by:
Dunbar Ivy,
University of Colorado Denver, United States
Sarah Moharem-Elgamal,
NIHR Bristol Cardiovascular Biomedical Research Unit, United Kingdom

***Correspondence:**
Junbao Du
junbaodu1@126.com

Specialty section:
This article was submitted to Pediatric Cardiology, a section of the journal Frontiers in Pediatrics

Received: *10 March 2019*
Accepted: *08 July 2019*
Published: *23 July 2019*

Citation:
Wang Y, Chen S and Du J (2019) Bosentan for Treatment of Pediatric Idiopathic Pulmonary Arterial Hypertension: State-of-the-Art. Front. Pediatr. 7:302. doi: 10.3389/fped.2019.00302

Pulmonary arterial hypertension (PAH) is a progressively deteriorative disease characterized by an increase of pulmonary vascular resistance (PVR) caused by the vascular structural remodeling of pulmonary arteries, likely causing right ventricular failure (1). Nowadays, the 6th WSPH Task Forces proposes (2) to include PVR equal to or over three Wood units in the definition of all forms of pre-capillary PH associated with mean pulmonary artery pressure (mPAP) > 20 mmHg (3). Idiopathic pulmonary arterial hypertension (IPAH) is one of the most common PAH categories in children (4). The damage of vascular endothelial function is one of the key factors in the pathogenesis of IPAH, although it has a complex pathogenesis (5). Increased levels of endothelin-1 (ET-1) in the plasma induce smooth muscle cell proliferation and fibrosis. The activation of endothelin receptors (ETRs) enhances the adhesion and chemotaxis of neutrophils that further aggravate vascular injury. Genetics (6), autoimmune-related pulmonary vascular injury, serotonin, and metalloproteinase damage to the vascular wall, and the inhibition of Kv channels are all involved in its pathogenesis.

In recent years, epidemiological characteristics of pediatric PH in the Netherlands and the United Kingdom showed that pediatric IPAH/HPAH accounted for 46–70 and 35–60% of PAH in children, respectively (7). In the Netherlands, the incidence of pediatric pulmonary hypertension is 3.0/1,000,000 and the prevalence rate is 20/1,000,000. In the United Kingdom and New Zealand, the incidences of IPAH are 0.48/1,000,000 and 0.7/1,000,000, and the prevalence rate is 2.1/1,000,000 and 4.4/1,000,000, respectively (8). However, 7.8% of children have a family history (UK). Without targeted treatment in children with IPAH, only 37% of patients survive within 1 year after diagnosis. According to the National Institutes of Health Registry, the median survival time of traditional treatment was only 10 months before 1995, and the 5 year survival rate was as low as 25% (9). However, with the progress of targeted therapy, IPAH treatment in children has undergone tremendous changes in the past decade (10) and has made great progress.

Meta-analysis reported that targeted therapy for PAH, including endothelin receptor antagonists, phosphodiesterase five inhibitors and prostacyclins, improved functional class, hemodynamics, and long-term prognosis in adults, but the efficacy has not yet been confirmed in children (10). In the past decade, the studies on bosentan, an endothelin receptor antagonist, for the treatment of pediatric IPAH have made new progress in several prospects (11–13).

PHARMACOLOGY OF BOSENTAN IN PEDIATRIC IPAH

Bosentan, the first orally active and dual antagonist for ETRs, was put onto use. By blocking the ETRs and inhibiting ET-1 function, it results in an inhibition of endothelial cell proliferation.

Introduction of Endothelin Receptors (14, 15)

The endothelium and ETRs play an important role in regulating pulmonary vascular development. ET-1 is a crucial part of endothelin isoforms, and has been detected in all types of vessel. ET-1 is comprised by 21 amino acids that are synthesized and released from endothelial cells with a three-step process: the gene encodes prepro-ET-1 by proteolytic cleaving the initial of the signal peptidase, and the generated pro-peptide is further cleaved by the enzyme furin convertase to big-ET-1 precursors. Big-ET-1 needs endothelin-converting enzyme (ECE) to biologically activate under particular conditions and transforms to mature form. Both physical and chemical stimuli contribute to alterations in the production. After that, ET-1 is secreted by constitutive pathway to interact with ET receptors to contribute to vasomotor tone or the regulated pathway in response to external stimuli from Weibel-Palade bodies.

ET-1 interacts with ET-A receptors on the smooth muscle to mediate constriction in all arteries and veins, while ET-B exhibits vascular contractions under normal physiologic conditions by releasing vasodilators such as nitric oxide. The above mechanisms make the homeostasis physiological.

ET-1 in IPAH (15)

In pediatric IPAH, plasma endothelin levels are elevated, and ECE activity is enhanced (16). ET-1 is highly expressed in the lung. The overproduction of ET or overactivation of ET-A receptors and reduced ET-B receptors under pathophysiological conditions will result in an intense vasoconstriction of vessels and an effect to stimulate matrix production and cell proliferation, which results in the fibrosis and inflammation of PAH. The levels of ET-1 correlated with the levels of PVR. As such, endothelin receptor antagonists likely play a role in the treatment of IPAH (17, 18).

Abbreviations: IPAH, Idiopathic pulmonary arterial hypertension; PVR, pulmonary vascular resistance; 6MWT, six-minute walking test; FC, functional class; mPAP, mean pulmonary artery pressure.

Mechanism for Bosentan in Treating PAH

Pulmonary arterial hypertension (PAH) is mainly developed according to three factors: pulmonary vasoconstriction, vascular remodeling caused by vascular smooth muscle proliferation, and inflammation. The following picture shows the main mechanism of bosentan in PAH (14, 19, 20) (**Figure 1**).

Pharmacokinetics of Bosentan (18, 21–24)

In adult, bosentan attains peak plasma concentrations in 3–5 h with the maximum plasma concentration (C_{max}) of ∼1,000 ng/ml. The terminal elimination half-life ($t_{1/2}$) is about 5.4 h and is unchanged at steady state in healthy adult subjects with a 50% bioavailability. The steady-state concentrations are achieved within 3–5 days after multiple-dose administration. Bosentan is ∼98% bound to albumin and multiple-dose administration has a volume of distribution of 30 L and a clearance of 17 L/h. Bosentan is mainly metabolized by CYP2C9 and 3A4 isoenzymes, and therefore, kidney function has a slight influence over it (18). The excretion of the metabolites via the bile constitutes the major pathway of elimination. The first-pass effect of bosentan is maximally 20% due to the clearance and the blood/plasma distribution ratio is 0.6.

The pharmacokinetics of bosentan in pediatric PAH patients and healthy adults are similar (24) according to the C_{max}, T_{max}, AUC, and values for $t_{1/2}$. The activity of CYP3A4 and P2C9 surges after birth, and reaches adult levels after 1 year-old. Furthermore, the extent of the reduction in exposure to bosentan in the pediatric patients is similar with adult.

Moreover, Beghetti et al. (25) showed that the dose of bosentan from 2 to 4 mg/kg did not alter the plasma concentrations in children, and also the concentration-time of doses of 2 and 4 mg/kg overlapped, suggesting that an exposure plateau was reached at a dose of 2 mg/kg, twice a day, likely due to the smaller size of their intestinal surface area and different absorption characteristics. The apparent $t_{1/2}$ of bosentan was similar to that in children based on the above research.

BOSENTAN AS A TARGETED THERAPY DRUG FOR PEDIATRIC IPAH

In European Medicines Agency (EMA), Food and Drug Administration (FDA), and China Food and Drug Administration (CFDA) highlight (26, 27), bosentan is indicated for the treatment of PAH to improve exercise capacity and symptoms in patients with WHO functional class III. The efficacy has been shown in primary PAH (idiopathic and familial), PAH secondary to scleroderma without significant interstitial pulmonary disease, congenital systemic-to-pulmonary shunts and Eisenmenger syndrome. In Europe and China, the recommended initial and maintenance dose is 2 mg/kg, although there are no data available on the safety and efficacy in pediatric cases. But bosentan has already been listed by the FDA as an indication for children at the age of 3 years old and older with IPAH or congenital PAH.

At present, numerous RCTs have shown that adult patients benefited from bosentan with respect to the six-minute walking

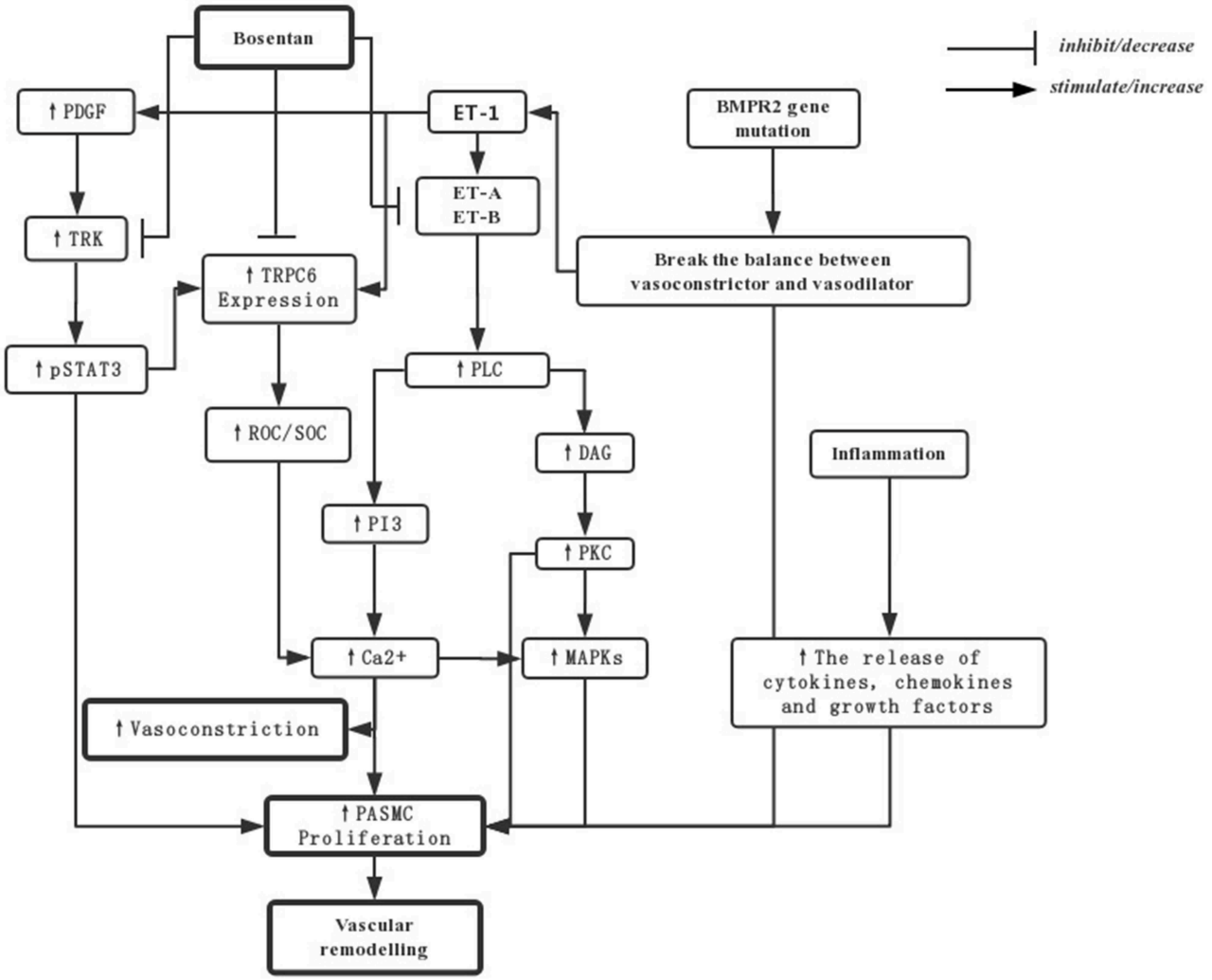

FIGURE 1 | The mechanisms for bosentan in treating PAH. PDGF-mediated activation of TRKs can upregulation of TRPC6 expression by activating of STAT3 phosphorylation. The resultant increase in the activity of pSTAT3 and ROCs and SOCs would increase Ca^{2+} to stimulate PASMCs and vasoconstriction. The over-expression of ET-1 can increase levels of PVR by ET-A and ET-B activation through PLC and the downstream in PI3 and DAG pathways. What's more, the balance between vasoconstrictive and vasodilatory mechanisms may be broken by the mutations in BMPR2, and the release of inflammation factors may also induce proliferation of cells. Bosentan, as an endothelin receptor antagonist, directly downregulates TRPC6 and TRK expression by repressing the gene transcription or translation, in addition to blockade of endothelin receptors and their downstream signal transduction pathway traditionally. PASMCs, pulmonary artery smooth muscle cells; DAG, diacylglycerol; PKC, protein kinase C; ROCs, Receptor-operated Ca^{2+} channels; SOCs, store-operated Ca^{2+} channels; TKRs, PDGF-mediated activation of tyrosine kinase receptors; pSTAT3, transcription-3 phosphorylation; PDGF, platelet-derived growth factor; TRPC, transient receptor potential channels.

test (6MWT), functional class (FC), safety and long-term prognosis (28–30), but the effects of bosentan on IPAH have not been completely defined in children. Due to the limitation of the investigation in child populations, there have been only a small number of cohort studies regarding the effect of bosentan in children with IPAH, although few RCT clinical studies have been conducted.

Yung et al. (31) performed a cohort study of 77 children with IPAH, indicating that the use of calcium channel blockers (CCB) in 31 children positive for acute vascular response (AVR-positive) resulted in 1, 5, and 10 year survival rates of 97, 97 and 81%, and treatment success rates of 84, 68, and 47%, respectively. Following the rise of the "New Drug Age" after 1995 (32, 33), drugs such as bosentan and sildenafil appeared on the market, yielding 1, 5, and 10 year survival rates of 97, 97, and 78%, and the treatment success rates of 93, 86, and 60%, respectively. These data support the view that new targeted drugs can improve the survival rate and quality of life of patients.

Change in Six-minute Walking Test Before and After Treatment of Bosentan

In 2006, Maiya et al. (34) examined the short-term effect of bosentan. They observed 10 pediatric IPAH patients who were treated with bosentan for 6 months. The six-minute walking test showed that five out of the 10 children improved substantially,

TABLE 1 | Six-minute walking distance (6MWD) of pediatric IPAH patients before and after the treatment of bosentan.

Numbers	F/M	Age, y	Treatment	6MWD before treatment	6MWD after treatment	References
8	4/4	12.8 (8.5–17.8)	Bosentan add-on after epoprostenol for >1 year	498 m	518 m	Ivy et al. (37)
20	15/5	8.0 (1.2–17.0)	Bosentan	6WMT: 245 m ($n = 10$)	6WMD: 421.8 m ($n = 10$)	Maiya et al. (34)
7	3/4	9.6 (1.0–16.0)	Sildenafil ($n = 5$) Bosentan ($n = 2$)	394.2 m	6 mon: 464.2 m 2 y: 526.7	Raposo-Sonnenfeld et al. (35)
64	26/38	4.3 (1.5–8.9)	Bosentan ($n = 23$) Prostanoids ($n = 15$) Sildenafil ($n = 9$) Combination therapy ($n = 11$) Calcium channel antagonists ($n = 6$)	6WMT: 285 m (19 out of 23 patients taking bosentan)	6WMD: 385 m (19 out of 23 patients taking bosentan)	Moledina et al. (36)
42	26/16	9.7	Bosentan	271 m	370 m	Hislop et al. (16)

F, Female; M, Male.

with a mean improvement of 176.8 m, and a mean improvement of 68 m among the entire group. Hislop et al. (16) confirmed that again in 2011, as demonstrated by a 6-minute walking distance increase from a baseline of 271 m to 370 m. To explore the long-term effects of targeted drug therapy, Raposo-Sonnenfeld et al. (35) reviewed seven patients in 2007, five of whom received sildenafil, and two received bosentan. All patients showed improvements in the 6-minute walking distance, from an average baseline of 394.2 m to 464.2 m in 6 months and 526.7 m after 2 years, demonstrating long-term period effects. Similar results were also seen in a 7 year retrospective cohort study in 2010 by Moledina et al. (36), which showed that 23 patients improved their 6-minute walking distance from 285 to 385 m after received bosentan treatment.

Additionally, bosentan was used for prostacyclin replacement therapy. Ivy et al. (37) conducted a cohort study of eight children with IPAH in 2004. Eight children received bosentan on the background of 1 year of prostacyclin treatment. At 6 months, the 6-minute walking distance increased from 498 m under the use of prostacyclin to 518 m. The 6-minute walking distance of IPAH children after bosentan treatment was increased by an average of 30–176 m in 6 months, and 100–132.5 m in 2 years. The cardiopulmonary function changed greatly in short and long periods (**Table 1**).

WHO Functional Class of Pediatric IPAH Patients Treated by Bosentan

Beghetti et al. (25) in 2009 showed that amongst 35 children treated with bosentan for 12 weeks, 29 of 35 remained (82.9%) unchanged, 5 of 35 (14.3%) upgraded one class, and one of 35 (2.9%) worsened one class. The cardiac function of patients also improved more significantly than before. Raposo-Sonnenfeld et al. (35) reported in 2007 that six of seven children with IPAH were graded III or IV prior to treatment with bosentan, whereas all seven children were graded I or II following 2 years of treatment. Similarly, Ivy et al. (38) retrospectively reviewed 36 children with IPAH treated with bosentan, of whom 14 (38%) children elevated by one functional class and 12 children remained unchanged. Berger et al. (39) reported similar proportions, in which 11 of 28 (39.3%) children improved from the baseline value, and two of 28 (7.1%) children worsened. Furthermore, Hislop et al. found that the WHO functional class changed from 2.8 to an average of 2.4 after 6 months of bosentan treatment (16).

For prostacyclin replacement, eight children with IPAH in the study by Ivy et al. (37) received prostacyclin treatment with an average functional class of 2.3 at baseline. When prostacyclin was reduced and bosentan added for 1 year, their average functional class improved to 2.0, and two out of eight cases who received prostacyclin replacement therapy increased their functional class by one grade, indicating that bosentan as a replacement therapy could increase functional class while reducing adverse effects. In 2006, Maiya et al. (34) obtained similar results.

To compare the effect of monotherapy and combined therapy, Rosenzweig et al. (40) conducted a 2-year study in which 38 patients used bosentan alone and 40 patients used prostaglandins in addition to bosentan for treatment. Overall, 36 (46%) patients improved by at least one class, 34 (44%) patients remained in the same class, and 8 (10%) patients worsened by one class. There was no statistical difference between the two groups, but the effect appeared more pronounced for bosentan alone than for combined prostaglandins.

In summary, after 6 months to 1 year of treatment with bosentan, the functional class in 20–46% patients improved, 44–55% patients remained unchanged, and a small number of patients declined due to progression of the original diseases. Bosentan demonstrated greater efficacy in treatment than prostaglandins and bosentan used in conjunction with prostaglandins (41) (**Table 2**).

Hemodynamic Parameters Change After Treatment of Bosentan

Barst et al. (24) showed that 19 pediatric IPAH patients showed significant improvement in hemodynamics after being treated with bosentan for 12 weeks. Raposo-Sonnenfeld et al. (35) reached the same conclusion. Two years later,

TABLE 2 | WHO functional class of pediatric IPAH patients treated by bosentan.

Numbers	F/M	Age, y	Treatment	WHO functional class before treatment	WHO functional class after treatment	References
8	4/4	12.8 (8.5–17.8)	Bosentan add-on after epoprostenol for >1 year.	The mean class before treatment is 2.3 WHO II: $n = 6$ WHO III: $n = 2$	The mean class after treatment is 2.0 WHO I: $n = 2$ WHO II: $n = 4$ WHO III: $n = 2$	Ivy et al. (37)
86	49/37	11.0 (0–18.0)	Bosentan concomitant Prostanoid ($n = 42$) Bosentan ($n = 44$)	WHO I: $n = 6$ WHO II: $n = 34$ WHO III: $n = 32$ WHO IV: $n = 6$	Improved one class: $n = 36$, remained stable: $n = 34$, worsened one class: $n = 8$ (78 out of 86 patients had WHO assessments)	Rosenzweig et al. (40)
20	15/5	8.0 (1.2–17.0)	Bosentan	WHO II: $n = 1$ WHO III: $n = 11$ WHO IV: $n = 8$	Improved one class: $n = 8$, remained stable: $n = 9$, worsened one class: $n = 2$	Maiya et al. (34)
7	3/4	9.6 (1.0–16.0)	Sildenafil ($n = 5$) Bosentan ($n = 2$)	WHO II: $n = 1$ WHO III: $n = 5$ WHO IV: $n = 1$	All of them are in Class I or II	Raposo-Sonnenfeld et al. (35)
36	15/21	7.0 (2.0–22.0)	Bosentan	WHO II: $n = 23$ WHO III: $n = 13$	Improved one class: $n = 5$ remained stable: $n = 29$, worsened one class: $n = 1$ WHO I: $n = 2$ WHO II: $n = 23$ WHO III: $n = 10$	Beghetti et al. (25)
64	26/38	4.3 (1.5–8.9)	Bosentan ($n = 23$) Prostanoid ($n = 15$) Sildenafil ($n = 9$) combined therapy ($n = 11$) Calcium channel antagonists ($n = 6$)	WHO II: $n = 12$ WHO III: $n = 34$ WHO IV: $n = 18$	They all get improved, and the mean class after treatment is 3.0	Moledina et al. (36)
36	16/20	10.5 (1.0–16.0)	Bosentan ($n = 11$) Bosentan concomitant prostanoid ($n = 25$)	WHO I: $n = 3$ WHO II: $n = 12$ WHO III: $n = 16$ WHO IV: $n = 3$	Improved one class: $n = 14$, remained stable: $n = 12$, worsened one class: $n = 6$ (32 out of 36 patients had assessments)	Ivy et al. (38)
42	26/16	9.7 (no data)	Bosentan	Mean class: 2.9 WHO I: $n = 2$ WHO II: $n = 8$ WHO III: $n = 25$ WHO IV: $n = 7$	The mean class is 2.4 No detailed data	Hislop et al. (16)
36	21/15	6.8 (2.0–12.0)	Bosentan	WHO II: $n = 17$ WHO III: $n = 11$	Improved one class: $n = 11$, remained stable: $n = 15$, worsened one class: $n = 2$	Berger et al. (39)

F, Female; M, Male.

the mPAP decreased from 91.2 mmHg to 86.2 mmHg. However, in a retrospective observational study by Hislop et al. (16), the hemodynamics did not significantly change but showed a downward trend: mPAP decreased from 48.8 to 48.3 mmHg, and PVR decreased from 16.5 $U.m^2$ to 14.1 $U.m^2$.

Later on, to know the hemodynamic differences between bosentan monotherapy and combined prostaglandin therapy, Rosenzweig et al. (40) studied 49 patients, including 25 treated with bosentan monotherapy. They found that those treated with bosentan monotherapy had a decrease in mPAP of 9 mmHg and a decrease in PVR of 6 $U.m^2$. Twenty-four patients treated with combined prostaglandin therapy showed a decrease in mPAP of 4 mmHg and a decrease in PVR of 3 $U.m^2$, which indicated that monotherapy resulted in better effects than when used in combination. Furthermore, bosentan had a better therapeutic effect than prostaglandins when used alone. Moledina et al. (36) found that the PVR of the bosentan group was decreased by 23% on average, and that of the prostaglandins group decreased by 17% (**Table 3**).

TABLE 3 | Hemodynamics at bosentan initiation and after at least 6 months of treatment.

Numbers	F/M	Age, y	Treatment	mPAP (mmHg) PVRi ($U.m^2$) before treatment	mPAP (mmHg) PVRi ($U.m^2$) after treatment	Conclusion	References
49	No data	11.0 (0–18.0)	Bosentan concomitant prostanoid ($n = 24$) Bosentan ($n = 25$)	mPAP: 64 PVR: 19	mPAP: 57 PVR: 15 In 25 patients taking bosentan: mPAP decreased by 9 mmHg, and PVR decreased by 6 mmHg	mPAP, PVR improved	Rosenzweig et al. (40)
20	15/5	8.0 (1.2–17.0)	Bosentan	mPAP: no data PVR: 21.7	mPAP: 61.45 PVR: 21.74	No significant change in PVR, mPAP	Maiya et al. (34)
7	3/4	9.6 (1.0–16.0)	Sildenafil ($n = 5$) Bosentan ($n = 2$)	mPAP: 91.2 PVR: no data	mPAP: 86.2 PVR: no data	mPAP improved	Raposo-Sonnenfeld et al. (35)
64	26/38	4.3 (1.5–8.9)	Bosentan ($n = 23$) Prostanoids ($n = 15$) Sildenafil ($n = 9$) Combination therapy ($n = 11$) Calcium channel antagonists ($n = 6$)	mPAP: 58 PVR: 19.7	mPAP: no data PVR: improved by 23% (23 patients taking bosentan)	PVRi improved	Moledina et al. (36)
42	26/16	9.7	Bosentan	mPAP: 48.8 PVR: 16.5	mPAP: 48.3 PVR: 14.1	No significant change in mPAP, PVRi	Hislop et al. (16)

F, Female; M, Male.

TABLE 4 | Patients' survival of treatment with bosentan.

Numbers	F/M	Age, y	Treatment	Survival	Conclusion	References
86	49/37	11.0 (0–18.0)	Bosentan concomitant Prostanoid ($n = 42$) Bosentan ($n = 44$)	The entire group: survival at 1- and 2-year was 100 and 88%, respectively Bosentan: 1- and 2-year survival was 98 and 94% Concomitant prostanoid: 1- and 2-year survival was 98 and 89%, respectively	Bosentan prolongs the life	Rosenzweig et al. (40)
7	6/1	7.4	Bosentan	The 3- and 5-year survival was 100 and 75%, respectively	Survival improved	Simpson et al. (43)
64	26/38	4.3 (1.5–8.9)	Bosentan ($n = 23$) Prostanoids ($n = 15$) Sildenafil ($n = 9$) Combined therapy ($n = 11$) Calcium channel antagonists ($n = 6$)	The entire group: 1-, 3-, and 5-year survival was 89, 84, and 75% for the entire group, respectively	The entire group improved, but with no data in bosentan, and there had no difference among bosentan, prostanoids, and sildenafil	Moledina et al. (36)
36	16/20	10.5 (1.0–16.0)	Bosentan ($n = 11$) Bosentan plus prostanoid ($n = 25$)	The entire group: survival at 1-, 2-, 3-, and 4-year was 98, 88, 82, and 82%, respectively	Most children improved in survival	Ivy et al. (38)
42	26/16	9.7	Bosentan	The survival values was 95, 95, 95, and 55% in 1, 2, 3, and 5 years, respectively	Effective in the long-term management	Hislop et al. (16)
122	73/49	15.0	53 out of 122 patients taking endothelin receptor antagonist: eight out of 53 received sitaxsentan, 45 out of 53 received bosentan	The survival of 122 patients in 6 months, 1- and 2-year was 99, 95, and 90%, respectively	Survival has been improved by targeted therapy	Barst et al. (30)
36	21/15	6.8 (2.0–12.0)	Bosentan	Estimated long-term survival at 2- and 4-year was 91.2 and 84.0%, respectively	There was an improvement in survival	Berger et al. (4)

F, Female; M, Male.

Survival in Patients Treated With Bosentan (42)

Ivy et al. (38) conducted a retrospective observational study in the USA. After the treatment with bosentan, in conjunction with or independent of other PAH-specific therapies, the survival at 1-, 2-, 3-, and 4- years was 98, 88, 82, and 82%, respectively. Despite the differences in children' drug response, bosentan therapy significantly prolonged survival time. A similar conclusion was obtained in the study by Barst et al. (30), Hislop et al. (16), and Berger et al. (4). Each study showed a significant survival benefit with bosentan in pediatric IPAH patients, and survival after bosentan treatment for 3 years was around 90%.

In addition, Simpson et al. (43) compared the survival between bosentan targeted therapy and historic therapy. They reviewed IPAH children at the Royal Melbourne Children's Hospital. Seven children received bosentan treatment and 12 children received historic treatment (such as aspirin, digoxin, CCB, etc.). Survival in the bosentan-treated group was 100% at 3 years and 75% at 5 years, compared with 33% at both time-points in the historic control group. Furthermore, Rosenzweig et al. (40) compared the therapeutic efficacy of bosentan with bosentan plus prostaglandin. They noticed that the 1 and 2 year survival rate of the entire group was 100 and 88%, respectively, 98 and 94% in the bosentan-treated group, and 98 and 89% in the bosentan plus prostaglandin-treated group, respectively. Moledina et al. (36) found that the survival in bosentan monotherapy appeared greater than in combined therapy, and the survival of the entire group was around 89% in 1 year, 84% in 3 years, and 75% in 5 years.

In conclusion, the survival of each group after bosentan treatment fluctuated from 89 to 100% in 1 year, from 89 to 95% in 2 years, and from 84 to 95% in 3 years. Survival was significantly higher than seen in traditional treatments, however there was no significant difference in survival between bosentan monotherapy and combined therapy (**Table 4**).

Safety and Tolerability in Treatment With Bosentan (44–47)

Common adverse reactions are respiratory tract infections, pyrexia, elevations of liver aminotransferases and liver failure (26).

Barst et al. (24) conducted a cohort study of 19 children with IPAH in 2003. Flushing, headache, edema, tachycardia, tremor, and increased liver transaminase levels were reported to be the most frequent adverse events in children who were treated with bosentan. These effects were also reported in the studies of Rosenzweig et al. (40), Simpson et al. (43), Ivy et al. (38), and Beghetti et al. (48).

No patients died during Barst's observation of bosentan treatment (22). However, in Rosenzweig et al. (40), two patients

TABLE 5 | Safety and tolerability in pediatric patients treated with bosentan.

Numbers	F/M	Age, y	Treatment	Safety and side effects	Death	References
19	10/9	3.0–15.0	10 out of 19 received bosentan	No data	No death	Barst et al. (24)
86	49/37	11.0 (0–18.0)	Bosentan concomitant Prostanoid ($n = 42$) Bosentan ($n = 44$)	No data	Bosentan + prostanoid: 3 patients died: two hemoptysis and acute respiratory distress syndrome, one worsening right heart failure Bosentan: two died from right heart failure	Rosenzweig et al. (40)
7	6/1	7.4	Bosentan	No data	One patient died of a pulmonary hypertensive crisis	Simpson et al. (43)
7	3/4	9.6 (1.0–16.0)	Sildenafil ($n = 5$) Bosentan ($n = 2$)	No patient suffered important side effects	No data	Raposo-Sonnenfeld et al. (35)
146	71/75	2.0–11.0	59 out of 146 patients received bosentan	30.8% had at least one safety signal	About 7.5% patients died in the entire group, but not related to bosentan	Beghetti et al. (48)
36	16/20	10.5 (1.0–16.0)	Bosentan ($n = 11$) Bosentan plus prostanoid ($n = 25$)	No data	Six died among 36 patients: one for right heart failure one for sudden death one for worsening pulmonary hypertension one for hemoptysis one for pulmonary hemorrhage one for thromboembolism	Ivy et al. (38)
36	21/15	6.8 (2.0–12.0)	Bosentan	Bosentan-related AEs occurred in 15 (41.7%) patients	Six deaths occurred, but unrelated to bosentan: three from worsen of PAH and cardiac complications, one from respiratory failure following pneumonia	Berger et al. (39)

F, Female; M, Male.

died from right heart failure in the bosentan treatment group, three died in the bosentan plus prostaglandins treatment group, two patients died from hemoptysis and acute respiratory distress syndrome, and one patient died from worsening right heart failure; and all deaths were considered as due to the clinical progression of IPAH. Similar results demonstrated by Simpson et al. (43), shows that three patients needed additional intravenous prostacyclin due to the poor efficacy of bosentan. However, lung transplant was not necessary. Unlike prior studies, among the seven children treated with bosentan in Raposo-Sonnenfeld et al. (35), there were no definite side effects with the exception of menorrhagia after 1 year of treatment. The side effects mentioned above were also seen in the studies by Ivy et al. (37) and Berger et al. (39), where six people died although causes were likely unrelated to bosentan.

In summary, causes for discontinuation of bosentan treatment for pediatric IPAH include worsening heart failure, and progressive pulmonary hypertension. Bosentan-related side effects were less than those related to prostacyclin, and most patients had no serious outcomes. The majority of patients' deaths was attributed to the progression of pulmonary hypertension (**Table 5**).

These retrospective studies demonstrate that bosentan improves efficacy over other targeted therapies, and the effect of bosentan monotherapy has a great influence on 6MWD and WHO functional class. The above data would provide new clinical evidence in hemodynamics and long-term efficacy. The use of bosentan (49, 50) lessened the side effects in prostacyclin with improvements in functional class and hemodynamics (51) on the basis of original prostacyclin treatment (52).

SUMMARY

Bosentan, as an ET-1 receptor antagonist, is an effective drug for children with IPAH. Further clinical studies of multicenter RCTs are needed to clarify its efficacy and safety, and explore the effective dosage for children (53). We look forward to novel breakthroughs in targeted therapy of IPAH in children.

AUTHOR CONTRIBUTIONS

JD, YW, and SC make substantial contributions to conception and design. YW and SC participate in drafting the article or revising it critically for important intellectual content. JD give final approval of the version to be submitted and any revised version.

FUNDING

This work was supported by Beijing Natural Science Foundation, China (7171010).

REFERENCES

1. Vanloon RLE, Roofthooft MTR, Delhaas T, Osch-Gevers MV, Harkel ADJ, Strengers JLM, et al. Outcome of pediatric patients with pulmonary arterial hypertension in the era of new medical therapies. *Am J Cardiol*. (2010) 106:117–24. doi: 10.1016/j.amjcard.2010.02.023
2. Simonneau G, Montani D, Celermajer DS, Denton CP, Gatzoulis MA, Krowka M, et al. Haemodynamic definitions and updated clinical classification of pulmonary hypertension. *Eur Respir J*. (2019) 53:1801913. doi: 10.1183/13993003.01913-2018
3. Qureshi AZ, Tulloh RMR. Paediatric pulmonary hypertension: aetiology, pathophysiology and treatment. *Paediatr Child Health*. (2017) 27:50–7. doi: 10.1016/j.paed.2016.10.001
4. Berger RMF, Beghetti M, Humpl T, Raskob GE, Ivy DD, Jing ZC, et al. Clinical features of paediatric pulmonary hypertension: a registry study. *Lancet*. (2012) 379:537–46. doi: 10.1016/S0140-6736(11)61621-8
5. Spindler M, Schmidt M, Geier O, Sandstede J, Hahn D, Ertl G, et al. Functional and metabolic recovery of the right ventricle during bosentan therapy in idiopathic pulmonary arterial hypertension. *J Cardiovasc Magn Reson*. (2005) 7:853–54. doi: 10.1080/10976640500295540
6. Liu Q, Zhang C, Li QQ, Zhu Y, Zhang D, Zhao WJ, et al. Analysis of prognosis and associated risk factors in pediatric idiopathic pulmonary arterial hypertension. *Chin J Pediatr*. (2018) 56:23–8. doi: 10.3760/cma.j.issn.0578-1310.2018.01.007
7. Douwes JM, Berger RM. Epidemiology of pediatric pulmonary hypertension. In: Cruz EM, editor. *Pediatric and Congenital Cardiology, Cardiac Surgery and Intensive Care*. London: Springer (2013). p. 2123–37. doi: 10.1007/978-1-4471-4619-3_204
8. Jin HF, Yang JY, Zhang QY, Du JB. Epidemiology and clinical management of pulmonary hypertension in children. *Korean Circ J*. (2012) 42:513–6. doi: 10.4070/kcj.2012.42.8.513
9. Tang Y, Yao L, Liu ZH, Ma XP, Luo Q, Zhao ZH, et al. Effect of calcium channel blockers evaluated by cardiopulmonary exercise testing in idiopathic pulmonary arterial hypertension responding to acute pulmonary vasoreactivity testing. *Clin Pharmacol Ther*. (2017) 43:26–31. doi: 10.1016/j.pupt.2017.01.012
10. Ivy DD, Saji BT. A new era in medical management of severe pediatric pulmonary arterial hypertension. *Pediatr Cardiol Cardiac Surg*. (2012) 26:206–18.
11. Vorhies EE, Ivy DD. Drug treatment of pulmonary hypertension in children. *Pediatr Drugs*. (2013) 16:43–65. doi: 10.1007/s40272-013-0052-2
12. Hall SM, Davie N, Klein N, Haworth SG. Endothelin receptor expression in idiopathic pulmonary arterial hypertension: effect of bosentan and epoprostenol treatment. *Eur Respir J*. (2011) 38:851–60. doi: 10.1183/09031936.00167010
13. Hansmann G, Apitz C. Treatment of children with pulmonary hypertension. Expert consensus statement on the diagnosis and treatment of paediatric pulmonary hypertension. The European Paediatric Pulmonary Vascular Disease Network, endorsed by ISHLT and DGPK. *Heart*. (2016) 102:ii67–85. doi: 10.1136/heartjnl-2015-309103
14. Chester AH, Yacoub MH. The role of endothelin-1 in pulmonary arterial hypertension. *Glob Cardiol Sci Pract*. (2014) 2014:62–78. doi: 10.5339/gcsp.2014.29
15. Davenport AP, Hyndman KA, Dhaun N, Southan C, Kohan DE, Pollock JS, et al. Endothelin. *Pharmacol Rev*. (2016) 68:357–418. doi: 10.1124/pr.115.011833
16. Hislop AA, Moledina S, Foster H, Schulze-Neick I, Haworth SG. Long-term efficacy of bosentan in treatment of pulmonary arterial hypertension in children. *Eur Respir J*. (2011) 38:70–7. doi: 10.1183/09031936.00053510
17. Hsu HH, Chen JS, Chen RJ, Ko WJ, Kuo SW, Wu ET, et al. Long-term outcome and effects of oral bosentan therapy in Taiwanese patients with advanced idiopathic pulmonary arterial hypertension. *Respir Med*. (2007) 101:1556–62. doi: 10.1016/j.rmed.2006.12.007
18. Huang B, Yang XH. Progress in targeted drug therapy for pulmonary hypertension in children. *J Practical Med*. (2015) 18:3106–8.

19. Kunichika N, Landsberg JW, Yu Y, Kunichika H, Thistlethwaite PA, Rubin LJ, et al. Bosentan inhibits transient receptor potential channel expression in pulmonary vascular myocytes. *Am J Respir Crit Care Med*. (2004) 170:1101–7. doi: 10.1164/rccm.200312-1668OC
20. Pullamsetti SS, Savai R, Janssen W, Dahal BK, Seeger W, Grimminger F, et al. Inflammation, immunological reaction and role of infection in pulmonary hypertension. *Clin Microbiol Infect*. (2011) 17:7–14. doi: 10.1111/j.1469-0691.2010.03285.x
21. Berger RMF, Gehin M, Beghetti M, Ivy D, Kusic-Pajic A, Cornelisse P, et al. A bosentan pharmacokinetic study to investigate dosing regimens in paediatric patients with pulmonary arterial hypertension: FUTURE-3. *Br J Clin Pharmacol*. (2017) 83:1734–44. doi: 10.1111/bcp.13267
22. Géhin M, Sidharta PN, Dingemanse J. Bosentan pharmacokinetics in pediatric patients with pulmonary arterial hypertension: comparison of dried blood spot and plasma analysis. *Pharmacology*. (2016) 98:111–4. doi: 10.1159/000446583
23. Dingemanse J, Giersbergen P.L.M. Clinical pharmacology of bosentan, a dual endothelin receptor antagonist. *Clin Pharmacokinet*. (2004) 43:1089-115. doi: 10.2165/00003088-200443150-00003
24. Barst RJ, Ivy D, Dingemanse J, Widlitz A, Schmitt K, Doran A, et al. Pharmacokinetics, safety, and efficacy of bosentan in pediatric patients with pulmonary arterial hypertension. *Clin Pharmacol Ther*. (2003) 73:372–82. doi: 10.1016/S0009-9236(03)00005-5
25. Beghetti M, Haworth SG, Bonnet D, Barst RJ, Acar P, Fraisse A, et al. Pharmacokinetic and clinical profile of a novel formulation of bosentan in children with pulmonary arterial hypertension: the FUTURE-1 study. *Br J Clin Pharmacol*. (2009) 68:948–55. doi: 10.1111/j.1365-2125.2009.03532.x
26. U. S. Food Drug Administration. Center for Drugs Evaluation Research (2019). *Approval Date(s) and History, Letters, Labels, Reviews for bosentan*. Washington, DC: Author. (Reference ID: 4434193). Retrieved from: https://www.accessdata.fda.gov/drugsatfda_docs/label/2019/021290s039, 209279s005lbl.pdf#page=30\protect\T1\textdollar\protect\T1\textdollar (accessed on 28, June 2019).
27. European Medicines Agency. Science Medicines Health (2014). *Tracleer*. Retrieved from: https://www.ema.europa.eu/en/documents/product-information/tracleer-epar-product-information_en.pdf (accessed on 28, June 2019).
28. Ogawa A, Ejiri K, Matsubara H. Long-term patient survival with idiopathic/heritable pulmonary arterial hypertension treated at a single center in Japan. *Open Life Sci*. (2014) 118:414–9. doi: 10.1016/j.lfs.2014.01.077
29. Adatia I, Haworth SG, Wegner M, Barst RJ, Ivy D, et al. Clinical trials in neonates and children: report of the pulmonary hypertension academic research consortium pediatric advisory committee. *Pulm Circ*. (2013) 3:252–66. doi: 10.4103/2045-8932.109931
30. Barst RJ, McGoon MD, Elliott CG, Foreman AJ, Miller DP, Ivy DD. Survival in childhood, pulmonary, arterial, hypertension: insights from the registry to evaluate early and long-term pulmonary arterial hypertension disease management. *Circulation*. (2012) 125:113–22. doi: 10.1161/CIRCULATIONAHA.111.026591
31. Yung D, Widlitz AC, Rosenzweig EB, Kerstein D, Maislin G, Barse RJ. Outcomes in children with idiopathic pulmonary arterial hypertension. *Circulation*. (2004) 110:660–5. doi: 10.1161/01.CIR.0000138104.83366.E9
32. Maron BA, Waxman AB, Opotowsky AR, Gillies H, Blair C, Aghamohammadzadeh R, et al. Effectiveness of spironolactone plus ambrisentan for treatment of pulmonary arterial hypertension (from the [ARIES] Study 1 and 2 Trials). *Am J Cardiol*. (2013) 112:720–5. doi: 10.1016/j.amjcard.2013.04.051
33. Lkehara S, Takatsuki S, Nakayama T, Naoi K, Matsuura H, Saji T. Clinical impact of main pulmonary artery dilatation on outcome in pediatric idiopathic and heritable pulmonary arterial hypertension. *Circ J*. (2018) 82:541–5. doi: 10.1253/circj.CJ-17-0092
34. Maiya S, Hislop AA, Flynn Y, Haworth SG. Response to bosentan in children with pulmonary hypertension. *Heart*. (2006) 92:664–70. doi: 10.1136/hrt.2005.072314
35. Raposo-Sonnenfeld I, Otero-Gonzalez I, Blanco-Aparicio M, Ferrer-Barba A, Medrano-Lopea C, et al. Treatment with sildenafil, bosentan, or both in children and young people with idiopathic pulmonary arterial hypertension and Eisenmenger's syndrome. *Rev Esp Cardiol*. (2007) 60:366–72. doi: 10.1016/S1885-5857(07)60169-8
36. Moledina S, Hislop AA, Foster H, Schulze-Neick I, Haworth SG. Childhood idiopathic pulmonary arterial hypertension: a national cohort study. *Heart*. (2010) 96:1401–6. doi: 10.1136/hrt.2009.182378
37. Ivy DD, Doran A, Claussen L, Bingaman D, Yetman A. Weaning and discontinuation of epoprostenol in children with idiopathic pulmonary arterial hypertension receiving concomitant bosentan. *Am J Cardiol*. (2004) 93:943–46. doi: 10.1016/j.amjcard.2003.12.031
38. Ivy DD, Rosenzweig EB, Lemarie JC, Brand M, Rosenberg D, Barst RJ. Long-term outcomes in children with pulmonary arterial hypertension treated with bosentan in real-world clinical settings. *Am J Cardiol*. (2010) 106:1332–8. doi: 10.1016/j.amjcard.2010.06.064
39. Berger RMF, Haworth SG, Bonnet D, Dulac Y, Fraisse A, Galie N, et al. FUTURE-2: Results from an open-label, long-term safety and tolerability extension study using the pediatric formulation of bosentan in pulmonary arterial hypertension. *Int J Cardio*. (2016) 202:52–8. doi: 10.1016/j.ijcard.2015.08.080
40. Rosenzweig EB, Ivy DD, Widlitz A, Doran A, Claussen LR, Yung D, et al. Effects of long-term bosentan in children with pulmonary arterial hypertension. *J Am Coll Cardiol*. (2005) 46:697–704. doi: 10.1016/j.jacc.2005.01.066
41. Hansmann G. Pulmonary hypertension in infants, children, and young adults. *J Am Coll Cardiol*. (2017) 69:2551–69. doi: 10.1016/j.jacc.2017.03.575
42. Zijlstra WMH, Douwes JM, Rosenzweig EB, Schokker S, Krishnan U, Roofthooft MTR, et al. Survival differences in pediatric pulmonary arterial hypertension. *J Am Coll Cardiol*. (2014) 63:2159–69. doi: 10.1016/j.jacc.2014.02.575
43. Simpson CM, Penny DJ, Cochrane AD, Davis AM, Rose ML, Wilson SE, et al. Preliminary experience with bosentan as initial therapy in childhood idiopathic pulmonary arterial hypertension. *J Heart Lung Transplant*. (2006) 25:469–73. doi: 10.1016/j.healun.2005.11.438
44. Takatsuki S, Nakayama T, Lkehara S, Matsuura H, Ivy DD, Saji T, et al. Pulmonary arterial capacitance index is a strong predictor for adverse outcome in children with idiopathic and heritable pulmonary arterial hypertension. *J Pediatr*. (2017) 180:75–9. doi: 10.1016/j.jpeds.2016.10.003
45. Akagi S, Matsubara H, Miyaji K, Ikeda E, Dan K, Tokunaga N, et al. Additional effects of bosentan in patients with idiopathic pulmonary arterial hypertension already treated with high-dose epoprostenol. *Circ J*. (2008) 72:1142–6. doi: 10.1253/circj.72.1142
46. Takatsuki S, Yanai S, Ikehara S, Nakayama T, Matsuura H. Clinical effects of syncope on disease severity and adverse outcomes in children with idiopathic and heritable pulmonary arterial hypertension. *Pediatr Cardiol*. (2019) 40:209–14. doi: 10.1007/s00246-018-1996-3
47. Gruening E, Michelakis E, Vachiery JL, Vizza CD, Meyer FJ, Doelberg M, et al. Acute hemodynamic effects of single-dose sildenafil when added to established bosentan therapy in patients with pulmonary arterial hypertension: Results of the COMPASS-1 study. *J Clin Pharmacol*. (2013) 49:1343–52. doi: 10.1177/0091270009341182
48. Beghetti M, Hoeper MM, Kiely DG, Carlsen J, Schwierin B, Segal ES, et al. Safety experience with bosentan in 146 children 2–11 years old with pulmonary arterial hypertension: results from the European postmarketing surveillance program. *Pediatr Res*. (2008) 64:200–4. doi: 10.1203/PDR.0b013e318179954c
49. Dyer KL, Pauliks LB, Das B, Shandas R, Ivy D, Shaffer EM, et al. Use of myocardial performance index in pediatric patients with idiopathic pulmonary arterial hypertension. *J Am Soc Echocardiogr*. (2006) 19:21–7. doi: 10.1016/j.echo.2005.07.010
50. Hoeper MM, Huscher D, Ghofrani HA, Delcroix M, Distler O, Schweiger C, et al. Elderly patients diagnosed with idiopathic pulmonary arterial hypertension: results from the COMPERA registry. *Int J Cardiol*. (2013) 168:871–80. doi: 10.1016/j.ijcard.2012.10.026
51. Sitbon O, Mclaughlin VV, Badesch DB, Barst RJ, Black C, Galie N, et al. Survival in patients with class III idiopathic pulmonary arterial hypertension treated with first line oral bosentan compared with an historical cohort

of patients started on intravenous epoprostenol. *Thorax.* (2005) 60:1025–30. doi: 10.1136/thx.2005.040618

52. Hsu HH, Wu ET, Chen JS, Wu MH, Wang JK, Ko WJ, et al. Bosentan is an alternative treatment option in a child with severe idiopathic pulmonary artery hypertension and abnormal liver enzymes. *Respir Med Extra*. (2005) 1:140–3. doi: 10.1016/j.rmedx.2005.08.004
53. Douwes JM, Roofthooft MTR, Vanloon RLE, Ploegstra MJ, Bartelds B, Hillege HL, et al. Sildenafil add-on therapy in paediatric pulmonary arterial hypertension, experiences of a national referral centre. *Heart.* (2014) 100:224–30. doi: 10.1136/heartjnl-2013-304895

Conflict of Interest Statement: The authors declare that the research was conducted in the absence of any commercial or financial relationships that could be construed as a potential conflict of interest.

frontiers in Pediatrics

ORIGINAL RESEARCH
published: 24 July 2019
doi: 10.3389/fped.2019.00288

MiR-223-3p Alleviates Vascular Endothelial Injury by Targeting IL6ST in Kawasaki Disease

Xiang Wang[1,2†], Yue yue Ding[1†], Ye Chen[1], Qiu qin Xu[1], Guang hui Qian[1,3], Wei guo Qian[1], Lei Cao[1], Wan ping Zhou[1], Miao Hou[1] and Hai tao Lv[1]*

[1] Department of Cardiology, Children's Hospital of Soochow University, Suzhou, China, [2] Department of Pediatrics, The Affiliated Huaian No.1 People's Hospital of Nanjing Medical University, Huaian, China, [3] Pediatric Research Institute of Soochow University, Suzhou, China

Background: Kawasaki disease (KD) is a self-limiting illness with acute systematic vascular inflammation. It causes pathological changes in mostly medium and small-sized arteries, especially the arteria coronaria, which adds the risk of developing coronary heart disease in adults.

Materials and methods: We detected the miR-223-3p expression in 30 KD patients combined with 12 normal controls using miRNA microarrays and RT-PCR. A KD mouse model was constructed using Candida albicans water insoluble substance (CAWS). We also checked the miR-223-3p's expression using qRT-PCR. The Luciferase reporting system was implemented to validate the correlation between miR-223-3p and Interleukin-6 receptor subunit beta (IL-6ST). TNF-α was used to stimulate human coronary artery endothelial cells (HCAECs), and miR-223-3p activator or inhibitor and KD serum were used to treat HCAECs. A Western blotting automatic quantitative analysis protein imprinting system was used to test the expression of signal transducer and the activator of transcription 3 (STAT3), phosphorylated-signal transducer and the activator of transcription 3 (pSTAT3) and NF-κB p65.

Results: Clinical trials found that miR-223-3p expressions were markedly different (more than 2-fold) between the acute KD group and the control group. E-selectin and intercellular cell adhesion molecule-1 (ICAM-1) levels were also significantly higher (about 2-fold) in KD especially with coronary artery lesions. MiR-223-3p could alleviate vascular endothelial damage in KD mice, and IL-6 (Interleukin-6), E-selectin and ICAM-1 were simultaneously negative. The values of IL-6, E-selectin, and ICAM-1 mRNA expressions decreased, while the value of IL-6ST was increased between the agonist treated mice and KD mice. The RT-qPCR consequences displayed that miR-223-3p explored the highest expression on the third day in both the KD mice as well as the agonist group. MiR-223-3p can directly combine with IL-6ST 3' untranslatable regions (UTR) and held back the IL-6's expression. Overexpression of miR-223 down regulated IL6ST expression and decreased the expression of p-STAT3 and NF-κB p65, while the miR-223 inhibitor could reverse the above process.

Conclusion: MiR-223-3p is an important regulatory factor of vascular endothelial damage in KD and could possibly become a potential target of KD treatment in the future.

Keywords: Kawasaki disease, MicroRNA-223-3p, IL6ST, vascular endothelial damage, STAT3

OPEN ACCESS

Edited by:
Hongfang Jin,
Peking University First Hospital, China

Reviewed by:
Giuseppina Milano,
Lausanne University Hospital (CHUV), Switzerland
Wei Sheng,
Children's Hospital, Fudan University, China
Zhong-Dong Du,
Beijing Children's Hospital, Capital Medical University, China

***Correspondence:**
Hai tao Lv
haitaosz@163.com

[†] These authors have contributed equally to this work

Specialty section:
This article was submitted to Pediatric Cardiology, a section of the journal Frontiers in Pediatrics

Received: *19 February 2019*
Accepted: *26 June 2019*
Published: *24 July 2019*

Citation:
Wang X, Ding Y, Chen Y, Xu Q, Qian G, Qian W, Cao L, Zhou W, Hou M and Lv H (2019) MiR-223-3p Alleviates Vascular Endothelial Injury by Targeting IL6ST in Kawasaki Disease. Front. Pediatr. 7:288. doi: 10.3389/fped.2019.00288

INTRODUCTION

Kawasaki disease (KD) is an acute systemic vascular inflammatory pathema, which largely impacts medium and small-sized arteries, particularly the arteria coronaria (1). Without early intervention, about 20% of children with KD may develop coronary artery aneurysms (2). Studies have found that the deregulation of innate immunity, vascular endothelial growth factor (VEGF) A and other reasons such as infectious factors are closely related to the pathogenesis of KD (3–5). However, the etiology of KD remains unclear. This underlines the need to reveal the potential pathogenesis mechanisms of KD, thus providing novel therapeutic targets for the condition.

MicroRNAs (miRNAs) are 18–25 small nucleotide non-coding RNAs which can adjust and control the genetic expression by imperfect hybridization to the 3′ untranslatable regions (UTR) of target mRNAs (6). miRNAs regulate nearly one third of the human gene function, and are involved in cell multiplication, growth, apoptosis, and the metabolism of important biological processes (7). For instance, in acute KD, microRNA-93 has been declared to regulate the expression of VEGF and is possibly involved in the pathogenesis of arteritis (8).

MiR-223 is deemed to be a cell–specific, hematopoietic lineage miRNA, which are exclusively expressed in blood cells such as blood platelets and leukocytes which are derived from bone marrow (9). Recent research has revealed that miR-223 participates in the development of atherosclerosis in experimental mice suffering from chronic kidney disease (CKD) (10). It has also been noted that as a receptor of the insulin-like growth factor 1, miR-223 can promote human umbilical vein endothelial cells apoptosis (11). These findings reveal that miR-223 could also be involved in vascular diseases such as KD which is explored in the present study. Results show that miR-223-3p plays a protective role against endothelial injury in KD, by targeting IL6ST and by regulating the STAT3-NF-κB signaling pathway, making it a potential target for the diagnosis and treatment of KD.

MATERIALS AND METHODS

Patient Characteristics

Plasma specimens were collected from KD children ($n = 6$; two males and four females, mean age, 24 months) and healthy controls ($n = 6$; two males and four females; mean age, 18 months) for miRNA microarray hybridization. Plasma specimens, used for the investigation, were collected from 30 patients [18 males and 12 females; median age: 18 months (range: 4–90 months)] with acute and subacute KD. Considering fever onset as the first day of the KD course, acute stage (prior treatment of intravenous human immunoglobulin, range: 1–10 days), subacute stage (post-treatment of intravenous human immunoglobulin, normothermia, range: 11–21 days). These groups were subdivided into coronary artery lesions (CALs) ($n = 10$) and no coronary artery lesions (nCALs) ($n = 20$) subgroups. CALs mainly include occlusion, localized stenosis, segmental stenosis, dilatation, and aneurysms during coronary angiography. In our study, echocardiography was utilized to detect cardiac vasodilation and coronary aneurysms at admission. The maximum inner diameters of both the left and right coronary arteries were measured in the two groups. CALs were defined as those whose maximum internal diameters were larger than 3.5 mm in those aged >9 y, larger than 3.0 mm in those aged 3–9 y, and larger than 2.5 mm in those aged <3 y. The diagnosis of KD was made on the basis of the criteria developed in 2004 by the American Heart Association. All patients, including those with KD and febrile controls, from the Cardiology Department, of the Children's Hospital of Soochow University (Suzhou, Jiangsu Province, China) were enrolled, from August 2015 to August 2016. In addition, plasma samples were collected from 24 controls comprising 12 healthy controls after routine physical examinations (male: $n = 8$; female: $n = 4$; median age:30 months) (12–84 months) and 12 febrile patients with proven respiratory infection (male: $n = 7$; female: $n = 5$; median age: 29 months) (range: 8–81 months). The whole blood sample (2 ml) was drawn into an EDTA-containing tube. After being centrifuged for 15 min at 3,500 rpm to spin down the blood cells, the supernatant was shifted into a clean microcentrifuge tube, followed with the second centrifugation to absolutely eliminate the cellular components. Plasma was then aliquoted and stored in a refrigerator at −80°C partitions for further use. All the study participants were obliged to provide signed informed consent, and the research was undertaken in light of the institutional ethics committees approved protocol and HIPAA regulations.

CAWS KD Mice Model

Kawasaki disease was simulated by intraperitoneal injection (20 mg/Kg; 5 consecutive days) of Candida albicans water-soluble fraction (CAWS) to C57BL/6 male mice of 4–6 weeks of age. miR-223-3p activator was purchased from GeneCopoeia (Rockville, MD, USA), and dispersed in PBS. KD mice received a tail vein injection of miR-223-3p activator (1 mg/kg). Seventy-two mice were divided into three groups randomly: ① The control group: normal saline intraperitoneal injection (0.1 ml;5 consecutive days). ② The KD group: CAWS intraperitoneal injection (0.1 ml, 20 mg/Kg; 5 consecutive days). ③ MiR-223-3p activator group: CAWS intraperitoneal injection (0.1 ml, 20 mg/Kg; 5 consecutive days) and tail vein injections of miR-223-3p activator (1 mg/kg, in the fifth day). Each group was sacrificed on the first day (6 day), third day (8 day), fifth day (10 day), seventh day (12 day), and tenth day (15 day), respectively. Post-sacrifice, whole blood from mice was drawn into EDTA-containing tubes and serum was extracted following the same protocol as with a patients' blood. Observation of the aorta was achieved under HE staining and a scanning electron microscope (SEM).

Cell Culture and Treatment

HCAECs were purchased from American Type Culture Collection (ATCC) (Manassas, VA, USA) and were cultured to confluence in RPMI 1640 medium (Gibco; Thermo Fisher Scientific, MA, USA) mixed with both 1% penicillin/streptomycin and 10% fetal bovine serum, in a humidified atmosphere with 5% CO_2 and the temperature was maintained at 37°C. HCAECs were then randomly and

transiently transfected with miR-223-3p activators, negative control oligonucleotides or miR-223-3p inhibitors (all were compounded by Shanghai Genechem Co. Ltd, Shanghai) acting on Lipofectamine 2000 reagent (Invitrogen; Thermo Fisher Scientific, Inc). HCAECs were seeded in a six-well plate, at 1×10^5 cells/ml. Transfection was performed after the cells reached 70% confluence. 20 nmol/L of miR-223 activators, negative control or miR-223 inhibitors were dispersed in Opti-MEM (Thermo Fisher Scientific) with twice the volume of Lipofectamine 2000. After 15 min quiescence at room temperature, the mixture was added into HCAECs 6 h post transfection, cells were given a PBS wash and the medium was replaced. The cells were then incubated in the aforementioned conditions and harvested after 24 h. For the KD serum stimulation assay, HCAECs were stimulated with acute phase KD serum and the healthy control group, respectively. Prior to use, we first used a 30 min long bath in 56°C water to inactivate the serum from holding back any immune response. Then the HCAECs were incubated in the serum-containing media for 48 h, after which they were harvested, and total mRNA was extracted from them. Finally, the RT-qPCR was utilized to celebrate the miR-223-3p expression level.

Reverse Transcription and Real-Time PCR

An MiRNeasy Serum/Plasma Kit (Qiagen) and miRNeasy Mini Kit (Qiagen, Hilden, Alemania) were used to extract the total RNA from the serum samples and the cells, respectively. An MiRNA specific Taqman MicroAssay (#4427975; ID 002619; Applied Biosystems) and Taqman miRNA Reverse Transcription Kit (Applied Biosystems) were used for reverse transcription. Specific primers used for all the microRNAs were obtained from Applied Biosystems [hsa-miR-16 (internal reference): upstream primer sequence 5′TAGCAGCACGTAAATATTG GCG3′; hsa-miR-223-3p: upstream primer sequence 5′TGT CAGTTTGTCAAATACCCCA3′;hsa-miR-765:upstream primer sequence 5′TGGAGGAGAAGGAAGGTGATG3′;hsa-miR-33b-3p:upstream primer sequence 5′CAGTGCCTCGG CAGTGCAGCCC3′; The downstream primer comes with the Qiagen kit]. These reactions were all carried out in duplicate in the 96-well plates, and the data were evaluated with the help of 7900HT Fast Real-Time PCR systems (Applied Biosystems).

MTT Assay

The proliferation rate of the transfected HCAECs was detected by the MTT assay. Briefly, 1×10^4 cells/well was suspended in 200 μl culture medium and seeded in a plate with 96-wells. After 24 h of cell seeding, we first used the serum-free medium containing 5 μg/ml MTT to replace the culture medium. Then, after further incubation for 4 h, the serum-free medium was replaced by DMSO, mixed well, and finally the SpectraMax 190 (Molecular Devices in Sunnyvale, CA, USA) was used to measure the optical density by recording the absorbance at 490 nm.

Luciferase Assay

HCAECs were seeded in a 24-well plate first. miR-223-3p and Mut 3′UTR or WT 3′UTR of IL6ST or the control mimics were co-transfected at the same time. After 48 h of incubation, cells were reaped using the DualLuciferase® Reporter Assay System (Promega, Madison, WI, USA) for Renilla and firefly luciferase activity assays.

Western Blotting

RIPA lysis buffer, supplemented with complete protease inhibitor cocktail (Beyotime, China) were employed to lyse the transfected HCAECs. Then we used the BCA Protein Assay Kit (Beyotime, China) to isolate the total protein. Immediately, 30 μg of total protein in the loading buffer were loaded per lane and separated by the Sodium Dodecyl Sulfate Polyacrylamide Gel Electrophoresis (SDS-PAGE) for immunoblotting. Polyvinylidene difluoride (PVDF) membranes were then used to transfer those separated proteins. After blocking the membrane for 60 min using 5% skimmed milk, we used those primary antibodies STAT3 (ab119352, abcam), pSTAT3 (phospho Y705, ab76315, abcam), NF-kB p65 (ab16502, abcam), β-actin (66009-1-Ig, Proteintech), IL6ST (ab202850, abcam) to incubate with the membranes overnight at 4°C. On the next day, post-wash, the membranes were incubated at room temperature with secondary antibodies for 2 h, then we used chemiluminescence to detect the protein bands.

Statistical Analysis

Data was presented as the mean ± standard deviation ($\bar{x}$±SD) or median (range: minimum, maximum) from at least three independent experiments. One-way analysis of variance (one-way ANOVA) with the Newman-Keuls comparison test was employed to determine the significant difference between groups. Statistical analysis was carried out using SPSS 17.0 software (IBM Corporation, Armonk, NY, USA). A level of $p < 0.05$ was considered as statistically significant.

RESULTS

The Expression Level of MiR-223-3p Is Upregulated in the Serum of Patients With KD

MiRNA microarrays revealed seven prominently upregulated miRNAs (hsa-let-7b-5p, hsa-miR-223-3p, hsa-miR-765, hsa-miR-4485, hsa-miR-4644, hsa-miR-4800-5p, sa-miR-6510-5p) and three remarkably downregulated miRNAs (hsa-miR-33b-3p, hsa-miR-4443, and hsa-miR-4515) among the plasma samples of six acute KD patients, compared with the levels detected in the healthy groups. So, the expression levels of these 10 miRNAs were accessed subsequently. Amongst 10 different miRNAs assessed, miR-223-3p was proved to be dramatically increased in the KD serum, almost about 9-fold higher ($p < 0.001$) in contrast to the healthy control group (**Figure 1A**).

HCAECs Stimulated With KD Serum

As an *in vitro* model, HCAECs were applied to study the vascular endothelium's function in our research. In order to test whether KD serum could increase miR-223-3p, KD acute stage serum was employed as a stimulant. The miR-223-3p expression level was determined followed by 48 h stimulation. The results revealed that there was a striking increase of the miR-223-3p level in those cultured with KD serum cells, but not for those in the healthy

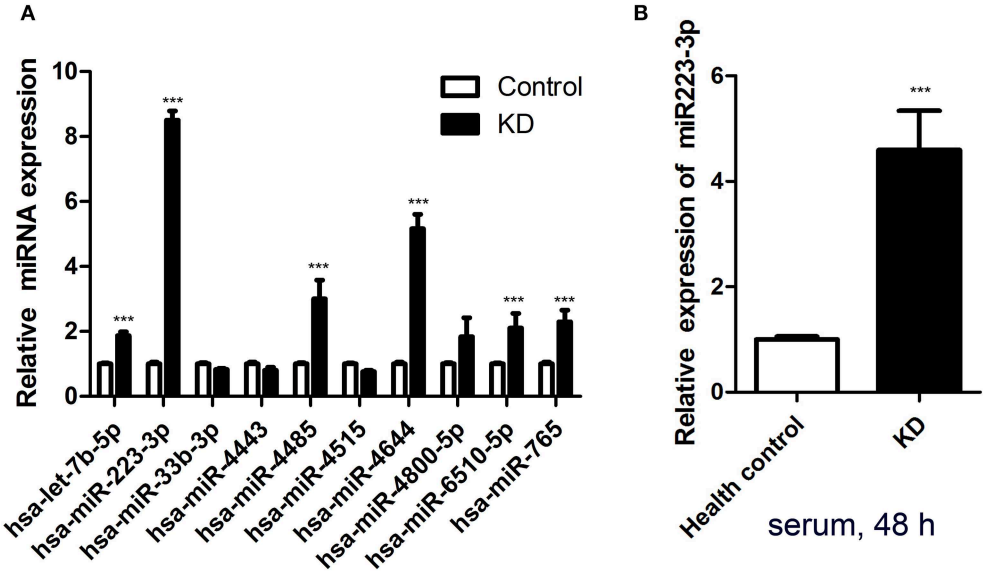

FIGURE 1 | Serum miR-223-3p was increased in patients with KD. **(A)** The result of Affymetrix microRNA microarrays for the expression of 10 miRNAs in Kawasaki disease acute stage plasma. **(B)** Expression of miR-223-3p was measured in HCAECs by RT-qPCR at 48 h following culture with 2 ml serum from KD patients and healthy controls ($n = 3$). Data are presented as mean ± standard error of mean, $^{***}P < 0.001$.

control group (**Figure 1B**). A probable mechanism of miR-223-3p was thus indicated in affecting the endothelial cells during the pathogenesis of KD.

Increased Expression of miR-223-3p Was Peculiar in Acute KD

We assessed the miR-223-3p expression level during both the acute and subacute stages of KD. Results displayed that the miR-223-3p expression level augmented 2-folds in the acute stage of KD ($p < 0.001$) and declined to 70% in the subacute stage of KD ($p = 0.021$), in comparison with the pyrexia control group (**Figure 2A**). Further, in acute KD serum, the miR-223-3p expression level was lower in the serum sample obtained from the CAL group than that in the nCAL group (**Figure 2E**). Similarly, we measured the variation in the expression levels of IL-6, ICAM-1, and E-selectin during different stages of KD at the same time. The trend was similar to miR-223-3p expression, where all the three molecules were found to be increasingly expressed in the acute stage KD serum sample while decreased in the subacute stage (**Figures 2B–D**). However, in contrast to the miR-223-3p expression levels in the acute KD serum, the expression of the three molecules increased in the CAL serum compared to that in the nCAL serum (**Figures 2F–H**).

IL6ST Was Found to be a Target Gene of miR-223-3p

To elucidate the underlying mechanism of miR-223-3p, we have planned to explore the miR-223-3p target genes with the help of the TargetScan bioinformatics algorithm. Based on putative target sequences at position 182-205 of the IL6ST 3′UTR, our analysis uncovered the fact that IL6ST is a potential target of miR-223-3p (**Figure 3A**). We then engineered luciferase reporter constructs containing the mutant (Mut) 3′UTR and the wild-type (WT) 3′UTR of the IL6ST to ascertain whether IL6ST can serve as a direct target spot of the miR-223-3p. The luciferase reporter assay data proves that miR-223-3p can remarkably decline the luciferase activity of the IL6ST 3′UTR but not the mutant IL6ST 3′UTR (**Figure 3C**). Additionally, the western blot analyses also revealed the fact that miR-223-3p overexpression dramatically downregulated the expression of IL6ST in HCAECs (**Figure 3B**). The relationship between IL6ST and miR-223-3p was further analyzed by detecting the relative expression level of IL6ST, and a significant negative correlation was observed between the miR-223-3p expression and IL6ST using the Spearman's correlation analysis (**Figure 3D**). Above all, we can conclude that IL6ST is the target gene of miR-223-3p in KD.

miR-223-3p Regulated the Inflammatory Factor Level in KD Mice

Six of the 24 rats died in the CAWS intraperitoneal injection group, and the mortality rate was between 10 and 30%. The majority of mice were found to have intestinal adhesion, intestinal mucosal swelling, obstruction, and even necrosis (**Supplementary Figure 1A**). The hair color of the CAWS groups became yellow and disorderly and they experienced a loss in appetite (**Supplementary Figures 1B,C**). One third of the intraperitoneal injection sites had visible scabs, and local skin erosion was visible in about 1/4 of sites (**Supplementary Figures 1D,E**). We observed two cases of aneurysmal dilatation on the seventh day in the KD group (**Supplementary Figures 1F,G**). By the tenth day, the mental reaction of mice had improved in both groups, the food intake

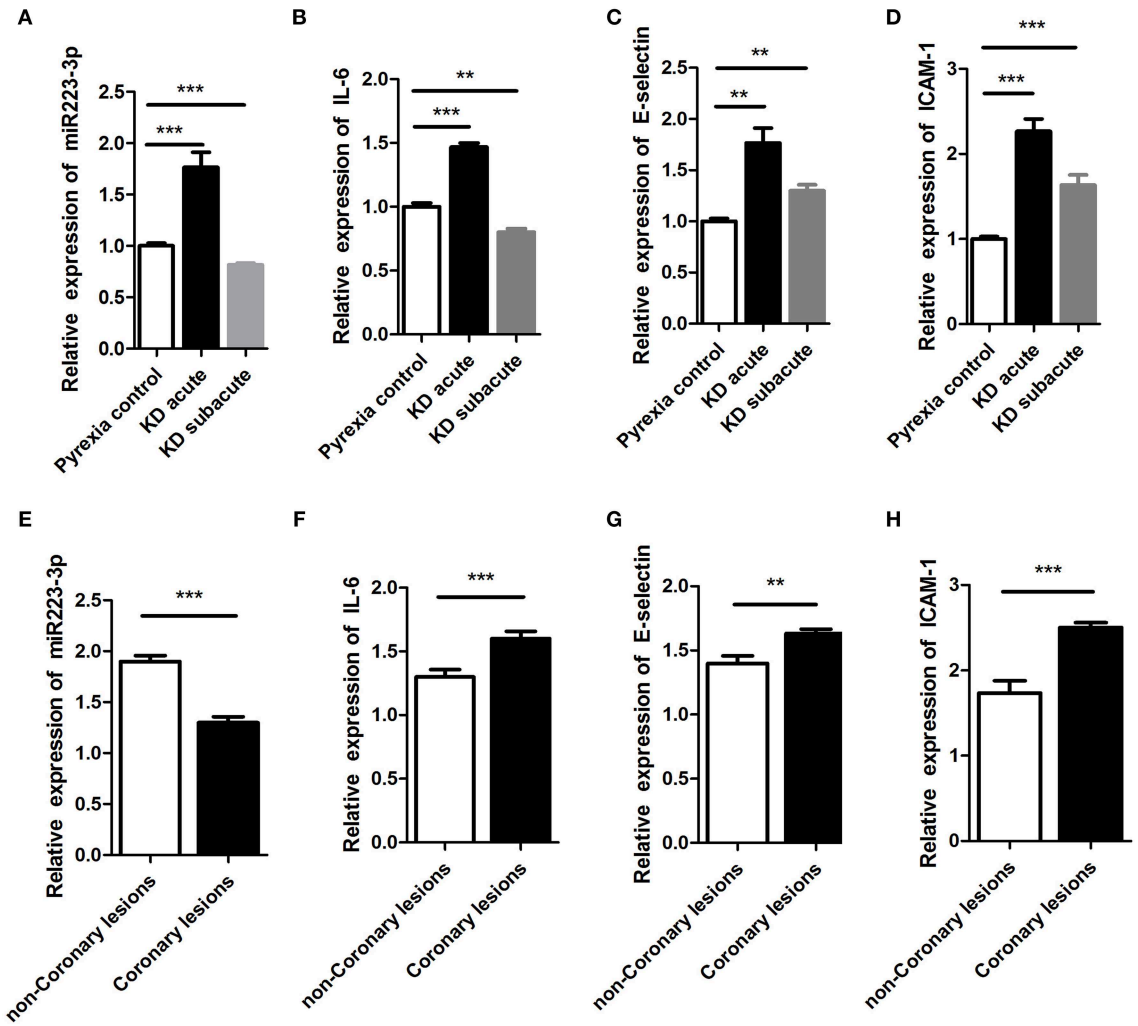

FIGURE 2 | The expression of miR-223-3p was seen to increase in acute stage of KD. panel **(A–D)** represent the relative expression levels of **(A)** miR-223-3p, **(B)** IL-6, **(C)** E-selectin, and **(D)** ICAM-1, respectively, in Pyrexia control, acute KD, and subacute KD. This figure represents the relative expression of **(E)** miR-223-3p, **(F)** IL-6, **(G)** E-selectin, and **(H)** ICAM-1 in coronary lesions group and non-coronary lesions group of KD. $^{**}P < 0.01$ and $^{***}P < 0.001$.

increased, and their hair color became dark and bright. One case of membranous peeling was observed at the end of the toe in the KD group (**Supplementary Figure 1H**). While two of the 24 rats died in the CAWS intraperitoneal injection combined with the miR-223-3p activator tail vein injection group. Obviously the mortality rate in the control group was markedly lower than that of the CAWS group. The results of these pathological specimens suggested that inflammation, thrombosis, and a thickening of the vascular wall were observed in the heart tissue of mice in the KD group, which is consistent with the pathological changes observed in Kawasaki disease vasculitis (**Supplementary Figures 2A–H**). However, there was no more severe vasculitis caused by lactobacillus caseate cell wall extract (LCWS) and the pathological picture was not so typical. In addition, we also compared the pathological discrepancy with HE staining at different time nodes between the KD and the miR-223-3p activator group, but the differences were not so obvious. As is evident by the SEM images (**Figure 4A**), after a period of 4 days post induction, the aorta showed intimal inflammation and the simultaneous appearance of a cavitation endothelial injury. After 6–8 days post induction, the vascular endothelium is shed off, cytoplasmic vacuolation occurs, and the endothelial injury reaches its peak. After a period of 10 days post induction, the inflammatory lesions begin to recede, and the mice enter the recovery phase.

To verify the particular function of miR-223-3p in vascular endothelial injury *in vivo*, the KD mice were injected with miR-223-3p activator. The RT-qPCR results revealed that miR-223-3p explored the highest expression on the third day in both the KD mice as well as the miR-223-3p activator treated KD mice. Both showed a subsequent decrease to the control level on the seventh day (**Figure 4B**). Although IL-6 showed a maximum expression on the third day, which then decreased to the control level on the seventh day. The highest levels of IL-6 were noted on the seventh day, after intraperitoneal injection with the miR-223-3p activator (**Figure 4C**). IL-6ST showed minimal expression on the third day

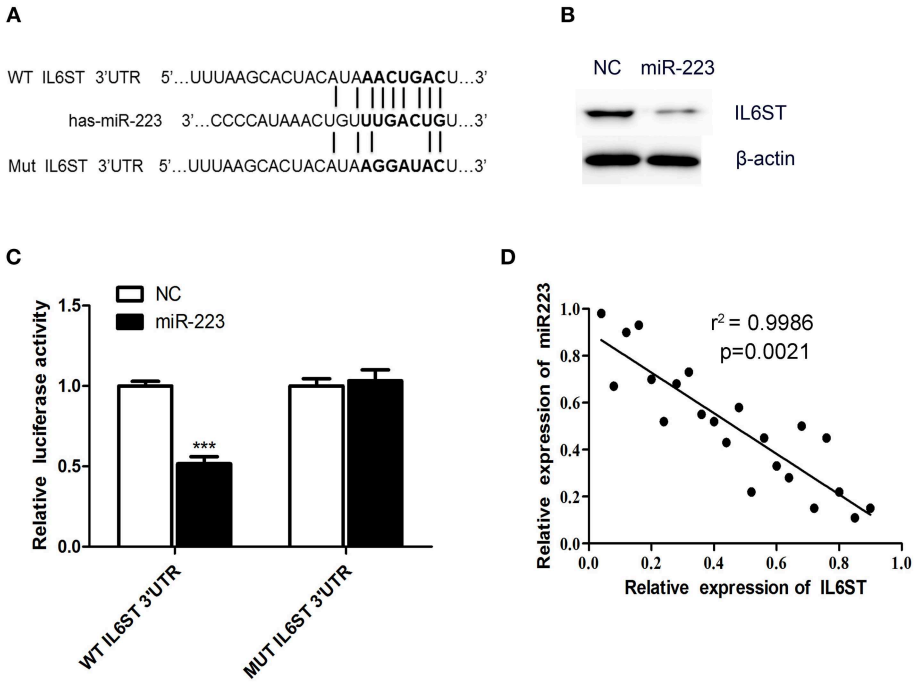

FIGURE 3 | IL6ST is a target gene of miR-223-3p. **(A)** Shows the IL6ST 3′UTR-containing reporter construct. Schematic representation of the miR-223-3p sequence, putative miR-223-3p targeting site in the 3′UTR of IL6ST, and the generated mutant IL6ST 3′UTR. **(B)** The western blot analysis shows that the cells transfected with miR-223 showed lower expression of IL6ST protein. **(C)** Luciferase reporter assay indicates the inhibitory effect that miR-223 has on the luciferase activity of IL6ST-3′UTR. **(D)** Correlation of the expression of IL6ST to that of miR-223-3p in KD samples using simple linear regression analysis. ***$P < 0.001$.

in both the KD mice and the miR-223-3p activator treated KD mice, and then showed an increased expression compared to the control level on the seventh day (**Figure 4D**). Our data revealed that the expression of STAT3 mRNA was highest on the third day in KD mice while the value was the lowest in mice who received a miR-223-3p activator injection (**Figure 4E**). The expression levels of E-selectin and ICAM-1 were also detected, and the results indicated that E-selectin and ICAM-1 both showed the highest expression level on the fifth day and their expression decreased subsequently. However, a notable feature was that the level of E-selectin and ICAM-1 would not decrease to the control level even 10 days post treatment (**Figures 4F,G**).

miR-223 Inhibited the Expression of IL-6ST in TNF-α

TNF-α being one of the most important inflammatory factors, was used for inducing inflammatory injury. We thus investigated the biological function of miR-223-3p in TNF-α treated HCAECs. First we disposed the HCAECs with different concentrations of TNF-α for 12 h, then the cell viability was detected, respectively. The result showed that 50 ng/ml TNF-α could significantly decrease the viability of HCAECs concentrations while when concentrations of TNF-α were higher than 50 ng/ml it could not decrease the cell viability any further (**Figure 5A**). A time-based experiment showed that cell viability began to decrease after being treated by 50 ng/ml of TNF-α for a period of 6 h. And when treated for 8 h or longer, it showed no further decrease in the cell viability anymore (**Figure 5B**). Thus, HCAECs were designed to be treated with 50 ng/ml TNF-α for 8 h in further experiments. Treatment of HCAECs with miR-223-3p activator showed that TNF-α could partially inhibit miR-223-3p expression under the influence of the miR-223-3p activator (**Figure 5C**). While the decrease of the miR-223-3p mRNA expression level was not significant ($p > 0.05$) in contrast to the control group (**Figure 5D**), this may possibly be due to the fact that the basic expression level of miR-223-3p was too low. However, when treated with TNF-α 50 ng/ml, the miR-223-3p inhibitor caused a dramatical decrease in the expression level of miR-223-3p (**Figure 5E**). The expression level of IL6ST mRNA was also detected and the results are as indicated in **Figures 5F,G**. The miR-223-3p activator significantly decreases the expression of IL6ST, when co-treated with TNF-α. IL6ST expression is much lower in this case compared to when treated with the miR-223-3p activator alone. The miR-223-3p inhibitor was seen to partially increase the expression of IL6ST. However, when co-treated with TNF-α, a slight decrease in the expression of IL-6ST was observed. The above results suggest that miR-223-3p significantly down-regulates the expression of IL-6ST in inflammatory conditions induced by TNF-α.

miR-223-3p Regulated STAT3 and NF-κB p65 Signaling Pathway

IL-1 and TNF-α can stimulate the activity of NF-κB to promote the secretion of IL-6 (12). The IL-6/IL6ST-STAT3 signaling

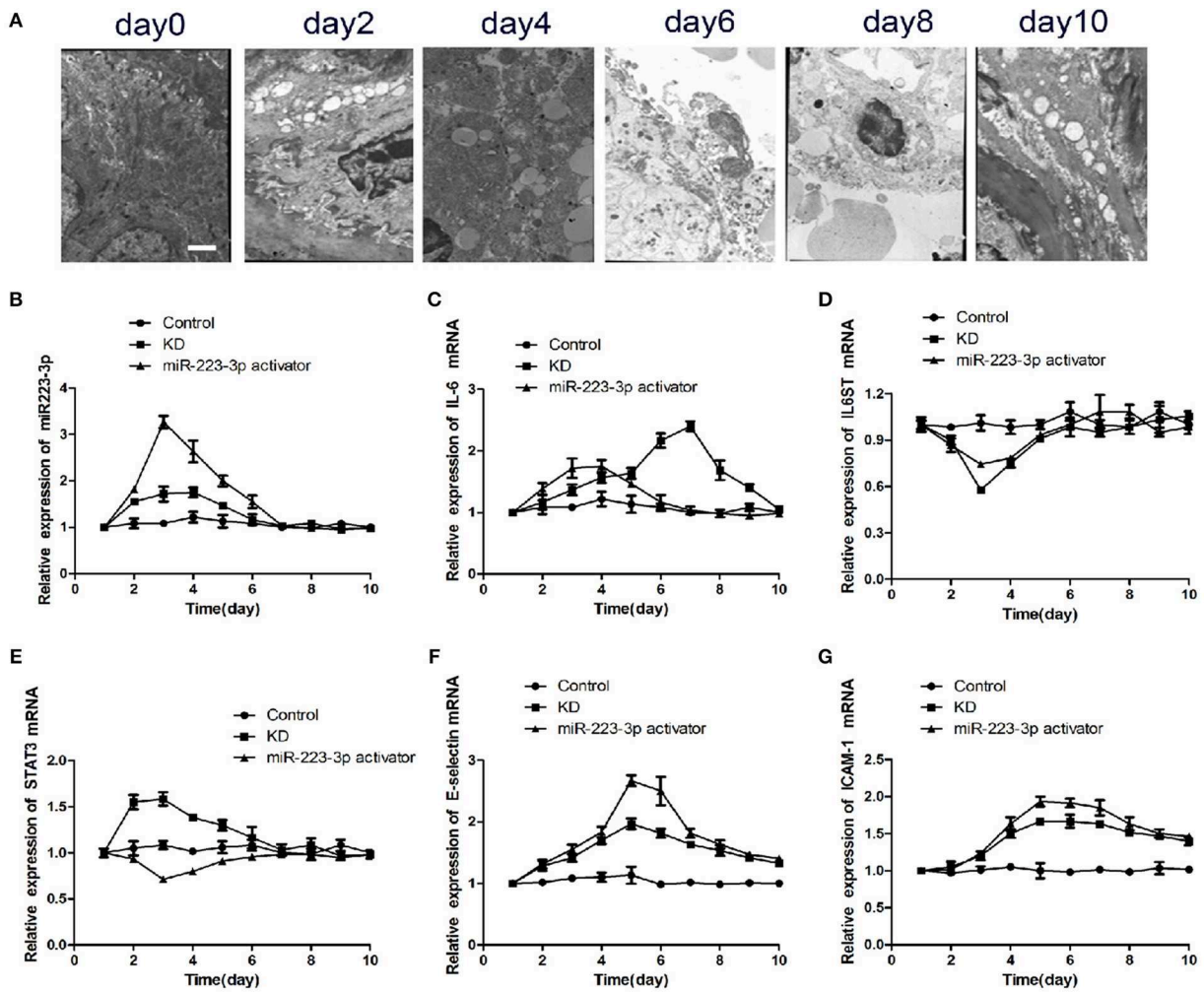

FIGURE 4 | miR-223-3p regulated the inflammatory factor levels in KD mice. **(A)** Representative SEM images of CAWS induced KD mice model at different stages. The Scale bar was "×5000." Relative expression levels of **(B)** miR-223-3p, **(C)** IL-6, **(D)** IL-6ST, **(E)** STAT3, **(F)** E-selectin, and **(G)** ICAM-1 in control mice, KD mice, and miR223-3p activator treated KD mice with respect to time.

pathway has been reported to be very crucial for inflammatory regulation (12). In the present study, the HCAECs were first treated with TNF-α, and the IL6ST expression was then suppressed by miR-223-3p. As expected, compared with the TNF-α induced group, miR-223-3p could significantly decrease the expression level of pSTAT3 and NF-κB p65 (**Figure 6A**). On the contrary, miR-223-3p inhibition could observably enhance the expression of pSTAT3 and NF-κB p65 at the same time (**Figure 6B**). In conclusion, these results imply that miR-223 can hold the activation of the STAT3 signaling pathway back, by targeting the inhibition of IL6ST, thus inducing vascular endothelial cell injury.

DISCUSSION

In recent years, KD has gradually turned into one of the major reasons for acquired heart diseases that affect children, which has attracted increased attention, while the vascular injury complication associated with KD has made it an important risk factor for adult ischemic heart disease (13). Unfortunately, our present understanding about the exact pathogenesis of vascular damage in KD is very limited and insufficient, and effective therapy strategies are still lacking. It is essential and crucially important for vascular biologists to study fresh mechanisms and to seek out therapeutic targets of KD-induced vascular endothelium damage, which are all crucial for both the investigation and the clinical therapy of KD.

Several research studies have been conducted to investigate the origin of KD and its correlation with the diseased state in patients (14–16). It has already been well-recognized that they are accompanied by numerous cellular inflammatory responses in the peripheral blood, composed of the activation of white blood cells and the release of their contents into the blood circulation in KD pathogenesis. As was previously reported,

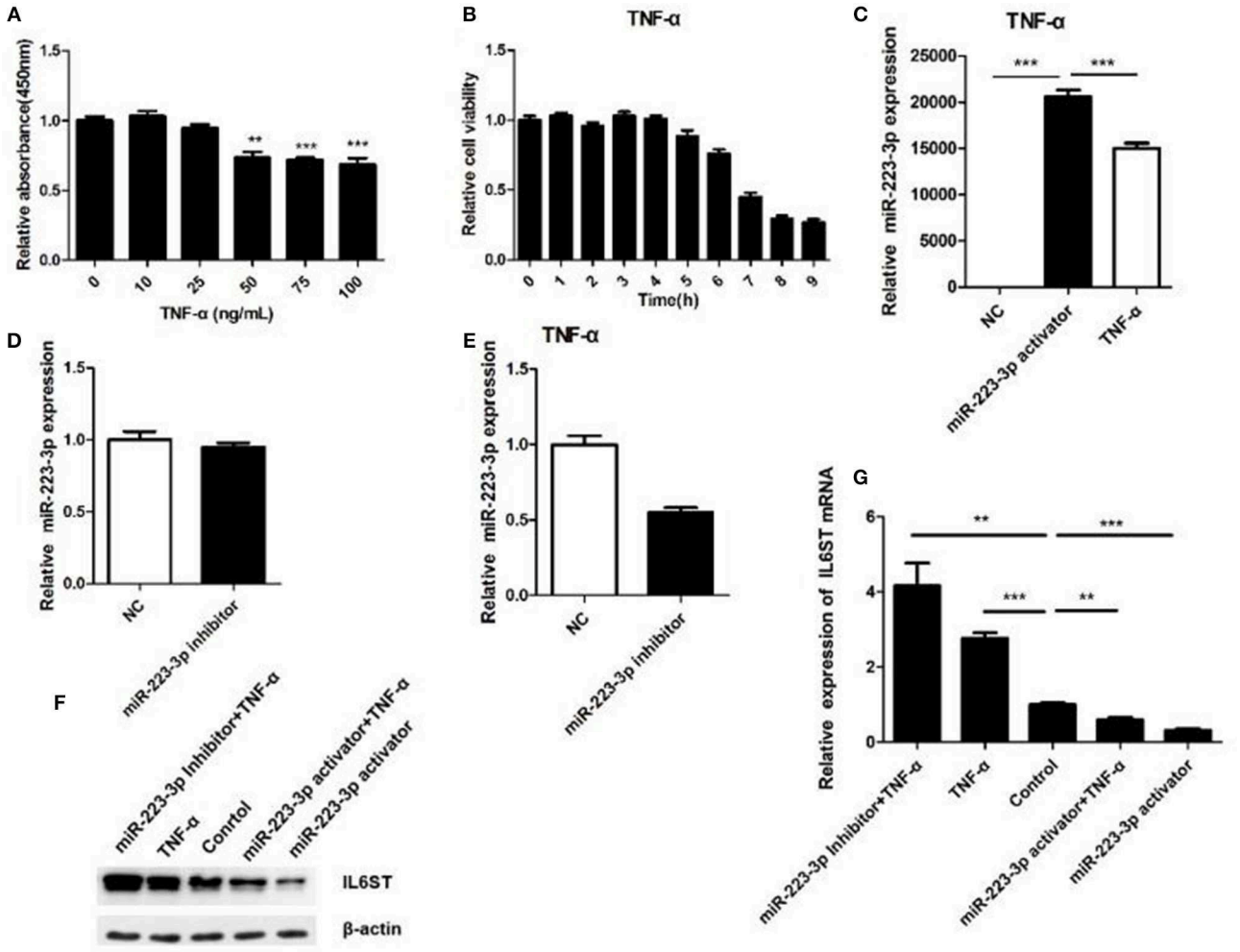

FIGURE 5 | Relationship between miR-223-3p and IL-6ST in TNF-α treatment. **(A)** Effect of different concentrations of TNF-α on the viability of HCAECs detected by the MTT assay. **(B)** The effect of TNF-α (concentration) on cell viability calculated for HCAECs with different time periods of exposure. The relative expression level of miR-223-3p post treatment with miR-223-3p and miR-223-3p activator combined with TNF-α. **(D)** miR-223-3p inhibitor. **(E)** miR-223-3p inhibitor and TNF-α. **(F)** The western blot indicates that the level of expression IL-6ST was least when treated with miR-223-3p and maximum when treated with the inhibitor in the presence of TNF-α. **(G)** Relative expression analysis of IL-6ST mRNA expression. $^{*}P < 0.05$, $^{**}P < 0.01$, and $^{***}P < 0.001$.

endothelial damage often occurs in the early stage of a coronary artery aneurysm during the course of KD (6) and the biological functions of these contents in KD and the vascular injuries caused by KD are yet to be elucidated. Studies have shown positive correlations between the elevation of EMP levels and TNF-α expression in the peripheral blood of patients with KD, suggesting that EMPs are likely to play a crucial part in the development of vasculitis in patients with KD (13, 16).

It has been reported that IL-6 is a key inflammatory factor in regulating the inflammatory reaction in KD. IL-6 plays a vital role in innate immunity, adaptive immunity, acute and chronic inflammation, KD occurrence and development. IL-6 can quickly activate the downstream STAT3 signaling pathway through its receptor protein coupling gp130 (17, 18). In addition, both IL-1 and TNF-α could promote the secretion of IL-6 by upregulating NF-κB activity, thereby indirectly activating STAT3 (19, 20). IL-17 increases the levels of IL-6, thus indirectly activates the STAT3 signaling pathway, significantly inducing inflammation and promoting the occurrence of tumors (21–23). So, the IL-6/IL-6ST and STAT3 signaling pathway is of great significance for the regulation of the inflammatory response in KD.

In a previous study, a few researchers found that miRNAs in KD were statistically changed, especially miR-223-3p (13, 24). MiR-223-3p was seen to cause a significant decline in the production of IL-1β and IL-6, while the miR-223-3p inhibitor revealed the opposite role in regulating IL-1β and IL-6 production (25). STAT3 siRNA exhibits a similar effect in cells. Studies have shown that in TLR-triggered macrophages, miR-223-3p has the ability to regulate the STAT3 expression, which is closely related to the inflammatory reactions in macrophages during the microorganism infection. In addition, several researchers have also shown that in RAW 264.7 cells

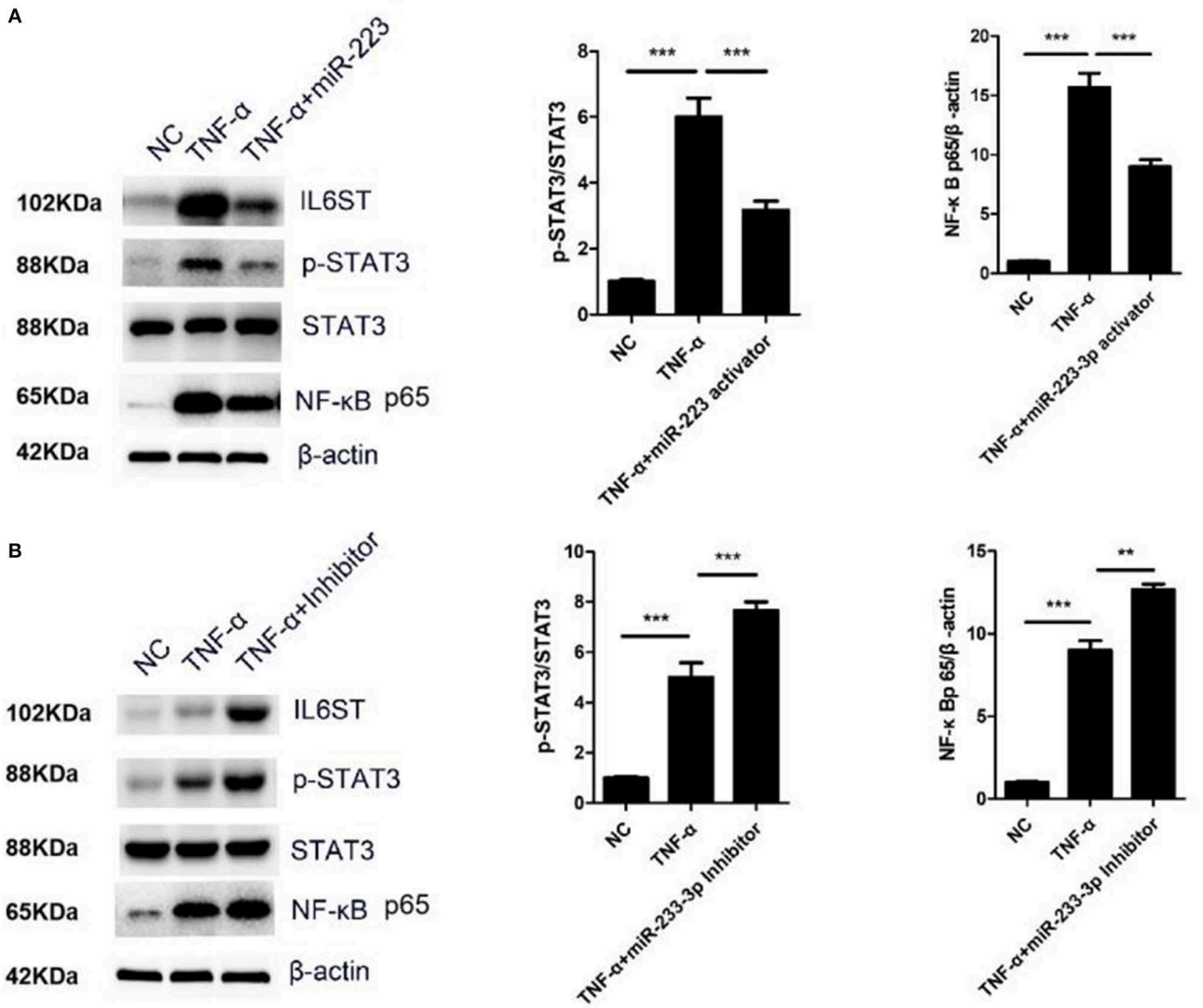

FIGURE 6 | miR-223-3p regulated STAT3 and NF-κB signaling pathway. **(A)** Western blot detection of the expression of p-STAT3/STAT3 and NF-κB p65 after miR-223-3p overexpression. **(B)** Western blot detection of the expression of p-STAT3/STAT3 and NF-κB p65 after treatment with miR-223-3p inhibitor. $^{**}P < 0.01$ and $^{***}P < 0.001$.

restraining STAT3 activity could hold back LPS-mediated IL-6 and IL-1β production as a priority, but not TNF-a (26). Data also proved that inhibiting STAT3 activity in gp130F/F mice, reduced the IL-6 expression level due to the response to LPS and then maintained the effect on STAT3 for promoting IL-6 gene transcription (27). All these studies indicate that the IL-6/STST3 signaling pathway plays a crucial role in the inflammatory responses.

KD is an important febrile illness causing multi-system vasculitis in childhood. Patients diagnosed with acute upper respiratory infection and herpangina, which mimic many of the clinical and laboratory findings in acute KD, were prospectively enrolled as febrile control subjects (14–16). In this research study, children with fever were selected as controls as well. We discovered that, miR-223-3p was highly expressed in the KD serum. The miR-223-3p expression level was high in acute stage KD and it was seen to decrease in coronary lesions of KD. IL-6 was confirmed as a target gene of miR-223-3p, and the miR-223-3p activator was thought to upregulate the expression of IL-6 and downregulate the expression of IL-6ST in KD mice. MiR-223-3p was observed to prohibit the expression of IL-6ST in an TNF-α induced inflammatory environment, and miR-223-3p was seen to regulate STAT3 and NF-κB p65 expression in the presence of TNF-α. This study yields an attractive molecular mechanism that indicates miR-223-3p's participation in KD pathogenesis through the adjustment and control of the IL6ST and STAT3 signaling pathways. Our research provides a reliable target gene for the clinical diagnosis and therapeutic treatment of Kawasaki disease.

DATA AVAILABILITY

The raw data supporting the conclusions of this manuscript will be made available by the authors, without undue reservation, to any qualified researcher.

ETHICS STATEMENT

This study was carried out in accordance with the recommendations of Medical ethics committee of Children's hospital of Soochow university and written informed consent was obtained from all subjects. All subjects gave written informed consent in accordance with the Declaration of Helsinki. The protocol was approved by the Medical ethics committee of Children's hospital of Soochow university.

The animal experiment study was also carried out in accordance with the recommendations of Medical ethics committee of Children's hospital of Soochow university. The related protocol were approved by medical ethics committee of Children's hospital of Soochow university too.

AUTHOR CONTRIBUTIONS

XW and YD contributed equally as co-first authors. XW contributed to designing the experiment and writing the manuscript. YD contributed to the design of the experiment. YC analyzed experimental results. QX established the animal model. GQ constructed the cell model. WQ performed statistic and analysis of data. LC performed bioinformatic analysis. WZ and MH collected and sorted out clinical case and experimental data. HL contributed to guiding, reviewing, inspecting of the experiments, and providing financial support.

FUNDING

The article was financially supported by the National Natural Science Foundation of China (Nos. 81570455, 8187021691, 31600695, and 81970436), the Natural Science Foundation of Young (Nos. 81600391, 81800437, 81570439, 81400222), and the Jiangsu Province Science Foundation (BE2017660), the Talent Foundation of Jiangsu Province (ZDRCA2016049 and No. WSN-070), the Jiangsu Provincial Medical Young Talents (QNRC2016764, QNRC2016756) and the Applied Foundational Research of Medical and Health Care of Suzhou City (SYS201633, SYS201642)

SUPPLEMENTARY MATERIAL

The Supplementary Material for this article can be found online at: https://www.frontiersin.org/articles/10.3389/fped.2019.00288/full#supplementary-material

REFERENCES

1. Kawasaki T, Kosaki F, Okawa S, Shigematsu I, Yanagawa H. A new infantile acute febrile mucocutaneous lymph node syndrome (MLNS) prevailing in Japan. *Pediatrics.* (1974) 54:271–6.
2. Yim D, Curtis N, Cheung M, Burgner D. Update on Kawasaki disease: epidemiology, aetiology and pathogenesis. *J Paediatr Child Health.* (2013) 49:704–8. doi: 10.1111/jpc.12172
3. Nakaoka H, Hirono K, Yamamoto S, Takasaki I, Takahashi K, Kinoshita K, et al. MicroRNA-145-5p and microRNA-320a encapsulated in endothelial microparticles contribute to the progression of vasculitis in acute Kawasaki disease. *Sci Rep.* (2018) 8:1016. doi: 10.1038/s41598-018-19310-4
4. Terai M, Yasukawa K, Narumoto S, Tateno S, Oana S, Kohno Y. Vascular endothelial growth factor in acute Kawasaki disease. *Am J Cardiol.* (1999) 83:337–9. doi: 10.1016/S0002-9149(98)00864-9
5. Ebata R, Abe J, Yasukawa K, Hamada H, Higashi K, Suwazono Y, et al. Increased production of vascular endothelial growth factor-D and lymphangiogenesis in acute Kawasaki disease. *Circ J.* (2011) 75:1455–62. doi: 10.1253/circj.CJ-10-0897
6. Jin J, Cai L, Liu ZM, Zhou XS. miRNA-218 inhibits osteosarcoma cell migration and invasion by down-regulating of TIAM1, MMP2 and MMP9. *Asian Pacif J Cancer Preven.* (2013) 14:3681–4. doi: 10.7314/APJCP.2013.14.6.3681
7. Du Z, Niu S, Xu X, Xu Q. MicroRNA31-NDRG3 regulation axes are essential for hepatocellular carcinoma survival and drug resistance. *Cancer Biomarkers.* (2017) 19:221–30. doi: 10.3233/CBM-170568
8. Saito K, Nakaoka H, Takasaki I, Hirono K, Yamamoto S, Kinoshita K, et al. MicroRNA-93 may control vascular endothelial growth factor A in circulating peripheral blood mononuclear cells in acute Kawasaki disease. *Pediatric Res.* (2016) 80:425–32. doi: 10.1038/pr.2016.93
9. Chen CZ, Li L, Lodish HF, Bartel DP. MicroRNAs modulate hematopoietic lineage differentiation. *Science.* (2004) 303:83–6. doi: 10.1126/science.1091903
10. Taibi F, Metzinger-Le Meuth V, M'Baya-Moutoula E, Djelouat MSE, Louvet L, Bugnicourt JM, et al. Possible involvement of microRNAs in vascular damage in experimental chronic kidney disease. *Bba-Mol Basis Dis.* (2014) 1842:88–98. doi: 10.1016/j.bbadis.2013.10.005
11. Pan Y, Liang HW, Liu H, Li DH, Chen X, Li LM, et al. Platelet-secreted MicroRNA-223 promotes endothelial cell apoptosis induced by advanced glycation end products via targeting the insulin-like growth factor 1 receptor. *J immunol.* (2014) 192:437–46. doi: 10.4049/jimmunol.1301790
12. Luo X, Zhang X, Zhao T, Zeng T, Liu W, Deng M, et al. A preliminary study on the proinflammatory mechanisms of *Treponema pallidum* outer membrane protein Tp92 in human macrophages and HMEC-1 cells. *Microb Pathog.* (2017) 110:176–83. doi: 10.1016/j.micpath.2017.06.046
13. Chu M, Wu R, Qin S, Hua W, Shan Z, Rong X, et al. Bone marrow-derived MicroRNA-223 works as an endocrine genetic signal in vascular endothelial cells and participates in vascular injury from Kawasaki disease. *J Am Heart Assoc.* (2017) 6:e004878. doi: 10.1161/JAHA.116.004878
14. Guiducci S, Ricci L, Romano E, Ceccarelli C, Distler JHW, Miniati I, et al. Microparticles and Kawasaki disease: a marker of vascular damage? *Clin Exp Rheumatol.* (2011) 29:S121–5.
15. Tan Z, Yuan Y, Chen S, Chen Y, Chen TX. Plasma endothelial microparticles, TNF-a and IL-6 in Kawasaki disease. *Indian Pediatr.* (2013) 50:501–3. doi: 10.1007/s13312-013-0152-7
16. Ding YY, Ren Y, Feng X, Xu QQ, Sun L, Zhang JM, et al. Correlation between brachial artery flow-mediated dilation and endothelial microparticle levels for identifying endothelial dysfunction in children with Kawasaki disease. *Pediatric Res.* (2014) 75:453–8. doi: 10.1038/pr.2013.240
17. Tadokoro T, Wang Y, Barak LS, Bai YS, Randell SH, Hogan BLM. IL-6/STAT3 promotes regeneration of airway ciliated cells from basal stem cells. *Proc Natl Acad Sci USA.* (2014) 111:E3641–9. doi: 10.1073/pnas.1409781111
18. Liu H, Ren GP, Wang TY, Chen YX, Gong CJ, Bai YF, et al. Aberrantly expressed Fra-1 by IL-6/STAT3 transactivation promotes colorectal cancer aggressiveness through epithelial-mesenchymal transition. *Carcinogenesis.* (2015) 36:459–68. doi: 10.1093/carcin/bgv017
19. Sironi M, Breviario F, Proserpio P, Biondi A, Vecchi A, Vandamme J, et al. Il-1 Stimulates Il-6 production in endothelial-cells. *J immunol.* (1989) 142:549–53.

20. Kaplanski G, Teysseire N, Farnarier C, Kaplanski S, Lissitzky JC, Durand JM, et al. IL-6 and IL-8 production from cultured human endothelial cells stimulated by infection with Rickettsia conorii via a cell-associated IL-1 alpha-dependent pathway. *J Clin Invest*. (1995) 96:2839–44. doi: 10.1172/JCI118354
21. Kabir S. The role of interleukin-17 in the *Helicobacter pylori* induced infection and immunity. *Helicobacter*. (2011) 16:1–8. doi: 10.1111/j.1523-5378.2010.00812.x
22. Wang L, Yi TS, Kortylewski M, Pardoll DM, Zeng DF, Yu H. IL-17 can promote tumor growth through an IL-6-Stat3 signaling pathway. *J Exp Med*. (2009) 206:1457–64. doi: 10.1084/jem.20090207
23. Jarnicki A, Putoczki T, Ernst M. Stat3: linking inflammation to epithelial cancer - more than a "gut" feeling? *Cell Div*. (2010) 5:14. doi: 10.1186/1747-1028-5-14
24. Chen Y, Ding YY, Ren Y, Cao L, Xu QQ, Sun L, et al. Identification of differentially expressed microRNAs in acute Kawasaki disease. *Mol Med Rep*. (2018) 17:932–8. doi: 10.3892/mmr.2017.8016
25. Chen QY, Wang H, Liu Y, Song YJ, Lai LH, Han Q, et al. Inducible microRNA-223 down-regulation promotes TLR-triggered IL-6 and IL-1 beta production in macrophages by targeting STAT3. *PLoS ONE*. (2012) 7:e42971. doi: 10.1371/journal.pone.0042971
26. Samavati L, Rastogi R, Du WJ, Huettemann M, Fite A, Franchi L. STAT3 tyrosine phosphorylation is critical for interleukin 1 beta and interleukin-6 production in response to lipopolysaccharide and live bacteria. *Mol Immunol*. (2009) 46:1867–77. doi: 10.1016/j.molimm.2009.02.018
27. Greenhill CJ, Rose-John S, Lissilaa R, Ferlin W, Ernst M, Hertzog PJ, et al. IL-6 trans-signaling modulates TLR4-dependent inflammatory responses via STAT3. *J Immunol*. (2011) 186:1199–208. doi: 10.4049/jimmunol.1002971

Conflict of Interest Statement: The authors declare that the research was conducted in the absence of any commercial or financial relationships that could be construed as a potential conflict of interest.

frontiers in Pediatrics

SYSTEMATIC REVIEW
published: 16 August 2019
doi: 10.3389/fped.2019.00342

Corticosteroids and Intravenous Immunoglobulin in Pediatric Myocarditis: A Meta-Analysis

Yining Li[1,2†], *Yuqing Yu*[1,2†], *Selena Chen*[3], *Ying Liao*[1*] *and Junbao Du*[1*]

[1] *Department of Pediatrics, Peking University First Hospital, Beijing, China,* [2] *Department of Basic Medical Sciences, Peking University School of Basic Medical Sciences, Beijing, China,* [3] *Division of Biological Sciences, University of California, San Diego, La Jolla, CA, United States*

Background: The efficacy of corticosteroids and intravenous immunoglobulin (IVIG) in pediatric myocarditis remains controversial.

Objectives: The authors performed a meta-analysis to assess the therapeutic efficacy of corticosteroids and IVIG in children with myocarditis.

Methods: We retrieved the trials on corticosteroids and IVIG therapy, respectively, in pediatric myocarditis from nine databases up to December 2018. Statistical analysis was performed using Review Manager 5.3.

Results: Our analysis included 8 studies and 334 pediatric patients. The data demonstrated that children receiving corticosteroids showed no significant improvement on left ventricular ejection fraction (LVEF) from 1 to 8 month-follow-up (MD = 5.17%, 95% CI = −0.26% to 10.60%, $P = 0.06$), and no significant improvement in death or heart transplantation incidence at the end of follow-up (OR = 1.33, 95% CI = 0.27–6.70, $P = 0.73$). However, children receiving IVIG revealed a statistically remarkable increase in LVEF at a follow-up over the course of 6 months to 1 year (MD = 18.91%, 95% CI = 11.74–26.08%, $P < 0.00001$), and a decrease in death or heart transplantation at the end of follow-up (OR = 0.31, 95% CI = 0.12–0.75, $P = 0.01$). Further comparisons showed that the mortality and heart transplantation rate of children with myocarditis treated with IVIG were significantly lower than those with corticosteroid therapy ($t' = 11.336$, $P < 0.001$).

Conclusions: IVIG might be beneficial to improve LVEF and survival for myocarditis in children. However, the present evidence does not support corticosteroids as superior to conventional therapy in children with myocarditis. Further randomized controlled trials with a larger sample size are required.

Keywords: myocarditis, children, corticosteroid, intravenous immunoglobulin, meta-analysis

OPEN ACCESS

Edited by:
Fu Lijun,
Shanghai Children's Medical Center, China

Reviewed by:
Muhammad Ali Mumtaz,
Baylor College of Medicine, United States
Federico Gutierrez-Larraya,
University Hospital La Paz, Spain

***Correspondence:**
Ying Liao
liaoyingwww@163.com
Junbao Du
junbaodu1@126.com

†These authors have contributed equally to this work

Specialty section:
This article was submitted to Pediatric Cardiology, a section of the journal Frontiers in Pediatrics

Received: *01 June 2019*
Accepted: *31 July 2019*
Published: *16 August 2019*

Citation:
Li Y, Yu Y, Chen S, Liao Y and Du J (2019) Corticosteroids and Intravenous Immunoglobulin in Pediatric Myocarditis: A Meta-Analysis. Front. Pediatr. 7:342. doi: 10.3389/fped.2019.00342

INTRODUCTION

Myocarditis is generally defined as the inflammatory cellular infiltration in the myocardium and subsequent cardiomyocyte necrosis of non-ischemic origin according to Dallas criteria (1, 2). It has a variety of clinical presentations (3). The exact incidence of myocarditis in children remains unknown (1). A multi-institutional analysis by Klugman et al. showed that myocarditis took up

about 0.05% among pediatric hospital discharges in the United States (4). Towbin and colleagues reported that the incidence of dilated cardiomyopathy (DCM) in children was 0.57 cases per 100,000 per year overall, 46% of which were caused by myocarditis (5). It is estimated that the prevalence of pediatric myocarditis is 0.3 cases per year per 100,000 children (6). Although myocarditis is not common in children, it can lead to significant morbidity and mortality (5).

It is generally believed that viral infection is a major cause of myocarditis. The pathophysiology of myocarditis consists of direct viral injury from viral proteins, the innate immune response including cytokines, toll-like receptors, and complements, and the acquired immune response involving T cells and antibodies. A chronic immune reaction related to molecular mimicry may lead to chronic dilated cardiomyopathy even without solid evidence of viral persistence (3, 7–9). Immunosuppressive therapy such as corticosteroids has been used in patients. In experimental models and some uncontrolled cases of myocarditis, intravenous immunoglobulin (IVIG) has shown to have antiviral and immunomodulatory effects (1). However, the efficacy of corticosteroids and IVIG remains controversial. Limited trials have been conducted on children, and the results are inconsistent. We therefore performed a meta-analysis of all qualified randomized or non-randomized controlled trials to determine the therapeutic efficacy of corticosteroids and IVIG in children with myocarditis.

METHODS

This meta-analysis was performed following the Preferred Reporting Items for Systematic Reviews and Meta-Analyses (PRISMA) statement (10).

Protocol of Searching

Studies were confirmed by searches from medical libraries or electronic reviews of published medical literature in our meta-analysis. The databases, including Cochrane (1943–2018), PubMed (1968–2018), Web of science (1970–2018), EMBASE (1991–2018), Chinese Biomed Database (1978–2018), the Latin American and Caribbean Health Science Information Database (LILACs) (1982–2018), the Cumulative Index to Nursing and Allied Health Literature (CINAHL) (1982–2018), WANFANG (1980–2018), and CNKI (1990–2018), were independently searched by two authors using medical subject heading (MeSH) terms (in English or Chinese) such as "myocarditis/inflammatory cardiomyopathy/dilated cardiomyopathy/carditis AND immunoglobulins/gammaglobulin/gamma-globulin/IVIG," "myocarditis/inflammatory cardiomyopathy/dilated cardiomyopathy/carditis AND anti-inflammatory agents/glucocorticoids/immunosuppressive agents/adrenal cortex hormones/predniso/dexamethason/hydrocortiso/methylprednison/steroid/corticostero/immunosuppress/glucocorticoid/mineralocorticoid/betamethason/budesonide/cortiso/fludrocortiso." We also narrowed the spectrum using the filters of clinical trial and child in the search strategy. No language restrictions were applied. Original articles were acquired from electronic databases or libraries.

Study Inclusion Criteria

We included English or Chinese studies that referred to randomized or retrospective conventional therapy-controlled trials for the treatment of myocarditis or DCM into our analysis. The diagnosis of myocarditis was made by established clinical, echocardiographic, cardiac MRI, histological, immunological, and immunohistochemical criteria. Trials involving Kawasaki disease, structural heart disease and other specific causes of acute cardiomyopathy as sepsis or drug toxicity were excluded. IVIG, corticosteroids or IVIG in combination with steroid agents were given to the treatment group while traditional therapy was used on the control group. The general characteristics of the subjects, the protocol of the trials and the process of the follow-up were illuminated in detail. Indicators for evaluating effects included the recovery of heart function after undergoing treatment, or the rate of death or heart transplantation during follow-up.

Study Exclusion Criteria

Studies without a clear standard of diagnosis of myocarditis or the use of other drugs in the control group were not selected. Additionally, studies in which subjects were not children, or the endpoints were not clearly described, were also eliminated. Some uncontrolled trials were excluded as well.

Study Quality Assessment

Two reviewers independently screened the title and abstract, selected the studies and assessed the quality of studies. Characteristics of subjects, design of trials, course of arrangement and analysis were abstracted and rated. Quality assessment of randomized controlled trials (RCTs) were based on the 7-point Modified Jadad Score, including 7 items on randomization, blinding, allocation concealment, withdrawals and dropouts. Studies were of high quality if they got 4 or more points. The quality of enrolled retrospective cohort studies was evaluated by the 9-star Newcastle-Ottawa Quality Assessment Scale, including 8 items on patient selection, comparability and outcome. Studies were interpreted as high-quality studies if they got 5 or more stars. Divergence was resolved by discussion, or by recourse to a third reviewer. Publication bias was assessed by Funnel plot.

Statistical Analysis

We used the Review Manager 5.3 software (The Nordic Cochrane Centre of The Cochrane Collaboration, Copenhagen, Denmark) available on international evidence-based medicine cooperative network for meta-analysis. We tested the heterogeneity of study data by forest plot, the Q-test as well as I^2 statistics. In the Q-test, the results of included studies were homogenous if $p > 0.05$, and a fixed effect model was applied; while if $p < 0.05$, the results were heterogeneous, and the outcome of systematic analysis was stated in a random effects model. $I^2 > 50\%$ indicated

Abbreviations: IVIG, intravenous immunoglobulin; DCM, dilated cardiomyopathy; LVEF, left ventricular ejection fraction; RCT, randomized controlled trial; ECMO, extracorporeal membrane oxygenation; MD, mean difference; CI, confidence interval; OR, odds ratio; SD, standard deviation; SE, standard error.

a significant heterogeneity. The final results were indicated in the form of vector images which combined mean difference (MD) or odds ratio (OR) with 95% confidence interval (CI). We also compared the two medicines by weighted independent *t*-test. $P < 0.05$ showed a statistically significant difference.

RESULTS

Basic Data of Included Studies

A total of 4,546 studies were retrieved using the retrieval methods mentioned above. Finally, there were eight studies (11–18) being adopted based on exclusion and inclusion criteria (**Figure 1**), consisting of two randomized controlled trials and six retrospective studies. All studies were published in English. **Table 1** shows the general background of eight studies and the list of characteristics of the subjects such as age. In total, 334 pediatric patients with myocarditis or DCM were included, consisting of 146 patients in the experimental group and 188 patients in the control group. The range of mean age of the research subjects was 0–17.7 years. All pediatric patients in these studies were diagnosed as myocarditis or DCM with or without corticosteroids or IVIG. Two of the eight studies regarded only left ventricular ejection fraction (LVEF) as the endpoint of follow-up, while four of the studies used only death or heart transplantation to indicate pharmaceutical effect. The remaining studies used both LVEF and death or heart transplantation to reflect the therapeutic efficacy. In studies mentioning the administration time, the mean time for corticosteroids administration varied from 1 to 8 months, while the range of mean time for IVIG administration was from 2 to 5 days. Follow-up duration lasted from 1 month to 5 years. The results of quality assessment showed that six of the eight studies were high-quality studies (**Table 1**).

Publication Bias

Funnel plot analysis indicates significant publication bias for the increase in LVEF and death or heart transplantation incidence (**Figure 2**). The number of articles available is likely a major contributing factor, which also limits our further test for funnel plot asymmetry.

Analysis of Left Ventricular Ejection Fraction

LVEF of children with myocarditis or dilated cardiomyopathy after intervention was reported in four trials. A total of 157 subjects were included, 81 in the treatment group and 76 in

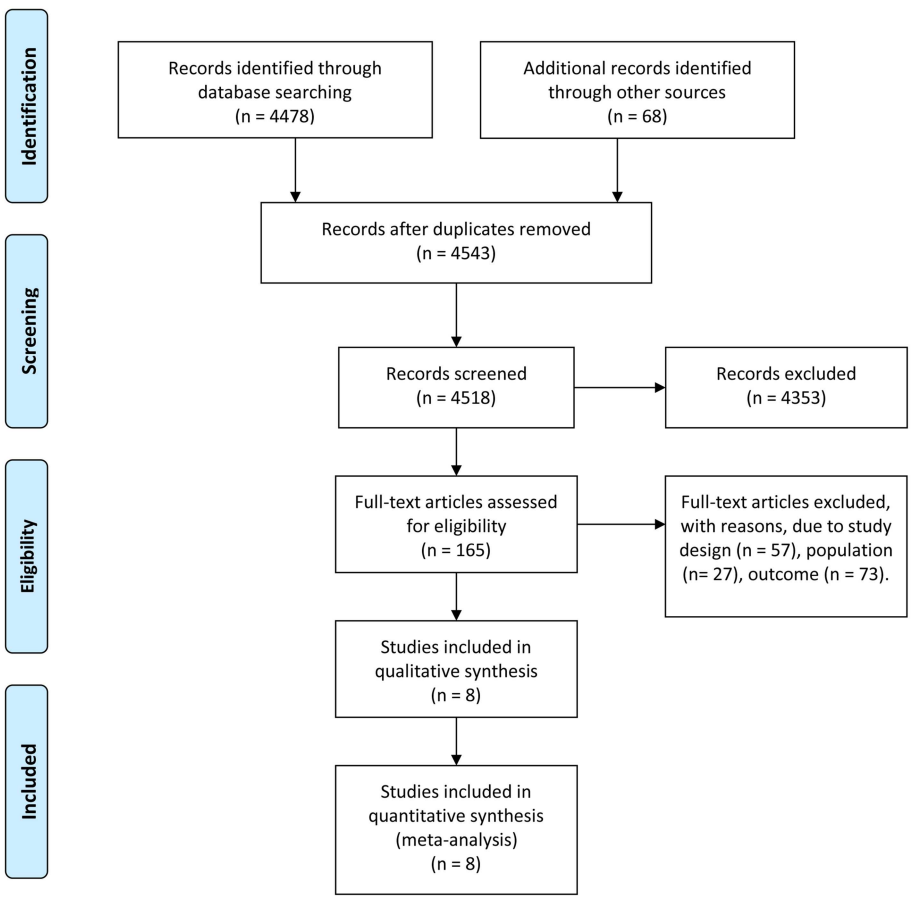

FIGURE 1 | Study flow diagram.

TABLE 1 | Basic data of eight included trials.

References	Study design	Groups		Age		Drugs	Dosing regimen	Control	Endpoint	Follow-up duration		*P*-value	Quality assessment
		T	C	T	C					T	C		
Aziz et al. (11)	RCT	44	24	3.4 ± 2.5 years	4.2 ± 3.4 years	Prednisolone	2 mg/kg/day for 1 month and then tapered off over a period of 15 days	Conventional therapy	LVEF	15.1 ± 9.2 months	13.6 ± 10.6 months	0.06	2
Camargo et al. (12)	RCT	12	9	0–15 years		Prednisolone	2.5 mg/kg/day for 1 week, 2.0 mg/kg/day for 3 weeks, 1.5 mg/kg/day for 4 weeks, and 1.0 mg/kg/day thereafter	Conventional therapy	LVEF, death or heart transplantation	8 months		>0.05	3
English et al. (13)	Retrospective	16	6	0–17.7 years		Steroids	2–10 mg/kg/day for a minimum of 3 days	Conventional therapy	Death or heart transplantation	60 months		—	7
Alrabte and Bezanti (14)	Retrospective	13	27	9 months		IVIG	0.4 g/kg/day for 5 days	Conventional therapy	LVEF	12 months		—	7
Atiq et al. (15)	Retrospective	16	20	2.39 ± 3.46 years	2.36 ± 1.75 years	IVIG	A single dose of 2 g/kg	Conventional therapy	Death or heart transplantation	12 months		0.2	9
Haque et al. (16)	Retrospective	12	13	7.3 ± 5.8 years	12.0 ± 4.9 years	IVIG	2 g/kg over 16–24 h on day of admission	Conventional therapy	Death or heart transplantation	—		0.04	7
Heidendael et al. (17)	Retrospective	21	73	10 (1, 51) months*	18 (2, 59) months*	IVIG	2 g/kg within 2 weeks after initial presentation	Conventional therapy	Death or heart transplantation	33 months		0.432	8
Prasad and Chaudhary, (18)	Retrospective	12	16	<12 years		IVIG	1 g/kg/day for 2 days	Conventional therapy	LVEF, death or heart transplantation	6 months		<0.05	8

**Age was given as median (interquartile range).*

Retrospective cohort studies were evaluated using 9-star Newcastle-Ottawa Quality Assessment Scale; RCT studies were evaluated using 7-point Modified Jadad Score; conventional therapy includes digitalis, diuretics, vasodilators, etc. T, treatment; C, control; RCT, randomized controlled trial; IVIG, intravenous immunoglobulin; LVEF, left ventricular ejection fraction.

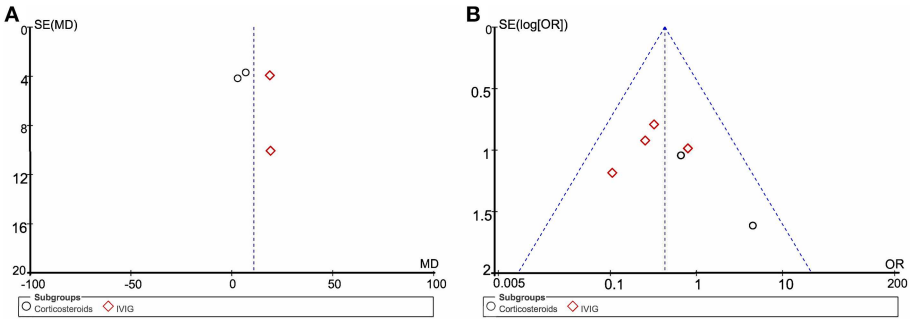

FIGURE 2 | Funnel plot of included studies. **(A)** The left funnel comprised of four dots representing studies using LVEF as the endpoint. **(B)** Funnel plot of six clinical trials using death or heart transplantation as the endpoint. MD, mean difference; OR, odds ratio; SE, standard error.

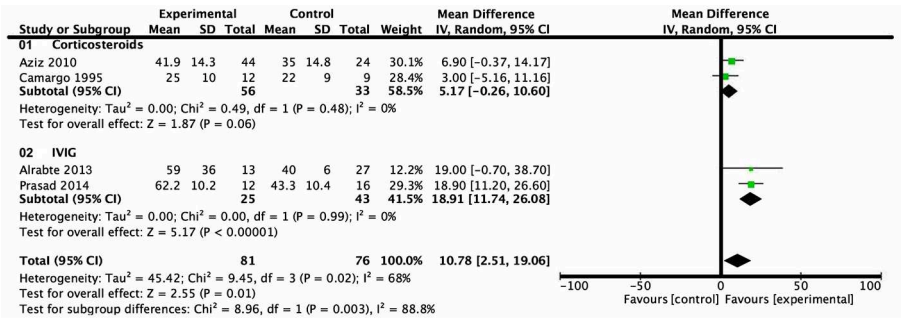

FIGURE 3 | Forest plot of four studies using LVEF as the endpoint. Comparison of drugs and conventional therapy on the outcome of left ventricular ejection fraction in pediatric myocarditis, excluding nonevent trials. Heterogeneity indicated a significant difference ($P = 0.02$, $I^2 = 68\%$). A random effects model was used. CI, confidence interval; SD, standard deviation.

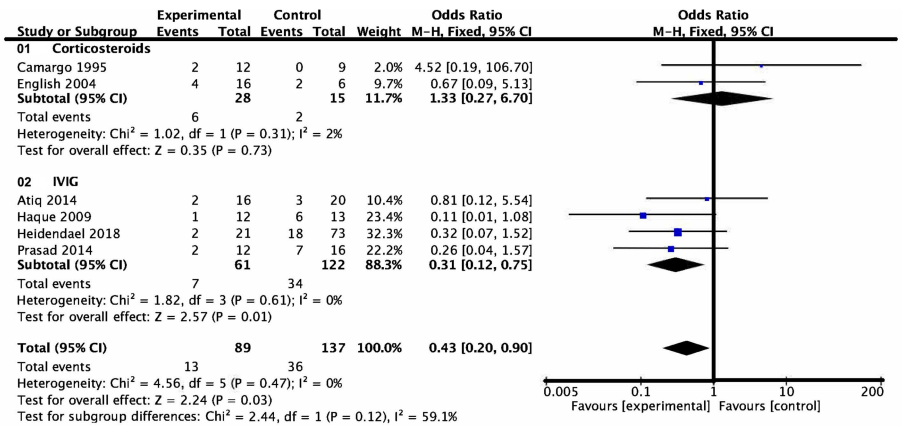

FIGURE 4 | Forest plot of six studies using death or heart transplantation as the endpoint. Drugs vs. conventional therapy on the outcome of rate of death or heart transplantation in pediatric myocarditis, excluding nonevent trials. Heterogeneity showed no significant differences ($P = 0.47$, $I^2 = 0\%$). Fixed effect model for combined effect size was used.

the control group. Heterogeneity analysis showed heterogeneity among the studies ($P = 0.02$, $I^2 = 68\%$) and a random effects model was used. Subgroup analysis showed that there was no statistical difference between the group treated with corticosteroids and the group treated with conventional therapy from 1 month- to 8 month-follow-up (mean difference = 5.17%, 95% CI = −0.26%–10.60%, $P = 0.06$). Patients treated with IVIG, on the other hand, revealed a higher level of LVEF compared with patients who received conventional therapy from a follow-up over the course of 6 months to 1 year (mean difference = 18.91%, 95% CI = 11.74–26.08%, $P < 0.001$) (**Figure 3**).

Analysis of Death and Transplantation

Six studies assigned death or heart transplantation as the endpoint of investigation, in which investigation of 49 patients ended with death or heart transplantation. This consisted of 13 patients in the medication group and 36 patients in the control group. Heterogeneity analysis showed no heterogeneity among the studies ($P = 0.47$, $I^2 = 0$) and a fixed effect model was used. The death or heart transplantation incidence was lower in the medication group than that in the control group (OR = 0.43, 95% CI = 0.20–0.90, $P = 0.03$). According to the subgroup analysis of the two types of drugs, the death or heart transplantation incidence in pediatric patients treated with IVIG was lower than that of patients treated with conventional therapy at the end of follow-up (OR = 0.31, 95% CI = 0.12–0.75, $P = 0.01$). On the contrary, there was no evidence of a significant difference in the death or heart transplantation incidence between the corticosteroids group and conventional therapy group at the end of follow-up (OR = 1.33, 95% CI = 0.27–6.70, $P = 0.73$) (**Figure 4**).

Further comparisons showed that the mortality and heart transplantation rate of children with myocarditis treated with IVIG were significantly lower than those with corticosteroid therapy ($t' = 11.336$, $P < 0.001$) (**Table 2**).

DISCUSSION

The results of our meta-analysis show that there is no significant difference in increased LVEF (from a 1 month- to 8 month- follow-up) and decreased death or heart transplantation incidence (at the end of follow-up) between the use of corticosteroids and that of conventional therapy in children with myocarditis or dilated cardiomyopathy. Compared to conventional therapy, additional IVIG treatment may be beneficial for the improvement of LVEF (at follow-up over the course from 6 months to 1 year) and for a decrease in death or heart transplantation rate (at the end of follow-up).

TABLE 2 | Comparisons of percentages of death and heart transplantation in children with myocarditis treated by corticosteroids and intravenous immunoglobulin.

Drugs	Reference	Percentage of death or heart transplantation (%)	Weighted mean percentage (%)
Corticosteroids	Camargo et al. (12)	16.7	21.4 ± 4.2
	English et al. (13)	25.0	
IVIG	Atiq et al. (15)	12.5	11.5 ± 3.0
	Haque et al. (16)	8.3	
	Heidendael et al. (17)	9.5	
	Prasad and Chaudhary, (18)	16.7	
Weighted independent *t'*-test*		$t' = 11.336$, $p < 0.001$	

**Weighted by number of the subjects; IVIG, intravenous immunoglobulin.*

The comparison between corticosteroids and IVIG in death or heart transplantation incidence reveals a statistical superiority of IVIG therapy.

Potential etiologies of myocarditis include infections, physical agents, toxins, medications, autoantigens and so on (19). Viral and post-viral myocarditis are major causes of dilated cardiomyopathy (1). The spectrum of viruses varies from enteroviruses (especially coxsackievirus), human herpesvirus 6, adenovirus, Epstein-Barr virus to parvovirus B19, hepatitis C and cytomegalovirus both in children and adults. *Trypanosoma cruzi* is a common cause of myocarditis in Central and South America (20). Our meta-analysis did not include this type of myocarditis because of its distinctive epidemiology, pathogenesis, treatment and management (21). After the initial infection period, patients may develop eosinophilic, lymphocytic, or giant cell/granulomatous inflammation of myocardium (22). Lymphocytic myocarditis is the most common viral myocarditis (9). Manifestations of myocarditis differ in children. Signs and symptoms can be sub-clinical, while patients sometimes experience chest pains similar to pericarditis or myocardial infarction, or even undergo sudden cardiac death from ventricular fibrillation. Moreover, symptoms of heart failure might occur when the disease develops into DCM, leading to death or heart transplantation.

The exact mechanisms for the injury during viral myocarditis have been studied for decades. Research on rodent models and isolated cell systems have shown three phases in the pathophysiology. During phase 1, viruses enter myocytes and macrophages through specific receptors and coreceptors and activate the innate immune response. Phase 2 involves viral replication and an acquired immune response. Protein products of viral genomes can also cause damage to myocardium. Phase 3 is either recovery or DCM. Cellular necrosis triggers the host's immune system and causes further degradation. Molecular mimicry possibly plays an important role in this autoimmune response. On most occasions, the status improves as viral titers decrease, whereas in some cases the disease evolves to chronic dilated cardiomyopathy and become irreversible. It is not clear whether viral persistence or reactivation of latent virus is involved in the chronic phase and eventual onset of DCM. Some viruses, such as parvovirus B19, can also cause myocarditis indirectly by infecting cardiac endothelial cells (1, 3, 9, 23). Genetic predisposition possibly works in viral and/or autoimmune myocarditis and later in DCM in humans (2).

The outcome, prognosis, and efficacy of treatment of myocarditis are closely related to etiology, clinical manifestations and the phase of disease. Conventional therapy includes optimal management of arrhythmia and of heart failure. In patients whose conditions deteriorate, mechanical circulatory support is required, such as extracorporeal membrane oxygenation (ECMO) or ventricular assist devices, as a bridge to recovery or heart transplantation.

As immunosuppressants, corticosteroids could be effective in the second phase of myocarditis with the three-phase pathological course. However, our meta-analysis shows that there is no significant difference in LVEF and death or heart transplantation ratio in children between the corticosteroids

group and the conventional treatment group. Corticosteroids use should depend on a prompt diagnosis and a clear assessment of the stage of myocarditis. In the three studies included, however, corticosteroids use varied among different stages of the patients, which likely resulted in no significant differences. In addition, using corticosteroids in acute myocarditis may exacerbate the situation through immunosuppression during the acute viremic phase (11–13). Although several previous randomized controlled trials (24, 25) and meta-analyses (26) have proven the efficacy of corticosteroids, these findings were based primarily on adults. The conclusion may not be conveniently extrapolated to the pediatric population as a result of different etiologies and different physical conditions.

On the other hand, our findings reveal that IVIG may have a therapeutic effect on pediatric myocarditis. Studies have shown that immunoglobulin G and polyvalent intravenous immunoglobulins IgG, IgA, and IgM exert proinflammatory effects, including the activation of immune cells, the complement system, and the opsonization of infective agents. They also have anti-inflammatory effects which comprise the neutralization of bacterial and other toxins, degradation products and an excess of complement factors and cytokines, which help to balance the proinflammatory process (27–29). IVIG can modulate the inflammatory and immune response without major side effects. Thus, if ongoing infection, a post-infectious inflammatory reaction, or a non-infectious process play a role, IVIG can be efficacious (30). However, additional and larger-scale randomized controlled trials on children are necessary for further investigation of IVIG use.

Theoretically, immunosuppressive therapy could lead to side-effects, including infectious diseases, hypertension, edema, an increase in body weight and so on (26). While IVIG therapy was principally associated with infusion-related side effects, all incidences were reported to be mild (30). We also took adverse drug reaction into account, although it was not comprehensively mentioned in the retrieved articles and reflects a limitation of these studies.

Considering the validity of medication targeting different periods of pathologic process, combination therapy may be a more effective option. However, far less research (13, 31) regarding steroid agents combined with IVIG for treating pediatric myocarditis was retrieved. Several studies indicated that combination treatment groups conferred advantages over the control group, while others showed no significant difference in therapeutic effects between the two groups. Therefore, performing more trials to study the efficacy and safety of combined treatment is necessary.

Most previously reported meta-analyses about the treatment for myocarditis (26, 32) targeted adults as research subjects. Moreover, most of these mentioned only IVIG or steroid agents, rather than both. On account of the significant morbidity and mortality rates of pediatric myocarditis, it is of great importance to further investigate more effective therapies. Additionally, our meta-analysis compared the efficacy of corticosteroids and IVIG, which might be taken as a reference for further researches.

STUDY LIMITATIONS

There were some limitations to the present study. The inverted funnel plot demonstrated an existence of publication bias. It is difficult to unify the diagnostic criteria and most studies lacked a clear assessment of the stage of myocarditis. Several different standards for judging the efficacy of medication were not all-inclusive in involved studies so that we could not estimate it completely. In addition, in biopsy-proven virus-negative patients whose condition deteriorates despite optimal conventional management, immunosuppressive therapy should be considered after ruling out the possible contraindications.

CONCLUSIONS

IVIG might be beneficial to improve LVEF and survival for myocarditis in children. However, the present evidence does not support corticosteroids as superior to conventional therapy in children with myocarditis. Further randomized controlled trials with a larger sample size are required to unambiguously delineate the clinical effect of corticosteroids and IVIG in the treatment of myocarditis in children.

DATA AVAILABILITY

The datasets generated for this study are available on request to the corresponding author.

AUTHOR CONTRIBUTIONS

YLi, YY, and JD contributed conception and design of the study. YLi and YY screened the title and abstract, selected the studies, assessed the quality of evidence, extracted the data, and performed the analysis. SC and YLia supervised study selection and data analysis. YLi and YY drafted the initial manuscript. All authors contributed to manuscript revision and read and approved the submitted version.

REFERENCES

1. Cooper LT Jr. Myocarditis. *N Engl J Med*. (2009) 360:1526–38. doi: 10.1056/NEJMra0800028
2. Caforio ALP, Pankuweit S, Arbustini E, Basso C, Gimeno-Blanes J, Felix SB, et al. Current state of knowledge on aetiology, diagnosis, management, and therapy of myocarditis: a position statement of the European Society of Cardiology Working Group on Myocardial and Pericardial Diseases. *Eur Heart J*. (2013) 34:2636–48. doi: 10.1093/eurheartj/eht210
3. D'Ambrosio A, Patti G, Manzoli A, Sinagra G, Di Lenarda A, Silvestri F, et al. The fate of acute myocarditis between spontaneous improvement and evolution to dilated cardiomyopathy: a review. *Heart*. (2001) 85:499–504. doi: 10.1136/heart.85.5.499

4. Klugman D, Berger JT, Sable CA, He J, Khandelwal SG, Slonim AD. Pediatric patients hospitalized with myocarditis: a multi-institutional analysis. *Pediatr Cardiol*. (2010) 31:222–8. doi: 10.1007/s00246-009-9589-9
5. Towbin JA, Lowe AM, Colan SD, Sleeper LA, Orav EJ, Clunie S, et al. Incidence, causes, and outcomes of dilated cardiomyopathy in children. *JAMA*. (2006) 296:1867–76. doi: 10.1001/jama.296.15.1867
6. Matsuura H, Ichida F, Saji T, Ogawa S, Waki K, Kaneko M, et al. Clinical features of acute and fulminant myocarditis in children – 2nd nationwide survey by Japanese Society of Pediatric Cardiology and Cardiac Surgery. *Circ J*. (2016) 80:2362–8. doi: 10.1253/circj.CJ-16-0234
7. Canter CE, Cunningham MW, Cooper LT. Recent clinical and translational research on pediatric myocarditis. *Prog Pediatr Cardiol*. (2011) 32:15–8. doi: 10.1016/j.ppedcard.2011.06.004
8. Qing-you Z, Jun-bao D. Recent clinical research on glucocorticoids and intravenous immunoglobulin therapy with myocarditis in children. *Chin Pediatr Emerg Med*. (2013) 20:459–63.
9. Rose NR. Viral myocarditis. *Curr Opin Rheumatol*. (2016) 28:383–9. doi: 10.1097/BOR.0000000000000303
10. Moher D, Liberati A, Tetzlaff J, Altman DG, The PG. Preferred reporting items for systematic reviews and meta-analyses: the PRISMA statement. *PLoS Med*. (2009) 6:e1000097. doi: 10.1371/journal.pmed.1000097
11. Aziz KU, Patel N, Sadullah T, Tasneem H, Thawerani H, Talpur S. Acute viral myocarditis: role of immunosuppression: a prospective randomised study. *Cardiol Young*. (2010) 20:509–15. doi: 10.1017/S1047951110000594
12. Camargo PR, Snitcowsky R, da Luz PL, Mazzieri R, Higuchi ML, Rati M, et al. Favorable effects of immunosuppressive therapy in children with dilated cardiomyopathy and active myocarditis. *Pediatr Cardiol*. (1995) 16:61–8. doi: 10.1007/BF00796819
13. English RF, Janosky JE, Ettedgui JA, Webber SA. Outcomes for children with acute myocarditis. *Cardiol Young*. (2004) 14:488–93. doi: 10.1017/S1047951104005049
14. Alrabte S, Bezanti K. Role of intravenous immunoglobulin in the treatment of acute myocarditis. *Cardiol Young*. (2013) 23:S96. doi: 10.1017/S104795111300036X
15. Atiq M, Hoda M, Aslam N. Effect of intravenous gamma globulin on short- and mid-term clinical outcome in acute viral myocarditis in children. *World J Cardiovasc Dis*. (2014) 4:39. doi: 10.4236/wjcd.2014.42007
16. Haque A, Bhatti S, Siddiqui FJ. Intravenous immune globulin for severe acute myocarditis in children. *Indian Pediatr*. (2009) 46:810–1.
17. Heidendael JF, Den Boer SL, Wildenbeest JG, Dalinghaus M, Straver B, Pajkrt D. Intravenous immunoglobulins in children with new onset dilated cardiomyopathy. *Cardiol Young*. (2018) 28:46–54. doi: 10.1017/S1047951117001561
18. Prasad AN, Chaudhary S. Intravenous immunoglobulin in children with acute myocarditis and/or early dilated cardiomyopathy. *Indian Pediatr*. (2014) 51:583–4. doi: 10.1007/s13312-014-0456-2
19. Heart Failure Society of America. Section 16: myocarditis: current treatment. *J Card Fail*. (2006) 12:e120–2. doi: 10.1016/j.cardfail.2005.11.021
20. Canter Charles E, Simpson Kathleen E. Diagnosis and treatment of myocarditis in children in the current era. *Circulation*. (2014) 129:115–28. doi: 10.1161/CIRCULATIONAHA.113.001372
21. Bern C. Chagas' disease. *N Engl J Med*. (2015) 373:456–66. doi: 10.1056/NEJMra1410150
22. Sally AH. Viral myocarditis and dilated cardiomyopathy: etiology and pathogenesis. *Curr Pharm Des*. (2016) 22:408–26. doi: 10.2174/1381612822666151222160500
23. Pollack A, Kontorovich AR, Fuster V, Dec GW. Viral myocarditis—diagnosis, treatment options, and current controversies. *Nat Rev Cardiol*. (2015) 12:670. doi: 10.1038/nrcardio.2015.108
24. Frustaci A, Russo MA, Chimenti C. Randomized study on the efficacy of immunosuppressive therapy in patients with virus-negative inflammatory cardiomyopathy: the TIMIC study. *Eur Heart J*. (2009) 30:1995–2002. doi: 10.1093/eurheartj/ehp249
25. Wojnicz R, Nowalany-Kozielska E, Wojciechowska C, Glanowska G, Wilczewski P, Niklewski T, et al. Randomized, placebo-controlled study for immunosuppressive treatment of inflammatory dilated cardiomyopathy: two-year follow-up results. *Circulation*. (2001) 104:39–45. doi: 10.1161/01.CIR.104.1.39
26. Lu C, Qin F, Yan Y, Liu T, Li J, Chen H. Immunosuppressive treatment for myocarditis: a meta-analysis of randomized controlled trials. *J Cardiovasc Med*. (2016) 17:631–7. doi: 10.2459/JCM.0000000000000134
27. Maisch B, Pankuweit S. Current treatment options in (peri)myocarditis and inflammatory cardiomyopathy. *Herz*. (2012) 37:644–56. doi: 10.1007/s00059-012-3679-9
28. Nimmerjahn F, Ravetch JV. Anti-inflammatory actions of intravenous immunoglobulin. *Annu Rev Immunol*. (2008) 26:513–33. doi: 10.1146/annurev.immunol.26.021607.090232
29. Maisch B, Alter P. Treatment options in myocarditis and inflammatory cardiomyopathy: focus on i. v. immunoglobulins. *Herz*. (2018) 43:423–30. doi: 10.1007/s00059-018-4719-x
30. Robinson J, Hartling L, Vandermeer B, Klassen TP. Intravenous immunoglobulin for presumed viral myocarditis in children and adults. *Cochrane Database Syst Rev*. (2015) 20:CD004370. doi: 10.1002/14651858.CD004370.pub3
31. Amabile N, Fraisse A, Bouvenot J, Chetaille P, Ovaert C. Outcome of acute fulminant myocarditis in children. *Heart*. (2006) 92:1269–73. doi: 10.1136/hrt.2005.078402
32. Liu C, Chen J, Liu K. Immunosuppressive treatment for inflammatory cardiomyopathy: meta-analysis of randomized controlled trials. *Int Heart J*. (2005) 46:113–22. doi: 10.1536/ihj.46.113

Conflict of Interest Statement: The authors declare that the research was conducted in the absence of any commercial or financial relationships that could be construed as a potential conflict of interest.

frontiers in Cardiovascular Medicine

CASE REPORT
published: 21 August 2019
doi: 10.3389/fcvm.2019.00121

Failing Homeostasis of Quadriceps Muscle Energy- and pH Balance During Bicycling in a Young Patient With a Fontan Circulation

Meindina G. Haarman[1†], Johannes D. L. Vos[1†], Rolf M. F. Berger[1], Tineke P. Willems[2] and Jeroen A. L. Jeneson[3]*

[1] Center for Congenital Heart Diseases, Department of Pediatric Cardiology, Beatrix Children's Hospital, University Medical Center Groningen, University of Groningen, Groningen, Netherlands, [2] Department of Radiology, University Medical Center Groningen, University of Groningen, Groningen, Netherlands, [3] Division of Neurosciences, Neuroimaging Center, University Medical Center Groningen, University of Groningen, Groningen, Netherlands

OPEN ACCESS

Edited by:
Fu Lijun,
Shanghai Children's Medical Center, China

Reviewed by:
Meena Nathan,
Boston Children's Hospital and Harvard Medical School, United States
Su-Zhen Dong,
Shanghai Children's Medical Center, China

***Correspondence:**
Meindina G. Haarman
m.g.haarman@umcg.nl

[†]These authors have contributed equally to this work

Specialty section:
This article was submitted to Pediatric Cardiology, a section of the journal Frontiers in Cardiovascular Medicine

Received: *30 April 2019*
Accepted: *06 August 2019*
Published: *21 August 2019*

Citation:
Haarman MG, Vos JDL, Berger RMF, Willems TP and Jeneson JAL (2019) Failing Homeostasis of Quadriceps Muscle Energy- and pH Balance During Bicycling in a Young Patient With a Fontan Circulation. Front. Cardiovasc. Med. 6:121. doi: 10.3389/fcvm.2019.00121

Aims: Patients with a congenital heart condition palliated with a Fontan circulation generally present with decreased exercise capacity due to impaired cardiopulmonary function. Recently, a study in patients with a Fontan circulation reported evidence for abnormal vascular endothelial function in leg muscle. We investigated if abnormal skeletal muscle hemodynamics during exercise play a role in the limited exercise tolerance of Fontan patients. If so, abnormalities in intramuscular energy metabolism would be expected both during exercise as well as during post-exercise metabolic recovery.

Methods: In a young patient with a Fontan circulation and his healthy twin brother we studied the *in vivo* dynamics of energy- and pH-balance in quadriceps muscle during and after a maximal in-magnet bicycling exercise challenge using 31-phosphorus magnetic resonance spectroscopy. An unrelated age-matched boy was also included as independent control.

Results: Quadriceps phosphocreatine (PCr) depletion during progressive exercise was more extensive in the Fontan patient than in both controls (95% vs. 80%, respectively). Importantly, it failed to reach an intermittent plateau phase observed in both controls. Quadriceps pH during exercise in the Fontan patient fell 0.3 units at low to moderate workloads, dropping to pH 6.6 at exhaustion. In both controls quadriceps acidification during exercise was absent but for the maximal workload in the twin brother (pH 6.8). Post-exercise, the rate of metabolic recovery in the Fontan patient and both controls was identical (time constant of PCr recovery 32 ± 4, 31 ± 2, and 28 ± 4 s, respectively).

Conclusion: Homeostasis of quadriceps energy- and pH-balance during a maximal exercise test failed in the Fontan patient in comparison to his healthy twin brother and an age-matched independent control. Post-exercise metabolic recovery was normal which does not support the contribution of significant endothelial dysfunction affecting adequate delivery of oxidative substrates to the muscle to the lower exercise capacity in this particular Fontan patient. These results suggest that mitochondrial ATP synthetic

capacity of the quadriceps muscle was intact but cardiac output to the leg muscles during exercise was insufficient to meet the muscular demand for oxygen. Therefore, improving cardiac output remains the main therapeutic target to improve exercise capacity in patients with a Fontan circulation.

Keywords: congenital heart disease, univentricular cardiac disease, exercise, phosphorus-31 magnetic resonance spectroscopy, metabolism

INTRODUCTION

Patients with a univentricular heart are commonly palliated with a Fontan circulation, where all systemic venous blood does not enter the heart but is diverted directly into the pulmonary arteries, without the interposition of a ventricle (1, 2). As a consequence, the single ventricular heart provides the systemic circulation in these individuals. Not surprisingly, these patients generally present with decreased exercise capacity (3–7). Classic work in exercise physiology has shown that cardiac reserve of the healthy human heart is insufficient to support adequate blood supply to the legs during maximal exercise (8, 9).

Cardiac output is, however, not the sole determinant of exercise capacity. Healthy vascular as well as skeletal muscle function also play a role (10–12). Recently, a study in patients with a Fontan circulation reported evidence for abnormal vascular endothelial function in leg muscle. On basis of this finding the authors hypothesized that decreased exercise capacity in Fontan patients may in part be caused by abnormal skeletal muscle hemodynamics (13).

Here, this matter was further investigated. In a young patient with a Fontan circulation and his healthy twin brother we studied the *in vivo* dynamics of energy- and pH-balance in quadriceps muscle during and after a maximal bicycling exercise challenge using 31-phosphorus magnetic resonance spectroscopy (31P-MRS). An unrelated sex- and age-matched boy was also studied as independent control. The aim was to investigate if abnormal skeletal muscle hemodynamics during exercise play a role in the limited exercise tolerance of Fontan patients. If so, abnormalities in intramuscular energy metabolism would be expected both during exercise as well as during post-exercise metabolic recovery.

MATERIALS AND METHODS

Ethics Statement

This study was conducted in accordance with the Declaration of Helsinki and was approved by the institutional ethics committee (University Medical Center Groningen). Informed consent for participation and publication was obtained from all study participants and/or their legally authorized representative(s).

Case Presentation

In this pilot study a young patient with a Fontan circulation, his healthy twin brother, and an unrelated sex- and age-matched control were included.

The patient, one of monozygotic twins, was diagnosed at birth with hypoplastic left heart syndrome due to mitral and aortic valve atresia for which he underwent a Norwood I procedure, followed by a bidirectional Glenn within the first year of life and subsequent completion into a Fontan circulation (with a fenestrated lateral tunnel) at the age of 4.5 years. Cardiac and developmental follow-up was uncomplicated and he leads an active lifestyle including weekly swimming classes, gymnastics, and biking, although his exercise tolerance is limited. Currently at the age of 11 years, he presented at the outpatient clinic.

Measurements

Patients with a Fontan circulation are followed with a standard follow-up protocol. This includes a 2-yearly echocardiography, cardiac magnetic resonance (CMR) imaging, pulmonary function test, and a cardiopulmonary exercise test (CPET). Also, information on height, weight, heart rate, blood pressure, and transcutaneous oxygen saturation at rest are reported.

CPET

CPET was performed on a stationary cycle ergometer with a ramp protocol with an increase of 20 W per minute. Arterial oxygen saturation was continuously monitored by transcutaneous pulse oximetry placed on the forehead. Oxygen uptake was measured using breath-by-breath analysis. The respiratory exchange ratio was calculated as the ratio between oxygen uptake (VO2) and carbon dioxide (VCO2) production at peak exercise. When an RER of >1.01 was reached, the performance was classified as adequate (14).

31P-MRS

Six weeks after the CPET, a second bicycling exercise test inside an MRI scanner was performed. Workload increments were derived from the results of the first CPET to ensure maximal exercise intensity was achieved within approximately 10 min. Dynamic *in vivo* 31P-MRS recordings of intramuscular energy metabolism and muscle pH were obtained from the vastus lateralis muscle at rest, during progressive exercise and subsequent metabolic recovery, respectively (15). Intramuscular phosphocreatine (PCr) concentration, a measure of muscular energy reserve, and pH were determined from the 31P-MRS recordings as described previously (15). The rate of post-exercise metabolic recovery, a measure of mitochondrial ATP synthetic function (16), was determined by non-linear curve-fitting of mono-exponential functions to the PCr and Pi time-course data weighted by SD of individual data points yielding estimates of the time constants tau_PCr and tau_Pi, respectively, as described previously (15).

The two healthy controls likewise performed the intra-MRI exercise test to obtain control data sets. Workload increments for these subjects were based on reference workload values for CPET (17).

RESULTS

The patient with a Fontan circulation reported no complaints of syncope, dizziness, palpitations, or chest pain. He swims once a week for 45 minutes. During gymnastics at school he sometimes needs to take a break. Besides methylphenidate, he did not use any medication. Anthropometric measurements were height: 157.8 cm (Z-score+1.00); weight: 40 kg (Z-score +0.7). Physical examination revealed that he was in good clinical condition. Blood pressures measured were 122/52 mmHg and 122/58 mmHg on his right arm and right leg, respectively. He had a normal respiratory rate and his oxygen saturation was 87%. Further physical examination showed no abnormalities besides a grade 2 systolic ejection murmur 2nd−4th left intercostal space and a palpable liver of 1 cm.

Echocardiography showed a moderate to normal systolic function of the systemic right ventricle, unobstructed cavopulmonary anastomoses, only mild atrioventricular valve insufficiency, and an open fenestration with a right to left shunt with an estimated mean pressure gradient of 6 mmHg.

During a maximal exercise test, confirmed by a RER of 1.1, oxygen saturation dropped from 88% at rest to 77% at maximal workload without any subsequent drop in O2 pulse. His maximal workload (108 Watt, 74% of predicted), maximal oxygen uptake adjusted for bodyweight (36.6 ml/kg/min, 76% of predicted), O2 pulse (77%), and maximal heart rate (164 bpm, 88% of predicted) were decreased compared to reference values (17). Patient's breathing reserve was 30% at 41 breaths/min. The VE/VCO2 slope was 40.4 and the anaerobic threshold was located at 68% of VO2 max. ECG monitoring showed a nodal cardiac rhythm at rest, rapidly converting into sinus rhythm during exercise.

31P-MRS Results

Total exercise time of the bicycling exercise test inside the MRI scanner of the patient, twin brother and second healthy control was 664, 632, and 608 seconds, respectively. PCr depletion was 95% in the Fontan patient vs. 80% in both healthy boys (**Figure 1**). End-exercise quadriceps pH was 6.6 in the Fontan patient vs. 6.8 and 6.9 in both healthy boys (**Figure 2**). In addition to these quantitative differences, we observed significant qualitative differences between the time-course of muscle PCr and pH in the patient and controls. Specifically, in both healthy boys, muscle PCr level attained a steady state value after an initial drop at the onset of exercise, followed by a monotonous progressive depletion at workloads above 70% (independent control) and 90% (healthy twin brother) of predicted Wmax (**Figure 1**). Strikingly, in the Fontan patient no such intermittent homeostatic plateau phase was observed (**Figure 1**). Similarly, homeostasis of quadriceps pH in both healthy boys was robust over almost the entire range of workloads, whereas in the patient progressive muscle acidification was manifest already at early

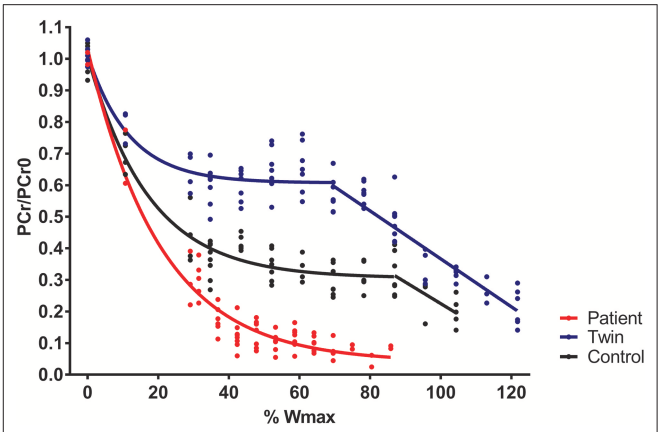

FIGURE 1 | Quadriceps phosphocreatine (PCr) content (scaled to resting content) during incremental exercise recorded in a young patient with a Fontan circulation (red trace), his healthy twin brother (blue trace), and a second age- and sex-matched healthy control (black trace). Quadriceps PCr content was determined from ^{31}P-magnetic resonance spectra as described elsewhere (15).

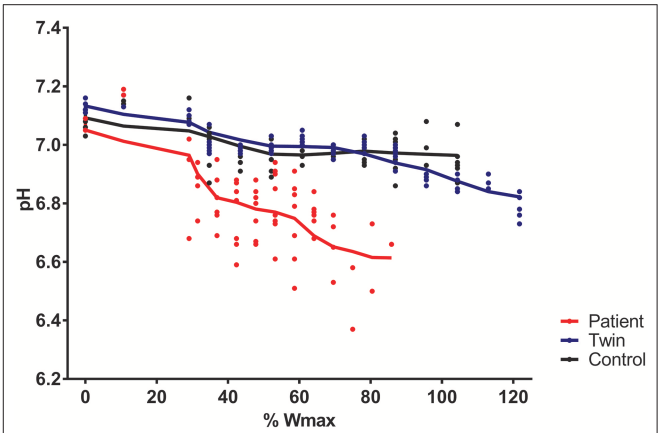

FIGURE 2 | Quadriceps pH during incremental exercise recorded in a young patient with a Fontan circulation (red trace), his healthy twin brother (blue trace), and a second age- and sex-matched healthy control (black trace). Quadriceps pH was determined from ^{31}P-magnetic resonance spectra as described elsewhere (15).

stages of the ramp exercise protocol (**Figure 2**). Post-exercise, the rates of metabolic recovery in the Fontan patient, his twin brother and the healthy control were identical (tau_PCr recovery 32 ± 4, 31 ± 2, and 28 ± 4 seconds, respectively; tau-Pi 24 ± 4, 32 ± 2, and 30 ± 6 seconds, respectively; **Supplementary Figure 1** showing the metabolic recovery in the Fontan patient). These rates are in good agreement with earlier findings in human quadriceps muscle (18, 19).

DISCUSSION

We have obtained *in vivo* evidence that exercise intolerance in a Fontan patient presenting with cyanosis and chronotropic

incompetence, is associated with failing homeostasis of quadriceps muscle energy balance and pH during exercise. Post-exercise metabolic recovery was completely normal. These findings impact the debate on the pathophysiological basis of exercise intolerance in patients with a univentricular heart palliated with a Fontan circulation. Firstly, we found no evidence for any endothelial dysfunction in the vascular bed of the leg muscles in this particular patient. Post-exercise metabolic recovery of resting PCr and Pi levels in the quadriceps muscle of the patient followed first-, not zero-, order kinetics. Moreover, the rate of recovery was identical to the rates measured in his healthy twin brother and a second, unrelated control. The latter finding also indicates that mitochondrial ATP-synthetic function in leg muscle of the patient was intact (16).

The presence of skeletal muscle hemodynamic abnormalities in response to exercise in Fontan patients was reported by Inai et al. (13). Their near-infrared spectroscopy (NIRS) observations in 50 patients palliated with a Fontan circulation showed that post-exercise recovery of muscle oxygenation in an unspecified Fontan patient was clearly dampened both in amplitude as well as rate [Figure 2 in (13)]. It has previously been shown that post-exercise metabolic recovery in muscle studied using NIRS typically correlates well with direct measurement of intramuscular metabolic recovery using 31P-MRS (20). Therefore, the fact that we failed to find any abnormalities in post-exercise metabolic recovery in our patient using 31P-MRS rules out that vascular dysfunction in skeletal muscle of single ventricle Fontan patients is a generic feature contributing to exercise limitations in this condition.

Our results of failing homeostasis of energy- and pH-balance in quadriceps muscle during exercise in the patient despite intact mitochondrial oxidative capacity suggest that cardiac output to the leg muscles during exercise was insufficient to meet the muscular demand for oxygen. Improving cardiac output therefore remains the main therapeutic target to improve exercise capacity in Fontan patients. The challenge will be to achieve this objective in a manner that is safe for the patient. The VO2 max depends on the function of the heart, the lungs and the muscles (17). Our results question the contribution of impaired mitochondrial oxidative capacity of the leg muscles in this particular Fontan patient. Although moderate-to-vigorous aerobic and resistance exercise training in Fontan patients has shown to improve venous return via an augmented peripheral muscle pump and to improve exercise capacity, the mechanism via which this is reached seems not to be an increase in mitochondrial oxidative capacity of the leg muscles (21).

Our results are based on a small sample size and therefore any definite conclusions cannot be drawn. Future studies should include more patients with a Fontan circulation. Also, using baseline CPET values in healthy controls would be worth considering. Future studies of this subject should preferably use additional methods, including dynamic MRI methodology, to investigate the presence of endothelial dysfunction in patients with a Fontan circulation (22, 23).

An alternative strategy could be to harness the metabolic power of dietary ketones to boost cardiac performance during exercise in Fontan patients. Indeed, ketone body suppletion in rodents was found to increase cardiac hydraulic work capacity by some 25% (24, 25). A recent study in athletes has found that ingestion of a synthetic ketone ester prior to physical exercise improved performance (26). Evidence suggests that the heart will switch almost completely to ketone oxidation when this oxidative substrate is available in the bloodstream (27, 28). In humans, mild nutritional ketosis may be safely achieved either by ingestion of ketone ester (26, 29) or medium-chain triglycerides [MCT; (30)]. As such, it may be interesting to study if mild nutritional ketosis during exercise may be beneficial in Fontan patients.

DATA AVAILABILITY

The datasets generated for this study are available on request to the corresponding author.

ETHICS STATEMENT

This study was conducted in accordance with the Declaration of Helsinki and was approved by the institutional ethics committee (University Medical Center Groningen). Informed consent for participation and publication was obtained from all study participants and/or their legally authorized representative(s).

AUTHOR CONTRIBUTIONS

MH, JV, JJ, and RB: substantial contributions to conception and design, acquisition of data, analysis, interpretation of data, drafting the article, and revising it critically for important intellectual content. RB and TW: revising the article critically for important intellectual content. All authors: final approval of the version to be published.

FUNDING

This work was funded by a grant from the Sebald Fund (to MH and JV) and a subcontract to NIH grant HL-072011 (to JJ).

SUPPLEMENTARY MATERIAL

The Supplementary Material for this article can be found online at: https://www.frontiersin.org/articles/10.3389/fcvm.2019.00121/full#supplementary-material

Supplementary Figure 1 | Quadriceps phosphocreatine (PCr) recovery after incremental exercise in a young patient with a Fontan circulation. Red line, a mono-exponential fit of the data (16); dotted blue lines, 95% confidence interval of the mono-exponential fit of the data ($R^2 = 0.84$; tau_PCr recovery = 32 ± 4 seconds). Quadriceps PCr content was determined from ^{31}P-magnetic resonance spectra as described elsewhere (15).

REFERENCES

1. Fontan F, Baudet E. Surgical repair of tricuspid atresia. *Thorax*. (1971) 26:240e248. doi: 10.1136/thx.26.3.240
2. Kreutzer G, Galíndez E, Bono H, De Palma C, Laura JP. An operation for the correction of tricuspid atresia. *J Thorax Cardiovasc Surg*. (1973) 66:613–21.
3. Wolff D, van Melle JP, Bartelds B, Ridderbos FS, Eshuis G, van Stratum EBHJ, et al. Fontan Circulation over Time. *Am J Cardiol*. (2017) 120:461–6. doi: 10.1016/j.amjcard.2017.05.005
4. Nir A, Driscoll DJ, Mottram CD, Offord KP, Puga FJ, Schaff HV, et al. Cardiorespiratory response to exercise after the Fontan operation, a serial study. *J Am Coll Cardiol*. (1993) 22:216–20. doi: 10.1016/0735-1097(93)90837-Q
5. Troutmann WB, Barstow TJ, Galindo AJ, Cooper DM. Abnormal dynamic cardiorespiratory response to exercise in pediatric patients after Fontan procedure. *J Am Coll Cardiol*. (1998) 27:668–79. doi: 10.1016/S0735-1097(97)00545-7
6. Zellers TM, Driscoll DJ, Mottram CD, Puga FJ, Schaff HV, Danielson GK. Exercise tolerance and cardiorespiratory response to exercise before and after the Fontan operation. *Mayo Clin Proc*. (1989) 64:1489–97. doi: 10.1016/S0025-6196(12)65704-8
7. Gewillig MH, Lundström UR, Bull C, Wyse RK, Deanfield JE. Exercise responses in patients with congenital heart disease after Fontan repair, patterns and determinants of performance. *J Am Coll Cardiol*. (1990) 15:1424–32. doi: 10.1016/S0735-1097(10)80034-8
8. Saltin B. Hemodynamic adaptations to exercise. *Am J Cardiol*. (1985) *55*:42D-7D. doi: 10.1016/0002-9149(85)91054-9
9. Bassett DR, Howley ET. Limiting factors for maximum oxygen uptake and determinants of endurance performance. *Med Sci Sports Exerc*. (2000) 32:70–84. doi: 10.1097/00005768-200001000-00012
10. Wasserman K, Hansen JE, Sue DY, Stringer WW, Sietsema KE, Sun X-G, et al. *Principles of Exercise Testing and Interpretation: Including Pathophysiology and Clinical Applications. Philadelphia, PA: Lippincott Williams & Wilkins* (2005).
11. Massie BM, Simonini A, Sahgal P, Wells L, Dudley GA. Relation of systemic and local muscle exercise capacity to skeletal muscle characteristics in men with congestive heart failure. *J Am Coll Cardiol*. (1996) 27:140–5. doi: 10.1016/0735-1097(95)00416-5
12. Cicoira M, Zanolla L, Franceschini L, Rossi A, Golia G, Zamboni M, et al. Skeletal muscle mass independently predicts peak oxygen consumption and ventilatory response during exercise in noncachectic patients with chronic heart failure. *J Am Coll Cardiol*. (2001) 37:2080–5. doi: 10.1016/S0735-1097(01)01306-7
13. Inai K, Saita Y, Takeda S, Nakazawa M, Kimura H. Skeletal muscle haemodynamics and endothelial function in patients after Fontan operation. *Am J Cardiol*. (2004) 93:792–7. doi: 10.1016/j.amjcard.2003.11.062
14. Shephard RJ. Methodology of exercise tests in healthy subjects and in cardiac patients. *Can Med Assoc J*. (1968) 99:354–9.
15. van Brussel M, van Oorschot JW, Schmitz JP, Nicolay K, van Royen-Kerkhof A, Takken T, et al. Muscle metabolic responses during dynamic in-magnet exercise testing: a pilot study in children with an idiopathic inflammatory myopathy. *Acad Radiol*. (2015) 22:1443–8. doi: 10.1016/j.acra.2015.06.013
16. Meyer RA. A linear model of muscle respiration explains monoexponential phosphocreatine changes. *Am J Physiol*. (1988) 254:C548–53. doi: 10.1152/ajpcell.1988.254.4.C548
17. Bongers BC, van brussel M, Hulzebos HJ, Takken T. *Paediatric Norms for Cardiopulmonary Exercise Testing in Relation to Gender and Age*. 's-Hertogenbosch: Boxpress (2014).
18. van Oorschot JW, Schmitz JP, Webb A, Nicolay K, Jeneson JA, Kan HE. 31P MR spectroscopy and computational modeling identify a direct relation between Pi content of an alkaline compartment in resting muscle and phosphocreatine resynthesis kinetics in active muscle in humans. *PLoS ONE*. (2013) 8:e76628. doi: 10.1371/journal.pone.0076628
19. van den Broek NM, De Feyter HM, de Graaf L, Nicolay K, Prompers JJ. Intersubject differences in the effect of acidosis on phosphocreatine recovery kinetics in muscle after exercise are due to differences in proton efflux rates. *Am J Physiol Cell Physiol*. (2007) 293:C228–37. doi: 10.1152/ajpcell.00023.2007
20. Ryan TE, Southern WM, Reynolds MA, McCully KK. A cross-validation of near-infrared spectroscopy measurements of skeletal muscle oxidative capacity with phosphorus magnetic resonance spectroscopy. *J Appl Physiol*. (2013) 115:1757–66. doi: 10.1152/japplphysiol.00835.2013
21. Cordina R, d'Udekem Y. Long-lasting benefits of exercise for those living with a Fontan circulation. *Curr Opin Cardiol*. (2019) *34*:79–86. doi: 10.1097/HCO.0000000000000582
22. Wary C, Nadaj-Pakleza A, Laforêt P, Claeys KG, Carlier R, Monnet A, et al. Investigating glycogenosis type III patients with multi-parametric functional NMR imaging and spectroscopy. *Neuromuscul Disord*. (2010) *20*:548–8. doi: 10.1016/j.nmd.2010.06.011
23. Bakermans AJ, Wessel CH, Zheng KH, Groot PFC, Stroes ESG, Nederveen AJ. Dynamic magnetic resonance measurements of calf muscle oxygenation and energy metabolism in peripheral artery disease. *J Magn Reson Imaging*. (2019). doi: 10.1002/jmri.26841. [Epub ahead of print].
24. Keon CA, Tuschiya N, Kashiwaya Y, Sato K, Clarke K, Radda GK, et al. Substrate dependence of the mitochondrial energy status in the isolated working rat heart. *Biochem Soc Trans*. (1995) 23:307S. doi: 10.1042/bst023307s
25. Sato K, Kashiwaya Y, Keon CA, Tsuchiya N, King MT, Radda GK, et al. Insulin, ketone bodies, and mitochondrial energy transduction. *FASEB J*. (1995) 9:651–8. doi: 10.1096/fasebj.9.8.7768357
26. Cox PJ, Kirk T, Ashmore T, Willerton K, Evans R, Smith A, et al. Nutritional ketosis alters fuel preference and thereby endurance performance in athletes. *Cell Metab*. (2016) 24:256–68. doi: 10.1016/j.cmet.2016.07.010
27. Little JR, Goto M, Spitzer JJ. Effect of ketones on metabolism of FFA by dog myocardium and skeletal muscle *in vivo*. *Am J Physiol*. (1970) 219:1458–63. doi: 10.1152/ajplegacy.1970.219.5.1458
28. Kim DK, Heineman FW, Balaban RS. Effects of beta-hydroxybutyrate on oxidative metabolism and phosphorylation potential in canine heart *in vivo*. *Am J Physiol*. (1991) 260:H1767–73. doi: 10.1152/ajpheart.1991.260.6.H1767
29. Stubbs BJ, Cox PJ, Evans RD, Santer P, Miller JJ, Faull OK, et al. On the metabolism of exogenous ketones in humans. *Front Physiol*. (2017) 8:848. doi: 10.3389/fphys.2017.00848
30. Freund G, Weinsier RL. Standardized ketosis in man following medium chain triglyceride ingestion. *Metabolism*. (1966) 15:980–91. doi: 10.1016/0026-0495(66)90046-1

Conflict of Interest Statement: The University Medical Center Groningen has contracts with Actelion and Lilly for consultancy-activities of RB, outside the submitted work.

The remaining authors declare that the research was conducted in the absence of any commercial or financial relationships that could be construed as a potential conflict of interest.

frontiers in Pediatrics

SYSTEMATIC REVIEW
published: 26 September 2019
doi: 10.3389/fped.2019.00374

Risk Factors of Coronary Artery Abnormality in Children With Kawasaki Disease: A Systematic Review and Meta-Analysis

Fan Yan[1], *Bo Pan*[1], *Huichao Sun*[1], *Jie Tian*[2,3,4,5] *and Mi Li*[1]*

[1] *Department of Cardiology, Children's Hospital of Chongqing Medical University, Chongqing, China,* [2] *Ministry of Education Key Laboratory of Child Development and Disorders, Chongqing, China,* [3] *National Clinical Research Center for Child Health and Disorders (Chongqing), Chongqing, China,* [4] *Chongqing Key Laboratory of Pediatrics, Chongqing, China,* [5] *China International Science and Technology Cooperation Base of Child Development and Critical Disorders, Chongqing, China*

While coronary artery abnormality (CAA) has been established as the most serious complication of Kawasaki disease (KD), there have been no detailed systematic reviews of the risk factors associated with this condition. We searched six databases and performed a systematic review and meta-analysis. Study-specific odds ratios (ORs) for each factor were pooled using a random effects model. We identified four risk factors for CAA children with KD: gender (OR, 1.75; 95% confidence interval [CI], 1.59–1.92), intravenous immunoglobulin (IVIG) resistance (OR, 3.43; 95% CI, 2.07–5.67), IVIG treatment beyond 10 days of onset of symptoms (OR, 3.65; 95% CI, 2.23–5.97), and increased C-reactive protein levels (OR, 1.02; 95% CI, 1.01–1.02). More number of the five typical symptoms of KD was identified as a protective factor against CAA (OR, 0.47; 95% CI, 0.33–0.66). Pediatric patients with IVIG resistant were more likely to develop CAA within 1 month of the onset of KD than the general population, even in patients with other risk factors for CAA. Thus, there is a potential risk of CAA misdiagnosis if echocardiography is not carried out frequently. In summary, we report four risk factors for CAA and a protective factor against CAA in children with KD. We recommend that pediatricians consider these factors much more closely. With accurate prediction and early preventive treatment in high-risk patients, we can expect a reduction in CAA rates. Further research is now required to investigate the associations between CAA and other factors including the interval between KD onset and IVIG administration, platelet count, and the duration of fever. We also need to confirm whether the frequency of echocardiography within a month of KD onset should be increased in IVIG-resistant patients.

Keywords: risk factors, coronary artery abnormality, Kawasaki disease, systematic review and meta-analysis, children

OPEN ACCESS

Edited by:
Xupei Huang,
Florida Atlantic University,
United States

Reviewed by:
Fangqi Gong,
ZheJiang University, China
Deepti Suri,
Post Graduate Institute of Medical Education and Research (PGIMER), India
Howard Prentice,
Florida Atlantic University,
United States
Wen Shen,
Florida Atlantic University,
United States

***Correspondence:**
Mi Li
lm_dhm@163.com

Specialty section:
This article was submitted to Pediatric Cardiology, a section of the journal Frontiers in Pediatrics

Received: *24 January 2019*
Accepted: *30 August 2019*
Published: *26 September 2019*

Citation:
Yan F, Pan B, Sun H, Tian J and Li M (2019) Risk Factors of Coronary Artery Abnormality in Children With Kawasaki Disease: A Systematic Review and Meta-Analysis. Front. Pediatr. 7:374. doi: 10.3389/fped.2019.00374

INTRODUCTION

Kawasaki disease (KD) is an acute self-limited disorder characterized by systemic vasculitis and predominantly occurs in early childhood (1, 2). The etiology of KD remains unknown and there are no specific diagnostic tests. Consequently, KD is characterized by fever in addition to numerous typical physical findings, including bilateral non-exudative conjunctivitis, erythema of the lips and.

oral mucosa, changes in extremities, rashes, cervical lymphadenopathy and laboratory evidence of a systemic inflammatory response (3, 4). Coronary artery abnormality (CAA) is the most serious complication occurring in 15–25% of untreated patients and is a persistent highlight in KD research (3)

Intravenous immunoglobulin (IVIG) is widely administered as the initial first-line treatment and some patients with a high risk of CAA are treated with adjunctive therapy such as corticosteroids and infliximab. However, despite these interventions, the reported incidence of CAA rate still exceeds 30% in some literatures. It is therefore very important to determine the potential risk factors of CAA in children with KD. Accordingly, previous research studies created a series of scoring systems to predict IVIG-resistant KD, considered as an important risk factor for CAA and the development of CAA in Japanese patients, such as the Harada, Kobayashi, Sano and Egami scoring systems (5–8). However, these systems were not as sensitive and specific in other populations as they were in the Japanese population (9). Moreover, these systems incorporate too many indicators and have never been systematically reviewed in detail except for a study concerning the incomplete presentation of KD and a meta-analysis investigating CAA risk factors in Chinese children (10, 11). Therefore, we conducted a systematic review and meta-analysis to investigate the risk factors of CAA in children with KD by analyzing the most up-to-date observational studies.

MATERIALS AND METHODS

Study Design

This systematic review and meta-analysis is reported in accordance with the Preferred Reporting Items for Systematic Reviews and Meta-Analyses (PRISMA) Statement (**Checklist S1**) and was registered in the International Prospective Register of Systematic Reviews (reference number: CRD42018076512).

Participants

Our analysis represented two groups: the control group—the KD patients without CAA, and the CAA group—the patients with onset of KD and CAA found in a given period of medical follow-up.

Search Strategy

We conducted a systematic literature search using electronic databases, including PubMed, Embase, Web of Science, Cochrane Library, and the National Institutes of Health Clinical Trial Databases up to the 16th May 2018. We also searched OvidMedline from 1946 to 16th May 2018. The search strategy used Medical Subject Headings (MeSH) terms or Emtree thesaurus terms combined with keywords for [(Mucocutaneous Lymph Node Syndrome) and (Coronary Artery)]. There was no language restriction. In addition, we manually searched the reference lists of original and review articles for further articles of interest. Some texts were unavailable online; in these cases, we attempted to contact the authors via email.

Inclusion and Exclusion Criteria

Our analysis included observational studies which fulfilled the following criteria: (1) Study participants were children diagnosed with KD, including both CKD and IKD; (2) All participants diagnosed with KD met the specific criteria published by the Japan Kawasaki Disease Research Committee (4th or 5th revised edition) or the American Heart Association (2001, 2004, or 2017 edition); (3) CAA was one of the outcome measures and was detected by ultrasonic cardiography as an existing abnormal body surface area adjusted by z-scores or abnormal internal lumen diameter according to criteria published by the Japanese Ministry of Health, American Heart Association, or by Chinese literature (3, 12); (4) Risk factors for CAA were investigated with no restriction to specific subgroups; (5) The study reported the odds ratio (OR) adjusted for at least one potential confounder and 95% confidence intervals (CIs) or allowed for the calculation of these parameters from the raw data presented in the article and (6) The article was written in English.

We excluded studies that examined risk factors for CAA in animal populations. We also excluded studies that were restricted to a specific clinical subgroup of KD patients, such as IVIG-resistant KD, atypical KD, recurrent KD or KD in pregnant women. We also excluded case reports, case series, reviews, letters, commentaries, conference papers and studies relating to the pathogenesis and genetics of KD.

Data Extraction and Quality Assessment

For each eligible study, two investigators (Fan Yan and Bo Pan) independently extracted the following information: author names, publication year, study design, follow-up duration (by echocardiography), study duration, study location, sample size, total number of CAA cases, diagnostic criteria used for KD, diagnostic criteria used for CAA, the definition of IVIG-resistant KD, risk factors and the methods used for statistical analysis. Quality assessments were also independently conducted by the two investigators (Fan Yan and Bo Pan) using the Newcastle-Ottawa Quality Assessment Scale for case control or cohort studies (**Checklist S2**, **Supporting Tables 1**, **2**); disagreements were resolved by group discussions.

Statistical Analysis

To control confounders, we included studies reporting estimates which adjusted for at least one potential confounder in their analysis; this strategy has been used in previous literature (13). We believe that this is a feasible approach for eliminating some publications with low evidence levels. When a reported risk factor was evaluated by three or more studies, considering the intrinsic differences of study design, we combined the adjusted ORs and 95% CIs with the random effects model to estimate pooled ORs and associated 95% CIs. The I^2 statistic was used to investigate the heterogeneity across studies; an I^2 value of $<25\%$ and $>50\%$ was considered to indicate low and high levels of heterogeneity, respectively (14). We also performed sensitivity analysis to assess the robustness of our results by omitting a single study in turn. We also conducted the Egger regression asymmetry test and the

Abbreviations: CI, Confidence intervals; CAA, Coronary artery abnormality; IVIG, Intravenous immunoglobulin; KD, Kawasaki disease; ORs, Odds ratios; PRISMA, Preferred Reporting Items for Systematic Reviews and Meta-Analyses.

Begg test to detect the presence of publication bias; this analysis showed that male gender was the only factor contributing to publication bias (all other factors were found in fewer than 10 studies). Statistical analyses were performed using STATA version 15 (StataCorp, College Station, TX).

RESULTS

In total, our initial search identified 1,970 articles. After removing duplicates and reviewing the titles and abstracts, 184 studies were potentially eligible for inclusion. After assessing the full text, 33 studies were found to conform to our specific inclusion criteria. Finally, 21 of the 33 studies were included in our meta-analysis; collectively, these studies included 26,684 participants, of which 4,461 were diagnosed with CAA, contributing 9 risk factors investigated in more than two studies (**Figure 1**). Specific characteristics of these data are summarized in **Table 1**.

Risk Factors

Gender

Meta-analysis of 10 studies that estimated the association between male gender and CAA identified that males had a significantly higher risk for CAA (OR, 1.75; 95% CI,

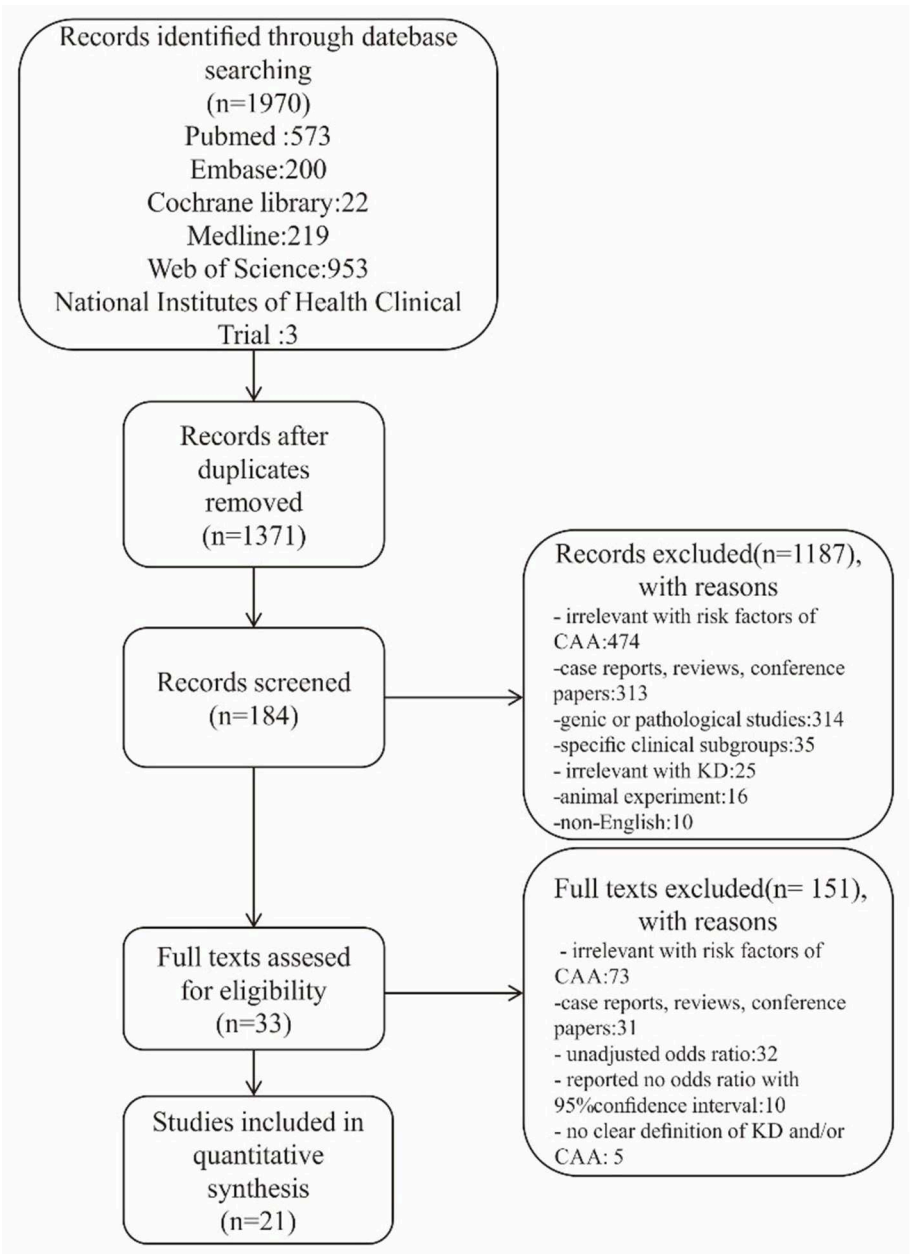

FIGURE 1 | Flow diagram of studies screened in the meta-analysis.

TABLE 1 | Summary of the included studies for quantitative synthesis.

Study	Study design	Duration of following-up (by echocardiogram)	Study duration	Study location	Population sample size	Total number of CAA	Diagnostic criteria of KD	Diagnostic criteria of CAA	Define of IVIG-resistant KD	Risk factors	Method of statistical analysis	NOS score
Yeo et al. (15)	Case-control	At least 2 months	2001–2006	Korea	136	16	AHA2004	JMH	ND	Days of fever, number of symptoms	Logistic regression analysis	7
Hamza et al. (16)	Case-control	Eight weeks	2012–2016	Egypt	64	34	AHA2017	Z score	ND	Platelet count	Logistic regression analysis	7
Wilder et al. (17)	Case-control	ND	1991–2002	America	324	21	AHA2004	Z score	ND	Diagnosis after illness day 10	Logistic regression analysis	7
Weng et al. (18)	Cohort study	Eight weeks	1993–2009	Taiwan	2,116	81	AHA2004	JMH	Fever for 3 days after initial IVIG	Neutrophil count,Dose of IVIG, platelet count	Logistic regression analysis	7
Tajima et al. (19)	Case-control	1 month	2006–2012	Japan	100	13	JKDRC	JMH	A second Dose IVIG	Delayed IVIG (≥6 days), IVIG-resistant	Logistic regression analysis	7
Song et al. (20)	Case-control	At least 2 months	2001–2007	Korea	221	30	AHA2004	JMH	fever for 2 days after initial IVIG	Number of symptoms, Post-IVIG fever, Harada score	Logistic regression analysis	7
Sabharwal et al. (21)	Case-control	6–8 weeks	1990–2007	Canada	1,374	266	AHA2004	JMH	Absence of fever within 36 h after initial IVIG	Age, male, duration of fever before diagnosis, albumin level, hemoglobin level, platelet count, IVIG-resistant	Logistic regression analysis	8
Ruan et al. (22)	Case-control	1 month	2003–2009	China	1,370	486	AHA2004	JMH	ND	Age (<6 months), Male, Time of IVIG, IVIG dose, platelet count and ESR	Logistic regression analysis	7
Qiu et al. (23)	Cohort study	ND	2009–2014	China	930	179	Similar to JKDRC	Chinese literatures criteria	ND	Treatment time, treatment time 10 days	Logistic regression analysis	7
Patel et al. (24)	Case-control	ND	1994–2008	Denmark	284	37	Similar to AHA2004	AHA	ND	Age, male, time of IVIG (>10 days)	Logistic regression analysis	7
Kim et al. (25)	Case-control	At least 2 months.	2001–2005	Korea	285	19	AHA2001	JMH	ND	Total days of fever >8 days	Logistic regression analysis	7
Young et al. (26)	Cohort study	6–8 weeks	2005–2013	Korea	703	266	AHA2004	Z score	Received more than one dose of IVIG	Male, fever duration (≥8 days), CRP (≥7 mg/dl), WBC count (>12 × 103/μL)	Logistic regression analysis	8

(Continued)

TABLE 1 | Continued

Study	Study design	Duration of following-up (by echocardiogram)	Study duration	Study location	Population sample size	Total number of CAA	Diagnostic criteria of KD	Diagnostic criteria of CAA	Define of IVIG-resistant KD	Risk factors	Method of statistical analysis	NOS score
Ghelani et al. (27)	Case-control	ND	2000–2002 and 2007–2009	America	203	33	AHA2004	Z score or JMH	Fever after one dose of IVIG and administration of additional IVIG or use of corticosteroids or TNF-alpha blockers	ESR, refractory Kawasaki disease	Logistic regression analysis	7
Chen et al. (28)	Case-control	1 month	2008–2012	China	2,302	365	JKDRC	JMH	ND	Male, age (≤1 year), IVIG unresponsiveness, time of IVIG	Logistic regression analysis	7
Lega et al. (29)	Case-control	6–8 weeks	1988–2007	France	194	64	AHA2004	AHA	Fever ≥36 h after complete IVIG infusion	Male, Age, PE, Hemoglobin level, IVIG resistance	Logistic regression analysis	7
Boudiaf and Achir (30)	Case-control	4–6 weeks	2005–2014	Algeria	133	30	AHA2004	Z score	ND	Duration of fever (>10 days), platelet count (>450,000/$mm^{3\cdot}$)	Logistic regression analysis	8
Berdej-Szczot et al. (9)	Case-control	No clear description	2003–2016	Poland	73	13	AHA	AHA	Fever >36 h after IVIG	Delay diagnosis, platelet count, additional symptom	Logistic regression analysis	8
Kim et al. (31)	Case-control	ND	2012–2014	Korea	5,151	524	AHA2004	JMH	A second dose of IVIG	CRP	Logistic regression analysis	7
Xu et al. (32)	Case-control	3 months	2009–2012	China	422	83	JKDRC	Chinese literatures Criteria	ND	RDW (>14.55%), IVIG resistance,Fever duration (>14 days)	Logistic regression analysis	8
Callinan et al. (33)	Case-control	ND	2000–2009	America	1,843	341	Similar to AHA2004	AHA	ND	Male, age, race, time of IVIG (>5 days)	Logistic regression analysis	7
Kim et al. (34)	Cohort study	3 months	ND	Korea	8,456	1,560	AHA2004	Z score or JMH	Existence of second-line treatment	Male, age, fever duration, incomplete presentation, recurrent illness, high/medium-dose ASA, non-response to first-line treatment, total bilirubin, CRP	Logistic regression analysis	6

NOS, Newcastle-Ottawa Quality Assessment Scale; AHA, American Heart Association; JMH, Japanese Ministry of Health; ND, no description; Z score, body surface area adjusted z-scores; JKDRC, Japan Kawasaki Disease Research Committee; ESR, erythrocyte sedimentation rate erythrocyte sedimentation rate; PE, pericardial effusion; CRP, C-reactive protein; RWD, red blood cell distribution width.

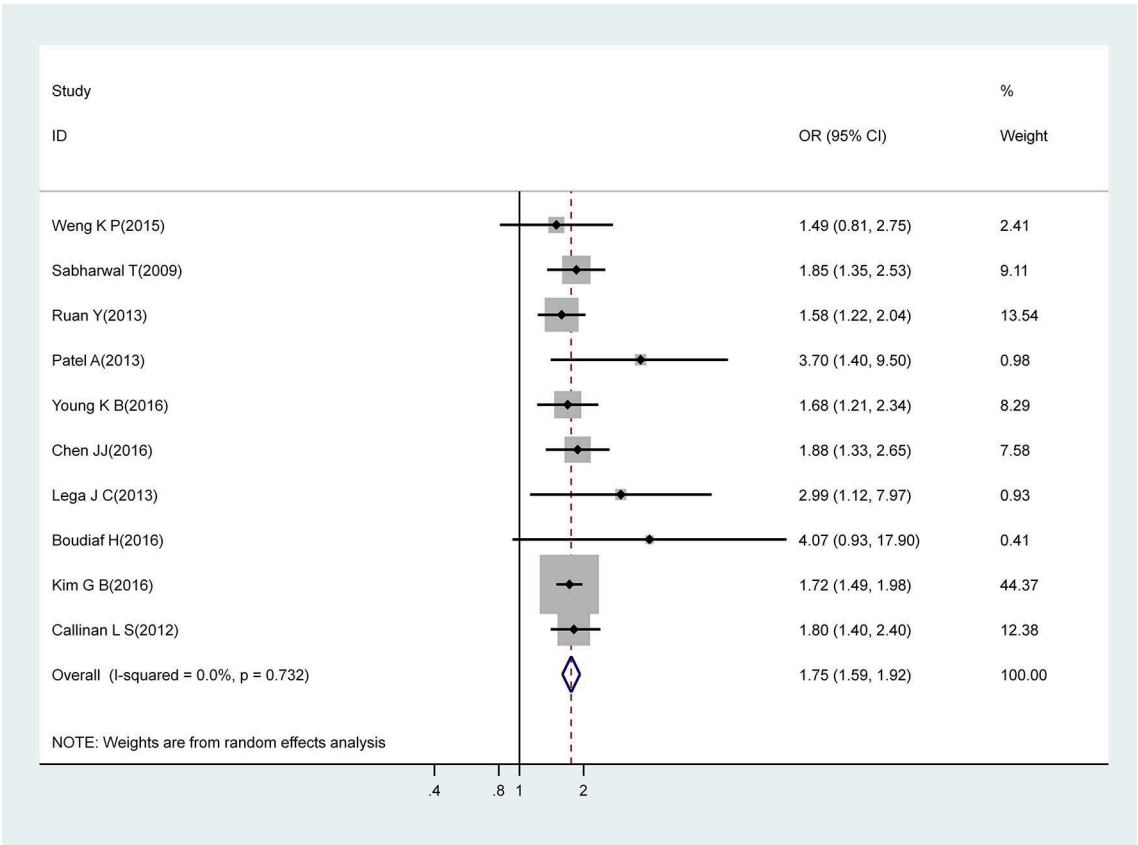

FIGURE 2 | Pooled odds ratio for CAA by gender (male vs. female).

1.59–1.92), with no evidence of heterogeneity ($I^2 = 0\%$; $P = 0.732$) (**Figure 2**).

IVIG Resistance

Pooled estimates from eight studies revealed that IVIG resistance markedly increased the risk for CAA (OR, 3.43; 95% CI, 2.07–5.67). However, there was significant heterogeneity between these eight studies ($I^2 = 76.7\%$; $P = 0.000$). Subgroup analysis showed that a follow-up duration of >1 month was an increased risk factor for CAA (OR, 2.19; 95% CI, 1.48–3.24) with acceptable levels of heterogeneity ($I^2 = 47.8\%$; $P = 0.105$). A follow-up duration of ≤1 month was associated with an increased risk for CAA (OR, 6.16; 95% CI, 3.79–10.00) with low levels of heterogeneity ($I^2 = 0\%$; $P = 0.560$) (**Figure 3**).

IVIG Treatment Beyond 10 Days of Onset of Symptoms

Meta-analysis of three studies showed that IVIG treatment beyond 10 days of onset of symptoms was associated with a significantly higher risk for CAA (OR, 3.65; 95% CI 2.23–5.97) with low levels of heterogeneity ($I^2 = 1.8\%$; $P = 0.361$) (**Figure 4**).

C-Reactive Protein (CRP)

Meta-analysis of pooled estimates from four studies revealed that a 1 mg/L increase in CRP levels was associated with a 0.02-fold increase in risk for CAA (OR, 1.02; 95% CI 1.01–1.02); with low levels of heterogeneity ($I^2 = 0.0\%$; $P = 0.441$) (**Figure 5**).

The Number of Symptoms

We investigated three studies which attempted to identify an association between the number of presenting symptoms and CAA. An increasing number of the five typical symptoms of KD was shown to represent a significant protective factor for CAA (OR, 0.47; 95% CI, 0.33–0.66), with no evidence of heterogeneity ($I^2 = 0.0\%$; $P = 0.753$) (**Figure 6**).

Other Factors

Our analysis identified several factors that were not significantly associated with CAA, including the interval between KD onset and IVIG administration (OR, 1.17; 95% CI, 0.99–1.38), platelet count (OR, 1.00; 95% CI, 1.00–1.01), the duration of fever (OR, 1.12; 95% CI, 0.99–1.27) and total bilirubin (OR, 1.06; 95% CI, 0.96–1.16) (**Figure 7**).

DISCUSSION

CAA is a commonly encountered and serious complication of KD and is considered as a leading cause of acquired heart disease in children. Identifying patients at high risk of developing CAA at an early stage after the onset of KD is important for determining a

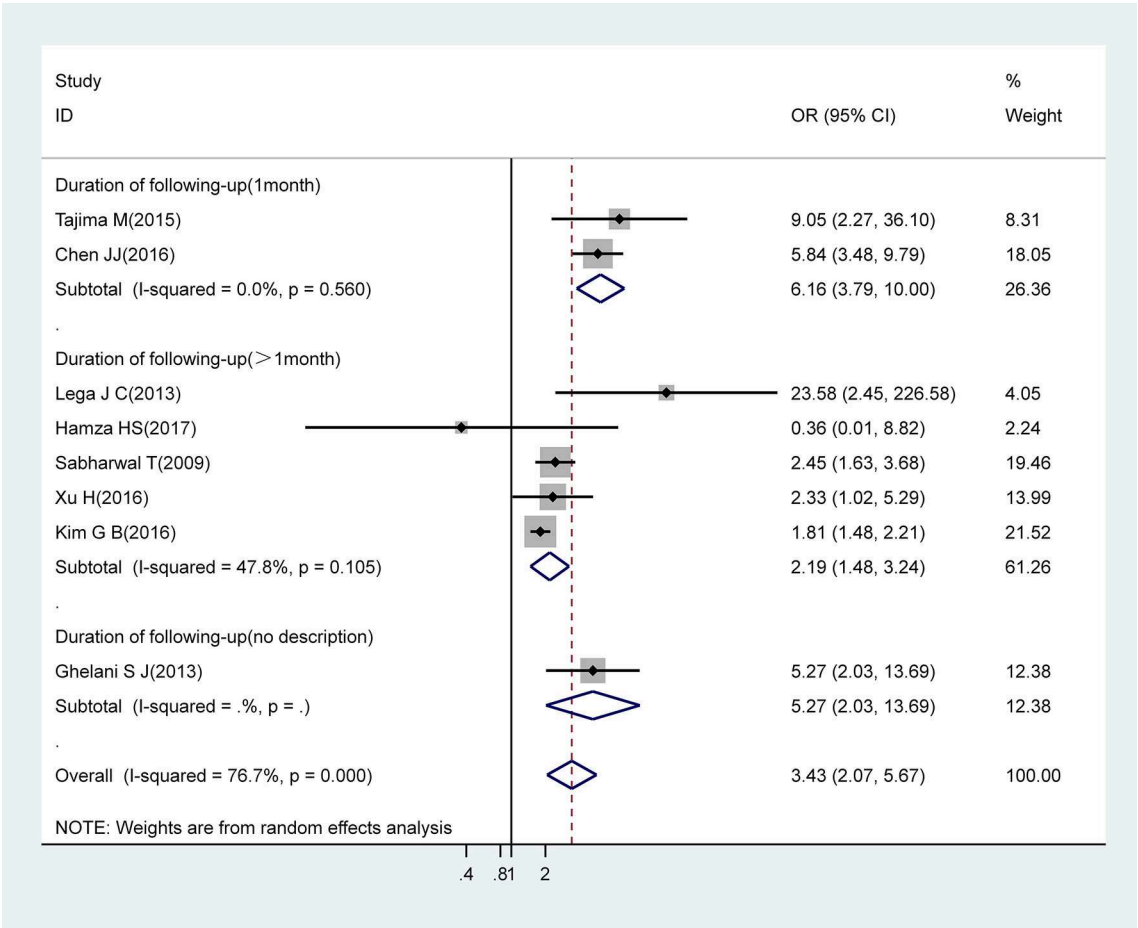

FIGURE 3 | Pooled odds ratio for CAA by IVIG-resistance (subgroup analysis basing on duration of following-up).

more intensive treatment, the duration of follow-up and targeted research studies aimed at identifying new therapeutic methods for KD. In this meta-analysis, we identified five factors, based on good evidence that were strongly associated with CAA: male gender, IVIG resistance, IVIG treatment beyond 10 days of onset of symptoms, increased CRP levels, and the number of presenting symptoms. To the best of our knowledge, our study is the first meta-analysis to comprehensively investigate the risk factors associated with CAA. Only two other related studies have been published: one investigated the incomplete presentation of KD as a risk factor for CAA, the other investigated risk factors for CAA in Chinese children but with non-convincing evidence (10, 11).

While previous studies failed to determine an association between CAA and gender (35, 36), we successfully identified male gender as a strong risk factor for CAA; this difference is likely to be due to the increasing number of multicenter studies being reported with large sample sizes. Epidemiological surveys, carried out in different biogeographical regions, also identified higher incidence rates of KD in males, the boys with KD outnumbered the girls with KD by the ratio approximately 1.5–1.7:1 (37, 38). Until now, there is no convincing explanation for this gender bias, although Kobayashi and Dallaire noted that healthy male children tended to have larger coronary arteries than female children (39, 40), thus making the diagnosis of KD and CAA easier in males when using the same diagnostic criteria. There are no obvious differences in terms of estrogen level when compared between genders in children, consequently it is difficult to explain the incidence of CAA in children with KD as an autoimmune disease by estrogen levels alone, as is the case for some autoimmune diseases in adults (41). However, it has been demonstrated that different genders express variable levels of miRNA expression and that these differences may play a role in the immune response and autoimmune diseases (42, 43).

IVIG treatment is a well-established primary treatment measure for KD, and several studies have linked IVIG factors (such as dose and brand) with a higher risk of CAA (18, 44). We found that IVIG resistance and IVIG treatment beyond 10 days of onset of symptoms was associated with an increased risk for CAA. IVIG is considered to alleviate coronary injury by regulating the immune system, including the reduction of cytokine levels and the suppression of endothelial cell activation (45, 46). However, studies have reported IVIG resistance rates as

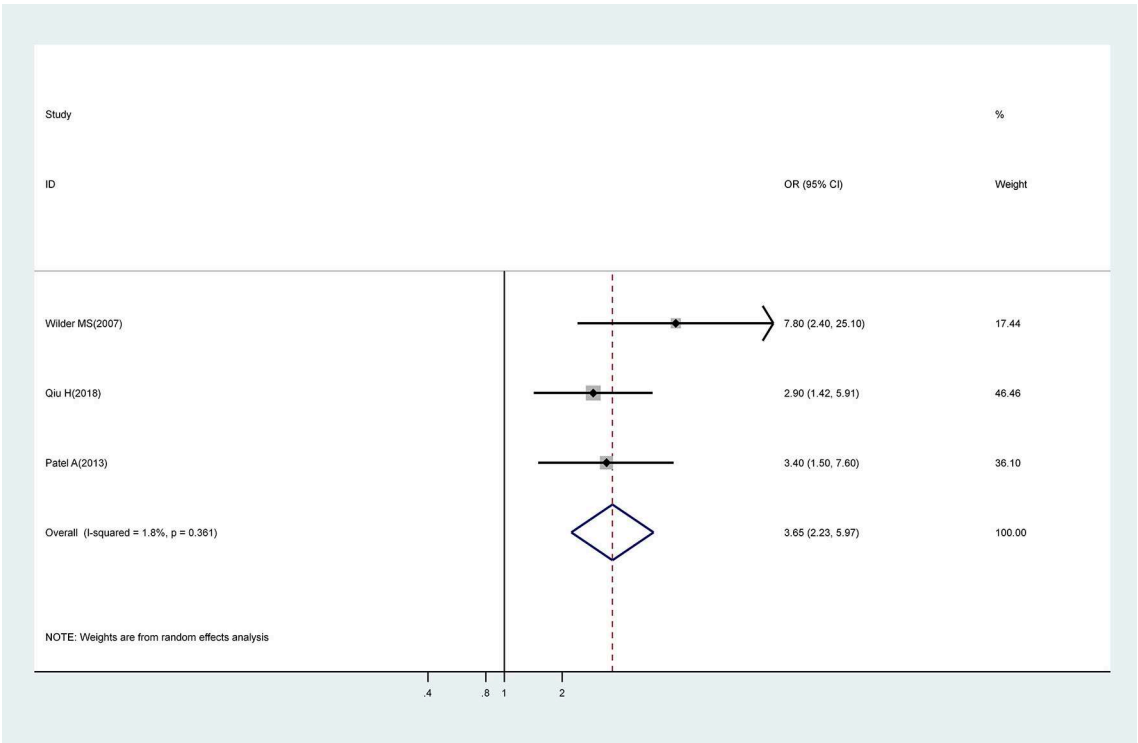

FIGURE 4 | Pooled odds ratio for CAA by time of initial IVIG treatment (IVIG > 10 days vs. IVIG ≤ 10 days).

high as 18–22%; accordingly, several scoring systems have been developed to predict IVIG-resistant KD. Because CAA usually occurs 7–10 days after the onset of KD onset (47, 48), the AHA published guidelines in 2004 which stated that "therapy should be instituted within the first 10 days of illness and, if possible, within 7 days of illness." However, some researchers believe that the status of the illness can potentially exert influence on the association between delayed IVIG treatment and CAA. For example, Qiu observed higher CRP levels and ESR in patients in which IVIG treatment was delayed (23). However, delayed IVIG treatment can cause increased CRP levels and ESR, and there is no good evidence to determine the causal factor between these factors. In contrast, higher CRP levels and ESR represent a more aggressive inflammatory response, causing a more typical manifestation of the illness with advanced intervention by IVIG treatment. Further studies are now required to clarify whether there is a correlation between the status of KD and delayed IVIG treatment.

We also noticed that patients with a 1 month follow-up period showed an obvious increase in the risk of CAA compared with those with a follow-up duration of >1 month among the IVIG-resistant population. AHA guidelines recommend that echocardiographic evaluation is recommended at the time of diagnosis, at 2 weeks, and at 6–8 weeks after the onset of disease. In a previous study, Tajima and Chen conducted echocardiographic examinations before and after IVIG treatment and 1 month after the diagnosis of KD (19, 28); this suggested that echocardiographic evaluations should be carried out more frequently within 1 month of the onset of KD than those recommended by the AHA guidelines. This could explain the differences between subgroups. Based on these findings, we attempted to verify whether this difference also existed in other populations. Unfortunately, with the limited number of studies included for other risk factors, we were only able to carry out the same subgroup analysis in the male population. However, in situations where studies included in our subgroup analysis were somewhat similar to the IVIG-resistant population, we found no noticeable difference in the risk of CAA when compared between shorter and longer follow-up periods (OR, 1.68; 95% CI, 1.37–2.06 vs. OR, 1.74; 95% CI, 1.55–1.96) (**Supporting Figure 1**). In summary, children with KD who were resistant to IVIG appeared to be more likely to develop CAA within 1 month after KD onset than the general population, even compared to patients with other risk factors for CAA. As a consequence, there are potential risks for the misdiagnosis of CAA when echocardiography is not carried out frequently. Whether echocardiography should be performed more often within 1 month of KD onset in an IVIG-resistant population remains to be confirmed by future studies.

Our meta-analysis found an apparently increased risk of CAA in children with elevated CRP levels. However, this did not appear to be a neglectable risk factor with a magnitude of 10 mg/L increasing frequently. When considered as a categorical variable, as in the present study and many others, an elevated CRP level is

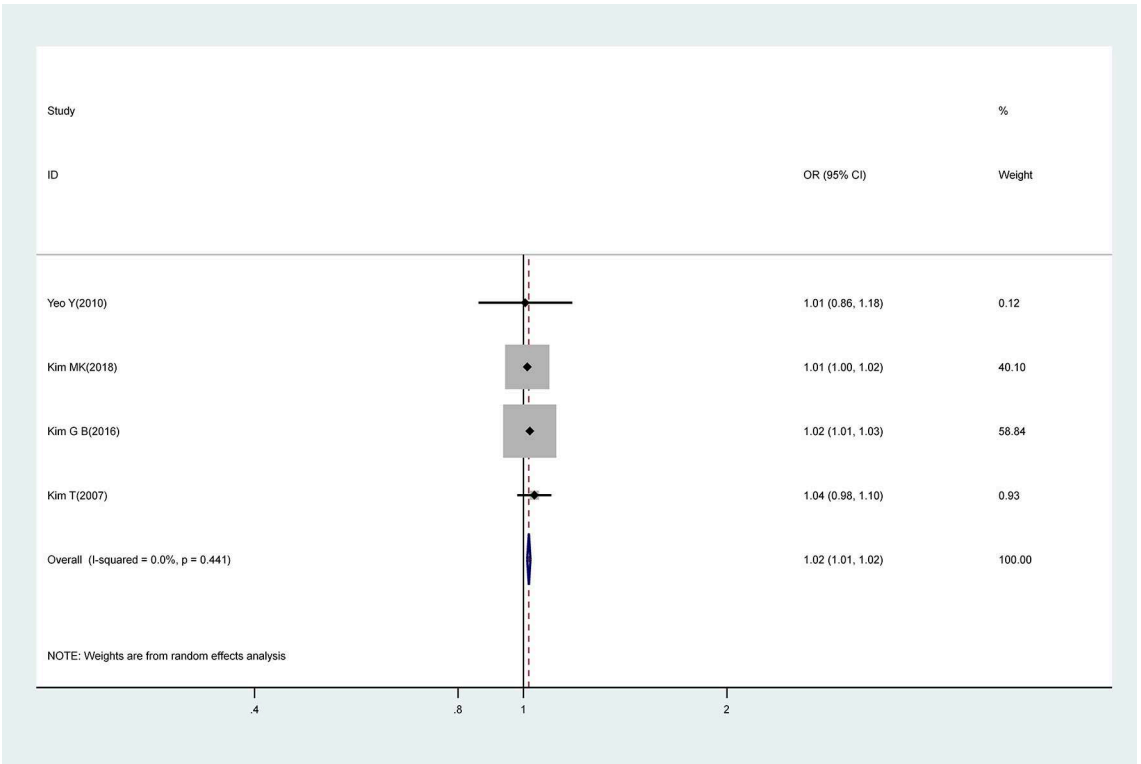

FIGURE 5 | Pooled odds ratio for CAA by CRP (mg/L).

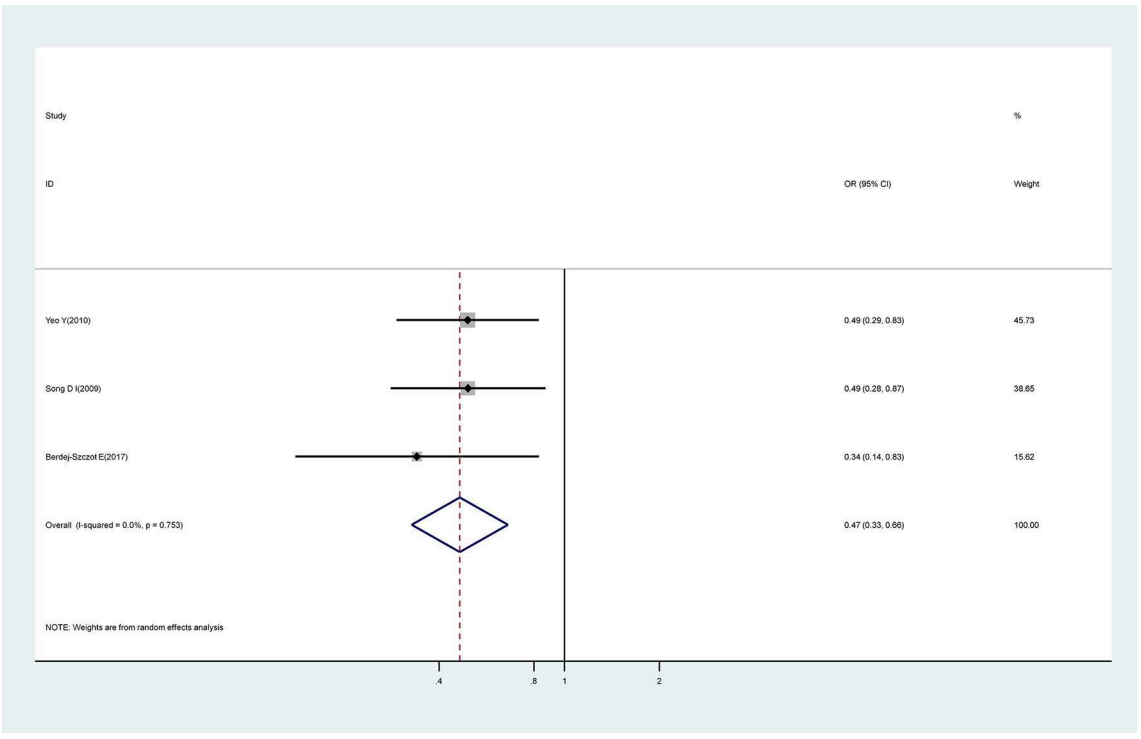

FIGURE 6 | Pooled odds ratio for CAA by number of the five typical symptoms of KD.

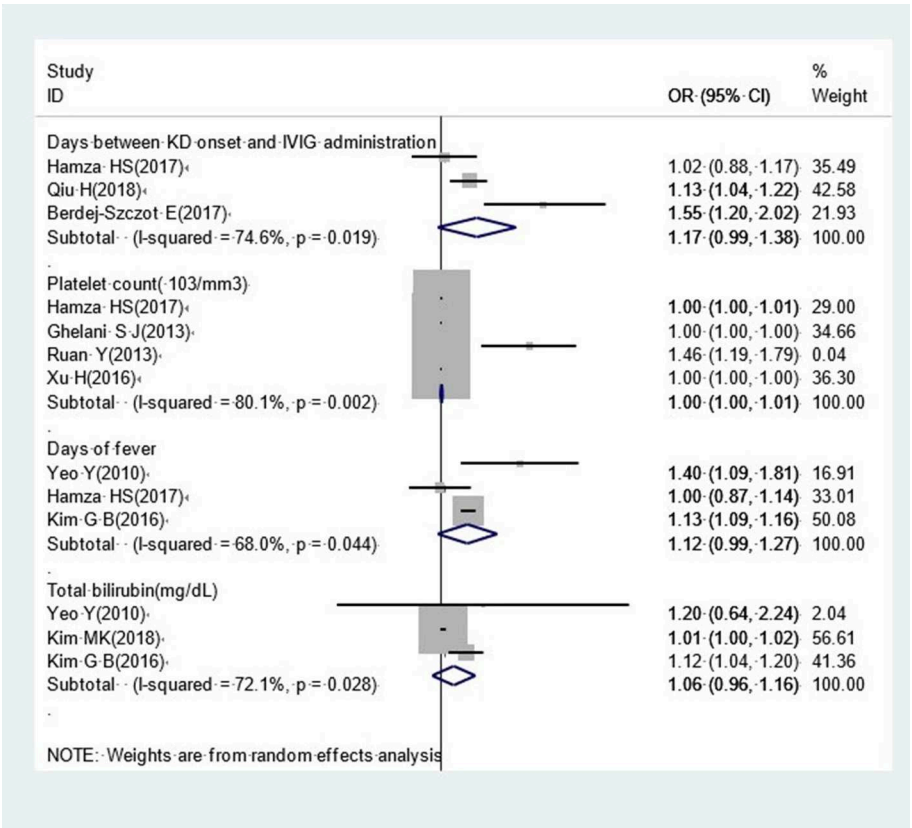

FIGURE 7 | Pooled odds ratios for CAA by other factors.

an important risk factor of CAA (5, 26, 49). Furthermore, some recent studies that have investigated the association between atherosclerosis and inflammatory status clearly recognized the fact that CRP is also a reliable marker of inflammation and the prediction of coronary events (50–52). However, in another study, Kim studied the genetic loci that influence the levels of CRP and identified a CRP locus that is associated with high CRP levels but without affecting the development of CAA (53). However, this result may have been due to the small sample size and the fact that this previous study focused only upon a single race (Korean); it is also possible that some other underlying cause may influence the development of CAA. Furthermore, one has to consider genotypic and phenotypic diversity and irrelevant factors associated with potential confounding factors, such as gender, the duration of IVIG treatment, and the number of symptoms. One may therefore speculate that determining the primary characteristics of individuals rather than the genetic features of KD is the key in making a specific and sensitive prediction regarding CAA.

Although we did not acquire sufficient studies with which to perform a meta-analysis for the relationship between atypical KD and CAA development, we still identified that more number of the five typical symptoms of KD was a strong protective factor for CAA. However, some previous studies have stated that delays in diagnosis and IVIG treatment are associated with atypical forms of KD (54, 55). Furthermore, children of a younger age have consistently been associated with atypical KD (24, 29). However, in all three of the studies included in our meta-analysis, no significant differences were identified in terms of age and/or interval between KD onset and IVIG administration when compared between CAA(+) and CAA(–) patients. Even after adjusting for such factors, more number of symptoms was clearly a protective factor of CAA. It seems reasonable to suggest that a lower number of symptoms relates to the manifestation of an immature or dysfunctional immune response during the onset of disease.

Although the interval between KD onset and IVIG administration, platelet count, and the duration of fever were not expected to show an obvious relationship with the development of CAA, the lower values of the narrow confidence intervals for these factors were very close to 1.0. Given that we could only include a limited number of studies to investigate these factors, it is possible that our final results could easily be changed by introducing more studies into our meta-analysis. As shown in **Figure 7**, the study reported Hamza was responsible for negative results in our meta-analysis relating to the interval between KD onset and the administration of IVIG and the duration of fever. Although this study scored 7 stars on the Newcastle-Ottawa Quality Assessment Scale, the sample size was small (64 participants); this may have had an impact upon the

on the accuracy of this research. As platelet counts can be as high as 150,000 to 450,000 platelets per microliter of blood, it is difficult to distinguish a remarkable effect with a 1,000-platelet increase in platelet count. Consequently, we considered that the adoption of an appropriate cut-off point could be helpful, as in previous studies (18, 30, 56). Hence, we cannot deny a potential connection between platelet count and CAA development, and further research is now needed to determine a stable relationship between these two factors. With regards to total bilirubin, only three previous studies have considered the potential role of bilirubin in CAA; these studies yield contradictory findings and therefore there is a lack of good evidence to support a potential relationship between these factors. We were unable to perform meta-analysis for some important continuous variables, such as lymphopenia, neutrophils, and eosinophils. This was because the cut-off point for these factors varied across different studies. In order to study risk factors in a more appropriate manner, it would be more meaningful for future studies to acquire uniform cut-off values for such continuous variables.

Strengths and Limitations

Our systematic review has several strengths. This is the first systematic review to comprehensively investigate the risk factors for CAA in children with KD. We used a strict search strategy to screen six databases, including PubMed, Embase, Web of Science, Cochrane Library, National Institutes of Health Clinical Trial Databases and OvidMedline. Based on the Newcastle-Ottawa Scale (NOS), 20/21 included studies scored $\geq$7 stars, suggested high-quality studies. We included a range of publications involving different ethnic populations from across the world to ensure the applicability of our findings and to investigate a wide range of risk factors for CAA. Furthermore, the application of adjusted ORs helped us to avoid the influence of confounding variables, at least in part. We also determined the heterogeneity between the studies included in sub-group analysis and found that apart from IVIG resistance, all other factors showed low levels of heterogeneity. Our sensitivity analysis showed that the sequential omission of a single study did not significantly influence the observed results and the magnitude of effects.

There are some important limitations to this systematic review that need to be considered. First, there are some differences in the criteria used to diagnose CAA. Second, although all of the publications involved in our meta-analysis were of high quality, all of these studies featured data that was acquired retrospectively. Thus, without cautious interpretation, these outcomes could exert a negative impact. Considering the limited number of studies for some factors, the accuracy and validity of the relationship between these factors and CAA may also be questionable. Besides, because of the intrinsic differences in the design of included studies, such as study types, duration of follow-up and so on, potential bias could not be completely ruled out. Finally, in terms of the assessment of publication bias, we were only able to show that there was no apparent publication bias with respect to male gender when using the Egger regression asymmetry test and the Begg test; we did not have a sufficient sample size to carry out similar tests for the other factors.

CONCLUSIONS

Although a number of indicators have been identified to predict the development of CAA development in pediatric KD patients, these studies have never been systematically reviewed. This can reduce the accuracy of prediction and create difficulties in applying these indicators in clinical scenarios. Our present study confirmed that gender, IVIG resistance, IVIG treatment beyond 10 days of onset of symptomsand increased CRP levels are all significant risk factors for CAA. We also identified reliable evidence to support the fact that more number of presenting symptoms is a protective factor against CAA. We recommend that pediatricians should consider these five reliable factors. By more accurate prediction, and earlier preventative treatment for high risk patients, we can expect a reduction in CAA rates. Further research is now needed to investigate the association between CAA and other factors including the interval between KD onset and IVIG administration, platelet count and the duration of fever. Future research should also aim to determine whether echocardiography should be performed more frequently within 1 month of the onset of KD in IVIG-resistant patients.

DATA AVAILABILITY STATEMENT

All datasets analyzed for this study are included in the manuscript/**Supplementary Files**.

ETHICS STATEMENT

This article does not feature any studies with human participants or animals that were carried out by the authors. This systematic review and meta-analysis is based on a collection of data retrieved from studies that have already been published. We did not collect individual patient data and did not have direct contact with any of the included patients.

AUTHOR CONTRIBUTIONS

FY, JT, and ML designed and conceived the experiments. FY and BP performed the experiments. FY, BP, and HS analyzed the data. FY and BP contributed reagents, materials, and analysis tools. FY, JT, and ML wrote the manuscript.

SUPPLEMENTARY MATERIAL

The Supplementary Material for this article can be found online at: https://www.frontiersin.org/articles/10.3389/fped.2019.00374/full#supplementary-material

Checklist S1 | The PRISMA Statement.

Checklist S2 | Newcastle-Ottawa Quality Assessment Scale for case control studies and cohort studies.

Supporting Figure 1 | Pooled odds ratio for CAA by gender (male vs. female, subgroup analysis according to the duration of follow-up).

Supporting Table 1 | The Newcastle-Ottawa Quality Assessment Scale for case control studies.

Supporting Table 2 | The Newcastle-Ottawa Quality Assessment Scale for cohort studies.

REFERENCES

1. Kawasaki T. [Acute febrile mucocutaneous syndrome with lymphoid involvement with specific desquamation of the fingers and toes in children]. *Allergy.* (1967) 16:178–222.
2. Sánchezmanubens J, Bou R, Anton J. Diagnosis and classification of Kawasaki disease. *J Autoimmun.* (2014) 48–49:113–7. doi: 10.1016/j.jaut.2014.01.010
3. Newburger JW, Takahashi M, Gerber MA, Gewitz MH, Tani LY, Burns JC, et al. Diagnosis, treatment, and long-term management of Kawasaki disease: a statement for health professionals from the Committee on Rheumatic Fever, Endocarditis and Kawasaki Disease, Council on Cardiovascular Disease in the Young, American Heart Association. *Circulation.* (2004) 110:2747–71. doi: 10.1161/01.CIR.0000145143.19711.78
4. Burns JC, Glodé MP. Kawasaki syndrome. *Lancet.* (2004) 364:533–44. doi: 10.1016/S0140-6736(04)16814-1
5. Harada K. Intravenous gamma-globulin treatment in Kawasaki disease. *Acta Paediatr.* (1991) 33:805–10. doi: 10.1111/j.1442-200X.1991.tb02612.x
6. Kobayashi T, Inoue Y, Takeuchi K, Okada Y, Tamura K, Tomomasa T, et al. Prediction of intravenous immunoglobulin unresponsiveness in patients with Kawasaki disease. *Circulation.* (2006) 113:2606. doi: 10.1161/CIRCULATIONAHA.105.592865
7. Seki M, Kobayashi T, Kobayashi T, Morikawa A, Otani T, Takeuchi K, et al. External validation of a risk score to predict intravenous immunoglobulin resistance in patients with kawasaki disease. *Pediatr Infect Dis J.* (2011) 30:145–7. doi: 10.1097/INF.0b013e3181f386db
8. Kobayashi T, Morikawa A, Ikeda K, Seki M, Shimoyama S, Ishii Y, et al. Efficacy of intravenous immunoglobulin combined with prednisolone following resistance to initial intravenous immunoglobulin treatment of acute Kawasaki disease. *J Pediatr.* (2013) 163:521–6. doi: 10.1016/j.jpeds.2013.01.022
9. Berdej-Szczot E, Małecka-Tendera E, Gawlik T, Firek-Pedras M, Szydłowski L, Gawlik A. Risk factors of immunoglobulin resistance and coronary complications in children with Kawasaki disease. *Kardiol Polska.* (2017) 75:261–6. doi: 10.5603/KP.a2016.0179
10. Ha KS, Jang G, Lee J, Lee K, Hong Y, Son C, et al. Incomplete clinical manifestation as a risk factor for coronary artery abnormalities in Kawasaki disease: a meta-analysis. *Eur J Pediatr.* (2013) 172:343–9. doi: 10.1007/s00431-012-1891-5
11. Zhao LL, Wang YB, Suo L. Meta-analysis of the risk factors for coronary artery lesion secondary to Kawasaki disease in Chinese children. *Zhonghua Er Ke Za Zhi.* (2011) 49:459–67.
12. Fu S, Gong F, Xie C, Zhu W, Wang W, Shen H, et al. S100A12 on circulating endothelial cells surface in children with Kawasaki disease. *Pediatr Res.* (2010) 68:165. doi: 10.1203/PDR.0b013e3181e67ce8
13. Autier P. Risk factors for breast cancer for women aged 40 to 49 years. *Ann Intern Med.* (2012) 157:529. doi: 10.7326/0003-4819-157-7-201210020-00016
14. Higgins JP, Thompson SG, Deeks JJ, Altman DG. Measuring inconsistency in meta-analyses. *BMJ.* (2003) 327:557–60. doi: 10.1136/bmj.327.7414.557
15. Yeo Y, Kim T, Ha K, Jang G, Lee J, Lee K, et al. Incomplete Kawasaki disease in patients younger than 1 year of age: a possible inherent risk factor. *Eur J Pediatr.* (2009) 168:157. doi: 10.1007/s00431-008-0722-1
16. Hamza HS, Raouf WA, Zaher AZ, Agha HM. Acute Kawasaki disease with emphasis on the echocardiographic profile: a single center experience. *Glob Cardiol Sci Pract.* (2017) 2017:e201727. doi: 10.21542/gcsp.2017.27
17. Wilder MS, Palinkas LA, Kao AS, Bastian JF, Turner CL, Burns JC. Delayed diagnosis by physicians contributes to the development of coronary artery aneurysms in children with Kawasaki syndrome. *Pediatr Infect Dis J.* (2007) 26:256–60. doi: 10.1097/01.inf.0000256783.57041.66
18. Weng KP, Hsieh KS, Huang SH, Ou SF, Ma CY, Ho TY, et al. Clinical relevance of the risk factors for coronary artery lesions in Kawasaki disease. *Kaohsiung J Med Sci.* (2012) 28:23–9. doi: 10.1016/j.kjms.2011.09.002
19. Tajima M, Shiozawa Y, Kagawa J. Early appearance of principal symptoms of kawasaki disease is a risk factor for intravenous immunoglobulin resistance. *Pediatr Cardiol.* (2015) 36:1159–65. doi: 10.1007/s00246-015-1136-2
20. Song D, Yeo Y, Ha K, Jang G, Lee J, Lee K, et al. Risk factors for Kawasaki disease-associated coronary abnormalities differ depending on age. *Eur J Pediatr.* (2009) 168:1315–21. doi: 10.1007/s00431-009-0925-0
21. Sabharwal T, Manlhiot C, Benseler SM, Tyrrell PN, Chahal N, Yeung RS, et al. Comparison of factors associated with coronary artery dilation only versus coronary artery aneurysms in patients with Kawasaki disease. *Am J Cardiol.* (2009) 104:1743–7. doi: 10.1016/j.amjcard.2009.07.062
22. Ruan Y, Ye B, Zhao X. Clinical characteristics of Kawasaki syndrome and the risk factors for coronary artery lesions in China. *Pediatr Infect Dis J.* (2013) 32:397–402. doi: 10.1097/INF.0b013e31829dd45e
23. Qiu H, He Y, Rong X, Ren Y, Pan L, Chu M, et al. Delayed intravenous immunoglobulin treatment increased the risk of coronary artery lesions in children with Kawasaki disease at different status. *Postgraduate Med.* (2018) 130:442. doi: 10.1080/00325481.2018.1468712
24. Patel A, Holman RC, Callinan LS, Sreenivasan N, Schonberger LB, Fischer TK, et al. Evaluation of clinical characteristics of Kawasaki syndrome and risk factors for coronary artery abnormalities among children in Denmark. *Acta Paediatr.* (2013) 102:385–90. doi: 10.1111/apa.12142
25. Kim T, Choi W, Woo CW, Choi B, Lee J, Lee K, et al. Predictive risk factors for coronary artery abnormalities in Kawasaki disease. *Eur J Pediatr.* (2007) 166:421–5. doi: 10.1007/s00431-006-0251-8
26. Kim BY, Kim D, Kim YH, Ryoo E, Sun YH, Jeon IS, et al. Non-responders to intravenous immunoglobulin and coronary artery dilatation in Kawasaki disease: predictive parameters in Korean children. *Korean Circ J.* (2016) 46:542–9. doi: 10.4070/kcj.2016.46.4.542
27. Ghelani SJ, Kwatra NS, Spurney CF. Can coronary artery involvement in Kawasaki disease be predicted? *Diagnostics.* (2013) 3:232–43. doi: 10.3390/diagnostics3020232
28. Chen JJ, Ma XJ, Liu F, Yan WL, Huang MR, Huang M, et al. Epidemiologic features of Kawasaki disease in Shanghai from 2008 through 2012. *Pediatr Infect Dis J.* (2016) 35:7–12. doi: 10.1097/INF.0000000000000914
29. Lega JC, Bozio A, Cimaz R, Veyrier M, Floret D, Ducreux C, et al. Extracoronary echocardiographic findings as predictors of coronary artery lesions in the initial phase of Kawasaki disease. *Arch Dis Childhood.* (2013) 98:97–102. doi: 10.1136/archdischild-2011-301256
30. Boudiaf H, Achir M. The clinical profile of Kawasaki disease in Algerian children: a single institution experience. *J Trop Pediatr.* (2016) 62:139–43. doi: 10.1093/tropej/fmv090
31. Kim MK, Song MS, Kim GB. Factors predicting resistance to intravenous immunoglobulin treatment and coronary artery lesion in patients with Kawasaki disease: analysis of the Korean nationwide multicenter survey from 2012 to 2014. *Korean Circ J.* (2018) 48:71–9. doi: 10.4070/kcj.2017.0136
32. Xu H, Fu S, Wang W, Zhang Q, Hu J, Gao L, et al. Predictive value of red blood cell distribution width for coronary artery lesions in patients with Kawasaki disease. *Cardiol Young.* (2016) 26:1151–7. doi: 10.1017/S1047951115002140
33. Callinan LS, Tabnak F, Holman RC, Maddox RA, Kim JJ, Schonberger LB, et al. Kawasaki syndrome and factors associated with coronary artery abnormalities in California. *Pediatr Infect Dis J.* (2012) 31:894–8. doi: 10.1097/INF.0b013e31825c4d7c
34. Kim GB, Yu JJ, Yoon KL, Jeong SI, Song YH, Han JW, et al. Medium- or higher-dose acetylsalicylic acid for acute Kawasaki disease and patient outcomes. *J Pediatr.* (2016) 184:125. doi: 10.1016/j.jpeds.2016.12.019
35. Ichida F, Fatica NS, Engle MA, O'Loughlin JE, Klein AA, Snyder MS, et al. Coronary artery involvement in Kawasaki syndrome in Manhattan, New York: risk factors and role of aspirin. *Pediatrics.* (1987) 80:828–35.
36. Koren G, Lavi S, Rose V, Rowe R. Kawasaki disease: review of risk factors for coronary aneurysms. *J Pediatr.* (1986) 108:388–92. doi: 10.1016/S0022-3476(86)80878-2
37. Holman RC, Curns AT, Belay ED, Steiner CA, Schonberger LB. Kawasaki syndrome hospitalizations in the United States, 1997 and 2000. *Pediatrics.* (2003) 112:495–501. doi: 10.1542/peds.112.3.495
38. Chang RK. The incidence of Kawasaki disease in the United States did not increase between 1988 and 1997. *Pediatrics.* (2003) 111:1124–5. doi: 10.1542/peds.111.5.1124
39. Kobayashi T, Fuse S, Sakamoto N, Mikami M, Ogawa S, Hamaoka K, et al. A new Z score curve of the coronary arterial internal diameter using the lambda-mu-sigma method in a pediatric population. *J Am Soc Echocardiogr.* (2016) 29:794–801.e29. doi: 10.1016/j.echo.2016.03.017
40. Dallaire F, Dahdah N. New equations and a critical appraisal of coronary artery Z scores in healthy children. J Am Soc Echocardiogr. (2011) 24:60–74. doi: 10.1016/j.echo.2010.10.004

41. Cattalini M, Soliani M, Caparello MC, Cimaz R. Sex differences in pediatric rheumatology. *Clin Rev Allergy Immunol.* (2019):293–307. doi: 10.1007/s12016-017-8642-3
42. Selmi C, Brunetta E, Raimondo MG, Meroni PL. The X chromosome and the sex ratio of autoimmunity. *Autoimmun Rev.* (2012) 11:A531–7. doi: 10.1016/j.autrev.2011.11.024
43. Menasha J, Levy B, Hirschhorn K, Kardon NB. Incidence and spectrum of chromosome abnormalities in spontaneous abortions: new insights from a 12-year study. *Genet Med.* (2005) 7:251–63. doi: 10.1097/01.GIM.0000160075.96707.04
44. Manlhiot C, Yeung RS, Chahal N, McCrindle BW. Intravenous immunoglobulin preparation type: association with outcomes for patients with acute Kawasaki disease. *Pediatr Allergy Immunol.* (2010) 21:515–21. doi: 10.1111/j.1399-3038.2010.00987.x
45. Kobayashi T, Saji T, Otani T, Takeuchi K, Nakamura T, Arakawa H, et al. Efficacy of immunoglobulin plus prednisolone for prevention of coronary artery abnormalities in severe Kawasaki disease (RAISE study): a randomised, open-label, blinded-endpoints trial. *Lancet.* (2012) 379:1613. doi: 10.1016/S0140-6736(11)61930-2
46. Kim HK, Oh J, Hong YM, Sohn S. Parameters to guide retreatment after initial intravenous immunoglobulin therapy in Kawasaki disease. *Korean Circ J.* (2011) 41:379–84. doi: 10.4070/kcj.2011.41.7.379
47. Zhang T, Yanagawa H, Oki I, Nakamura Y, Yashiro M, Ojima T, et al. Factors related to cardiac sequelae of Kawasaki disease. *Eur J Pediatr.* (1999) 158:694–7. doi: 10.1007/s004310051181
48. Yanagawa H, Tuohong Z, Oki I, Nakamura Y, Yashiro M, Ojima T, et al. Effects of gamma-globulin on the cardiac sequelae of Kawasaki disease. *Pediatr Cardiol.* (1999) 20:248–51. doi: 10.1007/s002469900458
49. Bai L, Feng T, Yang L, Zhang Y, Jiang X, Liao J, et al. Retrospective analysis of risk factors associated with Kawasaki disease in China. *Oncotarget.* (2017) 8:54357–63. doi: 10.18632/oncotarget.17530
50. Blake GJ, Ridker PM. Novel clinical markers of vascular wall inflammation. *Circ Res.* (2001) 89:763–71. doi: 10.1161/hh2101.099270
51. Ridker PM, Pare G, Parker A, Zee RY, Danik JS, Buring JE, et al. Loci related to metabolic-syndrome pathways including LEPR, HNF1A, IL6R, and GCKR associate with plasma C-reactive protein: the Women's Genome Health Study. *Am J Hum Genet.* (2008) 82:1185–92. doi: 10.1016/j.ajhg.2008.03.015
52. Ross R. Atherosclerosis–an inflammatory disease. *N Engl J Med.* (1999) 340:115. doi: 10.1056/NEJM199901143400207
53. Kim JJ, Yun SW, Yu JJ, Yoon KL, Lee KY, Kil HR, et al. Common variants in the CRP promoter are associated with a high C-reactive protein level in Kawasaki disease. *Pediatr Cardiol.* (2015) 36:438–44. doi: 10.1007/s00246-014-1032-1
54. Chang FY, Hwang B, Chen SJ, Lee PC, Meng CC, Lu JH. Characteristics of Kawasaki disease in infants younger than six months of age. *Pediatr Infect Dis J.* (2006) 25:241–4. doi: 10.1097/01.inf.0000202067.50975.90
55. Witt MT, Minich LL, Bohnsack JF, Young PC. Kawasaki disease: more patients are being diagnosed who do not meet American Heart Association Criteria. *Pediatrics.* (1999) 104:e10. doi: 10.1542/peds.104.1.e10
56. Chantasiriwan N, Silvilairat S, Makonkawkeyoon K, Pongprot Y, Sittiwangkul R. Predictors of intravenous immunoglobulin resistance and coronary artery aneurysm in patients with Kawasaki disease. *Paediatr Int Child Health.* (2018) 38:209–12. doi: 10.1080/20469047.2018.1471381

Conflict of Interest: The authors declare that the research was conducted in the absence of any commercial or financial relationships that could be construed as a potential conflict of interest.

frontiers in Pediatrics

ORIGINAL RESEARCH
published: 01 October 2019
doi: 10.3389/fped.2019.00388

The Clinical Features of Children With Acute Fulminant Myocarditis and the Diagnostic and Follow-Up Value of Cardiovascular Magnetic Resonance

Jianli Lv[1], *Bo Han*[1]*, *Cuiyan Wang*[2], *Jing Wang*[1], *Diandong Jiang*[1], *Lijian Zhao*[1], *Yingchun Yi*[1] *and Jianjun Zhang*[1]

[1] *Department of Pediatric Cardiology, Shandong Provincial Hospital Affiliated to Shandong University, Jinan, China,*
[2] *Shandong Medical Imaging Research Institute, Jinan, China*

OPEN ACCESS

Edited by:
Hongfang Jin,
Peking University First Hospital, China

Reviewed by:
Jie Tian,
Children's Hospital of Chongqing Medical University, China
Meirong Huang,
Shanghai Children's Medical Center, China
Dingding Xiong,
St. Vincent Mercy Medical Center, United States

****Correspondence:***
Bo Han
hanbo35@163.com

Specialty section:
This article was submitted to Pediatric Cardiology, a section of the journal Frontiers in Pediatrics

Received: *26 June 2019*
Accepted: *09 September 2019*
Published: *01 October 2019*

Citation:
Lv J, Han B, Wang C, Wang J, Jiang D, Zhao L, Yi Y and Zhang J (2019) The Clinical Features of Children With Acute Fulminant Myocarditis and the Diagnostic and Follow-Up Value of Cardiovascular Magnetic Resonance. Front. Pediatr. 7:388. doi: 10.3389/fped.2019.00388

Objective: To investigate the clinical features and the diagnostic and follow-up value of acute fulminant myocarditis (AFM) in children.

Methods: A total of 20 children diagnosed with AFM admitted to our department were reviewed, and the clinical manifestations; pathogenic examination results; myocardial injury biomarkers; and electrocardiography, echocardiogram, and cardiovascular magnetic resonance (CMR) results were analyzed.

Results: Twenty children with AFM, including 12 males and 8 females, aged 3–16 years, were analyzed. The initial symptoms were abdominal pain, vomiting, fatigue, syncope, and convulsions. All children had significantly increased hs-cTnT and NT-pro BNP. In addition to nonspecific ST-T changes, there were 10 cases of complete atrioventricular block, 2 cases of advanced atrioventricular block, and 1 case of ventricular tachycardia. Echocardiography showed an increase in the cardiac chamber sizes in 15 patients and a decrease in left ventricular ejection fraction (LVEF) in 17 patients. There were 16 patients with abnormal CMR findings, including 13 cases of high T2-weighted image (T2WI) signal and 14 cases of late gadolinium enhancement (LGE). In the patients who underwent CMR within 14 days of onset, the sensitivity of T2WI and LGE and the positive diagnosis rate were higher than in those who underwent CMR after 14 days, but the difference was not statistically significant. CMR was followed up in 10 patients: 7 patients returned to normal, 2 patients still had mild LGE, and 1 patient developed inflammatory dilated cardiomyopathy. All patients were treated with high-dose immunoglobulin, 11 of whom received high-dose immunoglobulin combined with glucocorticoids. Eight patients received temporary pacemakers, and 1 patient received ECMO. None of the patients died. The peak of hs-cTnT was significantly higher in the glucocorticoid group than in the unused glucocorticoid group (2853.4 ± 2217.2 and 1124.7 ± 527.3 pg/ml, respectively).

Conclusion: Children with AFM have unique clinical features. Early identification and effective treatment can reduce the mortality rate and improve the prognosis.

CMR is highly sensitive in the diagnosis of ARM, especially within 14 days of onset, and is a useful noninvasive imaging technique for the early identification of AFM in children. The dynamic observation and follow-up of children with AFM through CMR can guide clinical decision-making and prognosis assessment.

Keywords: children, acute fulminant myocarditis, cardiovascular magnetic resonance, pacemaker, ECMO

INTRODUCTION

Acute fulminant myocarditis (AFM) in children has a rapid onset and progresses rapidly. Most of the onsets are concealed. Extracardiac manifestations are predominant. It is difficult to make an early diagnosis. Various arrhythmias, Adams-Stokes syndrome, heart failure, cardiogenic shock, and even sudden cardiac death can occur within 24–48 h of onset. AFM is a clinically critical pediatric illness with a high mortality rate. A recent national survey in Japan found that the survival rate of children with AFM was only 48.6% (1). The key to affecting the mortality rate is related to early identification and effective treatment. Cardiovascular magnetic resonance (CMR) has received increasing attention in the diagnosis of children with AFM. It has been reported in the literature that the positive predictive value of CMR for acute myocarditis is over 90%. However, for patients with AFM, due to the serious condition and the inconvenience of the examination, the clinical application of CMR is greatly limited. Our early studies have shown that CMR is more sensitive than AFM in the diagnosis of conventional myocarditis. This study retrospectively analyzed the clinical data and CMR findings of 20 children with AFM and explored the clinical features of AFM in children and the value of CMR in diagnosis, treatment, and prognosis to provide valuable and important information for the diagnosis and treatment of this disease.

MATERIALS AND METHODS

Research Subjects

Twenty patients with AFM admitted to our hospital from November 2011 to March 2019 were enrolled, including 12 males and 8 females aged 3–16 years (8.4 ± 3.1 years).

Ethics Statements

This study was carried out in accordance with the recommendations of the Ethics Committee of Shandong Provincial Hospital Affiliated to Shandong University. All subjects gave written informed consent in accordance with the Declaration of Helsinki. The protocol was approved by the Ethics Committee of Shandong Provincial Hospital Affiliated with Shandong University.

The clinical data of the children were reviewed, including clinical manifestations; pathogenic examination results; myocardial injury biomarkers; electrocardiogram, echocardiography, and cardiac MRI results; treatment methods; and outcomes.

Inclusion criteria: ① a diagnosis of acute myocarditis in line with the criteria for the clinical diagnosis of myocarditis in the *Diagnostic Recommendations for Children with Myocarditis* (2018 edition) published by the Subspecialty Group of Cardiology of the Society of Pediatrics of Chinese Medical Association (2); and ② a diagnosis of AFM, which refers to clinical manifestations of severe heart failure within 2 weeks of onset (cardiac function level IV) and acute myocarditis requiring positive inotropic drugs, vasopressors, and/or mechanical circulation support to maintain heart function or blood pressure (3).

Exclusion criteria: nonischemic cardiomyopathy, congenital heart disease, myocardial infarctions and other diseases that can explain the clinical manifestations.

CMR

The machine used for the inspection was the 3.0T Skyra from Siemens. The heart rate is required to be 120 beats/min or less during the examination. The scan sequence includes gradient echo sequence, spin echo sequence, and inversion recovery fast spin echo sequence, first perfusion scan and late gadolinium enhancement (LGE). The contrast agent used in LGE was gadolinium-diethylenetriaminepentacetate (Gd-DTPA).

CMR Criteria for the Diagnosis of Myocarditis (4)

The diagnosis is established when the CMR performance meets two or more of the following three criteria: ① Regional or global myocardial signal intensity increases in T2-weighted images (T2WI); ② Increased global myocardial early enhancement ratio between the myocardium and skeletal muscle in gadolinium-enhanced T1-weighted images (T1WI); There is at least 1 focal lesion with nonischemic regional distribution in inversion recovery-prepared late gadolinium-enhanced T1WI (LGE).

Statistical Analysis

SPSS 25.0 statistical software was used, and the measured data are expressed as the range (mean ± standard deviation). The *t*-test was used to compare the two samples. Correlation analysis was performed with the Pearson correlation coefficient test. The count data are expressed by frequency (rate) and were analyzed by Fisher's exact probability method using the χ^2 test. $P < 0.05$ was considered statistically significant.

RESULTS

The main clinical data of 20 children with AFM are shown in **Table 1**.

Initial Symptoms

The initial symptoms were abdominal pain and vomiting in 12 patients (60%), chest tightness and fatigue in 4 patients (20%),

TABLE 1 | Main clinical data of 20 children with AFM.

Patient #	Age (yr)	Gender	Symptoms	Pathogens	hs-cTnT (pg/ml)	ECG	ECHO		CMR			Treatment		LOS
							CCE	LVEF (%)	FIT	T2WI	LGE	UOG	MCS	
1	9	F	Abdominal pain, vomiting	ASO	2,102	–	Yes	25	7	–	+	Yes	–	34
2	6	M	Vomiting	MP	1,632	CAVB	Yes	40	11	+	+	Yes	–	28
3	13	M	Syncope	–	1,967	CAVB	Yes	38	12	+	+	Yes	Pacemaker	33
4	7	M	Abdominal pain	–	2,783	CAVB	Yes	60	17	–	–	Yes	Pacemaker	16
5	8	F	Abdominal pain, vomiting	MP	6,457	–	Yes	33	13	+	+	Yes	–	29
6	10	F	Abdominal pain	ASO	269.2	–	Yes	30	24	–	–	Yes	–	32
7	12	F	Abdominal pain	–	1,791	CAVB	Yes	42	13	–	–	Yes	–	25
8	3	M	Abdominal pain, vomiting	–	1,864	AAVB	Yes	48	12	+	+	Yes	–	24
9	8	M	Convulsion	MP	956	CAVB	No	41	17	+	+	No	Pacemaker	22
10	16	F	Chest tightness	EBV	3,367	–	No	43	11	+	+	Yes	–	28
11	10	M	Fatigue	HHV6	1,550	CAVB	No	61	69	–	–	Yes	Pacemaker	34
12	9	M	Vomiting	MP	822.3	–	Yes	38	6	+	–	No	–	13
13	7	M	Palpitation	EBV, HHV6	212	–	Yes	37	20	+	+	No	–	26
14	5	M	Vomiting	MP	1,011	AAVB	Yes	50	12	-	+	No	–	19
15	10	F	Fatigue	–	1,164	–	Yes	35	10	+	+	No	–	22
16	9	F	Syncope	MP	1,477	CAVB	No	62	10	+	+	No	Pacemaker	23
17	7	F	Vomiting	ASO	1,105	CAVB	Yes	39	16	+	+	No	Pacemaker	19
18	3	M	Fatigue	–	1,188	CAVB	Yes	37	11	+	+	No	Pacemaker	31
19	7	M	Abdominal pain, vomiting	–	7,605	VT	Yes	20	23	+	+	Yes	ECMO	26
20	9	M	Vomiting	–	2,187	CAVB	No	45	38	–	+	No	Pacemaker	42

hs-cTnT, hypersensitive cardiac troponin T; CCE, cardiac chamber enlargement; LVEF, left ventricular ejection fraction; FIT, first inspection time; UOG, use of glucocorticoid; MCS, mechanical circulation support; LOS, length of stay; ASO, anti-streptolysin O; MP, mycoplasma pneumonia; EBV, Epstein-Barr virus; HHV6, human herpesvirus 6; CAVB, complete atrioventricular block; AAVB, advanced atrioventricular block; VT, ventricular tachycardia.

syncope and convulsion in 3 patients (15%), and palpitation in 1 patient (5%). The time from onset to admission was 0–7 days (3 ± 1.6 days). The most serious patients were often hospitalized within a few hours because of the deterioration of their condition, which manifested as heart failure, cardiogenic shock, Adams-Stokes syndrome, or severe arrhythmia.

Pathogen Examination

All patients underwent pathogen examinations after admission, including EBV, cytomegalovirus, coxsackie virus, parvovirus B19, adenovirus, HHV6, and hepatitis virus detection; influenza A and B virus nucleic acid detection; MP-IgM antibody and ASO detection; and sputum and blood bacterial culture analysis. There were a total of 12 abnormalities, including 6 patients positive for MP-IgM, 3 patients positive for ASO, 1 patient with EBV infection, 1 patient with HHV6 infection, and patient with mixed EBV and HHV6 infection.

hs-cTnT and NT-Pro BNP Results

hs-cTnT and NT-pro BNP were significantly increased in 20 children with AFM. Both peaked at 3–7 days (3.9 ± 1.0 days) after onset, then gradually decreased, and after 14–30 days (21.6 ± 5.5 days) returned to normal (**Figure 1**). Pearson correlation analysis confirmed that there was a significant correlation between hs-cTnT and NT-pro BNP (correlation coefficient 0.788–0.921, $P < 0.05$).

Electrocardiogram

Twenty patients underwent routine 12-lead ECG after admission. In addition to nonspecific ST-T abnormalities, there were 10 (50%) patients with CAVB, 2 (10%) with AAVB, and 1 (5%) with VT. The conduction block occurred within 0–4 days (1.2 ± 1.3 days) after onset, and conduction was mostly restored after 1–9 days (3.6 ± 2.5 days). However, there was still one patient with first-degree atrioventricular block combined with complete right bundle branch block during follow-up.

Echocardiography

Twenty patients were admitted to the hospital for echocardiography, and 18 patients (90%) had positive results for AFM. The diameter of the heart chamber was increased in 15 patients (75%), with 9 cases involving the left heart, 1 case involving the right heart, and 5 cases involving the whole heart. Except for 2 patients that did not return to normal, the remaining 13 patients returned to normal after 10–26 days (16.9 ± 4.9 days). Seventeen patients (85%) had a decreased LVEF (<60%) with an EF value of 20–50% (37.7 ± 7.7%):14 patients returned to normal within 30 days (16.4 ± 4.4 days), 2 patients returned to normal within 3 months, and 1 patient did not recover for half a year. Electrocardiography results from 10 patients (50%) showed a thickening of the ventricular wall that mainly involved the left ventricle. All patients had a reduction in wall motion, mainly in the interventricular septum and left ventricular inferior wall. There were 13 patients (65%) with

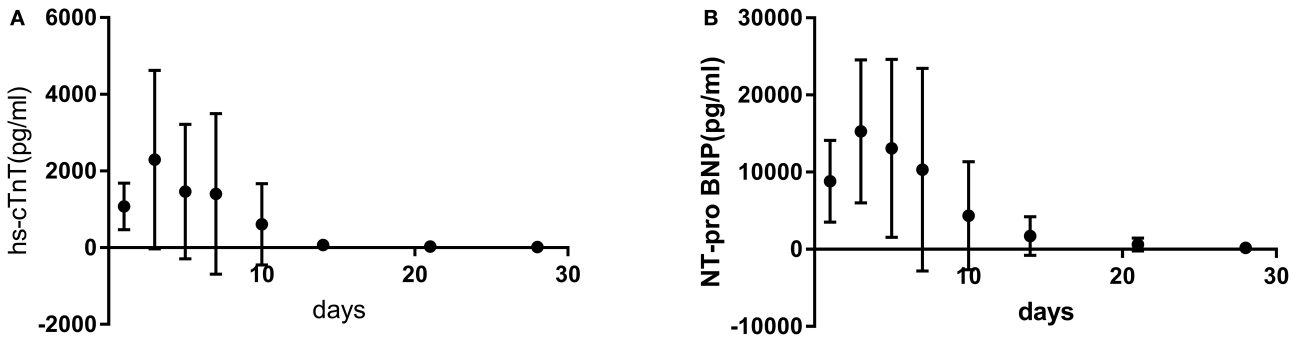

FIGURE 1 | The trend of hs-cTnT **(A)** and NT-pro BNP **(B)** with the course of disease.

pericardial effusion, mostly light, and only 1 case was moderate. Mitral regurgitation occurred in 17 patients (85%), mostly small or moderate. Myocardial thinning occurred in 4 patients, 3 of whom had thinning in the apex of the anterior wall and 1 in the ventricular septum.

CMR

Time and Safety of CMR Imaging

The 20 children with AFM were divided into group A (acute stage, onset within 14 days) and group B (recovery stage, onset after 14 days) according to the time of the first CMR examination. There were 12 patients (60%) in group A and 8 patients (40%) in group B. The examination time of group A was 6–13 days (10.7 ± 2.2 days) after onset and that of group B was 16–69 days (28.0 ± 18.0 days). Ten patients were followed up for 25–144 days (69.0 ± 38.6 days).

All the children successfully completed the CMR examination, and none of them had contrast agent allergy or other complications. Each examination took approximately 40 min to 1 h.

Total Inspection Results of Groups A and B

There were 16 patients (80%) with abnormal CMR imaging out of the 20 children with AFM. The main results were 13 cases (65%) of high T2WI signal, 14 cases (70%) of LGE, 5 cases of myocardial thinning, 6 cases of myocardial motility reduction, 6 cases of pericardial effusion, and 3 cases of myocardial perfusion defect.

CMR Results of Group A

Ten of the 12 patients in the acute phase who underwent CMR in the acute phase had abnormal results. There were 9 cases (75%) of high T2WI signal, including 7 cases in the ventricular septum and 2 cases in the left ventricle. LGE was found in 9 patients (75%), including in the ventricular septum in 2 patients, in the left ventricle in 5 patients, and in both the ventricular septum and left ventricle in 2 patients. The myocardium was thinned in 3 patients, including in the left ventricular wall in 2 patients and in the apex in 1 patient. Myocardial mobility was reduced in 4 patients. There were 5 cases of pericardial effusion, all of which were light.

Eight patients in group A underwent CMR follow-up, of whom 6 returned to normal after 25–63 days of onset, and 2 patients still had mild LGE at 33 and 46 days of onset, respectively, although the lesion range was smaller than before.

CMR Results of Group B

Six of the 8 patients in group B who underwent CMR during the recovery period had abnormal results. There were 4 cases (50%) of high T2WI signal, including 3 cases in the ventricular septum and 1 case in the left ventricle. LGE was found in 5 patients (62.5%), including in the ventricular septum in 3 patients and in both the ventricular septum and left ventricle in 2 patients. There were 3 cases of perfusion defects, including 1 case in the ventricular septum and 2 cases in the apex. Myocardial thinning occurred in 2 patients, including in the ventricular septum in 1 patient and in both the ventricular septum and left ventricular inferior wall in 1 patient. Myocardial mobility was reduced in 2 patients. Pericardial effusion occurred in one patient.

Two patients in group B underwent CMR follow-up. One of the patients had no abnormalities in the initial examination and follow-up examination. The other patient had significant cardiac enlargement, LVEF reduction, periventricular septal defect and LGE at 129 days of onset and was diagnosed with inflammatory dilated cardiomyopathy.

Comparison of T2WI, LGE Sensitivity, and Diagnostic Positive Rates Between Group A and B

There were 9 cases of T2WI high signal in the 12 patients of group A and 4 cases of T2WI high signal in the 8 patients of group B. There was no significant difference between the two groups ($P > 0.05$). There were 9 cases of LGE in the 12 patients of group A and 5 cases of LGE in the 8 patients of group B. There was also no significant difference between the two groups ($P > 0.05$). According to the Lake Louise criteria, 8 patients (66.7%) in group A were diagnosed with myocarditis (both T2WI high signal and LGE), and there were 4 patients with myocarditis (50%) in group B. There was no significant difference between the two groups ($P > 0.05$).

Treatment and Outcome

Twenty patients were treated with bed rest; oxygen; and anti-infection, myocardial nutrition, anti-heart failure, anti-arrhythmia, and other comprehensive treatments after admission. All patients were treated with high-dose human immunoglobulin (IVIG, total 2 g/kg, divided into 2–5 days). We used glucocorticoids in 11 patients who had no improvement in heart failure or a persistent increase in hs-cTnT after 2–3 days of routine treatment. The dosage of glucocorticoids was generally 1–2 mg/kg/d of prednisone, which was gradually decreased according to the condition of the patients. Six of these patients received an impact dose, methylprednisolone 10–30 mg/kg/d (total amount not exceeding 1 g), for 3 days. The total course of glucocorticoid treatment was 6–46 days (26.1 ± 12.9 days). The hs-cTnT peak in children in the glucocorticoid group was higher than that in the children in the unused glucocorticoid group (2853.4 ± 2217.2 and 1124.7 ± 527.3 pg/ml, respectively), and the difference was statistically significant ($P < 0.05$; **Table 2**). There was no significant difference between the length of stay (28.1 ± 5.4 vs. 24.1 ± 8.3 days) and the normal time of LVEF recovery (16.9 ± 5.2 vs. 27.3 ± 25.0 days) ($P > 0.05$) in the glucocorticoid group vs. the unused glucocorticoid group (**Table 2**). Eight patients were treated with a temporary pacemaker for 1–33 days (9.1 ± 10.2 days), and one patient was treated with ECMO for 4 days. All children were discharged, and no child died. In group A, in 2 patients with mild LGE during their CMR review, their cardiac size and function returned to normal after treatment with myocardial nutrition, beta-blocker, ACEI, aldosterone antagonist, or other drug therapy. Children who were treated with ECMO in group B did not recover at 5 months after treatment with the above method and were still in follow-up.

DISCUSSION

AFM is a cardiovascular crisis in children, and the incidence rate is increasing. In 1991, Lieberman et al. classified myocarditis into four types, fulminant, acute, chronic, and chronic, based on histological changes and the clinical manifestations of myocardial biopsy (5). In 2013, Ginsberg et al. defined AFM as acute myocarditis with clinical manifestations of sudden onset with severe hemodynamic disorders. Clinical symptoms markedly and rapidly worsen, requiring positive inotropic drugs, mechanical ventilation, or mechanical circulation aids to provide hemodynamic support (3). At present, the gold standard for AFM diagnosis is still endomyocardial biopsy (EMB), but because of its invasiveness and low sensitivity, it is not used as a first-line examination, especially for children (4, 6). Currently, the diagnosis of AFM mainly depends on the clinical manifestations; cardiac injury biomarkers; and electrocardiogram, chest X-ray and echocardiography results (7, 8). Therefore, this study chose to meet Ginsberg's definition of AFM as the research objective.

TABLE 2 | Comparison of the hs-cTnT peak and the length of stay between the glucocorticoid group and the unused glucocorticoid group.

	Glucocorticoid group ($n = 11$)	Unused glucocorticoid group ($n = 9$)	*P*
hs-cTnT peak (pg/ml)	2853.4 ± 2217.2	1124.7 ± 527.3	<0.05
Time of hs-cTnT to normal (days)	21.6 ± 5.9	22.0 ± 5.7	>0.05
Time of LVEF to normal (days)	16.9 ± 5.2	27.3 ± 25.0 ($n = 8$)	>0.05
Length of stay(days)	28.1 ± 5.4	24.1 ± 8.3	>0.05

The etiology and mechanism of this disease are unknown. Viral infection, autoimmune disease, drug poisoning, giant cell myocarditis, and sarcoidosis can induce AFM. Viral infection is the most common and difficult to foresee. There are a wide variety of pathogenic viruses, but due to the limitations of detection methods, only 10–20% of patients with acute myocarditis demonstrate the presence of viral genes in myocardial tissue upon detection. Myocarditis is usually caused by viral infections and postviral immune-mediated responses. With the development of new molecular technologies, such as polymerase chain reaction (PCR) and *in situ* hybridization, the most frequently detected viral profiles in EMB have changed from typical enteroviruses and adenoviruses to the major parvoviruses B19 (PVB19) and HHV6 (9, 10). In recent years, influenza viruses, especially influenza A viruses, are more common (11, 12). In addition, myocarditis can be caused by nonviral infections such as parasites, MP, *Streptococcus pneumoniae*, etc. (13–15). Mahfoud et al. studied the diagnostic value of viral serology and EMB viral genome detection in patients with clinically suspected myocarditis. Only 5 (4%) of 124 patients had serological evidence, and the same viral infection was detected by PCR in EMB samples (16). This result indicates that viral serology is not yet suitable for the diagnosis of myocardial infection in patients with suspected myocarditis. In our study, the pathogen examination was more common with MP-IgM and ASO. However, because EMB was not performed, we were unable to determine its relevance to AFM. However, clinicians are reminded to be alert to the possible pathogenesis of MP and *Streptococcus pneumonia* infection.

The initial symptoms of AFM often do not manifest as cardiovascular symptoms but as atypical symptoms such as vomiting, abdominal pain, cough, and syncope, and the clinical misdiagnosis rate is high. In this study, the initial symptoms of the digestive system, such as abdominal pain and vomiting, occurred in 60% of patients, respiratory symptoms such as chest tightness and fatigue occurred in 20%, and heart and other related symptoms occurred in only 5%. In clinical work, in patients with abdominal pain and chest tightness, especially in those with prodromal symptoms such as fever and cough, with hemodynamic disorder or malignant arrhythmia as the main manifestation, doctors should focus on whether the patient has AFM.

At present, the commonly used myocardial injury biomarkers are the creatine kinase isoenzyme and cardiac troponin (cTn). In the early stage of AFM, cTn increased more frequently than the creatine kinase isoenzyme (17), and the degree of cTn increase can help to judge the prognosis. cTn is a nonenzymatic serum marker with high specificity (90%) and high sensitivity for evaluating myocardial injury, and it is the preferred marker

for detecting myocardial injury (18). cTn usually rises within 2–4 h of onset and falls to normal for 2–3 weeks. The hs-cTnT level in this group reached a peak at 3–5 days after onset and rapidly decreased to normal after the disease improved, which was consistent with the above experience.

Typical manifestations of main electrocardiograms in the acute phase of AFM include extensive ST-T changes with atrioventricular block and various ectopic arrhythmias. A continuous prolongation of the QRS interval (>120 ms) is considered an independent predictor of cardiogenic death or heart transplantation (8). The most common atrioventricular block in this group was CAVB, most of which occurred within 3–5 days of onset, with an average return to normal within 3.6 ± 2.5 days. There was one case of continuous QRS interval (≥120 ms) that eventually developed into inflammatory dilated cardiomyopathy.

Echocardiography can assess ventricular size, wall thickness, the amplitude of motion, systolic and diastolic function, pericardial effusion, and endoluminal thrombosis in patients with AFM. Its most important role is to rule out other causes of heart failure, such as valvular heart disease or other cardiomyopathy (hypertrophic or restrictive cardiomyopathy) (19). Many previous studies have reported that the heart chamber size of patients with AFM is normal, and these patients mainly show an increase in the interval thickness due to acute myocardial edema, whereas the heart chamber of patients with common myocarditis is enlarged, and this helps to distinguish between AFM and common myocarditis (3, 20). The above studies are all results of adult AFM. In contrast, this group of children with AFM showed an increase in the diameter of the heart cavity in 75% of the patients, mainly a mild expansion. We consider that the reasons may be related to the following aspects: (1) the heart during childhood is still in the process of development, and the myocardial compliance is poor and cannot tolerate increased preload; (2) the sympathetic distribution of the myocardium is not mature enough to release enough catecholamine to regulate the response of the myocardium to the increased preload; (3) the conduction system of children with AFM is more susceptible, and atrioventricular block slows the heart rate and reduces cardiac output.

CMR is gaining increasing attention in the diagnosis of myocarditis. It can detect the location, extent and degree of myocardial injury, which cannot be detected by echocardiography. Abdel-Aty et al. reported that the sensitivity, specificity, and accuracy of T2WI in the diagnosis of myocarditis were 84, 74, and 79%, respectively; those of early enhancements were 80, 68, and 74.5%, respectively; and those of LGE were 44, 100, and 71%, respectively. Optimal diagnostic performance was produced when "any two" of the three sequences were positive in the same patient, with 76% sensitivity, 95.5% specificity, and 85% diagnostic accuracy (21). However, for patients with AFM, their options for clinical examination are greatly limited due to their poor condition and the inconvenience of the examination. We used CMR to examine the 20 patients with AFM, and the sensitivity of T2WI was 65% and that of LGE was 75%. Due to the criticality of the condition, CMR was performed only when the patient's hemodynamics were stable. Therefore, 20 patients had different examination times. We found that the sensitivity of CMR was different between the acute phase and the recovery phase: T2WI sensitivity was 75 and 50%, respectively, in the acute phase and the recovery phase, and LGE sensitivity was 75 and 62.5%, respectively, in the acute phase and the recovery phase, suggesting that myocardial edema began to resolve 14 days after onset while LGE was relatively delayed. In 2016, Wang et al. performed an early CMR examination and short-term follow-up of 8 children with AFM (22). It was found that CMR has certain value for the early diagnosis and short-term follow-up of children with AFM. Through the study of more patients and longer follow-up, we found that the sensitivity of CMR examination within 14 days was higher, and the sensitivity decreased significantly over 14 days. Therefore, we suggest that CMR should be performed as soon as possible if the patient's condition permits. In addition, we compared the results of echocardiography with those of CMR during follow-up, and these results confirmed that CMR could show abnormalities that could not be recognized by echocardiography and further confirmed that CMR had important value in the early diagnosis and long-term evaluation of children with AFM.

In terms of treatment, in recent years, an increasing number of small-scale studies and case reports have suggested that IVIG is beneficial for patients with AFM and inflammatory dilated cardiomyopathy and can improve LVEF and long-term prognosis with no obvious adverse reactions (14, 23). We performed IVIG treatment on this group of 20 children with AFM, and it also proved beneficial to these patients. Chen et al. conducted a controlled study of 719 patients with myocarditis and found that glucocorticoids may improve cardiac function but did not reduce mortality (24). In a long-term follow-up study (mean follow-up of 33 months), 21% of patients with myocarditis developed dilated cardiomyopathy (25). Studies by Kuhl et al. show that the persistence of the viral genome leads to chronic inflammation, which affects the recovery of LVEF (26) and may be related to progression to inflammatory dilated cardiomyopathy. However, some case reports and small-scale clinical studies have shown the beneficial effects of glucocorticoid therapy on AFM (27, 28). Therefore, the therapeutic effect of glucocorticoids on children with AFM is still controversial. Ginsberg et al. believe that immunosuppressive therapy should not be routinely used to treat myocarditis, but it is strongly recommended to use it after conventional anti-heart failure treatment (3). In this study, 11 patients with severe condition (mean hs-cTnT average 2853.4 ± 2217.2 pg/ml) were treated with IVIG and glucocorticoid therapy. The comparison of hospitalization time with children without glucocorticoids proved that glucocorticoids can improve children's condition but do not affect the prognosis. In theory, the use of immunosuppressive agents in the acute phase of viral replication may aggravate the direct damage of the virus to the myocardium, and the use of immunosuppressive agents during the acute phase of immune-mediated injury may bring some benefits, but how to grasp the timing still requires more research. In addition, 8 patients in this study received temporary

pacemakers, and 1 patient received ECMO to ensure effective tissue perfusion. Therefore, we recommend that patients with AFM with CAVB should receive temporary pacemakers in a timely manner, and those who cannot maintain the circulation stability for conventional treatment methods should receive ECMO and other mechanical circulation aids in time, which can play a crucial role in improving the prognosis of patients with AFM.

The limitations of this study are that the sample size is small and it is a retrospective clinical study, the accuracy and integrity of which cannot be guaranteed. AFM was only clinically diagnosed, EMB was not performed, and histopathological diagnosis and virus isolation were not used to determine the cause. In addition, although studies have shown that CMR has a high sensitivity for the diagnosis of AFM, it is necessary to conduct a randomized prospective trial to demonstrate its specificity in the diagnosis of these patients.

CONCLUSION

AFM has a rapid onset and can progress to heart failure and cardiogenic shock in a short period of time. The clinical presentation of symptoms of AFM in children are more commonly in the gastrointestinal and respiratory systems, and AFM is difficult to diagnose early and is easily misdiagnosed. CMR is highly sensitive for the diagnosis of AFM, especially within 14 days of onset. It can show not only the location of myocardial injury but also the degree and extent of myocardial inflammation, as well as the repair of fibrosis after inflammation, which is helpful for the early identification of children with AFM. The dynamic observation and follow-up of the course of AFM in children by cardiac MRI can be used to guide clinical decision-making and evaluate prognosis. The development of life support technologies such as emergency cardiac pacing and ECMO has reduced the mortality rate of children with AFM.

DATA AVAILABILITY STATEMENT

The raw data supporting the conclusions of this manuscript will be made available by the authors, without undue reservation, to any qualified researcher.

ETHICS STATEMENT

Written informed consent was obtained from the minor(s)' legal guardian/next of kin for the publication of any potentially identifiable images or data included in this article.

AUTHOR CONTRIBUTIONS

JL performed original literature search, developed methodology, performed statistics, summary and analysis of data, and prepared first draft of manuscript and revision. BH conceived the idea, performed original literature search, organized and coordinated the investigation, managed patients, and performed data analysis and manuscript revision. CW performed CMR and analyzed CMR data. JW performed literature search, data collection and data analysis, and provided critical advice on the manuscript. DJ managed patients and advised on data analysis and the manuscript. LZ, YY, and JZ managed patients and provided critical revision and advice on the research protocol and manuscript. All authors approved this version of the manuscript to be published and agreed to be accountable for all aspects of the work, thereby ensuring that questions related to the accuracy or integrity of any part of the work are appropriately investigated and resolved.

FUNDING

This work was supported by the National Natural Science Foundation of China (81873498) and the Taishan scholars (no. ts201511099).

REFERENCES

1. Matsuura H, Ichida F, Saji T, Ogawa S, Waki K, Kaneko M, et al. Clinical features of acute and fulminant myocarditis in children– 2nd nationwide survey by Japanese society of pediatric cardiology and cardiac surgery. *Circul J*. (2016) 80:2362–8. doi: 10.1253/circj.CJ-16-0234
2. Subspecialty Group of Cardiology tSoPCMA, Collaborating Group of Myocarditis tSGoCtSoPCMA, Editorial Board CJoP, Pediatric Cardiology Committee CCoCPCMDA. [Diagnostic recommendation for myocarditis in children (version 2018)]. *Zhonghua Er Ke Za Zhi*. (2019) 57:87–9. doi: 10.3760/cma.j.issn.0578-1310.2019.02.004
3. Ginsberg F, Parrillo JE. Fulminant myocarditis. *Crit Care Clin*. (2013) 29:465–83. doi: 10.1016/j.ccc.2013.03.004
4. Friedrich MG, Sechtem U, Schulz-Menger J, Holmvang G, Alakija P, Cooper LT, et al. Cardiovascular magnetic resonance in myocarditis: a JACC White Paper. *J Am Coll Cardiol*. (2009) 53:1475–87. doi: 10.1016/j.jacc.2009.02.007
5. Lieberman EB, Hutchins GM, Herskowitz A, Rose NR, Baughman KL. Clinicopathologic description of myocarditis. *J Am Coll Cardiol*. (1991) 18:1617–26. doi: 10.1016/0735-1097(91)90493-S
6. Ghelani SJ, Spaeder MC, Pastor W, Spurney CF, Klugman D. Demographics, trends, and outcomes in pediatric acute myocarditis in the United States, 2006 to 2011. *Circ Cardiovasc Qual Outcomes*. (2012) 5:622–7. doi: 10.1161/CIRCOUTCOMES.112.965749
7. Sankar J, Khalil S, Jeeva Sankar M, Kumar D, Dubey N. Short-term outcomes of acute fulminant myocarditis in children. *Pediatr Cardiol*. (2011) 32:885–90. doi: 10.1007/s00246-011-0007-8
8. Kindermann I, Barth C, Mahfoud F, Ukena C, Lenski M, Yilmaz A, et al. Update on myocarditis. *J Am Coll Cardiol*. (2012) 59:779–92. doi: 10.1016/j.jacc.2011.09.074
9. Breinholt JP, Moulik M, Dreyer WJ, Denfield SW, Kim JJ, Jefferies JL, et al. Viral epidemiologic shift in inflammatory heart disease: the increasing involvement of parvovirus B19 in the myocardium of pediatric cardiac transplant patients. *J Heart Lung Transplant*. (2010) 29:739–46. doi: 10.1016/j.healun.2010.03.003
10. Schultz JC, Hilliard AA, Cooper LT, Rihal CS. Diagnosis and treatment of viral myocarditis. *Mayo Clinic Proc*. (2009) 84:1001–9. doi: 10.4065/84.11.1001
11. Ukimura A, Satomi H, Ooi Y, Kanzaki Y. Myocarditis associated with influenza A H1N1pdm2009. *Influenza Res Treat*. (2012) 2012:351979. doi: 10.1155/2012/351979
12. Lobo MLS, Taguchi Â, Gaspar HA, Ferranti JF, Carvalho WBd, Delgado AF. Fulminant myocarditis associated with the H1N1 influenza virus: case

report and literature review. *Rev Bras Ter Intensiva.* (2014) 26:321–6. doi: 10.5935/0103-507X.20140046
13. Hidron A, Vogenthaler N, Santos-Preciado JI, Rodriguez-Morales AJ, Franco-Paredes C, Rassi A Jr. Cardiac involvement with parasitic infections. *Clin Microbiol Rev.* (2010) 23:324–49. doi: 10.1128/CMR.00054-09
14. Tsai YG, Ou TY, Wang CC, Tsai MC, Yuh YS, Hwang B. Intravenous gamma-globulin therapy in myocarditis complicated with complete heart block: report of one case. *Acta Paediatr Taiwan*. (2001) 42:311–3.
15. Wada H, Ogita M, Miyauchi K, Suwa S, Yamano M, Daida H. Case report: Fulminant myocarditis associated with overwhelming pneumococcal infection. *Int J Cardiol.* (2016) 223:706–7. doi: 10.1016/j.ijcard.2016.08.282
16. Mahfoud F, Gartner B, Kindermann M, Ukena C, Gadomski K, Klingel K, et al. Virus serology in patients with suspected myocarditis: utility or futility? *Eur Heart J.* (2011) 32:897–903. doi: 10.1093/eurheartj/ehq493
17. Lauer B, Niederau C, Kühl U, Schannwell M, Pauschinger M, Strauer B-E, et al. Cardiac troponin T in patients with clinically suspected myocarditis. *J Am Coll Cardiol.* (1997) 30:1354–9. doi: 10.1016/S0735-1097(97)00317-3
18. Ukena C, Kindermann M, Mahfoud F, Geisel J, Lepper PM, Kandolf R, et al. Diagnostic and prognostic validity of different biomarkers in patients with suspected myocarditis. *Clin Res Cardiol.* (2014) 103:743–51. doi: 10.1007/s00392-014-0709-z
19. Blauwet LA, Cooper LT. Myocarditis. *Prog Cardiovasc Dis*. (2010) 52:274–88. doi: 10.1016/j.pcad.2009.11.006
20. Felker GM, Boehmer JP, Hruban RH, Hutchins GM, Kasper EK, Baughman KL, et al. Echocardiographic findings in fulminant and acute myocarditis. *J Am Coll Cardiol.* (2000) 36:227–32. doi: 10.1016/S0735-1097(00)00690-2
21. Abdel-Aty H, Boye P, Zagrosek A, Wassmuth R, Kumar A, Messroghli D, et al. Diagnostic performance of cardiovascular magnetic resonance in patients with suspected acute myocarditis: comparison of different approaches. *J Am Coll Cardiol.* (2005) 45:1815–22. doi: 10.1016/j.jacc.2004.11.069
22. Wang H, Zhao B, Jia H, Gao F, Zhao J, Wang C. A retrospective study: cardiac MRI of fulminant myocarditis in children—can we evaluate the short-term outcomes? *PeerJ*. (2016) 4:e2750. doi: 10.7717/peerj.2750
23. Goland S, Czer LS, Siegel RJ, Tabak S, Jordan S, Luthringer D, et al. Intravenous immunoglobulin treatment for acute fulminant inflammatory cardiomyopathy: series of six patients and review of literature. *Can J Cardiol.* (2008) 24:571–4. doi: 10.1016/S0828-282X(08)70638-X
24. Chen HS, Wang W, Wu SN, Liu JP. Corticosteroids for viral myocarditis. *Cochrane Database Syst Rev.* (2013) 10:CD004471. doi: 10.1002/14651858.CD004471.pub3
25. D'Ambrosio A, Patti G, Manzoli A, Sinagra G, Lenarda AD, Silvestri F, et al. The fate of acute myocarditis between spontaneous improvement and evolution to dilated cardiomyopathy: a review. *Heart.* (2001) 85:499–504. doi: 10.1136/heart.85.5.499
26. Kuhl U, Pauschinger M, Seeberg B, Lassner D, Noutsias M, Poller W, et al. Viral persistence in the myocardium is associated with progressive cardiac dysfunction. *Circulation.* (2005) 112:1965–70. doi: 10.1161/CIRCULATIONAHA.105.548156
27. Moreels M, Delforge ML, Renard M. Fulminant myocarditis with dramatic response to corticoids. *Acta Cardiol.* (2010) 65:97–9. doi: 10.2143/AC.65.1.2045898
28. Nakashima H, Umeyama Y, Minami K. Successive immunosuppressive treatment of fulminant myocarditis that is refractory to mechanical circulatory support. *Am J Case Rep.* (2013) 14:116–9. doi: 10.12659/AJCR.889109

Conflict of Interest: The authors declare that the research was conducted in the absence of any commercial or financial relationships that could be construed as a potential conflict of interest.

frontiers in Pediatrics

ORIGINAL RESEARCH
published: 01 October 2019
doi: 10.3389/fped.2019.00387

Evaluation of Drug-Related Receptors in Children With Dilated Cardiomyopathy

Qing Guo[1], Jie Liu[1], Peng Zhu[2], Yali Liu[1], Nianguo Dong[2], Jiawei Shi[2] and Hua Peng[1]**

[1] Department of Pediatrics, Union Hospital, Tongji Medical College, Huazhong University of Science and Technology, Wuhan, China, [2] Department of Cardiovascular Surgery, Union Hospital, Tongji Medical College, Huazhong University of Science and Technology, Wuhan, China

OPEN ACCESS

Edited by:
Hongfang Jin,
Peking University First Hospital, China

Reviewed by:
Shiwei Yang,
Children's Hospital of Nanjing Medical University, China
Li Zi Pu,
Qingdao Women & Infants Hospital, China

***Correspondence:**
Jiawei Shi
shijiawei@21cn.com
Hua Peng
phua20120101@163.com

Specialty section:
This article was submitted to Pediatric Cardiology, a section of the journal Frontiers in Pediatrics

Received: *01 July 2019*
Accepted: *09 September 2019*
Published: *01 October 2019*

Citation:
Guo Q, Liu J, Zhu P, Liu Y, Dong N, Shi J and Peng H (2019) Evaluation of Drug-Related Receptors in Children With Dilated Cardiomyopathy. Front. Pediatr. 7:387. doi: 10.3389/fped.2019.00387

Background: Effective treatments for pediatric dilated cardiomyopathy (DCM) are limited. Currently, pediatric DCM therapy mainly includes supportive heart failure (HF) treatment. While the treatment for child DCM patients is generally the same as that for adult DCM patients, few randomized prospective studies on the clinical efficacy of treatments for pediatric DCM have been published. We explored the appropriate treatments for child patients.

Methods: The ultrastructure of pediatric DCM and control hearts was analyzed by electron microscopy and HE staining. Left ventricular tissues from children in the DCM and control groups were subjected to quantitative RT-PCR (qRT-PCR) to study the mRNA expression of receptors related to various treatments, including drugs targeting the renin-angiotensin-aldosterone system (RAAS) system, digoxin, milrinone, and β-receptor blockers, in child patients in the clinic. Furthermore, the differences in drug receptors in heart tissues between children and adults with DCM were analyzed.

Results: Compared with the control children, the children in the DCM group showed marked abnormalities in structure and organelles. The mRNA levels of angiotensin-converting enzyme (ACE), REN, prorenin receptor (PRR), NEP, ATP1A1, and phosphodiesterase3 (PDE3A) were higher in the pediatric DCM group than the control group. Interestingly, the mRNA expression of these treatment-related receptors was much higher in children than in adults.

Conclusion: ACE inhibitors, PRR or REN receptor inhibitors, PDE3 inhibitors and LCZ696 may be effective in children with DCM. However, β-receptor blockers are not valid treatments for pediatric DCM. Moreover, high receptor expression was observed in children. These data will improve the selection of drugs for DCM patients, enhance treatment, and increase the survival rate.

Keywords: children, dilated cardiomyopathy, receptors, treatment, RAAS

INTRODUCTION

Dilated cardiomyopathy (DCM) is a kind of cardiomyopathy that involves left ventricular (LV) dilation and systolic dysfunction without abnormal load conditions and severe coronary artery disease (1). The annual incidence of pediatric DCM is 0.58 cases per 100,000 person-years (2). Effective treatments for pediatric DCM are limited. Currently, therapy for DCM in children mainly includes supportive heart failure (HF) treatment. According to the current guidelines, pharmacotherapy involving ß-blockers and angiotensin-converting enzyme (ACE) inhibitors is the basis of pediatric HF therapy; however, viable randomized prospective studies are lacking (3). In addition, treatments such as furosemide, milrinone, and digoxin, which are commonly used to treat adult HF, are used to treat child HF. Although, the current treatment of adult HF has shown some success with these drugs, these same therapies do not seem to be effective for pediatric HF. Specifically, treatment of adult HF with PDE3A inhibitors led to an increased incidence of sudden death and arrhythmias (4). Treatment with PDE3A inhibitors improved symptoms in pediatric HF patients without increasing the incidence of arrhythmias or sudden death (5).

Activation of β-adrenergic and renin-angiotensin-aldosterone system (RAAS) receptors plays an important role in the treatment of adult HF and cardiac remodeling (6). RAAS is important regulator of blood pressure, and suppression of RAAS can decrease cardiac load and relieve HF. RAAS include some classic receptors such as NR3C2, prorenin receptor (PRR), ACE, REN. The β-adrenergic receptors of the myocardium play an important role in the regulation of heart function. Many studies reported that an over-expression of the ADRB1 (β1-adrenoceptor) are which is one of the main β-adrenergic receptors may contribute to heart failure. Treatment of HF and atrial fibrillation with cardiac glycosides can inhibit the Na+, K+-ATPase. A large catalytic subunit (alpha) and a small glycoprotein subunit (beta) compose Na+, K+-ATPase. The ATP1A1 gene encodes an alpha 1 subunit with good affinity for digoxin (7). These genes are involved in HF and LV remodeling (8). A member of the cGMP-inhibited cyclic nucleotide phosphodiesterase family is encoded by the PDE3A gene. Thus, inhibition of the protein encoded by the PDE3A gene may be an effective treatment for congestive HF (9). Neprilysin encoded by the NEP gene is a neutral endopeptidase that is a potential target for the treatment of HF and hypertension due to its functions in vasodilation, natriuresis, and fibrosis (10).

We suggest that the mechanisms of HF may be different in children and adults and that different cellular mechanisms may be involved in pediatric HF. We evaluated the effect of drugs on the treatment of children with DCM by measuring mRNA expression of the corresponding drug-related receptors in cardiomyocytes after HF treatment in this study.

MATERIALS AND METHODS

Human Samples

Child DCM samples ($n = 11$; age < 16 years) were obtained from Wuhan Union Hospital from January 2017 to October 2018 during heart transplantation due to end-stage idiopathic DCM. All cases of children DCM who underwent heart transplantation in this study were confirmed as primary DCM through discussion and approval by members of the heart transplantation committee. In addition, this research ethics has been approved by the medical ethics committee of Tongji medical college, Huazhong University of Science and Technology and all the patients' family members had signed informed consent before taking samples of this study. The clinical history and blood tests of these pediatric patients were available (**Table 1**). Adult DCM samples ($n = 10$; age 20–60 years) were obtained from Wuhan Union Hospital from January 2016 to 2018 from patients who underwent transplantation due to end-stage DCM and had no cardiac complications, such as hypertension, coronary atherosclerosis, and myocarditis. Control samples ($n = 7$) were from donor hearts that could not be transplanted for technical reasons (blood type or size mismatch) with normal LV function and active infection or no history of myocardial disease. The LV tissue underwent rapid dissection, rapid freezing, and preservation at −80°C when cardiac explants were taken from the operating room. Another LV sample was fixed in either 10% formalin or 2.5% glutaraldehyde.

Electron Microscopy

Cardiac specimens (2 mm^2) were fixed with 0.15 M cacodylate buffer at pH 7.4 containing 2 mM calcium chloride at 4°C overnight. Then, 0.15 M cacodylate buffer was used to rinse the specimens 3 times for 10 min each. Next, the specimens were fixed in 1% osmium tetroxide containing 1.5% potassium ferrocyanide in cacodylate buffer for 1 h. We used ultrapure water the wash samples 3 times and stained them en bloc for 1 h. Then, the samples were again washed with ultrapure water. Specimens were dehydrated in a graded acetone series (50, 70, 90, 100%) for 10 min twice. The specimens were fixed and incubated at 60°C for 48 h. We used a diamond trim tool (Daitome Ultra 45°) to trim each block. The slices were placed into 2% uranium acetate saturated alcohol solution and then lead citrate (15 min each staining) and were dried at room temperature overnight. An electron microscope (HITACHI HT7700) was used to observe and collect images.

qRT-PCR Assay

Total RNA was extracted from LV cardiac tissue by using TRIzol reagent according to the manufacturer's instructions (Sigma, St. Louis, MO), and reverse transcription reactions were performed using an All-in-One synthesis kit (GeneCopoeia, USA) according to the manufacturer's recommendations. RT-PCR was performed using a Bio-Rad CFX manager. A total reaction volume of 10 μl contained 1 μl of cDNA, 5 μl of All-in-One RT-PCR mix solution (GeneCopoeia, USA), 1 μl each of sense and antisense primers (10 μM), and up to 2 μl of ddH_2O. Primer sequences are listed (**Supplement 1**). The PCR amplification conditions were 95°C for 10 min and 39 cycles of 95°C for 10 s, 55°C for 30 s, and 72°C for 30 s, followed by 65°C for 5 s and 95°C for 5 s. GAPDH mRNA levels were used for normalization, and the relative mRNA expression was calculated by the $2^{-\Delta\Delta Ct}$ method.

TABLE 1 | Pediatric DCM descriptive data.

No	Age* (Year)	Sex	BMI (kg/m^2)	BNP (pg/ml)	Echocardiography			Medications					NYHA heart function
					LVDD (mm)	RVDD (mm)	EF %	β-blockers	Digoxin	ACEI	Diuretics	Aldosterone	
1	13.4	F	14.98	N	59	54	46	Y	Y	Y	Y	Y	Class IV
2	8.4	M	21.3	7,328	53	42	23	Y	Y	Y	Y	N	Class IV
3	13.9	M	14.27	N	61	50	16	N	Y	Y	N	Y	Class IV
4	12.33	M	13.22	N	53	47	28	Y	Y	Y	Y	Y	Class IV
5	10.67	M	19.63	140.9	60	32	26	Y	Y	Y	N	Y	Class IV
6	9.58	F	18.65	1,994.7	68	32	20	N	Y	Y	N	Y	Class IV
7	13.08	M	U	N	61	39	15	N	N	N	N	N	Class IV
8	11.5	F	U	1,612.5	70	49	12	Y	Y	N	N	Y	Class IV
9	14.83	M	U	5,408.8	74	44	21	Y	N	Y	Y	Y	Class III–IV
10	13.08	F	17.1	N	57	58	25	U	U	U	Y	Y	Class IV
11	16.83	M	16.85	N	60	55	25	N	Y	Y	Y	Y	Class III–IV

Age, age at tissue collection; F, female; M, male; Y, yes; N, no; U, unknown; BMI, body mass index; BNP, brain natriuretic peptide; LVDD, left ventricular end diastolic diameter; RVDD, right ventricular end diastolic diameter; EF, ejection fraction; ACEI, angiotensin converting enzyme inhibitor; NYHA, New York Heart Association.*

Data Analysis

All statistical analyses of qRT-PCR data were performed with GraphPad Prism software (GraphPad Software, Inc.). Variables were compared between the groups using comparison of two groups after analysis of variance (ANOVA). Statistical significance was set a priori at $p < 0.05$, and all data are presented as the mean ± SEM in the figures.

RESULTS

Children with DCM in this group who underwent heart transplantation had an age range of 8–17 years old, with an average age of 12.5 ± 2.4 years, and the ratio of males to females was 7:4. The LV ejection fraction (LVEF) ranged from 12% to 46%, with an average of 23 ± 9%. The average LV end diastolic diameter (LVDD) was 61.45 ± 6.684 mm, and the average right ventricular end diastolic diameter (RVDD) was 45.64 ± 8.8 mm. The mean BNP level in this group was 3,297 ± 2,967 pg/ml, while the normal value of BNP in our hospital was <100 pg/ml; the BNP value in the DCM group was at least 14 times higher than the normal value. All patients had a New York heart function of IV (**Table 1**).

Pathology and Ultrastructure in Pediatric DCM

We observed the pathology of HE-stained myocardial tissues by light microscopy. LV myocardial fibers in the DCM group showed a variable thickness with blurred transverse striae. Some myocardial fibers were thick, the nuclei were enlarged and hyperchromatic, and some areas between the myocardial tissues were obviously fibrotic (**Figures 1A,B**).

We observed the myocardial tissue ultrastructure in the groups with electron microscopy. Compared with those of the control myocardial tissue, Z bands of myofibrils from the pediatric DCM cardiac tissue appeared enlarged, loose, and fuzzy, and the sarcomeres disappeared. Some myofibrils showed dissolution or breakage. Compared with the normal group, the DCM group did not show an abnormal number of mitochondria, but some mitochondria were swollen and dissolved, and the mitochondrial cristae were empty, blurred or even absent (**Figure 2**).

The Gene Expression of Drug-Related Receptors on Cardiomyocytes in Children

Using qRT-PCR, we analyzed the expression of PRR, REN, ACE, and NR3C2 of the RAAS in the LV tissues from control and pediatric DCM hearts. We found that the expression of PRR, REN, ACE was higher in children with DCM than adults ($p < 0.05$) (**Figure 3**).

We measured the expression of ATP1A1, ADRA1, ADRB1, PDE3A, and NEP in the LV tissues from pediatric and normal hearts and found differences (**Figure 4**). ADRA1 and ADRB1 showed no significant differences between pediatric DCM samples and normal samples (**Figures 4A,B**). Both ATP1A1 and PDE3A levels were higher in pediatric DCM samples than in normal DCM samples ($p < 0.05$) (**Figures 4C,D**). NEP

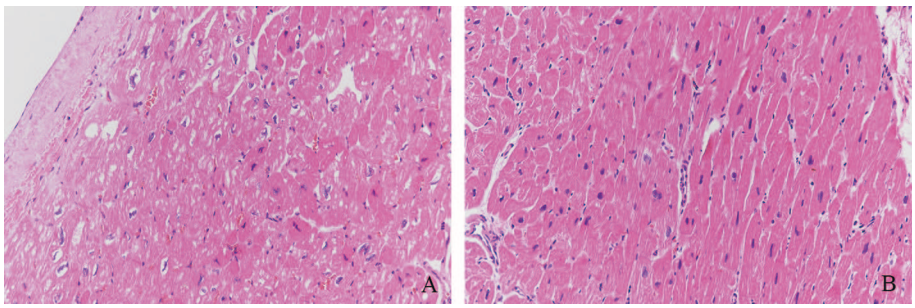

FIGURE 1 | Pathology of HE-stained myocardial tissue. **(A)** LV myocardial fibers of DCM samples showed variable thickness with blurred transverse striae. **(B)** Some myocardial fibers were thick, the nuclei were enlarged and hyperchromatic, and some areas between myocardial tissues were obviously fibrotic (Magnification = 200).

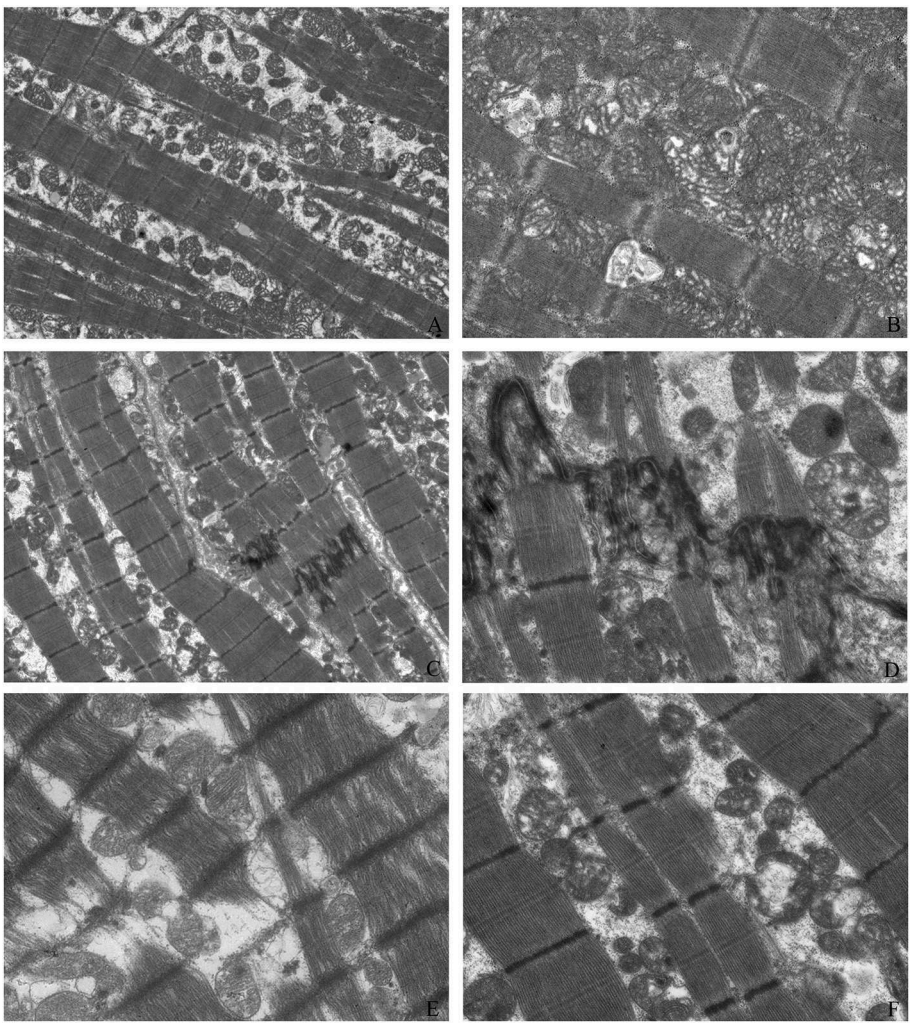

FIGURE 2 | Myocardial tissue ultrastructure. The ultrastructure of control myocardial tissue (**A**: magnification = 2,000, **B**: magnification = 5,000); Z bands of myofibrils from pediatric DCM cardiac tissue appeared enlarged, loose, and fuzzy, and the sarcomeres disappeared (**C**: magnification = 2,000, **D**: magnification = 5,000). Some myofibrils showed dissolution and breakage (**C,E**: magnification = 5,000). Compared with those of the normal group, some mitochondria were swollen and dissolved, and the mitochondrial cristae were empty, blurred, or even absent (**C,F**: magnification = 5,000).

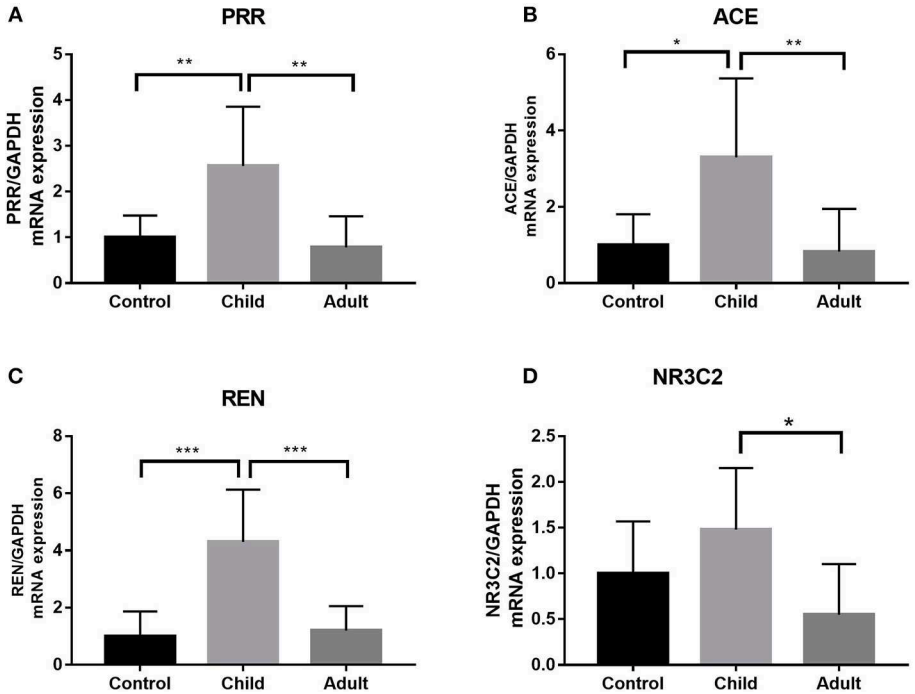

FIGURE 3 | Expression of PRR, ACE, REN, and NR3C2 in pediatric, adult DCM LV samples and control samples. **(A)** PRR expression was higher in pediatric DCM patients than controls. PRR expression was higher in pediatric DCM patients than adults. The significance was determined using comparison of two groups after ANOVA: $p = 0.009$, $p = 0.0023$. **(B)** ACE expression was higher in pediatric DCM patients than controls. ACE expression was higher in pediatric DCM patients than adults. The significance was determined using comparison of two groups after ANOVA: $p = 0.017$, $p = 0.008$. **(C)** REN expression was higher in pediatric DCM patients than controls. REN expression was higher in pediatric DCM patients than adults. The significance was determined using comparison of two groups after ANOVA: $p = 0.0003$, $p = 0.0006$. **(D)** NR3C2 expression was not higher in pediatric DCM patients than controls. Comparison of two groups after ANOVA determined that there was no difference in relative expression. NR3C2 expression was higher in pediatric DCM patients than adults. The significance was determined using comparison of two groups after ANOVA: $p = 0.015$. $^{*}P < 0.05$, $^{**}P < 0.01$, $^{***}P < 0.001$.

expression was significantly elevated in pediatric DCM compared to normal samples ($p = 0.0008$) (**Figure 4E**).

Gene Expression of the Drug-Related Receptors on Cardiomyocytes in Adults and Children

Using qRT-PCR, we analyzed the expression of PRR, REN, ACE, and NR3C2 of the RAAS in the LV tissues from adult and pediatric DCM hearts. These gene expression levels were higher in children with DCM than adults ($p < 0.05$) (**Figure 3**). We also measured the expression of ATP1A1, ADRA1, ADRB1, PDE3A, and NEP in child and adult hearts (**Figure 3**). ATP1A1, PDE3A, and NEP levels were increased in pediatric DCM and adult samples ($p < 0.05$) (**Figures 4C–E**). The expression of ADRA1 and ADRB1 was not significantly different between pediatric DCM and adult samples (**Figures 4A,B**).

DISCUSSION

The specimens selected in this study were all derived from the myocardial tissues of children with end-stage DCM. Even though the number of pediatric heart transplants has increasing in recent years, the number of pediatric heart transplants is still small relative to that of adult. So, it is not easy to get more samples of DCM heart. But this study firstly analyzed expression levels of drug relevant receptors and myocardial ultrastructure of DCM heart samples. Through electron microscopy, we observed that the end-stage myocardium in these children showed significant degeneration, the myofibrils focally dissolved and disappeared, and the mitochondria showed mitochondrial degeneration and vacuolation. Compared with that of adults, the myocardial ultrastructure in children with end-stage DCM was not significantly different (11).

The most common cause of pediatric HF is DCM, and the clinical prognosis of DCM is poor (12). The increase in the survival rate of these children is largely due to heart transplantation. While the preferred treatment for end-stage HF is transplantation, children on waiting lists for heart transplantation have some of the highest mortality rates because of the limited number of heart donors (13). Therefore, identification of a suitable drug treatment to prolong the survival time before heart transplantation is urgently needed.

Although, the myocellular mechanisms of DCM in children are mostly unexplored, treatment strategies for HF in children are consistent with those in adults. Some clinical studies have found that the treatment of adult patients with HF reduced mortality. However, the same treatment did not improve prognosis in

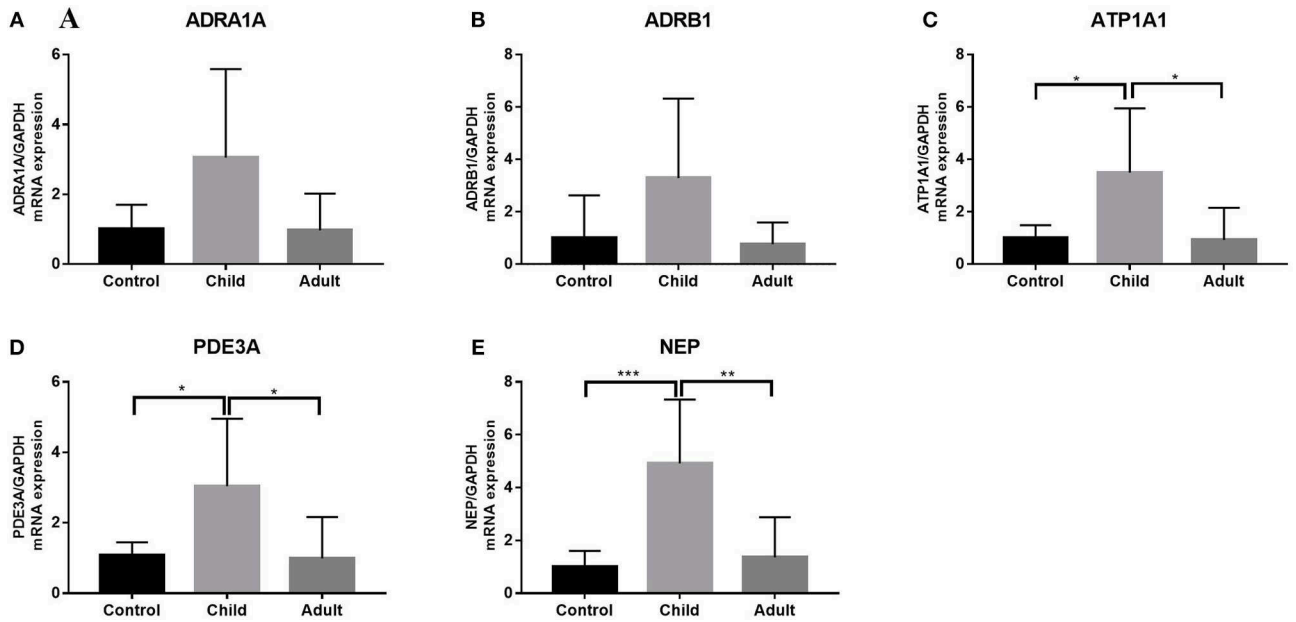

FIGURE 4 | Expression of ATP1A1, ADRA1, ADRB1, PDE3A, and NEP in pediatric, adult DCM LV, and control samples. **(A)** ADRA1 expression was not higher in pediatric DCM patients than controls. ADRA1 expression was not higher in pediatric DCM patients than adults. Comparison of two groups after ANOVA determined that there was no difference in relative expression. **(B)** ADRB1 expression was not higher in pediatric DCM patients than controls. ADRB1 expression was not higher in pediatric DCM patients than adults. Comparison of two groups after ANOVA determined that there was no difference in relative expression. **(C)** ATP1A1 expression was higher in pediatric DCM patients than controls. ATP1A1 expression was higher in pediatric DCM patients than adults. The significance was determined using comparison of two groups after ANOVA: $p = 0.021$, $p = 0.014$. **(D)** PDE3A expression was higher in pediatric DCM patients than controls. PDE3A expression was higher in pediatric DCM patients than adults. The significance was determined using comparison of two groups after ANOVA: $p = 0.041$, $p = 0.020$. **(E)** NEP expression was higher in pediatric DCM patients than controls. NEP expression was higher in pediatric DCM patients than adults. The significance was determined using comparison of two groups after ANOVA: $p = 0.0008$, $p = 0.0014$. $^{*}P < 0.05$, $^{**}P < 0.01$, $^{***}P < 0.001$.

children (14). In general, pharmacotherapy for DCM in children is consistent with pharmacotherapy for DCM in adults. A transition from almost total use of digoxin and diuretics to widespread use of ACE inhibitors occurred in the 1980s (15), and another transition to second- and third-generation β-AR blockers occurred in the 1990s. Milrinone, a PDE3 inhibitor, improves myocardial performance without increasing afterload. Therefore, milrinone can be used to improve cardiac function in children with end-stage HF (16). In addition, LCZ696 was more effective in lowering blood pressure in patients with hypertension and reduced all-cause mortality in patients with HF compared to valsartan or enalapril (17, 18). With the development of research, many researchers have realized that the mechanism of DCM in children and adults may not be the same. We measured the gene expression of the corresponding receptors of drugs used to treat HF on cardiomyocytes, which provides a reference for the treatment of pediatric DCM.

RAAS activation can cause fluid retention, pulmonary venous congestion, pleural effusion, cardiac dilatation, and myocardial fibrosis, leading to clinical symptoms of HF in humans. Active renin exclusively controls the firstrate limiting step in the RAAS cascade, i.e., conversion of angiotensinogen to angiotensin I (19, 20). The PRR binds renin and prorenin and induces profibrotic intracellular signal cascades (21). The NR3C2 gene, which encodes the mineralocorticoid receptor, mediates the effects of aldosterone on salt and water balance within restricted target cells to reduce the load on the heart. In this study, we observed higher expression of PRR, REN, and ACE of the RAAS in the LV tissues from pediatric DCM hearts compared to those of normal and adult hearts. To date, the most commonly used therapy targeting the RAAS system to treat heart disease in children is ACE inhibitors. Our study indicated that ACE inhibitors may block cardiomyocyte expansion and could significantly mitigate HF. In addition, either PRR or REN receptor inhibitors may be effective in DCM. In the future, we will further study the effects of either PRR or REN receptor inhibitors on DCM.

Adult HF patients respond well to treatment with β-blockers because AR-mediated adaptation plays an important role in heart abnormalities in adult HF. However, a growing body of literature suggests that β-blockers are not as effective in treating pediatric HF as adult HF (22). Our results showed that ADRA1 and ADRB1 expression in pediatric DCM was not strikingly different from expression in normal samples. Therefore, we hypothesized that there are different adaptive β-AR and adrenalin signaling pathways in children with DCM compared to adults with DCM. This finding may indicate that β-receptor blockers are not effective in treating pediatric DCM.

Our results showed that ATP1A1 expression in pediatric DCM is higher than expression in normal conditions. The ATP1A1 gene encodes an alpha 1 subunit with good affinity for digoxin.

Digoxin is a traditional medicine for the treatment of HF in children. Nakano et al. found that the level of myocardial cAMP in children treated with the PDE3 inhibitor milrinone increased, while the level of cAMP in adults treated with the PDE3 inhibitor remained low and unchanged (23). The results of our study confirmed the conclusions of previous studies and indicated that PDE3 inhibitor treatment is more effective in pediatric DCM than adult DCM.

In recent years, many studies have found that a combination of neprilysin/the RAAS inhibitor sacubitril/valsartan (LCZ696), which provides simultaneous neprilysin inhibition and angiotensin-II receptor blockade, was superior to ACEI/ARB therapy (24, 25). Our results showed that expression of the NEP gene, which encodes neprilysin, is higher than that in normal samples. This finding indicates that LCZ696 may be effective in treating children with DCM.

By comparing the expression of drug receptors related to heart disease in adult, child and normal myocardium, we confirmed that children and adults may not have the same response to DCM treatment in this study. ACE inhibitors, PRR or REN receptor inhibitors, PDE3 inhibitors and LCZ696 may be effective in children with DCM. However, β-receptor blockers are not valid treatments for pediatric DCM. Moreover, high receptor expression was observed in children. These data will improve drug selection for DCM patients, enhance DCM treatment and increase the survival rate.

DATA AVAILABILITY STATEMENT

All datasets analyzed for this study are included in the manuscript/**Supplementary Files**.

ETHICS STATEMENT

The studies involving human participants were reviewed and approved by Drug clinical trial ethics committee of Huazhong University of Science and Technology. Written informed consent to participate in this study was provided by the participants' legal guardian/next of kin.

AUTHOR CONTRIBUTIONS

JS and HP conception and design of the study. JL and YL performed the statistical analysis. PZ and ND collect sample. QG wrote the first draft of the manuscript. All authors contributed to manuscript revision, read and approved the submitted version.

ACKNOWLEDGMENTS

We are grateful for the support in sample collection and preparation provided by Yuan Yin, Wang Qiupeng, and Zhang Rong. The authors would also like to thank and acknowledge the Tongji Medical College, Huazhong University of Science and Technology of Heart Transplant Team for their contributions. This project was made possible by funding provided by the National Youth Natural Science Foundation of China (81500218).

SUPPLEMENTARY MATERIAL

The Supplementary Material for this article can be found online at: https://www.frontiersin.org/articles/10.3389/fped.2019.00387/full#supplementary-material

REFERENCES

1. Pinto YM, Elliott PM, Arbustini E, Adler Y, Anastasakis A, Bohm M, et al. Proposal for a revised definition of dilated cardiomyopathy, hypokinetic non-dilated cardiomyopathy, and its implications for clinical practice: a position statement of the ESC working group on myocardial and pericardial diseases. *Eur Heart J*. (2016) 37:1850–8. doi: 10.1093/eurheartj/ehv727
2. Wilkinson JD, Landy DC, Colan SD, Towbin JA, Sleeper LA, Orav EJ, et al. The pediatric cardiomyopathy registry and heart failure: key results from the first 15 years. *Heart Fail Clin*. (2010) 6:401–13, vii. doi: 10.1016/j.hfc.2010.05.002
3. Kirk R, Dipchand AI, Rosenthal DN, Addonizio L, Burch M, Chrisant M, et al. The International Society for Heart and Lung Transplantation Guidelines for the management of pediatric heart failure: executive summary. *J Heart Lung Transplant*. (2014) 33:888–909. doi: 10.1016/j.healun.2014.06.002
4. Packer M, Carver JR, Rodeheffer RJ, Ivanhoe RJ, DiBianco R, Zeldis SM, et al. Effect of oral milrinone on mortality in severe chronic heart failure. The PROMISE study research group. *N Engl J Med*. (1991) 325:1468–75. doi: 10.1056/NEJM199111213252103
5. Price JF, Towbin JA, Dreyer WJ, Moffett BS, Kertesz NJ, Clunie SK, et al. Outpatient continuous parenteral inotropic therapy as bridge to transplantation in children with advanced heart failure. *J Card Fail*. (2006) 12:139–43. doi: 10.1016/j.cardfail.2005.11.001
6. Jiang X, Sucharov J, Stauffer BL, Miyamoto SD, Sucharov CC. Exosomes from pediatric dilated cardiomyopathy patients modulate a pathological response in cardiomyocytes. *Am J Physiol Heart Circ Physiol*. (2017) 312:H818–26. doi: 10.1152/ajpheart.00673.2016
7. Hauck C, Potter T, Bartz M, Wittwer T, Wahlers T, Mehlhorn U, et al. Isoform specificity of cardiac glycosides binding to human Na+,K+-ATPase alpha1beta1, alpha2beta1 and alpha3beta1. *Eur J Pharmacol*. (2009) 622:7–14. doi: 10.1016/j.ejphar.2009.08.039
8. Dorn GW II. Adrenergic pathways and left ventricular remodeling. *J Card Fail*. (2002) 8:S370–3. doi: 10.1054/jcaf.2002.129267
9. Hambleton R, Krall J, Tikishvili E, Honeggar M, Ahmad F, Manganiello VC, et al. Isoforms of cyclic nucleotide phosphodiesterase PDE3 and their contribution to cAMP hydrolytic activity in subcellular fractions of human myocardium. *J Biol Chem*. (2005) 280:39168–74. doi: 10.1074/jbc.M506760200
10. Levin ER, Gardner DG, Samson WK. Natriuretic peptides. *N Engl J Med*. (1998) 339:321–8. doi: 10.1056/NEJM199807303390507
11. Paterick TE, Tajik AJ. Left ventricular noncompaction: a diagnostically challenging cardiomyopathy. *Circ J*. (2012) 76:1556–62. doi: 10.1253/circj.CJ-12-0666
12. Towbin JA, Lowe AM, Colan SD, Sleeper LA, Orav EJ, Clunie S, et al. Incidence, causes, and outcomes of dilated cardiomyopathy in children. *JAMA*. (2006) 296:1867–76. doi: 10.1001/jama.296.15.1867
13. Almond CSD, Thiagarajan RR, Piercey GE, Gauvreau K, Blume ED, Bastardi HJ, et al. Waiting list mortality among children listed for heart transplantation in the United States. *Circulation*. (2009) 119:717–27. doi: 10.1161/CIRCULATIONAHA.108.815712
14. Kantor PF, Abraham JR, Dipchand AI, Benson LN, Redington AN. The impact of changing medical therapy on transplantation-free survival in pediatric dilated cardiomyopathy. *J Am Coll Cardiol*. (2010) 55:1377–84. doi: 10.1016/j.jacc.2009.11.059

15. Dzau VJ, Colucci WS, Williams GH, Curfman G, Meggs L, Hollenberg NK. Sustained effectiveness of converting-enzyme inhibition in patients with severe congestive heart failure. *N Engl J Med*. (1980) 302:1373–9. doi: 10.1056/NEJM198006193022501
16. Alousi AA, Canter JM, Montenaro MJ, Fort DJ, Ferrari RA. Cardiotonic activity of milrinone, a new and potent cardiac bipyridine, on the normal and failing heart of experimental animals. *J Cardiovasc Pharmacol*. (1983) 5:792–803. doi: 10.1097/00005344-198309000-00014
17. McMurray JJ, Packer M, Desai AS, Gong J, Lefkowitz MP, Rizkala AR, et al. Angiotensin-neprilysin inhibition versus enalapril in heart failure. *N Engl J Med*. (2014) 371:993–1004. doi: 10.1056/NEJMoa1409077
18. Solomon SD, Zile M, Pieske B, Voors A, Shah A, Kraigher-Krainer E, et al. The angiotensin receptor neprilysin inhibitor LCZ696 in heart failure with preserved ejection fraction: a phase 2 double-blind randomised controlled trial. *Lancet*. (2012) 380:1387–95. doi: 10.1016/S0140-6736(12)61227-6
19. Schroten NF, Gaillard CA, van Veldhuisen DJ, Szymanski MK, Hillege HL, de Boer RA. New roles for renin and prorenin in heart failure and cardiorenal crosstalk. *Heart Fail Rev*. (2012) 17:191–201. doi: 10.1007/s10741-011-9262-2
20. Weber KT. Aldosterone in congestive heart failure. *N Engl J Med*. (2001) 345:1689–97. doi: 10.1056/NEJMra000050
21. Peters J. The (pro)renin receptor and its interaction partners. *Pflugers Arch*. (2017) 469:1245–56. doi: 10.1007/s00424-017-2005-z
22. Miyamoto SD, Stauffer BL, Nakano S, Sobus R, Nunley K, Nelson P, et al. Beta-adrenergic adaptation in paediatric idiopathic dilated cardiomyopathy. *Eur Heart J*. (2014) 35:33–41. doi: 10.1093/eurheartj/ehs229
23. Nakano SJ, Miyamoto SD, Movsesian M, Nelson P, Stauffer BL, Sucharov CC. Age-related differences in phosphodiesterase activity and effects of chronic phosphodiesterase inhibition in idiopathic dilated cardiomyopathy. *Circ Heart Fail*. (2015) 8:57–63. doi: 10.1161/CIRCHEARTFAILURE.114.001218
24. Li B, Zhao Y, Yin B, Helian M, Wang X, Chen F, et al. Safety of the neprilysin/renin-angiotensin system inhibitor LCZ696. *Oncotarget*. (2017) 8:83323–33. doi: 10.18632/oncotarget.18312
25. Desai AS, Claggett BL, Packer M, Zile MR, Rouleau JL, Swedberg K, et al. Influence of sacubitril/valsartan (LCZ696) on 30-day readmission after heart failure hospitalization. *J Am Coll Cardiol*. (2016) 68:241–8. doi: 10.1016/j.jacc.2016.04.047

Conflict of Interest: The authors declare that the research was conducted in the absence of any commercial or financial relationships that could be construed as a potential conflict of interest.

frontiers in Pediatrics

REVIEW
published: 18 October 2019
doi: 10.3389/fped.2019.00419

Recurrent Pericarditis in Children and Adolescents

Enrico Tombetti[1]*, *Teresa Giani*[2,3], *Antonio Brucato*[1] and *Rolando Cimaz*[4,5]

[1] Department of Medicine, Azienda Socio Sanitaria Territoriale (ASST) Fetebenefratelli-Sacco and Department of "Biomedical and Clinical Sciences Luigi Sacco", Milan University, Milan, Italy, [2] Rheumatology Unit, Department of Pediatrics, Anna Meyer Children's Hospital, University of Florence, Florence, Italy, [3] Department of Medical Biotechnology, University of Siena, Siena, Italy, [4] Department of Clinical Sciences and Community Health, University of Milan, Milan, Italy, [5] Azienda Socio Sanitaria Territoriale (ASST) G.Pini, Milan, Italy

Recurrent pericarditis (RP) is a clinical syndrome characterized by recurrent attacks of acute pericardial inflammation. Prognosis *quoad vitam* is good, although morbidity might be significant, especially in children and adolescents. Multiple potential etiologies result in RP, in the vast majority of cases through autoimmune or autoinflammatory mechanisms. Idiopathic RP is one of the most frequent diagnoses, that requires the exclusion of all known etiologies. Therapeutic advances in the last decade have been significant with the recognition of the effectiveness of anti IL1 therapy, but a correct diagnostic and therapeutic algorithm is of key importance. Unfortunately, most of evidence comes from studies in adult patients. Here we review the etiopathogenesis, diagnosis and management of RP in pediatric patients.

Keywords: pericarditis, myopericarditis, children, adolescents, pediatric, autoinflammatory diseases

OPEN ACCESS

Edited by:
Hongfang Jin,
Peking University First Hospital, China

Reviewed by:
George Lazaros,
Hippokration General Hospital, Greece
Dingding Xiong,
St. Vincent Mercy Medical Center, United States

***Correspondence:**
Enrico Tombetti
enrico.tombetti@unimi.it

Specialty section:
This article was submitted to Pediatric Cardiology, a section of the journal Frontiers in Pediatrics

Received: *29 July 2019*
Accepted: *02 October 2019*
Published: *18 October 2019*

Citation:
Tombetti E, Giani T, Brucato A and Cimaz R (2019) Recurrent Pericarditis in Children and Adolescents. Front. Pediatr. 7:419. doi: 10.3389/fped.2019.00419

PERICARDITIS: DEFINITIONS

Pericarditis is a clinical syndrome characterized by pericardial inflammation with or without concurrent pericardial effusion.

According to the European Society of Cardiology (ESC) guidelines (1), diagnosis of acute pericarditis requires at least two of the objective criteria listed in **Table 1**. The clinical course is distinguished into acute, incessant, recurrent and chronic pericarditis by temporal cut-offs defined by expert consensus (**Table 1**). Acute pericarditis accounts for 5% of the presentations to the emergency department for chest pain in pediatric patients (3). After the attack has subsided, acute pericarditis may recur leading to recurrent pericarditis (RP) in about 15–30% of adult patients (4, 5) and in 35% of pediatric patients (6). Recurrences are frequently less severe than the first attack.

Most of evidence about pericarditis comes from studies on adults. However, RP in children and adolescents is frequent, and has important specificities that will be review here.

ETIOLOGY, EPIDEMIOLOGY, AND DIAGNOSIS

Clinical and Etiological Classification

Acute pericarditis recognizes multiple etiologies, including infections, autoimmunity, autoinflammation, genetic abnormalities, drugs, cardiac injuries, and undetermined causes resulting in idiopathic pericarditis (**Table 2**). Most frequent etiologies show geographical variation and depend on the clinical course. Worldwide, tuberculosis is the most common cause of pericarditis. In developed countries, a viral infection is the most common cause of the first pericarditis attack, while idiopathic RP (IRP) accounts for about 80% of adults and 70% of children with RP.

TABLE 1 | Definition and diagnostic criteria for pericarditis.

	Definition and diagnostic criteria
Acute Pericarditis	Acute (lasting <4–6 weeks) inflammatory pericardial syndrome to be diagnosed by ≥2 of the following: a) Pericardial chest pain* (prevalence in pediatric cases 90–95%) b) Pericardial rubs (prevalence in pediatric cases 30%) c) New widespread ST-elevation or PR depression on ECG (prevalence in pediatric cases 40–50%) d) Pericardial effusion (new or worsening, prevalence in pediatric cases 70–80%) Additional supporting findings: - Elevated inflammatory markers (e.g., C-reactive protein, erythrocyte sedimentation rate, and white blood cell count) - Pericardial inflammation at imaging (CT, CMR)
Recurrent pericarditis	Recurrence of acute pericarditis after a documented first episode and a symptom-free interval of ≥4–6 weeks

Adapted from Adler et al. (1) and Imazio et al. (2).
CT, computed tomography; ECG, electrocardiogram; CMR, cardiac magnetic resonance.
**Pericardial chest pain: typically sharp and with pleuritic features; improved by sitting and leaning forward.*

TABLE 2 | Most common etiologies of acute pericarditis in the pediatric age.

Infectious[#]	Purulent – pyogenic bacteria Tubercular Viral* (adenovirus, enterovirus, parvovirus, influenza A, cytomegalovirus, Epstein-Barr Virus, human herpesvirus-6) Other: Lyme's disease, *Histoplasma capsulatum*, and opportunistic infections in immunocompromised patients
Autoimmune	Connective tissue diseases* (systemic lupus erythematous [SLE], dermatomyositis) Arthritis (Systemic-onset juvenile idiopathic arthritis [so-JIA]*, rheumatic fever*) Vasculitis* (Takayasu, Kawasaki, Behçet disease and ANCA-associated vasculitides) Sarcoidosis* Inflammatory bowel diseases*
Autoinflammatory	Familiar Mediterranean Fever (FMF)* TNF receptor-associated periodic syndrome (TRAPS)*
Other genetic conditions	Camptodactyly–arthropathy–coxa vara–pericarditis (CACP) syndrome
Iatrogenic	Chemotherapy- and radiotherapy- related Immune checkpoint-inhibitors (7) Drug-related SLE (8) Hypersensitivity (e.g., penicillins, mesalamine, sulfasalazine, infliximab)
Post-cardiac injury	Myocardial infarction, pericardiotomy*, pericardial bleeding*, percutaneous coronary intervention*, pacemaker lead insertion*, radiofrequency ablation*, chest trauma*
Miscellaneous	Malignancies Uremia Mixedema Anorexia nervosa
Idiopathic	*

**Potential evolution to recurrent pericarditis.*
[#]Potentially favored by inherited or acquired immune deficiencies.

Idiopathic Recurrent Pericarditis (IRP)

Limited epidemiologic data are available for pediatric IRP. Acute idiopathic pericarditis equally affects male and female children, while being more prevalent in male among adolescents (9). The reported incidence in the general population of acute pericarditis is 30–150/10^5 per year (10, 11). Considering the probability of recurrence and of alternative etiologies, the incidence of IRP can be estimated at about 5–35/10^5 per year. After the first recurrence, up to 50% of patients undergo further pericarditis attacks (12, 13).

IRP is a diagnosis of exclusion, that can be made only after an exhaustive screening. Invasive procedures (e.g., pericardiocentesis and pericardial biopsy) allow to increase the sensitivity for specific etiologies (14), but are rarely performed and there is no consensus about which tests should be performed before concluding for IRP.

Despite that the term "idiopathic" reflects our ignorance about the etiology of these conditions, recent advances have allowed an increased awareness about the autoimmune/autoinflammatory pathogenesis and about patients heterogeneity. In our experience, there are three extreme phenotypes within IRP:

i) Recurrent attacks of pericarditis followed by complete resolution with highly symptomatic serositis, high fever and strikingly elevated acute-phase reactants. This phenotype is particularly frequent in pediatric cases (2) and typically shows a spectacular response to anti-interleukin-1 (IL1) therapies such as anakinra (15). Important similarities with autoinflammatory conditions (see below), suggests a similar pathogenesis.
ii) Recurrent attacks with a subacute course, moderate to high elevation of acute-phase reactants, frequent autoantibody positivity (anti-nuclear antibodies, ANA, anti-heart antibodies, AHA, and anti-intercalated disk autoantibodies) and presence of other features occurring in systemic autoimmune diseases (e.g., arthralgias, xeroftalmia, Raynaud's phenomenon, discoid lupus, uveitis). Autoimmune mechanisms are believed to play an important role in these patients. However, we highlight that autoantibodies are not a specific markers of an autoimmune pathogenesis, as they may be an epiphenomenon of pericardial inflammation.
iii) Patients with mild attacks with a subacute or grumbling course, smoldering elevation of inflammatory markers, and no evidence of autoimmunity.

Post-cardiac Injury Recurrent Pericarditis

Post-cardiac injury syndromes are characterized by pleuro-pericarditis occurring after myocardial infarction, chest trauma, cardiac surgery, and percutaneous procedures including angioplasty/coronary stenting, cardiovascular implantable electronic device lead insertion and radiofrequency ablation (16–18). Among these, post-pericardiotomy (PP) pericarditis is the best-characterized condition. PP pericarditis occurs after heart surgery in about 15–30% of subjects (19, 20), typically within 3 months. The observed risk to develop RP after the first attack ranges between 1 and 2% in the studies performed in the

last decade (19, 20) and 50% in those performed in the early 90s' (50%) (21).

It is debated whether pediatric patients have a higher risk than adults to develop PP-pericarditis and PP-RP. Observational studies on pediatric cohorts of RP have reported that PP cases account for about 10% of children and adolescents with PR (2). The risk of development of PP-pericarditis in children undergoing heart surgery might be particularly high after surgical repair of atrial septal defects (22); being reported to range between 10 and 28% (23–25), which is similar to what observed in adults.

Secondary RP

RP in Systemic Autoimmune Disorders

Pericarditis is a frequent finding in patients with systemic autoimmune disorders (**Table 2**). In general, pericarditis in the setting of systemic autoimmunity might follow ether a chronic or an acute/subacute course reflecting the inflammatory activity of the underlying disease with multiple potential recurrences. On average, pericardial effusion tends to be larger but less symptomatic than that observed in idiopathic or viral pericarditis (26).

In the setting of systemic autoimmunity, the diagnostic work-up should screen for involvement of other heart structures, and consider specific complications related to immunosuppression such as lymphoproliferative diseases or infections.

Systemic lupus erythematosus (SLE) and connective-tissue diseases

SLE is the prototypic connective tissue disease, mainly affecting young women with a chronic-relapsing course. Up to 20% of SLE patients experience disease onset during infancy of adolescence (27). Heterogeneity in terms of disease severity and pattern of involvement is substantial, as SLE can involve most body tissues and organs. Prevalence of symptomatic pericarditis is about 25% in adults (28), and appears to be even higher in childhood-onset SLE (29). Although pericardial involvement is the most common cause of symptomatic heart disease in SLE, it is frequently asymptomatic and seldom results in major complications such as cardiac tamponade or pericardial constriction (26, 30, 31).

Idiopathic inflammatory myopathies, in particular dermatomyositis, are another connective tissue diseases that may affects pediatric patients (32–34). Although the skin and striated muscles are typical disease targets, pericardial involvement and pericarditis have been described, with lower frequency than SLE (26).

Systemic-onset juvenile idiopathic arthritis

Juvenile idiopathic arthritis (JIA) represent a heterogeneous group of diseases that globally accounts for most of childhood chronic rheumatic conditions (35). Systemic-onset JIA (SoJIA, also known as Still's disease) is characterized by polyarthritis, high-spiking fever with prominent acute-phase response, a fleeting pink skin rash, generalized lymphadenopathy, hepatosplenomegaly, and sometimes serositis. SoJIA pathogenesis include dysregulation in innate and adaptive immunity, thus presenting features of both autoimmune and autoinflammatory conditions. Cardiac involvement, predominantly pericarditis, is estimated to occur clinically in 10% of cases, and echocardiographic signs are observed in more than 30% of the cases (36, 37). Pericardial tamponade is uncommon, especially after therapy has been undertaken (38). Children and adolescents suffering from other forms of JIA might have asymptomatic pericardial effusion or a typically mild and benign pericarditis in up to 30 and 10% of cases, respectively (39).

Rheumatic fever (RF)

RF is a relapsing autoimmune disorder triggered by group-A streptococci infection in predisposed subjects. Inflammation typically affects the joints and the heart, and sometimes also the skin and the brain basal ganglia (40). Pathogenesis is due to molecular mimicry between streptococcal M protein and self-antigens. Pericarditis during RF is a sign of rheumatic carditis. Usually, it occurs at the initial episode, within 1 week after appearance of fever and arthritis (26), but sometimes is the presenting manifestation of RF or can present during relapses of RF (41). Pericarditis usually resolves without sequelae and does not require a specific management in addition to that for rheumatic carditis (antibiotics to eradicate streptococcal infection, salicilates, glucocorticoids, and management of valvulopathy and heart failure) (40).

Vasculitis

Pediatric vasculitides might uncommonly result in pericarditis. Despite being the most common pediatric vasculitis, Henoch-Schonlein purpura is not associated with pericarditis, as coexistence of the two has been reported only once (42).

Kawasaki disease is an acute, self-limiting muco-cutaneous febrile illness typically affecting children and characterized by small- and medium-sized arteries and frequently resulting in remodeling of coronary artery with stenosis or aneurysm. Pericardial effusion is frequently observed and is predictive of coronaritis and coronary artery remodeling (43). However, overt pericarditis is uncommon and typically uniphasic (44).

Takayasu arteritis is the prototypic large-vessel vasculitis (45, 46), and is the third most frequent pediatric vasculitis (47). Takayasu arteritis might be associated with pericarditis at disease onset or in the case of very high disease activity (48).

Behçet's disease can affect arteries and veins of variable size, skin and oral/genital mucosa, the bowel, the eye and the CNS (49). Five to ten percent of patients experience disease onset during childhood (50). Despite that Behçet's disease seldom affects the heart, pericarditis is the most common type of heart involvement (51).

ANCA-associated vasculitides (AAVs) are small-vessel vasculitides that can rarely affect pediatric patients. Although infrequently, pericarditis may be associated with active AAVs (26, 52).

Sarcoidosis

Sarcoidosis is the prototypic idiopathic granulomatous disease and affects multiple organs, mainly the lymph nodes and the lungs (53). Disease onset during childhood or adolescence

occurs in <10% of subjects. Heart involvement might lead to cardiomyopathy with heart failure, conduction abnormalities, and arrhythmias. Mild to moderate pericardial effusion is frequently present during active sarcoidosis, while pericarditis is rare but can occur with a relapsing course (26).

Inflammatory bowel diseases

Inflammatory bowel diseases (IBDs) are chronic-relapsing inflammatory conditions, mainly represented by Crohn's disease and ulcerative colitis, that primarily affect the gut. Pediatric onset occurs in about 15–20% of subjects and portend a poorer prognosis (54). Extra-intestinal inflammatory involvement occurs in about a third of patients. Pericarditis is the most frequent extra-intestinal manifestation of IBDs, being reported in about 70% of subjects with cardiovascular complications (55). Pericarditis in the setting of IBD might follow a relapsing course and sometimes has onset before intestinal manifestations (56). Concurrent myocardial involvement is not rare and frequently depends on hypersensitivity to aminosalicylate therapy with mesalamine or sulfasalazine (55, 57–59).

RP in Autoinflammatory Disorders

Autoinflammatory diseases are a recently-recognized group of disorders in which inflammation results from dysregulated innate immunity rather than from autoimmunity. Many autoinflammatory diseases have been recognized as genetic disorders caused by mutations in key regulators of innate immunity. Although not being part of the typical disease features, pericarditis has been described in the setting of multiple autoinflammatory conditions, including Hyperimmunoglobulinemia D with periodic fever syndrome (HIDS) (60), NOD2-associated autoinflammatory syndrome (61), and chronic atypical neutrophilic dermatosis with lipodystrophy and elevated temperature (CANDLE) (62). On the contrary, two autoinflammatory conditions, namely Familial Mediterranean Fever (FMF) and TNF receptor-associated periodic syndrome (TRAPS), are closely related to IRP because of clinical similarities and a similar response to colchicine and anti-IL1 therapies such as anakinra.

Familiar Mediterranean Fever (FMF)

FMF is the most common monogenic autoinflammatory disease. It characterized by episodes lasting 1–3 days with fever, systemic inflammation, serositis and oligoarthritis (63). Overt peritonitis occurs in more than 90% of cases, pleuritis in about 40%, and pericarditis in about 5% (64–66). Subclinical pericardial disease might be more prevalent, as echocardiographic signs of pericardial effusion or thickening are present in up to 27% of patients (67). Pericarditis attacks during FMF often have a benign course without sequelae and tend to occur later in life (68).

TRAPS

TRAPS is a genetic condition characterized by febrile attacks lasting several days to weeks, associated with migratory erythema with underlying myalgia, ocular inflammation, arthralgia and/or arthritis, and serositis (69). Clinical and genetic heterogeneity of TRAPS is substantial, and attacks with isolated pericarditis have been described. Indeed, TRAPS mutations sometimes are identified in subjects with colchicine-refractory or steroid-dependent RP (70).

TABLE 3 | Prognostic factors predictive of complication or recurrence (1).

Major	Fever > 38°C Subacute onset Large pericardial effusion (>20 mm) Cardiac tamponade Lack of response to Aspirin or NSAID after ≥1 week of treatment
Minor	Myocardial involvement Immunosuppression Trauma Anticoagulant therapy

RP Secondary to Other Pediatric Disorders

Camptodactyly–Arthropathy–Coxa Vara–Pericarditis (CACP) Syndrome

CACP syndrome is characterized by symmetrical, non-inflammatory arthropathy, synovial hyperplasia, congenital or early-onset camptodactyly, progressive coxa vara, and pericarditis. It is caused by mutations in the *proteoglycan 4* gene, which encodes lubricin, a lubricating glycoprotein of synovial fluid, articular cartilage and pericardium. Lubricin absence results in pericardial adhesions and fibrosis (71).

Non-inflammatory pericardial effusion is reported in up to 30% cases of CACP syndrome. Ascites and pleural effusions are uncommon. Pericarditis has a variable course, from a self-limiting condition to a chronic and constrictive evolution requiring surgical intervention.

Diagnostic Specificities in the Pediatric Age

The ESC guidelines highlight that search for etiology is not mandatory at the first pericarditis attack in the absence of factors for a poor prognosis (**Table 3**) or of features suggestive of specific causes (1). However, RP represents a different scenario especially in children, where specific etiologies occur most frequently than in adults. In pediatric patients, high attention should be paid to identify genetic causes that might entail a specific management. Red flags for considering genetic screening for FMF or TRAPS are: (i) familiarity for RP or autoinflammatory diseases, (ii) a personal history of periodic fever, or (iii) colchicine-refractory or steroid-dependent RP.

PATHOGENESIS

IRP results from an interplay between environmental triggers, genetic predisposition and the immune system. The triggers of recurrence remain to be clarified. Recurrences are not associated with clinical features suggestive of a concurrent viral infection: it has been proposed that a tolerance break toward pericardial antigens at the first attack may pave the way for subsequent relapses. According to this view, dysregulated adaptive immunity and autoimmunity have a central role in IRP pathogenesis. This paradigm is supported by several

observations, such as: (a) the occurrence of pericarditis in autoimmune diseases (72, 73), (b) the association of IRP with cardiac-specific and non-cardiac specific autoantibodies, such as antinuclear antibodies (ANA), anti-heart antibodies (AHA) and anti-intercalated disk antibodies (AIDA) (74), (c) the efficacy of steroids, of immunosuppressive agents targeting cellular immunity (e.g., azathioprine) and of immune-modulatory drugs such as intravenous immunoglobulin (75–79), and (d) the association of IRP with specific alleles in the human leukocyte antigen (HLA)–A, -C, and -DQB1 (80). Recently, this traditional view of IRP as an autoimmune disorder has been challenged by the discovery that dysregulated innate immunity is the driver of a group of inflammatory conditions, thus named "autoinflammatory diseases."

Innate immunity is triggered by germ-line encoded receptors expressed by multiple cell lines and results in an inflammatory response. These receptors recognize signals derived from microbial constituents (PAMPs, pathogen-associated molecular patterns) or from damaged tissue components (DAMPs, damage-associated molecular patterns). A crucial step in modulation of inflammation is the regulation of inflammasome activity (81). Inflammasomes are a family of multimeric complexes that activate caspase-1 and other proteases involved in inflammation. Inflammasomes are activated by specific sensor proteins belonging to the nucleotide-binding oligomerisation domain-like receptor (NLR) family. Upon stimulation, sensor proteins self-assemble into complexes (the inflammasomes) that recruit pro-caspase 1 (81). The adaptor protein ASC (Apoptosis Speck-like protein with a CARD domain) facilitates assembly and is typically required for efficient caspase 1 activation. One of the best-characterized inflammasomes derives from the sensor protein NLRP3 (NLR pyrine domain-containing-3). Recognition of multiple viral PAMPs and several DAMPs, such as urate crystals in gout and cholesterol in atherosclerosis (82–84), results in NLRP3 inflammasome activation and IL1 production (**Figure 1**). Gain-of-function mutations in the gene encoding pyrine, another sensor protein, may cause hyperactivity of pyrin inflammasome and result in FMF. A different inflammatory mechanism underlies TRAPS, which is caused by gain-of-function mutations in the receptor for Tumor Necrosis Factor (TNF)-α (69). Relatives of patients with TRAPS are frequently diagnosed with IPR, suggesting an overlap these conditions, especially for patients with low-penetrance mutations that may have a delayed disease onset or an incomplete TRAPS phenotype (85, 86).

The recognition that sterile pericarditis may derive from either dysregulated adaptive or innate immunity led to the proposal of an autoimmune and an autoinflammatory phenotype of IRP (87). However, distinction between the two is not is not always straightforward, due to the absence of specific biomarkers and to the strong overlap between innate and adaptive immunity, which are intrinsically co-entangled.

Similarly, the pathogenesis of post-cardiac injury pericarditis is poorly understood (16, 17). An autoimmune mechanism has been proposed to explain the onset of relapsing inflammation after tissue damage. Indeed, cardiac injury may result in the presentation of cardiac antigens in an immunogenic context. However, post-cardiac injury pericarditis has been observed in severely immunocompromised children after heart transplantation (88), suggesting that mechanisms alternative to autoimmunity can sustain inflammation. It logical to speculate that strong pathogenic similarities exist between IRP and post-cardiac injury RP, both resulting from dysregulated innate and/or adaptive immunity.

PROGNOSIS OF RECURRENT PERICARDITIS IN THE PEDIATRIC AGE

Prognosis of IRP is good in terms of mortality. No deaths were observed in children hospitalized for acute idiopathic or viral pericarditis in the pediatric health information system (PHIS) database (9). However, morbidity is significant due to multiple recurrences, medication side effects, or occurrence of complications such as cardiac tamponade, pericardial constriction and myocardial involvement. Prognostic factors associated with an increased risk of recurrences or of complications have been identified (**Table 3**), although they have been derived from unselected cohorts of patients with pericarditis and never validated in pediatric cohorts.

Cardiac tamponade typically occurs upon rapid accumulation of fluid in the pericardium, such as in the case of neoplastic pericarditis. Cardiac tamponade is much rarer (about 1–2% of cases) in idiopathic or in viral acute pericarditis (89). Cardiac tamponade complicates the first pericarditis attack more frequently than recurrences (90). Prevalence of tamponade in post-cardiac injury pericarditis is higher, being reported in 5–20% of subjects (19, 91, 92). Cardiac tamponade warrants prompt pericardiocentesis, but subsequent clinical course is similar to uncomplicated pericarditis (75).

Pericardial constriction is a hemodynamic condition due to hampering of diastolic filling of ventricles by a fibrotic and inextensible pericardium. Occurrence of pericardial constriction is rare (1–2% at 6 years of follow-up) in patients with idiopathic or viral pericarditis, relatively infrequent (2–13%) in those with post-cardiac injury pericarditis or pericarditis in the settings of other systemic autoimmune disorders, and frequent (20–30%) in the case of tubercular, purulent or post-actinic pericarditis (91, 93). Pericardial constriction has never been reported in IRP (90, 94). Severe constriction requires surgical pericardiectomy, although medical therapy with NSAIDs sometimes results in improvement in the case of viral, idiopathic or immune-mediated pericarditis (95, 96).

Myocardial involvement during acute pericarditis occurs in about 15% of adult subjects (75) and up to 35% of pediatric patients (97). Myocardial inflammation is revealed by increased troponin levels or by myocardial inflammation/fibrosis at cardiac magnetic resonance (MR). It has been proposed to distinguish two conditions with concomitant pericardial and myocardial inflammation: myopericarditis and perimyocarditis. The former is characterized by predominant pericardial inflammation extending from the epicardial fat to the myocardium. Myopericarditis has clinical features highly similar to pericarditis and usually follow a benign course with a

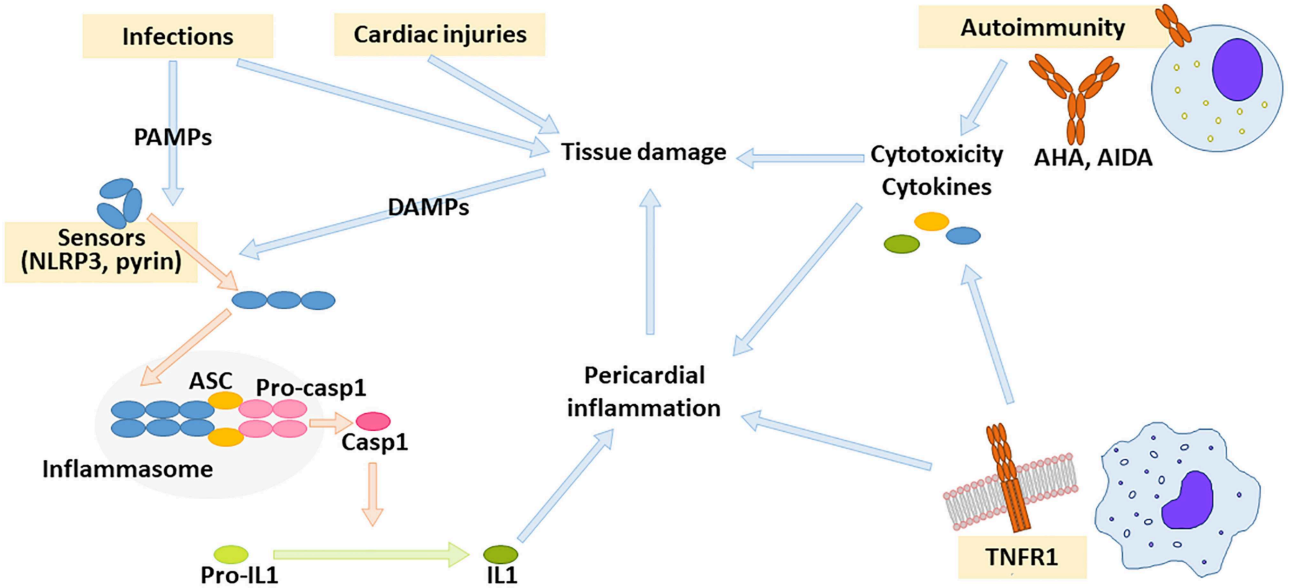

FIGURE 1 | Drivers of pericardial inflammation. Autoimmunity against cardiac antigens as well as dysregulated innate immunity might result in pericardial inflammation. Innate immunity is activated by receptors for pathogen- or damage-associated molecular patterns (PAMPs and DAMPs, respectively). Crucial innate immunity pathways leading to pericardial inflammation depend on inflammasome activity and on TNF receptor-1 (TNFR1). The inflammasome is a multimolecular complex composed of sensor protein such as NLRP3 or pyrin (that self-assemble upon activation), stimuli such as NLRP3 or pyrin, adaptor proteins such as ASC, and pro-caspase-1. Upon inflammasome assembly, pro-caspase 1 releases active caspase 1, which can process pro-IL1 to active IL1. AHA: anti-heart antibodies, AIDA: anti-intercalated disc antibodies.

reduced risk of recurrences or cardiac tamponade. Conversely, perimyocarditis patients tend to have less intense pericardial pain and elevation of acute-phase reactants but prominent myocardial inflammation with regional or global reduction in systolic function (98). Most of these patients recover a normal left ventricular function after the resolution of the attack.

ROLE OF IMAGING

In patients with cardio-respiratory symptoms, chest X-ray may reveal concomitant conditions or alternative diagnosis to pericarditis, or identify pleural and pericardial effusion. Thus, chest X-ray is the first imaging technique usually performed, although it is inaccurate in the quantification of the amount of pericardial fluid, and it is unable to assess the cardiac function and to differentiate among the various etiologies of pericarditis.

Echocardiography is the technique of choice, it is widely and rapidly available, and can be repeated during follow-up. It allows to study the dimensions and functions of cardiac chambers and valves. Signs suggestive of active pericarditis are pericardial effusion and hyperechoic pericardium. In addition, echocardiography may quantify pericardial effusion and reveal potential complications such as cardiac tamponade, systolic dysfunction as well as signs of pericardial constriction.

In selected cases, cardiac MR might be complementary to echocardiography, thanks to its ability to (i) provide an excellent depiction of cardiac and pericardial morphology together with a good quantification of pericardial effusion and ventricular or valvular function, (ii) characterize myocardial and pericardial tissue in terms of inflammation, edema and fibrosis, and (iii) reveal findings suggestive for concomitant diseases, such in the case of autoimmune diseases, large-vessels vasculitis, thoracic lymphadenopathies, or cardiac tumors. Acquisition protocols specific for pediatric patients may require to take into account small heart dimension and fast heart rates and to ensure reliable breath-holding (99). Briefly, specific signs of active pericardial inflammation at MR are pericardial edema (hyperintensity on T2-weighted short-tau inverted recovery [STIR] sequences) and pericardial late gadolinium enhancement (LGE, meaning pericardial signal enhancement in T1-weighted sequences obtained 10 min after contrast medium administration). Pericardial thickening (>4 mm) is not considered a specific sign of active pericarditis because it can be observed in multiple pericardial disorders including pericardial constriction or neoplasms. Cardiac MR might also revel concomitant myocarditis. It is proposed that the kinetic of gadolinium ingress and egress differs between the pericardium and the myocardium. Accordingly, active myocardial inflammation is heralded by edema and early gadolinium enhancement (observed on T1-weighted sequences obtained after about 2 min after contrast medium administration). Differently from the pericardium, myocardial late gadolinium-enhancement reveals fibrosis (75).

Given the specificities of cardiac MR, its indications in the setting of pericarditis are: (i) atypical cases, to confirm pericarditis or identify alternative diagnoses, (ii) pericardial constriction or myocardial involvement, and (iii) RP associated to specific etiologies such as large-vessel vasculitis (100), and (iv)

TABLE 4 | Medical therapy for recurrent pericarditis in children.

Agent	Starting dose
NSAID	
Ibuprofen	30–50 mg/kg daily, divided every 6–8 h
Indomethacin	2 mg/kg daily, divided every 6–12 h
Colchicine	0.5 mg/day before 5 years of age
	1–1.5 mg/day after 5 year of age
Anakinra	1–2 mg/kg daily up to 100 mg daily subcutaneously
	Start tapering not before 3–6 months of remission
Prednisone	0.5–2 mg/kg daily
IVIG	400–500 mg/kg for 5 days (repeatable once a month)

need to tailor therapy according to the intensity or persistence of pericardial inflammation (101).

Computed tomography (CT) is another complementary technique. Similarly to MR, CT provides good anatomic images and may quantify pericardial thickness, the volume of pericardial effusion or the presence of localized effusion. In addition, CT can assess the presence of pericardial calcifications and define the attenuation values of the pericardial fluid which might be of help in the diagnostic workup: high values suggest hemorrhage, intermediate values exudative effusions and low values trasudative effusions (102). CT is particularly useful in the initial diagnostic work-up to exclude specific etiologies including malignancies and tuberculosis, and in the preoperative planning of pericardiectomy.

MANAGEMENT OF RECURRENT PERICARDITIS IN THE PEDIATRIC AGE

Management of pediatric patients with RP is derived from the experience with adult patients: it includes medical and interventional therapies, and lifestyle recommendations. After correct diagnostic workflow, therapy should be targeted to the underlying etiopathogenesis as much as possible, aiming at inducing remission and preventing recurrences and complications. Primary prevention of pericarditis (e.g., in the setting of cardiac surgery) is beyond the scope of this review. Available evidence has not suggested important differences in the management of recurrences and remission phases of post-cardiac injury RP and IRP.

Management of Acute Attacks

Admission should be considered in presence of severe pain or predictors of poor prognosis (**Table 3**) (1). Acute pericarditis should be treated with high-dose NSAIDs in combination with colchicine, except for specific etiologies requiring alternative treatments or for refractory subjects (1). High-dose aspirin is generally not used in pediatric patients, due to concerns about the risk of Reye syndrome. In this setting, ibuprofen (30–50 mg/kg daily, divided every 6–8 h) or indomethacin (2 mg/kg daily, divided every 6–12 h, **Table 4**) are valid options. Intravenous administration might be useful to achieve rapid pain control in hospitalized patients.

Colchicine is an anti-gout medication that is also active for FMF (103) and pericarditis. Colchicine concentrates within leukocytes (especially granulocytes) and inhibits microtubule assembly, thus limiting cell motility, phagocytosis, and degranulation. Moreover, colchicine downregulates NLRP3 inflammasome by antagonizing caspase-1 activity and potential triggering factors (e.g., P2X2 and P2X7 channels and Reactive Oxygen Species) (104). Gastrointestinal intolerance is the most common side effect, it is dose-dependent and reported in about 5–10% of adults (5, 12, 13), although children might tolerate higher per kilo doses than adults. Studies have shown that colchicine hastens the response to treatment and decreases the risk of recurrences of about 50% (105). Moreover, colchicine reduces the risk of pericardial constriction in PP pericarditis (91). Unfortunately, little evidence is available about colchicine in pediatric patients with RP (106): a recent observational study reported a 65% reduction of recurrences (2). Moreover, colchicine therapy in pregnant women with IRP raised no concerns about fetal toxicity (107). Despite this encouraging data about safety and efficacy in children with RP, colchicine remains underprescribed in the pediatric population (9, 108).

Currently, steroids are used as second line therapy in adults with sever acute pericarditis or with colchicine-refractory RP: they are rapidly effective but they favor recurrences and steroid-dependence, especially if used at high doses (109, 110). In children, steroids may cause growth retardation, acne, *striae rubrae*, and predisposition to osteoporosis. Therefore, steroids should be avoided as much as possible in pediatric IRP by means of the following recommendations: (i) to use NSAIDs at the maximum tolerated does or (ii) to intravenously administer NSAIDs in hospitalized patients, and (iii) to consider the use of anti-IL1 therapy after failure of high dose NSAIDs combined with colchicine. Alternatively, steroids should be started at the lowest effective dose, and slowly tapered after remission has been obtained.

Anti-IL1 therapy with anakinra (1–2 mg/kg daily subcutaneously) is the most important advance in the last decade for the field (111). Anakinra is efficacious for multiple autoinflammatory diseases including FMF. Thus, it has been initially used in children with refractory IRP. Subsequent experience including a clinical trial has shown that anakinra has spectacular effects in refractory or steroid-dependent IRP with raised acute-phase reactants (2, 15, 112–114). Children with IRP frequently have an "autoinflammatory phenotype" (2) that is particularly responsive to anakinra. Anakinra has a very good safety profile, due to its short half-life and low risk of infections and of reactivation of tuberculosis. Severe reactions are rare, but injections site-reactions are frequent in the first month of treatment, and then disappear (111). Thus, anakinra should be considered as a second line agent for children and adolescents with IRP with raised acute-phase reactants that is refractory to NSAIDs and colchicine.

Intravenous immunoglobulins (IVIG) are used for refractory cases at the dose of is 400–500 mg/kg for 5 days, potentially repeatable after 1 month (2, 77–79). A systematic review about IVIG for RP including 19 adults and 11 pediatric patients, showed good efficacy and safety of IVIG (79). The main limitations

TABLE 5 | Tapering of glucocorticoids in children.

Daily dose*	Tapering
>0.7 mg/kg	0.14 mg/kg*day every 1–2 weeks
0.35–0.7 mg/kg	0.7–14 mg/kg*day every 1–2 weeks
0.2–35 mg/kg	0.035 mg/kg*day every 2–4 weeks
< 0.2 mg/kg	0.017–0.035 mg/day every 2–6 weeks

Doses are expressed as prednisone-equivalents.

of IVIG are costs, the intravenous administration and the administration schedule. Since anti-IL1 therapy has become available for IRP, the role of IVIG is mainly limited to patients with autoimmune features.

RP in the setting of specific etiologies should be treated accordingly to the underlying disease. Specifically, RP in the setting of FMF should be treated with colchicine and anti-IL1 therapies (anakinra, rilonacept, canakinumab) for refractory cases (63). In RP due to TRAPS patients should be treated with NSAIDs, steroids and anti-IL1 treatments or etanercept (115, 116). SLE-associated RP should be treated with a combination of hydroxychloroquine, a brief steroid course and immunosuppressive agents such as azathioprine and mycophenolate mofetil (117, 118).

Prevention of Recurrences and Other Complications

After complete remission (absence of symptoms and of raised acute-phase reactants) has been achieved, therapy can be slowly tapered, reducing a single class of drug at a time. Steroids and high-dose NSAIDs are tapered first. **Table 5** shows the steroid-tapering schedule that we follow in pediatric patients with IRP, directly derived from recommendations for adult patients (1). Recurrences are particularly frequent when steroids are tapered below 0.2 mg/kg*day of prednisone-equivalent, and small decrements are advisable every at least 2–6 weeks (e.g., reductions of 1–2.5 mg on alternate days). Tapering of anakinra should not start before 3–6 months of sustained remission, and should be performed very slowly due to high risk of recurrences.

Slow-acting medications including hydroxicloroquine or immunosuppressive agents such as azathioprine, mycophenolate or cyclosporine (2, 76), have been proposed as 3rd or 4th line medications to prevent recurrences in the cases of refractoriness to anakinra or of features suggestive of autoimmune pathogenesis.

With the exception of acute-phase reactants, we lack biomarkers to guide therapeutic tapering during remission and to predict future exacerbations. Cardiac MR has been proposed at this purpose, although its use in young children might be troublesome because of durations of acquisition and capability to ensure adequate breath holds.

Interventional Therapy for Relapsing Pericarditis

Cardiac tamponade requires emergent pericardiocentesis to restore adequate heart filling. Selected cases of acute pericarditis (mainly at the first episode) might require diagnostic pericardiocentesis if specific etiologies are suspected, including neoplasms or bacteria.

Surgical pleuropericardial window is another options that might be considered for subjects at risk of recurrent pericardial tamponade. In the case of severe or chronic pericardial constriction or of RP refractory to multiple therapeutic lines, surgical pericardiectomy might be of help. However, evidence about pericardiectomy for refractory RP is limited to adults (119), and this procedures should be considered only as an *extrema ratio* in pediatric patients.

Lifestyle Recommendations

Based on expert recommendations, children should avoid physical activity after acute attacks until the resolution of symptoms and acute-phase reactants. Moreover, resumption of competitive sports should occur not before 3 months after complete remission of pericarditis. In case of frequent recurrences avoidance of physical activity in children in our opinion is less stringent, since it is important to allow a normal or near-normal life in these children; the focus should be on a therapy able to control the disease more than on restriction of physical activity.

Exacerbations of SLE or autoinflammatory diseases are sometimes associate with specific triggers, including sunlight for SLE, and exercise, local injury, infection, cold exposure, emotional stress, surgery and hormonal changes for FMF and TRAPS. Patients with RP associated with these condition should be advised to avoid potential triggers, especially if they have been involved in previous disease flares.

The recommended vaccination schedule (120) may not require changes for most children with RP. Prevention of recurrences by influenza vaccination is not demonstrated, reflecting that influenza is a rare trigger of RP. Subjects treated with immunosuppressive agents might benefit from all available inactivated vaccines, although immunogenicity might be reduced and additional administrations be required. On the contrary, a careful balance of the degree of immunocompromised, the risk of natural exposure and the availability of non-live alternatives, may be required for attenuated vaccines.

CONCLUSIONS

RP in children and adolescences has significant morbidity. Multiple potential causes exist, although most of them are related to either autoimmune or autoinflammatory mechanisms. Recent advances allow to manage RP effectively in almost all patients. However, a careful diagnostic work-up and a correct therapeutic algorithm are required to maximize efficacy while limiting avoidable costs and side effects.

AUTHOR CONTRIBUTIONS

ET, TG, AB, and RC designed the study and drafted the manuscript. All authors agree to be accountable for the content of the work.

REFERENCES

1. Adler Y, Charron P, Imazio M, Badano L, Barón-Esquivias G, Bogaert J, et al. 2015 ESC Guidelines for the diagnosis and management of pericardial diseases. *Eur Heart J.* (2015) 36:2921–64. doi: 10.1093/eurheartj/ehv318
2. Imazio M, Brucato A, Pluymaekers N, Breda L, Calabri G, Cantarini L, et al. Recurrent pericarditis in children and adolescents. *J Cardiovasc Med.* (2016) 17:707–12. doi: 10.2459/JCM.0000000000000300
3. Geggel RL. Conditions leading to pediatric cardiology consultation in a tertiary academic hospital. *Pediatrics.* (2004) 114:e409–17. doi: 10.1542/peds.2003-0898-L
4. Imazio M, Bobbio M, Cecchi E, Demarie D, Demichelis B, Pomari F, et al. Colchicine in addition to conventional therapy for acute pericarditis. *Circulation.* (2005) 112:2012–6. doi: 10.1161/CIRCULATIONAHA.105.542738
5. Imazio M, Brucato A, Cemin R, Ferrua S, Maggiolini S, Beqaraj F, et al. A randomized trial of colchicine for acute pericarditis. *N Engl J Med.* (2013) 369:1522–8. doi: 10.1056/NEJMoa1208536
6. Ratnapalan S, Brown K, Benson L. Children presenting with acute pericarditis to the emergency department. *Pediatr Emerg Care.* (2011) 27:581–5. doi: 10.1097/PEC.0b013e31822251ba
7. Altan M, Toki MI, Gettinger SN, Carvajal-Hausdorf DE, Zugazagoitia J, Sinard JH, et al. Immune checkpoint inhibitor–associated pericarditis. *J Thorac Oncol.* (2019) 14:1102–8. doi: 10.1016/j.jtho.2019.02.026
8. Harnett DT, Chandra-Sekhar HB, Hamilton SF. Drug-induced lupus erythematosus presenting with cardiac tamponade: a case report and literature review. *Can J Cardiol.* (2014) 30:247.e11–247.e12. doi: 10.1016/j.cjca.2013.11.011
9. Shakti D, Hehn R, Gauvreau K, Sundel RP, Newburger JW. Idiopathic pericarditis and pericardial effusion in children: contemporary epidemiology and management. *J Am Heart Assoc.* (2014) 3:e001483. doi: 10.1161/JAHA.114.001483
10. Søgaard KK, Farkas DK, Ehrenstein V, Bhaskaran K, Bøtker HE, Sørensen HT. Pericarditis as a marker of occult cancer and a prognostic factor for cancer mortality. *Circulation.* (2017) 136:996–1006. doi: 10.1161/CIRCULATIONAHA.116.024041
11. Imazio M, Cecchi E, Demichelis B, Chinaglia A, Ierna S, Demarie D, et al. Myopericarditis versus viral or idiopathic acute pericarditis. *Heart.* (2008) 94:498–501. doi: 10.1136/hrt.2006.104067
12. Imazio M, Bobbio M, Cecchi E, Demarie D, Pomari F, Moratti M, et al. Colchicine as first-choice therapy for recurrent pericarditis: results of the CORE (COlchicine for REcurrent pericarditis) trial. *Arch Intern Med.* (2005) 165:1987–91. doi: 10.1001/archinte.165.17.1987
13. Imazio M, Belli R, Brucato A, Cemin R, Ferrua S, Beqaraj F, et al. Efficacy and safety of colchicine for treatment of multiple recurrences of pericarditis (CORP-2): a multicentre, double-blind, placebo-controlled, randomised trial. *Lancet.* (2014) 383:2232–7. doi: 10.1016/S0140-6736(13)62709-9
14. Maisch B, Rupp H, Ristic A, Pankuweit S. Pericardioscopy and epi- and pericardial biopsy—a new window to the heart improving etiological diagnoses and permitting targeted intrapericardial therapy. *Heart Fail Rev.* (2013) 18:317–28. doi: 10.1007/s10741-013-9382-y
15. Picco P, Brisca G, Traverso F, Loy A, Gattorno M, Martini A. Successful treatment of idiopathic recurrent pericarditis in children with interleukin-1beta receptor antagonist (anakinra): an unrecognized autoinflammatory disease? *Arthritis Rheum.* (2009) 60:264–8. doi: 10.1002/art.24174
16. Imazio M, Hoit BD. Post-cardiac injury syndromes. An emerging cause of pericardial diseases. *Int J Cardiol.* (2013) 168:648–52. doi: 10.1016/j.ijcard.2012.09.052
17. Imazio M. The post-pericardiotomy syndrome. *Curr Opin Pulm Med.* (2012) 18:366–74. doi: 10.1097/MCP.0b013e32835311a2
18. Tamarappoo BK, Klein AL. Post-pericardiotomy syndrome. *Curr Cardiol Rep.* (2016) 18:116. doi: 10.1007/s11886-016-0791-0
19. Imazio M, Trinchero R, Brucato A, Rovere ME, Gandino A, Cemin R, et al. COlchicine for the Prevention of the Post-pericardiotomy Syndrome (COPPS): a multicentre, randomized, double-blind, placebo-controlled trial. *Eur Heart J.* (2010) 31:2749–54. doi: 10.1093/eurheartj/ehq319
20. Imazio M, Brucato A, Ferrazzi P, Pullara A, Adler Y, Barosi A, et al. Colchicine for prevention of postpericardiotomy syndrome and postoperative atrial fibrillation: the COPPS-2 randomized clinical trial. *JAMA.* (2014) 312:1016–23. doi: 10.1001/jama.2014.11026
21. Horneffer PJ, Miller RH, Pearson TA, Rykiel MF, Reitz BA, Gardner TJ. The effective treatment of postpericardiotomy syndrome after cardiac operations. A randomized placebo-controlled trial. *J Thorac Cardiovasc Surg.* (1990) 100:292–6.
22. Raatikka M, Pelkonen PM, Karjalainen J, Jokinen E V. Recurrent pericarditis in children and adolescents: report of 15 cases. *J Am Coll Cardiol.* (2003) 42:759–64. doi: 10.1016/S0735-1097(03)00778-2
23. Heching HJ, Bacha EA, Liberman L. Post-pericardiotomy syndrome in pediatric patients following surgical closure of secundum atrial septal defects: incidence and risk factors. *Pediatr Cardiol.* (2015) 36:498–502. doi: 10.1007/s00246-014-1039-7
24. Rabinowitz EJ, Meyer DB, Kholwadwala P, Kohn N, Bakar A. Does prophylactic ibuprofen after surgical atrial septal defect repair decrease the rate of post-pericardiotomy syndrome? *Pediatr Cardiol.* (2018) 39:1535–9. doi: 10.1007/s00246-018-1926-4
25. Elias MD, Glatz AC, O'Connor MJ, Schachtner S, Ravishankar C, Mascio CE, et al. Prevalence and risk factors for pericardial effusions requiring readmission after pediatric cardiac surgery. *Pediatr Cardiol.* (2017) 38:484–94. doi: 10.1007/s00246-016-1540-2
26. Imazio M. Pericardial involvement in systemic inflammatory diseases. *Heart.* (2011) 97:1882–92. doi: 10.1136/heartjnl-2011-300054
27. Aggarwal A, Srivastava P. Childhood onset systemic lupus erythematosus: how is it different from adult SLE? *Int J Rheum Dis.* (2015) 18:182–91. doi: 10.1111/1756-185X.12419
28. Moder KG, Miller TD, Tazelaar HD. Cardiac involvement in systemic lupus erythematosus. *Mayo Clin Proc.* (1999) 74:275–84. doi: 10.4065/74.3.275
29. Chang JC, Xiao R, Mercer-Rosa L, Knight AM, Weiss PF. Child-onset systemic lupus erythematosus is associated with a higher incidence of myopericardial manifestations compared to adult-onset disease. *Lupus.* (2018) 27:2146–54. doi: 10.1177/0961203318804889
30. Doria A, Iaccarino L, Sarzi-Puttini P, Atzeni F, Turriel M, Petri M. Cardiac involvement in systemic lupus erythematosus. *Lupus.* (2005) 14:683–6. doi: 10.1191/0961203305lu2200oa
31. Langley RL, Treadwell EL. Cardiac tamponade and pericardial disorders in connective tissue diseases: case report and literature review. *J Natl Med Assoc.* (1994) 86:149–53.
32. Mendez EP, Lipton R, Ramsey-Goldman R, Roettcher P, Bowyer S, Dyer A, et al. US incidence of juvenile dermatomyositis, 1995–1998: results from the National Institute of Arthritis and Musculoskeletal and Skin Diseases Registry. *Arthritis Rheum.* (2003) 49:300–5. doi: 10.1002/art.11122
33. Orandi AB, Baszis KW, Dharnidharka VR, Huber AM, Hoeltzel MF. Assessment, classification and treatment of calcinosis as a complication of juvenile dermatomyositis: a survey of pediatric rheumatologists by the childhood arthritis and rheumatology research alliance (CARRA). *Pediatr Rheumatol.* (2017) 15:71. doi: 10.1186/s12969-017-0199-4
34. Shah M, Mamyrova G, Targoff IN, Huber AM, Malley JD, Rice MM, et al. The clinical phenotypes of the juvenile idiopathic inflammatory myopathies. *Medicine.* (2013) 92:25–41. doi: 10.1097/MD.0b013e31827f264d
35. Prakken B, Albani S, Martini A. Juvenile idiopathic arthritis. *Lancet.* (2011) 377:2138–49. doi: 10.1016/S0140-6736(11)60244-4
36. Ward SC, Wiselka MJ, Nicholson KG. Still's disease and myocarditis associated with recent mumps infection. *Postgrad Med J.* (1988) 64:693–5. doi: 10.1136/pgmj.64.755.693
37. Sachs RN, Talvard O, Lanfranchi J. Myocarditis in adult Still's disease. *Int J Cardiol.* (1990) 27:377–80. doi: 10.1016/0167-5273(90)90295-G
38. Ben Ghorbel I, Lamloum M, Miled M, Aoun N, Houman M-H, Pouchot J. [Adult-onset Still's disease revealed by a pericardial tamponade: report of two cases]. *La Rev Med Interne.* (2006) 27:546–9. doi: 10.1016/j.revmed.2006.03.027

39. Koca B, Sahin S, Adrovic A, Barut K, Kasapcopur O. Cardiac involvement in juvenile idiopathic arthritis. *Rheumatol Int.* (2017) 37:137–42. doi: 10.1007/s00296-016-3534-z
40. Karthikeyan G, Guilherme L. Acute rheumatic fever. *Lancet.* (2018) 392:161–74. doi: 10.1016/S0140-6736(18)30999-1
41. Howard A, Sutton MD L, Fergie J. Rheumatic fever presenting as recurrent pericarditis and cardiac tamponade. *Clin Pediatr.* (2017) 56:870–2. doi: 10.1177/0009922817715938
42. Cimaz R, Boccazzi A, Milone V, Careddu P. Pericarditis as a presenting feature of Henoch-Schönlein purpura. *Clin Exp Rheumatol.* (2000) 18:785.
43. Maggio MC, Corsello G, Prinzi E, Cimaz R. Kawasaki disease in Sicily: clinical description and markers of disease severity. *Ital J Pediatr.* (2016) 42:92. doi: 10.1186/s13052-016-0306-z
44. Marchesi A, Tarissi de Jacobis I, Rigante D, Rimini A, Malorni W, Corsello G, et al. Kawasaki disease: guidelines of the Italian Society of Pediatrics, part I - definition, epidemiology, etiopathogenesis, clinical expression and management of the acute phase. *Ital J Pediatr.* (2018) 44:102. doi: 10.1186/s13052-018-0536-3
45. Tombetti E, Manfredi A, Sabbadini MG, Baldissera E. Management options for Takayasu arteritis. *Expert Opin Orphan Drugs.* (2013) 1:685–93. doi: 10.1517/21678707.2013.827570
46. Tombetti E, Mason JC. Takayasu arteritis: advanced understanding is leading to new horizons. *Rheumatology.* (2019) 58:206–19. doi: 10.1093/rheumatology/key040
47. Barut K, Sahin S, Kasapcopur O. Pediatric vasculitis. *Curr Opin Rheumatol.* (2016) 28:29–38. doi: 10.1097/BOR.0000000000000236
48. Melboucy-Belkhir S, Compain C, Sacré K, Bussone G, Chauveheid M-P, Pasi N, et al. Recurrent acute pericarditis in *Takayasu arteritis*. *Int J Cardiol.* (2013) 166:263–5. doi: 10.1016/j.ijcard.2012.09.106
49. Jennette JC, Falk RJ, Bacon PA, Basu N, Cid MC, Ferrario F, et al. 2012 revised international Chapel Hill consensus conference nomenclature of vasculitides. *Arthritis Rheum.* (2013) 65:1–11. doi: 10.1002/art.37715
50. Sarica R, Azizlerli G, Köse A, Dişçi R, Ovül C, Kural Z. Juvenile Behçet's disease among 1784 Turkish Behçet's patients. *Int J Dermatol.* (1996) 35:109–11. doi: 10.1111/j.1365-4362.1996.tb03272.x
51. Demirelli S, Degirmenci H, Inci S, Arisoy A. Cardiac manifestations in Behcet's disease. *Intractable Rare Dis Res.* (2015) 4:70–5. doi: 10.5582/irdr.2015.01007
52. Iudici M, Pagnoux C, Quartier P, Büchler M, Cevallos R, Cohen P, et al. Childhood- versus adult-onset ANCA-associated vasculitides: a nested, matched case–control study from the French Vasculitis Study Group Registry. *Autoimmun Rev.* (2018) 17:108–14. doi: 10.1016/j.autrev.2017.11.014
53. Valeyre D, Prasse A, Nunes H, Uzunhan Y, Brillet P-Y, Müller-Quernheim J. Sarcoidosis. *Lancet.* (2014) 383:1155–67. doi: 10.1016/S0140-6736(13)60680-7
54. Oliveira SB, Monteiro IM. Diagnosis and management of inflammatory bowel disease in children. *BMJ.* (2017) 357:j2083. doi: 10.1136/bmj.j2083
55. Mitchell NE, Harrison N, Junga Z, Singla M. Heart under attack: cardiac manifestations of inflammatory bowel disease. *Inflamm Bowel Dis.* (2018) 24:2322–6. doi: 10.1093/ibd/izy157
56. Bunu D-M, Timofte C-E, Ciocoiu M, Floria M, Tarniceriu C-C, Barboi O-B, et al. Cardiovascular manifestations of inflammatory bowel disease: pathogenesis, diagnosis, and preventive strategies. *Gastroenterol Res Pract.* (2019) 2019:1–14. doi: 10.1155/2019/3012509
57. Sentongo TA, Piccoli DA. Recurrent pericarditis due to mesalamine hypersensitivity: a pediatric case report and review of the literature. *J Pediatr Gastroenterol Nutr.* (1998) 27:344–7. doi: 10.1097/00005176-199809000-00015
58. Nair AG, Cross RR. Mesalamine-induced myopericarditis in a paediatric patient with Crohn's disease. *Cardiol Young.* (2015) 25:783–6. doi: 10.1017/S1047951114001048
59. Brown G. 5-Aminosalicylic acid-associated myocarditis and pericarditis: a narrative review. *Can J Hosp Pharm.* (2016) 69:466–72. doi: 10.4212/cjhp.v69i6.1610
60. Breda L, Nozzi M, Di Marzio D, De Sanctis S, Gattorno M, Chiarelli F. Recurrent pericarditis in hyper-IgD syndrome. *Clin Exp Rheumatol.* (2009) 27:695.
61. Yao Q, Zhou L, Cusumano P, Bose N, Piliang M, Jayakar B, et al. A new category of autoinflammatory disease associated with NOD2 gene mutations. *Arthritis Res Ther.* (2011) 13:R148. doi: 10.1186/ar3462
62. Cavalcante MP V., Brunelli JB, Miranda CC, Novak G V., Malle L, Aikawa NE, et al. CANDLE syndrome: chronic atypical neutrophilic dermatosis with lipodystrophy and elevated temperature—a rare case with a novel mutation. *Eur J Pediatr.* (2016) 175:735–40. doi: 10.1007/s00431-015-2668-4
63. Padeh S, Berkun Y. Familial Mediterranean fever. *Curr Opin Rheumatol.* (2016) 28:523–9. doi: 10.1097/BOR.0000000000000315
64. Ozen S, Demirkaya E, Amaryan G, Koné-Paut I, Polat A, Woo P, et al. Results from a multicentre international registry of familial Mediterranean fever: impact of environment on the expression of a monogenic disease in children. *Ann Rheum Dis.* (2014) 73:662–7. doi: 10.1136/annrheumdis-2012-202708
65. Sarı İ, Birlik M, Kasifoğlu T. Familial Mediterranean fever: an updated review. *Eur J Rheumatol.* (2014) 1:21–33. doi: 10.5152/eurjrheum.2014.006
66. Tutar E, Yalçinkaya F, Ozkaya N, Ekim M, Atalay S. Incidence of pericardial effusion during attacks of familial Mediterranean fever. *Heart.* (2003) 89:1257–8. doi: 10.1136/heart.89.10.1257
67. Dabestani A, Noble LM, Child JS, Krivokapich J, Schwabe AD. Pericardial disease in familial Mediterranean fever: an echocardiographic study. *Chest.* (1982) 81:592–5. doi: 10.1378/chest.81.5.592
68. Kees S, Langevitz P, Zemer D, Padeh S, Pras M, Livneh A. Attacks of pericarditis as a manifestation of familial Mediterranean fever (FMF). *QJM.* (1997) 90:643–7. doi: 10.1093/qjmed/90.10.643
69. Magnotti F, Vitale A, Rigante D, Lucherini OM, Cimaz R, Muscari I, et al. The most recent advances in pathophysiology and management of tumour necrosis factor receptor-associated periodic syndrome (TRAPS): personal experience and literature review. *Clin Exp Rheumatol.* (2013) 31 (3 Suppl. 77):141–9.
70. Cantarini L, Lucherini OM, Cimaz R, Baldari CT, Bellisai F, Rossi Paccani S, et al. Idiopathic recurrent pericarditis refractory to colchicine treatment can reveal tumor necrosis factor receptor-associated periodic syndrome. *Int J Immunopathol Pharmacol.* (2009) 22:1051–8. doi: 10.1177/039463200902200421
71. Peters B, Schuurs-Hoeijmakers JHM, Fuijkschot J, Reimer A, van der Flier M, Lugtenberg D, et al. Protein-losing enteropathy in camptodactyly-arthropathy-coxa vara-pericarditis (CACP) syndrome. *Pediatr Rheumatol Online J.* (2016) 14:32. doi: 10.1186/s12969-016-0093-5
72. Tselios K, Urowitz MB. Cardiovascular and pulmonary manifestations of systemic lupus erythematosus. *Curr Rheumatol Rev.* (2017) 13:206–18. doi: 10.2174/1573397113666170704102444
73. Ryu S, Fu W, Petri MA. Associates and predictors of pleurisy or pericarditis in SLE. Lupus Sci Med. (2017) 4:e000221. doi: 10.1136/lupus-2017-000221
74. Caforio ALP, Brucato A, Doria A, Brambilla G, Angelini A, Ghirardello A, et al. Anti-heart and anti-intercalated disk autoantibodies: evidence for autoimmunity in idiopathic recurrent acute pericarditis. *Heart.* (2010) 96:779–84. doi: 10.1136/hrt.2009.187138
75. Cremer PC, Kumar A, Kontzias A, Tan CD, Rodriguez ER, Imazio M, et al. Complicated pericarditis. *J Am Coll Cardiol.* (2016) 68:2311–28. doi: 10.1016/j.jacc.2016.07.785
76. Vianello F, Cinetto F, Cavraro M, Battisti A, Castelli M, Imbergamo S, et al. Azathioprine in isolated recurrent pericarditis: a single centre experience. *Int J Cardiol.* (2011) 147:477–8. doi: 10.1016/j.ijcard.2011.01.027
77. del Fresno MR, Peralta JE, Granados MA, Enriquez E, Dominguez-Pinilla N, de Inocencio J. Intravenous immunoglobulin therapy for refractory recurrent pericarditis. *Pediatrics.* (2014) 134:e1441–6. doi: 10.1542/peds.2013-3900
78. Moretti M, Buiatti A, Merlo M, Massa L, Fabris E, Pinamonti B, et al. Usefulness of high-dose intravenous human immunoglobulins treatment for refractory recurrent pericarditis. *Am J Cardiol.* (2013) 112:1493–8. doi: 10.1016/j.amjcard.2013.06.036
79. Imazio M, Lazaros G, Picardi E, Vasileiou P, Carraro M, Tousoulis D, et al. Intravenous human immunoglobulins for refractory recurrent pericarditis. *J Cardiovasc Med.* (2016) 17:263–9. doi: 10.2459/JCM.0000000000000260

80. Lazaros G, Karavidas A, Spyropoulou M, Tsiachris D, Halapas A, Zacharoulis A, et al. The role of the immunogenetic background in the development and recurrence of acute idiopathic pericarditis. *Cardiology.* (2011) 118:55–62. doi: 10.1159/000324309
81. de Torre-Minguela C, Mesa del Castillo P, Pelegrín P. The NLRP3 and pyrin inflammasomes: implications in the pathophysiology of autoinflammatory diseases. *Front Immunol.* (2017) 8:43. doi: 10.3389/fimmu.2017.00043
82. Martinon F, Pétrilli V, Mayor A, Tardivel A, Tschopp J. Gout-associated uric acid crystals activate the NALP3 inflammasome. *Nature.* (2006) 440:237–41. doi: 10.1038/nature04516
83. Muruve DA, Pétrilli V, Zaiss AK, White LR, Clark SA, Ross PJ, et al. The inflammasome recognizes cytosolic microbial and host DNA and triggers an innate immune response. *Nature.* (2008) 452:103–7. doi: 10.1038/nature06664
84. Duewell P, Kono H, Rayner KJ, Sirois CM, Vladimer G, Bauernfeind FG, et al. NLRP3 inflammasomes are required for atherogenesis and activated by cholesterol crystals. *Nature.* (2010) 464:1357–61. doi: 10.1038/nature08938
85. Cantarini L, Lucherini OM, Baldari CT, Laghi Pasini F, Galeazzi M. Familial clustering of recurrent pericarditis may disclose tumour necrosis factor receptor-associated periodic syndrome. *Clin Exp Rheumatol.* (2010) 28:405–7.
86. Cantarini L, Vitale A, Lucherini OM, De Clemente C, Caso F, Costa L, et al. The labyrinth of autoinflammatory disorders: a snapshot on the activity of a third-level center in Italy. *Clin Rheumatol.* (2015) 34:17–28. doi: 10.1007/s10067-014-2721-0
87. Brucato A, Imazio M, Cremer PC, Adler Y, Maisch B, Lazaros G, et al. Recurrent pericarditis: still idiopathic? The pros and cons of a well-honoured term. *Intern Emerg Med.* (2018) 13:839–44. doi: 10.1007/s11739-018-1907-x
88. Cabalka AK, Rosenblatt HM, Towbin JA, Price JK, Windsor NT, Martin AB, et al. Postpericardiotomy syndrome in pediatric heart transplant recipients. Immunologic characteristics. *Texas Hear Inst J.* (1995) 22:170–6.
89. Imazio M, Cecchi E, Demichelis B, Ierna S, Demarie D, Ghisio A, et al. Indicators of poor prognosis of acute pericarditis. Circulation. (2007) 115:2739–44. doi: 10.1161/CIRCULATIONAHA.106.662114
90. Imazio M, Brucato A, Adler Y, Brambilla G, Artom G, Cecchi E, et al. Prognosis of idiopathic recurrent pericarditis as determined from previously published reports. *Am J Cardiol.* (2007) 100:1026–8. doi: 10.1016/j.amjcard.2007.04.047
91. Alraies MC, Al Jaroudi W, Shabrang C, Yarmohammadi H, Klein AL, Tamarappoo BK. Clinical features associated with adverse events in patients with post-pericardiotomy syndrome following cardiac surgery. *Am J Cardiol.* (2014) 114:1426–30. doi: 10.1016/j.amjcard.2014.07.078
92. van Osch D, Dieleman JM, Bunge JJ, van Dijk D, Doevendans PA, Suyker WJ, et al. Risk factors and prognosis of postpericardiotomy syndrome in patients undergoing valve surgery. *J Thorac Cardiovasc Surg.* (2017) 153:878–85.e1. doi: 10.1016/j.jtcvs.2016.10.075
93. Imazio M, Brucato A, Maestroni S, Cumetti D, Belli R, Trinchero R, et al. Risk of constrictive pericarditis after acute pericarditis. *Circulation.* (2011) 124:1270–5. doi: 10.1161/CIRCULATIONAHA.111.018580
94. Brucato A, Brambilla G, Moreo A, Alberti A, Munforti C, Ghirardello A, et al. Long-term outcomes in difficult-to-treat patients with recurrent pericarditis. *Am J Cardiol.* (2006) 98:267–71. doi: 10.1016/j.amjcard.2006.01.086
95. Haley JH, Tajik AJ, Danielson GK, Schaff H V, Mulvagh SL, Oh JK. Transient constrictive pericarditis: causes and natural history. *J Am Coll Cardiol.* (2004) 43:271–5. doi: 10.1016/j.jacc.2003.08.032
96. Feng D, Glockner J, Kim K, Martinez M, Syed IS, Araoz P, et al. Cardiac magnetic resonance imaging pericardial late gadolinium enhancement and elevated inflammatory markers can predict the reversibility of constrictive pericarditis after antiinflammatory medical therapy. *Circulation.* (2011) 124:1830–7. doi: 10.1161/CIRCULATIONAHA.111.026070
97. Perez-Brandão C, Trigo C, Pinto FF. Pericarditis – clinical presentation and characteristics of a pediatric population. *Rev Port Cardiol.* (2019) 38:97–101. doi: 10.1016/j.repce.2018.05.014
98. Imazio M, Brucato A, Barbieri A, Ferroni F, Maestroni S, Ligabue G, et al. Good prognosis for pericarditis with and without myocardial involvement: results from a multicenter, prospective cohort study. *Circulation.* (2013) 128:42–9. doi: 10.1161/CIRCULATIONAHA.113.001531
99. Etesami M, Gilkeson RC, Rajiah P. Utility of late gadolinium enhancement in pediatric cardiac MRI. *Pediatr Radiol.* (2016) 46:1096–113. doi: 10.1007/s00247-015-3526-2
100. Tombetti E, Mason JC. Application of imaging techniques for *Takayasu arteritis*. *Presse Med.* (2017) 46:e215–23. doi: 10.1016/j.lpm.2017.03.022
101. Alraies MC, AlJaroudi W, Yarmohammadi H, Yingchoncharoen T, Schuster A, Senapati A, et al. Usefulness of cardiac magnetic resonance–guided management in patients with recurrent pericarditis. *Am J Cardiol.* (2015) 115:542–7. doi: 10.1016/j.amjcard.2014.11.041
102. Maggiolini S, De Carlini CC, Ferri LA, Colombo GI, Gentile G, Meles E, et al. The role of early contrast-enhanced chest computed tomography in the aetiological diagnosis of patients presenting with cardiac tamponade or large pericardial effusion. *Eur Heart J Cardiovasc Imaging.* (2016) 17:421–8. doi: 10.1093/ehjci/jev225
103. Zemer D, Pras M, Sohar E, Modan M, Cabili S, Gafni J. Colchicine in the prevention and treatment of the amyloidosis of familial mediterranean fever. *N Engl J Med.* (1986) 314:1001–5. doi: 10.1056/NEJM198604173141601
104. Schenone AL, Menon V. Colchicine in pericardial disease: from the underlying biology and clinical benefits to the drug-drug interactions in cardiovascular medicine. *Curr Cardiol Rep.* (2018) 20:62. doi: 10.1007/s11886-018-1008-5
105. Verma S, Eikelboom JW, Nidorf SM, Al-Omran M, Gupta N, Teoh H, et al. Colchicine in cardiac disease: a systematic review and meta-analysis of randomized controlled trials. *BMC Cardiovasc Disord.* (2015) 15:96. doi: 10.1186/s12872-015-0068-3
106. Alabed S, Pérez-Gaxiola G, Burls A. Colchicine for children with pericarditis: systematic review of clinical studies. *Arch Dis Child.* (2016) 101:953–6. doi: 10.1136/archdischild-2015-310287
107. Brucato A, Pluymaekers N, Tombetti E, Rampello S, Maestroni S, Lucianetti M, et al. Management of idiopathic recurrent pericarditis during pregnancy. *Int J Cardiol.* (2019) 282:60–5. doi: 10.1016/j.ijcard.2019.02.003
108. Tarantino G, Delogu AB, De Rosa G, Rigante D. A possible still role for colchicine in children with idiopathic recurrent acute pericarditis? *Intern Emerg Med.* (2019) 14:331–2. doi: 10.1007/s11739-018-1997-5
109. Imazio M, Brucato A, Cumetti D, Brambilla G, Demichelis B, Ferro S, et al. Corticosteroids for recurrent pericarditis. *Circulation.* (2008) 118:667–71. doi: 10.1161/CIRCULATIONAHA.107.761064
110. Artom G, Koren-Morag N, Spodick DH, Brucato A, Guindo J, Bayes-de-Luna A, et al. Pretreatment with corticosteroids attenuates the efficacy of colchicine in preventing recurrent pericarditis: a multi-centre all-case analysis. *Eur Heart J.* (2005) 26:723–7. doi: 10.1093/eurheartj/ehi197
111. Brucato A, Emmi G, Cantarini L, Di Lenarda A, Gattorno M, Lopalco G, et al. Management of idiopathic recurrent pericarditis in adults and in children: a role for IL-1 receptor antagonism. *Intern Emerg Med.* (2018) 13:475–89. doi: 10.1007/s11739-018-1842-x
112. Brucato A, Imazio M, Gattorno M, Lazaros G, Maestroni S, Carraro M, et al. Effect of anakinra on recurrent pericarditis among patients with colchicine resistance and corticosteroid dependence. *JAMA.* (2016) 316:1906. doi: 10.1001/jama.2016.15826
113. Gaspari S, Marsili M, Imazio M, Brucato A, Di Blasi Lo Cuccio C, Chiarelli F, et al. New insights in the pathogenesis and therapy of idiopathic recurrent pericarditis in children. *Clin Exp Rheumatol.* (2013) 31:788–94.
114. Finetti M, Insalaco A, Cantarini L, Meini A, Breda L, Alessio M, et al. Long-term efficacy of interleukin-1 receptor antagonist (anakinra) in corticosteroid-dependent and colchicine-resistant recurrent pericarditis. *J Pediatr.* (2014) 164:1425-1431.e1. doi: 10.1016/j.jpeds.2014.01.065
115. Sag E, Bilginer Y, Ozen S. Autoinflammatory diseases with periodic fevers. *Curr Rheumatol Rep.* (2017) 19:41. doi: 10.1007/s11926-017-0670-8
116. ter Haar NM, Oswald M, Jeyaratnam J, Anton J, Barron KS, Brogan PA, et al. Recommendations for the management of autoinflammatory diseases. *Ann Rheum Dis.* (2015) 74:1636–44. doi: 10.1136/annrheumdis-2015-207546

117. Groot N, De Graeff N, Avcin T, Bader-Meunier B, Brogan P, Dolezalova P, et al. European evidence-based recommendations for diagnosis and treatment of childhood-onset systemic lupus erythematosus: the SHARE initiative. *Ann Rheum Dis.* (2017) 76:1788–96. doi: 10.1136/annrheumdis-2016-210960
118. Fanouriakis A, Kostopoulou M, Alunno A, Aringer M, Bajema I, Boletis JN, et al. 2019 update of the EULAR recommendations for the management of systemic lupus erythematosus. *Ann Rheum Dis.* (2019) 78:736–45. doi: 10.1136/annrheumdis-2019-215089
119. Khandaker MH, Schaff H V, Greason KL, Anavekar NS, Espinosa RE, Hayes SN, et al. Pericardiectomy vs medical management in patients with relapsing pericarditis. *Mayo Clin Proc.* (2012) 87:1062–70. doi: 10.1016/j.mayocp.2012.05.024
120. CDC. *Birth-18 Years Immunization Schedule*. (2018). Available online at: https://www.cdc.gov/vaccines/schedules/hcp/imz/child-adolescent.html (accessed October 8, 2019).

Conflict of Interest: AB declares unrestricted research grants by ACARPIA e SOBI.

The remaining authors declare that the research was conducted in the absence of any commercial or financial relationships that could be construed as a potential conflict of interest.

The reviewer GL declared a past collaboration with one of the authors AB to the handling editor.

frontiers in Pediatrics

SYSTEMATIC REVIEW
published: 07 November 2019
doi: 10.3389/fped.2019.00460

Efficacy of β-Blockers on Postural Tachycardia Syndrome in Children and Adolescents: A Systematic Review and Meta-Analysis

Xinwei Deng [1,2,3†], Yuyang Zhang [1,2†], Ying Liao [1] and Junbao Du [1,3*]*

[1] Department of Pediatrics, Peking University First Hospital, Beijing, China, [2] Peking University Health Sciences Centre, Beijing, China, [3] Research Unit of Clinical Diagnosis and Treatment of Pediatric Syncope and Cardiovascular Diseases, Chinese Academy of Medical Sciences, Beijing, China

Background: Postural tachycardia syndrome (POTS) is a severe health problem in children. Short-term β-blockers are recommended for pharmaceutical treatment. However, there have been contradictory data about its efficacy among pediatric patients.

Methods and Results: Eight studies comparing β-blockers to conventional treatments for children with POTS were selected, where 497 cases of pediatric POTS were included. The efficacy of β-blockers was evaluated using the effective rate, the change of symptom score, the change of heart rate difference and adverse events. The results were stated as relative ratio (RR) and mean difference (MD) with a 95% confidence interval (95% CI). A random-effects meta-analysis for the effective rate indicated that β-blockers were more effective in treating pediatric POTS than controlled treatment (79.5 vs. 57.3%, RR = 1.50, 95%CI: 1.15–1.96, $P < 0.05$). A fixed-effects model analysis showed that β-blockers were more effective in lowering the symptom score and the heart rate increment during standing test than controlled treatment with a mean difference of 0.81 (95% CI: 0.44–1.18, $P < 0.05$) and 3.78 (95% CI: 2.10–5.46, $P < 0.05$), respectively. There were no reported severe adverse events in included studies.

Conclusion: β-blockers are effective in treating POTS in children and adolescents, alleviating orthostatic intolerance, and improving hemodynamic abnormalities.

Keywords: efficacy, β-blockers, metoprolol, children, POTS

OPEN ACCESS

Edited by:
Fu Lijun,
Shanghai Children's Medical Center, China

Reviewed by:
Cheng Wang,
Central South University, China
Fangqi Gong,
ZheJiang University, China
Cuifen Zhao,
Qilu Hospital, Shandong University, China

***Correspondence:**
Ying Liao
liaoyingwww@163.com
Junbao Du
junbaodu1@126.com

†These authors have contributed equally to this work

Specialty section:
This article was submitted to Pediatric Cardiology, a section of the journal Frontiers in Pediatrics

Received: *02 August 2019*
Accepted: *22 October 2019*
Published: *07 November 2019*

Citation:
Deng X, Zhang Y, Liao Y and Du J (2019) Efficacy of β-Blockers on Postural Tachycardia Syndrome in Children and Adolescents: A Systematic Review and Meta-Analysis. Front. Pediatr. 7:460. doi: 10.3389/fped.2019.00460

INTRODUCTION

Postural tachycardia syndrome (POTS) is common in children, featuring an abnormal increment in heart rate of over 40 beats per minute (bpm) within the first 10 min of head-up tilt (HUT) or standing test accompanied by symptoms of orthostatic intolerance such as dizziness, headache, palpitation, chest discomfort, blurred vision, tremor, and profuse perspiration (1). The prevalence of POTS in Chinese children is ∼6.8%, with a peak age of onset around 15–25 years old (2). Children are more easily affected than adults, with recurrent syncope attacks most often resulting in physical and psychological damage.

Currently used drugs for POTS include β-adrenoreceptor blockers, α-adrenoreceptor agonists, pyridostigmine and fludrocortisone, each of which has a distinct while overlapping mechanism underlying its observed clinical efficacy (3). Decreased intravascular volume, elevated plasma norepinephrine levels, attenuated sympathetic vasoconstrictor responsiveness, and peripheral

autonomic neuropathy are important factors contributing to tachycardia in POTS patients (4–6). Through reducing cardiac baroreceptor activation, lowering blood norepinephrine level, and inhibiting sympathetic nerve activity, it is likely reasonable that β-blockers might be a promising therapeutic option for the treatment of POTS (7).

Although several randomized controlled trials of relatively high quality may have provided physicians with reasons to consider treating adult POTS patients with β-blockers, it is not the case with children (8, 9). Inconsistent results have been published in recent years, most of which are non-randomized, or of small sample size. A randomized controlled trial (RCT) of Lin et al. (10) in the treatment of 54 children with POTS using metoprolol showed that the treatment group was significantly more effective than the control group (72.2 vs. 48.0%), while Chen et al. (11) found that the efficacy of a same drug was unproved, also in an RCT that involved 19 POTS children. Therefore, the present study was undertaken to carry out a systematic review and meta-analysis to present updated evidence for clinical reference and hopefully to provide guidance for further research in this field.

METHODS

Criteria for Considering Studies

Types of Studies

The studies included the analysis of the RCTs and non-randomized controlled trials (Non-RCTs). We only included prospected studies on the treatment of POTS in children and adolescents, comparing β-blockers to conventional therapies.

Types of Participants

We included pediatric patients aged below 20 years old, who were diagnosed as POTS by HUT or standing test. We excluded patients with any systematic diseases, metabolic disturbances, or cardiogenic diseases.

Types of Interventions

Studies that compared treatment of oral administration of β-blockers using standard pediatric doses and duration with conventional therapies were included. Conventional therapies for control group referred to non-pharmacological measures such as oral rehydration salts (ORS) and patient education. We allowed additional interventions in trials such as α-adrenergic receptor agonist if there was a comparison with β-blockers. We excluded trials with short duration of therapeutic course <1 month.

Types of Outcome Measures

Our primary outcome was the effective rate, a dichotomous variable defined as the ratio of participants whose symptoms were relieved after the treatment. This outcome was equal to the cure rate plus the improvement rate. Our secondary outcomes included: (1) the change of symptom score (Δ heart rate difference): defined as the reduction in symptom score according to Winker symptom scale (WSS) and expressed as mean ± standard deviation; (2) the change of heart rate difference (Δ heart rate difference): the heart rate difference is defined as the increment of heart rate during HUT, while Δ heart rate difference stands for the heart rate difference after the treatment minus the baseline heart rate difference. The results were expressed as mean ± standard deviation; (3) adverse events: defined as drug-related adverse effects. Our study documented the adverse effects reported in each trial explicitly.

Search Strategy

We searched the following databases till 24 June 2019 without any restriction on the published years: Cochrane Library, EMBASE, Pubmed, and Sinomed. The databases were searched by two professional co-workers using search terms (in English or Chinese) such as "postural tachycardia syndrome/ postural orthostatic tachycardia syndrome/POTS" AND "treatment/therapy/intervention/management/β-blocker/metoprolol/propranol/betaloc/atenolol." Original articles were obtained through downloads from electronic databases or copies from libraries. References of relevant articles were also searched by the two authors independently.

Data Collection and Analysis

Data Extraction and Management

Two reviewers (DXW and ZYY) independently conducted the search according to the pre-designed inclusion and exclusion criteria. Necessary data and information from included studies were extracted by one reviewer and checked by the other. Discrepancies were jointly resolved by the two members.

Data Analysis

We used Review Manager 5.3 for the analysis of the extracted data. Along with 95% confidence interval (95%CI), the dichotomous outcomes were analyzed by relative ratio (RR)

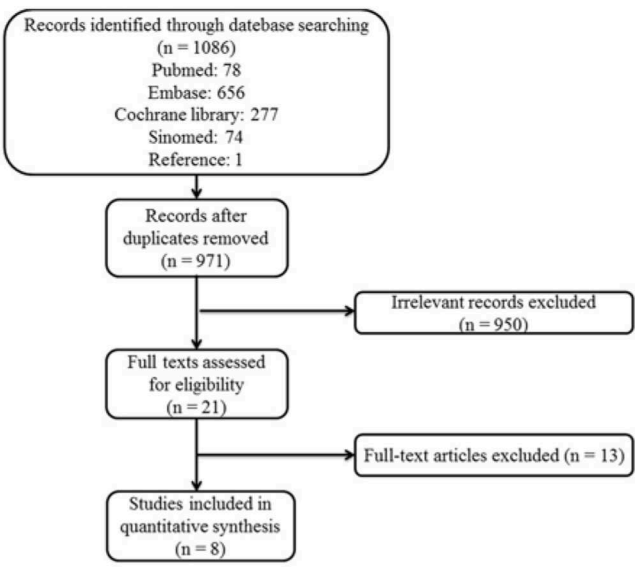

FIGURE 1 | Study selection flow chart: Flow chart of the literature selection process for studies enrolled in this systematic review and meta-analysis. POTS, postural tachycardia syndrome.

TABLE 1 | Characteristics of included studies.

Reference	Trial design	Participants (n)			Age (y), Mean ± SD	Treatment		Outcoms	Symptom tool	Efficacy
		Total	β-blockers	Control		β-blockers	Control			
Chen et al. (12)	RCT	54	32	22	12.0 ± 2.6	Metoprolol 0.5 mg/(kg·d) bid; 3-6 months	ORS	-Effective rate	Improvement: Syncope decreased ≥50%	84.4 vs 40.9%
Chen et al. (11)	RCT	53	19	15	12.2 ± 2.4	Metoprolol 0.5 mg/(kg·d) bid; 3-6 months	Conventional therapy	-Symptom score -Blood pressure -ΔHR -Effective rate	Improvement: Symptom score decreased ≥50%	57.9 vs 53.3%
Lin et al. (10)	Non-RCT	192	54	54	11.4 ± 2.5	Metoprolol 12.5 mg/d bid; 3 months	ORS 500 ml	-Symptom score -Blood pressure -ΔHR -Effective rate	Improvement: Symptom score decreased ≥50%	72.2 vs 48.0%
Liu et al. (13)	RCT	21	14	7	9.24 ± 3.76	Metoprolol 1.0 mg/(kg·d) bid; 3 months	Oryzanol 10 mg/d tid	-Symptom score -Blood pressure -ΔHR -Effective rate	Improvement: Symptom score decreased by 2 points	85.7 vs 28.6%
Sun et al. (14)	RCT	92	34	26	13.2 ± 2.2	Metoprolol 1.0 mg/(kg·d) bid; 2 months	NS 250 ml bid	-Symptom score -Blood pressure -ΔHR -Effective rate	Improvement: Symptom score decreased ≥50%	94.1 vs 38.5%
Yang et al. (15)	Non-RCT	244	66	75	11.6 ± 2.5	Metoprolol 1.0 mg/(kg·d) bid; 3 months	ORS 500 ml	-Symptom score -Blood pressure -ΔHR -Effective rate	Improvement: Symptom score decreased by 2 points	80.3 vs 72.0%
Zhang et al. (16)	Non-RCT	30	20	10	13 ± 2	Metoprolol 1.0 mg/(kg·d) bid; 3 months	NS 250 ml bid	-Symptom score -Blood pressure -ΔHR -Effective rate	Improvement: Symptom score decreased by 2 points	80.0 vs 40.0%
Zhang et al. (17)	Non-RCT	118	10	39	11.4 ± 2.6	Metoprolol 1.0 mg/(kg·d) bid; 3 months	ORS 500 ml	-Symptom score -Blood pressure -ΔHR -Effective rate	Improvement: Symptom score decreased by 2 points	80.0 vs 74.4%

RCT, randomized controlled trial; Non-RCT, non-randomized controlled trial; SD, standard deviation; ORS, oral rehydration salts; NS, normal saline; HR, heart rate; bid, twice a day.

and the continuous outcomes by mean difference (MD). We evaluated heterogeneity by Chi-square test and I^2 statistic calculation. We formulated our cut-off level at 50% for I^2. When $I^2 > 50\%$ or $P < 0.05$, indicating high heterogeneity among studies, the random-effects model was employed for meta-analysis. Otherwise, we chose the fixed-effects model since low heterogeneity was confirmed (18). We calculated the standard deviation for continuous outcomes as suggested by Cochrane (18). Study results were displayed through forest plots. Additionally, $P < 0.05$ indicated that the difference was statistically significant.

Assessment of Risk of Bias in Included Studies

Using a 12-category assessment of risk of bias, the quality of each eligible study was rated by two reviewers (DXW and ZYY) independently and defined as high, low, or unclear risk of bias. The criteria were recommended by Cochrane Back Review Group (19). Studies with an overall low risk of bias in six or more dimensions were classified as high-quality studies. Publication bias was estimated by funnel plot. Disagreements were resolved following discussion among the reviewers.

RESULTS

Description of Studies

A total of 1,086 original articles were identified initially from Cochrane, EMBASE, Pubmed and Sinomed databases. After removing duplicated studies, screening titles and abstracts as well as reviewing the full texts, 1078 articles were excluded and eight articles were accepted in our final analysis including four

RCTs and four Non-RCTs. The flow chart of study selection is summarized in **Figure 1**.

The general characteristics of included studies are presented in **Table 1**. Of these eight trials, seven (10, 12–17) were reported in Chinese and one (11) in English. All of the studies focused on children and adolescents at an average age of 9.2–13.2 years. The β-blockers used in the selected studies were metoprolol, although in various dosages—0.5 mg/(kg·d) in two publications (11, 12), 12.5 mg/d in one (10) and 1.0 mg/(kg·d) for the others. The studies included shared similar intervention duration between 3 and 6 months. In terms of efficacy evaluation, seven studies referred to the WSS (20). Treatments that resulted in a reduction of 2-points or above in symptom score [four studies (13, 15–17)] or decrease in symptom score by 50 percent or above [three studies (10, 11, 14)] were defined, respectively, as effective. Only in one study (12) the treatment efficacy was evaluated by measuring the reduction of syncope frequency.

Risk of Bias in Included Studies

We evaluated risk of bias in all enrolled studies using the criteria suggested by Cochrane Back Review Group. Because of unreported details, the risks of bias of most studies were defined as unclear. There is high risk of selection bias in four studies (10, 15–17) on account of non-randomized sequence generation. Four studies (10, 12, 14, 15) were decided as high risks of attrition bias due to incomplete outcomes. Five studies (12–15, 17) that failed to present all the pre-determined primary and secondary outcomes were considered as high risks of reporting bias. The study by Chen et al. (11) was the only study with low risk of bias in six categories of our bias assessment system, and therefore determined as overall high-quality. Our risk of bias estimation is summarized in **Figures 2**, **3**.

Allocation

Of the four studies (11–14) reporting a random sequence generation, only Chen et al. (11) described the randomization process in detail. The other four studies (10, 15–17) that failed to mention allocation concealment were considered as high risk of bias under allocation category.

Blinding

None of the included studies stated a blinding process of participants, personnel, or outcome assessors.

Incomplete Outcome Data

There was no missing outcome data in two studies (11, 16). Four studies (10, 12, 14, 15) suggested a high risk of drop outs in outcome data and a lack of information for the intention to treat analysis. The risk of bias of the rest two studies (13, 17) was unclear due to no explicit statements in some of the outcomes regarding the number of participants.

Selective Reporting

Five studies (1, 12–15) that failed to report secondary outcomes such as the symptom score or the change of the heart rate were defined as high risks of selective reporting bias. The risk of bias assessment of the other three studies was classified as unclear due to unavailable study protocols.

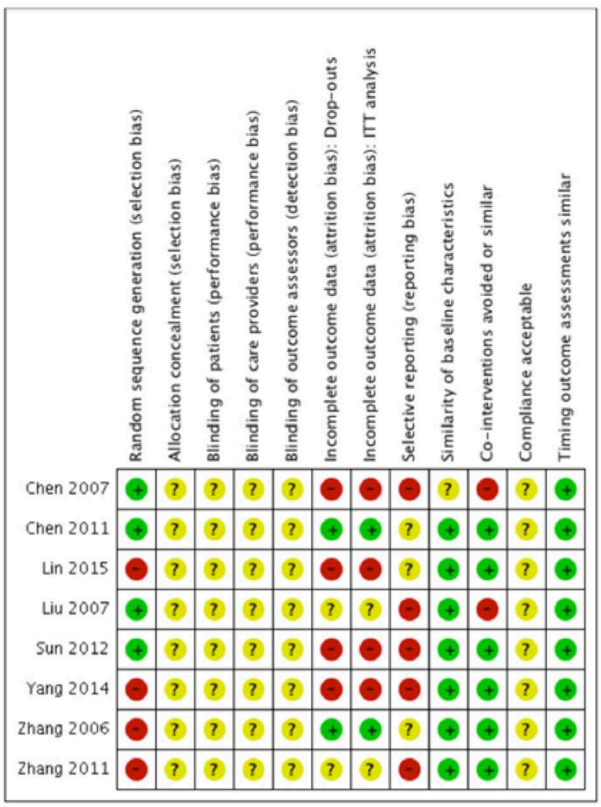

FIGURE 2 | Risk of bias summary: Review author's judgments about each risk of bias item for each included study. "+" indicates certain criterion has been met and therefore suggests a low risk of bias; "–" indicates certain criterion has not been met and therefore suggests a high risk of bias; "?" indicates unclear risk of bias for lack of relative information.

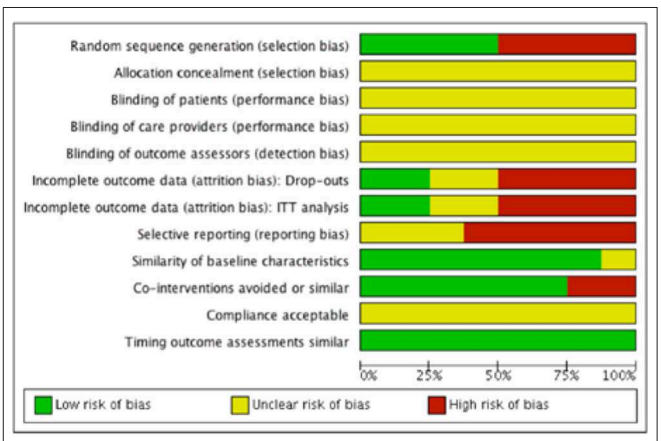

FIGURE 3 | Risk of bias graph: Review author's judgments about each risk of bias item presented as percentages across all included studies.

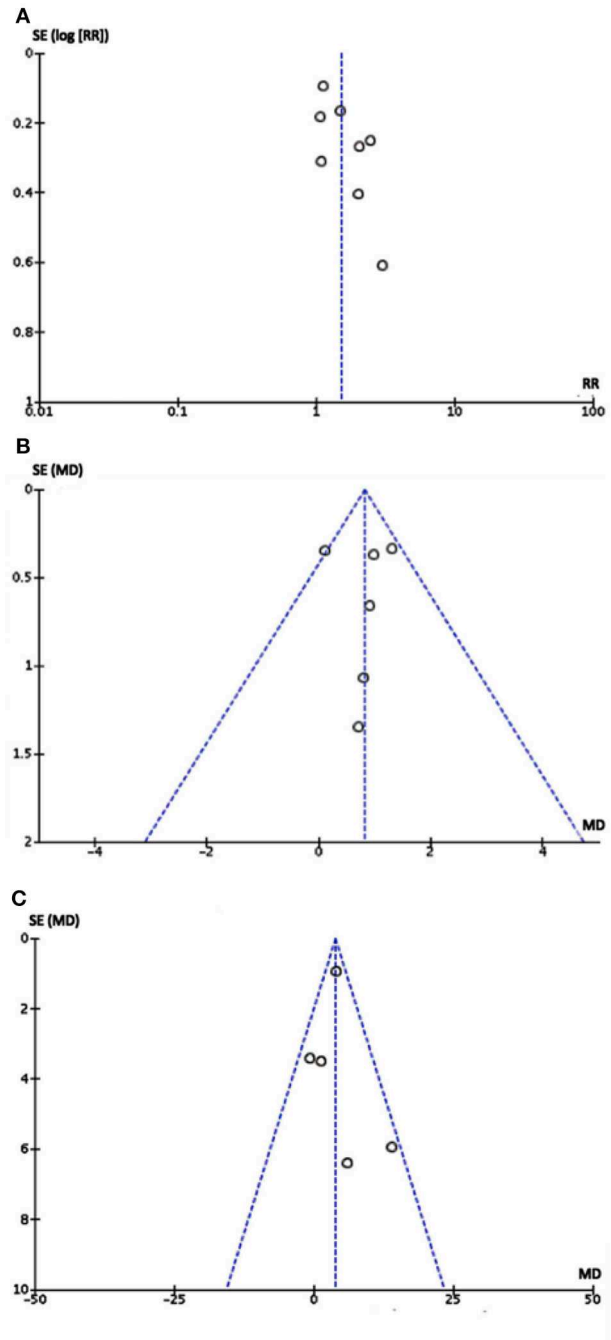

FIGURE 4 | Funnel plot of eight studies: Each dot stood for one study. The distance between each dot and the upright line indicated the bias in each study. **(A)** Funnel plot of comparison between metoprolol with controls in therapeutic effect. **(B)** Funnel plot of comparison between metoprolol with controls in Δ symptom score. **(C)** Funnel plot of comparison between metoprolol with controls in Δ heart rate difference. As the funnel plots of three outcomes were visually symmetric implying that publication bias may not exist.

Publication Bias

No publication bias was detected from the funnel plot (**Figure 4**) of primary and secondary outcomes visually, implying that the publication bias might not exist among the included studies.

Other Potential Sources of Bias

Baseline characteristics are similar between groups on demographic factors and important hemodynamic data in all studies except for the study by Chen et al. (12) which did not report this. As for "Co-intervention," metoprolol was compared to conventional therapies including ORS (10, 12, 15, 17), oral normal saline (11, 14, 16) and oryzanol (13). In one study (12), metoprolol was used alone in the experimental group without parallel treatment as its control. Timing of outcome assessments was similar in all studies. Performance bias could not be assessed for that no descriptions of patient compliance could be found in any of the included studies.

Outcomes

Primary Outcomes

In respect of effective rate, data were available for all the studies. A random-effects model was conducted for meta-analysis. The Chi² value for heterogeneity test of the risk ratio (RR) was 19.82 ($P = 0.006$) and I^2 statistic 65%, which suggests statistical heterogeneity across studies. The studies enrolled reported 497 cases of pediatric POTS with 340 children improved after treatment, including 198 of the metoprolol group and 142 of the control group. The effective rate at the end of short-term follow-up in the metoprolol group was significantly higher than that of the control group (79.5 vs. 57.3%, RR = 1.50, 95% CI: 1.15–1.96, $P = 0.002$; **Figure 5**).

Secondary Outcomes

Δ *Heart Rate Difference*

There were five articles (10, 11, 15–17) describing heart rate difference during standing test. We calculated the decrement in heart rate different (Δ heart rate difference) in each trial with fixed-effects model to analyze the results. Heterogeneity analysis of the subgroup showed a low level of heterogeneity (Chi² = 5.39, $P = 0.25$, $I^2 = 26\%$). After the treatment, there was a reduction in the heart rate difference during standing test in both groups, but the heart rate change of the metoprolol group was significantly greater than the control group (MD = 3.78, 95% CI: 2.10–5.46, $P < 0.0001$; **Figure 6A**).

Δ *Symptom Score*

There were six articles (10, 11, 14–17) describing the symptom score outcome before and after treatment. We calculated the decrement in symptom score (Δ symptom score) in each trial and analyzed the results using a fixed-effects model. Heterogeneity analysis of the subgroup showed a low level of heterogeneity (Chi²=6.64, $P = 0.25$, $I^2 = 25\%$). The symptom score after treatment in both groups was lower than that before treatment, but the reduction of the symptom score was significantly greater in the metoprolol group than that of the control group (MD = 0.81, 95% CI: 0.44–1.18, $P < 0.0001$; **Figure 6B**).

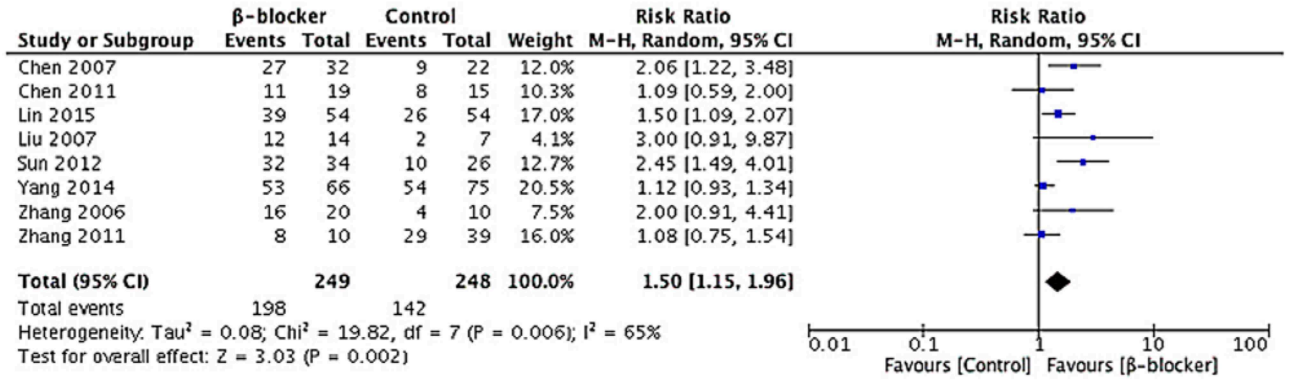

FIGURE 5 | Forest plot of eight studies in efficacy rate for metoprolol vs. comparator: Heterogeneity analysis showed statistical heterogeneity among the studies ($p < 0.05$). A random-effects model was conducted. The analysis of total effects presented in the bottom. Risk ratio of efficacy rate analyzed by Mantel-Haensze test was summarized on the right. Each little square represented the RR value of each study along with a transverse line representing 95% CI. The rhombus below stood for the overall result of meta-analysis.

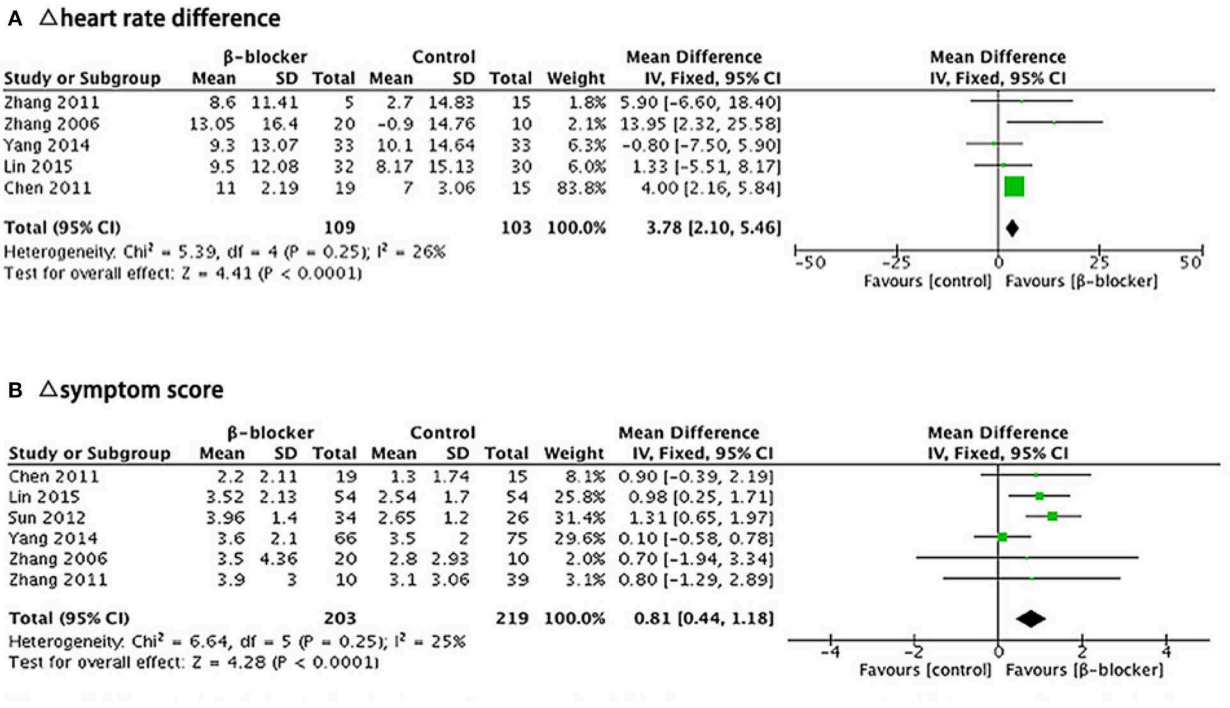

FIGURE 6 | Forest plot for sub-group analysis: **(A)** Five studies, comparing Δ heart rate difference between β-blockers and comparator. **(B)** Six studies, comparing Δ symptom score for two groups. The analysis of total effects were presented in the bottom. Mean difference analyzed by inverse variance method was summarized on the right. Each little square represented the mean difference of each study along with a transverse line representing 95% CI. The rhombus below stood for the overall result of meta-analysis.

Adverse Events

There was one article (14) missing the description of adverse events. Others had a record of that. Three studies (11, 13, 16) did not appear to report any side effects during the drug treatment. Chen et al. (12) showed that bradycardia occurred in three children without subjective symptoms. Lin et al. (10) reported that one child presented with fatigue and chest tightness. Yang et al. (15) discovered that three children complained of abdominal pain and one patient presented with decreased blood pressure. Zhang et al. (17) discovered that two children had stomach discomfort. None of the aforementioned adverse events were severe and all of the children went through full course of treatment.

DISCUSSION

In this systematic review and meta-analysis, we included eight studies that assessed β-blockers efficacy in treating POTS children and adolescents. All the eight trials collecting data on the effective rate of β-blockers showed that the efficacy of β-blockers were significantly higher than those of their comparable control treatments (79.5 vs. 57.3%, RR = 1.50, 95% CI: 1.15–1.96, $P = 0.002$), mainly with ORS or normal saline. In addition to this, β-blockers might also be more effective than controlled treatments in lowering the heart rate increment during standing test (MD = 3.78, 95% CI: 2.10–5.46, $P < 0.0001$). Finally, the decrement in symptom score is significantly greater than controlled treatments in the β-blocker group (MD = 0.81, 95% CI: 0.44–1.18, $P < 0.0001$). There was no reporting of severe adverse events that led to treatment discontinuation. However, the influence of the relatively small sample sizes and short follow-up period in most enrolled studies should not be neglected. All in all, we concluded that β-blockers are effective in treating POTS in children and adolescents, alleviating orthostatic intolerance, and improving hemodynamic abnormalities.

Postural tachycardia is the main hemodynamic feature of POTS children. When moving from a supine to a standing position, a healthy man would have blood pooling in the lower limbs due to the law of gravity, which is not perceivable thanks to the delicate regulatory mechanism culminating in a crucial increment of heart rate of 10–15 bpm. Unfortunately, owing to complex factors such as hypovolemia, autonomic dysfunction and neurohumoral dysregulation, POTS children often have a hard time making this normal adjustment through cardiac output compensation, resulting in a marked rise in heart rate, symptoms of orthostatic intolerance, and even cerebral hypoperfusion (21, 22).

Based on current understanding of potential etiology, several non-pharmacological treatments have been introduced into POTS treatment, such as reducing venous pooling by wearing lower-body compression garments or practicing resistance training for the thighs (23). Apart from that, studies have shown that 70% of POTS children have decreased intravascular volume, whose symptoms of orthostatic intolerance could be attenuated by increasing consumption of water and salt (24). In our review, we also found that ORS treatment was proved effective in most control groups. There is, still, a noticeable amount of POTS children who are not responding to the classic non-pharmacological ORS treatment (16), indicating the existence of other hemodynamic factors contributing to the clinical presentation of tachycardia.

The role of hyper-adrenergic state in the development of POTS has gained more and more attention in recent years. Zhang et al. (25) discovered that norepinephrine in some POTS patients increased significantly, the level of which was positively correlated with the severity of clinical presentation. Earlier studies reported that mutation of norepinephrine transporter (NET) might be one of the reasons for the elevated norepinephrine level (26). Other than that, the clearance mechanism of norepinephrine in POTS patients is damaged and their sympathetic activation is prominent (27, 28).

β-blockers were introduced into clinical practice based on the reasons listed above, the efficacy of which has been recognized to a certain extent, mainly through clinical observations and application experience. Under this context, we performed an updated review of the available evidence. Among the 249 POTS children treated with metoprolol, 198 cases reported symptom improvement. The pooled efficacy of metoprolol is 79.5%, which is significantly greater than the control group (57.3%), indicating that β-blocker is an effective way to treat POTS in children. The efficacy of β-blockers implies symptoms improvement as well as tachycardia alleviation.

There are two possible reasons supporting the efficacy of β-blockers. On one side, they could block cardiac β1 receptors, thus serving a negative inotropic effect. On the other side, they are capable of inhibiting renin secretion through the inhibition of β1 receptors of juxtaglomerular cells, resulting in a lowered norepinephrine level. Then, autonomic activity was reduced, followed by a decreased heart rate and improved orthostatic tolerance (29).

Although the theoretical basis for the efficacy of β-blockers seems rather solid, there are inconsistent results among the studies. The reasons might be multi-faceted. First of all, POTS is a heterogeneous disorder with complicated nosogenesis. Some researchers made the distinction between partial dysautonomic POTS and hyperadrenergic POTS, while others preferred the division of three subtypes (7, 30–32). Different pathogenesis among POTS subtypes indicates that individual patient may have different response to the same treatment. It has been reported that the plasma level of norepinephrine might serve as an efficacy predictor of metoprolol therapy for POTS in children and adolescents (25). None of the included studies described the baseline plasma norepinephrine level of POTS children, which might partly account for the individual difference in response to β-blockers. Secondly, the discrepancy between POTS diagnostic standards and the diversity of efficacy evaluation methods may contribute to the inconsistent results. Except for the study by Lin et al. (10) in which the latest diagnostic criteria of POTS (6) (an increment of heart rate of over 40 bpm within the first 10 min of HUT) were adopted, other seven studies uniformly determined a value of over 30 bpm heart rate elevation as standard, which could lead to heterogeneity in baseline hemodynamic level. As for efficacy assessment, all of the studies except for that by Chen et al. (12) used symptom score for the evaluation, but different standards were adopted when defining the key word "effective."

Finally, the general limitation of trial design cannot be neglected. All studies included score of their targeted patients according to the WSS, which is a scoring system that requires self-evaluation of various symptoms at different time points. The WSS scale's relatively strong subjectivity and its generalization of symptoms of different severity could cripple the accuracy of the calculated efficacy that were held as the primary outcome for all studies. It is indeed worth pondering whether this WSS could evaluate the severity of POTS symptoms and efficacy of certain drugs both comprehensively and objectively.

Two systematic reviews and meta-analysis were published previously (33, 34). However, our present study showed that β-blocker was an effective therapeutic option for the treatment of

POTS in children. With respect to the study inclusion criteria, we excluded the studies (35) that were ambiguous about the efficacy evaluation standard, while adding the studies (10) with larger sample-sized and more rigorous trial design. As for the pooled outcome, apart from the therapeutic efficacy that was adopted by both aforementioned reviews, we took on two new outcome assessment indexes—the "symptom score" and the "heart rate difference" in the evaluation.

In addition to the promising efficacy of metoprolol, its tolerance and safety seems rather acceptable. In our study, the rate of drug-related adverse effects in the metoprolol group was 4.0% (10/249), including abdominal discomfort, bradycardia, decreased blood pressure, fatigue and chest tightness. Although the present dosage of metoprolol, which is about 0.5–1 mg per kg everyday, presented a rare occurrence of unexpected events, a higher dose might be less well tolerated (8). Larger studies of longer follow-up period would be further required to identify rare or late-occurred adverse events.

Our review has several limitations that must be acknowledged. First of all, only articles written in English or Chinese are included in our study, leading to the inappropriate exclusion of trials published in other languages. Secondly, of the eight studies included, there are only four RCTs and the number of the studies with multi-center design and number of included sample size are not large enough. There are selective reporting with respect to symptom score in two studies and hemodynamic changes in three studies. Four studies lacked long-term follow-up, and the description of blinding process and patient compliance was unavailable in most articles. All of the above might affect the result.

At present, β-blockers have been used to in treating POTS children in many studies, but it is unclear whether there are any significant differences in its therapeutic efficacy over age. Convincing evidence derived from large scale RCTs that supports its efficacy is still a vacancy (36, 37). Through this systematic review and meta-analysis, we concluded that β-blocker was effective in treating POTS in children and adolescents, alleviating orthostatic intolerance, and improving hemodynamic abnormalities. However, limited by the disease's elusive pathogenesis, baseline difference of patients and the overall deficiency in study design, more studies of RCT and/or multicenter-based clinical studies are still in need before reaching a solid consensus. As for the research direction, we recommend that more efforts should be made for the establishment of a uniform standard for efficacy assessment, and also for the exploration of potential connections between symptoms and their underlying mechanisms, in order to offer reliable basis for a more evidence-based management of this complex disorder.

CONCLUSION

β-blockers are effective in treating POTS in children and adolescents, alleviating orthostatic intolerance, and improving hemodynamic abnormalities.

AUTHOR CONTRIBUTIONS

XD and YZ conceived the study, performed the data extraction, and coordinated data collection and analysis. Initial manuscript was drafted by XD and YZ collectively. YL and JD reviewed and critically revised the drafts of the manuscript and approved the final version as submitted.

FUNDING

This work was supported by Science and Technology Program of Beijing (Z171100001017253), Peking University Clinical Scientist Program (BMU2019LCKXJ001), and the Fundamental Research Funds for the Central Universities.

ACKNOWLEDGMENTS

The authors thank Dingyu Wang and Yuchen Wang from Peking University Health Science Center for their assistance with the methodology and data analysis. We also appreciate Xiaoyu Chen for her generous help with the article modification.

REFERENCES

1. Boris JR. Postural orthostatic tachycardia syndrome in children and adolescents[J]. *Auton Neurosci.* (2018) 215:97–101. doi: 10.1016/j.autneu.2018.05.004
2. Lin J, Han Z, Li X, Ochs T, Zhao J, Zhang X, et al. Risk factors for postural tachycardia syndrome in children and adolescents. *PLoS ONE.* (2014) 9:e113625. doi: 10.1371/journal.pone.0113625
3. Miller AJ, Raj SR. Pharmacotherapy for postural tachycardia syndrome. *Auton Neurosci.* (2018) 215:28–36. doi: 10.1016/j.autneu.2018.04.008
4. Benarroch EE. Postural tachycardia syndrome: a heterogeneous and multifactorial disorder. *Mayo Clin Proc.* (2012) 87:1214–25. doi: 10.1016/j.mayocp.2012.08.013
5. Mathias CJ, Low DA, Iodice V, Owens AP, Kirbis M, Grahame R. Postural tachycardia syndrome—current experience and concepts. *Nat Rev Neurol.* (2011) 8:22–34. doi: 10.1038/nrneurol.2011.187
6. Sheldon RS, Grubb BP, Olshansky B, Shen WK, Calkins H, Brignole M, et al. 2015 Heart Rhythm Society expert consensus statement on the diagnosis and treatment of postural tachycardia syndrome, inappropriate sinus tachycardia, and vasovagal syncope. *Heart Rhythm.* (2015) 12:e41–63. doi: 10.1016/j.hrthm.2015.03.029
7. Raj SR, Black BK, Biaggioni I, Paranjape SY, Ramirez M, Dupont WD, et al. Propranolol decreases tachycardia and improves symptoms in the postural tachycardia syndrome: less is more. *Circulation.* (2009) 120:725–34. doi: 10.1161/CIRCULATIONAHA.108.846501
8. Arnold AC, Okamoto LE, Diedrich A, Paranjapem SY, Raj SR, Biaggioni I, et al. Low-dose propranolol and exercise capacity in postural tachycardia syndrome: a randomized study. *Neurology.* (2013) 80:1927–33. doi: 10.1212/WNL.0b013e318293e310
9. Moon J, Kim DY, Lee WJ, Lee HS, Lim JA, Kim TJ, et al. Efficacy of propranolol, bisoprolol, and pyridostigmine for postural tachycardia syndrome: a randomized clinical trial. *Neurotherapeutics.* (2018) 15:785–95. doi: 10.1007/s13311-018-0612-9
10. Lin J, Liu P, Wang Y, Jin H, Yang J, Zhao J, et al. A signal center follow-up study on the treatment of postural tachycardia syndrome in children. *Chin J Appl Clin Pediatr.* (2015) 30:983–87.

11. Chen L, Wang L, Sun J, Qin J, Tang C, Jin H, et al. Midodrine hydrochloride is effective in the treatment of children with postural orthostatic tachycardia syndrome. *Circ J.* (2011) 75:927–31. doi: 10.1253/circj.CJ-10-0514
12. Chen L, Du J, Zhang Q, Wang C, Du Z, Wang H, et al. A multicenter study on treatment of autonomous nerve-mediated syncope in children with beta-receptor blocker. *Chin J Pediatr.* (2007) 45:885–88.
13. Liu Y, Zhai Y. Therapeutic effect of beta receptor blocker in the treatment of children with postural orthostatic tachycardia syndrome. *Chin J Prac Diag Ther.* (2007) 21:778–9.
14. Sun W. Comparison of the efficacies of metoprolol and midodrine hydrochloride in treating children with postural orthostatic tachycardia syndrome. *J Prac Med.* (2012) 28:1701–3.
15. Yang J, Liao Y, Zhang F, Chen L, Du J, Jin H. The follow up study on the treatment of children with postural orthostatic tachycardia syndrome. *Int J Pediatr.* (2014) 41:76–9.
16. Zhang Q, Du J, Wang Y. Efficacy of beta receptor blocker plus oral saline in the treatment of postural orthostatic tachycardia syndrome in children. *J Clin Pediatr.* (2006) 24:357–60.
17. Zhang F, Liao Y, Li X, Chen L, Jin H, Du J. Therapies for postural tachycardia syndrome in children. *Chin J Pediatr.* (2011) 49:428–32.
18. Higgins JPT, Green S (editors). *Cochrane Handbook for Systematic Reviews of Interventions Version 5.1.0*. The Cochrane Collaboration (2011). Available online at: https://training.cochrane.org/handbook (accessed Jul 24, 2019).
19. Furlan AD, Pennick V, Bombardier C, van Tulder M, Editorial Board, Cochrane Back Review Group. 2009 updated method guidelines for systematic reviews in the cochrane back review group. *Spine.* (2009) 34:1929–41. doi: 10.1097/BRS.0b013e3181b1c99f
20. Winker R, Barth A, Dorner W, Mayr O, Pilger A, Ivancsits S, et al. Diagnostic management of orthostatic intolerance in the workplace. *Int Arch Occup Environ Health.* (2003) 76:143–50. doi: 10.1007/s00420–002-0395–4.
21. Pianosi PT, Schroeder DR, Fischer PR. Cardiac responses to exercise distinguish postural orthostatic tachycardia syndrome variants. *Physiol Rep.* (2016) 4:e13040. doi: 10.14814/phy2.13040
22. Távora-Mehta MZ, Mehta N, Magajevski A, Oliveira L, Maluf DL, Concato L, et al. Reduced systolic volume: main pathophysiological mechanism in patients with orthostatic intolerance? *Arq Bras Cardiol.* (2016) 107:354–64. doi: 10.5935/abc.20160135
23. Fu Q, Levine BD. Exercise and non-pharmacological treatment of POTS. *Auton Neurosci.* (2018) 215:20–7. doi: 10.1016/j.autneu.2018.07.001
24. Arnold AC, Ng J, Lei L, Raj SR. Autonomic dysfunction in cardiology: pathophysiology, investigation, and management. *Can J Cardiol.* (2017) 33:1524–34. doi: 10.1016/j.cjca.2017.09.008
25. Zhang Q, Chen X, Li J, Du J. Orthostatic plasma norepinephrine level as a predictor for therapeutic response to metoprolol in children with postural tachycardia syndrome. *J Transl Med.* (2014) 12:249. doi: 10.1186/s12967-014-0249-3
26. Nickander KK, Carlson PJ, Urrutia RA, Camilleri M, Low PA. A screen of candidate genes and influence of beta2-adrenergic receptor genotypes in postural tachycardia syndrome. *Auton Neurosci.* (2005) 120:97–103. doi: 10.1016/j.autneu.2005.05.001
27. Crnošija L, Krbot Skorić M, Lovrić M, Junaković A, Miletić V, Alfirev RŠ, et al. Differences in neurohumoral and hemodynamic response to prolonged head-up tilt between patients with high and normal standing norepinephrine forms of postural orthostatic tachycardia syndrome. *Auton Neurosci.* (2017) 205:110–4. doi: 10.1016/j.autneu.2017.05.007
28. Crnošija L, Krbot Skorić M, Adamec I, Lovrić M, Junaković A, Mišmaš A, et al. Hemodynamic profile and heart rate variability in hyperadrenergic versus non-hyperadrenergic postural orthostatic tachycardia syndrome. *Clin Neurophysiol.* (2016) 127:1639–44. doi: 10.1016/j.clinph.2015.08.015
29. Zheng X, Chen Y, Du J. Recent advances in the understanding of the mechanisms underlying postural tachycardia syndrome in children:practical implications for treatment. *Cardiol Young.* (2017) 27:413–7. doi: 10.1017/S1047951116002559
30. Ross AJ, Ocon AJ, Medow MS, Stewart JM. A double-blind placebo-controlled cross-over study of the vascular effects of midodrine in neuropathic compared with hyperadrenergic postural tachycardia syndrome. *Clin Sci.* (2014) 126:289–96. doi: 10.1042/CS20130222
31. Freitas J, Santos R, Azevedo E, Costa O, Carvalho M, de Freitas AF. Clinical improvement in patients with orthostatic intolerance after treatment with bisoprolol and fludrocortisone. *Clin Auton Res.* (2000) 10:293–9. doi: 10.1007/BF02281112
32. Stewart JM, Munoz J, Weldon A. Clinical and physiological effects of an acute α1 adrenergic agonist and a β1 adrenergic antagonist in chronic orthostatic intolerance. *Circulation.* (2002) 106:2946–54. doi: 10.1161/01.CIR.0000040999.00692.F3
33. Lu W, Xu W, Du J. Meta-analysis of effect of beta-blockers on treatment of postural orthostatic tachycardia syndrome in children. *Chin J Appl Clin Pediatr.* (2015) 30:1415–9.
34. Deng W, Du J. A meta-analysis of α-adrenoceptor agonists and beta-blockers for the treatment of postural orthostatic tachycardia syndrome in children. *Chin J Appl Clin Pediatr.* (2013) 28:357–60.
35. Zuo Y, Wu Q, Gao J, Zhang J, Guo Y. Therapeutic effect of metoprolol combined with oral rehydration salts in the treatment of children with postural tachycardia syndrome. *Chin J Misdiagn.* (2009) 9:8089–90.
36. Wang C, Li Y, Liao Y, Tian H, Huang M, Dong X, et al. Chinese Pediatric Cardiology Society (CPCS) guideline for diagnosis and treatment of syncope in children and adolescents. *Sci Bull.* (2018) 63:1558–64.
37. Tao C, Liu X, Zhang C, Chen Y, Huang Y. Comments on 2018 CPCS guideline for diagnosis and treatment of syncope in children and adolescents. *Sci Bull.* (2019) 64:291–2. doi: 10.1016/j.scib.2019.01.008

Conflict of Interest: The authors declare that the research was conducted in the absence of any commercial or financial relationships that could be construed as a potential conflict of interest.

frontiers in Pediatrics

ORIGINAL RESEARCH
published: 20 November 2019
doi: 10.3389/fped.2019.00465

Arrhythmia and/or Cardiomyopathy Related to Maternal Autoantibodies: Descriptive Analysis of a Series of 16 Cases From a Single Center

Benzhen Wang[1,2†], *Sujuan Hu*[3†], *Degong Shi*[4], *Zhen Bing*[2] *and Zipu Li*[1,2*]

[1] School of Medicine, Shandong University, Jinan, China, [2] Heart Center, Qingdao Women and Children's Hospital, Affiliated to Qingdao University, Qingdao, China, [3] Department of Pediatrics, The Affiliated Hospital of Qingdao University, Qingdao, China, [4] Department of Pediatrics, The Traditional Chinese Medical Hospital of Huangdao District, Qingdao, China

OPEN ACCESS

Edited by:
Fu Lijun,
Shanghai Children's Medical Center, China

Reviewed by:
Giuseppe Limongelli,
Second University of Naples, Italy
Yanmin Zhang,
University of Manchester, United Kingdom

***Correspondence:**
Zipu Li
apuqd@sina.com

[†]These authors have contributed equally to this work

Specialty section:
This article was submitted to Pediatric Cardiology, a section of the journal Frontiers in Pediatrics

Received: 09 June 2019
Accepted: 24 October 2019
Published: 20 November 2019

Citation:
Wang B, Hu S, Shi D, Bing Z and Li Z (2019) Arrhythmia and/or Cardiomyopathy Related to Maternal Autoantibodies: Descriptive Analysis of a Series of 16 Cases From a Single Center. Front. Pediatr. 7:465. doi: 10.3389/fped.2019.00465

Objective: To describe the clinical characteristics of maternal autoantibody-mediated arrhythmia and/or cardiomyopathy, and to explore the therapeutic role of glucocorticoids in these diseases.

Methods: This was a retrospective observational study of 2 fetuses and 14 children who presented with autoantibody-mediated arrhythmia and/or cardiomyopathy in our hospital from September 2010 to December 2018.

Results: In total, 16 patients were identified, including 2 fetuses, and 14 children. One mother suffered from Sjogren's syndrome, two suffered from systemic lupus erythematosus (SLE), and the remaining 13 were asymptomatic carriers of autoantibodies. Two fetuses were diagnosed with complete congenital heart block (CHB) and had mean heart rates of 45 and 50 bpm. In the 14 surviving children, third-degree CHB was detected in 4 children, second- to third-degree CHB in 4, corrected QT interval (QTc) prolongation in 1, atrioventricular dissociation, and junctional ectopic tachycardia in 1, complete left bundle branch block (CLBBB) with dilated cardiomyopathy (DCM) in 3, and endocardial fibroelastosis (EFE) in 1. All of the 14 surviving babies received intravenous immunoglobulin and glucocorticoids. None of the children received pacemaker implantation. During the follow-up, one 3-month-old girl who had complete CHB, DCM, and Torsades de pointes almost recovered after the administration of prednisone for ∼8 years. Three cases with complete CHB had no improvement after 3–5 years of follow-up. One case with EFE and three cases with CLBBB and DCM were in stable condition now. Children with QTc prolongation and junctional ectopic tachycardia returned to a regular rhythm.

Conclusions: Autoantibody-mediated arrhythmias and/or cardiomyopathy are severe complications related to maternal autoantibodies, and the administration of steroid may be beneficial in reversing complete CHB.

Keywords: autoantibody, congenital heart block, cardiomyopathy, steroid, neonatal lupus

INTRODUCTION

Autoantibody-mediated heart disease, the most common manifestation of neonatal lupus, includes congenital heart block (CHB), and involvement beyond the atrioventricular node such as myocarditis, dilated cardiomyopathies (DCM), valvular abnormalities, and endocardial fibroelastosis (EFE) (1–3). Heart involvement of neonatal lupus carries an increased mortality and morbidity rate (4), and the mortality is between 16 and 23%, mostly *in utero* or during the first year of life (5).

Heart involvement in neonatal lupus is often accompanied by the presence of maternal autoantibodies in the fetal and neonatal circulation (6). The signature cardiac lesion is an atrioventricular block seen as a CHB, but 15–20% of these cases have associated fatal cardiomyopathy (7, 8). Autoimmune congenital heart block (ACHB), a rare condition that occurs in ∼1 out of every 20,000 pregnancies (9), is associated with the transplacental passage of maternal autoantibodies such as anti-Ro/SSA and/or anti-La/SSB antibodies in more than 80% of affected neonates (3). ACHB might be detected *in utero* as a first- or second-degree atrioventricular block (AVB), but the majority have a potentially lethal complete AVB (CAVB) (10).

Atrioventricular block most commonly develops during the 18–24 weeks of gestation, and may be found using fetal Doppler echocardiography (11). The disease can continue to develop after birth, even during infancy and early childhood (12). At the same time, ∼20% of affected fetuses can develop more diffuse myocardial disease manifested as cardiomyopathy and usually associated with endocardial fibroelastosis (EFE) (1, 2, 13); unfortunately, information relating to these conditions is sparse (2, 13, 14).

The majority of studies suggest that autoantibodies damage fetal conduction tissues leading to inflammation, calcification, and fibrosis, which can block signal conduction at the atrioventricular node without the requirement for additional structural abnormalities (2, 3). Indeed, increasing experimental, and clinical evidence has shown how these autoantibodies can critically interfere with cardiac electrical function and promote the development of life-threatening arrhythmic events by affecting the function of cardiac ion channels (7, 15).

The current curative CHB treatment is very controversial, and various therapeutic approaches including corticosteroids (especially fluorinated steroids, such as betamethasone or dexamethasone), intravenous immunoglobulin (IVIG), plasmapheresis, and beta-adrenergic agents have been reported (3, 5, 16). However, several studies have cast doubt on the efficacy of these therapies, and ultimately, a pacemaker is required in ∼80% of newborns with congenital third-degree AVB (17–19).

This study aims to present our single-center experience describing the clinical characteristics of maternal autoantibody-mediated arrhythmia and/or cardiomyopathy. In addition, we describe one interesting case where the mother had systemic lupus erythematosus (SLE), and the obstetric history demonstrated fetal bradycardia, complete AVB, Torsades de pointes (Tdp), and DCM in the third month after birth, but had almost returned to normal following the long-term administration of corticosteroids.

MATERIALS AND METHODS

Patient Identification

Clinical data on 16 cases were collected by performing a retrospective observational study of the patients at the Heart Center of Qingdao Women and Children's Hospital from September 2010 to December 2018. This study was approved by the ethics committee of Qingdao Women and Children's Hospital, and written informed consent was obtained from the parents of the study participants.

Inclusion criteria were as follows: The presence of maternal autoantibodies, such as anti-Ro/SSA and/or anti-La/SSB antibodies; and the confirmation of arrhythmia [including second- and third-degree heart block, prolonged QT interval, and complete left bundle branch block (CLBBB)] and/or cardiomyopathy (autoantibody-mediated EFE or DCM) in the patients, as documented by fetal echocardiography, electrocardiogram, or Holter monitoring performed in our center, and excluding other causes, such as myocarditis, complications from heart surgery, inherited cardiomyopathy, trauma, or toxication (1, 13, 20–22).

Selected Variables for Analysis

For the 16 mothers included in this study, demographic characteristics such as the age at diagnosis of CHB and type of autoimmune disease, and immunologic features such as the presence of anti-nuclear antibody, anti-Ro/SSA, anti-Ro/SSB, anti-Ro52, and anti-Ro 60 were collected when the children's diseases were first diagnosed. A screening of autoimmune diseases was also performed in asymptomatic carriers of autoantibodies.

Among the 16 fetuses and children, the gestation age at CHB diagnosis, age at CHB diagnosis, and type of CHB were collected. In addition, among the surviving children, we collected data on the sex, birth weight, heart rate, heart malformation, type of cardiomyopathy, clinical manifestation, presence of autoantibodies, erythrocyte sedimentation rate (ESR), size of ventricular cavity, heart function, treatment, and the follow-up.

Statistical Methods

The results from continuous variables are presented as median (range), while those from categorical data are presented as percentages.

RESULTS

A total of 16 women, accounting for 2 fetuses and 14 children with arrhythmia and/or cardiomyopathy, were identified from the cohort of the obstetrics clinic and the department of pediatrics in our hospital (**Table 1**). Termination of pregnancy (TOP) was performed in two women because of the persistence of complete CHB, and 14 live-born infants were delivered at full-term.

Unfortunately, data to calculate the incidence of maternal autoantibody-mediated arrhythmia and/or cardiomyopathy in the heart center (from 2010 to 2018) are not available.

TABLE 1 | Features of mothers, fetuses, and children.

Maternal features	
Mean age (years)	30 (27–35)
Systemic autoimmune disease	
Sjogren's syndrome	1 (6.2%)
Systemic lupus erythematosus	2 (12.5%)
Asymptomatic carrier	13 (81.3%)
Autoantibodies	
ANA + Anti-Ro/SSA	3 (18.8%)
ANA + Anti-Ro/SSB	1 (6.2%)
ANA + Anti-Ro/SSA + Anti-Ro/SSB + Anti-Ro/52	3 (18.8%)
ANA + Anti-Ro/SSA + Anti-Ro/52	5 (31.2%)
ANA + Anti-Ro/SSA + Anti-Ro/52 + Anti-Scl-70	1 (6.2%)
ANA + Anti-Ro/SSA + Anti-Ro/52 + Anti-nucleosome antibody	1 (6.2%)
Anti-Ro/52 + Anti-PM-SCL antibody	1 (6.2%)
Anti-Ro/SSA + Anti-Ro/52	1 (6.2%)
Features of fetuses and children	
Gestation age at the diagnosis (weeks, 2 fetuses)	28, 36
Mean age at diagnosis after birth (months, 14 surviving children)	14 (3–108)
Sex	
Female	10 (71.4%)
Male	4 (28.6%)
NA	2 (12.5%)
Clinical manifestation of surviving children	
Retardation	6 (42.9%)
Seizure	1 (7.1%)
None	7 (50%)
Type of Arrhythmia of surviving children	
Third-degree AVB	4 (28.5%)
Second→ third-degree AVB	4 (28.5%)
CLBBB	3 (21.4%)
AV dissociation + functional ectopic tachycardia	1 (6.2%)
QTc prolongation	1 (6.2%)
None	1 (6.2%)
Type of cardiomyopathy of Surviving children	
EFE	1 (7.1%)
DCM	3 (21.4%)
None	10 (71.4%)
Autoantibodies of surviving children	
Anti-nuclear antibody	2 (14.3%)
Anti-Ro/52	2 (14.3%)
DS-DNA	1 (7.1%)
Anti-PM-SCL	1 (7.1%)
None	8 (57.1%)

NA, not applicable; ANA, antinuclear antibodies; AVB, atrial ventricular block; AV, atrial ventricular; CLBBB, complete left bundle branch block; DS-DNA, double-stranded deoxyribonucleic acid; EFE, endocardial fibroelastosis; DCM, dilated cardiomyopathies.

Maternal Features

The traits of the women whose children were diagnosed with arrhythmia and/or cardiomyopathy are shown in **Table 1**. The median age at diagnosis of autoimmune abnormality was 30 years (range, 27–35 years). Three of the 16 women suffered from autoimmune disease, of whom one (6.2%) had Sjogren's syndrome and two (12.5%) had SLE. However, the remaining 13 women were asymptomatic carriers of autoantibodies. All of the mothers had positive autoantibodies, of whom 14 (85.7%) had positive anti-nuclear antibody (ANA), 13 (78.6%) had positive anti-Ro/SSA, 11 (64.3%) had positive anti-Ro52, 4 (25%) had positive anti-Ro/SSB, and 3 (18.8%) had positive anti-Ro 60. Only one case (7.7%) had positive anti-nucleosome antibodies, anti-scl-70, and anti-PM-Scl. Both mothers of fetus had positive anti-Ro/SSA and anti-Ro52, and erythrocyte sedimentation rate (ESR) of one of them reached 80 mm/h. The cases with coexisting antibodies are shown in **Table 1**.

Features of Children and Fetuses

The main characteristics of the children and fetuses are shown in **Tables 1**, **2**. The gestational age at the diagnosis of complete CHB in the two aborted fetuses was 28 and 30 weeks, and the mean heart rate at diagnosis of CHB was 45 and 50 bpm. In the 14 surviving children, 12 (85.7%) were full-term infants and 2 were premature infants. Ten cases were female and four cases were male. The median birth weight was 3,000 g (range, 2,000–3,700 g), and the median age at diagnosis was 14 months (range, 3–108 months). The data confirmed third-degree AVB in four babies, second- to third-degree AVB in four, QTc prolongation in one, junctional ectopic tachycardia in one, EFE in one, and CLBBB combined with DCM in three (**Table 1**). Case 4 was a special case who manifested with third-degree AVB, Tdp, and DCM; this case is described in detail below.

Among the 14 survivors, convulsions were the initial symptom in one case, and development retardation was the most common symptom in six children. The mean heart rates were below 100 bpm, and the median heart rate was 77 bpm (range, 50–99 bpm) in seven children. Four of the 14 surviving babies were diagnosed with congenital heart disease, including secundum atrial septal defect (ASD) (the sizes of the defects were 8 mm × 7 mm and 13 mm × 15 mm) and patent ductus arteriosus (PDA) (the ductal diameters were 3 and 2 mm) in two children. An echocardiogram was also used to assess ventricular size and ejection fraction (EF), and 8 of the 14 babies had an enlarged left ventricle, with a left ventricular end-diastolic dimension (LVEDD) of between 34 and 58 mm, and of whom five babies had left ventricular systolic dysfunction with a left ventricular ejection fraction (LVEF) below 40%.

The 14 surviving babies were all tested for autoantibodies, and the results showed that two babies were positive for ANA coexisting with anti-Ro/SSA, and double-stranded deoxyribonucleic acid (DS-DNA) and anti-PM-SCL antibodies were positive in one baby. However, the other babies had no significant level of autoantibodies. Furthermore, ESR and thyroid function were normal in all of the surviving babies (**Table 1**).

All of the surviving babies received IVIG and glucocorticoid (methylprednisolone and/or prednisolone) treatment. The IVIG was applied five times in total. The first dose of IVIG was 2 g/kg, then 1 g/kg was applied after 2 weeks, and then 1 g/kg per time was applied every other month for three

TABLE 2 | Clinical characteristics of 16 cases with autoantibody-mediated heart disease.

Case	Age at diagnosis (gestational age)	Delivery	Sex	Birth weight (g)	Type of disease (degree of AVB)	FHR (beats/min)	NT-proBNP (ng/ml)	LVEDD (mm)	LVEF (%)	Treatment	Outcome
1	19 months	Full-Term	F	3700	3	NA	218.7	34	N	IVIG + GC + SAL + ATR	Stay
2	4 months	Full-Term	F	3600	3	NA	624	N	N	IVIG + GC + SAL + ATR	Stay
3	14 months	Full-Term	F	3400	2→ 3 + ASD	98	323	N	N	IVIG + GC + SAL + ATR + Surgery	Improve
4	3 months	Full-Term	F	3100	3 + Tdp + DCM	80	6000	35	33	IVIG + GC + SAL + CAP	Improve (nearly cured)
5	60 months	Full-Term	F	3200	3 + PDA	55	103	35	N	IVIG + GC + SAL + ATR+ Intervention	Stay
6	32 weeks	TOP	NA	NA	3	40	NA	NA	NA	NA	NA
7	108 months	Full-Term	F	3300	2→ 3	N	63	N	N	IVIG + GC + SAL	Stay
8	6 months	Full-Term	F	2800	2→ 3 + ASD	N	NA	N	N	IVIG + GC + SAL+ Intervention	Improve
9	39 months	Full-Term	F	3000	2→ 3 + PDA	N	248	N	N	IVIG + GC + SAL + CAP	Stay
10	3 months	Full-Term	F	3000	CLBBB + DCM	N	2000	39	30	IVIG + GC + SAL + CAP + D	Improve
11	5 months	Full-Term	M	2200	CLBBB + DCM	N	> 35000	56	24	IVIG + GC + SAL + CAP + D	Improve
12	56 months	Full-Term	F	3000	CLBBB + DCM	N	2000	58	31	IVIG + GC + SAL + CAP + D	Stay
13	3 months	Full-Term	M	3550	EFE	N	> 35000	39	20	IVIG + GC + SAL + CAP + D	Improve
14	36 weeks	Pre-Term	M	3000	AV dissociation + JT	200	8613	N	N	IVIG + GC + AMI	Improve
15	28 weeks	TOP	NA	NA	3	50	NA	NA	NA	NA	NA
16	34 weeks	Pre-Term	M	2000	QTc prolongation	70	14774	N	N	IVIG + GC + SAL	Recover

N, normal; NA, not applicable; FHR, fetal heart rate; NT-proBNP, N-terminal pro B-type natriuretic peptide; LVEDD, left ventricular end-diastolic dimension; LVEF, left ventricular ejection fraction; AVB, atrioventricular block; AV, atrioventricular; Tdp, Torsades de pointes; TOP, termination of pregnancy; EFE, endocardial fibroelastosis; DCM, dilated cardiomyopathy; F, female; M, male; ASD, atrial septal defect; PDA, patent ductus arteriosus; CLBBB, complete left bundle branch block; JT, junctional tachycardia; IVIG, intravenous immunoglobulin; GC, glucocorticoid; SAL, salbutamol; CAP, captopril; AMI, amiodarone; D, diuretic; ATR, atropine.

times. Methylprednisolone is generally selected as glucocorticoid (prednisolone approximate equivalent dose conversion with methylprednisolone is 4:5), 2 mg/kg for 1 week, then reduced to 1 mg/kg for 1 month, and then reduced to 0.5 mg/kg for 2–6 months (the duration of application is adjusted according to the condition of the disease; poor response to treatment led us to suspend the drug, and conversely, the treatment will be maintained). Five children with third-degree CHB were administrated salbutamol and atropine, and those with cardiac dysfunction were given diuretics, captopril, and symptomatic treatment and one boy with EFE also received digoxin. None of the babies underwent pacemaker implantation; one child had surgical repair of ASD, and two children had transcatheter closure of ASD or PDA. At the follow-up, no improvement was found in four of the five cases with third-degree CHB, and one case with EFE and three cases with CLBBB combined with DCM were in a stable condition with the exception of growth retardation; however, no significant improvement in the enlarged left ventricle was noticed. Two newborns with QTc prolongation or atrioventricular dissociation recovered to a regular rhythm after the administration of IVIG and glucocorticoids (**Table 2**).

Case 4 was an interesting case; she had convulsion as the initial clinical manifestation in the third month after birth, and was diagnosed with third-degree AVB (**Figure 1A**), Tdp (**Figure 1B**), and DCM, and the obstetric history of her mother revealed fetal bradycardia during labor; unfortunately, we did not obtain the result of the fetal heart ultrasound. Her mother was diagnosed with SLE because a laboratory investigation showed an ESR of 80 mm/h, an ANA titer of 1:1,000, and positive anti-Ro/SSA and anti-Ro/52 antibodies; however, no autoantibodies were found in the baby. An electrocardiogram showed that the baby had a ventricular rate of 60 bpm and an atrial rate of 140 bpm, paroxysmal ventricular tachycardia, and TdP. An echocardiogram showed normal cardiac anatomy with an enlarged left ventricle (LVEDD 35 mm) (**Figure 2A**), diminished contractility (LVEF 42%), moderate mitral regurgitation, and mild pulmonary hypertension with a pulmonary artery systolic pressure of 33 mmHg. The baby was treated using steroids (prednisone), intravenous immunoglobulin, salbutamol, atropine, diuretic (furosemide), and captopril, but no permanent pacemaker was implanted. During her 8-year clinic visit, the electrocardiogram and echocardiogram showed an improvement in heart rhythm and function, and the dosage of prednisone was subsequently reduced from 2 mg/kg/day to 0.5 mg/kg once every other day step-by-step. At the same time, salbutamol, and atropine were gradually decreased, and was ceased at the relief of symptoms. Finally, her third-degree AVB completely disappeared, no further ventricular tachycardia or Tdp was observed, her heart rhythm restored to sinus rhythm, and her mean heart rate increased to 75 bpm. Only the complete right bundle branch block (CRBBB) with abnormal Q wave on leads II, III, avF, and V6 remained (**Figure 3**). On the other hand, an echocardiogram revealed a relatively normal heart size (LVEDD 45 mm) and function (LVEF 63%) (**Figure 2B**).

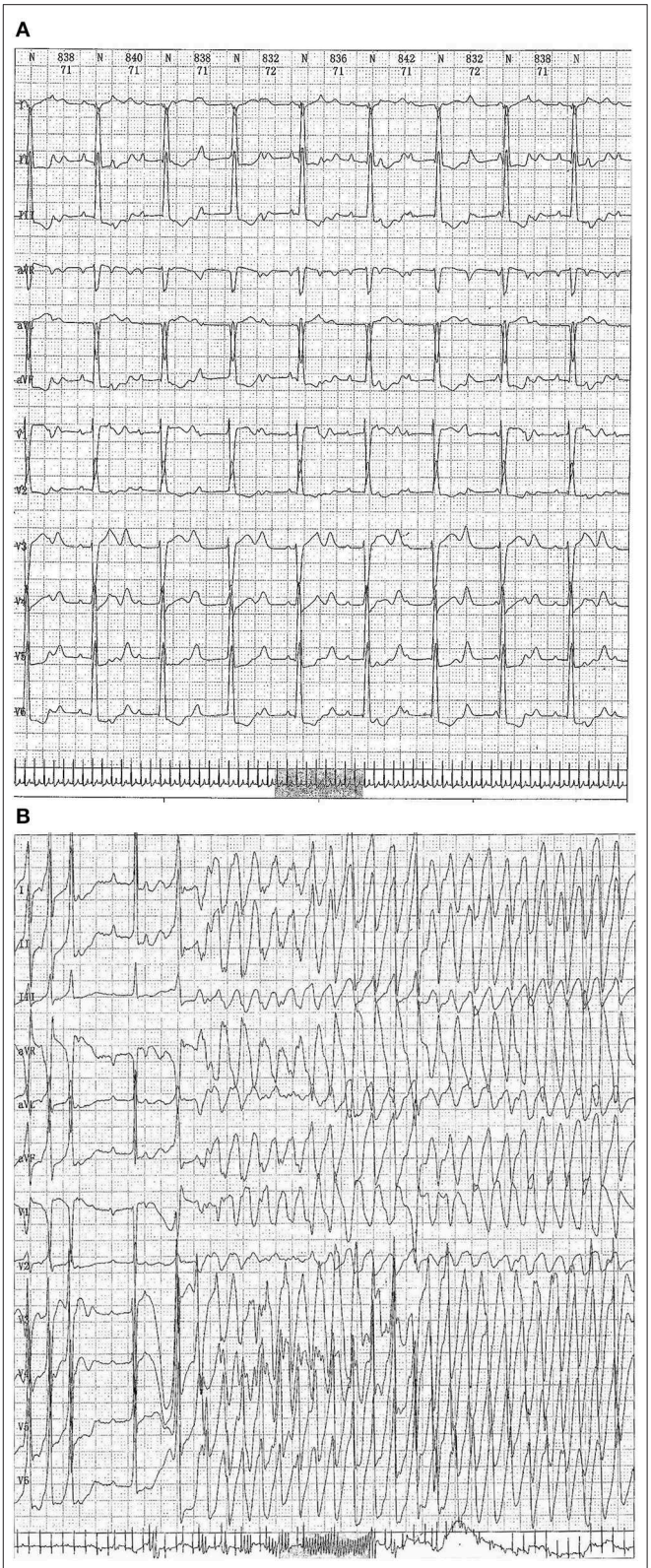

FIGURE 1 | (A) Echocardiograph showing a third-degree atrioventricular block. **(B)** Electrocardiography showing a third-degree atrioventricular block combined with Torsades de pointes (Tdp) (up to a maximum duration of 68 s).

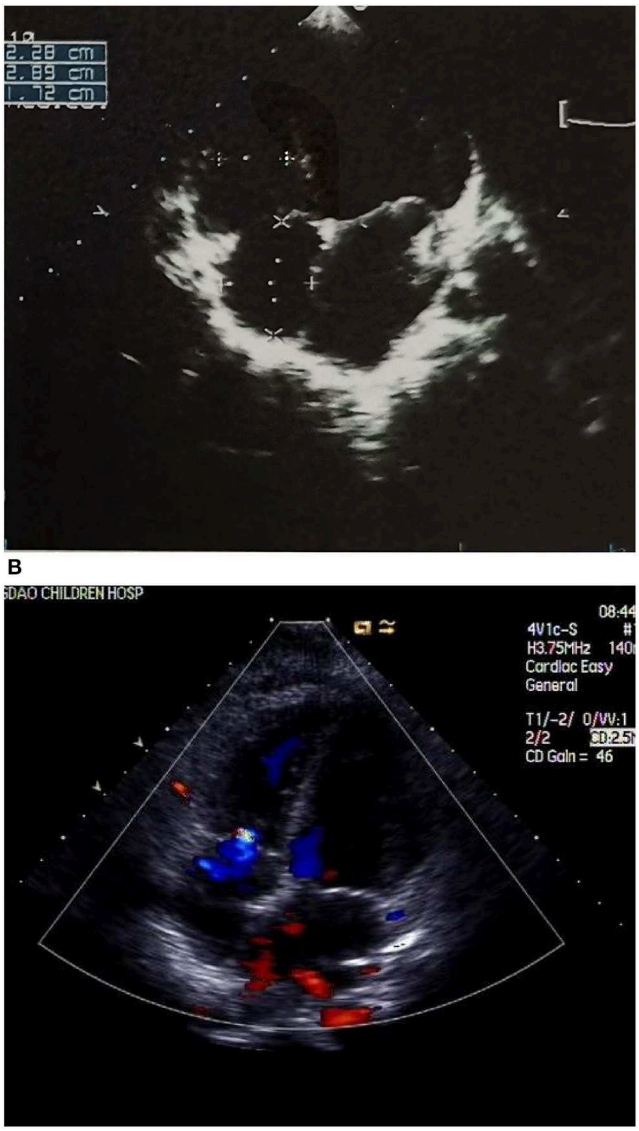

FIGURE 2 | (A) Echocardiograph showing an enlarged left ventricle (LVEDD 35 mm) **(B)** Echocardiograph showing a relatively normal heart size (LVEDD 45 mm) and a mild tricuspid regurgitation.

DISCUSSION

In this study, we describe the clinical and immunological characteristics of maternal autoantibody-mediated arrhythmia and/or cardiomyopathy in "children" rather than neonates. Combined with the children's electrocardiogram and echocardiographic features and significant abnormalities of the maternal immune system, we considered whether the diagnosis of autoantibody-mediated arrhythmia and/or cardiomyopathy was appropriate for the children included in our study. This was considered even in cases where we missed the optimal time to confirm the transplacental passage of maternal autoantibodies. Interestingly, in China, a delay in the management of high-grade AVB or other arrhythmias in the perinatal period is very common. There are several possible reasons for this situation. First, the testing for autoantibodies is not routinely performed during antenatal care. Second, techniques such as fetal Doppler echocardiography are not being performed effectively and screening for cardiovascular disease is often the weak link in newborn screening. Our report is consistent with the previous study that demonstrated that the majority of autoantibody-positive mothers who deliver a child with ACHB are asymptomatic for autoimmune disease (3). This situation increases the difficulty for prenatal diagnosis of autoantibody-mediated disease. Three mothers in our series were positive for anti-Scl-70, anti-nucleosome antibody, and anti-PM-SCL antibody; however, no previous studies have focused on the relationship between these antibodies and autoantibody-mediated arrhythmia or cardiomyopathy.

Autoimmune cardiac channelopathies are a novel and increasingly recognized mechanism of cardiac arrhythmias and/or cardiomyopathy; these are mediated by circulating autoantibodies that interfere with the function of various cardiac ion channels (15). Indeed, autoantibodies critically interfere with cardiac electrical function and promote the development of life-threatening arrhythmic events by affecting the function of cardiac ion channels (15). A large number of studies have clearly demonstrated that anti-Ro/SSA autoantibody cross-reactivity with L-type Ca^{2+} channels, and subsequent inhibition of I_{CaL} in the fetal heart conduction system are crucial pathogenic mechanisms through which these autoantibodies lead to the development of ACHB (15, 23–25). Increasing evidence indicates that the hERG1 K^+ channel is also a specific target of anti-Ro/SSA, which constitutes a novel form of acquired long QT syndrome (LQTS) of autoimmune origin (15, 26). Moreover, there are several other autoantibodies capable of disturbing various ion channels such as the anti-T-type Ca^{2+} channel, anti-KCNQ1 K^+ channel, and the anti-Na^+ channel; all of the above antibodies might lead to arrhythmia and/or cardiomyopathy (15). In terms of maternal demographic and clinical data, our results are generally consistent with the majority of previous studies in that the vast majority of the mothers had anti-Ro/SSA antibodies and four mothers also had anti-La/SSB antibodies.

Dilated cardiomyopathies can be diagnosed *in utero* together with autoimmune CHB, or may develop after birth; when DCM develops after the neonatal period, it is referred to as late-onset or delayed DCM (20, 22, 27). Morel et al. found that 22 of 174 (12.7%) children with CHB had no signs of DCM, either at birth or during the neonatal period, but ultimately developed late-onset DCM during the follow-up. However, neonatal DCM was observed in 13 children with CHB (6.9%) (20). It is noteworthy that three (21.4%) children had CLBBB complicated with DCM in our series. To date, there are no data regarding the incidence of new-onset LBBB in young patients with DCM; generally, the conduction abnormalities are a part of the natural history of DCM (28). The previous study has shown that myocardial fibrosis correlates with CLBBB (29). Based on the available evidence, it is difficult to determine whether DCM or CLBBB was the initial problem for these three babies. In addition, EFE

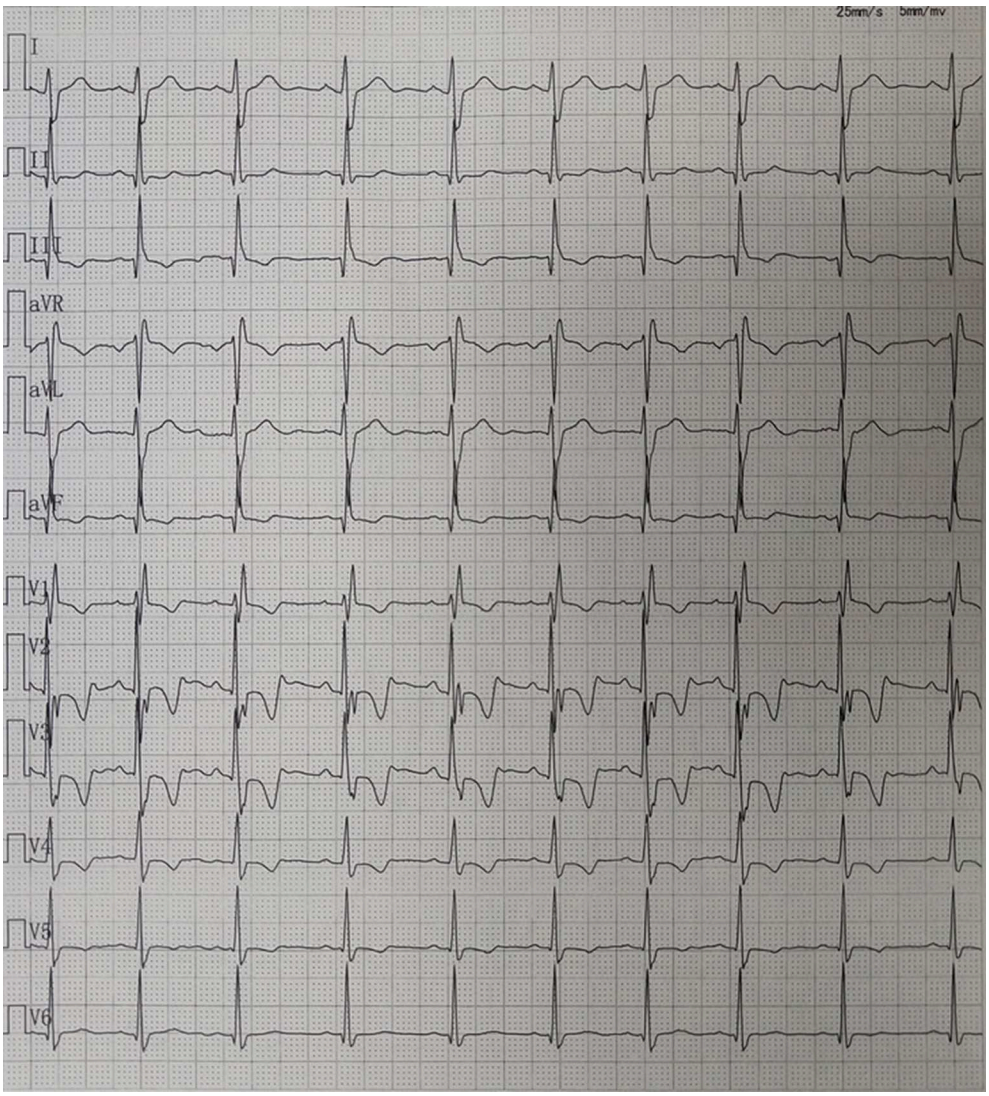

FIGURE 3 | Electrocardiography showing sinus rhythm and complete right bundle branch block (CRBBB) with abnormal Q wave on leads II, III, avF, and V6.

also occupies a certain proportion of the cardiac manifestation of neonatal lupus (9, 20) and isolated EFE associated with maternal antibodies can be present in the absence of CAVB (13). In our study, a 3-month-old boy whose mother had Sjogren's syndrome was diagnosed with EFE without conduction abnormalities; fortunately, the IVIG and glucocorticoid achieved some positive clinical effects. Although information relating to DCM or EFE caused by autoantibodies remains sparse, we believe that the incidence of this condition induced by autoantibodies is relatively common in clinical practice. Therefore, further research is needed to explore the relationship between cardiomyopathy and autoantibodies, especially maternal autoantibodies.

The therapeutic principle is extremely similar for heart block and other heart involvements of neonatal lupus, including corticosteroids, and intravenous immunoglobulin. Additionally, beta-adrenergic agents, and pacemaker implantation are particularly crucial for patients with third-degree AVB and an extremely low heart rate (1, 3, 5, 6, 12, 18, 19). To date, a series of studies have shown that the IVIG might be effective in preventing the passively acquired autoimmune CHB by several potential mechanisms: First, by lowering or even eliminating maternal antibodies in the fetal circulation; then, by decreasing the placental transport of maternal antibodies; and finally, by regulating the fetal and neonatal immune system (6, 17–19). Although not uniformly effective, corticosteroids, especially fluorinated steroids, have been associated with the reversal of first- and second-degree heart block; however, third-degree heart block has not yet been reversed with any treatment (1, 5, 19). Furthermore, considering the side effects of steroids, the routine administration of steroids remains controversial.

To the best of our knowledge, case 4 in our study is the first case of CAVB, Tdp, and DCM that has been almost cured by

the long-term administration of glucocorticoid; this case also provides us with some insight into the effect of steroids. The 3-month-old girl had third-degree heart block, Tdp, and DCM; after a relatively long duration of prednisone treatment, the heart block, severe ventricular tachycardia, as well as the heart size and function gradually restored to almost normal. So far, the growth and development of this girl are similar to that of her peer group and no obvious side effects have been observed. This therapeutic effect reflects the immune-mediated nature of this disease and suggests that steroids might actually have the capacity to reverse complete heart block. More importantly, this is the newest and most remarkable evidence for a possibility that complete heart block may be recoverable rather than irreversible. Although this opinion is contrary to all previous research (1, 5, 19), it is an exciting area that should be investigated further. Despite the success of this case, this approach also has great risks and is not recommended as a regular treatment in clinical practice without ample evidence.

Our study has a number of limitations owing to its retrospective design, the rarity of autoantibody-mediated arrhythmia, and/or cardiomyopathy and the lack of *in utero* details, which limit the power of the analyses. Furthermore, we were unable to determine the exact date when the heart involvement occurred. Ultimately, since only one child had a significant improvement with the usage of steroids, we could not evaluate the underlying mechanism and full effect of this therapy. Thus, more research, both experimental and clinical, should be conducted in order to fully elucidate these points.

In conclusion, autoantibody-mediated arrhythmias and/or cardiomyopathy are severe complications related to maternal autoantibodies, mainly anti-Ro/SSA and anti-La/SSB antibodies. Although the administration of steroids may have the ability to reverse complete AVB, further studies are needed to understand the mechanisms and to determine the security and validity of these findings.

DATA AVAILABILITY STATEMENT

All datasets generated for this study are included in the article/supplementary material.

ETHICS STATEMENT

The studies involving human participants were reviewed and approved by the ethics committee of Qingdao Women and Children's Hospital. Written informed consent to participate in this study was provided by the participants' legal guardian/next of kin. Written informed consent was obtained from the individual(s), and minor(s)' legal guardian/next of kin, for the publication of any potentially identifiable images or data included in this article.

AUTHOR CONTRIBUTIONS

BW was responsible for interpretation of the data, statistical analysis, drafting of the manuscript, and approval of the final version to be published. SH, DS, ZB, and ZL were responsible for the study conception, data collection and interpretation, revision of the manuscript, and approval of the final version to be published. All authors read and approved the final manuscript.

FUNDING

This study was supported by the Qingdao Outstanding Health Professional Development Fund (Qingdao FPCSE 2017-4).

REFERENCES

1. Trucco SMM, Jaeggi EM, Cuneo BM, Moon-Grady AJM, Silverman EM, Silverman NM, et al. Use of intravenous gamma globulin and corticosteroids in the treatment of maternal autoantibody-mediated cardiomyopathy. *JACC*. (2011) 57:715–23. doi: 10.1016/j.jacc.2010.09.044
2. Nield LE, Silverman ED, Taylor GP, Smallhorn JF, Mullen JB, Silverman NH, et al. Maternal anti-Ro and anti-La antibody-associated endocardial fibroelastosis. *Circulation*. (2002) 105:843–8. doi: 10.1161/hc0702.104182
3. Brito-Zeron P, Izmirly PM, Ramos-Casals M, Buyon JP, Khamashta MA. The clinical spectrum of autoimmune congenital heart block. *Nat Rev Rheumatol*. (2015) 11:301–12. doi: 10.1038/nrrheum.2015.29
4. Tincani A, Rebaioli CB, Taglietti M, Shoenfeld Y. Heart involvement in systemic lupus erythematosus, anti-phospholipid syndrome and neonatal lupus. *Rheumatology*. (2006) 45(Suppl 4): iv8–iv13. doi: 10.1093/rheumatology/kel308
5. Brucato A, Tincani A, Fredi M, Breda S, Ramoni V, Morel N, et al. Should we treat congenital heart block with fluorinated corticosteroids?*Autoimmun Rev*. (2017) 16: 1115–8. doi: 10.1016/j.autrev.2017.09.005
6. Buyon JP, Clancy RM, Friedman DM. Cardiac manifestations of neonatal lupus erythematosus: guidelines to management, integrating clues from the bench and bedside. *Nat Clin Pract Rheumatol*. (2009) 5:139–48. doi: 10.1038/ncprheum1018
7. Lee HC, Huang KT, Wang XL, Shen WK. Autoantibodies and cardiac arrhythmias. *Heartrhythm*. (2011) 8:1788–95. doi: 10.1016/j.hrthm.2011.06.032
8. Moak JP, Barron KS, Hougen TJ, Wiles HB, Balaji S, Sreeram N, et al. Congenital heart block: development of late-onset cardiomyopathy, a previously underappreciated sequela. *JACC*. (2001) 37:238–42. doi: 10.1016/S0735-1097(00)01048-2
9. Buyon JP, Clancy RM. Neonatal lupus: basic research and clinical perspectives. *Rheum Dis Clin North Am*. (2005) 31:299–313. doi: 10.1016/j.rdc.2005.01.010
10. Strasburger JF, Wakai RT. Fetal cardiac arrhythmia detection and in utero therapy. *Nat Rev Cardiol*. (2010) 7:277–90. doi: 10.1038/nrcardio.2010.32
11. Buyon JP, Hiebert R, Copel J, Craft J, Friedman D, Katholi M, et al. Autoimmune-associated congenital heart block: demographics, mortality, morbidity and recurrence rates obtained from a national neonatal lupus registry. *JACC*. (1998) 31:1658–66. doi: 10.1016/S0735-1097(98)00161-2
12. Ruffatti A, Marson P, Svaluto-Moreolo G, Marozio L, Tibaldi M, Favaro M, et al. A combination therapy protocol of plasmapheresis, intravenous immunoglobulins and betamethasone to treat anti-Ro/La-related congenital atrioventricular block. A case series and review of the literature. *Autoimmun Rev*. (2013) 12:768–73. doi: 10.1016/j.autrev.2013.01.002
13. Nield LE, Silverman ED, Smallhorn JF, Taylor GP, Mullen JB, Benson LN, et al. Endocardial fibroelastosis associated with maternal anti-Ro and anti-La antibodies in the absence of atrioventricular block. *JACC*. (2002) 40:796–802. doi: 10.1016/S0735-1097(02)02004-1

14. Nield LE, Silverman ED, Taylor GP. Maternal anti-Ro and anti-La antibody associated endocardial fibroelastosis. *Acccurr J Rev*. (2002) 11:103. doi: 10.1016/S1062-1458 (02) 00756-0
15. Lazzerini PE, Capecchi PL, Laghi-Pasini F, Boutjdir M. Autoimmune channelopathies as a novel mechanism in cardiac arrhythmias. *Nat Rev Cardiol*. (2017) 14:521–35. doi: 10.1038/nrcardio.2017.61
16. Gleicher N, Elkayam U. Preventing congenital neonatal heart block in offspring of mothers with anti-SSA/Ro and SSB/La antibodies: a review of published literature and registered clinical trials. *Autoimmun Rev*. (2013) 12:1039–45. doi: 10.1016/j.autrev.2013.04.006
17. Friedman DM, Llanos C, Izmirly PM, Brock B, Byron J, Copel J, et al. Evaluation of fetuses in a study of intravenous immunoglobulin as preventive therapy for congenital heart block: Results of a multicenter, prospective, open-label clinical trial. *Arthritis Rheum*. (2010) 62:1138–46. doi: 10.1002/art.27308
18. Friedman DM, Kim MY, Copel JA, Llanos C, Davis C, Buyon JP. Prospective evaluation of fetuses with autoimmune-associated congenital heart block followed in the PR Interval and Dexamethasone Evaluation (PRIDE) Study. *Am J Cardiol*. (2009) 103:1102–6. doi: 10.1016/j.amjcard.2008.12.027
19. Ruffatti A, Cerutti A, Favaro M, Del RT, Calligaro A, Hoxha A, Marson P, et al. Plasmapheresis, intravenous immunoglobulins and bethametasone - a combined protocol to treat autoimmune congenital heart block: a prospective cohort study. *Clin Exp Rheumatol*. (2016) 34:706–13. Available online at: https://www.clinexprheumatol.org/abstract.asp?a=10107
20. Morel N, Lévesque K, Maltret A, Baron G, Hamidou M, Orquevaux P, et al. Incidence, risk factors, and mortality of neonatal and late-onset dilated cardiomyopathy associated with cardiac neonatal lupus. *Int J Cardiol*. (2017) 248:263–9. doi: 10.1016/j.ijcard.2017.07.100
21. Doti PI, Escoda O, Cesar-Diaz S, Palasti S, Teixido I, Sarquella-Brugada G, et al. Congenital heart block related to maternal autoantibodies: descriptive analysis of a series of 18 cases from a single center. *Clin Rheumatol*. (2016) 35:351–6. doi: 10.1007/s10067-016-3174-4
22. Villain E, Coastedoat-Chalumeau N, Marijon E, Boudjemline Y, Piette JC, Bonnet D. Presentation and prognosis of complete atrioventricular block in childhood, according to maternal antibody status. *JACC*. (2006) 48:1682–7. doi: 10.1016/j.jacc.2006.07.034
23. Santos-Pardo I, Villuendas R, Salvador-Corres I, Martinez-Morillo M, Olive A, Bayes-Genis A. Anti-Ro/SSA antibodies and cardiac rhythm disturbances: Present and future perspectives. *Int J Cardiol*. (2015) 184:244–50. doi: 10.1016/j.ijcard.2014.11.002
24. Ambrosi A, Sonesson S, Wahren-Herlenius M. Molecular mechanisms of congenital heart block. *Exp Cell Res*. (2014) 325:2–9. doi: 10.1016/j.yexcr.2014.01.003
25. Karnabi E, Boutjdir M. Role of calcium channels in congenital heart block. *Scand J Immunol*. (2010) 72:226–34. doi: 10.1111/j.1365-3083.2010.02439.x
26. Boutjdir M, Lazzerini PE, Capecchi PL, Laghi-Pasini F, El-Sherif N. Potassium channel block and novel autoimmune-associated long QT syndrome. *Card Electrophysiol Clin*. (2016) 8:373–84. doi: 10.1016/j.ccep.2016.02.002
27. Udink TCF, Breur JM, Cohen MI, Boramanand N, Kapusta L, Crosson JE, et al. Dilated cardiomyopathy in isolated congenital complete atrioventricular block: early and long-term risk in children. *JACC*. (2001) 37:1129–34. doi: 10.1016/S0735-1097(00)01209-2
28. Aleksova A, Carriere C, Zecchin M, Barbati G, Vitrella G, Di Lenarda A, et al. New-onset left bundle branch block independently predicts long-term mortality in patients with idiopathic dilated cardiomyopathy: data from the Trieste Heart Muscle Disease Registry. *Europace*. (2014) 16:1450–9. doi: 10.1093/europace/euu016
29. Mahmod M, Karamitsos TD, Suttie JJ, Myerson SG, Neubauer S, Francis JM. Prevalence of cardiomyopathy in asymptomatic patients with left bundle branch block referred for cardiovascular magnetic resonance imaging. *Int J Cardiovasc Imaging*. (2012) 28:1133–40. doi: 10.1007/s10554-011-9931-1

Conflict of Interest: The authors declare that the research was conducted in the absence of any commercial or financial relationships that could be construed as a potential conflict of interest.

frontiers in Pediatrics

ORIGINAL RESEARCH
published: 11 December 2019
doi: 10.3389/fped.2019.00514

A New Scoring System for Prediction of Intravenous Immunoglobulin Resistance of Kawasaki Disease in Infants Under 1-Year Old

Shu Wu[1,2†], Yuan Long[3†], Selena Chen[4], Yaqian Huang[1], Ying Liao[1], Yan Sun[1], Qingyou Zhang[1], Chunyu Zhang[1], Hui Yan[1], Jianguang Qi[1], Xueqin Liu[1], Yonghong Chen[1], Yong Zhang[3] and Junbao Du[1,5*]*

[1] Department of Pediatrics, Peking University First Hospital, Beijing, China, [2] Research Unit of Clinical Diagnosis and Treatment of Pediatric Syncope and Cardiovascular Diseases, Chinese Academy of Medical Sciences, Beijing, China, [3] Department of Pediatric Cardiology, Wuhan Children's Hospital (Wuhan Maternal and Child Healthcare Hospital), Tongji Medical College, Huazhong University of Science and Technology, Wuhan, China, [4] Division of Biological Sciences, University of California, San Diego, San Diego, CA, United States, [5] Key Laboratory of Molecular Cardiovascular Sciences, Ministry of Education, Beijing, China

OPEN ACCESS

Edited by:
Fu Lijun,
Shanghai Children's Medical Center, China

Reviewed by:
Mingguo Xu,
Shenzhen Children's Hospital, China
Yu Xianyi,
China Medical University, China

***Correspondence:**
Yong Zhang
1539210298@qq.com
Junbao Du
junbaodu1@126.com

[†]These authors have contributed equally to this work

Specialty section:
This article was submitted to Pediatric Cardiology, a section of the journal Frontiers in Pediatrics

Received: 26 October 2019
Accepted: 27 November 2019
Published: 11 December 2019

Citation:
Wu S, Long Y, Chen S, Huang Y, Liao Y, Sun Y, Zhang Q, Zhang C, Yan H, Qi J, Liu X, Chen Y, Zhang Y and Du J (2019) A New Scoring System for Prediction of Intravenous Immunoglobulin Resistance of Kawasaki Disease in Infants Under 1-Year Old. Front. Pediatr. 7:514. doi: 10.3389/fped.2019.00514

Background: Children with Kawasaki disease (KD) under 1-year old are at high risk for intravenous immunoglobulin (IVIG) resistance. The study was designed to explore the predictive measure of IVIG resistance in infants under 1-year old with KD.

Methods: This study enrolled children under 1-year old suffering from KD in Peking University First Hospital and Wuhan Children's Hospital. All infants were divided into IVIG-responsive and IVIG-resistant groups. The differences in demographic characteristics, clinical features, and laboratory examinations were compared and the risk factors of IVIG resistant KD were analyzed. Furthermore, a scoring system was developed for predicting IVIG resistance in KD infants and an external validation was performed.

Result: A total of 282 infants (194 boys, median age of 7.0 months) were enrolled in this study, of whom 23 children were IVIG-resistant. Compared with IVIG-responsive infants, those in the IVIG-resistant group had a high neutrophil-to-lymphocyte ratio (NLR), high platelet-to-lymphocyte ratio (PLR), high mean platelet volume-to-lymphocyte ratio (MPVLR) in peripheral blood, and low serum albumin, and low serum sodium before IVIG therapy (all $P < 0.01$). Multiple regression analysis indicated that high levels of peripheral NLR and MPVLR, and low levels of serum albumin and serum sodium were independent risk factors for IVIG resistant KD infants. A scoring system, which included peripheral NLR $\geq$ 2.69 (1 point), MPVLR $\geq$ 2.78 (1 point), serum albumin $\leq$ 30.7 g/L (1 point), and serum sodium $\leq$ 135.2 mmol/L (1 point), was established. A cut-off value of a total score of 2 points or higher yielded a sensitivity of 87.0% and a specificity of 78.4%, with an area under the curve of 0.891. External validation with clinical diagnostic standard showed that a cut-off value of total score of 2 points or higher for predicting the IVIG-resistance yielded a sensitivity of 70.0% and a specificity of 75.1%.

Conclusion: For the first time, we proposed a predictive model of IVIG resistance in KD infants under 1-year old. The scoring system, which accounts for baseline peripheral NLR, MPVLR, and serum albumin and sodium, predicts with relatively high sensitivity and specificity for IVIG-resistant infants with KD under 1-year old.

Keywords: Kawasaki disease, infants under 1-year old, intravenous immunoglobulin resistance, scoring system, prediction

INTRODUCTION

Kawasaki disease (KD) commonly presents as an acute autoimmune vasculitis in childhood (1). Serious complications include coronary dilatation and coronary aneurysm, which may result in myocardial infarction (2, 3). Intravenous immunoglobulin (IVIG) with oral aspirin can significantly reduce the incidence of coronary artery complications (4). It is a standardized treatment for KD that is widely accepted (5). However, some children are resistant to IVIG therapy and have recurrent or persistent fever 36–48 h after the first dose of IVIG (4). The incidence of IVIG resistance was about 4.9–38.3% in different regions according to particular definition (4, 6–9). IVIG resistance represents severe inflammatory response and it is also an independent predictor for coronary artery lesions (10–12).

The peak incidence of IVIG resistance occurs at ages <1-year old, especially between 9 and 11 months old (9). Kobayashi et al. have shown that ages under 1-year old are an independent risk factor for not only IVIG resistance (13) but also coronary artery lesions (8). In recent years, randomized, open-label, blinded-endpoints trials have confirmed that IVIG therapy combined with other immunosuppressive agents such as glucocorticoid and cyclosporine effectively reduce the incidence of coronary artery complications in children predicted with IVIG resistance before treatment (14, 15). Therefore, it is important to determine an efficient predictive scoring system of IVIG resistance for KD infants under 1-year old.

Classic indicators previously identified to predict IVIG resistance include young ages, a high peripheral neutrophil percentage, high c-reactive protein, serum alanine transaminase (ALT), glutamyl transpeptidase, and total bilirubin levels, and low peripheral hemoglobin, serum albumin, and serum sodium levels (13, 16–21). Investigators have reported several scoring systems predicting IVIG resistance, for instance, the scoring systems by Sano, Kobayashi, and Egami scoring systems in Japan and San Diego scoring system in the United States. However, they showed unsatisfactory predictive abilities when validated externally in Chinese (22, 23). Recent studies showed that the neutrophil-to-lymphocyte ratio (NLR), platelet-to-lymphocyte ratio (PLR), and mean platelet volume-to-lymphocyte ratio (MPVLR) in peripheral blood could reflect the severity of inflammatory and cardiovascular disease (24–26). The basic pathological manifestation of KD is systemic vasculitis, and the increase of peripheral NLR and PLR are closely related to IVIG resistance (24, 27). However, at present the relationship between MPVLR and IVIG resistance remains unexplored. A previous study showed that in patients at all ages with KD, NLR $\geq$ 2.8 was a high risk factor for IVIG resistance (28), but the peripheral lymphocyte count or neutrophil count markedly changes with respect to the age groups in children. This has a significant influence on the predictive value of IVIG-resistant patients with KD.

Therefore, considering the specific impact of the peripheral lymphocyte count or neutrophil count according to age, and understanding that the peak incidence of IVIG resistance occurs at ages younger than 12 months old, the present study was undertaken to explore the predictive indicators of IVIG resistance to establish a Chinese scoring system predicting IVIG resistant KD infants under 1-year old.

MATERIALS AND METHODS

Study Population

This research was a double-center-based retrospective study. The medical data of children under 1-year old diagnosed with KD in the department of pediatrics at Peking University First Hospital from January 2008 to August 2019 and Wuhan Children's Hospital from January 2018 to August 2019 were collected for constructing the predictive scoring system. Furthermore, the medical data of children under 1-year old diagnosed with KD in Wuhan Children's Hospital from January 2016 to December 2017 were used for external validation. All children met the KD diagnostic criteria by the American Academy of Pediatrics and the American Heart Association (29). The first day of illness was defined as the first day of fever. The following cases were excluded: (1) patients with illness days longer than 10 days; (2) patients treated with IVIG before admission; (3) patients without use of IVIG after admission; (4) patients with incomplete data (**Figure 1**). A total of 469 children were enrolled, receiving IVIG of 2 g/kg combined with oral aspirin of 30–50 mg/kg/d initially. IVIG resistance was defined as infants with KD having persistent or recrudescent fever ($\geq$38°C) 48 h after completion of the first IVIG infusion (18). Two hundred eighty-two infants (259 IVIG-responsive cases and 23 IVIG-resistant cases) were used for the scoring system development to predict IVIG resistance in KD infants, and another 187 infants (177 IVIG-responsive cases and 10 IVIG-resistant cases) for the external validation (**Figure 1**). This study was approved by the Ethics Committee of Peking University First Hospital, China and the Ethics Committee of Wuhan Children's Hospital.

Data Collection

Data referring to demographic characteristics, clinical manifestations, laboratory examinations before IVIG therapy,

and echocardiography results were documented. The peripheral white blood cell count (WBC), neutrophil count, lymphocyte count, hemoglobin, platelet count, mean platelet volume, NLR, PLR, and MPVLR, together with ALT, albumin, and sodium in serum were recorded. We used echocardiography by two-dimensional ultrasound during hospitalization to assess coronary

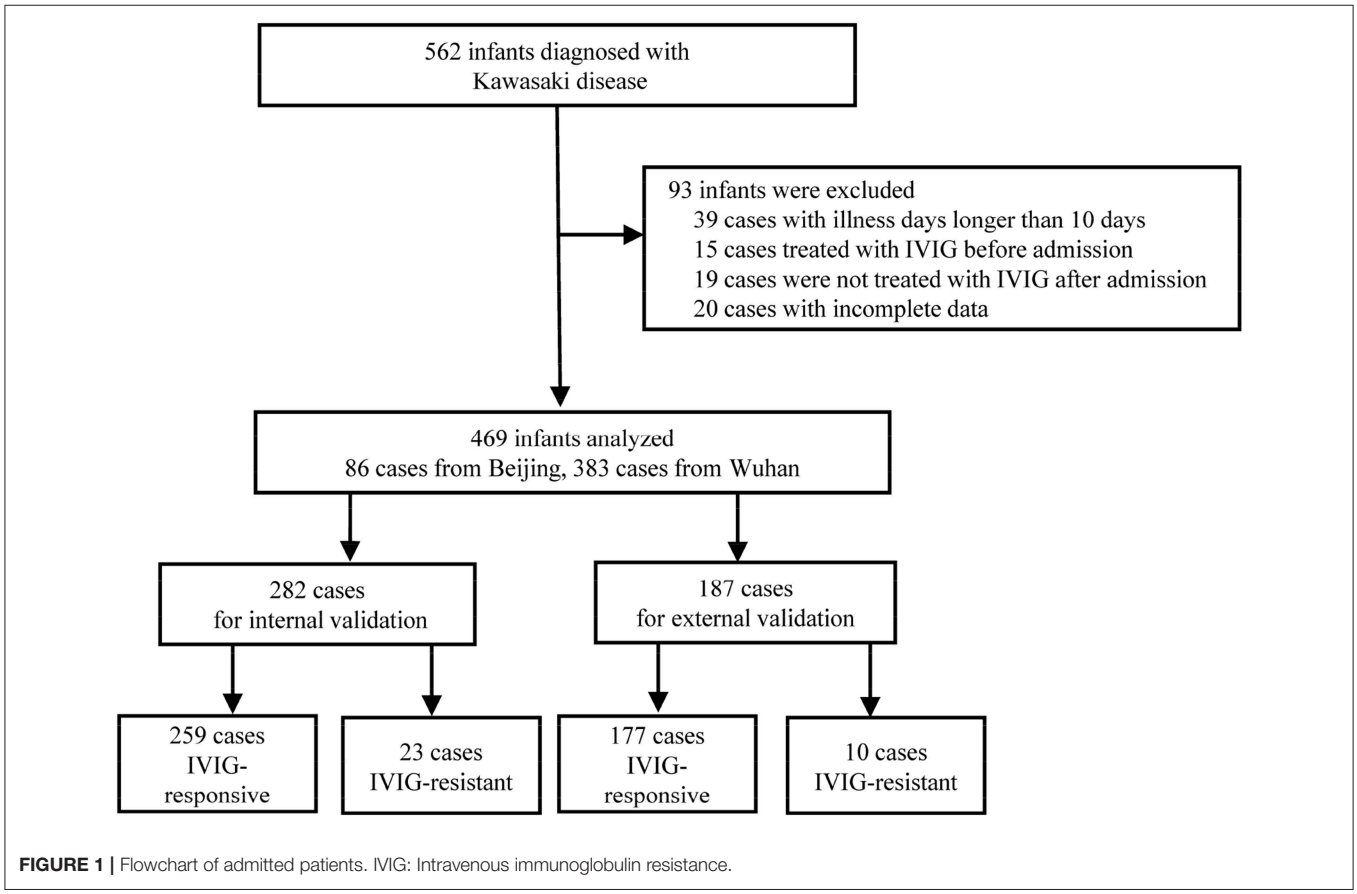

FIGURE 1 | Flowchart of admitted patients. IVIG: Intravenous immunoglobulin resistance.

TABLE 1 | Comparison of clinical characteristics between IVIG-responsive and IVIG-resistant cases.

Variable	Total (n = 282)	IVIG-responsive (n = 259)	IVIG-resistant (n = 23)	P-value
Gender (M/F)	194/88	175/84	19/4	0.136
Age, months	7.00 (4.00, 9.00)	7.00 (4.00, 9.00)	8.00 (5.00, 10.00)	0.152
cKD/iKD	145/137	132/127	13/10	0.609
No. CAL	59 (20.9%)	53 (20.5%)	6 (26.1%)	0.525
White blood cell, 10^9/L	14.55 (11.26, 18.85)	14.49 (11.20, 18.79)	14.71 (11.31, 22.63)	0.577
Neutrophil count, 10^9/L	8.42 (5.91, 11.31)	8.13 (5.56, 11.14)	9.76 (8.14, 15.78)	0.009
Lymphocyte count, 10^9/L	4.50 (3.06, 6.05)	4.63 (3.23, 6.16)	2.60 (1.88, 3.34)	<0.001
Hemoglobin, g/L	101.02 ± 11.93	101.10 ± 11.99	100.13 ± 11.48	0.709
Platelet count, 10^9/L	402.00 (318.00, 513.00)	404.00 (324.00, 518.00)	324.00 (230.00, 484.00)	0.028
Mean platelet volume, fl	9.70 (9.10, 10.30)	9.70 (9.10, 10.30)	9.60 (9.30, 10.60)	0.628
NLR	1.93 (1.22, 2.90)	1.79 (1.20, 2.61)	4.86 (2.74, 6.26)	<0.001
PLR	94.59 (69.86, 125.14)	91.29 (69.55, 121.59)	132.74 (87.94, 198.08)	0.006
MPVLR	2.14 (1.57, 3.24)	2.07 (1.53, 3.00)	3.64 (2.78, 5.21)	<0.001
Alanine transaminase, IU/L	24.00 (15.00, 42.00)	23.00 (15.00, 40.00)	33.00 (23.00, 45.00)	0.057
Serum albumin, g/L	37.42 ± 4.42	37.68 ± 4.28	34.55 ± 5.03	0.001
Serum sodium, mmol/L	137.37 (135.50, 139.30)	137.60 (135.68, 139.40)	134.80 (133.21, 137.50)	0.001

IVIG, intravenous immunoglobulin; cKD, complete Kawasaki disease; iKD, incomplete Kawasaki disease; No. CAL, numbers of coronary artery lesions; NLR, neutrophil-to-lymphocyte ratio; PLR, platelet-to-lymphocyte ratio; MPVLR, mean platelet volume-to-lymphocyte ratio.

artery lesions. Coronary artery luminal diameters of the left main coronary artery and the right coronary artery were converted to body surface area-adjusted Z-scores. If the maximum Z-score of the coronary artery was >2.5, a coronary artery lesion was determined (29).

Statistical Analysis

Statistical analysis was performed by SPSS version 25.0. We used frequency (percentage) to describe categorical variables and a χ^2-test was used to analyze the difference between the 2 groups. For continuous variables, normally distributed variables were expressed as the mean ± standard deviation and assessed by independent sample *t*-test, and non-normally distributed variables were shown as median (interquartile range) and compared by the Mann-Whitney U test. Univariable analysis was performed to determine the differences in age (months), gender, peripheral WBC, hemoglobin, NLR, PLR, and MPVLR, and serum ALT, albumin, and sodium between two groups, and the continuous variables were converted to categorical variables first. Variables selected by the univariate analysis ($p < 0.05$) were applied for multivariate logistic regression to screen out independent risk factors for IVIG resistance. To construct the scoring system, the score of independent risk factors were determined by the odd ratios, and each patient obtained a total score. The cut-off point was chosen by the receiver-operator characteristic (ROC) curves and adjusted by the previous classical literature and clinical practice. The cut-off score was chosen at the highest Youden index and the sensitivity and specificity of the scoring system were analyzed. A value of $P < 0.05$ was considered statistically significant.

RESULTS

Demographic and Clinical Features

One hundred ninety-four boys and 88 girls at a median age of 7.0 (4.0, 9.0) months were analyzed for establishing the scoring system in this study. There were 259 IVIG responders and 23 IVIG non-responders. IVIG resistance occurred in 8.16% of the study subjects. The IVIG-responsive group included 175 boys (67.6%) and 84 girls (32.4%) at a median age of 7.0 (4.0, 9.0) months. The IVIG-resistant group included 19 boys (82.6%) and 4 girls (17.4%) at a median age of 8.0 (5.0, 10.0) months. The percentage of patients with incomplete KD and coronary artery abnormalities between two groups did not differ ($P > 0.05$, **Table 1**). Compared with the IVIG-responsive group, the levels of peripheral neutrophil count, NLR, PLR, and MPVLR were significantly increased in IVIG-resistant patients, and the levels of peripheral lymphocyte and platelet count, serum albumin and sodium levels were significantly decreased ($P < 0.01$, except for the platelet count, $P < 0.05$; **Table 1**).

Univariate Analysis

Ten categorical variables were analyzed in the univariate analysis. The cut-off point for each variable was as follows: (1) age ≤6

TABLE 2 | Univariate analysis between IVIG-responsive and IVIG-resistant cases.

Variable	Cut-off point	IVIG-responsive ($n = 259$)	IVIG-resistant ($n = 23$)	χ^2	*P*-value
Age, months	≤6.0	158 (61.0%)	16 (69.6%)	0.655	0.418
Gender	Male	175 (67.6%)	19 (82.6%)	2.226	0.136
White blood cell, 10^9/L	≥14.5	129 (49.8%)	12 (52.2%)	0.047	0.828
Hemoglobin, g/L	≤100.5	122 (47.1%)	11 (47.8%)	0.004	0.947
NLR	≥2.69	63 (24.3%)	18 (78.3%)	30.017	<0.001
PLR	≥110.92	83 (32.0%)	16 (69.6%)	13.052	<0.001
MPVLR	≥2.78	74 (28.6%)	19 (82.6%)	27.907	<0.001
Alanine transaminase, IU/L	≥40.0	64 (24.7%)	9 (39.1%)	2.289	0.130
Serum albumin, g/L	≤30.7	17 (6.6%)	9 (39.1%)	26.768	<0.001
Serum sodium, mmol/L	≤135.2	52 (20.1%)	13 (56.5%)	15.819	<0.001

IVIG, intravenous immunoglobulin; NLR, neutrophil-to-lymphocyte ratio; PLR, platelet-to-lymphocyte ratio; MPVLR, mean platelet volume-to-lymphocyte ratio.

TABLE 3 | Independent factors identified by multiple logistic regression analysis for prediction of IVIG resistance.

Variables	Logistic coefficient (β)	SE	*Wald* χ^2	*P*-value	Odd ratio (95% CI)	Score point
NLR ≥ 2.69	1.393	0.619	5.064	0.024	4.027 (1.197, 13.548)	1
PLR ≥ 110.92	0.551	0.594	0.860	0.354	1.735 (0.542, 5.557)	–
MPVLR ≥ 2.78	1.351	0.687	3.863	0.049	3.860 (1.004, 14.846)	1
Serum Albumin ≤ 30.7 g/L	1.194	0.600	3.961	0.047	3.300 (1.018, 10.693)	1
Serum Sodium ≤ 135.2 mmol/L	1.308	0.527	6.165	0.013	3.700 (1.317, 10.393)	1

IVIG, intravenous immunoglobulin; CI, confidence interval; NLR, neutrophil-to-lymphocyte ratio; PLR, platelet-to-lymphocyte ratio; MPVLR, mean platelet volume-to-lymphocyte ratio.

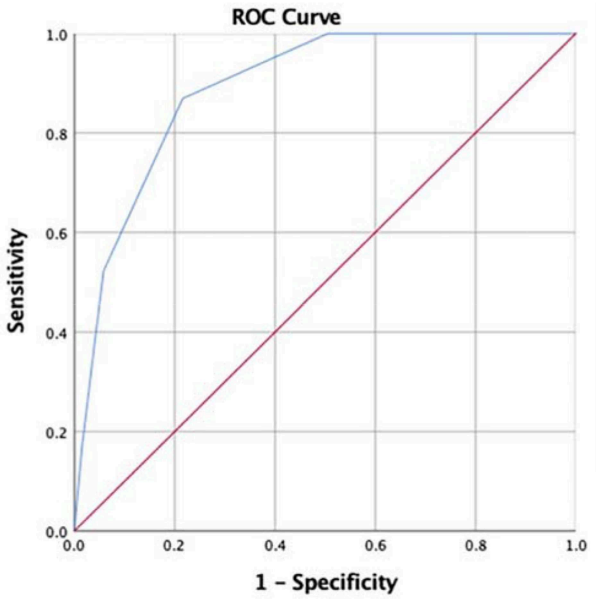

FIGURE 2 | Receiver operating characteristic (ROC) curve of our scoring system for prediction of intravenous immunoglobulin (IVIG) resistance in Kawasaki disease (KD) patients under 1-year old. For the cut-off value of 2 points or more, the sensitivity and specificity were 87.0% and 78.4%, and the area under the curve (AUC) was 0.891 (95% confidence interval 0.837–0.945, $p < 0.001$).

months; (2) gender, male; (3) peripheral WBC $\geq 14.5 \times 10^9$/L; (4) peripheral hemoglobin $\leq$100.5 g/L; (5) peripheral NLR $\geq$ 2.69; (6) peripheral PLR $\geq$ 110.92; (7) peripheral MPVLR $\geq$ 2.78; (8) serum ALT $\geq$ 60 IU/L; (9) serum albumin $\leq$ 30.2 g/L; and (10) serum sodium $\leq$ 135.2 mmol/L. Peripheral NLR, PLR, and MPVLR, and serum albumin and sodium levels were significantly different between the two groups ($P < 0.01$, **Table 2**).

Multivariate Logistic Regression Analysis

Peripheral NLR, PLR, and MPVLR, and serum albumin and sodium were analyzed by multivariate logistic regression. The results indicated that peripheral NLR ($\geq$ 2.69), MPVLR ($\geq$ 2.78), serum albumin ($\leq$ 30.7 g/L), and sodium ($\leq$ 135.2 mmol/L) were independent risk factors for IVIG resistance with OR values of 4.027, 3.860, 3.300, and 3.700, respectively (**Table 3**).

Scoring System for Predicting IVIG Resistance

To construct the predictive scoring system, peripheral NLR ($\geq$2.69), MPVLR ($\geq$2.78), serum albumin ($\leq$30.7 g/L), and serum sodium ($\leq$135.2 mmol/L) were all given 1 point depending upon the proximity of their odds ratio values. The total scores were calculated for each patient with KD. ROC analysis showed that the area under the curve (AUC) was 0.891 (95% confidence interval, 0.837–0.945; $P < 0.001$), and a cut-off score of 2 points or higher yielded the sensitivity of 87.0% and specificity of 78.4% to predict IVIG resistance (**Figure 2**).

TABLE 4 | External validation of predictive scoring system.

Prediction of IVIG resistance		Clinical standard-based outcome, *n* (%)	
		IVIG-resistant	IVIG-responsive
Predictive scoring system-based outcome ($\geq$2 points), *n* (%)	IVIG-resistant	7 (70%)	44 (24.9%)
	IVIG-responsive	3 (30%)	133 (75.1%)

IVIG, intravenous immunoglobulin.

External Validation Studies

One hundred eighty-seven infants were enrolled in the externally validated population. External validation with clinical diagnostic standard showed that a cut-off value of total score of 2 points or higher for predicting the IVIG-resistance yielded a sensitivity of 70.0% and a specificity of 75.1% (**Table 4**).

DISCUSSION

Patients under 1-year of age diagnosed with KD are prone to be resistant to the initial IVIG treatment and develop coronary artery lesions. Our predictive model is the first scoring system for predicting IVIG-resistant patients with KD under 1-year old. The scoring system includes peripheral NLR $\geq$ 2.69 (1 point), peripheral MPVLR $\geq$ 2.78 (1 point), serum albumin $\leq$ 30.7 g/L (1 point) and serum sodium $\leq$ 135.2 mmol/L (1 point), and a total score $\geq$ 2 points yielded a sensitivity and a specificity of 87.0 and 78.4%, respectively, for predicting IVIG-resistance, and in external validation the sensitivity and specificity of predicting IVIG-resistance in KD infants were 70.0% and 75.1%, respectively.

The major pathological changes of KD were systemic vasculitis affecting small and medium-size arteries. Elevated peripheral NLR and MPVLR and decreased serum albumin and sodium represent the severity of inflammation. NLR stands for the ratio of absolute neutrophil count to lymphocyte count in peripheral blood. During systemic inflammation, increased neutrophil production in the bone marrow and circulation into blood, as well as delayed apoptosis, result in neutrophilia. Neutrophils play a critical role in the progression of vascular inflammation by migrating to the site of inflammation and releasing inflammatory cytokines and activating T cells. Meanwhile, accelerated apoptosis results from immunosuppression induced lymphocytopenia (30, 31). In consequence, a high level of peripheral NLR indicates the severity of the clinical course. Peripheral MPVLR represents the ratio of mean platelet volume to lymphocyte count, and high peripheral MPV values have been found in a variety of inflammatory diseases (32). Elevated MPVLR was shown in previous studies to predict the poor prognosis of patients with cardiovascular disease, especially for coronary heart disease (25, 33). This present study is the first to report that high MPVLR ($\geq$2.78) is an independent risk indicator for predicting IVIG resistance in infants with KD under 1-year old.

The mechanisms of hypoalbuminemia consist of the following: first, increased vascular permeability leading to leakage of albumin (34, 35); second, liver dysfunction resulting in decreased albumin synthesis; and third, a lack of essential amino acids due to low nutrient intake or malnutrition, resulting in reduced albumin synthesis (36). IVIG non-responders tend to have more severe vascular leakage and liver damage, inducing lower albumin levels. The cause of hyponatremia is still unknown. Lim et al. found that there was a strong negative correlation between the level of serum sodium and inflammatory factors including c-reactive protein and interleukin-6 (IL-6) in children with KD (37). In addition to KD, studies referring to patients with inflammatory disease such as pneumonia, urinary tract infection, and lupus erythematosus also demonstrated that hyponatremia is an important marker for the severity and prognosis (38–40). The most probable pathophysiological mechanism for hyponatremia is non-osmotic secretion of antidiuretic hormone (ADH). Several studies have confirmed that the release of ADH is promoted by IL-6 and tumor necrosis factor-α (TNF-α) during inflammation (41). IL-6, TNF-α as well as other cytokines participate in inflammation of KD patients in the acute phase (42), suggesting that hyponatremia may be associated with inappropriate release of ADH. The marked increase in plasma IL-6 and TNF-α in IVIG-resistant infants compared with IVIG-responsive patients (43, 44) may explain the significant hyponatremia in IVIG non-responders. More serious inflammatory reactions at the acute phase in IVIG non-responders than in IVIG responders supports our findings that the inflammation-related indicators, including high peripheral NLR and MPVLR, and low serum albumin and sodium, could be used for predicting IVIG-resistant infants with KD under 1-year old effectively.

The indicators in our scoring system for predicting IVIG resistance, which include peripheral NLR and MPVLR and serum albumin and sodium, have significant advantages. They are inexpensive and easy-to-operate as routine examinations. Moreover, the peripheral neutrophil and lymphocyte are less influenced by age during the first 12 months. Our scoring system would have evident practical value for clinical applications due to its relatively high sensitivity and specificity.

There are some limitations to this study. The results may have bias as it was a retrospective study. The sample size was not large enough and a large-scaled external validation of our scoring system will be required in the future. However, the predictive model consisting of peripheral NLR ($\geq$2.69) and MPVLR ($\geq$2.78) and serum albumin ($\leq$30.7 g/L) and sodium ($\leq$135.2 mmol/L) prior to IVIG therapy showed relatively high sensitivity and specificity for the prediction of IVIG-resistant infants with KD under 1-year old.

DATA AVAILABILITY STATEMENT

The raw data supporting the conclusions of this article will be made available by the authors, without undue reservation, to any qualified researcher.

ETHICS STATEMENT

The studies involving human participants were reviewed and approved by the Ethics Committee of Peking University First Hospital and the Ethics Committee of Wuhan Children's Hospital. Written informed consent for participation was not provided by the participants' legal guardians/next of kin because this is a retrospective study.

AUTHOR CONTRIBUTIONS

SW, YLo, YZ, and JD designed the study and analyzed the data. SW, YLo, YLi, YH, YS, CZ, HY, QZ, JQ, YC, XL, and YZ acquired the data. SW and YZ organized the database. SW, SC, and JD drafted the manuscript. YLo, YLi, YS, CZ, HY, QZ, JQ, YC, XL, YZ, and YH read and revised the manuscript. All authors contributed to all study data, write and approved the final version of the manuscript.

REFERENCES

1. Saguil A, Fargo M, Grogan S. Diagnosis and management of Kawasaki disease. *Am Fam Physician.* (2015) 91:365–71.
2. Bayers S, Shulman ST, Paller AS. Kawasaki disease: part II. complications and treatment. *J Am Acad Dermatol.* (2013) 69:513.e1–8; quiz 21–2. doi: 10.1016/j.jaad.2013.06.040
3. Shulman ST, Rowley AH. Kawasaki disease: insights into pathogenesis and approaches to treatment. *Nat Rev Rheumatol.* (2015) 11:475–82. doi: 10.1038/nrrheum.2015.54
4. McCrindle BW, Rowley AH, Newburger JW, Burns JC, Bolger AF, Gewitz M, et al. Diagnosis, treatment, and long-term management of Kawasaki disease: a scientific statement for health professionals from the American Heart Association. *Circulation.* (2017) 135:e927–99. doi: 10.1161/CIR.0000000000000484
5. Kainth R, Shah P. Kawasaki disease: origins and evolution. *Arch Dis Child.* (2019). doi: 10.1136/archdischild-2019-317070. [Epub ahead of print].
6. Research Committee of the Japanese Society of Pediatric Cardiology, Cardiac Surgery Committee for Development of Guidelines for Medical Treatment of Acute Kawasaki Disease. Guidelines for medical treatment of acute Kawasaki disease: report of the research committee of the Japanese society of pediatric cardiology and cardiac surgery (2012 revised version). *Pediatr Int.* (2014) 56:135–58. doi: 10.1111/ped.12317
7. Phuong LK, Curtis N, Gowdie P, Akikusa J, Burgner D. Treatment options for resistant Kawasaki disease. *Paediatr Drugs.* (2018) 20:59–80. doi: 10.1007/s40272-017-0269-6
8. Chen JJ, Ma XJ, Liu F, Yan WL, Huang MR, Huang M, et al. Epidemiologic features of Kawasaki disease in Shanghai from 2008 through 2012. *Pediatr Infect Dis J.* (2016) 35:7–12. doi: 10.1097/INF.0000000000000914
9. Makino N, Nakamura Y, Yashiro M, Kosami K, Matsubara Y, Ae R, et al. Nationwide epidemiologic survey of Kawasaki disease in Japan, 2015–2016. *Pediatr Int.* (2019) 61:397–403. doi: 10.1111/ped.13809
10. Xie LP, Yan WL, Huang M, Huang MR, Chen S, Huang GY, et al. Epidemiologic features of Kawasaki disease in Shanghai from 2013 through 2017. *J Epidemiol.* (2019). doi: 10.2188/jea.JE20190065. [Epub ahead of print].
11. Hua W, Ma F, Wang Y, Fu S, Wang W, Xie C, et al. A new scoring system to predict Kawasaki disease with coronary artery lesions. *Clin Rheumatol.* (2018) 38:1099–107. doi: 10.1007/s10067-018-4393-7
12. Tang Y, Gao X, Shen J, Sun L, Yan W. Epidemiological and clinical characteristics of Kawasaki disease and factors associated with coronary artery

abnormalities in east China: nine years experience. *J Trop Pediatr.* (2016) 62:86–93. doi: 10.1093/tropej/fmv077
13. Kobayashi T, Inoue Y, Takeuchi K, Okada Y, Tamura K, Tomomasa T, et al. Prediction of intravenous immunoglobulin unresponsiveness in patients with Kawasaki disease. *Circulation.* (2006) 113:2606–12. doi: 10.1161/CIRCULATIONAHA.105.592865
14. Kobayashi T, Saji T, Otani T, Takeuchi K, Nakamura T, Arakawa H, et al. Efficacy of immunoglobulin plus prednisolone for prevention of coronary artery abnormalities in severe Kawasaki disease (RAISE study): a randomised, open-label, blinded-endpoints trial. *Lancet.* (2012) 379:1613–20. doi: 10.1016/S0140-6736(11)61930-2
15. Hamada H, Suzuki H, Onouchi Y, Ebata R, Terai M, Fuse S, et al. Efficacy of primary treatment with immunoglobulin plus ciclosporin for prevention of coronary artery abnormalities in patients with Kawasaki disease predicted to be at increased risk of non-response to intravenous immunoglobulin (KAICA): a randomised controlled, open-label, blinded-endpoints, phase 3 trial. *Lancet.* (2019) 393:1128–37. doi: 10.1016/S0140-6736(18)32003-8
16. Egami K, Muta H, Ishii M, Suda K, Sugahara Y, Iemura M, et al. Prediction of resistance to intravenous immunoglobulin treatment in patients with Kawasaki disease. *J Pediatr.* (2006) 149:237–40. doi: 10.1016/j.jpeds.2006.03.050
17. Sano T, Kurotobi S, Matsuzaki K, Yamamoto T, Maki I, Miki K, et al. Prediction of non-responsiveness to standard high-dose gamma-globulin therapy in patients with acute Kawasaki disease before starting initial treatment. *Eur J Pediatr.* (2007) 166:131–7. doi: 10.1007/s00431-006-0223-z
18. Tremoulet AH, Best BM, Song S, Wang S, Corinaldesi E, Eichenfield JR, et al. Resistance to intravenous immunoglobulin in children with Kawasaki disease. *J Pediatr.* (2008) 153:117–21. doi: 10.1016/j.jpeds.2007.12.021
19. Tang Y, Yan W, Sun L, Huang J, Qian W, Ding Y, et al. Prediction of intravenous immunoglobulin resistance in Kawasaki disease in an East China population. *Clin Rheumatol.* (2016) 35:2771–6. doi: 10.1007/s10067-016-3370-2
20. Tan XH, Zhang XW, Wang XY, He XQ, Fan C, Lyu TW, et al. A new model for predicting intravenous immunoglobin-resistant Kawasaki disease in Chongqing: a retrospective study on 5277 patients. *Sci Rep.* (2019) 9:1722. doi: 10.1038/s41598-019-39330-y
21. Yang S, Song R, Zhang J, Li X, Li C. Predictive tool for intravenous immunoglobulin resistance of Kawasaki disease in Beijing. *Arch Dis Child.* (2019) 104:262–7. doi: 10.1136/archdischild-2017-314512
22. Song R, Yao W, Li X. Efficacy of four scoring systems in predicting intravenous immunoglobulin resistance in children with Kawasaki disease in a children's hospital in Beijing, North China. *J Pediatr.* (2017) 184:120–4. doi: 10.1016/j.jpeds.2016.12.018
23. Qian W, Tang Y, Yan W, Sun L, Lv H. A comparison of efficacy of six prediction models for intravenous immunoglobulin resistance in Kawasaki disease. *Ital J Pediatr.* (2018) 44:33. doi: 10.1186/s13052-018-0475-z
24. Kawamura Y, Takeshita S, Kanai T, Yoshida Y, Nonoyama S. The combined usefulness of the neutrophil-to-lymphocyte and platelet-to-lymphocyte ratios in predicting intravenous immunoglobulin resistance with Kawasaki disease. *J Pediatr.* (2016) 178:281–4.e1. doi: 10.1016/j.jpeds.2016.07.035
25. Kurtul A, Acikgoz SK. Usefulness of mean platelet volume-to-lymphocyte ratio for predicting angiographic no-reflow and short-term prognosis after primary percutaneous coronary intervention in patients with ST-segment elevation myocardial infarction. *Am J Cardiol.* (2017) 120:534–41. doi: 10.1016/j.amjcard.2017.05.020
26. Gasparyan AY, Ayvazyan L, Mukanova U, Yessirkepov M, Kitas GD. The platelet-to-lymphocyte ratio as an inflammatory marker in rheumatic diseases. *Ann Lab Med.* (2019) 39:345–57. doi: 10.3343/alm.2019.39.4.345
27. Yuan YD, Sun J, Li PF, Wei CL, Yu YH. Values of neutrophil-lymphocyte ratio and platelet-lymphocyte ratio in predicting sensitivity to intravenous immunoglobulin in Kawasaki disease. *Zhongguo Dang Dai Er Ke Za Zhi.* (2017) 19:410–3. doi: 10.7499/j.issn.1008-8830.2017.04.010
28. Hua W, Sun Y, Wang Y, Fu S, Wang W, Xie C, et al. A new model to predict intravenous immunoglobin-resistant Kawasaki disease. *Oncotarget.* (2017) 8:80722–9. doi: 10.18632/oncotarget.21083
29. Newburger JW, Takahashi M, Gerber MA, Gewitz MH, Tani LY, Burns JC, et al. Diagnosis, treatment, and long-term management of Kawasaki disease: a statement for health professionals from the committee on rheumatic fever, endocarditis and Kawasaki disease, council on Cardiovascular disease in the Young, American Heart Association. *Circulation.* (2004) 110:2747–71. doi: 10.1161/01.CIR.0000145143.19711.78
30. Zahorec R. Ratio of neutrophil to lymphocyte counts–rapid and simple parameter of systemic inflammation and stress in critically ill. *Bratisl Lek Listy.* (2001) 102:5–14.
31. Hwang SY, Shin TG, Jo IJ, Jeon K, Suh GY, Lee TR, et al. Neutrophil-to-lymphocyte ratio as a prognostic marker in critically-ill septic patients. *Am J Emerg Med.* (2017) 35:234–9. doi: 10.1016/j.ajem.2016.10.055
32. Korniluk A, Koper-Lenkiewicz OM, Kaminska J, Kemona H, Dymicka-Piekarska V. Mean platelet volume (MPV): new perspectives for an old marker in the course and prognosis of inflammatory conditions. *Mediat Inflamm.* (2019) 2019:9213074. doi: 10.1155/2019/9213074
33. Hudzik B, Szkodzinski J, Lekston A, Gierlotka M, Polonski L, Gasior M. Mean platelet volume-to-lymphocyte ratio: a novel marker of poor short- and long-term prognosis in patients with diabetes mellitus and acute myocardial infarction. *J Diabetes Complications.* (2016) 30:1097–102. doi: 10.1016/j.jdiacomp.2016.04.010
34. Kuo HC, Liang CD, Wang CL, Yu HR, Hwang KP, Yang KD. Serum albumin level predicts initial intravenous immunoglobulin treatment failure in Kawasaki disease. *Acta Paediatr.* (2010) 99:1578–83. doi: 10.1111/j.1651-2227.2010.01875.x
35. Soeters PB, Wolfe RR, Shenkin A. Hypoalbuminemia: pathogenesis and clinical significance. *JPEN J Parenter Enteral Nutr.* (2019) 43:181–93. doi: 10.1002/jpen.1451
36. Arques S. Human serum albumin in cardiovascular diseases. *Eur J Intern Med.* (2018) 52:8–12. doi: 10.1016/j.ejim.2018.04.014
37. Lim GW, Lee M, Kim HS, Hong YM, Sohn S. Hyponatremia and syndrome of inappropriate antidiuretic hormone secretion in kawasaki disease. *Korean Circ J.* (2010) 40:507–13. doi: 10.4070/kcj.2010.40.10.507
38. Park SW, Shin SM, Jeong M, Cho DH, Lee KH, Eisenhut M, et al. Hyponatremia in children with respiratory infections: a cross-sectional analysis of a cohort of 3938 patients. *Sci Rep.* (2018) 8:16494. doi: 10.1038/s41598-018-34703-1
39. Park SJ, Oh YS, Choi MJ, Shin JI, Kim KH. Hyponatremia may reflect severe inflammation in children with febrile urinary tract infection. *Pediatr Nephrol.* (2012) 27:2261–7. doi: 10.1007/s00467-012-2267-9
40. Il Shin J, Park SJ, Suh CH, Lee GH, Hur MW, Han SY, et al. Hyponatremia in patients with systemic lupus erythematosus. *Sci Rep.* (2016) 6:25566. doi: 10.1038/srep25566
41. Kim JH, Park JH, Eisenhut M, Yu JW, Shin JI. Inflammasome activation by cell volume regulation and inflammation-associated hyponatremia:a vicious cycle. *Med Hypotheses.* (2016) 93:117–21. doi: 10.1016/j.mehy.2016.05.018
42. Agarwal S, Agrawal DK. Kawasaki disease: etiopathogenesis and novel treatment strategies. *Expert Rev Clin Immunol.* (2017) 13:247–58. doi: 10.1080/1744666X.2017.1232165
43. Hu P, Jiang GM, Wu Y, Huang BY, Liu SY, Zhang DD, et al. TNF-alpha is superior to conventional inflammatory mediators in forecasting IVIG nonresponse and coronary arteritis in Chinese children with Kawasaki disease. *Clin Chim Acta.* (2017) 471:76–80. doi: 10.1016/j.cca.2017.05.019
44. Wu Y, Liu FF, Xu Y, Wang JJ, Samadli S, Wu YF, et al. Interleukin-6 is prone to be a candidate biomarker for predicting incomplete and IVIG nonresponsive Kawasaki disease rather than coronary artery aneurysm. *Clin Exp Med.* (2019) 19:173–81. doi: 10.1007/s10238-018-00544-5

Conflict of Interest: The authors declare that the research was conducted in the absence of any commercial or financial relationships that could be construed as a potential conflict of interest.

frontiers in Pediatrics

CASE REPORT
published: 17 December 2019
doi: 10.3389/fped.2019.00506

Transcatheter Closing Atrial Septal Defect in a Child With Hereditary Spherocytosis

Zhixian Ji†, Na Liu†, Zhanhui Du, Gang Luo, Zhen Bing, Quansheng Xing and Silin Pan**

Heart Center, Qingdao Women and Children's Hospital, Qingdao University, Qingdao, China

A 3-year-old girl was admitted to our hospital for the correction of atrial septal defect (ASD). Open heart operation with cardiopulmonary bypass is dangerous because the patient also had hereditary spherocytosis, which put her at risk for hemolytic anemia. Therefore, percutaneous transcatheter closure for ASD was chosen and performed successfully, which avoided the erythrocyte damage caused by cardiopulmonary bypass. This is the first time such a case has been reported, and we present an alternative approach for ASD with hereditary spherocytosis.

Keywords: atrial septal defect, hereditary spherocytosis, percutaneous transcatheter closure, cardiopulmonary bypass, hemolysis

OPEN ACCESS

Edited by:
Hongfang Jin,
Peking University First Hospital, China

Reviewed by:
Mingguo Xu,
Shenzhen Children's Hospital, China
Ju Liu,
Shandong University, China

****Correspondence:***
Quansheng Xing
xingqs0532@163.com
Silin Pan
silinpan@126.com

†These authors have contributed equally to this work

Specialty section:
This article was submitted to Pediatric Cardiology, a section of the journal Frontiers in Pediatrics

Received: *20 October 2019*
Accepted: *22 November 2019*
Published: *17 December 2019*

Citation:
Ji Z, Liu N, Du Z, Luo G, Bing Z, Xing Q and Pan S (2019) Transcatheter Closing Atrial Septal Defect in a Child With Hereditary Spherocytosis. Front. Pediatr. 7:506. doi: 10.3389/fped.2019.00506

INTRODUCTION

Hereditary spherocytosis (HS) is a genetic blood disease characterized by hemolysis, anemia, jaundice, and splenomegaly (1). Atrial septal defect (ASD) is one of most common congenital heart defects (2). However, concomitant ASD and HS is rare. Patient with HS undergoing traditional open heart surgery has a high risk of perioperative hemolysis and secondary renal dysfunction because of the deleterious effects of cardiopulmonary bypass (CPB) (3).

At present, transcatheter closure of ASD has been accepted worldwide as an alternative to surgical closure due to the ease of interventional therapy and the often increased perioperative risk from surgery (4, 5). There is no published report about children with HS undergoing interventional closure for structural heart disease. Here, we reported a case of a 3-year-old girl manifested with ASD and HS undergoing transcatheter ASD closure.

CASE REPORT

The patient was brought to the heart center of our hospital after a diagnosis of ASD and HS. The patient had been suffering from repeated attacks of hemolytic anemia since she was born. She was intermittently treated in the local hospitals for 2 years with the medicine "Yinzhihuang" (a traditional Chinese Medicine), L-carnitine, Vitamin B12, etc., and her hemoglobin level was maintained at 90 g/L with normal liver function. The patient presented to a local hospital 2 years ago because of the upper respiratory tract infection, and was found to have a heart murmur during the physical examination. The followed echocardiographic examination revealed an ASD, and the patient was suggested to go to check-up regularly. One month ago, the patient was sent to the local hospital for anemia and was diagnosed with HS based on the laboratory findings of the patient's blood smear and the osmotic fragility test. Then, the patient was introduced to our hospital for further treatments.

On admission, the patient was anemic and icteric. She weighed 14.5 kg. Physical examination revealed a systolic ejection murmur at the left second intercostal space and hepatosplenomegaly. Laboratory findings showed a hemoglobin level of 82 g/L, and red blood cell (RBC) count of 3.26×10^{12}/L. The total serum bilirubin was 89.4 μM, direct bilirubin was 11.8 μM,

and indirect bilirubin was 77.6 μM. Elevations of the liver enzymes were not found. A peripheral blood smear revealed RBC size disparity and the presence of spherocytes (12%, **Figure 1**). RBC osmotic fragility was increased (hemolysis began at 0.55% NaCl and was complete at 0.50% NaCl). Additionally, a bone marrow examination was done, which showed erythroblastic hyperplasia dominated with rubricyte and metarubricyte. Echocardiography showed a left to right shunt, enlargement of right atrium and right ventricle, dilatation of main pulmonary artery, and fossa ovalis ASDs.

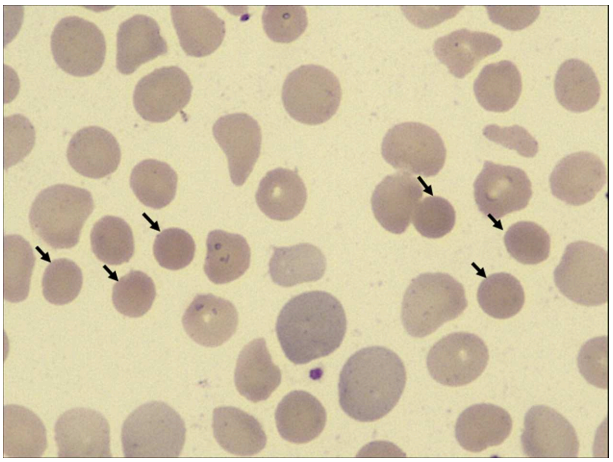

FIGURE 1 | High-power view (×100 magnification) of peripheral blood smears from the patient. Spherocytes are indicated by black arrows.

Concomitant ASD and HS is rare. Surgical intervention for ASD using CPB might exacerbate hemolysis and subsequent renal dysfunction because of the deleterious effects of CPB. Therefore, we consulted the hematologist and cardiac surgeons, and got a unanimous decision to perform transcatheter closure of ASD for the patient. Her parents were informed of the purpose and risk of the treatment, and written informed consent was obtained before intervention operation.

Percutaneous transcatheter closure of ASD was performed under general anesthesia. Echocardiography showed that the diameter of ASD was 14 × 10 mm (**Figures 2A,B**). The whole process of cardiac catheterization was smooth, and a 16-mm ASD occluder was placed through 8F delivery sheath (**Figures 2C,D**). From the first day of operation, sodium bicarbonate (2 ml/kg) was given daily to alkaline blood for 3 days and aspirin (3 mg/kg/day) was taken orally for 6 months. Multiple retests of blood routine and urine analysis had been undertaken after closure, and the results showed no decrease in hemoglobin and the results of urine analysis were normal. Echocardiography showed that the location of occluder was fixed and there was no pericardial effusion. Gradually, the patient recovered and was discharged from the hospital. One-month follow-up result showed that the level of hemoglobin remained stable and no hemoglobinuria occurred. Echocardiography showed no residual ASD and a normal state of heart function.

DISCUSSION

HS is a genetic, frequently familial hemolytic blood disease (1). One of the major concerns for children with HS undergoing open-heart surgery for congenital heart disease is accentuation

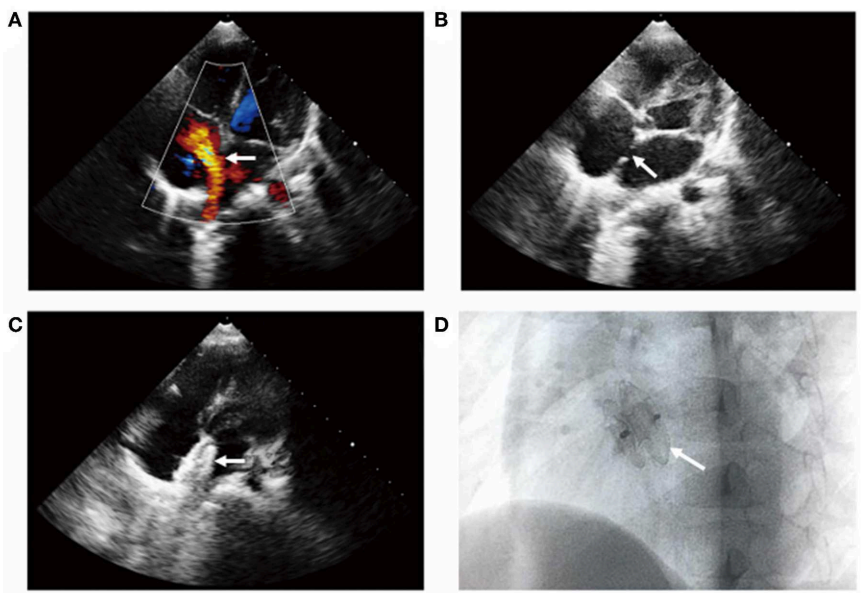

FIGURE 2 | Transcatheter closure of ASD shown by transthoracic color Doppler echocardiography. The apical four-chamber section showed **(A)** left to right shunt at the level of atrial septum, **(B)** the continuous interruption of the atrial septum with a loss of about 14 mm, and **(C)** the atrial septal occluder was well-positioned without residual shunt (see arrow). **(D)** X-ray examination of left anterior oblique position after interventional closure showed that the occluder was fixed and the shape was normal (see arrow).

of the risk of perioperative hemolysis. Several patients with HS undergoing open-heart surgery under CPB have been reported so far (3, 6–10). Based on previous reports, cardiac surgery has been successfully performed in all the patients. However, the potential worsening concern from CPB in HS and trauma from open-heart surgery is a big problem. A variety of approaches have been proposed for HS patients to avoid hemolysis during surgery, such as preemptive splenectomy (7). Although splenectomy is an effective treatment for reducing hemolysis, it has a high risk of infection in children under 2 years of age (10, 11). Because our patient was only 3 years old, it was not recommended to undergo splenectomy before cardiac surgery in order to maintain her immune function.

In the last 20 years, ASD transcatheter occlusion technique has been accepted worldwide as an alternative to surgery for its major advantages, such as the short hospital stay as well as evading thoracotomy, CPB, intensive care, and long scars (4, 5). Though there is also a risk of hemolysis after transcatheter closure, most scholars believe that there will be no damage to RBCs due to the hemodynamic characteristics of ASD (3). The pressure gradient between the left atrium and right atrium is small, which usually does not produce high-speed blood flow and high shear force, even if there is a small residual shunt after closure. According to the conclusion discussed by our heart center experts, the first choice for the patient to close ASD was interventional therapy by cardiac catheterization. The most important thing was to choose the appropriate occluder to avoid the use of large ASD occluder (12). The measures for preventing hemolysis and corresponding treatment were formulated in detail, and sodium bicarbonate and rehydration were used for the treatment of hydrated alkali on the day after catheterization. The level of hemoglobin and the state of heart function were observed closely. If there was severe anemia, hemolysis, and deterioration of cardiac function, aspirin could be discontinued. High dose of steroid could be used to stabilize cell membrane. If necessary, surgical removal of occluder and even splenectomy would be performed (13). The hemoglobin level of the patient was maintained at about 90 g/L, and the hematocrit was maintained at about 30%. No obvious extravascular hemolysis occurred. Additionally, there have been reported cases of HS that could lead to congestive heart failure (14). Hence, the patient still need close follow-up of the degree of hemolytic anemia and the station of cardiac function.

In conclusion, an extremely rare condition of having both ASD and HS in a same patient and successful therapeutic interventions by cardiac catheterization has been reported.

DATA AVAILABILITY STATEMENT

The raw data used to support the findings of this study are available from the corresponding author upon request.

ETHICS STATEMENT

Written informed consent was obtained from patient's parents for publication of this case report and any potentially identifying information.

AUTHOR CONTRIBUTIONS

ZJ and NL drafted the initial manuscript. ZD, GL, and ZB collected the samples, clinical data, and analyzed the data. QX and SP conceived and designed the study, and revised the manuscript.

FUNDING

This work was supported by grants from National Natural Science Foundation of China (81770316) and Taishan Scholars Project of Shandong Province (2017).

REFERENCES

1. Perrotta S, Gallagher PG, Mohandas N. Hereditary spherocytosis. *Lancet*. (2008) 372:1411–26. doi: 10.1016/s0140-6736(08)61588-3
2. Vyas-Read S, Guglani L, Shankar P, Travers C, Kanaan U. Atrial septal defects accelerate pulmonary hypertension diagnoses in premature infants. *Front Pediatr*. (2018) 6:342. doi: 10.3389/fped.2018.00342
3. Matsuzaki Y, Tomioka H, Saso M, Azuma T, Saito S, Aomi S, et al. Open-heart surgery using a centrifugal pump: a case of hereditary spherocytosis. *J Cardiothorac Surg*. (2016)11:138. doi: 10.1186/s13019-016-0534-8
4. Butera G, De Rosa G, Chessa M, Rosti L, Negura DG, Luciane P, et al. Transcatheter closure of atrial septal defect in young children: results and follow-up. *J Am Coll Cardiol*. (2003) 42:241–5. doi: 10.1016/s0735-1097(03)00589-8
5. Zanjani KS, Zeinaloo A, Malekan-Rad E, Kiani A, Bagheri MM. Transcatheter atrial septal defect closure under transthorasic echocardiography in children. *Iran J Pediatr*. (2011) 21:473–8.
6. deLeval MR, Taswell HF, Bowie EJ, Danielson GK. Open heart surgery in patients with inherited hemoglobinopathies, red cell dyscrasias, and coagulopathies. *Arch Surg*. (1974) 109:618–22. doi: 10.1001/archsurg.1974.01360050016005
7. Gayyed NL, Bouboulis N, Holden MP. Open heart operation in patients suffering from hereditary spherocytosis. *Ann Thorac Surg*. (1993) 55:1497–500. doi: 10.1016/0003-4975(93)91097-7
8. Aoyagi S, Kawano H, Tomoeda H, Hiratsuka R, Kawara T. Open heart operation in a patient with hereditary spherocytosis: a case report. *Ann Thorac Cardiovasc Surg*. (2001) 7:375–7.
9. Dal A, Kumar RS. Open heart surgery in presence of hereditary spherocytosis. *J Cardiovasc Surg*. (1995) 36:447–8.
10. Kawahira Y, Kishimoto H, Iio M, Ikawa S, Ueda H, Kayatani F, et al. Open heart operation in a young child with spherocytosis. *Ann Thorac Surg*. (1994) 58:1166–8. doi: 10.1016/0003-4975(94)90481-2
11. Bolton-Maggs PH, Stevens RF, Dodd NJ, Lamont G, Tittensor P, King MJ. Guidelines for the diagnosis and management of hereditary spherocytosis. *Br J Haematol*. (2004) 126:455–74. doi: 10.1111/j.1365-2141.2004.05052.x
12. Rana BS. Echocardiography guidance of atrial septal defect closure. *J Thorac Dis*. (2018) 10:S2899–908. doi: 10.21037/jtd.2018.07.126
13. Das A, Bansal D, Das R, Trehan A, Marwaha RK. Hereditary spherocytosis in children: profile and post-splenectomy outcome. *Indian Pediatr*. (2014) 51:139–41.doi: 10.1007/s13312-014-0348-5

14. Alter P, Maisch B. Non-compaction cardiomyopathy in an adult with hereditary spherocytosis. *E J Heart Fail.* (2007) 9:98–9. doi: 10.1016/j.ejheart.2006.03.008

Conflict of Interest: The authors declare that the research was conducted in the absence of any commercial or financial relationships that could be construed as a potential conflict of interest.

frontiers in Pediatrics

ORIGINAL RESEARCH
published: 14 February 2020
doi: 10.3389/fped.2020.00024

Kawasaki Disease in Children Older Than 10 Years: A Clinical Experience From Northwest India

Ankur Kumar Jindal[1†], Rakesh Kumar Pilania[1†], Sandesh Guleria[1], Pandiarajan Vignesh[1], Deepti Suri[1], Anju Gupta[1], Manphool Singhal[2], Amit Rawat[1] and Surjit Singh[1]*

[1] Allergy Immunology Unit, Department of Pediatrics, Advanced Pediatrics Centre, Postgraduate Institute of Medical Education and Research (PGIMER), Chandigarh, India, [2] Department of Radiodiagnosis and Imaging, Postgraduate Institute of Medical Education and Research (PGIMER), Chandigarh, India

Background: Kawasaki disease (KD) is predominantly seen in young children (<5 years). Diagnosis of KD is often delayed in older children and adolescents, leading to a higher risk of coronary artery abnormalities (CAAs). There is a paucity of literature on KD in older children.

Methods: Data were collated from a review of records of patients diagnosed with KD who were aged ≥10 years at the time of diagnosis, during the period from January 1994 to June 2019.

Results: Eight hundred and sixty five patients were diagnosed with KD during this period. Of these, 46 (5.3%; 26 boys and 20 girls) were aged 10 years or older at the time of diagnosis. The median age at diagnosis was 11 years (range of 10–30 years). The median interval between the of fever and the diagnosis of KD was 12 days (range of 4–30 days). Eight patients (17.4%) presented with hypotensive shock. Coronary artery abnormalities (CAAs) were seen in six patients (13.04%), and three patients had myocarditis. Patients with CAAs were found to have significantly higher median platelet counts and higher median C-reactive protein levels. First-line treatment included intravenous immunoglobulin. Adjunctive therapy was given in five patients (infliximab in four patients and steroids in one patient). The median time between the onset of fever and the administration of IVIg was 13.5 days (range of 6–2). The total duration of follow up is 2,014.5 patient-months.

Conclusion: Diagnosis of KD in children older than 10 years is usually delayed, and these patients are thus at a higher risk of CAAs.

Keywords: adolescents, coronary artery abnormalities, intravenous immunoglobulin, Kawasaki disease, older children

OPEN ACCESS

Edited by:
Hongfang Jin,
Peking University First Hospital, China

Reviewed by:
Elumalai Appachi,
Baylor College of Medicine, United States
Mingguo Xu,
Shenzhen Children's Hospital, China

***Correspondence:**
Surjit Singh
surjitsinghpgi@rediffmail.com

[†]These authors have contributed equally to this work and share first authorship

Specialty section:
This article was submitted to Pediatric Cardiology, a section of the journal Frontiers in Pediatrics

Received: *07 August 2019*
Accepted: *17 January 2020*
Published: *14 February 2020*

Citation:
Jindal AK, Pilania RK, Guleria S, Vignesh P, Suri D, Gupta A, Singhal M, Rawat A and Singh S (2020) Kawasaki Disease in Children Older Than 10 Years: A Clinical Experience From Northwest India. Front. Pediatr. 8:24. doi: 10.3389/fped.2020.00024

INTRODUCTION

Kawasaki disease (KD), a medium vessel vasculitis, is commonly seen in children below the age of 5. Cardiac involvement in the form of coronary artery abnormalities (CAAs) is the most significant long-term complication of KD (1, 2). In developed countries, KD is the most common cause of acquired heart disease in children. Even in developing countries, KD is now being increasingly reported, and it is emerging as one of the leading causes of acquired heart disease in children

(3–5). However, no age group seems to be exempt from developing KD, and this disease can at times affect adolescents and adults as well. Diagnosis of KD often gets missed in these age groups, as many physicians may not consider KD an upfront clinical possibility in a febrile patient. This often leads to delays in diagnosis and initiation of therapy, thereby increasing the risk of developing CAAs (6).

Manlhiot et al. reported a higher incidence of CAAs in adolescents with KD, as compared to children ages 1–9 years (6). A similar study published in Indonesia found that adolescents with KD often had incomplete forms of the disease and had a higher risk of CAAs (7). A recent Japanese survey of KD, administered nationwide, has shown that 1.2% of all patients with KD were aged more than 10 years (8).

There is a paucity of literature on the clinical profile and cardiac complications of KD in adolescents and adults, especially from developing countries. We herein report our experience of KD in older patients over the last 25 years.

PATIENTS AND METHODS

Data were collated from a review of records for patients diagnosed with KD who were aged >10 years at the time of diagnosis during the period of January 1994 to June 2019 in the Pediatric Allergy Immunology Unit, Advanced Pediatrics Centre, Postgraduate Institute of Medical Education and Research (PGIMER), Chandigarh, India. Our center is a tertiary care, not-for-profit, federally funded institute in Northwest India.

Case files of patients were retrieved and clinical details were recorded on a predesigned proforma. The study was approved by the Departmental Review Board and Institute Ethics Committee. The diagnosis of KD was based on guidelines given by the American Heart Association (AHA) (1, 9). Laboratory investigations that were carried out in these patients included acute phase reactants (complete blood count, erythrocyte sedimentation rate [ESR], C-reactive protein [CRP]), urine examination, biochemistry work-up (blood urea, serum creatinine, and liver function tests), chest radiograph, and an electrocardiogram (depending on clinical requirements). 2D-echocardiography was usually performed at admission, and then again on follow up after 4–8 weeks. CAAs were initially classified based on absolute coronary artery dimensions. Since 2015, we have been using body-surface-area-based "Z" scores for the purpose of classifying the severity of CAAs. Use of 128-slice dual source computed tomography coronary angiography (CTCA) was initiated in 2014, and this imaging modality has been performed in select patients who had large or unusual CAAs, or where the visualization of coronaries was difficult because of a thick chest wall (10). Assay of serum N-terminal pro-brain natriuretic peptide (NT-proBNP) levels was initiated in our laboratory in 2014 (11).

Patients were managed using standard treatment guidelines as given by the AHA (1, 9). Intravenous immunoglobulin (IVIg−2 g/kg) given over 12–24 h was used as first-line therapy, along with oral aspirin [initially in anti-inflammatory doses (30–50 mg/kg/day) followed by antiplatelet doses (3–5 mg/kg/day)]. IVIg was not given to patients who were afebrile at presentation and who had presented late after acute stage of illness when inflammatory parameters had normalized. Adjunctive therapy (infliximab or corticosteroids) was used in selected patients with IVIg resistance or significant myocardial dysfunction.

RESULTS

Clinical Profile

Eight hundred and sixty five patients were diagnosed to have KD during this period. Of these, 46 (5.3%; 26 boys and 20 girls) were aged 10 years or more at time of diagnosis (**Table 1**, **Figure 1**). The median age at diagnosis was 11 years (range 10–30 years). All patients had a fever at presentation, and the median duration of a fever was 10 days (range 2–30 days). The median interval between the onset of fever and diagnosis of KD was 12 days (range 4–30). Eight patients (17.4%) presented with hypotensive shock. Pulmonary presentation was seen in 4 out of 46 (8.7%) patients in this group. All four patients with pulmonary presentation had pneumonia with synpneumonic effusion. Nine children (19.6%) developed arthritis. Infection-triggered KD was seen in 10 (21.7%) patients—*Staphylococcus aureus* in three patients, *Streptococcus pneumoniae* in one patient, *Mycobacterium tuberculosis* in one patient, *Pseudomonas aeruginosa* in one patient, Mycoplasma in one patient, *Burkholderia cepacia* in one patient, and *Klebsiella pneumoniae* in one patient. One patient had pyogenic skin and soft infection, but no microorganism could be isolated. BCG scar reactivation was observed in one patient.

TABLE 1 | Clinical features of children with Kawasaki disease (KD) aged ≥10 years at the time of diagnosis.

Patient characteristics	Results
Median age at diagnosis (range), years	11 (10-30)
Sex	Male: 26; Female: 20
Fever	46/46 (100%)
Median duration of fever	10 (2-30)
Day of diagnosis (days)	12 (4-30)
Rash	34/46 (73.9%)
Oral cavity and mucosal changes	36/46 (78.3%)
Conjunctival redness	29/46 (63%)
Cervical lymphadenopathy	28/46 (60.9%)
Dorsal edema	11/46 (23.9%)
Periungual desquamation	45/46 (97.8%)
Day of desquamation (days)	10 (5-20)
Irritability	3/46 (6.5%)
Arthritis	9/46 (19.6%)
Hypotensive shock	8/46(17.4%)
Sterile pyuria	6/46 (13%)
Pulmonary manifestations	4/46 (8.7%)
Significant myocardial dysfunction	3/46 (6.5%)
Infection-triggered KD	10/46 (21.7%)

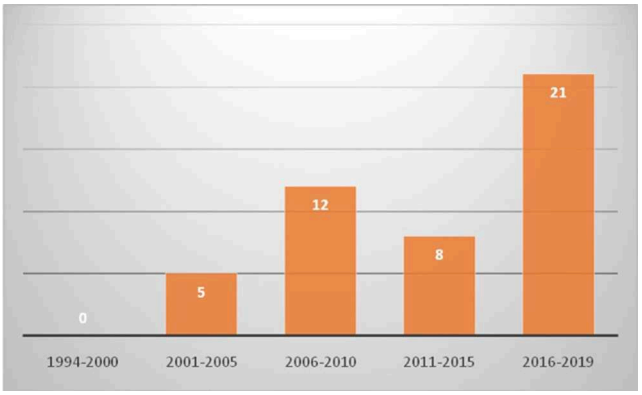

FIGURE 1 | Trends of diagnosis of Kawasaki disease in children aged 10 years or older in Chandigarh, India (1994–2019) [x axis shows years and y axis shows number of cases].

TABLE 2 | Laboratory investigations.

Characteristics	Results
Hemoglobin (g/L); Mean ± SD	106.7 ± 18.3
White blood cell counts ($\times 10^9$/L); Median (range)	13.45 (2.20–38.65)
Platelet counts at admission ($\times 10^9$/L); Median (range)	333 (21.5, 1121)
Maximum platelet counts ($\times 10^9$/L); Median (range)	541 (183, 1470)
Erythrocyte sedimentation rate (mm/hour); Median (range)	42.5 (2, 118)
C-reactive protein (<6 mg/L); Median (range)	43 (1.24, 269)
Procalcitonin (<0.50 ng/mL); Median (range)	1.18 (0.05, 33)
Aspartate transaminase (<40 U/L); Median (range)	37 (9, 585)
Alanine transaminase (<41 U/L); Median (range)	36.5 (7, 866)
Serum albumin (mg/dL); Mean ± SD	3.07 ± 0.70
Sterile pyuria, *n* (%)	6/42 (14.3%)

TABLE 3 | Treatment details.

Characteristics	*n* = 46 (%)
Treatment with IVIg	39/46 (84.7%)
Adjunctive treatment	5/46 (10.9%)
(i) Infliximab	3 (6.5%)
(ii) Second dose of IVIg and infliximab	1 (2.2%)
(iii) Methylprednisolone pulse followed by tapering doses of prednisolone	1 (2.2%)

IVIg, intravenous immunoglobulin.

Laboratory Characteristics

Laboratory investigations of patients at the time of diagnosis are shown in **Table 2**. The mean hemoglobin concentration was 106.7 ± 18.3 g/L. The median value of maximum platelet count was 541 × 10^9/L. Five patients had thrombocytopenia at time of presentation, and of these, two patients had CAAs and one patient had low ejection fraction. Median ESR and CRP were 42.5 mm in the first hour and 43 mg/L, respectively. Aspartate (AST) and alanine transaminase (ALT) values were available in 41 and 39 patients, respectively. AST and ALT values were elevated in 18 out of 41 patients (43.9%) and 18 out of 39 (46.2%) patients, respectively. Most patients had mild elevation in transaminases (i.e., <2 times). Six patients had significant elevations in transaminases, and of these, one patient had levels more than 10 times the normal level. Transaminase levels normalized after treatment. We were able to monitor serum procalcitonin in 14 patients, and median levels were 1.18 ng/mL (range 0.05–33) (Normal <0.5). Nine out of fourteen patients (64.3%) had elevated procalcitonin value, and of these, four had infection-triggered KD. In 21 patients, we were able to perform NT-pro-BNP, and the median value was 225 pg/mL (range 29–9,435) (Normal < 125). NT-pro-BNP values were found to be elevated in 16 out of 21 (76.2%) patients.

Cardiac Complications

CAAs were seen in six (13.04%) patients: two had isolated left main coronary artery (LMCA) aneurysms; one had isolated left anterior descending artery (LAD) aneurysms; one had LAD and right coronary artery (RCA) aneurysms; one had aneurysms in LMCA, LAD, and RCA; and one had aneurysms in all four coronary arteries. Frequency of involvement of coronary arteries was as follows: LMCA−4 out of 12 (33.3%); LAD−4 out of 12 (33.3%); RCA−3 out of 12 (25%); and left circumflex coronary artery (LCx)−1 out of 12 (8.3%). Giant aneurysms were seen in two patients—one had involvement of the LAD and RCA, while the other had involvement of the LAD, RCA, and LCx. Three patients had severe myocardial dysfunction secondary to myocarditis. One patient had a stormy course of illness and developed ventricular premature complexes, severe myocarditis, pericardial effusion with tamponade; this patient required a pleuro-pericardial window.

Treatment

Median time between onset of fever and administration of IVIg was 13.5 days (range 6–32 days). Seven patients were not offered treatment, as they had presented late in convalescent phase when the fever had subsided, inflammatory markers had settled, and 2D-echocardiography was normal. Adjunctive therapy was required in five patients (repeat IVIg and infliximab in one; infliximab alone in three; and methylprednisolone in one) (**Table 3**). Total duration of follow up was 2,014.5 patient-months. Five patients were not on regular follow up at time of this analysis. However, none of them had developed CAAs during the acute phase. No mortality was seen in this cohort, and none of the patients with CAAs developed thrombosis or acute coronary artery events on follow up.

We compared the clinical profile of patients with and without CAAs (**Table 4**). Patients with CAAs were found to have significantly higher median maximum platelet count and higher median CRP. Pulmonary presentation was significantly more common in patients with CAAs, and these patients required adjunctive therapy more commonly. Although the median time between onset of fever and diagnosis of KD was relatively higher in patients with CAAs as compared to those without CAAs (14.5 days vs. 12 days), the difference was not statistically

TABLE 4 | Comparison of clinical and laboratory features of patients of Kawasaki disease (KD) with and without coronary artery abnormalities (CAAs).

Characteristics	KD without CAAs ($n = 40$)	KD with CAAs ($n = 6$)	*p*-value
Interval between onset of fever and diagnosis (days), Median (IQR)	12 (10,20)	14.5 (6, 15.5)	0.53
Hypotensive shock, *n* (%)	7/40 (17.5%)	1/6 (16.7%)	0.96
Arthritis, *n* (%)	8/40 (20%)	0	0.23
Infections, *n* (%)	9/40 (22.5%)	2/6 (33.3%)	0.56
Pulmonary presentation, *n* (%)	2/40 (5%)	3/6 (50%)	**0.001**
Diarrhea, *n* (%)	8/40 (20%)	1/6 (16.7%)	0.82
Hemoglobin (g/L), Mean ± SD	102.5 ± 13.5	107.4 ± 18.9	0.458
Total leucocyte count ($\times 10^9$/L), Median (IQR)	12.7 (8.67, 18.4)	15.9 (13.7, 23.8)	0.09
Platelet counts at admission ($\times 10^9$/L), Median (IQR)	333.0 (233.0, 464.7)	359.5 (103.7, 931.3)	1.00
Thrombocytopenia at admission ($<150 \times 10^9$/L), *n* (%)	3/40 (7.5%)	2/6 (33.3%)	0.06
Maximum recorded platelet count ($\times 10^9$/L), Median (IQR)	502.0 (409.0, 649.0)	817.5 (635.2, 994.5)	**0.04**
Erythrocyte sedimentation rate (mm/hour), Median (IQR)	36 (20.5, 60.0)	59 (44.3, 77.3)	0.18
C-reactive protein (mg/L), Median (IQR)	40.0 (6.59, 64.5)	115.0 (48.5, 249.0)	**0.05**
Albumin (g/L), Mean ± SD	2.81 ± 0.75	3.12 ± 0.70	0.337
Aspartate transaminase (U/L), Median (IQR)	34 (24.0, 51.0)	76.0 (32.3, 82.3)	0.13
Alanine transaminase (U/L), Median (IQR)	35 (29.5, 64.7)	51.0 (26.3, 67.0)	0.66
NT-Pro BNP (pg/mL), Median (IQR)	225.0 (122.2, 600.0)	231.5 (116.3, 447.3)	0.788
Adjunctive therapy, *n* (%)	2/40 (5%)	3/6 (50%)	**0.001**
Day of administration of IVIg, Median (IQR)	13.5 (10.8, 21.3)	15.0 (10.3, 17.0)	0.743

CAAs, coronary artery abnormalities; IQR, interquartile range; IVIg, intravenous immunoglobulin; pg, pictogram; KD, Kawasaki disease; NT-Pro BNP, N-terminal pro-brain natriuretic peptide; SD, standard deviation. Bold values indicate p value < 0.05.

significant. Thrombocytopenia during the acute stage of KD was also found to be more common in patients with CAAs. All other clinical features and laboratory findings were similar in the two groups.

DISCUSSION

KD is the most common childhood vasculitis, and it usually affects children below the age of 5. Diagnosis of KD at extremes of age can, however, pose several diagnostic and therapeutic problems. We, along with others, have previously reported our experience of KD in infants below 6 months of age (12, 13). These studies have shown that infants with KD are at a high risk of developing CAAs despite timely diagnosis and treatment. Incomplete forms of KD are also very common in this age group (12, 13).

Diagnosis of KD in older children and adolescents is often challenging, as the treating physician may not consider this condition during their differential diagnosis of a febrile child. There is a paucity of literature on the clinical presentation of KD in older children and adolescents from developing countries. Manlhiot et al. have recently published their experience on KD occurring in extremes of age and have shown that 6% of patients in their cohort were aged 9 years or older—making their findings similar to ours (6). However, a recent nationwide Japanese survey has shown that only 1% of patients with KD were aged more than 10 years at the time of diagnosis (8). Similarly, a study by Advani et al. has found that 17 out of 1,150 (1.5%) of such cases involved patients aged more than 10 years (7). The percentage of cases of KD in older age groups varies from 1 to 7% in different studies (6, 7, 14–17), but Cai et al. have reported a figure as high as 17%. However, they have included children above the age of 5 in their analysis (17).

We have a cohort of 865 patients that were diagnosed with KD from the period of January 1994 to June 2019. Forty-six (5.3%) amongst these were aged 10 years or older at the time of diagnosis. One possible explanation for the relatively higher proportion of older patients with KD in our cohort is that we may be missing KD in infants and young children, in whom this condition often gets confused with febrile exanthemata (18, 19).

The clinical profile of patients with KD in this cohort has been compared with previously published studies (**Table 5**). Amongst the principal clinical features, periungual desquamation was found in 98% of cases, followed by oral cavity and lip changes (78%), skin rash (74%), conjunctival injection (63%), lymphadenopathy (61%), and dorsal edema (24%). However, as several patients had presented late, it is possible that some of the clinical features may have been missed altogether.

Diagnosis of KD should ideally be made before day 10 of illness, so that timely treatment can be instituted to prevent the development of CAAs (1, 20). In our cohort, the median day of diagnosis was 12 days. Manhliot et al. have also shown that the diagnosis of KD in children older than 9 years was delayed until day 12 (6). Seven patients in our cohort (15.2%) were not offered treatment, as they had presented late and their fever had already subsided. Similarly, 19% of the patients were not treated in the study published by Manlihot et al. (6), and 22% of the patients in the study published by Stockheim et al. (15).

The most significant morbidity in patients with KD is due to development of CAAs. Approximately 25% of KD cases develop CAAs if the disease remains untreated. With timely initiation of IVIg, <5% patients will go on to develop CAAs (1). Risk of CAAs is higher in older children with KD as compared to their younger counterparts (6, 15–17). Delay in diagnosis and initiation of treatment is considered to be the most important risk factor for development of CAAs in these patients (6). In the present cohort, 13% of cases developed CAAs. Our results are in consonance with the findings of previous studies (6, 7, 15–17).

It has also been observed by several authors that incomplete presentations are more common in older patients with KD (up to 59% in various series) (6, 7, 14, 17). We observed incomplete KD in 43% of our patients. Delay in diagnosis of KD has been found to be the most important risk factor for the development

TABLE 5 | A review of all reported studies on Kawasaki disease in older age groups.

	Momenah et al. Canada (16)	Stockheim et al. USA (15)	Cai et al. China (17)	Nagamori et al. Japan (14)	Manlihot et al. USA (6)	Advani et al. Indonesia (7)	Present study
Total no. of patients	133	500	113	650	1,374	1,150	865
No. of patients in older age group (%)	10 (7.5)	28 (5.6)	20 (17.7)	14 (2.2)	87 (6)	17 (1.5)	46 (5.3)
Age group (years)	≥9	≥8	≥5	>7	>9	>10	≥10
Median age in years (range)	NR	9 (8-15)	NR	8	NR	11.2 (10-16)	11 (10-30)
Mean age in years	10.9 ± 0.46	NR	8.22 ± 3	NR	NR	11.25 ± 1.2	16.3 ± 4.1
Male: female	1:1	2.5:1	2.33:1	NR	2:1	4.6:1	1.3:1
Fever duration (median, days)	10.8	10.5	10.8	5 (3-12)	9 (5-42)	NR	10 (2-30)
Rash (%)	NR	25 (89)	14 (70)	NR	69 (83)	10 (59)	34 (73.9)
Conjuctival injection (%)	NR	28 (100)	17 (85)	NR	70 (84)	11 (65)	29 (63)
Oral mucosal changes (%)	NR	27(96)	18 (90)	NR	73 (88)	13(77)	36 (78.3)
Cervical adenopathy (%)	NR	17 (61)	17 (85)	5 (36)	49 (59)	14 (82)	28 (60.9)
Extremity changes (%)	NR	28 (100)	17 (85)	9 (64)	63 (76)	7 (41)	45(97.8)
Hemodynamic instability/KDSS	NR	NR	NR	NR	NR	NR	8 (17.4)
Incomplete KD (%)	NR	1 (3.57)	5 (25)	4 (29)	36	10 (59)	20 (43)
IVIG used (%)	10 (100)	22 (78.6)	19 (95)	14 (100)	68 (81)	NR	39 (84.8)
IVIG resistance (%)	2 (20)	–	6 (30)	1 (7.14)	14 (17)	NR	none
Coronary abnormalities (%)	8 (40)	6 (21)	12 (60)	2 (14)	22 (25)	8 (47)	6 (13.04)

IVIG, intravenous immunoglobulin; KDSS, Kawasaki Disease Shock Syndrome; NR, not reported.

of CAAs in this age group. Manlihot et al. reported that unlike young infants, these patients have not been found to have other risk factors contributing to the development of CAAs, such as low serum albumin, hemoglobin, and platelet counts. The mean hemoglobin levels seen in the study by Manlihot et al. were 123 ±_15 g/L (6), while the mean levels in our cohort were 106.7 ± 18.3 g/L. Mean albumin concentration seen in our series was 31 ± 7 g/L. This was also lower than mean serum albumin level as reported by Manlihot et al. (38 ± 8 g/L) (6). It is likely that the underlying nutritional status of our cohort was responsible for these apparent differences. Mean hemoglobin and mean albumin levels were not found to be different in children with or without CAAs in our study. Median platelet counts in the study by Manlihot et al. were reported to be 268 × 10^9/L (6), while the median platelet count at presentation in our cohort was 333 × 10^9/L. We also observed that the median CRP was significantly higher in our patients who developed CAAs, as compared to our patients who did not develop CAAs.

In our cohort, the children who developed CAAs had a relatively higher median interval between the onset of fever and the diagnosis of KD when compared to children who did not develop CAAs. Similarly, pulmonary presentation was more common in patients with CAAs. We have previously reported that delays in diagnosis and initiation of treatment are more common in patients with KD who also have a pulmonary presentation (21). Although this increased risk of CAAs in KD in older age groups can be ascribed to delays in diagnosis and treatment, one cannot be categorical (as there may be several confounding factors at play). Further, it would be imprudent to draw conclusions when the numbers are small.

Eladawy et al. reported that 48.5% of patients with KD had one or more liver enzyme abnormalities. The authors have also shown that most liver enzyme elevations were subclinical and <2 times above the reference values. Elevation of liver enzymes were found to be associated with increased risk of IVIg resistance (22). In our study, elevated liver transaminases were seen in 46% of patients, and there was no difference in the frequency of liver enzyme abnormalities in patients with and without CAAs (**Table 4**).

Approximately 5% of children with KD can also present with hemodynamic instability and hypotensive shock—termed KD Shock Syndrome (KDSS) (1, 23, 24). In our study, 8 out of the 46 cases (17.4%) had KDSS-like presentation and initially, the possibility of toxic shock syndrome was considered in all of them. There was a significant delay in the diagnosis of KD in these patients—in one case the diagnosis was delayed until 3 weeks while in two cases the diagnosis cold be made only after 4 weeks. CAAs were seen in one patient with KDSS. The relatively higher proportion of patients with KDSS in our cohort could be a reflection of late diagnosis as well as delays in the initiation of therapy.

While managing patients with KD in older age groups, it needs to be kept in mind that getting an appropriate acoustic window for coronary artery evaluation may be difficult. In such situations, it may be difficult to rely completely on 2D-echocardiography findings, and one may have to pre-emptively carry out CTCA in selected patients (25). We carried out this investigation in 8 out of 46 patients.

In conclusion, our study shows that 5.3% of patients with KD were aged 10 years or older at time of diagnosis. Older children with KD appear to have significant delays in diagnosis of the disease and a higher chance of development of CAAs. The strength of this study is that all patients have been diagnosed and treated on the basis of uniform protocols and by a team with more than 25 years of experience of managing this condition. The obvious lacuna is the small cohort size and the fact that it is a single center retrospective study. Multicenter, large-sample,

prospective studies would help in further understanding the significance of our findings.

DATA AVAILABILITY STATEMENT

The datasets generated for this study are available on request to the corresponding author.

ETHICS STATEMENT

The study protocol was approved by the Departmental Review Board and Institutional Ethics Committee of the Postgraduate Institute of Medical Education and Research, Chandigarh, India. Diagnosis of KD was based on guidelines given by American Heart Association (AHA) (1, 9). As this manuscript pertains to collation of anonymized retrospective data from clinic records, acquiring consent was not necessary.

AUTHOR CONTRIBUTIONS

AJ and RP: conceptualization of the study, data collection, patient management, writing of the initial draft, editing of the manuscript, and review of the literature. SG, PV, DS, AG, and AR: patient management and review of literature, revision of manuscript. MS: radiological investigations, patient management, and review of literature. SS: conceptualization of the study, data collection, patient management, critical revision of manuscript, review of literature, and final approval of the manuscript.

REFERENCES

1. McCrindle BW, Rowley AH, Newburger JW, Burns JC, Bolger AF, Gewitz M, et al. Diagnosis, treatment, and long-term management of Kawasaki disease: a scientific statement for health professionals from the american heart association. *Circulation*. (2017) 135:e927–99. doi: 10.1161/CIR.0000000000000484
2. Singh S, Jindal AK, Pilania RK. Diagnosis of Kawasaki disease. *Int J Rheum Dis*. (2018) 21:36–44. doi: 10.1111/1756-185X.13224
3. Singh S, Vignesh P, Burgner D. The epidemiology of Kawasaki disease: a global update. *Arch Dis Child*. (2015) 100:1084–8. doi: 10.1136/archdischild-2014-307536
4. Singh S, Newburger JW, Kuijpers T, Burgner D. Management of Kawasaki disease in resource-limited settings. *Pediatr Infect Dis J*. (2015) 34:94–6. doi: 10.1097/INF.0000000000000600
5. Basha A, Rawat A, Jindal AK, Gupta A, Anand S, Garg R, et al. Autoantibody profile in children with Kawasaki disease on long-term follow-up: A prospective study from North India. *Int J Rheum Dis*. (2018) 21:2036–40. doi: 10.1111/1756-185X.13372
6. Manlhiot C, Yeung RSM, Clarizia NA, Chahal N, McCrindle BW. Kawasaki Disease at the extremes of the age spectrum. *Pediatrics*. (2009) 124:e410–5. doi: 10.1542/peds.2009-0099
7. Advani N, Santoso LA, Sastroasmoro S. Profile of Kawasaki disease in adolescents: is it different? *Acta MedicaIndones*. (2019) 51:42–6.
8. Makino N, Nakamura Y, Yashiro M, Kosami K, Matsubara Y, Ae R, et al. Nationwide epidemiologic survey of Kawasaki disease in Japan, 2015-2016. *Pediatr Int Off J JpnPediatr Soc*. (2019) 61:397–403. doi: 10.1111/ped.13809
9. Newburger JW, Takahashi M, Gerber MA, Gewitz MH, Tani LY, Burns JC, et al. Diagnosis, treatment, and long-term management of Kawasaki disease: a statement for health professionals from the committee on rheumatic fever, endocarditis and kawasaki disease, council on cardiovascular disease in the young, American Heart Association. *Circulation*. (2004) 110:2747–71. doi: 10.1161/01.CIR.0000145143.19711.78
10. Singhal M, Singh S, Gupta P, Sharma A, Khandelwal N, Burns JC. Computed tomography coronary angiography for evaluation of children with Kawasaki disease. *Curr Probl Diagn Radiol*. (2018) 47:238–44. doi: 10.1067/j.cpradiol.2017.09.013
11. Reddy M, Singh S, Rawat A, Sharma A, Suri D, Rohit MK. Pro-brain natriuretic peptide (ProBNP) levels in North Indian children with Kawasaki disease. *Rheumatol Int*. (2016) 36:551–9. doi: 10.1007/s00296-016-3430-6
12. Singh S, Agarwal S, Bhattad S, Gupta A, Suri D, Rawat A, et al. Kawasaki disease in infants below 6 months: a clinical conundrum? *Int J Rheum Dis*. (2016) 19:924–8. doi: 10.1111/1756-185X.12854
13. Salgado AP, Ashouri N, Berry EK, Sun X, Jain S, Burns JC, et al. High risk of coronary artery aneurysms in infants younger than 6 months of age with Kawasaki disease. *J Pediatr*. (2017) 185:112–6.e1. doi: 10.1016/j.jpeds.2017.03.025
14. Nagamori Y, Ogihara Y, Sato K, Ebato T, Otani K, Nakamura S, et al. Abstract 16: a clinical study of older children with Kawasaki disease. *Circulation*. (2015) 131(suppl. 2):A16.
15. Stockheim JA, Innocentini N, Shulman ST. Kawasaki disease in older children and adolescents. *J Pediatr*. (2000) 137:250–2. doi: 10.1067/mpd.2000.105150
16. Momenah T, Sanatani S, Potts J, Sandor GG, Human DG, Patterson MW. Kawasaki disease in the older child. *Pediatrics*. (1998) 102:e7. doi: 10.1542/peds.102.1.e7
17. Cai Z, Zuo R, Liu Y. Characteristics of Kawasaki disease in older children. *Clin Pediatr*. (2011) 50:952–6. doi: 10.1177/0009922811409027
18. Singh S, Aulakh R, Bhalla AK, Suri D, Manojkumar R, Narula N, et al. Is Kawasaki disease incidence rising in Chandigarh, North India? *Arch Dis Child*. (2011) 96:137–40. doi: 10.1136/adc.2010.194001
19. Singh S, Bansal A, Gupta A, Kumar RM, Mittal BR. Kawasaki disease: a decade of experience from North India. *Int Heart J*. (2005) 46:679–89. doi: 10.1536/ihj.46.679
20. Pilania RK, Jindal AK, Guleria S, Singh S. An update on treatment of Kawasaki disease. *Curr Treat Options Rheumatol*. (2019) 5:36–55. doi: 10.1007/s40674-019-00115-z
21. Singh S, Gupta A, Jindal AK, Gupta A, Suri D, Rawat A, et al. Pulmonary presentation of Kawasaki disease-A diagnostic challenge. *Pediatr Pulmonol*. (2018) 53:103–7. doi: 10.1002/ppul.23885
22. ElAdawy M, Dominguez SR, Anderson MS, Glodé MP. Abnormal liver panel in acute Kawasaki disease. *Pediatr Infect Dis J*. (2011) 30:141–4. doi: 10.1097/INF.0b013e3181f6fe2a
23. Kanegaye JT, Wilder MS, Molkara D, Frazer JR, Pancheri J, Tremoulet AH, et al. Recognition of a Kawasaki disease shock syndrome. *Pediatrics*. (2009) 123:e783–9. doi: 10.1542/peds.2008-1871
24. Pilania RK, Jindal AK, Srikrishna VV, Samprathi M, Singhal M, Singh S. Hypotension in a febrile child-beware of Kawasaki disease shock syndrome. *J Clin Rheumatol*. (2019). doi: 10.1097/RHU.0000000000001002. [Epub ahead of print].
25. Singhal M, Gupta P, Singh S, Khandelwal N. Computed tomography coronary angiography is the way forward for evaluation of children with Kawasaki disease. *Glob Cardiol Sci Pract*. (2017) 2017:e201728. doi: 10.21542/gcsp.2017.28

Conflict of Interest: The authors declare that the research was conducted in the absence of any commercial or financial relationships that could be construed as a potential conflict of interest.

frontiers in Pediatrics

CASE REPORT
published: 20 February 2020
doi: 10.3389/fped.2020.00051

A Large Isolated Congenital Left Circumflex Artery-to-Right Atrial Fistula in a 9-Year-Old Child

Xin Li[1,2], *Jun An*[3], *Shuai Wang*[4,5], *Wanli Lu*[2], *Zhigang Liu*[2,6], *Yili Wu*[4,5,7]* and *Fengjuan Jiao*[4,5]*

[1] Department of Pediatrics, TEDA International Cardiovascular Hospital, TEDA, Tianjin, China, [2] Department of Pediatric Cardiac Surgery, TEDA International Cardiovascular Hospital, TEDA, Tianjin, China, [3] Department of Biochemistry and Molecular Biology, College of Life Sciences, Nankai University, Tianjin, China, [4] Shandong Collaborative Innovation Center for Diagnosis, Treatment and Behavioral Interventions of Mental Disorders, Institute of Mental Health, Jining Medical University, Jining, China, [5] Shandong Key Laboratory of Behavioral Medicine, School of Mental Health, Jining Medical University, Jining, China, [6] Department of Great Blood Vessel and Cardiac Surgery, TEDA International Cardiovascular Hospital, TEDA, Tianjin, China, [7] Collaborative Innovation Center for Birth Defect Research and Transformation of Shandong Province, Jining Medical University, Jining, China

Isolated congenital coronary artery fistula (ICCAF) is an exceedingly rare anomaly in which there is a direct abnormal connection between a coronary artery and other cardiac chambers or any of great vessels. The left circumflex artery (LCX) is the least common source of ICCAF. Here we reported a rare case of large ICCAF originated from the LCX in a 9-year-old boy. He presented fatigability, murmurs and NYHA class II. Echocardiography and cardiac CT revealed that an aneurysmal dilatation of the LCX along with the dilated coronary sinus entered into the right atrium (RA) through the great cardiac vein. However, it showed that the dilated LCX directly drained into the RA by coronary angiography, which was confirmed by the surgery. During the surgical procedure, the LCX fistula was identified in a 3*3 cm bulbous structure, the aneurysmal dilation of RA tissue. The end of fistula was located in the lower-middle interatrial septum, which was near the coronary sinus and above the opening of inferior vena cava (IVC). Transcardiac chamber closure with cardiopulmonary bypass (CPB) was successfully performed for the correction of the fistula. It indicated that preoperative angiography is essential to define the details of large ICCAF with aneurysmal dilation. Moreover, transcardiac chamber closure with CPB is the optimal procedure for the treatment of large ICCAF, while interventional catheterization is not feasible due to the presence of aneurysmal dilation of the LCX. The description of this rare case might have great value for the diagnosis and treatment of large ICCAF originated from the LCX.

Keywords: coronary artery fistula, congenital, heart defects, pediatrics, surgical procedures

OPEN ACCESS

Edited by:
Hongfang Jin,
Peking University First Hospital, China

Reviewed by:
Muhammad Ali Mumtaz,
Baylor College of Medicine, United States
Dingding Xiong,
St. Vincent Mercy Medical Center, United States

***Correspondence:**
Yili Wu
yili_wu2004@yahoo.ca
Fengjuan Jiao
jiaofengjuan8516@163.com

Specialty section:
This article was submitted to Pediatric Cardiology, a section of the journal Frontiers in Pediatrics

Received: *09 June 2019*
Accepted: *03 February 2020*
Published: *20 February 2020*

Citation:
Li X, An J, Wang S, Lu W, Liu Z, Wu Y and Jiao F (2020) A Large Isolated Congenital Left Circumflex Artery-to-Right Atrial Fistula in a 9-Year-Old Child. Front. Pediatr. 8:51. doi: 10.3389/fped.2020.00051

BACKGROUND

Isolated congenital coronary artery fistula (ICCAF) is an exceedingly rare anomaly in which there is a direct abnormal connection between a coronary artery and one of the four cardiac chambers or any of great vessels without other abnormal cardiac structure (1–3). The incidence of ICCAF is 0.002% in the general population and ICCAF accounts for 0.4% in patients with cardiac

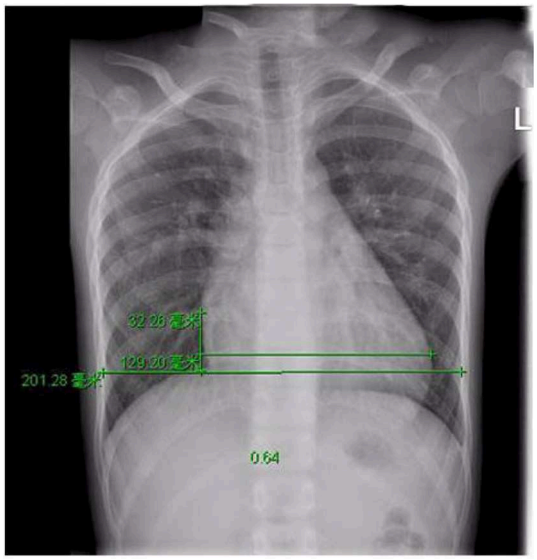

FIGURE 1 | Pre-operative Chest X-ray film view showed increased pulmonary flow and cardiomegaly, with a cardiothoracic area ratio of 0.64.

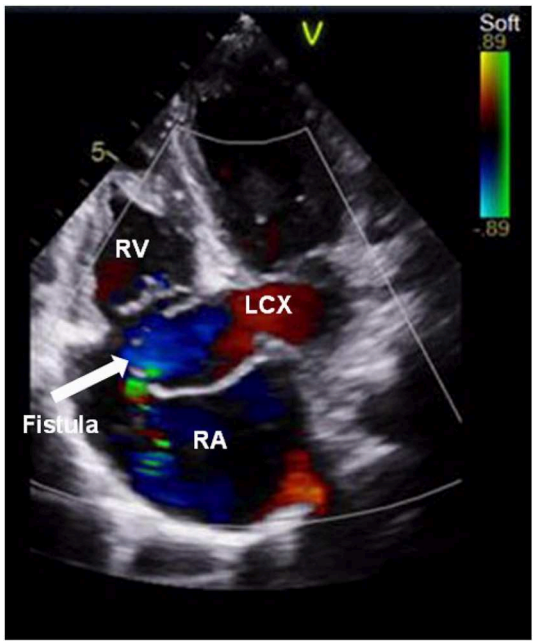

FIGURE 2 | Color Doppler examination showed a coronary artery fistula from the left circumflex artery to the right atrium. The arrow points to the fistula. RV, right ventricle; LCX, left circumflex artery; RA, right atrium.

malformations (4–6). The left circumflex artery (LCX) fistula is the most rare type of ICCAF (7, 8). Here we reported a rare case of large ICCAF originated from the LCX in a 9-year-old boy.

CASE PRESENTATION

A 9-year-old boy (weight 29.55 kg and height 139 cm) entered the hospital because of easy fatigability in the past 3 years. Continuous blowing murmur was found in the precordial region, and NYHA class II was defined. On auscultation, a grade 2/6 continuous blowing murmur could be heard at the third and fourth right intercostal spaces close to the sternum. The chest film demonstrated increased peripheral pulmonary vascularity and moderate to marked cardiomegaly, especially the right heart, with a cardiothoracic ratio of 0.64 (**Figure 1**). The electrocardiogram result showed sinus arrhythmia. In echocardiography and contrast-enhanced computed tomography (cardiac CT), the left main and circumflex coronary arteries showed an aneurysmal dilatation, which joined with the dilated coronary sinus (15 mm) through the great cardiac vein, and then entered into the right atrium (RA) (**Figures 2**, **3**). Subsequent coronary angiography revealed the distal LCX with an aneurysmal dilatation directly extended into the RA, while it failed to delineate the anatomy of the fistula (**Figure 4**). The surgery is necessary for this patient to keep healthy. Because the location of the fistula could not be defined by echocardiography and coronary angiography, the surgical operation was necessary to locate the fistula and treat it.

Median sternotomy and pericardiotomy were performed. External cardiac exploration showed that the end of LCX was a long segment ectasia that was connected to RA. Under cardiopulmonary bypass (CPB), the specific location of the LCX-RA fistula was determined. The CPB was instituted with bicaval drainage and aorta cannulation with mild hypothermia (33–35°C). During parallel circulation process, the RA was opened. A 3*3 cm bulbous structure was found. On the side surface of bulbous structure, there was a 4 mm opening that sprayed more blood and the coronary sinus opening compressed by the bulbous structure was located inferiorly and posteriorly. The left heart was vented via the atrial septum. The bulbous structure was opened, and a communication with LCX distal segment was found in the deep, that was the location of the LCX fistula. The end of fistula was located in the lower-middle interatrial septum, which was near the coronary sinus and above the opening of inferior vena cava (IVC). Then we found the component of the bulbous structure was RA tissue with aneurysmal dilation (**Figure 5**). Several interrupted pledgeted stitches was used to close the fistula and there was no any effluent blood, while the cardioplegia was repeatedly given. The fistula was repaired, and the aneurysmal wall was resected and trimmed subsequently.

The whole 157 min procedure involved 35 min cross-clamp and 62 min CPB.120 min ventilation and 18 h ICU stay were applied postoperatively. After weaning from CPB, no electrocardiographic change of myocardial ischemia was detected. The postoperative ECG showed that sinus rhythm was recovered. The postoperative course was uneventful. Oral aspirin was given for 12 months. No thrombus was found at 9 month follow-up, although a thrombus was found at the end of LCX at 1 and 3 months postoperative follow-up, respectively. Twelve months after the operation, cardiac CT showed that the diameter of proximal LCX and left main coronary artery was significantly reduced, and there was no abnormal connection between the LCX and the RA (**Figure 6**).

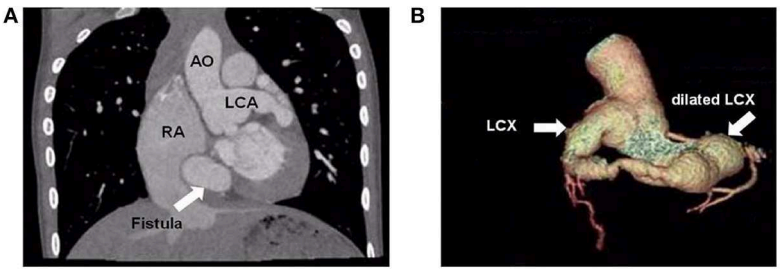

FIGURE 3 | Cardiac computed tomographic view the dilated left main coronary artery and circumflex artery. **(A)** Cardiac computed controlled X-ray shows dilated left main coronary artery and right atrium. The arrow points to the fistula. **(B)** Three-dimensional reconstructed computed tomographic demonstrates the dilated left circumflex artery. The distal left circumflex artery showed an aneurysmal dilatation. AO, aorta; LCA, left coronary artery; RA, right atrium; LCX, left circumflex artery.

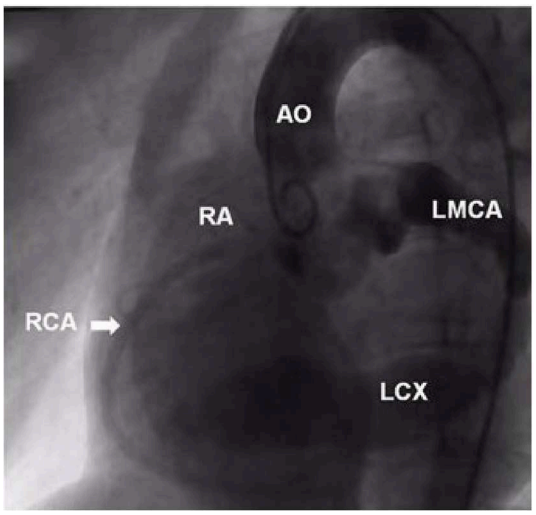

FIGURE 4 | Ascending aorta and coronary angiography view showed the dilated left main and circumflex coronary arteries. The distal LCX showed a stage of aneurysmal dilatation. AO, aorta; RA, right atrium; RCA, right coronary artery; LMCA, left main coronary artery; LCX, left circumflex artery.

DISCUSSION

Coronary artery fistula (CAF) can be congenital or acquired. Non-isolated congenital CAF was associated with other congenital heart diseases including tetralogy of Fallot or pulmonary atresia, while isolated congenital coronary artery fistula (ICCAF) occurs in structurally normal hearts (9). Patients with ICCAF are usually asymptomatic in pediatric population, and have symptoms or complications more than 20 years old (2). The duration and severity of the clinical symptoms depend on the amount of blood shunt, the size of the fistula and the resistance of the drainage chamber. Clinically, patients with ICCAF may present with palpitations, cyanosis, dyspnea on exertion, symptoms of angina, bacterial endocarditis or heart failure (10). Moreover, continuous murmur with local tremor or systolic and diastolic murmurs at the precardiac area could be heard in most patients with ICCAF (11). In this case, the patient was easy fatigability and presented with a continuous heart murmur in precordium area, and NYHA class II, which may be associated with the large blood flow of the fistula.

The LCX was the least common source of ICCAF, and the right heart chambers were the most common location of drainage (1, 8). Up until now, clinical experience with this rare anomaly have been published in fewer case reports or short series involving a few patients (12). However, most of the reports described the circumflex artery fistulae in patients aged more than 20 years and had clinical symptoms, such as congestive heart failure (13), palpitations and dyspnea (14), atrial fibrillation and angina (15). Hou and colleagues reported 29 LCX fistulas patients in which LCX to the RA fistulas accounted for 41% (12 of 29), whereas they didn't describe the key factors of the cases, e.g., their age, gender, whether they had a large isolated congenital LCX-to-RA fistula, and whether they had obvious clinical symptoms and associated cardiac diseases (16). A large ICCAF draining from the LCX to the RA was found in this pediatric patient, and the end of the ICCAF was located in the lower-middle interatrial septum, which was near the coronary sinus and above the opening of inferior vena cava (IVC).

Echocardiography is an important primary non-invasive tool for identifying the anomalous origin of CAF. In general, echocardiography can show the location and type of the CAF, including the course and drainage site of coronary artery, while it didn't delineate the exact anatomy of the fistula. So far, coronary angiography remains the golden standard imaging tool for diagnosing coronary anomalies and can be used as a diagnostic and therapeutic procedure (17). In this case, echocardiography and cardiac CT showed that the dilated coronary artery was connected with dilated coronary sinus and outlet stenosis of coronary sinus, while coronary angiography showed the ICCAF draining from the distal aneurysm-like LCX to the RA. However, the location of the fistula was not delineated. Liang and Ko (18) reported that a pediatric CAF leading to a dilated coronary artery and secondary aneurysmal formation may be considered as an indication for surgical treatment.

The coronary arteriovenous fistulas are divided into five types according to the chamber or vessel into which they drain: Type I (draining into the right atrium), Type II (draining into the right ventricle), Type III (draining into the pulmonary artery),

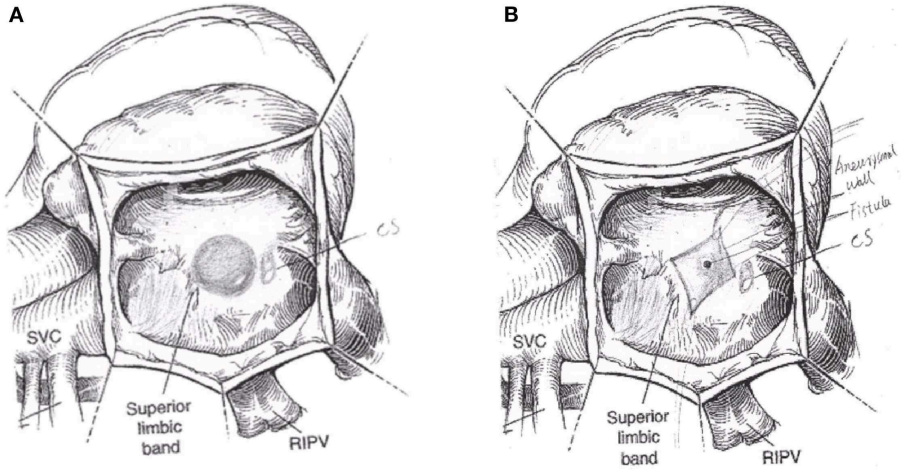

FIGURE 5 | The operation schematic diagram showed the distal aneurysm-like left circumflex artery was exposed within the right atrium **(A)**. The LCX fistula was shown by cutting the aneurysm **(B)**. CS, coronary sinus; SVC, superior vena cava; RIPV, right inferior pulmonary vein.

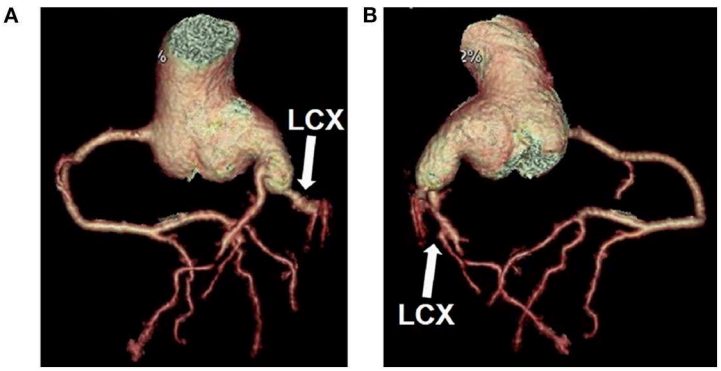

FIGURE 6 | Cardiac computed tomographic showed constriction of the left coronary artery and circumflex artery **(A,B)**. LCX, left circumflex artery.

Type IV (draining into the left atrium), and Type V (draining into the left ventricle) (3). The ICCAF of this patient belongs to Type I coronary arteriovenous fistula, and the ligation of the CAF distal to the origin, a type of surgery without CPB, was recommended for the correction of the fistula. Because it was difficult to make sure the specific location of the LCX-RA fistula, so transcardiac chamber closure with CPB was performed for the correction of the fistula (3). The left main coronary artery and the LCX were dilated obviously, and the end of LCX enters into the RA with aneurysmal dilatation. The LCX fistula was identified in the 3*3 cm bulbous structure, the aneurysmal dilation of RA tissue. The end of fistula was located in the lower-middle interatrial septum, which was near the coronary sinus and above the opening of inferior vena cava (IVC). The coronary sinus opening was compressed by the bulbous structure, which may be the main reason for the abnormal dilation of the coronary sinus. Transcardiac chamber closure with CPB was successfully performed without any complications listed in the studies that Hou and colleagues had been reported (16).

CONCLUSIONS

Herein, we present a pediatric case with a large ICCAF stemmed from the aneurysmal LCX and draining into the RA. Due to the special anatomical structure of the ICCAF in this case, the position of the fistula was not accurately defined by echocardiography, cardiac CT and coronary angiography. Based on the clinical presentation and special cardiac pathology, individualized therapeutic strategy was chosen. Transcardiac chamber closure with CPB was successfully performed without any complication. The description of this rare case might have great value for the diagnosis and treatment of large ICCAF originated from the LCX.

DATA AVAILABILITY STATEMENT

All datasets generated for this study are included in the article/supplementary material.

ETHICS STATEMENT

This study was carried out in accordance with the recommendations of clinical practice guidelines of China (Chinese Medical Association) with written informed consent from all subjects. All subjects gave written informed consent in accordance with the Declaration of Helsinki. The protocol was approved by the Ethical Committee of TEDA International Cardiovascular Hospital.

AUTHOR CONTRIBUTIONS

XL, JA, and SW collected and analyzed the data. XL and FJ wrote the manuscript. XL, YW, and FJ revised the manuscript. XL and WL managed the patient. WL and ZL participated in the surgery. WL provided a photo of the operation and answers the operation questions.

FUNDING

This work was supported by grants from the Natural Science Foundation of Shandong Province of China ZR2018BC022 to FJ and ZR2016HM30 to YW, Key Scientific and Technological Support Projects of Tianjin Binhai New Area Health and Family Planning Commission YJ-KY-Lix01-2018006 and 2017BWKZ008 to XL. Supporting Fund for Teachers' Research of Jining Medical University JY2017JS006 to FJ.

ACKNOWLEDGMENTS

We thank the patient and his family's support and the written informed consent was obtained from his parents for the publication of this case report. We also thank Kaixin Qiu and Yuqing Wang for the helpful comments.

REFERENCES

1. Lowe JE, Oldham HN Jr, Sabiston DC Jr. Surgical management of congenital coronary artery fistulas. *Ann Surg.* (1981) 194:373–80. doi: 10.1097/00000658-198110000-00001
2. Liberthson RR, Sagar K, Berkoben JP, Weintraub RM, Levine FH, Congenital coronary arteriovenous fistula. Report of 13 patients, review of the literature and delineation of management. *Circulation.* (1979) 59:849–54. doi: 10.1161/01.CIR.59.5.849
3. Sakakibara S, Yokoyama M, Takao A, Nogi M, Gomi H, Coronary arteriovenous fistula. Nine operated cases. *Am Heart J.* (1966) 72:307–14. doi: 10.1016/S0002-8703(66)80004-2
4. Peters C, Wacker-Gussmann A, Strasburger JF, Cuneo BF, Gotteiner NL, Gulecyuz M, et al. Electrophysiologic features of fetal ventricular aneurysms and diverticula. *Prenatal diagnosis*. (2015) 35:129–36. doi: 10.1002/pd.4501
5. Dodge-Khatami A, Mavroudis C, Backer CL. Congenital heart surgery nomenclature and database project: anomalies of the coronary arteries. *Ann Thorac Surg.* (2000) 69:S270–97. doi: 10.1016/S0003-4975(99)01248-5
6. Ponthier L, Brenot P, Lambert V, Petit J, Riou JY, Baruteau AE. Closure of isolated congenital coronary artery fistula: long-term outcomes and rate of re-intervention. *Pediatr Cardiol.* (2015) 36:1728–34. doi: 10.1007/s00246-015-1224-3
7. Vavuranakis M, Bush CA, Boudoulas H. Coronary artery fistulas in adults: incidence, angiographic characteristics, natural history. *Cathet Cardiovasc Diagn.* (1995) 35:116–20. doi: 10.1002/ccd.1810350207
8. Kamiya H, Yasuda T, Nagamine H, Sakakibara N, Nishida S, Kawasuji M, et al. Surgical treatment of congenital coronary artery fistulas: 27 years' experience and a review of the literature. *J Card Surg.* (2002) 17:173–7. doi: 10.1111/j.1540-8191.2002.tb01195.x
9. Said SA, Lam J, van der Werf T. Solitary coronary artery fistulas: a congenital anomaly in children and adults. A contemporary review. *Congen Heart Dis.* (2006) 1:63–76. doi: 10.1111/j.1747-0803.2006.00012.x
10. Darwazah AK, Hussein IH, Hawari MH. Congenital circumflex coronary arteriovenous fistula with aneurysmal termination in the pulmonary artery. *Tex Heart Inst J.* (2005) 32:56–9; discussion: 58–9.
11. Teno LA, Santos JL, Bestetti RB, Zanardi AM, Ceccon C, Castilho OT. Congenital circumflex coronary artery fistula with drainage into the left ventricle. *Tex Heart Inst J.* (1993) 20:304–6.
12. Forker AD, Weaver WF, Carveth SW, Reese HE. Congenital left circumflex coronary artery fistula to right atrium without a murmur. *Nebr Med J.* (1973) 58:38–41.
13. Sato Y, Mitsui M, Takahashi H, Miyazawa T, Okabe H, Inoue F, et al. A giant left circumflex coronary artery–right atrium arteriovenous fistula detected by multislice spiral computed tomography. *Heart Vessels.* (2004) 19:55–6. doi: 10.1007/s00380-003-0707-y
14. Gan H, Liu Y, Liu L, He Y, Zhang S. Coronary artery fistula between the left circumflex artery and right atrium: Multimodal imaging. *Wien Klin Wochenschr.* (2018) 130:738–9. doi: 10.1007/s00508-018-1409-x
15. Arani DT, Greene DG, Klocke FJ. Coronary artery fistulas emptying into left heart chambers. *Am Heart J.* (1978) 96:438–43. doi: 10.1016/0002-8703(78)90152-7
16. Hou B, Ma WG, Zhang J, Du M, Sun HS, Xu JP, et al. Surgical management of left circumflex coronary artery fistula: a 25-year single-center experience in 29 patients. *Ann Thorac Surg.* (2014) 97:530–6. doi: 10.1016/j.athoracsur.2013.09.015
17. Abdelmoneim SS, Mookadam F, Moustafa SE, Holmes DR. Coronary artery fistula with anomalous coronary artery origin: a case report. *J Am Soc Echocardiogr.* (2007) 20:333 e1–4. doi: 10.1016/j.echo.2006.09.012
18. Liang CD, Ko SF. Midterm outcome of percutaneous transcatheter coil occlusion of coronary artery fistula. *Pediatr Cardiol.* (2006) 27:557–63. doi: 10.1007/s00246-006-1317-0

Conflict of Interest: The authors declare that the research was conducted in the absence of any commercial or financial relationships that could be construed as a potential conflict of interest.

frontiers in Pediatrics

ORIGINAL RESEARCH
published: 21 February 2020
doi: 10.3389/fped.2020.00054

Sympathetic Overactivation From Supine to Upright Is Associated With Orthostatic Hypertension in Children and Adolescents

Yang Hu[1,2†], Yuanyuan Wang[1†], Bing He[3†], Yaru Wang[1], Zhenhui Han[4], Chunyan Tao[1], Hongxia Li[1], Yi Jiang[1], Chaoshu Tang[5] and Junbao Du[1,5]*

[1] Department of Pediatrics, Peking University First Hospital, Beijing, China, [2] Research Unit of Clinical Diagnosis and Treatment of Pediatric Syncope and Cardiovascular Diseases, Chinese Academy of Medical Sciences, Beijing, China, [3] Department of Pediatrics, People's Hospital of Wuhan University, Hubei, China, [4] Department of Pediatrics, Children's Hospital of Kaifeng, Henan, China, [5] Key Laboratory of Cardiovascular Sciences, Ministry of Education, Beijing, China

OPEN ACCESS

Edited by:
Fu Lijun,
Shanghai Children's Medical Center, China

Reviewed by:
Runmei Zou,
Central South University, China
Jie Tian,
Children's Hospital of Chongqing Medical University, China

***Correspondence:**
Junbao Du
junbaodu1@126.com

[†] These authors have contributed equally to this work

Specialty section:
This article was submitted to Pediatric Cardiology, a section of the journal Frontiers in Pediatrics

Received: 19 December 2019
Accepted: 05 February 2020
Published: 21 February 2020

Citation:
Hu Y, Wang Y, He B, Wang Y, Han Z, Tao C, Li H, Jiang Y, Tang C and Du J (2020) Sympathetic Overactivation From Supine to Upright Is Associated With Orthostatic Hypertension in Children and Adolescents. Front. Pediatr. 8:54. doi: 10.3389/fped.2020.00054

There are no prior publications or submissions with any overlapping information, including studies and patients. The study data have not been presented as an abstract or poster before the submission.

Objectives: The study was conducted to analyze the changes of baroreflex sensitivity and heart rate variability from supine to upright standing in children and adolescents with orthostatic hypertension to explore whether and how the autonomic nerve regulation was involved in the development of pediatric orthostatic hypertension.

Methods: This case-control study included twenty-five children with orthostatic hypertension (the patient group) and twenty-six healthy controls (the control group). All subjects underwent a standing test, during which their hemodynamic parameters were continuously monitored by a Finapres Medical System, and baroreflex sensitivity and heart rate variability were calculated.

Results: The demographic characteristics, supine baroreflex sensitivity, and supine heart rate variability including time domain and frequency domain indices did not differ between the patients with orthostatic hypertension and healthy subjects ($P > 0.05$). However, a more obvious drop of baroreflex sensitivity and a greater increase of low frequency/high frequency ratio from supine to upright were observed in subjects with orthostatic hypertension compared with those in the healthy children ($P < 0.001$ and $P < 0.01$, respectively). Changes of baroreflex sensitivity were negatively related to mean arterial pressure changes from supine to upright in all subjects ($P < 0.01$), and the increases in low frequency/high frequency ratio from supine to standing were positively correlated with those in mean arterial pressure in the study subjects ($P < 0.001$).

Conclusion: Upright sympathetic overactivation is associated with pediatric orthostatic hypertension.

Keywords: baroreflex sensitivity, heart rate variability, orthostatic hypertension, orthostatic intolerance, pediatrics

INTRODUCTION

Orthostatic hypertension (OHT) refers to a significant blood pressure (BP) elevation in the upright position compared to supine or sitting position, which reflects abnormal regulation of BP during postural changes. Streeten et al. (1) first put forward the concept of OHT and studied its pathogenesis in the 1980s. Subsequently, multiple studies in adults with OHT show that OHT is seen in the elderly with essential hypertension or diabetes and patients with dysautonomias and also occurs in young adults with normal supine BP (2–5). Furthermore, OHT is closely related to the subsequent cardiovascular and cerebrovascular diseases and central nervous system damage, and it was regarded as a new risk factor for cardiovascular and cerebrovascular diseases in adults (3, 6–10). Therefore, increasing attention has been paid to OHT.

While, in adolescents and children, OHT has been recognized recently and it is now considered as an important cause of orthostatic intolerance (OI) (11–13). Our research group reported OHT in children for the first time in 2012. We discovered that most children with OHT were in the period of puberty, with OI symptoms as their main clinical manifestations, such as dizziness, headache or even syncope, etc (11). Kang et al. conducted a head-up tilt (HUT) test on 2,089 children with unexplained syncope, headache, dizziness, chest tightness, and sighing, and found that the prevalence of OHT was high in these children in the middle-south part of China (12). The abovementioned symptoms were often induced by postural change from supine to upright or prolonged standing (11, 13). The recurrent symptoms of OHT greatly impact on the academic performance and daily life in children and adolescents (11). Moreover, previous studies showed that OHT in young adults was associated with elevated risk of suffering from essential hypertension in the future (5, 14), which also drew focus on adolescents and children with OHT. However, up to now, the mechanism for pediatric OHT is poorly understood (13, 15, 16).

OHT stands for the hypertension occurring from supine to upright, and the autonomic nervous system regulates and maintains BP and heart rate (HR) during postural changes via baroreceptors (17). Hence, baroreflex sensitivity (BRS) and heart rate variability (HRV) are two widely accepted measures to assess the autonomic activity, and spectral analysis of HRV is used to reflect the balance between sympathetic and vagal tone (18). However, the changes in BRS and HRV indices from supine to upright in children and adolescents with OHT have not been yet clear.

Therefore, this study was aimed to examine the possible changes in BRS and HRV indices from supine to upright in children and adolescents with OHT, and reveal the role of autonomic regulation in the development of pediatric OHT.

METHODS

Subjects

This case-control study enrolled 25 children with OHT (the OHT group) and 26 healthy children (the control group). The OHT group included 11 girls and 14 boys, from age 8 to 17 (12.5 $\pm$ 0.5) years old. All patients with OHT were admitted to the Department of Pediatrics at Peking University First Hospital from October 2015 to June 2019 with OI symptoms as their chief complaints and were diagnosed with OHT according to the published guidelines (19, 20). Specifically, the diagnostic criteria of OHT were as follows: mainly occurs in older children; associated with predisposing factors in most patients, such as prolonged standing, emotional stress, and crowded or stuffy environment; often associated with OI symptoms after upright; with a positive HUT test or standing test result (see *Standing test*); and exclusion of other diseases that cause OI symptoms (19, 20). The control group consisted of 12 girls and 14 boys, aged from 10 to 14 (12.0 $\pm$ 0.3) years old. They were recruited from elementary and junior high schools in two cities of China. They were considered healthy based on the medical history, physical examination and the standing test, and none of them had experienced OI symptoms within 3 months of the enrollment in the study.

Standing Test

All subjects underwent a standing test. Before the test, all subjects were confirmed as not having any structural heart disease, arrhythmias, or neurologic disease and not taking any medication or food that might have influence on autonomic nervous function. The test was conducted in a quiet and dimly lit room. The children were asked to lay supine on the testing bed for 10 min, then stand upright on their own for another 10 min, and still then return to the supine position (19, 20) at the termination of the test. During the test, all subjects were asked to remain silent and breathe normally.

A positive OHT response to the standing test was defined as follows: normal supine BP; during the initial 3 min of the standing test, increased systolic BP (SBP)$\geq$ 20 mmHg and/or increased diastolic BP (DBP) $\geq$ 25 mmHg (in children 6–12 years old) or $\geq$ 20 mmHg (in adolescents 13–18 years old) from supine to upright standing; or during upright standing, BP $\geq$ 130/90 mmHg (in children 6–12 years old) or $\geq$ 140/90 mmHg (in adolescents 13–18 years old) (19, 20).

Data Recording and Analysis

During the standing test, HR, BP, and standard three-lead electrocardiograph were taken and recorded with a Dash 2000 Multi-lead Physiological Monitor (General Electric, New York, NY, USA). The last BP measured in supine position and the BP measured at 3 min after standing served as supine BP and upright BP, respectively. R-R interval (RRI) data obtained from electrocardiograph were visually reviewed, and five-min segments free of ectopic beats and artifacts severally in supine and upright position were used for further analysis.

Meanwhile, the Finapres Medical System (Finometer PRO, FMS Company, Netherlands) was applied to continuously and non-invasively record beat-to-beat BP data during the standing test and calculating hemodynamic parameters and BRS afterwards. Using a finger plethysmogram, beat-to-beat BP measures of SBP, DBP, and pulse intervals were collected. Then, stroke volume (SV) was computed with the model flow method.

HR was calculated as the inverse of the pulse interval, and cardiac output (CO) was calculated as HR multiplying SV. Mean arterial pressure (MAP) was computed as the true integral of the arterial pressure wave over one beat, and total peripheral vascular resistance (TPVR) was calculated from MAP divided by CO. Average CO and TPVR taken from the last 1 min of the supine period was regarded as the supine values, and the upright CO and TPVR were computed as a 1-min average in the third minute after standing. The reliability of beat-to-beat BP measurements was validated using a Finapres system (21).

Cross-correlation was used to derive a form of sequential BRS. The correlation between interbeat interval and beat-by-beat SBP, with delays of 0–5 s for interval, was sampled and computed. When the correlation was significant at $P < 0.01$, the slope between SBP and interbeat interval was documented as one BRS value (22). Average supine and upright BRS values were taken consistent with the rule of CO and TPVR described above.

Five-min segments of RRI data were used to calculate time domain and frequency domain parameters of HRV. Standard deviation of RRI (SDNN) and root mean square of successive differences (RMSSD) of RRI were analyzed. Original RRI series was altered to equidistantly sampled sequence by a cubic spline interpolation method. Fast Fourier transformation was then used to obtain power spectral density (PSD) functions with Welch's periodogram method. Total power (TP) in the frequency range from 0.0 to 0.4 Hz was composed of very low frequency (VLF, 0.0–0.04 Hz), low frequency (LF, 0.04–0.15 Hz) and high frequency (HF, 0.15–0.4 Hz) bands. Powers of each band were computed as integrals under the respective PSD functions. The ratio between normalized LF power and HF power was calculated as LF/HF ratio.

Statistical Analysis

Statistical analyses were carried out with SPSS 20.0 software (SPSS, Chicago, IL, USA). All data are expressed as means ± SE, and $P < 0.05$ (2-tailed) indicated a statistically significant difference. The independent *t* test was applied for the comparisons between groups in the same position, and the paired *t* test was utilized to compare the corresponding parameters before and at standing for the same person. The Chi-squared test was used to compare categorical variables. Covariance analysis was adopted to compare all autonomic measures (BRS and HRV) after adjusting for gender, age and body mass index (BMI). Pearson correlation analysis was used for linear correlations and partial correlation analysis was adopted to correct the influence of gender, age, and BMI.

RESULTS

Subject Characteristics

The sex ratio, age, height, weight, or BMI between the subjects in OHT and in control groups did not significantly differ ($P > 0.05$, **Table 1**).

TABLE 1 | Demographic characteristics of the OHT group and control group.

Groups	*n*	Gender (M/F)	Age (years)	Height (cm)	Weight (kg)	BMI (kg/m^2)
OHT	25	14/11	12.5 ± 0.5	159.0 ± 3.2	53.5 ± 3.0	20.7 ± 0.6
Control	26	14/12	12.0 ± 0.3	158.4 ± 1.6	48.1 ± 1.5	19.1 ± 0.5
t /χ^2	–	0.024	0.810	0.166	1.599	1.925
P-value	–	0.877	0.424	0.869	0.119	0.060

Values are expressed as means ± SE. BMI, body mass index; OHT, orthostatic hypertension.

Changes in Hemodynamic Parameters During the Standing Test

As seen in **Figure 1**, in the supine position, all of the hemodynamic measures did not differ between the patients with OHT and the control group. While, HR, SBP, DBP, and MAP increased after standing in both groups ($P < 0.001$ for all variables). However, at 3 min of standing, the patients with OHT exhibited significantly higher SBP, DBP, and MAP than the control subjects ($P < 0.01$ for DBP, and $P < 0.001$ for SBP, and MAP). In addition, from supine to standing, OHT patients experienced an obvious decrease in CO ($P < 0.01$) and a marked increase in TPVR ($P < 0.01$), while the CO and TPVR of the control group did not show any significant changes upon standing ($P > 0.05$).

Changes in BRS and HRV Measures During the Standing Test

BRS and HRV changes from supine to upright are shown in **Figure 2**. At rest, there were no statistical differences in BRS and HRV estimates between the two groups. After standing, the BRS of the OHT patients decreased more significantly than that of the controls ($P < 0.001$), and the upright BRS in the OHT group was significantly lower than that in the control group after controlling for gender, age and BMI ($P < 0.001$). As for HRV indices, SDNN, RMSSD, TP, and HF power markedly decreased upon standing in all subjects, but at standing, SDNN, RMSSD, TP, LF power, or HF power did not significantly differ between the two groups. While, the elevation in LF/HF ratio from supine to upright was significantly greater in the OHT subjects compared with the healthy children, after controlling for gender, age and BMI ($P < 0.01$). Specific values in **Figures 1**, **2** are displayed in the **Supplementary Table 1**.

Association of Changes in BRS and LF/HF Ratio With the Changes in Blood Pressure From Supine to Upright

Pearson correlation analysis showed that changes in BRS were negatively correlated with changes in MAP from supine to upright in all subjects ($P < 0.01$, **Figure 3**). While, changes in LF/HF ratio were positively correlated with the MAP elevations from supine to standing ($P < 0.001$, **Figure 3**). In partial correlation analysis, the correlation coefficients were −0.442 and 0.709, respectively, after adjusting for gender, age and BMI.

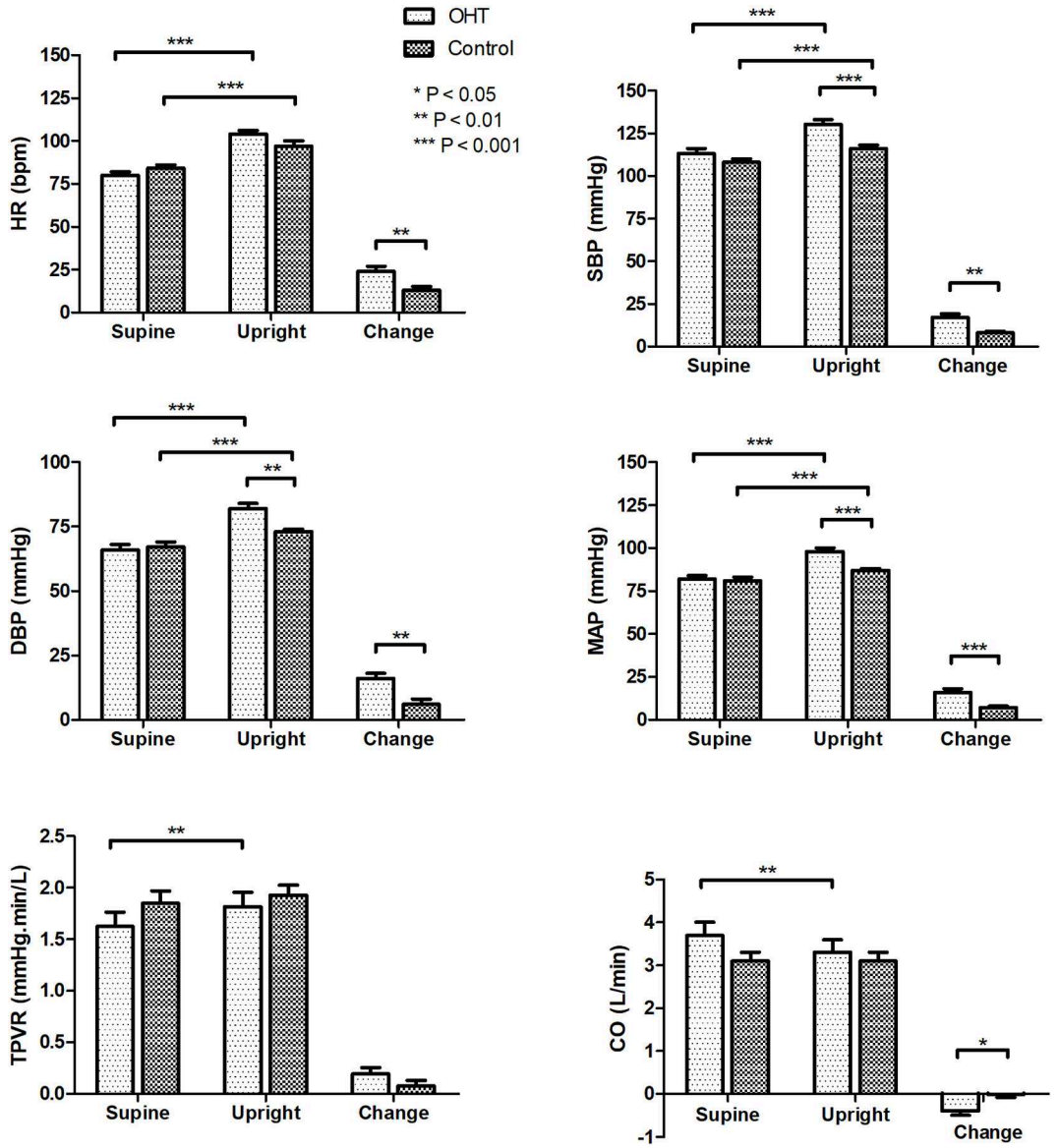

FIGURE 1 | Hemodynamic changes of the study subjects during the standing test. Values are means ± SE. *$P < 0.05$, **$P < 0.01$, ***$P < 0.001$. OHT, orthostatic hypertension; HR, heart rate; SBP systolic blood pressure; DBP, diastolic blood pressure; MAP, mean arterial pressure; TPVR, total peripheral vascular resistance; CO, cardiac output.

DISCUSSION

For the first time in this study, we explored the alterations in the autonomic nervous tone from supine to standing through BRS and HRV indices in children and adolescents with OHT and healthy controls, and found a significant drop in BRS but an obvious rise in LF/HF ratio from supine to upright in the patients with OHT after controlling for confounding variables. The results suggested a sympathetic overdrive upon standing in pediatric OHT patients and greatly contributed to the understanding of the mechanisms for pediatric OHT.

The mechanisms responsible for the development of pediatric OHT have not been clear. Kario et al. (8) measured changes in plasma norepinephrine (NE) levels in OHT patients before and after tilting. In their study, after tilting, the plasma NE level was significantly higher in the OHT group than that in the controls, while the supine plasma NE levels were comparable between the two groups. Moreover, α-receptor blockers have been shown to be capable of reducing the upright BP without effecting baseline BP in clinical studies (8, 23). Based on the above facts, we hypothesized that the abnormal autonomic nervous system control is likely associated with OHT. Therefore, the present study was designed to analyze the possible involvement of

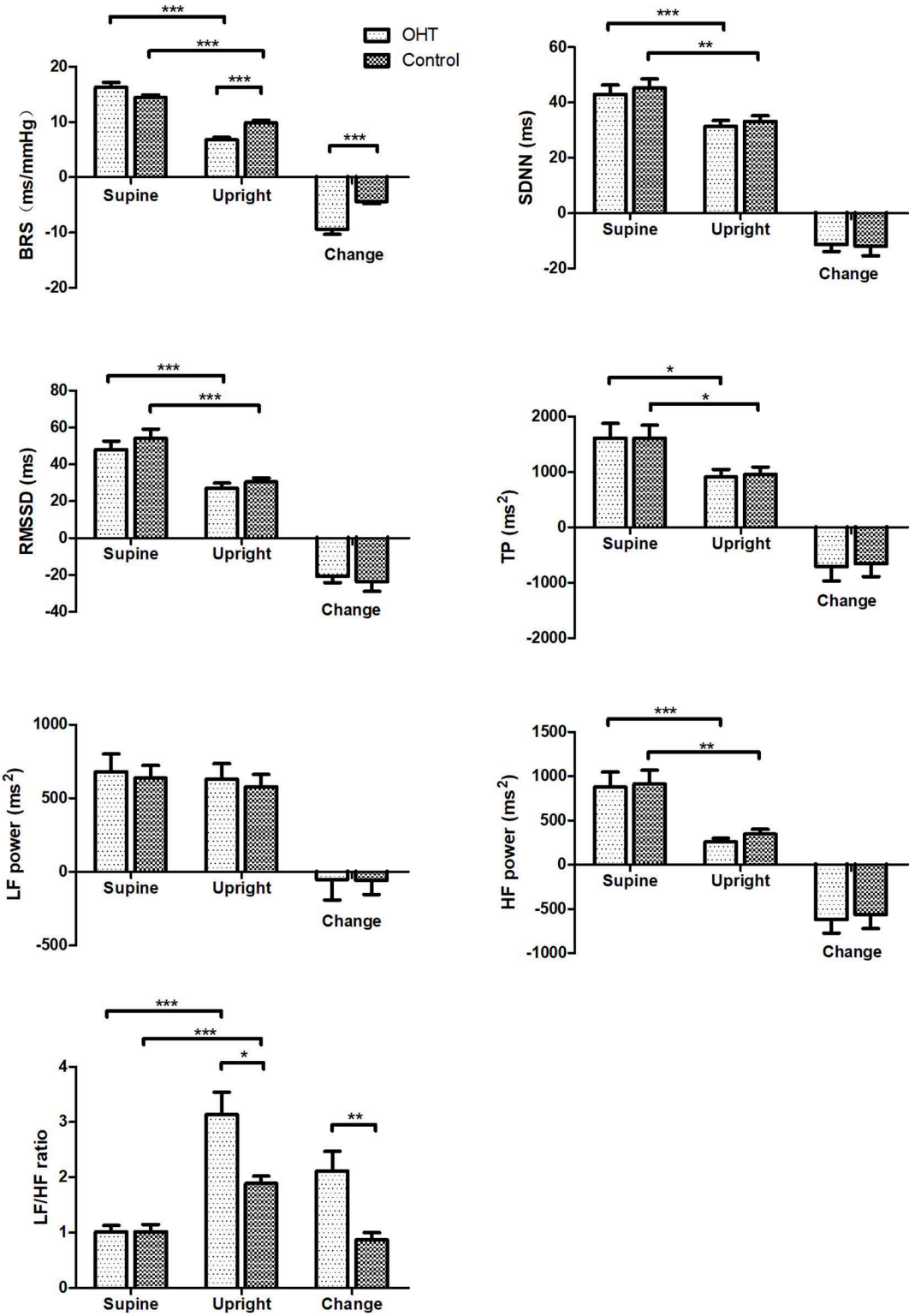

FIGURE 2 | Changes in BRS and HRV measures of the study subjects during the standing test. Values are means ± SE. *$P < 0.05$, **$P < 0.01$, ***$P < 0.001$. OHT, orthostatic hypertension; BRS, baroreflex sensitivity; SDNN, standard deviation of R-R intervals; RMSSD, root mean square of successive differences; TP, total power; LF, low frequency; HF, high frequency.

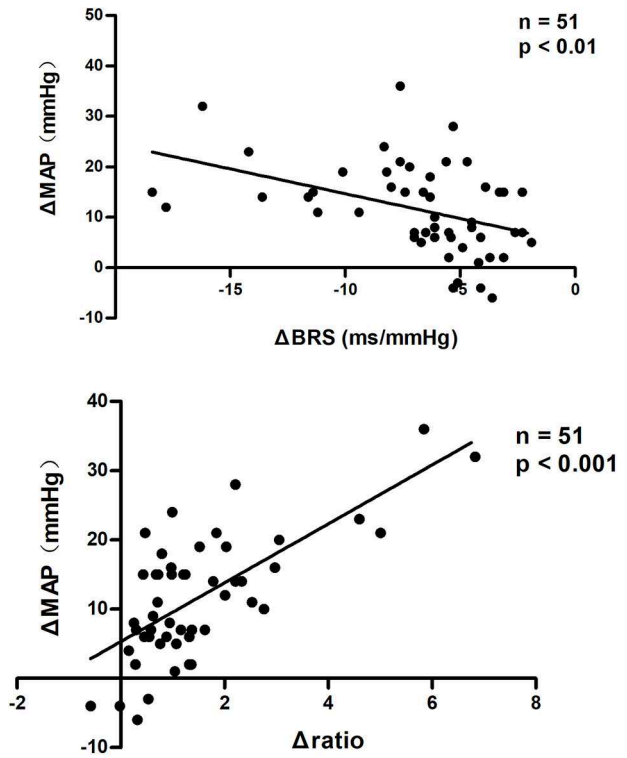

FIGURE 3 | Pearson correlation analysis of changes in BRS and LF/HF ratio with BP changes from supine to upright. MAP changes from supine to upright were negatively correlated with BRS changes and positively correlated with LF/HF ratio changes in all subjects. BRS, baroreflex sensitivity; MAP, mean arterial pressure. ΔBRS, upright BRS – supine BRS; ΔMAP, upright MAP – supine MAP; Δratio, upright LF/HF ratio – supine LF/HF ratio.

autonomic nervous dysfunction in the development of pediatric OHT by detecting the changes in autonomic measures from supine to upright. BRS and HRV are two commonly used measures of autonomic nerve function. Baroreflex is essential in the instant regulation of BP (24, 25), and LF/HF ratio reflects the predominant component among sympathetic and vagal tone (18). Normally, BRS and RRI variability decrease but LF/HF ratio increases after standing (17, 18, 26). However, both the decrease in BRS and the increase in LF/HF ratio from supine to upright were significantly greater in pediatric patients with OHT than those in controls. The reduction of BRS is associated with the sympathetic activation (17, 26, 27), and the increased LF/HF ratio indicates an obvious sympathetic predominance. Therefore, the significant drop of BRS and the remarkably increased LF/HF ratio at standing in the OHT patients demonstrated sympathetic overactivity in adolescents with OHT when upright. Furthermore, we found that both the changes in BRS and the changes in LF/HF ratio from supine to upright were linearly correlated with the changes in MAP in all subjects, which indicated that the severity of BP elevation was related to the degree of sympathetic activation. In addition, it is worth noting that we recorded a decrease in CO and an increase in TPVR after standing in adolescents with OHT, while CO and TPVR did not change significantly in healthy controls from supine to upright. The decrease in CO upon upright might be the trigger for sympathetic overactivation in OHT patients. The previous studies showed that, after wearing inflatable pressure suits to increase returned blood volume, the upright DBP of the OHT patients was lower than before (1). Besides, we controlled the gender, age and BMI when analyzing autonomic measures to exclude their influence on autonomic activity (23, 24, 28).

In this research, no significant differences in supine BRS and RRI variability were found between the individuals with and without OHT. In contrast to our results, Yoshinari et al. (29) reported that the coefficient of variation of the RRI at rest was higher in diabetic patients with OHT than in diabetic patients without OHT, suggesting an increased baseline BRS level in OHT patients. However, they only recorded the RRI for 200 beats on the electrocardiogram in the supine position, and did not compute BRS directly. More importantly, the participants were quite different from ours, since diabetes mellitus affected autonomic nervous function itself. In a pilot study on children with OI, Wagoner et al. (30) found that there was no significant difference in BRS measures between OI and non-OI subjects in the supine position, and BRS decreased in OI subjects upon standing, but they did not subgroup the OI subjects. As for HRV measures, Yang et al. analyzed Holter ECG results of children with OHT, and found that LF/HF ratio in the OHT group was higher than that in the control group (31). However, they did not show the comparisons of HRV measures among different positions, including the upright position.

To date, there have been no reports of medication therapy for pediatric OHT since the mechanism for pediatric OHT is poorly understood (13). However, despite suffering from recurrent OI symptoms, children with OHT might have increased potential of developing hypertension in the future as the frequent fluctuations of BP might damage the function of the vascular wall and endothelial cells (32). Therefore, children and adolescents with OHT urgently need assessment for the necessity of medication. Our results provided a potential therapeutic target, an excessive activation of the sympathetic nervous system, though more research evidence is needed in the future.

The limitations of our study would be that first, the non-invasive methods (BRS and HRV analysis) that we used for assessing the autonomic nervous function, due to the difficulties in the implementation of invasive methods in children, are not the most direct. Muscle sympathetic nerve activity (MSNA) detected by microneurography is another reliable way of evaluating sympathetic activity, which is more direct, but it is hard to conduct and not included in the present study due to the invasiveness of testing (33). The coherence between HRV and MSNA spontaneous variability at rest and during orthostatic challenge has been proved before, and HRV is easier to obtain compared with MSNA (34). Second, the sample size in our study is relatively small, which might lead to the increase of sampling error. Therefore, multiple-center based and large-sample sized studies will be needed in the future to further validate the role of autonomic nervous regulation in the development of pediatric OHT.

In conclusion, our study provided new insight into the vital role of sympathetic hyper-activation upon standing in pediatric OHT. The data would greatly further the

understanding of the mechanisms for OHT in children and adolescents.

DATA AVAILABILITY STATEMENT

The datasets generated for this study are available on request to the corresponding author.

ETHICS STATEMENT

The studies involving human participants were reviewed and approved by The Ethics Committee of Peking University First Hospital. Written informed consent to participate in this study was provided by the participants' legal guardian/next of kin.

AUTHOR CONTRIBUTIONS

JD, BH, and CTan contributed to the conception and design of the study, revise of the manuscript, and final approval of the version to be published. YH, YuW, YaW, YJ, ZH, CTao, CTan, and HL analyzed and interpretated the data, and drafted the article. YyW, BH, YaW, ZH, CTao, and HL undertook the test and acquired the data. JD, YJ, and CTan revised the manuscript critically for important intellectual content.

FUNDING

This study was supported by National Natural Science Foundation of China (81622004), Peking University Clinical Scientist Program (BJMU2019LCKXJ001), and Fundamental Research Funds for the Central Universities.

SUPPLEMENTARY MATERIAL

The Supplementary Material for this article can be found online at: https://www.frontiersin.org/articles/10.3389/fped.2020.00054/full#supplementary-material

REFERENCES

1. Streeten DH, Richardson RL, Thomas FD, Miller JW. Orthostatic hypertension. Pathogenetic studies. *Hypertension*. (1985) 7:196–203. doi: 10.1161/01.HYP.7.2.196
2. Robertson D. Orthostatic hypertension: the last hemodynamic frontier. *Hypertension*. (2011) 57:158–9. doi: 10.1161/HYPERTENSIONAHA.110.163485
3. Magkas N, Tsioufis C, Thomopoulos C, Dilaveris P, Georgiopoulos G, Doumas M, et al. Orthostatic hypertension: from pathophysiology to clinical applications and therapeutic considerations. *J Clin Hypertens.* (2019) 21:426–33. doi: 10.1111/jch.13491
4. Mesquita P, Queiroz D, Lamartine de Lima Silva V, Texeira Vde C, Vilaca de Lima YR, Junior ER, et al. Prevalence of orthostatic hypertension in elderly patients with type 2 diabetes. *Int J Endocrinol.* (2015) 2015:463487. doi: 10.1155/2015/463487
5. Thomas RJ, Kiang L, Jacobs DR, Bild DE, Kiefe CI, Hulley SB. Positional change in blood pressure and 8-year risk of hypertension: the CARDIA Study. *Mayo Clin Proc.* (2003) 78:951–8. doi: 10.4065/78.8.951
6. Kazuomi K. Orthostatic hypertension-a new haemodynamic cardiovascular risk factor. *Nat Rev Nephrol.* (2013) 9:726–38. doi: 10.1038/nrneph.2013.224
7. Eguchi K, Kario K, Hoshide S, Hoshide Y, Ishikawa J, Morinari M, et al. Greater change of orthostatic blood pressure is related to silent cerebral infarct and cardiac overload in hypertensive subjects. *Hypertens Res.* (2004) 27:235–41. doi: 10.1291/hypres.27.235
8. Kario K, Eguchi K, Hoshide S, Hoshide Y, Umeda Y, Mitsuhashi T, et al. U-curve relationship between orthostatic blood pressure change and silent cerebrovascular disease in elderly hypertensives: orthostatic hypertension as a new cardiovascular risk factor. *J Am Coll Cardiol.* (2002) 40:133–41. doi: 10.1016/S0735-1097(02)01923-X
9. Fan XH, Wang Y, Sun K, Zhang W, Wang H, Wu H, et al. Disorders of orthostatic blood pressure response are associated with cardiovascular disease and target organ damage in hypertensive patients. *Am J Hypertens.* (2010) 23:829–37. doi: 10.1038/ajh.2010.76
10. Agnoletti D, Valbusa F, Labat C, Gautier S, Mourad JJ, Benetos A. Evidence for a prognostic role of orthostatic hypertension on survival in a very old institutionalized population. *Hypertension*. (2016) 67:191–6. doi: 10.1161/HYPERTENSIONAHA.115.06386
11. Zhao J, Yang J, Jin H, Du J. Clinical analysis of orthostatic hypertensin in children. *Clin J Pediatr.* (2012) 50:839–42. doi: 10.3760/cma.j.issn.0578-1310.2012.11.010
12. Kang M, Xu Y, Wang C, Wu L, Zhu L, Ran J, et al. Differences of age and gender in children with orthostatic hypertension. *Clin J Appl Clin Pediatr.* (2013) 28:24–6. doi: 10.3760/cma.j.issn.2095-428X.2013.01.008
13. Duan H, Zhou K, Hua Y. Clinical progress of orthostatic hypertension in children. *Chin Med J.* (2014) 127:3825–8. doi: 10.3760/cma.j.issn.0366-6999.20132969
14. Lee H, Kim HA. Orthostatic hypertension: an underestimated cause of orthostatic intolerance. *Clin Neurophysiol.* (2016) 127:2102–7. doi: 10.1016/j.clinph.2015.12.017
15. Zhao J, Du SX, Yang JY, Lin J, Jin HF, Du JB. Changes in plasma nitric oxide and nitric oxide synthase activity in children with orthostatic hypertension. *Chin J Appl Clin Pediatr.* (2014) 29:971–3. doi: 10.3760/j.issn.2095-428X.2014.13.005
16. Zhao J, Yang J, Du S, Tang C, Du J, Jin H. Changes of atrial natriuretic peptide and antidiuretic hormone in children with postural tachycardia syndrome and orthostatic hypertension: a case control study. *Chin Med J.* (2014) 127:1853–7. doi: 10.3760/cma.j.issn.0366-6999.20140336
17. Cooper VL, Hainsworth R. Effects of head-up tilting on baroreceptor control in subjects with different tolerances to orthostatic stress. *Clin Sci.* (2002) 103:221–6. doi: 10.1042/cs1030221
18. Finley JP, Nugent ST, Hellenbrand W. Heart-rate variability in children. Spectral analysis of developmental changes between 5 and 24 years. *Can J Physiol Pharmacol.* (1987) 65:2048–52. doi: 10.1139/y87-320
19. Chinese Pediatric Cardiology Society and Editorial Board of Chinese Journal of Pediatrics, Subspecialty Group of Cardiology, the Society of Pediatrics, Beijing Medical Association and Professional Board of Syncope in Children, Pediatrician Society, Chinese Medical Doctor Association. Guideline of diagnosis of syncope in children. *Clin J Pediatr.* (2016) 54:246–50. doi: 10.3760/cma.j.issn.0578-1310.2016.04.003
20. Wang C, Li Y, Liao Y, Tian H, Huang M, Dong X, et al. 2018 Chinese Pediatric Cardiology Society. (CPCS) guideline for diagnosis and treatment of syncope in children and adolescents. *Sci Bull.* (2018) 63:1558–64. doi: 10.1016/j.scib.2018.09.019
21. Omboni S, Parati G, Frattola A, Mutti E, Rienzo M, Castiglioni P, et al. Spectral and sequence analysis of finger blood pressure variability. Comparison with analysis of intra-arterial recordings. *Hypertension*. (1993) 22:26–33. doi: 10.1161/01.HYP.22.1.26
22. Westerhof BE, Gisolf J, Stok WJ, Wesseling KH, Karemaker JM. Time-domain cross-correlation baroreflex sensitivity: performance on the EUROBAVAR data set. *J Hypertens.* (2004) 22:1371–80. doi: 10.1097/01.hjh.0000125439.28861.ed

23. Hoshide S, Parati G, Matsui Y, Shibazaki S, Eguchi K, Kario K. Orthostatic hypertension: home blood pressure monitoring for detection and assessment of treatment with doxazosin. *Hypertens Res.* (2012) 35:100–6. doi: 10.1038/hr.2011.156
24. Fitzgibbon LK, Coverdale NS, Phillips AA, Shoemaker JK, Klentrou P, Wade TJ, et al. The association between baroreflex sensitivity and blood pressure in children. *Appl Physiol Nutr Metab.* (2012) 37:301–7. doi: 10.1139/h11-163
25. Dietrich A, Riese H, van Roon AM, Van EK, Ormel J, Neeleman J, et al. Spontaneous baroreflex sensitivity in (pre)adolescents. *J Hypertens.* (2006) 24:345–52. doi: 10.1097/01.hjh.0000200517.27356.47
26. Honzikova N, Zavodna E. Baroreflex sensitivity in children and adolescents: physiology, hypertension, obesity, diabetes mellitus. *Physiol Res.* (2016) 65: 879–89.
27. Straznicky NE, Eikelis N, Lambert EA, Esler MD. Mediators of sympathetic activation in metabolic syndrome obesity. *Curr Hypertens Rep.* (2008) 10:440–7. doi: 10.1007/s11906-008-0083-1
28. Lenard Z, Studinger P, Mersich B, Kocsis L, Kollai M. Maturation of cardiovagal autonomic function from childhood to young adult age. *Circulation*. (2004) 110:2307–12. doi: 10.1161/01.CIR.0000145157.07881.A3
29. Yoshinari M, Wakisaka M, Nakamura U, Yoshioka M, Uchizono Y, Iwase M. Orthostatic hypertension in patients with type 2 diabetes. *Diabetes Care.* (2001) 24:1783–6. doi: 10.2337/diacare.24.10.1783
30. Wagoner AL, Olson JD, Westwood BM, Fortunato JE, Diz DI, Shaltout HA. Children with orthostatic intolerance exhibit elevated markers of inflammation in the dorsal medulla. *Am J Physiol Heart Circ Physiol.* (2019) 317:H323–9. doi: 10.1152/ajpheart.00680.2018
31. Zhixiang Y, Cheng W, Jibing X, Bisheng G, Ming X, Deyu L. Ambulatory blood pressure monitoring in children suffering from orthostatic hypertension. *Biomed Eng Online.* (2018) 17:129. doi: 10.1186/s12938-018-0530-4
32. Rizzoni D, Porteri E, Platto C, Rizzardi N, De CC, Boari GE, et al. Morning rise of blood pressure and subcutaneous small resistance artery structure. *J Hypertens.* (2007) 25:1698–703. doi: 10.1097/HJH.0b013e328172dc41
33. Dutoit AP, Hart EC, Charkoudian N, Wallin BG, Curry TB, Joyner MJ. Cardiac baroreflex sensitivity is not correlated to sympathetic baroreflex sensitivity within healthy, young humans. *Hypertension*. (2010) 56:1118–23. doi: 10.1161/HYPERTENSIONAHA.110.158329
34. Furlan R, Porta A, Costa F, Tank J, Baker L, Schiavi R, et al. Oscillatory patterns in sympathetic neural discharge and cardiovascular variables during orthostatic stimulus. *Circulation*. (2000) 101:886–92. doi: 10.1161/01.CIR.101.8.886

Conflict of Interest: The authors declare that the research was conducted in the absence of any commercial or financial relationships that could be construed as a potential conflict of interest.

frontiers in Pediatrics

ORIGINAL RESEARCH
published: 11 March 2020
doi: 10.3389/fped.2020.00098

Reduced 24-h Sodium Excretion Is Associated With a Disturbed Plasma Acylcarnitine Profile in Vasovagal Syncope Children: A Pilot Study

Jinqing Song[1†], Chunyan Tao[1†], Guozhen Chen[1,2], Selena Chen[3], Wenrui Xu[1], Junbao Du[1], Yanling Yang[1*] and Yaqian Huang[1*]*

[1] Department of Pediatrics, Peking University First Hospital, Beijing, China, [2] Department of Pediatrics, The Affiliated Yantai Yuhuangding Hospital of Qingdao University, Yantai, China, [3] Division of Biological Sciences, University of California, San Diego, La Jolla, CA, United States

OPEN ACCESS

Edited by:
Xupei Huang,
Florida Atlantic University,
United States

Reviewed by:
Ju Liu,
Shandong University, China
Cheng Wang,
Central South University, China

***Correspondence:**
Wenrui Xu
xuwenrui10@126.com
Yanling Yang
yanlinggy@vip.sina.com
Yaqian Huang
yaqianhuang@126.com

[†] These authors have contributed equally to this work

Specialty section:
This article was submitted to Pediatric Cardiology, a section of the journal Frontiers in Pediatrics

Received: 31 December 2019
Accepted: 26 February 2020
Published: 11 March 2020

Citation:
Song J, Tao C, Chen G, Chen S, Xu W, Du J, Yang Y and Huang Y (2020) Reduced 24-h Sodium Excretion Is Associated With a Disturbed Plasma Acylcarnitine Profile in Vasovagal Syncope Children: A Pilot Study. Front. Pediatr. 8:98. doi: 10.3389/fped.2020.00098

Objective: To investigate if the low sodium intake is associated with the plasma carnitine and acylcarnitine profile in children with vasovagal syncope (VVS).

Materials and Methods: Twenty-six children suffering from VVS were recruited in the present study and divided into a group of low urinary sodium excretion or a group of normal urinary sodium excretion according to the excretion of 24-h urinary sodium <3 or 3–6 g, respectively. The excretion of 24-h urinary sodium was detected with ion-selective electrode approach. Plasma carnitine and acylcarnitine concentrations were measured with tandem mass spectrometry. Each participant completed the head-up tilt test. The demographics, clinical characteristics, hemodynamic parameters and plasma carnitine and acylcarnitine concentrations were compared between the two groups. A bivariate correlation between plasma acylcarnitine profiles and the excretion of 24-h urinary sodium was conducted with Spearman's correlation coefficients.

Results: Of the enrolled VVS patients, 14 patients were assigned to the group of low urinary sodium excretion and the remaining 12 patients were assigned to the group of normal urinary sodium excretion. Symptoms of fatigue were more prevalent in the group of low urinary sodium excretion than in the group of normal urinary sodium excretion ($p = 0.009$). Aside from fatigue, no other differences in the demographics, clinical characteristics or hemodynamic parameters during the head-up tilt test were found between the two groups ($p > 0.05$). Concentrations of plasma tiglylcarnitine (C5:1), hydroxyhexadecanoylcarnitine (C16OH), hydroxyoctadecanoylcarnitine (C18OH), and carnitine C22 were significantly higher in the group of low urinary sodium excretion than in the group of normal urinary sodium excretion (all p-values = 0.048); moreover, they were all negatively correlated with 24-h urinary sodium levels (all p-values = 0.016). There were no differences between the two groups in other acylcarnitines or free carnitine.

Conclusions: Reduced excretion of 24-h urinary sodium is associated with a disturbed plasma acylcarnitine profile in children with VVS. The findings suggest that restricted sodium intake-induced disturbance of plasma acylcarnitines and related cellular energy metabolism might be involved in the pathogenesis of VVS in children.

Keywords: carnitine, acylcarnitine, low sodium intake, vasovagal syncope, children

INTRODUCTION

Vasovagal syncope (VVS) is the main form of syncope in children and adolescents and is characterized by syncopal attack and hemodynamic abnormalities during the head-up tilt test (HUTT), including systemic arterial hypotension, bradycardia, or both. It has been reported that VVS accounts for more than 60% of all pediatric syncopal cases (1, 2). Approximately 30% of affected individuals suffer from recurrent syncopal episodes, which significantly impair their quality of life (3, 4). Under such circumstances, efficient interventions are required. However, the exact underlying mechanisms of VVS are not fully understood, which results in an unsatisfactory outcome of treatment to some extent (5, 6). Therefore, elucidation of the complex mechanisms of VVS is particularly important. Fatigue, which is related to energy metabolic dysfunction, is common in patients with VVS (7). Moreover, it has been established that skeletal muscle extensively accumulates carnitine and acylcarnitines, which are pivotal in cellular energy production because of their role in transporting long-chain fatty acids from the cellular matrix into the matrix of mitochondrion for subsequent beta-oxidation (8, 9). Nevertheless, it is unclear whether a disturbance of carnitine and acylcarnitine profiles is associated with the pathogenesis of VVS. Low sodium intake is one proposed mechanism of VVS and leads to hypovolemia and alterations in biologically active substances which are likely to contribute to syncopal occurrence, including renin, aldosterone, and catecholamine (10–12). As a result, supplementation of fluid and sodium is a rationally efficient method to treat VVS (13). A possible relationship between the metabolism of carnitine and acylcarnitines and the reducing intake of sodium was mentioned among adults with hypertension (14). However, it is unclear whether low sodium intake in patients with VVS leads to abnormal changes in carnitine and acylcarnitines, which mediates the occurrence of syncope.

Therefore, the present research was undertaken to explore if the low sodium intake is associated with the plasma carnitine and acylcarnitine profile in pediatric VVS patients and discuss the possible underlying mechanisms.

MATERIALS AND METHODS

Study Subjects

Twenty-six patients (19 girls and 7 boys, aged 12.5 ± 2.7 years old) with VVS were enrolled in the present research. They visited the Child Syncope Center at Peking University First Hospital from August 2018 to September 2019. All patients underwent an excretion test of 24-h urinary sodium. Based on the excretion levels of 24-h urinary sodium, patients were divided into the group of low urinary sodium excretion (excretion level <3 g) or the group of normal urinary sodium excretion (excretion level between 3 and 6 g) (2). No patients were overweight or obese, nor had associated disorders of diabetes mellitus, thyroid dysfunction, renal dysfunction, hepatic dysfunction, or cardiac dysfunction or symptoms and signs of fever, vomiting, diarrhea or dehydration. The criteria for the diagnosis of pediatric VVS were as follows: (1) syncopal events that were often induced by predisposing factors including rapid postural alterations, long-term standing, and emotional stimulation, etc.; (2) a positive response to the HUTT; as well as (3) excluding other syncopal disorders (15, 16). The Ethics Committee of Peking University First Hospital approved this study. We conducted the study in line with the ethical criteria in the Declaration of Helsinki. The legal guardians of each patient signed the informed consent.

Abbreviations: VVS, vasovagal syncope; HUTT, head-up tilt test.

Protocol for the HUTT

All enrolled patients underwent strict inspections to exclude cardiogenic, neurological, and metabolic disorders. Patients then completed the HUTT. This test was conducted in a dimly lit, warm and quiet room between 8:30 and 12:00 a.m. Patients were required to fast and the medication impacting autonomic nervous function was avoided at least 5 half-life times before the HUTT. They were placed on an autonomic stretcher (HUT-821; Beijing Juchi, Beijing, China) for 10–20 min to maintain a stable hemodynamic condition. Then, they were positioned at 60° passively for as long as 45 min or until a positive response occurred. A positive response to the HUTT was according to the criteria described previously (15, 16).

Protocol for the 24-h Urinary Sodium Excretion Test

Each patient as well as his/her caretakers were introduced to a standard urine collection process in advance. Girls were required to make a collection of 24-h urine samples during non-menstrual periods. The sodium-selective electrode approach (Cobas 6000, Roche, Basel, Switzerland) was done for measuring the excretion of 24-h urinary sodium. The formula is as follows (17): excretion of 24-h urinary sodium = concentration of sodium × total 24-h urine volume.

Measurement of Plasma Carnitine and Acylcarnitines

All VVS patients fasted for at least 4 h before blood sampling at ∼8:00 a.m. Two milliliters of blood were drawn by venipuncture and collected in an ethylenediaminetetraacetic acid anticoagulant tube. After being centrifugated at 2,000 g for 20 min, plasma was extracted at 4°C and then preserved at −80°C until tested. The collected plasma was thawed at one time for the measurement of the carnitine and acylcarnitine profile on a tandem mass spectrometer (MS/MS, API3200, Applied Biosystems, California, USA). The concentrations of carnitine and acylcarnitines were calculated automatically using Chemo View software (NeoLynx, Waters, Massachusetts, USA). All the testing work was done by a professionally trained investigator.

Statistical Analysis

The data were processed with SPSS software 22.0 (IBM Corp., NY, USA). Continuous variables are stated as the mean ± SD. And between two groups, the differences were measured by Student's *t*-test or Mann-Whitney *U*-test according to the Shapiro-Wilk test consequences. Categorical variables are presented as numbers, and Fisher's exact test was applied for

TABLE 1 | Baseline characteristics and hemodynamics in the head-up tilt test in vasovagal syncope patients.

Items	Low urinary sodium excretion group ($n = 14$)	Normal urinary sodium excretion group ($n = 12$)	$t/Z/\chi^2$ value	p-value
Gender (n, M/F)	3/11	4/8	—†	0.665
Age (years)	12.1 ± 3.0	13.0 ± 2.4	−0.788	0.439
Body mass index (kg/m^2)	17.6 ± 2.3	20.0 ± 3.9	−1.916	0.067
Symptom duration (months)	29.6 ± 37.1*	17.1 ± 19.5*	−0.646	0.518
Numbers of syncope (times)	4 ± 3*	4 ± 2*	−1.157	0.247
Duration of unconsciousness (min)	5.2 ± 8.3*	1.5 ± 1.7*	−1.066	0.286
Fatigue (n, yes/no)	13/1	5/7	—†	0.009
Supine HR (beats/min)	77 ± 14*	77 ± 14	−0.180	0.857
Supine SBP (mmHg)	106 ± 9	110 ± 11*	−1.185	0.236
Supine DBP (mmHg)	62 ± 6	66 ± 9	−1.070	0.295
Time to positive response in HUTT (min)	31 ± 11*	26 ± 13	−1.159	0.246
Positive HR in HUTT (beats/min)	116 ± 32	114 ± 16	0.270	0.789
Positive SBP in HUTT (mmHg)	72 ± 5	71 ± 5	0.567	0.576
Positive DBP in HUTT (mmHg)	48 ± 7*	48 ± 4	−0.438	0.661

HR, heart rate; SBP, systolic blood pressure; DBP, diastolic blood pressure; HUTT, head-up tilt test; Data are mean ± SD or numbers.
**Non-normality.*
† Fisher's exact test.

comparison. A bivariate correlation between data with non-normal distribution was conducted with Spearman's correlation coefficients. Significance was considered when p-value <0.05.

RESULTS

Basic Information of VVS Patients

Among the enrolled VVS patients, the group of low urinary sodium excretion included 14 patients with a 24-h urinary sodium excretion of 0.8–2.7 g (mean 2.1 ± 0.6 g), and the group of normal urinary sodium excretion included 12 children with a 24-h urinary sodium excretion of 3.1–5.9 g (mean 3.8 ± 0.8 g). No differences existed in the demographics, and clinical and hemodynamic characteristics between the two groups ($p > 0.05$, **Table 1**). However, more children in the group of low urinary sodium excretion reported fatigue than in the group of normal urinary sodium excretion ($p = 0.009$, **Table 1**).

Plasma Carnitine and Acylcarnitine Profile in VVS Patients

Levels of several acylcarnitines, namely tiglylcarnitine (C5:1) ($p = 0.048$), hydroxyhexadecanoylcarnitine (C16OH) ($p = 0.048$), hydroxyoctadecanoylcarnitine (C18OH) ($p = 0.048$), and carnitine C22 ($p = 0.048$), were higher in the group of low urinary sodium excretion than in the group of normal urinary sodium excretion (**Table 2**). No statistically significant differences were showed between the two groups in other acylcarnitines or free carnitine (C2, $p = 0.504$; C3, $p = 0.777$; C3DC, $p = 0.803$; C4, $p = 0.620$; C5, $p = 1.000$; C5DC, $p = 0.912$; C5OH, $p = 0.654$; C6, $p = 0.312$; C6DC, $p = 0.354$; C8, $p = 0.288$; C8:1, $p = 0.313$; C10, $p = 0.359$; C10:1, $p = 0.086$; C10:2, $p = 0.192$; C12, $p = 0.720$; C12:1, $p = 0.083$; C14, $p = 0.845$; C14:1, $p = 0.565$; C14:2, $p = 0.146$; C14DC, $p = 0.181$; C14OH, $p = 0.234$; C16, $p = 0.897$; C16:1, $p = 0.863$; C16:1OH, $p = 0.725$; C18, $p = 0.958$; C18:1, $p = 0.813$; C18:1OH, $p = 0.481$; C18:2, $p = 0.813$; C20, $p = 0.105$; C24, $p = 0.457$; C26, $p = 0.355$; C5/C2, $p = 0.297$; C2/C0, $p = 0.366$; C3/C2, $p = 0.602$; C3/C0, $p = 1.000$; C8/C2, $p = 0.867$; C14:1/C16, $p = 0.909$; free carnitine, $p = 0.897$, **Table 2**).

Correlations Between the Excretion of 24-h Urinary Sodium and Plasma Acylcarnitines

Further examining the association between the excretion levels of 24-h urinary sodium and the abovementioned plasma acylcarnitines with significant difference, negative Spearman's correlation coefficients were found (C5:1, $r = -0.469$, $p = 0.016$; C16OH, $r = -0.469$, $p = 0.016$; C18OH, $r = -0.469$, $p = 0.016$; and C22, $r = -0.469$, $p = 0.016$) in all study patients.

DISCUSSION

In mitochondria, carnitine and acylcarnitines are a series of essential molecules that play an obligatory part in the long-chain fatty acid beta-oxidation. Analyzing carnitine and acylcarnitine profile may help in the investigation and elucidation of metabolic derangements. The acylcarnitine profile displays a characteristic alteration in inherited metabolic diseases, such as short chain and medium chain acyl coenzyme A dehydrogenase deficiency, and carnitine acylcarnitine translocase deficiency (18). Moreover, it was reported that changes in the acylcarnitine profile were related to the development of IgA nephropathy and diabetes mellitus (19, 20). In the study, we observed that in VVS patients, some plasma acylcarnitines (C5:1, C16OH, C18OH, C22) were higher in the group of low urinary sodium excretion than in the group of normal

TABLE 2 | Plasma carnitine and acylcarnitines in vasovagal syncope patients.

Items	Low urinary sodium excretion group ($n = 14$)	Normal urinary sodium excretion group ($n = 12$)	*t*/*Z* value	*p*-value
Free carnitine	23.657 ± 5.937	23.388 ± 4.33	0.130	0.897
C2	3.110 ± 1.237	2.885 ± 1.005*	−0.669	0.504
C3	0.204 ± 0.066	0.206 ± 0.071*	−0.284	0.777
C3DC	0.019 ± 0.010*	0.018 ± 0.006*	−0.249	0.803
C4	0.101 ± 0.039	0.108 ± 0.038	−0.502	0.620
C5	0.045 ± 0.015	0.045 ± 0.016	0.000	1.000
C5:1	0.013 ± 0.005*	0.010 ± 0.000	−1.974	0.048
C5DC	0.054 ± 0.023*	0.047 ± 0.010*	−0.110	0.912
C5OH	0.029 ± 0.010*	0.027 ± 0.005*	−0.448	0.654
C6	0.032 ± 0.012	0.029 ± 0.012*	−1.012	0.312
C6DC	0.052 ± 0.022*	0.041 ± 0.007*	−0.926	0.354
C8	0.068 ± 0.026	0.061 ± 0.032*	−1.063	0.288
C8:1	0.125 ± 0.035	0.122 ± 0.064*	−1.009	0.313
C10	0.086 ± 0.033	0.073 ± 0.035	0.935	0.359
C10:1	0.102 ± 0.023	0.092 ± 0.034*	−1.715	0.086
C10:2	0.021 ± 0.006*	0.018 ± 0.006*	−1.305	0.192
C12	0.029 ± 0.012	0.028 ± 0.015*	−0.359	0.720
C12:1	0.052 ± 0.015*	0.043 ± 0.014*	−1.732	0.083
C14	0.019 ± 0.010*	0.018 ± 0.012*	−0.195	0.845
C14:1	0.047 ± 0.013	0.045 ± 0.012*	−0.575	0.565
C14:2	0.019 ± 0.007*	0.016 ± 0.009*	−1.452	0.146
C14DC	0.011 ± 0.004*	0.010 ± 0.000	−1.336	0.181
C14OH	0.006 ± 0.005*	0.003 ± 0.005*	−1.190	0.234
C16	0.114 ± 0.118*	0.110 ± 0.095*	−0.130	0.897
C16:1	0.016 ± 0.012*	0.015 ± 0.008*	−0.173	0.863
C16:1OH	0.006 ± 0.008*	0.004 ± 0.005*	−0.352	0.725
C16OH	0.003 ± 0.005*	0.000 ± 0.000	−1.974	0.048
C18	0.036 ± 0.032*	0.038 ± 0.037*	−0.053	0.958
C18:1	0.118 ± 0.125*	0.101 ± 0.100*	−0.237	0.813
C18:1OH	0.003 ± 0.005*	0.002 ± 0.004*	−0.704	0.481
C18:2	0.076 ± 0.073*	0.063 ± 0.056*	−0.236	0.813
C18OH	0.003 ± 0.005*	0.000 ± 0.000	−1.974	0.048
C20	0.004 ± 0.005*	0.001 ± 0.003*	−1.620	0.105
C22	0.003 ± 0.005*	0.000 ± 0.000	−1.974	0.048
C24	0.009 ± 0.003*	0.008 ± 0.004*	−0.743	0.457
C26	0.009 ± 0.003*	0.010 ± 0.000	−0.926	0.355
C5/C2	0.014 ± 0.006*	0.017 ± 0.007*	−1.043	0.297
C2/C0	0.121 ± 0.043*	0.108 ± 0.029*	−0.905	0.366
C3/C2	0.069 ± 0.027*	0.075 ± 0.028	−0.522	0.602
C3/C0	0.010 ± 0.000	0.010 ± 0.000	0.000	1.000
C8/C2	0.021 ± 0.009	0.022 ± 0.006*	−0.167	0.867
C14:1/C16	0.736 ± 0.373	0.717 ± 0.465	0.116	0.909

Data are mean ± SD.
**Non-normality.*

urinary sodium excretion. Moreover, the excretion of 24-h urinary sodium was negatively correlated with these plasma acylcarnitines. Patients suffering from VVS with low urinary sodium excretion were more susceptible to experiencing symptoms of fatigue than those in the group of normal urinary sodium excretion.

The mechanisms by which low sodium loading results in a disturbed acylcarnitine profile have not been explored. Derkach et al. also found a phenomenon in a DASH-sodium trial among participants with high blood pressure, that plasma metabolites of acylcarnitines (butyrylcarnitine and valerylcarnitine) were increased with sodium reduction (14). On the other hand,

some studies showed a significant increase in renin-angiotensin-aldosterone system activity with low sodium intake (12). The activated renin-angiotensin-aldosterone system is capable of inducing oxidative stress (21, 22), which could diminish the activity of enzymes in metabolic processes. Therefore, we inferred that low sodium loading might impair the activity of enzymes involved in the long-chain fatty acid beta-oxidation. The inefficient long-chain fatty acid beta-oxidation could promote the accumulation of acylcarnitine byproducts from substrate catabolism, which are capable of passing across the mitochondrial membrane and the cell membrane (19, 23, 24). More convincingly, 24-h urinary sodium excretion was found to be negatively correlated with the concentration of several acylcarnitines in our study, which suggested that reduced dietary sodium intake might be associated with abnormal fatty acid metabolism.

As a high-energy-consuming organ, skeletal muscle needs fatty acids to supplement essential energy during exercise or stress (25). Insufficient energy leads to fatigue. Large numbers of VVS patients complain of fatigue before or after syncope occurrence (7). In our Syncope Unit, we also observed several patients experiencing fatigue for long durations of time. In the present study, patients with low urinary sodium excretion were more prone to experience fatigue than those with normal urinary sodium excretion. This highlights that some VVS patients are disturbed by energy metabolism dysfunction, which is likely induced, at least in part, by low sodium intake.

The excretion of 24-h urinary sodium, a standard criterion for the measurement of sodium intake (26), is applied in many investigations to explore the relationship between sodium intake and development of diverse disorders. Kieneker et al. conducted a study in 7,330 individuals and found a strong relationship between low urinary sodium level and an increased stroke risk (27). Moreover, many investigations have showed that abnormal sodium intake is related to increased mortality and cardiovascular events (28, 29). The relationship between sodium intake and outcomes of health should be a U-shape, where high and low sodium intake indicated a risk factor for negative outcomes. We suggested that low sodium intake might decrease the long-chain fatty acid beta-oxidation rate and increase the plasma concentration of acylcarnitines in VVS patients. Additional and longer investigations should be performed to determine whether low sodium intake can predict the outcomes of affected individuals.

In summary, increased plasma concentration of acylcarnitines in VVS patients with low urinary sodium excretion was reported for the first time. In addition to VVS, postural tachycardia syndrome is another subtype of orthostatic intolerance with fatigue, palpitation and dizziness as well as syncope in the childhood (30, 31). Furthermore, some postural tachycardia syndrome patients are also characterized with low sodium intake (32, 33). As such, we speculate that the restricted sodium intake-induced disturbance of plasma acylcarnitines and cellular energy metabolism might be associated with the pathogenesis of not only VVS, but also other subtypes of orthostatic intolerance in children, which merits further investigations. Also, there were some limitations, such as a small sample size, the single-center observational study design and the lack of healthy control participants. Future multicenter-based, larger sample-sized and mechanistic studies should be performed to explore the significance of low-sodium-intake-associated energy metabolism in pathogenesis of VVS.

DATA AVAILABILITY STATEMENT

The datasets generated for this study are available on request to the corresponding author.

ETHICS STATEMENT

The studies involving human participants were reviewed and approved by the Ethics Committee of Peking University First Hospital. Written informed consent to participate in this study was provided by the participants' legal guardian/next of kin.

AUTHOR CONTRIBUTIONS

JS had the primary responsibility for the protocol development, examined the plasma concentrations of carnitine and acylcarnitines. CT was responsible for patient enrollment, data collection, and preliminary data analysis. JS and CT wrote the drafted manuscript. GC, SC, JD, and WX assisted with the data collection and data analysis. GC, JD, and SC revised the manuscript and gave important advice on the subject. WX, YY, and YH supervised the design and execution of this study, checked data analysis, revised the manuscript, and had a final approval of the submitted manuscript. All authors have read and approved the final manuscript and assumed full responsibility for its contents.

FUNDING

This study was supported by Peking University Clinical Scientist Program (BJMU2019LCKXJ001) and the Fundamental Research Funds for the Central Universities.

ACKNOWLEDGMENTS

The authors thank all the children as well as their caretakers for participating in this study.

REFERENCES

1. Romme JJ, van Dijk N, Boer KR, Dekker LR, Stam J, Reitsma JB, et al. Influence of age and gender on the occurrence and presentation of reflex syncope. *Clin Auton Res*. (2008) 18:127–33. doi: 10.1007/s10286-008-0465-0
2. Alderman MH. Dietary sodium: where science and policy diverge. *Am J Hyperten*. (2016) 29:424–7. doi: 10.1093/ajh/hpu256
3. Ng J, Sheldon RS, Ritchie D, Raj V, Raj SR. Reduced quality of life and greater psychological distress in vasovagal syncope patients compared to healthy individuals. *Pacing Clin Electrophysiol*. (2019) 42:180–8. doi: 10.1111/pace.13559

4. Anderson JB, Czosek RJ, Knilans TK, Marino BS. The effect of paediatric syncope on health-related quality of life. *Cardiol Young*. (2012) 22:583–8. doi: 10.1017/S1047951112000133
5. Vyas A, Swaminathan PD, Zimmerman MB, Olshansky B. Are treatments for vasovagal syncope effective? A meta-analysis. *Int J Cardiol*. (2013) 167:1906–11. doi: 10.1016/j.ijcard.2012.04.144
6. Romano S, Branz L, Fondrieschi L, Minuz P. Does a therapy for refex vasovagal syncope really exist? *High Blood Press Cardiolvasc Prev*. (2019) 26:273–82. doi: 10.1007/s40292-019-00327-3
7. Legge H, Norton M, Newton JL. Fatigue is significant in vasovagal syncope and is associated with autonomic symptoms. *Europace*. (2008) 10:1095–101. doi: 10.1093/europace/eun164
8. Almannai M, Alfadhel M, El-Hattab AW. Carnitine inborn errors of metabolism. *Molecules*. (2019) 24:E3251. doi: 10.3390/molecules24183251
9. Tamai I, Ohashi R, Nezu J, Yabuuchi H, Oku A, Shimane M, et al. Molecular and functional identification of sodium ion-dependent, high affinity human carnitine transporter OCTN2. *J Biol Chem*. (1998) 273:20378–82. doi: 10.1074/jbc.273.32.20378
10. Mosqueda-Garcia R, Furlan R, Tank J, Fernandez-Violante R. The elusive pathophysiology of neurally mediated syncope. *Circulation*. (2000) 102:2898–906. doi: 10.1161/01.CIR.102.23.2898
11. El-Sayed H, Hainsworth R. Salt supplement increases plasma volume and orthostatic tolerance in patients with unexplained syncope. *Heart*. (1996) 75:134–40. doi: 10.1136/hrt.75.2.134
12. Graudal NA, Hubeck-Graudal T, Jurgens G. Effects of low sodium diet versus high sodium diet on blood pressure, renin, aldosterone, catecholamines, cholesterol, and triglyceride. *Cochrane Database Syst Rev*. (2011) doi: 10.1002/14651858.CD004022.pub3.
13. Chu W, Wang C, Wu L, Lin P, Li F, Zou R. Oral rehydration salts: an effective choice for the treatment of children with vasovagal syncope. *Pediatr Cardiol*. (2015) 36:867–72. doi: 10.1007/s00246-015-1097-5
14. Derkach A, Sampson J, Joseph J, Playdon MC, Stolzenberg-Solomon RZ. Effects of dietary sodium on metabolites: the Dietary Approaches to Stop Hypertension (DASH)-Sodium Feeding Study. *Am J Clin Nutr*. (2017) 106:1131–41. doi: 10.3945/ajcn.116.150136
15. Tao C, Chen S, Li H, Wang Y, Wang Y, Liu P, et al. Value of immediate heart rate alteration from supine to upright in differential diagnosis between vasovagal syncope and postural tachycardia syndrome in children. *Front Pediatr*. (2018) 6:343. doi: 10.3389/fped.2018.00343
16. Wang C, Li Y, Liao Y, Tian H, Huang M, Dong XY, et al. 2018 Chinese Pediatric Cardiology Society (CPCS) guideline for diagnosis and treatment of syncope in children and adolescents. *Sci Bull*. (2018) 63:1558–64. doi: 10.1016/j.scib.2018.09.019
17. Tao C, Lu W, Lin J, Li H, Li X, Tang C, et al. Long-term outcomes of children and adolescents with postural tachycardia syndrome after conventional treatment. *Front Pediatr*. (2019) 7:261. doi: 10.3389/fped.2019.00261
18. Peng L, Liu L, Peng M, Jiang M. Application of acylcarnitine analysis on the screening and diagnosis of inherited metabolic diseases. *J Appl Clin Pediatr*. (2012) 27:1617–20. doi: 10.3969/j.issn.1003-515X.2012.20.025
19. Zhang X, Zhang C, Chen L, Han X, Ji L. Human serum acylcarnitine profiles in different glucose tolerance states. *Diabetes Res Clin Pract*. (2014) 104:376–82. doi: 10.1016/j.diabres.2014.04.013
20. Xia F, Zhu L, Xu C, Wu Q, Chen W, Zeng R, et al. Plasma acylcarnitines could predict prognosis and evaluate treatment of IgA nephropathy. *Nutr Metab (Lond)*. (2019) 16:2. doi: 10.1186/s12986-018-0328-1
21. Münzel T, Gori T, Keaney JF Jr, Maack C, Daiber A. Pathophysiological role of oxidative stress in systolic and diastolic heart failure and its therapeutic implications. *Eur Heart J*. (2015) 36:2555–64. doi: 10.1093/eurheartj/ehv305
22. Haas MJ, Onstead-Haas L, Lee T, Torfah M, Mooradian AD. Angiotensin II receptor one (AT1) mediates dextrose induced endoplasmic reticulum stress and superoxide production in human coronary artery endothelial cells. *Int J Cardiol*. (2016) 220:842–50. doi: 10.1016/j.ijcard.2016.06.094
23. Koves TR, Ussher JR, Noland RC, Slentz D, Mosedale M, Ilkayeva O, et al. Mitochondrial overload and incomplete fatty acid oxidation contribute to skeletal muscle insulin resistance. *Cell Metab*. (2008) 7:45–56. doi: 10.1016/j.cmet.2007.10.013
24. Adams SH, Hoppel CL, Lok KH, Zhao L, Wong SW, Minkler PE, et al. Plasma acylcarnitine profiles suggest incomplete long-chain fatty acid beta-oxidation and altered tricarboxylic acid cycle activity in type 2 diabetic African-American women. *J Nutr*. (2009) 139:1073–81. doi: 10.3945/jn.108.103754
25. Lu Km, Nishimori H, Nakamura Y, Shima K, Kuwajima M. A missense mutation of mouse OCTN2, a sodium-dependent carnitine cotransporter, in the juvenile visceral steatosis mouse. *Biochem Biophys Res Commun*. (1998) 252:590–4. doi: 10.1006/bbrc.1998.9708
26. McLean RM. Measuring population sodium intake: a review of methods. *Nutrients*. (2014) 6:4651–62. doi: 10.3390/nu6114651
27. Kieneker LM, Eisenga MF, Gansevoort RT, de Boer RA, Navis G, Dullaart RPF, et al. Association of low urinary sodium excretion with increased risk of stroke. *Mayo Clin Proc*. (2018) 93:1803–9. doi: 10.1016/j.mayocp.2018.05.028
28. Graudal N, Jürgens G, Baslund B, Alderman MH. Compared with usual sodium intake, low- and excessive-sodium diets are associated with increased mortality: a meta-analysis. *Am J Hypertens*. (2014) 27:1129–37. doi: 10.1093/ajh/hpu028
29. O'Donnell M, Mente A, Rangarajan S, McQueen MJ, Wang X, Liu L, et al. Urinary sodium and potassium excretion, mortality, and cardiovascular events. *N Engl J Med*. (2014) 317:612–23. doi: 10.1056/NEJMoa1311889
30. Goodman BP. Evaluation of postural tachycardia syndrome (POTS). *Auton Neurosci*. (2018) 215:12–9. doi: 10.1016/j.autneu.2018.04.004
31. Bryarly M, Phillips LT, Fu Q, Vernino S, Levine BD. Postural orthostatic tachycardia syndrome: JACC focus seminar. *J Am Coll Cardiol*. (2019) 73:1207–28. doi: 10.1016/j.jacc.2018.11.059
32. Zhang Q, Liao Y, Tang C, Du J, Jin H. Twenty-four-hour urinary sodium excretion and postural orthostatic tachycardia syndrome. *J Pediatr*. (2012) 161:281–4. doi: 10.1016/j.jpeds.2012.01.054
33. Mar PL, Raj SR. Postural orthostatic tachycardia syndrome: mechanisms and new therapies. *Annu Rev Med*. (2020) 71:235–48. doi: 10.1146/annurev-med-041818-011630

Conflict of Interest: The authors declare that the research was conducted in the absence of any commercial or financial relationships that could be construed as a potential conflict of interest.

frontiers in Pediatrics

ORIGINAL RESEARCH
published: 05 May 2020
doi: 10.3389/fped.2020.00221

Clinical Characteristics for Differentiating Febrile Children With Suspected Kawasaki Disease Diagnosis

*Jia-Huei Yan [1,2,3], Ling-Sai Chang [1,2], Yi-Ju Lin [1,2], Mindy Ming-Huey Guo [1,2], Ying-Hsien Huang [1,2] and Ho-Chang Kuo [1,2]**

[1] Department of Pediatrics, Kaohsiung Chang Gung Memorial Hospital and Chang Gung University College of Medicine, Kaohsiung, Taiwan, [2] Kawasaki Disease Center, Kaohsiung Chang Gung Memorial Hospital, Kaohsiung, Taiwan, [3] Department of Pediatrics, Chiayi Chang Gung Memorial Hospital, Chiayi, Taiwan

Background: Kawasaki disease (KD) is a form of vasculitis that primarily affects children under the age of 5 years old. Patients may be missed or diagnosis delayed when initial clinical symptoms do not fulfill the traditional criteria or a normal echocardiography was found. In this study, we aimed to analyze factors that clinicians could use to differentiate febrile children suspected of KD.

Method: We retrospectively enrolled in this study a total of 50 febrile children who were initially suspected of KD, but they did not meet the American Heart Association (AHA) criteria for a diagnosis. However, some of these patients were diagnosed with KD during their second visit. We analyzed patients' characteristics, clinical symptoms, and laboratory data (initial data in the first visit).

Results: In total, 50 patients were enrolled in the study. Of those, ten patients were diagnosed with KD on their second visit (group 1), while the other 40 patients still did not fit a KD diagnosis (group 2). A higher neutrophil-to-lymphocyte ratio (NLR, $p = 0.037$) and higher C-reactive protein levels (CRP, $p = 0.02$) were found in group 1 when compared to group 2. A patient with a NLR >1.33 combined with a CRP more than 33 mg/L was more likely to have KD (Sensitivity 90%, specificity 69.2%, $p = 0.001$; Odds ratio 20.25, 95% confident interval 2.3–178.25).

Conclusion: Among patients suspected of KD that did not initially meet the criteria, clinicians should pay special attention to elevated neutrophil-to-lymphocyte ratios and CRP levels and closely follow up such patients.

Keywords: clinical characteristics, febrile children, kawasaki disease, C-reactive protein, neutrophil-to-lymphocyte ratio

OPEN ACCESS

Edited by:
Ruth Heying,
University Hospital Leuven, Belgium

Reviewed by:
Elumalai Appachi,
Baylor College of Medicine, United States
Lijian Xie,
Shanghai Children's Hospital, China

***Correspondence:**
Ho-Chang Kuo
erickuo48@yahoo.com.tw

Specialty section:
This article was submitted to Pediatric Cardiology, a section of the journal Frontiers in Pediatrics

Received: *15 May 2019*
Accepted: *14 April 2020*
Published: *05 May 2020*

Citation:
Yan J-H, Chang L-S, Lin Y-J, Guo MM-H, Huang Y-H and Kuo H-C (2020) Clinical Characteristics for Differentiating Febrile Children With Suspected Kawasaki Disease Diagnosis. Front. Pediatr. 8:221. doi: 10.3389/fped.2020.00221

INTRODUCTION

Kawasaki disease (KD) is characterized as a medium-sized vasculitis that particularly involves the coronary arteries. It is the most common cause of acquired heart disease in children under the age of 5 years old (1). The etiology of KD is still not completely known. The incidence of KD is higher in Asia than in the United States and Europe and has been increasing in recent decades (2, 3).

In Taiwan and Japan, the incidence is 3 to 15 times higher than in North America (1). KD can lead to coronary artery anomalies (CAA) if not properly treated with intravenous immunoglobulin (IVIG). In the pre-IVIG era, the CAA incidence rate was 20–25%, but IVIG therapy has reduced that to 3–5% (1, 4). Delaying both diagnosis and treatment are major risk factors of CAA persistence and such adverse cardiac events as myocardial ischemia and sudden cardiac arrest (4). The importance of early differentiation of KD from other fever patients cannot be overlooked.

KD diagnostic criteria is currently based on clinical findings, echocardiogram, and AHA supplementary laboratory data, so that clinicians can exclude other similar diseases (1). However, KD diagnosis can often be missed or postponed in the case of atypical or incomplete clinical presentation. The characteristic clinical features of KD include prolonged fever that lasts more than 5 days, and four of the following five symptoms: oral changes, non-exudative conjunctivitis, skin rash, extremity changes, and cervical lymphadenopathy (1, 5). Nevertheless, these symptoms and signs may appear at different times during the febrile period, and the presentation of illness is often not apparent in infants younger than 6 months old or incomplete KD patients (1, 6, 7). Pyuria may be treated as a urinary tract infection while subsequent skin rash, injected eyes, or red lips may be considered a reaction to antibiotics. KD may cause retropharyngeal edema and KD shock syndrome, which are often mistaken as being bacterial in origin (8). In this study, we reviewed suspected KD patients that did not fulfill the criteria at their first clinic visit, comparing and differentiating their clinical findings regarding KD diagnosis between it and their second visit.

METHOD

Study Design

We retrospectively reviewed 50 children who were suspected of KD by pediatric clinicians, but whose clinical conditions did not meet the American Heart Association's (AHA) criteria for diagnosing typical KD or incomplete KD (1) on the first visit. The cases were divided into two groups based on whether they fit the KD diagnosis on the second visit. For this study, we examined patients that visited Kaohsiung Chang-Gung Memorial Hospital from November 2008 to September 2018, and patients without complete medical chart records were excluded.

The AHA criteria for typical KD diagnosis is based on fever $\geq$5 days and the presence of $\geq$4 of the 5 clinical features (as our rapid memory method 1-2-3-4-5) (5): oral changes (1 mouth) (strawberry tongue, erythematous or cracking of lip, and/or erythema of oral mucosa), non-exudative bilateral bulbar conjunctival injection (2 eyes), cervical lymphadenopathy (3 fingers to check neck lymph node $\geq$1.5 cm diameter, usually unilateral), 4 limbs extremity changes (erythema and edema of the hands and feet and/or periungual desquamation), and dysmorphism skin rash (5 means many rashes). Incomplete KD is defined as children with fever $\geq$5 days, CRP $\geq$ 30 mg/L, and/or ESR $\geq$ 40 mm/hour, as well as two or three compatible criteria plus a positive echocardiogram finding or three or more of six laboratory features (anemia by age, platelet count $\geq$450000/mm^3 after 7th day of fever, albumin $\leq$ 3g/dL, elevated ALT level, WBC count $\geq$ 15000/mm^3, urine $\geq$ 10 WBC/high power field). Based on the AHA recommendations for an incomplete KD diagnosis, an echocardiogram finding is considered positive if any of the following three conditions are met (1): left anterior descending (LAD) coronary artery or right coronary artery (RCA) Z score of $\geq$2.5; presence of a coronary artery aneurysm in the echocardiogram; or the presence of $\geq$3 other suggestive features, including decreased left ventricular function, mitral regurgitation, pericardial effusion, or Z scores in LAD coronary artery or RCA of 2 to 2.5. This study was approved the Institutional Review Board of Chang Gung Memorial Hospital (102-0364B).

TABLE 1 | Patients' characteristics and clinical symptoms and signs.

	KD (Group 1)	Not KD (Group 2)	*P*-value
Total (*N*)	10	40	
Age [year; median (IQR)]	2.2 (1.5–4.3)	1.4 (0.8–3.2)	0.121
Gender Male	5	27	0.463
female	5	13	
Days of fever* [median (IQR)]	4.5 (3–5)	4 (3–6)	0.555
Initial clinical symptoms and signs [*N* (%)]			
Oral change	7 (70%)	25 (62.5%)	0.73
Non-exudative conjunctivitis	8 (80%)	26 (65%)	0.468
Extremity change	4 (40%)	20 (50%)	0.728
Skin rash	5 (50%)	30 (75%)	0.143
Lymphadenopathy	1 (10%)	4 (10.3%)	1

**Days of fever before first visit to our clinic.*

Data Analysis

We analyzed the patients' characteristics, clinical symptoms, and laboratory data (initial data of first visit) (**Tables 1**, **2**). Characteristics include patients' age, gender, and days of fever before their first visit. We compared clinical symptoms based on KD diagnostic criteria, including oral changes, non-exudative conjunctivitis, extremity changes, skin rash, and lymphadenopathy (>1.5 cm). We used the Kolmogorov-Smirnova test to examine the data and reveal non-normal distributions. We analyzed continuous variables using the Mann-Whitney test, while the chi-square test and Fisher's exact test were adopted for categorical variables. The cut-off point was determined through the ROC curve and Youden index. All data are presented by percentage and median with interquartile range (IQR). We considered $p < 0.05$ statistically significant. All statistical tests were performed using SPSS 22.0 (SPSS, Inc., Chicago, Illinois).

RESULTS

We enrolled 50 patients in this study, including 32 boys and 18 girls, 10 of which were diagnosed as KD with a positive echocardiogram finding or one or more new clinical features in their second visit (group 1) and 40 non-KD patients (group 2). The mean interval between first visit and second visit was 8.4 days. In group 1, five cases were diagnosed by a

TABLE 2-1 | Patients' laboratory data [median (IQR)] at first visit.

	KD (Group 1)	Not KD (Group 2)	*P*-value
Total (*N*)	10	40	
WBC (1000/mm^3)	11 (8.8–13)	11.5 (9–15.4)	0.594
Hemoglobulin(g/dL)	11.3 (10.7–12)	11.5 (11–12.2)	0.481
Platelet (1000/mm^3)	297.5 (248.5–408.5)	313.5 (259.5–392.8)	0.799
Neutrophil (%)	63.7 (51.9–77)	53 (43–65)	0.051
Lymphocyte (%)	29.7 (14–32.7)	37.9 (25.2–49.9)	0.048*
Neutrophil to lymphocyte ratio	2.1 (1.5–5.5)	1.39 (0.85–2.6)	0.037*
CRP (mg/L)	62.3(35.7–99.9)	26 (8.3–48.9)	0.020*
GOT (IU/L)	33 (24–52)	35.5 (28–44)	0.617
GPT (IU/L)	21 (12–55.8)	22 (14.8–32)	0.949
Albumin (g/dL)	4.1 (3.8–4.2)	4.2 (4–4.4)	0.098
Urine WBC (/μL)	6 (0–29)	1 (0–3)	0.200

*$p < 0.05$.

TABLE 2-2 | Patients' laboratory data [median (IQR)] at second visit.

	KD (Group 1)	Not KD (Group 2)	*P*-value
Patient numbers	10/10	7/40	
WBC (1000/mm^3)	11.1 (9.6–13.0)	9.6 (7.4–11.7)	0.299
Hemoglobulin (g/dL)	11.0 (10.0–11.7)	11.5 (10.7–12.2)	0.252
Platelet (1000/mm^3)	544.0 (403.5–591.5)	484.0 (327.0–527.0)	0.299
Neutrophil (%)	55.1 (35.5–69.0)	36.8 (19.0–56.0)	0.299
Lymphocyte (%)	32.0 (20.8–59.0)	53.8 (25.0–66.0)	0.470
Neutrophil to lymphocyte ratio	1.67(0.59-3.55)	0.68(0.29–2.32)	0.408
CRP (mg/L)	10.3 (2.5–26.4)	1.1 (0.2–10.1)	0.070
GOT (IU/L)	33.0 (26.8–42.3)	32.0 (25.0–50.0)	0.887
GPT (IU/L)	14.0 (8.5–42.0)	21.0 (15.0–52.0)	0.417
Albumin (g/dL)	3.9 (3.8–4.4)	¶	
Urine WBC (/μL)	0 (0–0)	¶¶	

¶ only 2 patients in group 2 obtained albumin (3.7, and 4.0 g/uL, respectively) in not KD group in second visit.
¶¶ only 1 patient obtained U-WBC data (61/uL) in not-KD group in second visit.
**p < 0.05.*

positive echocardiogram, four cases were diagnosed by new clinical features, and one case was diagnosed by both a positive echocardiogram and new features in the second visit (**Figure 1**); Of the 10 patients, 6 of them were atypical KD on the diagnosis in second visit. Moreover, in group 1, nine of them had normal echocardiography result and 1 did not perform echocardiography during 1st visit. However, 6 of them had coronary arteries dilatation or aneurysms formation at second visit. The mean ages were 2.2 (1.5–4.3) years and 1.4 (0.8–3.2) years old, and the days of fever before the first visit were 4.5 (3–5) days and 4 (3–6) days for group 1 and group 2, respectively. We found no statistically significant differences regarding age, gender, days of fever, and initial clinical symptoms between the two groups (**Table 1**).

We further analyzed laboratory data and found a higher neutrophil-to-lymphocyte ratio (NLR, $p = 0.037$) and higher C-reactive protein levels (CRP, $p = 0.02$) in group 1 compared to group 2 (**Table 2**). Cut-off points determined by ROC curve presented NLR > 1.33 (AUC = 0.715, sensitivity 100%, specificity 47.5%, $p = 0.008$, Odds ratio 1.48, 95% confident interval 1.16–1.88) and CRP > 33 mg/L (AUC = 0.74, sensitivity 90%, specificity 59%, $p = 0.011$, Odds ratio 12.94, 95% confident interval 1.49–112.44), both of which have a probability of predicting KD. By combining NLR > 1.33 and CRP > 33 mg/L, we found a higher odds ratio of 20.25 (95% confident interval 2.30–178.25) of KD predicting probability, as well as 90% sensitivity and 69.2% specificity ($P = 0.001$) (**Table 3**).

DISCUSSION

In this study, we demonstrated patients who were suspected of KD but did not meet either AHA diagnostic criteria. A diagnosis of KD consists of refractory and prolonged fever for more than 5 days and traditional four of five clinical presentation symptoms. However, patients with atypical or incomplete KD pose a challenge for pediatricians, particularly young infants <6 months old and older children at high risk of CAA development (1, 9). Atypical or incomplete presentation refers to patients with prolonged fever that only fit two or three clinical features. Symptoms may be dispersed over a period of time; for example, desquamation of the fingers and toes is a late finding that appears at 2∼3 weeks after onset of fever (10). KD may be misdiagnosed without careful clinical observation or echocardiogram finding. The current treatment recommendation is administering IVIG therapy within 10 days of the onset of illness (1, 11), and postponed treatment is the leading cause of CAA formation (4, 7, 9–11). Clinicians should closely follow up patients who are suspected of KD but do not fit the criteria.

The neutrophil-to-lymphocyte ratio (NLR) is considered the absolute neutrophil count divided by the absolute lymphocyte count and is a simple and inexpensive test to perform. Neutrophils reflect ongoing inflammation and enhanced inflammatory mediator secretion; on the other hand, lymphocytes represent immune regulatory response (12). NLR is a vital biomarker of the balance between inflammation and immune regulation and has been studied with regard to the prognostic and risk factors of cardiovascular diseases and cancer (13–15). Furthermore, previous studies have also demonstrated its predictive value for KD. A higher NLR is associated with IVIG-resistant KD and CAA formation (16–19). Our study demonstrated that the cut-off value of NLR of 1.33 has an odds ratio of 1.48 to predict KD with high sensitivity. Such higher sensitivity can indicate that clinicians should follow up with patients more closely and help them make a real KD diagnosis earlier.

CRP levels are responsible for a patient's inflammation status and can serve as a differentiating factor in this study. According to AHA guidelines for incomplete KD diagnosis, CRP > 3.0 mg/dL (=30 mg/L) and/or ESR ≥ 40 mm/hour is considered supplementary laboratory data (1). We determined that the CRP cut-off point of more than 33 mg/L can also be a predicting factor of KD, with an odds ratio of 12.94 (95% confident interval 1.49–112.44, sensitivity 90%, specificity 59%, $p = 0.011$). However, CRP levels are elevated not only in the case of inflammation but also in patients with an infectious disease. Clinicians must cautiously interpret CRP levels and rule out the possibility of

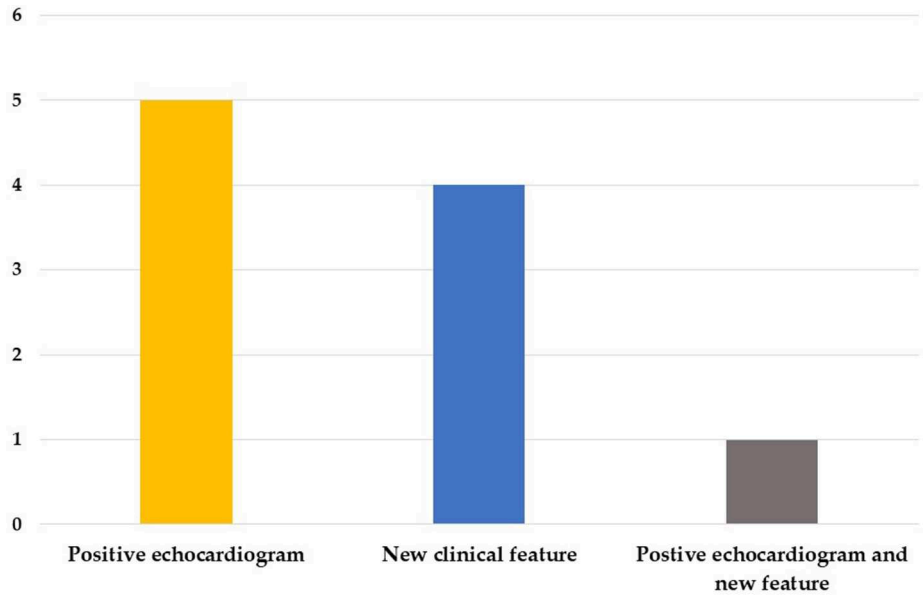

FIGURE 1 | Factors for diagnosis of KD based on the second visit.

TABLE 3 | The sensitivity, specificity and odds ratio of cut-points.

	NLR > 1.33	CRP > 33 mg/dL	NLR > 1.33 plus CRP > 33 mg/dL
Sensitivity	100%	90%	90%
Specificity	47.5%	59%	69.2%
P-value	0.008	0.011	0.001
Odds ratio (95% confident interval)	1.48 (1.16–1.88)	12.94 (1.49–112.44)	20.25 (2.30–178.25)

pathogen invasion and other systemic inflammation diseases, while a CRP level <33 mg/L is common in refractory febrile children with infection. Therefore, we combined the two cut-off values of both NLR and CRP to achieve a higher odds ratio of 20.25, a mildly lower sensitivity but better specificity than using NLR or CRP independently (95% confident interval 2.30–178.25, sensitivity 90% and specificity 69.2%, $P = 0.001$). For patients suspected of KD but that do not meet either of the AHA criteria for typical or incomplete KD, pediatric clinicians should pay particular attention to elevated NLR and CRP levels and closely follow up with those patients. As mentioned in the **Table 1**, the febrile days before 1st visit ranged from 3 to 6 days. It meant that we should pay attention and check NLR and CRP when we raise the suspicion to KD as early as fever longer than 3 days. A high sensitivity and odds ratio can provide clinicians with a useful tool for differentiation.

This study has certain limitations. First, this study was a retrospectively reviewed study, and the symptoms and onset of febrile days may have had recall bias from patients and family; furthermore, some medical records did not present complete data. Second, the number of patients diagnosed with KD on the second visit was small, which may weaken the study's statistical power, and we hope to obtain more cases to conduct a larger study in the future. Third, this study has a single center, so our results should be examined in another hospital or managed as a cohort study in the future. Further research is still needed about the clinical factors that can distinguish KD from other febrile diseases.

CONCLUSION

Identifying atypical presentations of KD in a timely manner poses a challenge for pediatricians. Delaying treatment can result in cardiovascular sequalae. NLR and CRP are both biomarkers that represent inflammation and immune regulatory pathways and can be used as predictive tools of KD. Among patients suspected of KD that did not initially meet the criteria, clinicians should be aware of an elevated neutrophil-to-lymphocyte ratio, as well as CRP levels, and follow up those patients closely.

DATA AVAILABILITY STATEMENT

The datasets generated and analyzed during the current study are not publicly available due to strict ethical regulation of information privacy in Taiwan. Requests to access these datasets should be directed to Dr. Ho-Chang Kuo, erickuo48@yahoo.com.tw.

ETHICS STATEMENT

We retrospectively reviewed those cases' medical records, so we did not obtain the informed consent. On the other hand, our

study was approved by Institutional Review Board of Chang Gung Memorial Hospital (102-0364B).

AUTHOR CONTRIBUTIONS

All authors were involved in drafting the article or revising it critically and all authors approved the final version to be published. MG, Y-HH, and H-CK contributed to conceptualization and study design of the study, J-HY and Y-JL interpreted and statistically analyzed the data, J-HY was the major contributor in writing the manuscript. L-SC and H-CK were responsible for monitoring and data management, reviewing and editing the manuscript.

FUNDING

This study was partly supported by grants from the Ministry of Science and Technology, Taiwan (MOST: 105-2314-B-182-050-MY3) and Chang Gung Memorial Hospital (CMRPG8E0211, CMRPG8E0212, and CORPG8F0011-2). These organizations had no role in the study design, data collection and analysis, decision to publish, or preparation of this manuscript.

ACKNOWLEDGMENTS

We would like to thank the Biostatistics Center, Kaohsiung Chang Gung Memorial Hospital for its statistical work.

REFERENCES

1. McCrindle BW, Rowley AH, Newburger JW, Burns JC, Bolger AF, Gewitz M, et al. Diagnosis, treatment, and long-term management of kawasaki disease: a scientific statement for health professionals from the American Heart Association. *Circulation.* (2017) 135:e927–99. doi: 10.1161/CIR.0000000000000484
2. Lin MT, Wu MH. The global epidemiology of Kawasaki disease: review and future perspectives. *Glob Cardiol Sci Pract.* (2017) 2017:e201720. doi: 10.21542/gcsp.2017.20
3. Uehara R, Belay ED. Epidemiology of Kawasaki disease in Asia, Europe, and the United States. *J Epidemiol.* (2012) 22:79–85. doi: 10.2188/jea.JE20110131
4. Friedman KG, Gauvreau K, Hamaoka-Okamoto A, Tang A, Berry E, Tremoulet AH, et al. Coronary artery aneurysms in kawasaki disease: risk factors for progressive disease and adverse cardiac events in the US Population. *J Am Heart Assoc.* (2016) 5:e003289. doi: 10.1161/JAHA.116.003289
5. Kuo HC. Preventing coronary artery lesions in Kawasaki disease. *Biomed J.* (2017) 40:141–6. doi: 10.1016/j.bj.2017.04.002
6. Anderson MS, Todd JK, Glode MP. Delayed diagnosis of Kawasaki syndrome: an analysis of the problem. *Pediatrics.* (2005) 115:e428–33. doi: 10.1542/peds.2004-1824
7. Minich LL, Sleeper LA, Atz AM, McCrindle BW, Lu M, Colan SD, et al. Delayed diagnosis of Kawasaki disease: what are the risk factors? *Pediatrics.* (2007) 120:e1434–40. doi: 10.1542/peds.2007-0815
8. Vervoort D, Donne M, Van Gysel D. Pitfalls in the diagnosis and management of Kawasaki disease: an update for the pediatric dermatologist. *Pediatr Dermatol.* (2018) 35:743–7. doi: 10.1111/pde.13620
9. Son MBF, Newburger JW. Kawasaki Disease. *Pediatr Rev.* (2013) 34:151–62. doi: 10.1542/pir.34-4-151
10. Zhu FH, Ang JY. The clinical diagnosis and management of Kawasaki disease: a review and update. *Curr Infect Dis Rep.* (2016) 18:32. doi: 10.1007/s11908-016-0538-5
11. Bal AK, Prasad D, Umali Pamintuan MA, Mammen-Prasad E, Petrova A. Timing of intravenous immunoglobulin treatment and risk of coronary artery abnormalities in children with Kawasaki disease. *Pediatr Neonatol.* (2014) 55:387–92. doi: 10.1016/j.pedneo.2013.11.007
12. Azab B, Zaher M, Weiserbs KF, Torbey E, Lacossiere K, Gaddam S, et al. Usefulness of neutrophil to lymphocyte ratio in predicting short- and long-term mortality after non-ST-elevation myocardial infarction. *Am J Cardiol.* (2010) 106:470–6. doi: 10.1016/j.amjcard.2010.03.062
13. Bhat T, Teli S, Rijal J, Bhat H, Raza M, Khoueiry G, et al. Neutrophil to lymphocyte ratio and cardiovascular diseases: a review. *Expert Rev Cardiovasc Ther.* (2013) 11:55–9. doi: 10.1586/erc.12.159
14. Faria SS, Fernandes PC, Jr, Silva MJ, Lima VC, Fontes W, et al. The neutrophil-to-lymphocyte ratio: a narrative review. *Ecancermedicalscience.* (2016) 10:702. doi: 10.3332/ecancer.2016.702
15. Guthrie GJ, Charles KA, Roxburgh CS, Horgan PG, McMillan DC, Clarke SJ. The systemic inflammation-based neutrophil-lymphocyte ratio: experience in patients with cancer. *Crit Rev Oncol Hematol.* (2013) 88:218–30. doi: 10.1016/j.critrevonc.2013.03.010
16. Cho HJ, Bak SY, Kim SY, Yoo R, Baek HS, Yang S, et al. High neutrophil: lymphocyte ratio is associated with refractory Kawasaki disease. *Pediatr Int.* (2017) 59:669–74. doi: 10.1111/ped.13240
17. Demir F, Karadeniz C, Ozdemir R, Yozgat Y, Celegen K, Karaaslan U, et al. Usefulness of neutrophil to lymphocyte ratio in prediction of coronary artery lesions in patients with Kawasaki Disease. *Balkan Med J.* (2015) 32:371–6. doi: 10.5152/balkanmedj.2015.151108
18. Ha KS, Lee J, Jang GY, Lee J, Lee KC, Son CS, et al. Value of neutrophil-lymphocyte ratio in predicting outcomes in Kawasaki disease. *Am J Cardiol.* (2015) 116:301–6. doi: 10.1016/j.amjcard.2015.04.021
19. Takeshita S, Kanai T, Kawamura Y, Yoshida Y, Nonoyama S. A comparison of the predictive validity of the combination of the neutrophil-to-lymphocyte ratio and platelet-to-lymphocyte ratio and other risk scoring systems for intravenous immunoglobulin (ivig)-resistance in Kawasaki disease. *PLoS ONE.* (2017) 12:e0176957. doi: 10.1371/journal.pone.0176957

Conflict of Interest: The authors declare that the research was conducted in the absence of any commercial or financial relationships that could be construed as a potential conflict of interest.

frontiers in Pediatrics

ORIGINAL RESEARCH
published: 05 May 2020
doi: 10.3389/fped.2020.00186

Hypoperfusion With Vomiting, Abdominal Pain, or Dizziness and Convulsions: An Alert to Fulminant Myocarditis in Children

Angang Zhu[1†], *Tian Zhang*[2†], *Xiaobi Hang*[3], *Xiaoguang Zhang*[2], *Yingying Xiong*[1], *Tao Fang*[4] *and Mingwu Chen*[1,4*]

[1] Department of Pediatrics, Anhui Provincial Hospital, Wannan Medical College, Hefei, China, [2] Department of Pediatrics, Anhui Provincial Hospital Affiliated to Anhui Medical University, Hefei, China, [3] Department of Pediatrics, Anhui Provincial Children's Hospital, Hefei, China, [4] Division of Life Sciences and Medicine, Department of Pediatrics, The First Affiliated Hospital of USTC, Anhui Provincial Hospital, University of Science and Technology of China, Hefei, China

OPEN ACCESS

Edited by:
Hongfang Jin,
Peking University First Hospital, China

Reviewed by:
Lijian Xie,
Shanghai Children's Hospital, China
Yusheng Pang,
First Affiliated Hospital of Guangxi Medical University, China

***Correspondence:**
Mingwu Chen
chenmingwu01@126.com

[†] These authors share first authorship

Specialty section:
This article was submitted to Pediatric Cardiology, a section of the journal Frontiers in Pediatrics

Received: 31 January 2020
Accepted: 30 March 2020
Published: 05 May 2020

Citation:
Zhu A, Zhang T, Hang X, Zhang X, Xiong Y, Fang T and Chen M (2020) Hypoperfusion With Vomiting, Abdominal Pain, or Dizziness and Convulsions: An Alert to Fulminant Myocarditis in Children. Front. Pediatr. 8:186. doi: 10.3389/fped.2020.00186

Objective: To investigate the clinical features, treatment methods, and outcomes of fulminant myocarditis (FM) in children.

Methods: The clinical data of 23 children with FM hospitalized in the First Affiliated Hospital of USTC, Division of Life Sciences and Medicine, University of Science and Technology of China (Anhui Provincial Hospital) and Anhui Provincial Children's Hospital from January 2011 to September 2019 were retrospectively analyzed.

Results: Among the 23 patients analyzed, 10 were male and 13 were female. The patients aged from 6 months to 14 years old (6.5 ± 3.4 years), and 18 patients were over 3 years old. There were 14 cases with respiratory symptoms, 16 cases with gastrointestinal symptoms, 15 cases with neurological symptoms, and 19 cases with hypoperfusion manifestations. Creatine kinase MB (CK-MB) and cardiac troponin I (CTnI) levels were increased in 19 and 21 cases, respectively. Electrocardiography (ECG) showed ST-T changes in 18 cases and atrioventricular blocks (AVB) in 15 cases. Echocardiography (ECHO) showed cardiac chamber enlargement (CCE) in eight cases, left ventricular systolic dysfunction in five cases, decrease in left ventricular ejection fraction (LVEF) in four cases, reduction in wall motion in two cases, and pericardial effusion in seven cases. Intravenous immunoglobulin (IVIG) and glucocorticoids were administered to 19 and 20 patients, respectively. Fourteen patients were treated with temporary pacemakers, one patient received extracorporeal membrane oxygenation (ECMO), one patient received continuous renal replacement therapy (CRRT), and one patient received ECMO combined with CRRT. Twenty patients improved at discharge, and three patients died.

Conclusion: Preschool and school-age children showing hypoperfusion symptoms, such as paleness, cold, clammy limbs, and capillary refill time (CRT) extension, accompanied by vomiting, abdominal pain, dizziness, convulsions, and other symptoms, should be carefully examined for FM. CK-MB, CTnI, ECG, and echocardiogram need

to be performed at the earliest opportunity. In the early stages of FM, vital signs should be actively monitored, high-dose IVIG and glucocorticoids should be administered, and life support technologies such as temporary pacemakers, ECMO, and CRRT should be used to increase the survival rate of children with FM as needed.

Keywords: hypoperfusion, fulminant, myocarditis, children, retrospective analysis

INTRODUCTION

Fulminant myocarditis (FM) is an inflammatory process of the myocardium that is an important cause of cardiac dysfunction in children and is characterized by abrupt onset, fast progress, and high mortality (1, 2). Patients may present with acute heart failure, cardiogenic shock, Adams-Stokes syndrome, or fatal arrhythmia in a short time and are usually admitted to the hospital with digestive system symptoms such as vomiting and abdominal pain or neurological symptoms such as dizziness and convulsions (3). The initial clinical symptoms are often atypical and can easily be misdiagnosed. The aim of this study was to improve our understanding of the diagnosis and treatment of FM by analyzing the clinical features, treatment methods, and outcomes in children with FM.

MATERIALS AND METHODS

Research Subjects

Data from 23 children with a diagnosis of FM hospitalized in the First Affiliated Hospital of USTC, Division of Life Sciences and Medicine, University of Science and Technology of China (Anhui Provincial Hospital) and Anhui Provincial Children's Hospital from January 2011 to September 2019 were retrospectively analyzed.

Ethics Statements

This study was approved by the ethics committee of the First Affiliated Hospital of USTC, Division of Life Sciences and Medicine, University of Science and Technology of China (Anhui Provincial Hospital) and Anhui Provincial Children's Hospital, and written informed consent was obtained from the parents of the study participants.

Inclusion Criteria

All selected children were diagnosed with FM and were younger than 16 years old. The diagnosis of FM was based on clinical manifestations, electrocardiography (ECG), and echocardiography, which is in line with the criteria for the clinical diagnosis of myocarditis in the Diagnostic Recommendations for Children with Myocarditis (2018 edition) (4) and the diagnostic criteria for FM recommended by Ammirati et al. (5). The following clinical manifestations were considered for the diagnosis of FM: acute onset, cardiac hemodynamic instability, hemodynamic or circulatory support to maintain heart function or blood pressure, and evidence of myocardial damage suggesting cardiac dysfunction, such as changes in CK-MB levels, CTnI levels, ECG, and echocardiography.

Exclusion Criteria

Congenital heart disease, non-ischemic cardiomyopathy, endocardial elastic fibrosis, and myocardial infarction.

Research Methods

The following clinical data of the 23 children were reviewed: age; gender; clinical manifestations; myocardial injury biomarkers, such as CK-MB, CTnI, N-terminal pro-B-type natriuretic peptide (NT-pro-BNP), and B-type natriuretic peptide (BNP) levels; ECG; echocardiography; treatment methods; outcomes.

Clinical Treatment

All 23 children received treatments including bed rest, oxygen, anti-infective therapy, myocardial nutrition, anti-shock treatment, anti-heart failure treatment, anti-arrhythmia treatment, and other comprehensive treatments after admission. IVIG, glucocorticoids, temporary pacemakers, ECMO, and CRRT were administered according to the condition of the patients.

Statistical Analysis

The SPSS 21.0 statistical software was used for statistical analysis. The measured data are expressed as mean ± standard deviation, and the count data are expressed as percentages (%).

RESULTS

The main clinical data of the 23 children with FM are shown in **Table 1**.

Age and Gender

Among the 23 patients analyzed, 10 were male and 13 were female. The patients were aged from 6 months to 14 years old (6.5 ± 3.4 years). Five patients (22%) were under the age of 3. Eighteen patients (78%) were over 3 years old, of which seven patients (30%) were aged between 3 and 7 years old, and 11 patients (48%) were aged over 7 years old (**Figure 1**).

Clinical Manifestations

The initial symptoms of children with FM were varied. Respiratory symptoms such as fever and cough occurred in 14 patients (61%); digestive system symptoms such as nausea, vomiting, and abdominal pain occurred in 16 patients (70%); 15 patients (65%) presented with neurological symptoms such as headache, dizziness, syncope, convulsion, drowsiness, and coma. Regarding the circulatory symptoms, there were 19 patients (83%) with hypoperfusion manifestations, such as paleness, cold, clammy limbs, and capillary refill time (CRT) extension (>3 s), and 10 patients (43%) with chest pain, chest tightness, and

TABLE 1 | Main clinical data of 23 children with FM.

Patient	Age	Gender	Symptoms	CK-MB (IU/L)	CTnI (μg/L)	ECG	ECHO		Treatment	Outcome
							Changes	LVEF (%)		
1	8 years	M	H, NSS, DSS	72	20.069	ST-T change, AVB	/	67	IVIG, GC, TP	Improve
2	7 years	F	H, NSS, DSS, RSS	129	>50	AVB	PE, RIWM	48	IVIG, TP, CRRT	Died
3	35 months	F	DSS, RSS	118	38.13	ST-T change, AVB	/	53	IVIG, GC, TP	Died
4	8 years	F	H, NSS, DSS	95	8.762	ST-T change, AVB	PE	53	IVIG, GC, TP	Improved
5	11 years	F	H, NSS, DSS, RSS	11	23.476	ST-T change, AVB	PE	61	IVIG, GC, TP	Improved
6	7 years	M	H, NSS, DSS, RSS	806	4.67	ST-T change, AVB	PE	58	IVIG, GC, TP	Improved
7	32 months	F	H, DSS, RSS	24	0.03	ST-T change, AVB	/	73	IVIG, GC, TP	Improved
8	11 years	M	/	47	15.955	ST-T change, AVB	/	62	IVIG, GC, TP	Improved
9	9 years	F	H	39	8.51	ST-T change	RIWM	36	IVIG, GC	Improved
10	8 years	F	DSS	67	18.296	ST-T change	/	75	IVIG, GC	Improved
11	8 years	F	H	30	3.089	ST-T change	/	62	/	Improved
12	10 years	M	H, NSS, RSS	8.3	0.06	ST-T change, AVB	CCE	66	GC, TP	Improved
13	6 months	F	DSS, RSS	20	0.017	AVB	/	66	IVIG, GC	Improved
14	8 years	F	H, NSS, DSS, RSS	82	52.2	ST-T change, AVB	/	65	IVIG, GC, TP	Improved
15	14 years	M	H, NSS, RSS	116.5	2.9	/	CCE	72	IVIG, GC	Improved
16	5 years	M	H, NSS, RSS	39.83	3.4	ST-T change, AVB	LVSD, CCE	67	IVIG, GC, TP	Improved
17	1 years	M	H, NSS	46.4	6.25	ST-T change	/	/	/	Died
18	4 years	M	H, DSS	26.5	13.3	ST-T change	LVSD, PE, CCE	53	IVIG, GC	Improved
19	3 years	F	H, NSS, DSS, RSS	56.3	8.7	ST-T change, AVB	/	59	IVIG, GC, TP	Improved
20	7 years	F	H, NSS, DSS, RSS	156.19	29.9	ST-T change, AVB	LVSD, PE, CCE	58	IVIG, GC, TP, ECMO	Improved
21	1 years	F	H, NSS, DSS, RSS	11.49	1.84	ST-T change	LVSD, CCE	22	IVIG, GC, ECMO, CRRT	Improved
22	10 years	M	H, NSS, DSS	15.08	0.993	AVB	CCE	64	GC, TP	Improved
23	5 years	M	H, NSS, DSS, RSS	22	1.77	/	LVSD, PE, CCE	26	IVIG, GC	Improved

CK-MB, creatine kinase MB; CTnI, cardiac troponin I; ECG, electrocardiography; ECHO, echocardiography; LVEF, left ventricular ejection fraction; H, hypoperfusion; NSS, neurological system symptoms; DSS, digestive system symptoms; RSS, respiratory system symptoms; AVB, atrioventricular block; PE, pericardial effusion; RIWM, reduction in wall motion; CCE, cardiac chamber enlargement; LVSD, left ventricular systolic dysfunction; IVIG, intravenous immunoglobulin; GC, glucocorticoid; TP, temporary pacemaker; CRRT, continuous renal replacement therapy; ECMO, extracorporeal membrane oxygenation.

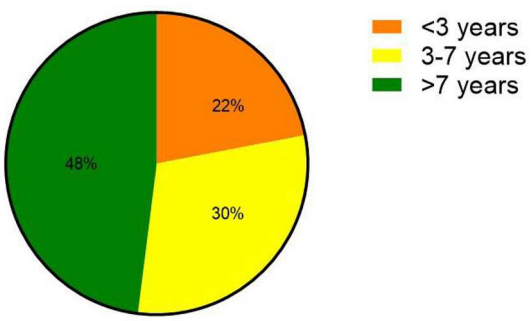

FIGURE 1 | Age distribution of children with FM.

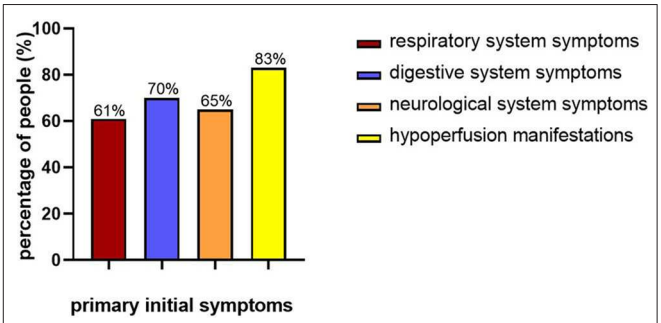

FIGURE 2 | Primary initial symptoms of children with FM.

palpitation (**Figure 2**). The time from onset to admission was 0–5 days (2.4 ± 1.3 days). Fourteen patients (61%) suffered from low blood pressure, eight patients (35%) had heart failure, and five patients (22%) had hepatosplenomegaly. One child was admitted to the hospital due to fever and convulsions, accompanied by pale complexion and hypotension, and then quickly developed shock and heart failure, and finally died after 2 h.

Myocardial Injury Biomarkers

Twenty-three children were admitted to the hospital for testing myocardial injury biomarkers. CK-MB levels (normal physiological range: 0–16 IU/L) were increased in 19 children (83%), which peaked at 1–8 days (3.4 ± 2.3 days) after onset and returned to the normal range in 14 patients after 3–17 days (8.7 ± 4.3 days). CTnI levels (normal physiological range: 0–0.03 g/L) were increased in 21 cases (91%), peaking at 1–6 days (3.0 ± 1.6

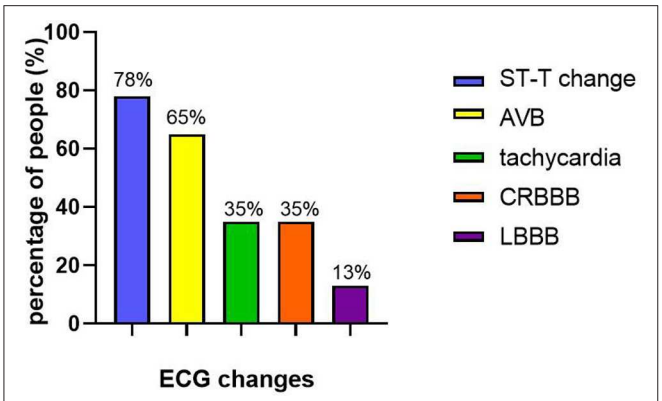

FIGURE 3 | ECG changes of children with FM.

days) after onset and returning to the normal range in 19 patients after 7–29 days (14.4 ± 6.7 days). An NT-pro-BNP examination was completed for 10 patients, and the resulting value was high in eight patients (>300 pg/mL). BNP examination results are available for seven patients, and the value was high in six patients (>100 pg/mL).

ECG

All children were examined using a standard 12-lead ECG after admission. ST-T abnormalities were found in 18 children (78%). There were 15 cases (65%) with atrioventricular blocks (AVB), of which three cases (13%) were second-degree AVB and 12 cases (52%) were third-degree AVB. The AVB occurred between days 1 and 6 (3.6 ± 1.6 days) after onset, and the patients recovered after 1–14 days (6.9 ± 4.3 days). There were eight cases (35%) with tachycardia, most of which were sinus tachycardia cases. The manifestations of the child who died quickly were ST-T changes and sinus tachycardia, quickly progressing into cardiac arrest. Complete right bundle branch block (CRBBB) occurred in eight children (35%), and left bundle branch block (LBBB) occurred in three children (13%). At the time of discharge, there were six children with CRBBB and two children with LBBB (**Figure 3**).

Echocardiography

Twenty-two children underwent echocardiography examination (the child who died quickly did not undergo this examination). Cardiac chamber enlargement (CCE) occurred in eight cases (36%): there were three cases of left cardiac enlargement and five cases of total cardiac enlargement. Four patients with CCE recovered after 12–19 days (14.8 ± 2.9 days), and the other patients did not recover, even at discharge. Five cases (23%) presented with left ventricular systolic dysfunction: two recovered within 10 days, one recovered after 19 days, and two did not recover even at discharge. Four cases (18%) had a decreased left ventricular ejection fraction (LVEF) (<50%), of which it was restored in two cases (one died, and one did not recover). Two cases (9%) had a reduction in wall motion, and seven cases (32%) had mild pericardial effusion.

Treatment and Outcome

All patients were treated with conventional treatments, including bed rest, oxygen, anti-infective therapy, myocardial nutrition, anti-shock, anti-heart failure, and anti-arrhythmia treatments. IVIG (total 2 g/kg over a period of 2 days) was used in 19 patients (83%). Twenty patients (87%) were treated with glucocorticoid therapy (methylprednisolone 10 mg/kg/d for 3 days and prednisolone 2 mg/kg/d, decreased gradually and maintained for 18–24 weeks based on the condition). IVIG combined with glucocorticoids was administered to 18 patients (78%). The CTnI levels decreased after treatment with IVIG and/or glucocorticoids in 19 patients. Of the 15 patients with second-degree AVB or third-degree AVB, 14 (61%) received temporary pacemakers for 2–24 days (9.3 ± 6.6 days), and the remaining one patient rejected pacemaker implantation. For the patients with cardiogenic shock after conventional therapy, the following treatments were used: ECMO was used in one patient for 7 days, CRRT was used in one patient for 8 h, ECMO combined with CRRT was used in one patient for 5 days, and the child who was only treated with CRRT developed multiple organ failure leading to death. Overall, 20 (87%) of the 23 patients improved, and three patients (13%) died. Clinical symptom recovery was achieved in the children who survived, and most examination indicators were gradually restored to the normal range. ECG was assessed after 6 months of follow-up in nine children, of which six were cured and two presented with CRBBB, and the status of one was unknown (the cellphone had no service).

DISCUSSION

Myocarditis is usually related to viral infections and post-viral immune-mediated responses. FM is the most severe type of viral myocarditis. It has been reported that the mechanisms of this disease progression are associated with an immunoreaction. Viral infection results in damage to myocardial cells, which can induce immune responses causing cardiac damage. Necrotic myocardial cells may release autoantigens, which can activate the immune reaction leading to the obstruction of nerve-body fluid regulation, myocardial remodeling, and myocardial dysfunction. In more serious instances, it can cause heart failure, cardiogenic shock, and sudden death (1). FM can occur in all age groups of children. In this study, 78% of children with FM were over 3 years old, showing that the majority were preschool and school-age children. At the onset, 70% of patients had digestive system symptoms, and 65% had neurological symptoms. The non-cardiac manifestations mainly included digestive system symptoms, such as vomiting and abdominal pain or neurological system symptoms such as dizziness and convulsions, which was consistent with the results reported in other studies (6). FM can cause extensive or localized necrosis of myocardial cells or tissues, severe heart pumping dysfunction, and decreased cardiac output, leading to a decrease in effective blood volume (1, 7), which results in a series of hypoperfusion manifestations of organs and tissues. The inadequacy of effective circulatory blood volume can start the compensatory mechanism of the body and activate

the sympathetic-adrenal medulla system, subsequently raising the level of catecholamines. This hormone can cause cutaneous vasoconstriction and reduce cutaneous blood flow, leading to a pale complexion. At the same time, the secretion of sweat glands is increased, and the skin becomes wet, which manifests as cold, clammy limbs. Low blood volume affects the recovery of capillary blood flow after being pressed (8). Around 83% of children showed paleness, cold, clammy limbs, and CRT extension, which were considered to be connected with heart-pumping function dysfunction due to FM. These clinical manifestations, which are often ignored at the first visit, should be paid more attention.

Biomarkers of myocardial injury are widely used in the clinical diagnosis of heart diseases. Creatine kinase (CK) and CTnI are common markers for detecting myocardial injury. Wang et al. reported that the rise of CK is an early feature of FM (9). Earlier studies found that the levels of CK-MB and CTnI in patients with FM were elevated more significantly than in patients without FM and that CTnI values were more sensitive and specific (10). In addition, recent studies have shown that NT-Pro-BNP and BNP levels can reflect impaired cardiac function, which is conducive to the early identification of FM. Levels of CTnI >1 μg/L and high BNP levels are risk factors that influence the prognosis of patients (3, 11). In this study, the biomarkers of myocardial injury were increased diversely in most children in the early stages of FM, which is useful since it is suggested that early detection is helpful for the diagnosis of this disease. After treatment, these indicators gradually returned to the normal range, showing that it can be used to judge recovery and prognosis.

ECG and echocardiography are important techniques for the diagnosis of FM. Electrocardiography of patients with FM was characterized by ST-T changes, AVB, and various ectopic arrhythmias in the acute phase (12); 65% of children with FM presented ST-T changes with AVB, and second-degree AVB was more common. The main echocardiography findings in children with FM were decreased ventricular wall motion and ejection fraction, thickened ventricular wall, heart dilation, pericardial effusion, valvular regurgitation, and endoluminal thrombosis (13). The decrease in ejection fraction indicates cardiac insufficiency, and the reduction of ventricular wall motion amplitude and ejection fraction can reflect the severity of FM, which are important indicators for evaluating the prognosis of children with FM (14). Decreased LVEF, pericardial effusion, and decreased ventricular wall motion amplitude occurred in a small number of patients in this study. The small number of samples or the non-acute phase of the disease at the time of testing may be the reason for the low positivity rate of echocardiography. Endomembrane biopsy (EMB) is important for diagnosing FM, but it is invasive (15). In the current practice, EMB is seldom used to diagnose myocarditis because of the unstable hemodynamics in patients and the risks inherent to the procedure. In addition, cardiac magnetic resonance (CMR) is a valuable non-invasive method that can be applied for the diagnosis of FM with high sensitivity and specificity (16). Myocardial perfusion imaging is also helpful (17).

Of the 19 patients with hypoperfusion, 15 showed increased CK-MB levels, 17 showed increased CTnI levels, 17 had positive findings on ECG, and 13 had positive results on echocardiography for FM, suggesting that the manifestations of hypoperfusion have implications for the diagnosis of FM. The positivity rate of various checks in patients who had neurological symptoms or gastrointestinal symptoms was similar to that in patients with hypoperfusion. Therefore, we recommend that patients who present hypoperfusion accompanied by neurological symptoms or digestive system symptoms should be alerted to the possibility of FM.

Early comprehensive treatment of FM is essential. Treatment with bed rest, oxygen, anti-infective therapy, myocardial nutrition, anti-shock, anti-heart failure, and anti-arrhythmia treatments should be used to maintain heart function. One study has indicated that the early use of glucocorticoids in large doses is effective in the treatment of FM and can reduce mortality (18). Chen et al. found that glucocorticoids may improve cardiac function but cannot reduce mortality (19). Studies have shown that IVIG is beneficial for the treatment of FM and can improve LVEF and long-term prognosis of patients with this disease (20, 21). However, the use of IVIG and glucocorticoids as immunotherapy for this condition remains controversial. Around 78% of patients received an early application of IVIG combined with glucocorticoids, leading to only one child death (of the three children who died, one died soon after admission without the application of glucocorticoids and IVIG, and glucocorticoids alone were used for the other), suggesting that early immunotherapy can effectively improve the success rate of rescue. In recent years, temporary pacemakers, ECMO, CRRT, and other life support technologies have been gradually applied to FM. Patients can manifest Adams-stokes syndrome in a short period of time and even suffer cardiac shock and cardiac arrest. The installation of a temporary pacemaker is a quick and effective treatment measure to save lives. The timing of temporary pacemaker implantation directly determines the treatment effect and prognosis (22). Fourteen patients with AVB received temporary pacemakers to maintain stable hemodynamics, of which only one patient died. Lorusso et al. pointed out that ECMO could provide strong circulatory support for patients with FM and cardiogenic shock on the basis of 5 years of multi-institutional experience (23). A weighted meta-analysis of 170 patients with FM indicated that the survival rate at discharge was nearly 66.9% after ECMO treatment (24). For patients who are not hemodynamically stable with conventional treatments or even pacemakers, ECMO combined with CRRT may be a solution to the problem (25). One patient who was treated with ECMO and one patient who received ECMO combined with CRRT were alive at discharge. However, one patient with hemodynamic instability only accepted CRRT and soon died of multiple organ failure. Our data suggest that immunotherapy is important for treating FM; temporary pacemakers should be used in patients with AVB, and ECMO combined with CRRT should be applied to patients with circulation instabilities after conventional treatments.

There are some limitations to our study. This is a small-sized retrospective clinical study. The conclusions of this study still need to be proven in more multicenter and large-scale clinical studies. Due to technical and financial issues, CMR or myocardial perfusion imaging could not be performed.

CONCLUSION

The onset of FM is rapid, and the clinical manifestations vary, which can quickly lead to the death of children with cardiogenic shock. Therefore, early and accurate diagnosis is essential. When preschool and school-age children present with hypoperfusion manifestations such as paleness, cold, clammy limbs, and CRT extension, accompanied by vomiting, abdominal pain, dizziness, convulsions, and other such symptoms, they should be carefully examined for FM. Timely measurements of CK-MB and CTnI levels, together with ECG and echocardiogram, are essential. Reasonable treatment is of great significance in improving the prognosis of children with FM. In the early stage of FM, vital signs should be actively monitored, high-dose IVIG and glucocorticoids should be administered, and life support technologies such as temporary pacemakers, ECMO, and CRRT should be used to increase the survival rate of children with FM as and when needed.

DATA AVAILABILITY STATEMENT

All datasets generated for this study are included in the article/supplementary material.

ETHICS STATEMENT

The studies involving human participants were reviewed and approved by the Ethics Committee of the First Affiliated Hospital of USTC, Division of Life Sciences and Medicine, University of Science and Technology of China (Anhui Provincial Hospital) and Anhui Provincial Children's Hospital. Written informed consent to participate in this study was provided by the participants' legal guardian/next of kin.

AUTHOR CONTRIBUTIONS

AZ has obtained the approval of all other co-authors to submit this article. All the authors have contributed to the manuscript.

FUNDING

The study was supported by the Natural Science Foundation of Anhui Province (grant no. 21608085MH196).

ACKNOWLEDGMENTS

We would like to thank the patients and their families for their generous participation in this study.

REFERENCES

1. Di Filippo S. Improving outcomes of acute myocarditis in children. *Expert Rev Cardiovasc Ther.* (2016) 14:117–25. doi: 10.1586/14779072.2016.1114884
2. Nakamura T, Ishida K, Taniguchi Y, Nakagawa T, Seguchi M, Wada H, et al. Prognosis of patients with fulminant myocarditis managed by peripheral venoarterial extracorporeal membranous oxygenation support: a retrospective single-center study. *J Intensive Care.* (2015) 3:5. doi: 10.1186/s40560-014-0069-9
3. Lee EY, Lee HL, Kim HT, Lee HD, Park JA. Clinical features and short-term outcomes of pediatric acute fulminant myocarditis in a single center. *Korean J Pediatr.* (2014) 57:489–95. doi: 10.3345/kjp.2014.57.11.489
4. Subspecialty Group of Cardiology tSoPCMA, Collaborating Group of Myocarditis tSGoCtSoPCMA, Editorial Board CJoP, Pediatric Cardiology Committee CCoCPCMDA. Diagnostic recommendation for myocarditis in children (version 2018). *Zhonghua Er Ke Za Zhi.* (2019) 57:87–9. doi: 10.3760/cma.j.issn.0578-1310.2019.02.004
5. Ammirati E, Cipriani M, Lilliu M, Sormani P, Varrenti M, Raineri C, et al. Survival and left ventricular function changes in fulminant versus nonfulminant acute myocarditis. *Circulation.* (2017) 136:529–45. doi: 10.1161/CIRCULATIONAHA.117.026386
6. Pei L, Yang N, Yang YH, Guo ZY, Xu W, Liu CF. Clinical features and prognostic factors in children with fulminant myocarditis. *Zhongguo Dang Dai Er Ke Za Zhi.* (2015) 17:1232–6. doi: 10.7499/j.issn.1008-8830.2015.11.016
7. Rose NR. Viral myocarditis. *Curr Opin Rheumatol.* (2016) 28:383–9. doi: 10.1097/BOR.0000000000000303
8. McGee WT, Headley JM, Frazier JA, Lichtenthal PR. *Quick Guide to Cardiopulmonary Care.* Irvine, CA: Edwards Critical Care Education (2014).
9. Wang Z, Wang Y, Lin H, Wang S, Cai X, Gao D. Early characteristics of fulminant myocarditis vs non-fulminant myocarditis: A meta-analysis. *Medicine.* (2019) 98:e14697. doi: 10.1097/MD.0000000000014697
10. Smith SC, Ladenson JH, Mason JW, Jaffe AS. Elevations of cardiac troponin I associated with myocarditis experimental and clinical correlates. *Circulation.* (1997) 95:163–68. doi: 10.1161/01.CIR.95.1.163
11. Sachdeva S, Song X, Dham N, Heath DM, Debiasi RL. Analysis of clinical parameters and cardiac magnetic resonance imaging as predictors of outcome in pediatric myocarditis. *Am J Cardiol.* (2015) 115:499–504. doi: 10.1016/j.amjcard.2014.11.029
12. Lv J, Han B, Wang C, Wang J, Jiang D, Zhao L, et al. The clinical features of children with acute fulminant myocarditis and the diagnostic and follow-up value of cardiovascular magnetic resonance. *Front Pediatr.* (2019) 7:388. doi: 10.3389/fped.2019.00388
13. Ginsberg F, Parrillo JE. Fulminant myocarditis. *Crit Care Clin.* (2013) 29:465–83. doi: 10.1016/j.ccc.2013.03.004
14. Shillcutt SK, Thomas WR, Sullivan JN. Fulminant myocarditis: the role of perioperative echocardiography. *Anesth Analg.* (2015) 120:296–9. doi: 10.1213/ANE.0000000000000508
15. Ghelani SJ, Spaeder MC, Pastor W, Spurney CF, Klugman D. Demographics, trends, and outcomes in pediatric acute myocarditis in the United States, 2006 to 2011. *Circ Cardiovasc Qual Outcomes.* (2012) 5:622–7. doi: 10.1161/CIRCOUTCOMES.112.965749
16. Ryu DR, Heo JW, Lee SH, Lee W, Choi JW, Kim HY, et al. Fulminant myocarditis: the role of cardiac magnetic resonance imaging. *Int J Cardiol.* (2013) 68:e58–9. doi: 10.1016/j.ijcard.2013.07.002
17. Ziółkowska L, Kawalec W, Biernatowicz M, Swiatek E, Kaminska A, Turska-Kmieć A. The usefulness of scintigraphy with 99mTc–Anti–Granulocyte antibody for diagnosis and follow–up in children with myocarditis. *Kardiol Pol.* (2012) 70:1243–9.
18. Bjelakovic B,Vukomanovic V. Fulminant myocarditis in children successfully treated with high dose of methyl-prednisolone. *Ind J Pediatr.* (2016) 83:268–9. doi: 10.1007/s12098-015-1831-2
19. Chen HS, Wang W, Wu SN, Liu JP. Corticosteroids for viral myocarditis. *Cochrane Database Syst Rev.* (2013) 10:CD004471. doi: 10.1002/14651858.CD004471.pub3
20. Tsai YG, Ou TY, Wang CC, Tsai MC, Yuh YS, Hwang B. Intravenous gammaglobulin therapy in myocarditis complicated with complete heart block: report of one case. *Acta Paediatr Taiwan.* (2001) 42:311–3.
21. Goland S, Czer LS, Siegel RJ, Tabak S, Jordan S, Luthringer D, et al. Intravenous immunoglobulin treatment for acute fulminantinflflammatory cardiomyopathy: series of six patients and review of literature.

Can J Cardiol. (2008) 24:571–4. doi: 10.1016/S0828-282X(08)70638-X

22. Chien SJ, Liang CD, Lin IC, Lin YJ, Huang CF. Myocarditis complicated by complete atrioventricular block: nine years' experience in a medical center. *Pediatr Neonatol.* (2008) 49:218–22. doi: 10.1016/S1875-9572(09)60014-0
23. Lorusso R, Centofanti P, Gelsomino S, Barili F, Di Mauro M, Orlando P, et al.Venoarterial extracorporeal membrane oxygenation for acute fulminant myocarditis in adult patients: A 5-year multi-institutional experience. *Ann Thorac Surg.* (2016) 101:919–26. doi: 10.1016/j.athoracsur.2015.08.014
24. Cheng R, Hachamovitch R, Kittleson M, Patel J, Arabia F, Moriguchi J, et al. Clinical outcomes in fulminant myocarditis requiring extracorporeal membrane oxygenation: a weighted meta-analysis of 170 patients. *J Card Fail.* (2014) 20:400–6. doi: 10.1016/j.cardfail.2014.03.005
25. Zhou YP, Shi JY, Wang F, Cui Y, Xu TT, Wang CX, et al. Continuous renal replacement therapy combined with extracorporeal membrane oxygenation for pediatric cardiopulmonary failure. *Zhonghua Er Ke Za Zhi.* (2018) 56:336–41. doi: 10.3760/cma.j.issn.0578-1310.2018.05.006

Conflict of Interest: The authors declare that the research was conducted in the absence of any commercial or financial relationships that could be construed as a potential conflict of interest.

frontiers in Pediatrics

ORIGINAL RESEARCH
published: 28 May 2020
doi: 10.3389/fped.2020.00274

CT Coronary Angiography Studies After a Mean Follow-up of 3.8 Years in Children With Kawasaki Disease and Spontaneous Defervescence

Santosh Dusad[1†], *Manphool Singhal*[2†], *Rakesh Kumar Pilania*[1†], *Deepti Suri*[1] *and Surjit Singh*[1*]

[1] *Allergy Immunology Unit, Department of Pediatrics, Advanced Pediatrics Centre, Post Graduate Institute of Medical Education and Research, Chandigarh, India,* [2] *Department of Radiodiagnosis and Imaging, Postgraduate Institute of Medical Education and Research, Chandigarh, India*

Background: There is paucity of literature on follow-up of children with Kawasaki disease (KD) who have spontaneous defervescence during the acute stage and do not receive intravenous immunoglobulin. We report herein the role of computed tomography coronary angiography (CTCA) as an imaging modality in such situations.

Methods: This prospective observational study was carried out during the period January 2016–June 2017. Children underwent CTCA on 128-slice Dual Source CT (DSCT) scanner (Somatom Definition Flash, Siemens; Germany), and 2D-echocardiography on the same day.

Results: Mean age at time of diagnosis was 6.52 ± 3.13 years; range 2–14 years. Mean age at time of study was 11.03 ± 5.10 years; range 3.75–23.30 years. Mean interval between diagnosis of KD and time of present study was 3.84 ± 2.27 years. None of the patients showed any coronary artery abnormalities on either 2D-echocardiography or CTCA. While assessment of proximal segments of left main coronary artery, proximal right coronary artery, and left anterior descending artery was comparable on both 2D-echocardiography and CTCA, left circumflex artery, and distal right coronary artery could be clearly visualized only on CTCA.

Conclusion: In our experience, patients with KD who have spontaneous defervescence during the acute stage and do not receive IVIg may not have significant long-term coronary sequelae. CTCA is a useful imaging modality for delineation of coronary artery in patients with KD on long term follow-up especially in older children with thick chest walls and poor acoustic windows.

Keywords: Kawasaki disease, spontaneous defervescence, dual source computed tomography coronary angiography, coronary artery abnormalities, 2D-echocardiography

OPEN ACCESS

Edited by:
Xupei Huang,
Florida Atlantic University,
United States

Reviewed by:
Ziyad M. Hijazi,
Rush University, United States
Anju Gupta,
All India Institute of Medical Sciences, India

***Correspondence:**
Surjit Singh
surjitsinghpgi@rediffmail.com

†These authors have contributed equally to this work and share first authorship

Specialty section:
This article was submitted to Pediatric Cardiology, a section of the journal Frontiers in Pediatrics

Received: *15 January 2020*
Accepted: *30 April 2020*
Published: *28 May 2020*

Citation:
Dusad S, Singhal M, Pilania RK, Suri D and Singh S (2020) CT Coronary Angiography Studies After a Mean Follow-up of 3.8 Years in Children With Kawasaki Disease and Spontaneous Defervescence. Front. Pediatr. 8:274. doi: 10.3389/fped.2020.00274

INTRODUCTION

KD is an acute, systemic childhood vasculitis syndrome that mainly affects small children and has a predilection for coronary arteries. Diagnosis of KD is purely clinical and there are no laboratory tests available to confirm the diagnosis. Delays in diagnosis of patients with KD are not unusual and are more common in developing countries like India where awareness about this disorder is

still low (1–6). Coronary artery abnormalities (CAAs) are known to develop in 15–25% of children with KD who do not receive appropriate and prompt treatment with IVIg. CAAs account for most of the morbidity and mortality associated with the disease (1, 7–9).

When a patient with KD presents in convalescent phase after spontaneous defervescence, decisions regarding initiation of treatment with intravenous immunoglobulin (IVIg) can be difficult and need to be individualized (1, 10). There is paucity of literature on long-term follow-up studies in children with KD who have had spontaneous defervescence. It was hitherto believed that patients with KD who have spontaneous defervescence tend to have a benign course (11, 12). However, recent studies have shown that KD patients with spontaneous defervescence may not always have milder phenotypes of the disease—in fact, the converse may well be true as incidence of CAAs in such situations may be higher than in patients who have been treated with IVIg (13, 14).

Echocardiography is considered to be the imaging modality of choice in acute stage as well as during follow-up of KD. Sensitivity and specificity rates of 95 and 99% have been reported for identification of coronary aneurysms by echocardiography (15). However, this imaging modality has several inherent limitations—these include poor visualization of middle and distal segments of coronaries, difficulties in visualization of left circumflex artery (LCx), chances of inter-observer variation, operator dependency, and poor acoustic windows in older children because of thick chest wall (12–14).

CTCA on dual source CT (DSCT) is a non-invasive tool that, under expert hands, has low radiation exposure and can accurately demonstrate CAAs in both proximal and distal coronaries. CTCA on DSCT has recently emerged as a non-invasive tool that has low radiation exposure and can accurately demonstrate the coronary wall anatomy and intraluminal abnormalities like thrombosis, stenosis, and calcification (16–18). There is, however, paucity of literature on CTCA performed during follow-up of children with KD who have had spontaneous defervescence.

We report herein the role of CTCA on a 128-slice DSCT platform in detecting CAAs in patients with KD who had spontaneous defervescence during the acute stage and did not receive IVIg for one or more reasons.

METHODS

This prospective observational study was carried out during the period January 2016–June 2017. Nineteen children (15 boys; four girls) with KD who had not received IVIg and were on regular follow up at Pediatric Allergy Immunology Unit, Advanced Pediatrics Centre, Postgraduate Institute of Medical Education and Research, Chandigarh, India were included in the study (19). Our institute is a not-for-profit federally funded tertiary care teaching hospital in North-West India.

Diagnosis of KD was based on diagnostic criteria given by AHA (4). These patients had not received IVIg because they either presented late in convalescent phase or had already became afebrile at time of presentation and had normal inflammatory markers. The study was approved by the Institute Ethics Committee, Institute Thesis Committee, and the Departmental Review Board. A written informed consent was obtained from the parents prior to enrolment. Children underwent CTCA on 128-slice Dual Source CT (DSCT) scanner (Somatom Definition Flash, Siemens; Germany), and 2D-echocardiography on the same day. The minimum and maximum dose length product (DLP) was 21 and 182 mGycm with mean DLP of 86.11 ± 48.02 mGycm. The scan time was 3.72 ± 0.60 s; range 2.85–4.76 s. Effective radiation dose was 1.19 ± 0.29 mSv; range 0.25–2.58 mSv. Diameters of major coronary arteries were recorded and coronary artery lesions, if any, were noted. Calcium scoring through DSCT was also carried out. Results of 2D-echocardiography that had been carried out at time of diagnosis were also taken into account. Seven patients had also undergone stress myocardial perfusion scintigraphy at initial diagnosis.

Findings of echocardiography were compared with those of CTCA. Paired sampled *t*-test was used to compare the average diameter of coronaries obtained by the two imaging modalities.

TABLE 1 | Clinical profile of children with Kawasaki disease in the study ($n = 19$).

Characterstics	Present
Fever	19 (100%)
Rash	10 (52.6%)
Rash ≤ 1 week of fever onset	10 (100%)
Cervical lymphadenapathy	10 (52.6%)
Conjuctival injection	2 (10.5%)
Desquamation	19 (100%)
Lip and oral changes	6 (31.6%)

RESULTS

Baseline Demographics

Mean age at time of diagnosis was 6.52 ± 3.13 years; range 2–14 years. Mean age of at time of study was 11.03 ± 5.10 years; range 3.75–23.30 years. The most common symptom present in this cohort of patients with KD was fever, that was present in all patients (100%). Mean duration of fever was 6.47 ± 5.44 days. Mean duration of symptoms before presentation to our institute was 21.79 ± 14.27 days. Sixteen patients (84.2%) were classified as incomplete KD. Principal clinical features included lip and oral cavity changes (31.6%), cervical lymphadenopathy in (52.6%), conjunctival injection (10.5%), polymorphous rash (52.6%), desquamation of fingers and/or toes (100%). Mean interval between diagnosis of KD and time of present study was 3.84 ± 2.27 years; range 2.4 months to 7.3 years. Seven patients had interval <2 years, 7 had interval between 2 and 5 years while five had interval more than 5 years (**Table 1**).

Characteristics

Findings of echocardiography that had been carried out at initial admission were also taken into account. Prior to 2014 we had not been recording *Z* scores of coronary arteries. At that time,

TABLE 2 | Mean coronary artery diameter by DSCT coornary angiography and 2D-echocardiography.

Mean coronary artery diameter in mm	2D-Echocardiography	DSCT coronary angiography
LMCA (Mean ± *SD*)	2.46 ± 0.47; (*n* = 16)	2.62 ± 0.46; (*n* = 19)
RCA (Mean ± *SD*)	2.14 ± 0.52; (*n* = 15)	2.28 ± 0.47; (*n* = 19)
LAD (Mean ± *SD*)	1.84 ± 0.31; (*n* = 15)	1.93 ± 0.28; (*n* = 18)
LCX (Mean ± *SD*)	1.46 ± 0.35; (*n* = 11)	1.70 ± 0.37; (*n* = 18)

DSCT, Dual Source Computed tomography; LMCA, Left main coronary artery; RCA, Right coronary artery; LAD, Left anterior descending artery; LCx, Left circumflex coronary artery; SD, Standard Deviation.

TABLE 3 | Comparison between DSCT coronary angiography and 2D-echocardiography.

Coronary artery	Mean ± *SD* in mm on DSCT Coronary angiography	Mean ± *SD* in mm on 2D-Echocardiography	Correlation	*p*-value
LMCA (*n* = 16)	2.54 ± 0.45	2.47 ± 0.47	0.77	0.36
RCA (*n* = 15)	2.25 ± 0.50	2.15 ± 0.53	0.92	0.08
LAD (*n* = 15)	1.89 ± 0.30	1.84 ± 0.31	0.50	0.51
LCX (*n* = 11)	1.56 ± 0.28	1.46 ± 0.35	0.76	0.18

DSCT, Dual Source Computed tomography; LMCA, Left main coronary artery; RCA, Right coronary artery; LAD, Left anterior descending artery; LCx, Left circumflex coronary artery; SD, Standard Deviation.

CAAs were categorized based on absolute internal diameter of vessels. Initial echocardiograms carried out at time of diagnosis showed normal coronary arteries in 16 of 19 children enrolled in the study. However, three children had CAAs—while two had mild dilatation of LMCA, one had irregular lumen of LAD with loss of distal tapering. All three patients had presented late to our institute in convalescent phase of disease and two of three had incomplete forms of KD. These changes had normalized on repeat echocardiography and CTCA performed at time of present study.

None of the patients in this series showed any CAA on either 2D-echocardiography or CTCA. While assessment of proximal segments of left main coronary artery (LMCA), proximal right coronary artery (RCA), and left anterior descending artery (LAD) was comparable on both 2DE and DSCT, left circumflex (LCx) and distal RCA could be clearly visualized only on CTCA.

Coronary artery diameters could be easily measured in all subjects by CTCA. However, on echocardiography LMCA diameter at the time of follow-up could be assessed accurately in 16, RCA and LAD in 15, and LCx in 11 subjects only (**Table 2**). All patients, except one, in whom coronary arteries were not visualized were aged more than 10 years and impaired visualization of coronary arteries was because of thick chest walls. Mean diameters of coronary artery measured by 2D-echocardiography and DSCT were comparable (**Table 3**).

Stress myocardial perfusion scintigraphy was reported normal in six and showed mildly reduced perfusion defect in one child (20). Calcium scores were normal in all 19 patients.

DISCUSSION

The diagnosis of KD is always based on clinical criteria and there is no laboratory marker that can serve as a gold standard for diagnosis of this condition (21). A significant proportion of children with KD (25–50% in various series) have incomplete KD (7, 22–25). And this proportion would be higher in situations wherein the patients have reported late for diagnosis, as was the case in the present series (12, 13). Although 16/19 patients had incomplete KD at time of diagnosis, it is possible that some of the clinical features of KD may have disappeared by the time the children reported to us. Takahashi et al. have reported that incomplete forms of KD are more common in children who have had spontaneous defervescence as compared to those who have received IVIg (59.2 vs. 13.5%) (12). Hu et al. have also reported similar findings (13).

Delineation of coronary arteries in children with KD can be carried out by several imaging techniques. 2D-echocardiography is the preferred imaging modality both during the acute phase as well as during convalescence (1, 2, 4, 24, 26). However, there has been increasing interest about other imaging modalities that can address the limitations of echocardiography as described above. These include catheter angiography (CA), CTCA and magnetic resonance coronary angiography (MRCA) (16–18).

In this study we have assessed role of CTCA done on DSCT in evaluation of CAAs in patients with KD on follow-up. These children had had spontaneous defervescence during the acute stage and did not receive IVIg. Spontaneous defervescence is known to occur in a small proportion of patients with KD (1). CTCA is superior to 2DE for distal coronary artery visualization and for evaluation of the LCx. Further, assessment of the wall of coronary arteries is more accurate on CTCA than on 2DE. In older children, 2DE is often not very useful for evaluation of coronary arteries because of thick chest walls and the resultant poor acoustic window. In the present study, echocardiography could not visualize LCx and distal segments of coronary arteries in older children. CTCA accurately delineated the anatomy and lumen of coronary arteries and was especially useful for assessing distal segments of coronary arteries that are usually not visualized on 2DE.

Management of patients with KD and spontaneous defervescence is contentious and there is no consensus (1, 11, 12). Lin et al. had shown that regression of CAAs within 1 month of KD was more likely among patients who had been treated with IVIg compared to those who did not receive such treatment. However, authors have shown that late coronary outcome in these two group were comparable (11). Takahashi et al. retrospectively reviewed patients with KD who had had spontaneous defervescence. It was noted that there was no difference in development of CAAs between those that received IVIg therapy, and the ones who experienced spontaneous defervescence (12). Recently, Hu et al. have published data on outcomes of 37 children with KD who had spontaneous defervescence within 10 days. The incidence of CAAs at 1 month after disease onset was higher in patients with KD who had spontaneous defervescence as compared to those treated with IVIg (18.9 vs. 5.1%). Furthermore, it has been shown that new

emergence of CAAs became significantly higher if they had not received IVIg therapy (due to spontaneous defervescence) when compared with those who did (13). These findings are a matter of serious concern and require further studies for confirmation.

CT calcium scoring is a technique that identifies calcium deposition in coronary arteries without the need of intravenous contrast. Calcium deposition is considered a surrogate marker for previous coronary artery involvement in patients with KD. Kahn et al. have shown that calcium deposition was not seen in patients with KD who did not develop CAAs during acute phase of disease (27). The authors have shown that calcium scoring by CT is also a useful tool for identification of unrecognized CAAs in patients with a remote history of KD. In the present study we have also performed calcium scoring and did not find any abnormalities. Our findings are in consonance with the results of Kahn et al. (27).

To conclude, this study shows that patients with KD who had spontaneous defervescence did not develop any significant long-term coronary sequelae. This is reassuring. The strengths of our study are that all diagnoses were confirmed by one individual (the senior author—SS) and there was uniformity of data collection as this was a single center cohort. Further, CTCAs were performed under direct supervision of the consultant radiologist (MS) in all cases using radiation optimized protocols. The number of patients included in the study is undoubtedly small. However, this is due to the fact that we have only enrolled children with KD who had spontaneous defervescence during the acute stage and did not receive IVIg. In our experience CTCA is a useful imaging modality for delineation of coronary arteries in patients with KD on long term follow-up, especially in older children who have thick chest walls and poor acoustic windows. Further long-term and multicentric large cohort studies are warranted on this aspect of KD.

DATA AVAILABILITY STATEMENT

All datasets generated for this study are included in the article/supplementary material.

ETHICS STATEMENT

The studies involving human participants were reviewed and approved by Institute Ethics Committee, Postgraduate Institute of Medical Education and Research, Chandigarh, India.

AUTHOR CONTRIBUTIONS

SD, MS, and RP wrote the initial draft of manuscript and were also involved in editing and revision of manuscript at all stages of its production. SD and RP collected data, performed statistical calculations, analyzed, and critically interpreted the results. DS reviewed the literature and contributed to editing of manuscript. SS conceived the idea, reviewed the literature, critically reviewed and edited the manuscript at all stages of its production. All authors discussed the results and read and approved the final manuscript.

REFERENCES

1. Newburger JW, Takahashi M, Gerber MA, Gewitz MH, Tani LY, Burns JC, et al. Diagnosis, treatment, and long-term management of Kawasaki disease: a statement for health professionals from the committee on rheumatic fever, endocarditis and Kawasaki disease, council on cardiovascular disease in the young, American heart association. *Circulation.* (2004) 110:2747–71. doi: 10.1161/01.CIR.0000145143.19711.78
2. Singh S, Sharma A, Jiao F. Kawasaki disease: issues in diagnosis and treatment–a developing country perspective. *Indian J Pediatr.* (2016) 83:140–5. doi: 10.1007/s12098-015-1890-4
3. Singh S, Newburger JW, Kuijpers T, Burgner D. Management of Kawasaki disease in resource-limited settings. *Pediatr Infect Dis J.* (2015) 34:94–6. doi: 10.1097/INF.0000000000000600
4. Pilania RK, Bhattarai D, Singh S. Controversies in diagnosis and management of Kawasaki disease. *World J Clin Pediatr.* (2018) 7:27–35. doi: 10.5409/wjcp.v7.i1.27
5. Singh S, Vignesh P, Burgner D. The epidemiology of Kawasaki disease: a global update. *Arch Dis Child.* (2015) 100:1084–8. doi: 10.1136/archdischild-2014-307536
6. Singh S, Bhattad S. Kawasaki disease incidence at Chandigarh, North India, during 2009-2014. *Rheumatol Int.* (2016) 36:1391–7. doi: 10.1007/s00296-016-3543-y
7. Jindal AK, Pilania RK, Prithvi A, Guleria S, Singh S. Kawasaki disease: characteristics, diagnosis and unusual presentations. *Expert Rev Clin Immunol.* (2019) 15:1089–104. doi: 10.1080/1744666X.2019.1659726
8. Singh S, Bhattad S, Gupta A, Suri D, Rawat A, Rohit M. Mortality in children with Kawasaki disease: 20 years of experience from a tertiary care centre in North India. *Clin Exp Rheumatol.* (2016) 34(3 Suppl.97):S129–33.
9. Pilania RK, Jindal AK, Guleria S, Singh S. An update on treatment of Kawasaki disease. *Curr Treat Options Rheumatol.* (2019) 5:36–55. doi: 10.1007/s40674-019-00115-z
10. Research Committee of the Japanese Society of Pediatric Cardiology, Cardiac Surgery Committee for Development of Guidelines for Medical Treatment of Acute Kawasaki Disease. Guidelines for medical treatment of acute Kawasaki disease: report of the research committee of the Japanese society of pediatric cardiology and cardiac surgery (2012 revised version). *Pediatr Int.* (2014). 56:135–58. doi: 10.1111/ped.12317
11. Lin M-T, Sun L-C, Wu E-T, Wang J-K, Lue H-C, Wu M-H. Acute and late coronary outcomes in 1073 patients with Kawasaki disease with and without intravenous γ-immunoglobulin therapy. *Arch Dis Child.* (2015) 100:542–7. doi: 10.1136/archdischild-2014-306427
12. Takahashi T, Sakakibara H, Morikawa Y, Miura M. Development of coronary artery lesions in indolent Kawasaki disease following initial spontaneous defervescence: a retrospective cohort study. *Pediatr Rheumatol Online J.* (2015) 13:44. doi: 10.1186/s12969-015-0042-8
13. Hu Y-C, Liu H-M, Lin M-T, Chen C-A, Chiu S-N, Lu C-W, et al. Outcomes of Kawasaki disease children with spontaneous defervescence within 10 days. *Front Pediatr.* (2019) 7:158. doi: 10.3389/fped.2019.00158
14. Hayakawa I, Miura M. Giant coronary aneurysms in incomplete Kawasaki disease with early spontaneous defervescence. *J Clin Rheumatol.* (2016) 22:40. doi: 10.1097/RHU.0000000000000337
15. Hiraishi S, Misawa H, Takeda N, Horiguchi Y, Fujino N, Ogawa N, et al. Transthoracic ultrasonic visualisation of coronary aneurysm, stenosis, and occlusion in Kawasaki disease. *Heart.* (2000) 83:400–5. doi: 10.1136/heart.83.4.400
16. Chu WCW, Mok GCF, Lam WWM, Yam M-C, Sung RYT. Assessment of coronary artery aneurysms in pediatric patients with Kawasaki disease by multidetector row CT angiography: feasibility

and comparison with 2D echocardiography. *Pediatr Radiol.* (2006) 36:1148–53. doi: 10.1007/s00247-006-0281-4
17. Singhal M, Gupta P, Singh S, Khandelwal N. Computed tomography coronary angiography is the way forward for evaluation of children with Kawasaki disease. *Glob Cardiol Sci Pract.* (2017) 2017:e201728. doi: 10.21542/gcsp.2017.28
18. Singhal M, Singh S, Gupta P, Sharma A, Khandelwal N, Burns JC. Computed tomography coronary angiography for evaluation of children with Kawasaki disease. *Curr Probl Diagn Radiol.* (2018) 47:238–44. doi: 10.1067/j.cpradiol.2017.09.013
19. European society congress. Proceedings of the 24th paediatric rheumatology European society congress: part one. *Pediatr Rheumatol Online J.* (2017). 15(Suppl.2):65. doi: 10.1186/s12969-017-0185-x
20. Kashyap R, Mittal BR, Bhattacharya A, Manojkumar R, Singh S. Exercise myocardial perfusion imaging to evaluate inducible ischaemia in children with Kawasaki disease. *Nucl Med Commun.* (2011) 32:137–41. doi: 10.1097/MNM.0b013e3283411c67
21. Reddy M, Singh S, Rawat A, Sharma A, Suri D, Rohit MK. Pro-brain natriuretic peptide (ProBNP) levels in North Indian children with Kawasaki disease. *Rheumatol Int.* (2016) 36:551–9. doi: 10.1007/s00296-016-3430-6
22. Singh S, Agarwal S, Bhattad S, Gupta A, Suri D, Rawat A, et al. Kawasaki disease in infants below 6 months: a clinical conundrum? *Int J Rheum Dis.* (2016) 19:924–8. doi: 10.1111/1756-185X.12854
23. Jindal AK, Pilania RK, Guleria S, Vignesh P, Suri D, Gupta A, et al. Kawasaki disease in children older than 10 years: a clinical experience from Northwest India. *Front Pediatr.* (2020) 8:24. doi: 10.3389/fped.2020.00024
24. Singh S, Jindal AK, Pilania RK. Diagnosis of Kawasaki disease. *Int J Rheum Dis.* (2018) 21:36–44. doi: 10.1111/1756-185X.13224
25. Guleria S, Pilania RK, Jindal AK, et al. Clinico-laboratory profile of Kawasaki disease with arthritis in children. *Eur J Pediatr.* (2020) 179:875–9. doi: 10.1007/s00431-020-03582-y
26. Routhu SK, Singhal M, Jindal AK, Kumar V, Yadav AK, Singh S. Assessment of endothelial dysfunction in acute and convalescent phases of Kawasaki disease using automated edge detection software: a preliminary study from North India. *J Clin Rheumatol.* (2019). doi: 10.1097/RHU.0000000000001233. [Epub ahead of print].
27. Kahn AM, Budoff MJ, Daniels LB, Jimenez-Fernandez S, Cox AS, Gordon JB, et al. Calcium scoring in patients with a history of Kawasaki disease. *JACC Cardiovasc Imaging.* (2012) 5:264–72. doi: 10.1016/j.jcmg.2011.12.010

Conflict of Interest: The authors declare that the research was conducted in the absence of any commercial or financial relationships that could be construed as a potential conflict of interest.

frontiers in Cardiovascular Medicine

REVIEW
published: 28 May 2020
doi: 10.3389/fcvm.2020.00094

Antibodies and Immunity During Kawasaki Disease

Mark Daniel Hicar[1,2,3]*

[1] University at Buffalo, Buffalo, NY, United States, [2] John R. Oishei Children's Hospital, Buffalo, NY, United States, [3] Department of Pediatrics, Jacobs School of Medicine and Biomedical Sciences, University at Buffalo, Buffalo, NY, United States

The cause of Kawasaki disease (KD), the leading cause of acquired heart disease in children, is currently unknown. Epidemiology studies support that an infectious disease is involved in at least starting the inflammatory cascade set off during KD. Clues from epidemiology support that humoral immunity can have a protective effect. However, the role of the immune system, particularly of B cells and antibodies, in pathogenesis of KD is still unclear. Intravenous immunoglobulin (IVIG) and other therapies targeted at modulating inflammation can prevent development of coronary aneurysms. A number of autoantibody responses have been reported in children with KD and antibodies have been generated from aneurysmal plasma cell infiltrates. Recent reports show that children with KD have similar plasmablast responses as other children with infectious diseases, further supporting an infectious starting point. As ongoing studies are attempting to identify the etiology of KD through study of antibody responses, we sought to review the role of humoral immunity in KD pathogenesis, treatment, and recovery.

Keywords: kawasaki disease, antibodies-monoclonal, B cells, plasmablast, immunoglobulin intravenous

OPEN ACCESS

Edited by:
Xupei Huang,
Florida Atlantic University,
United States

Reviewed by:
Howard Prentice,
Florida Atlantic University,
United States
Junjun Quan,
Children's Hospital of Chongqing
Medical University, China

***Correspondence:**
Mark Daniel Hicar
markhica@buffalo.edu

Specialty section:
This article was submitted to Pediatric Cardiology, a section of the journal Frontiers in Cardiovascular Medicine

Received: *08 July 2019*
Accepted: *30 April 2020*
Published: *28 May 2020*

Citation:
Hicar MD (2020) Antibodies and Immunity During Kawasaki Disease. Front. Cardiovasc. Med. 7:94. doi: 10.3389/fcvm.2020.00094

INTRODUCTION

The cause of Kawasaki disease (KD) continues to perplex clinicians and researchers. Also known as Kawasaki syndrome or mucocutaneous lymph node syndrome, KD is the leading cause of acquired cardiac disease in children. Recent murine and human clinical trials are enhancing our understanding of this disorder (1). The mainstay of treatment has been intravenous immunoglobulin (IVIG), initially implying a major role for humoral immunity. However, newer therapies that also have broad immunomodulatory effects have become widely used for refractory cases (2). Studies from different fields, from maternal immunity to genome-wide association studies, also imply a role of humoral immunity (3–6). This review will give an overview of the present knowledge of the field directed toward the etiology of KD and what role B cells and antibodies may play in treatment, pathogenesis, and diagnosis.

REVIEW WITH A FOCUS ON B CELLS AND ANTIBODIES

Clinical Presentation

Diagnosis is purely clinical, as there are no adequately specific or sensitive tests available. The "classic" diagnosis involves 5 days of fever and having four of the five following criteria: mucous membrane inflammation, rash, hands and feet swelling, conjunctivitis, and a solitary inflamed lymph node mass (6–9). If left untreated, roughly one-quarter of the children meeting clinical criteria will go on to have coronary artery inflammation, including aneurysms. Incomplete cases, those which do not fulfill four of five of the classic criteria, have similar risk of coronary aneurysms

(10). Treating affected patients with IVIG reduces the rates of coronary aneurysms, with a minority seemingly resistant to treatment (6–8, 11–14). Although most aneurysms resolve, some defects are retained. Initial studies done on adults with a history of KD implies there is a greater lifetime risk of cardiac issues and early mortality (15–18). To add to the diagnostic confusion, several infectious etiologies have also been independently associated with aneurysms (19). It remains a frustrating diagnosis because of the unknown etiology, clinical variability, lack of specific testing, and unclear pathogenesis.

Epidemiology

There appears to be a genetic influence in exhibiting KD. Incidence is higher in some genetic backgrounds and consistently appears in males greater than females within those backgrounds (20). By age five in the United States, 1 in 1,000 African-American children and 1 in 2,000 Caucasian children will have been affected (21–23). In general, Asians have a much higher rate of KD; which is especially evident in Japanese children, whose lifetime incidence rate is near 1% (24). This predisposition holds even for those persons of Japanese heritage raised in foreign lands, such as the United States (20). Sibling can have a 10–30-fold higher risk of KD compared to the general population (25).

The etiology of KD is unknown (6, 26, 27). However, there is a proposed relation to an infectious agent. Epidemiological evidence for this comes from the fact that there are seasonal peaks of KD during winter and spring months and outbreaks have been described (27–34). Siblings have a 10–30-fold higher rate, with most occurring within 1 year of each other (35), and up to 50% of sibling cases are within 10 days of each other (25).

Recent studies support a protective role for humoral immunity. There is a lower incidence in breastfed infants (4) and KD is rare in both newborns and individuals over 5 years of age. This implies a maternally derived protective immunity to a ubiquitous infectious agent (36). Trans-placental passage of maternal antibodies is thought to be protective and explain the paucity of cases in infancy (3).

Proposed Etiologies

It is possible that there is not one cause of KD, but multiple etiologies that result in similar pathogenesis. This may explain the clinical variability and lack of discovery of a definitive agent, however, the low recurrence rate even in high prevalent areas speaks against a large number of infectious causes (37).

Previously proposed infectious agents include Herpesviridae (HHV-6, Epstein Barr Virus, Cytomegalovirus), human coronavirus, retroviruses, Parvovirus B19, bocavirus, and bacterial infections such as staphylococci, streptococci, *Bartonella*, and *Yersinia* infections (15, 20). Some of these agents have been independently associated with aneurysm formation (19), with the Epstein Barr Virus most commonly associated (38). Several non-infectious agents have also been proposed such as carpet shampoos, mercury exposure and living near bodies of water (15, 20). Additionally, the recent report of tropospheric wind patterns correlating with outbreaks in Japan would not be consistent with many of the viruses that have been proposed (26, 34, 39). These reports imply a relationship to an environmental antigen, as either a priming or inciting event. This "two-hit" hypothesis is also suggested by similar data from Canada (40).

If a ubiquitous childhood pathogen is the cause of KD, the mode of entry would likely be a common mode of infection such as fecal-oral or respiratory spread. Outbreaks in the United States have been associated with preceding viral illness (41). To note, mild upper respiratory symptoms and gastrointestinal complaints have been described in up to 35 and 61% of cases, respectively (42). Rare but more significant pulmonary disease has also been reported (43). Notably, however, concomitant respiratory viruses are near 10% of cases (44, 45). A persistent infection has been theorized (46). Although numerous viruses that can reactivate during stress (Herpesviridae family) or are considered "slow" viral infections (47), the failure of numerous attempts to identify a specific infectious agent argues against a prolonged infection. There are difficult to culture viruses, such as coronavirus which had also enjoyed a short-lived consideration as the cause of KD (48). An abnormal response to normal flora has been proposed (49, 50) and studies on a relationship to the emerging field of microbiome research have recently been reviewed (51).

Human Biomarkers

Currently, diagnosis is aided by utilizing sensitive but not specific biomarkers such as C-reactive protein, sedimentation rate, liver function tests, urine leukocytes, platelets, leukocyte count, and hemoglobin (2). As highlighted by recommendations for diagnosis of incomplete cases, many biomarkers do not reveal the nature of the underlying illness. A number of traditional laboratory and clinical findings have been built into scoring systems to predict IVIG resistance that are used in Japanese populations (52). These scoring systems (*Sano, Kobayashi, Egami*) all have relatively high sensitivity, near 80%, in Asian populations; however, they have poor predictive ability in heterogenous lower pretest probability populations of North America (53).

Numerous other biomarkers have been proposed to aid in diagnosis of KD and have been recently reviewed (54). Although some of the transcriptomic approaches mirror genomic findings, intriguingly, there has been a disconnect between proteomics and genomic associations. A recent study using serum mass spectrometry to look at differentially expressed proteins showed lipopolysaccharide binding protein (LBP), leucine rich alpha-2 glycoprotein (LRG1), and angiotensinogen were higher in acute phase, and retinol binding protein was diminished (55). The marker of tenascin, involved in tissue remodeling, is promising as a marker of coronary involvement during acute KD (56, 57).

Numerous cytokine associations in KD have been shown, and those with unique B cell associations will be reviewed. IL-10 has long been shown to be elevated during acute KD (58, 59). This is likely a natural anti-inflammatory response, as recent studies show supplementing IL-10 via an AAV vector protected against aneurysms in the *Candida albicans* murine model (60). IL-10 is produced by myeloid dendritic cells and regulatory B cells, and recently has been shown to drive plasmablast responses (discussed later) (61). IP-10, an activator of B cells and

macrophages, has also been associated with clinical KD. Notably, this group did not see peripheral IL-1B elevation. (62). IL-21, produced mainly by T cells and Natural Killer cells (63, 64), has recently been proposed as a specific marker in KD in a Korean cohort of children when compared to prolonged fevers from mononucleosis (65). IL-21 modulates immunoglobulin isotype switching and is involved in the differentiation of both naïve and memory B cells into mature plasma cells (66). However, in a study of IL-21 levels in children presenting to a North American emergency room with fever, KD and febrile children could not be distinguished by IL-21 levels (67).

Biomarkers Supporting Innate Immunity

A number of transcriptomic approaches show some promise in distinguishing KD from viral infections. Initial studies that look at IVIG response in PBMCs and monocytes suggested monocyte regulation was a main role of IVIG (68) FCGR1a, FCGR3A, CCR2, S100A9, S100A12, and adrenomedullin were notably effected. FCGR2A transcripts were reduced, but surface expression on monocytes was variable. The S100A9 and S100A12 are involved in monocyte adhesion and chemotaxis. Adrenomedullin, important for vascular integrity, was shown in monocytes by gene array as well (69) and these were both supported in other studies (70). Transcriptome analysis of PBMCs showed upregulation of NAIP, IPAF, S100A9, FCGR1A, and GCA which is also supportive of a role for the innate immune system (71).

Transcriptomics Supportive of a Role for B Cells in KD

Pathway significance analysis of blood lymphocyte-specific gene markers revealed that PI3K signaling in B lymphocytes was the most significant finding; however, T cell receptor signaling, B cell receptor signaling, T helper cell differentiation, and natural killer cell signaling were also significantly down-regulated in KD compared to febrile control patients (72). On whole blood expression analysis, comparing acute vs. convalescent samples, numerous upregulated pathways involved in innate immunity (particularly IL-1 and the Nlrp3 inflammasome) were shown in the acute phase. IL-10 was notably the highest association, and will be reviewed later. For pathways downregulated, outside of EIF2/p70S6K/MTOR pathways, "B cell development" was the most significant. As mTOR is essential in signaling through PI3K/Akt activity after B cell receptor (BCR) engagement, this association also supports that B cells may be playing a role. A number of these associations; however, were also seen in their controls. There was a surprising similarity with influenza and virally infected individuals. Of the pathways completely unique to KD, most of the specific associations related to myofibroblast migration (paxillin signaling, G-protein coupled receptor signaling, triacylglycerol and relaxin signaling) but PI3K/AKT signaling pathway showed a minor association. Lastly, there was surprisingly few transcript differences noted in those with and without aneurysms (73). A recent similar study comparing KD to adenovirus did not show much specific overlap with previous studies, but was also consistent with relation to a number of inflammatory pathways (74).

Overall, transcriptomics and cytokine profiling suggest a significant, but not exclusive, role for B cells in the pathogenesis of KD.

Models Systems of KD (See Table 1)

The first KD model system developed depended on intraperitoneal *Candida albicans* alkaline extract injections in susceptible mouse strains (75). Injection of the water soluble fraction of this, (CAWS) had increased incidence of arteritis which can be partially blocked by IVIG. IL-1 inhibition also diminishes the coronary inflammation (76). Notably this vasculitis is a panvasculitis predominantly and also effects the aortic root, which has not been described in KD cases (77).

Similarly, mice develop coronary artery inflammation after intraperitoneal injection with *Lactobacillus casei* cell wall extract (LCWE) (78, 79). Pathogenesis in this model parallels KD in that younger mice are more predisposed to develop arteritis and there is a favorable response to IVIG treatment. This disease exhibits mostly a T-cell infiltrate in coronary arterial specimens (79). In fact, in both RAG-1 (80) and TCR-α (81) deficient mice, this arteritis is diminished (82). Etanercept completely blocked these lesions and this was apparently related to signaling through

TABLE 1 | Comparison of human KD to common murine models of KD.

	Human KD	CAWS	LCWE
Pathogenesis	Unknown	Superantigen	Superantigen
Etiology	Unknown	*Candida albicans* water soluble injection	*Lactobacillus casei* cell wall extract injection
Animal	Human	Mice	Mice
Arteritis	medium-sized, muscular arteries, includes epicardial coronary arteries	Targets elastic arteries, including aortic root	Elastic arteries, aortitis, proximal coronary arteritis, abdominal aorta dilatations.
Histology	Early neutrophils, mixed data on granulomas	Monocytes, macrophages, neutrophils	Granulomatous
Myocarditis	Subclinical, Tachycardia	Significant	Significant, CK-MB and troponin rise, late myofibrosis
Timing	Adventia/intima to pan vasculitis	Progresses from initial intima layer slowly to panvasculitis	np
Therapy that reduces coronary inflammation	IVIG shows efficacy, Cyclosporine A efficacious in higher risk individuals	TNF a blocks arteritis IVIG partially blocks arteritis IVIG timing influences effect	Diminished by IVIG, anti-TNFα, anti-IL-1
Long term findings	Unclear associations Limited pathologic samples, mixed reports	np	Atherosclerosis, myofibrosis

np, not published.

TNFRI (83). Blocking IL-1 can also prevent progression of coronary pathology (84, 85). TNFα can drive metalloproteinase mmp9 activity to cause elastin breakdown. Doxycycline has been shown to prevent this (86), and human data will come from the currently open trial (87). A number of studies show marked myocarditis in these models with late fibrosis (88); however, following troponins is generally not clinically relevant. One group did associate serum troponins and ck-mb (89) but others have not seen that association. A number of the model systems have granulomatous changes, which have variably been seen in human specimens (90, 91). Other models depend on immune complex deposition. This was observed after bovine serum albumin injection into rabbits, which exhibited a disease similar to serum sickness (92). Presently, there is not a model system consistent with direct infectious coronary artery invasion.

No model system exactly replicates the pathologic changes seen in humans, and the utility of these models have been called into question (93). Although most data from model systems are supportive of superantigen involvement, studies from human peripheral lymphocyte responses as reviewed are variable and inconsistent (94). These models and other data are driving clinical trials, but results seen in the models aren't equitably transferable to treatment modalities (reviewed later). Since the cause in humans is unknown, it is still unclear if any of these models of arteritis are truly applicable.

The Superantigen Theory

A superantigen response was considered by numerous groups and is supported by murine models (79, 95–99). Certain bacterial infections contain proteins that non-specifically bind effector cell receptors causing a more generalized polyclonal expansion and inflammation, termed a superantigen effect. Polyclonality of T cell receptor usage has been shown in KD (100, 101); however, the reports are variable as to which subset of T cell receptors are effected (102). Other studies support a traditional oligoclonal response consistent with an immune response against a specific etiologic agent. Oligoclonal expansion of CD8+ T cells (103) and peripheral IgM+ B cell responses have been shown (9, 104). Numerous other studies have not shown superantigen associated expansions of cell subsets (103, 105, 106). Overall, there is not a clear role for a superantigen response during KD.

Genetic Implications

Inflammation during KD is universally present, so it is no surprise that a recent network and pathway analysis was consistent with global activation of the immune response (107). Large dataset and related human genomic studies have been performed to look for associated genes with KD incidence and treatment response. These study co-segregation of single nucleotide polymorphisms (SNPs) with the disease state to define significance. These are excellent hypothesis generating techniques, as each dataset generated has numerous implicated genes, but assigning biological significance can at times be difficult. These have been more successful in more homogenous populations and, for KD, have been recently reviewed (108–110).

Genome wide association studies (GWAS) offer unbiased approaches to explore genetic associations. A SNP (rs28493229) near inositol 1, 4, 5-trisphosphate 3-kinase (ITPKC, 19q13) was implicated first by a linkage disequilibrium study in siblings (111). ITPKC modifies the IP3 pathway leading to activation of NFAT transcription factor. A number of GWAS studies were negative or needed metanalysis to confirm this finding (112, 113) or showed a different SNP (rs2290692) association in the area (114). This may be an effect of differing genetic backgrounds in these studies. Other studies associate this gene area with coronary artery risk (115) and a number of SNPs associated with ITPKC were also seen in a study that initially identified FCRG2a (116). Caspase 3 (rs113420705) has been proposed to act downstream of ITPKC, and a genetic variance in the enhancer has been associated (rs72689236) (117, 118). Single-nucleotide polymorphisms (SNPs) in ITPKC (rs28493229) and caspase-3 (CASP3, rs113420705), when analyzed together, associate with increased risk for aneurysms (119). Separately they show a trend of overrepresentation in IVIG non-responders and together with coronary risk (120). These two genes could work on a similar calcium influx pathway. The polymorphism rs28493229 has been shown to effect ITPKC protein levels and thereby IL-1β and inflammasome NLRP3 expression, which was shown by studying murine models, KD subject samples, and EBV transformed B cells (121). There is a general lack of studies in non-Asian populations and disparate results can be seen depending on the genetic background. One of the first studies of this nature showed NAALADL2 and ZFHX3 highly associated with susceptibility in Dutch Caucasians. Reanalysis implicated other genes as well (DGKB, PPP1R14C, LNX1, CAMK2D, CSMD1, and TCP1) and network analysis could associate a number of these with CAMK2D (122).

The most significant and repeatedly associated susceptibility genes are FCGR2A, BLK and CD40, as reviewed in (110). The rs1801274 SNP is a functional polymorphism associated in the IgG receptor gene FCGR2A, which is a cell surface receptor found on phagocytic cells such as macrophages and neutrophils (116, 123). This receptor is a low-affinity receptor for immunoglobulin and is involved in the process of phagocytosis and clearing of immune complexes. Intriguingly, male gender influences the association of the FCRG2a (124). Genome-wide genetic marker association studies show that specific polymorphisms in CD40 and in the B lymphoid tyrosine kinase genes associate with KD (5, 6). One of the more consistent findings from GWAS data has been identifying SNPs in the region of the B lymphocyte kinase (BLK) (123, 125). BLK encodes a non-receptor protein tyrosine kinase and of the Src family of tyrosine kinases that acts downstream of the B cell receptor. Functional validation shows BLK is induced during acute KD (from patient samples) and the protective genotype of this SNP correlates with lower BLK expression on induction of EBV transformed B cells. Intriguingly, on a recent meta-analysis rs2736340 of BLK is also associated with systemic lupus erythematosus and rheumatoid arthritis-associated (126). Hypothesizing the importance of B cells based solely on BLK association is tenuous, as Blk knockout mice also suggest a role for Blk in the development of γδ TCR^+ T cells (127) and marginal zone B cells (128). The association of CD40 would also potentially point to a more specific B cell function (5, 123, 125), although CD40 is expressed on a number of cell types and functional inference of this association is lacking. The association of BLK and FCGR2a were recently confirmed;

TABLE 2 | Notable therapies and trials for treatment to prevent coronary aneurysms in Kawasaki Disease.

Therapy	Mechanism and cohort	Clinical trials, National Clinical Trial (NCT) #, name (if applicable)	Results summary/comments
Infliximab	TNFα blockade, most studied in refractory cases	2298062; 00271570; 00760435; 01596335; 03065244-KIDCARE	Given with IVIG, Improved defervescence, well-tolerated, variable z score reduction, (132). In refractory, Improved defervescence, well-tolerated, (133). KIDCARE recruiting
Etanercept	In conjunction with IVIG	00841789	Study awaiting results
Anakinra	IL-1 blockade, Refractory cases	02179853 02390596-KAWAKINRA	KAWAKINRA recruiting
Cyclosporine A	In conjunction with IVIG in predicted high risk individuals	Japan Medical Association, JMA-IIA00174- KAICA	Efficacy shown in preventing more severe coronary involvement (134), (135)
IVIG dosage		00000520; 02439996	Single dose of IVIG is better than splitting doses (136)
IVIG + pulsed steroids	Primary cases	00132080	No difference shown (137)
IVIG + 5 days prednisolone	For refractory cases	03200561- RAST	Proposal published (138); recruiting
IVIG without Aspirin	Primary cases	02951234	Proposal published (139); recruiting
Doxycycline	Decreases MMP degradation of elastin, supported by murine model	01917721-DEAL	Proposal published (87); recruiting
Statins	For those with severe coronary artery involvement	03915795	Recruiting
Rituximab	Anti-CD20 targets B cells	na	Case report (140)
Plasma Exchange	Broad effects, decreases cytokines, increase of T regs	na	No active studies (141)

na, not applicable.

however, did not seem to correlate with incomplete or cases from children older than 5 years of age (129).

A recent meta-analysis did see nominal associations with four previously noted genes (FCGR2A rs1801274, TCP1 rs3818298, BLK rs2736340, and CD40 rs4813003) but did not replicate a number of these associations (ZFHX3 rs9937546, NAALADL2 rs1870740, CAMK2D rs4834340, LNX1 rs6554112, MIA-RAB4B rs2233152, HLA-DQB-HLA-DOB rs2857151) (130). When specifically studying susceptibility to cardiac aneurysms, a number of intergenic associations were also shown, highlighting the complex organization and influence of chromatin structure (131). The most review and meta-analysis of available data supports a role for in susceptibility for genetic variations of ACE, BLK, CASP3, CD40, FCGR2A, FGb, HLA-E, IL1A, IL6, ITPKC, LTA, MPO, PD1, SMAD3, TARC/CCL17, and TNF. Also, genetic variations in BTNL2, CASP3, FCGR2A, FGF23, FGb, GRIN3A, HLA-E, IL10, ITPKC, and TGFBR2 may serve as biomarkers of CALs in KD (109).

Overall, association with a variety of pathways is not surprising for a disease with a likely complex pathogenesis. However, most of the major repetitively associated and/or validated genomic findings could support a role for B cells and antibodies influencing susceptibility (110).

Clues From Treatment (See Table 2)

Intravenous Immunoglobulin (IVIG)

The first implication of humoral immunity possibly being involved in KD was the response to immunoglobulin infusions. IVIG was started after success with preparations in Immune thrombocytopenic purpura and was shown to protect against cardiac involvement (142). After discovery that aneurysms are associated with KD, studies, including randomized controlled trials, supported a protective effect of IVIG (136). IVIG is known to broadly effect numerous mechanisms that have been outlined in recent reviews, including: direct neutralization of organism or toxin, inhibition of autoantibodies, inhibition of the complement cascade, inhibition of adhesion molecules on vascular endothelium, modulation of cytokine response, expansion of T regulatory cells, modulation of dendritic cell responses, and decreasing pro-inflammatory effects of monocytes by FC interaction (143–146). Possible mechanisms are detailed in **Figure 1.** The exact mechanism that correlates with clinical improvement seems to depend on the underlying disorder. On the most simplistic level, supplementation of a specific necessary immune response is still theorized for KD (147).

However, it is unclear how IVIG actually functions during KD and if specific antibody responses are responsible for pathogenesis. Early studies focused on dosing regimens and showed single large infusions (2 grams/kg) are superior to smaller more frequent doses (136). It is possible that a high level of antibody is needed to clear a pathogen, or to improve diffusion to certain areas; however, why this difference is unclear. The mechanism of loading of the neonatal FcRn receptor may require such high volume administration. Other Fc receptor modulation, particularly upregulation of FcγRIIB has also been proposed (148, 149). Without knowledge of the cause of KD, the mechanism of action will remain difficult to prove. The anti-inflammatory properties of IVIG also treat many infectious

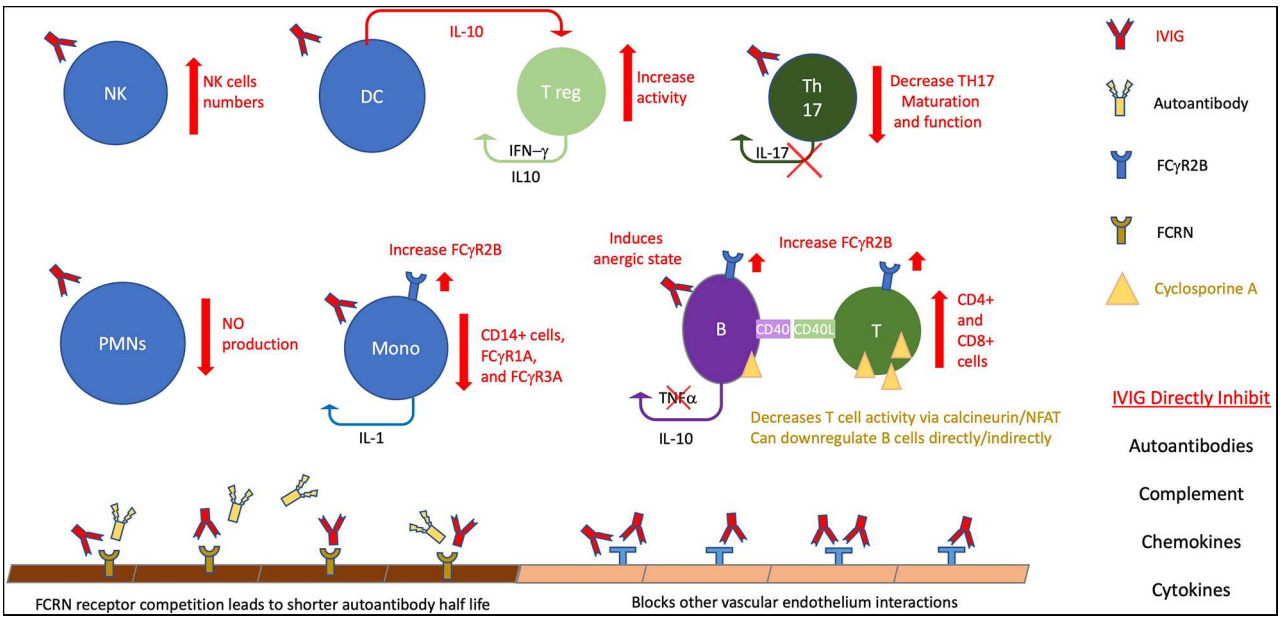

FIGURE 1 | The many and varied potential activities in KD. This figure highlight potential therapeutic effects on B cell activity, particularly for IVIG. IVIG effects are noted by red elements, cyclosporin A noted by gold. B, B cells; T, T cells; T reg, T regulatory cells, DC, dendritic cells; nk, natural killer; PMNs, polymorphonuclear cells; Mono, monocytes, NO, Nitric Oxide.

agents so a clinical response to IVIG is not definitive proof of the diagnosis of KD (147).

Recent studies show specific immune changes induced by treatment with IVIG. TH17 cells and IL-17 levels are elevated during acute KD, which is seen in autoimmune disorders, and this can be improved after IVIG (150, 151). T regulatory cells (T regs) are reduced during acute KD, and this is improved with IVIG (152). These cells, as well as myeloid dendritic cells are expanded by IVIG (145). In a study comparing IVIG to aspirin treatment alone group, IVIG treatment showed increase CD4, restoration of CD8 to normal control levels, and a significant suppression of CD19 cells below that of normal controls (153). Other studies also have explored diminished CD8 T cells in acute KD (154). Abnormal elevations of BAFF, which is in involved in survival of and proliferation of B cells, are decreased after treatment with IVIG (155). In what authors termed, "functional silencing," IVIG suppressed phosphoinositide 3-kinase signaling (via NFAT) which would affect calcium signaling, coreceptor activation, and BCR activation (156). This finding supportive of B cell signaling involvement in KD could potentially link some of the genomic and transcriptomic associations.

Other Treatments

Adjunct steroids showed efficacy in certain populations (157). Meta-analysis of this and other clinical trials, mostly from Japan, support the use of steroids along with IVIG in high-risk patients (158). Since it is difficult to predict risk in heterogenous populations outside of Japan, and historical studies have shown worse outcomes with steroid use (159), there is not a universal recommendation to give adjunct steroids (2). Even in the revised 2012 guidelines from the Japanese Society of Pediatric Cardiology, "controversy remains" on universal initial steroid use (160). Aspirin is begun at anti-inflammatory doses initially, then is changed to a lower dose to prevent complications of coronary involvement (2). As this has not been shown to effect development of aneurysms, other platelet- aggregation inhibitors such as Clopidogrel or dipyridamole, can be considered in special situations (2). The main treatment modalities hoped to target prevention of coronary aneurysms used for refractory treatment are second doses of IVIG, steroids, calcineurin inhibitors, anti-IL-1 monoclonal antibodies, and anti-TNF monoclonal antibodies; all of which have broad immunological effects (53, 161).

Success with anti-TNFα treatment seemingly argues against a significant role of B cells, as this would affectively release a suppressive action of TNFα on B cell proliferation. The main treatments studied have been infliximab, a humanized mouse monoclonal antibody, and etanercept, a human recombinant mimic of the TNFα receptor (162). TNFα produced from B cells is implicated in atherosclerosis, so perhaps B cell derived TNFα is targeted (163). Notably, IVIG decreases TNFα production. The status of clinical trials have been recently reviewed (164). Although tolerance and improved defervescence are clear in trials with infliximab, there is less clarity of efficacy for improvement of aneurysms (132, 133). The KIDCARE trial, which is focused on recalcitrant cases may prove to be more insightful than previous trials. Etanercept has also undergone recent phase II randomized trial, but publications of results have not been done to date. A recent meta-analysis of twelve studies showed that both IV methylprednisolone and infliximab were not superior to a second

dose of IVIG for prevention of aneurysms (165). The other main class of biologics used are Interluekin-1 (IL 1) inhibitors. These obviously have a broad inflammatory response (145) with notable effects on B cell activity (166) There is support in the *Lactobacillus casei* mouse model for IL-1 playing a role (167).

Genetic associations and data from murine models have supported targeting of NFAT with calcineurin inhibitors, and treatment protocols for KD have been developed (168). A recent Japanese clinical trial (135) show that addition of Cyclosporine A to IVIG in high risk patients is efficacious in prevention of the largest of aneurysms. Cyclosporine A mainly targets T cell activity by inhibition of calcineurin and its downstream transcription factor NFAT. This downregulation of T cell activity has been shown to decrease B cell immunoglobulin production (169). Although encouraging, the applicability of this treatment outside of the highest risk individuals is unclear. Limited reports of successful treatment with anti-B cell monoclonal antibodies (anti-CD20) also support a role for B cell activation in KD pathogenesis (140). Based on data regarding MMP in murine models, doxycycline is also being used (87). Supplementation with statins also has a currently recruiting trial ongoing. Plasma exchange, which also has a broad range of activity, is used in some centers, particularly in Japan (2). Recent data suggests restitution of circulating T regulatory cells occurs which aligns with other mechanisms similar to IVIG (141).

The broad effects of most treatments make drawing specific conclusions about correlation with pathogenesis (see **Figure 1**); however, a number of treatments and reported success with anti-CD20 monoclonal antibodies supports a significant role for B cells.

Autoimmune Antibodies in KD

A role for B cells could imply a significant autoimmune component in KD (170). Self-antigen responses to a variety of targets have actually been well-described in KD. These include recent reports of antibody responses to type III collagen, myosin (171), cardiolipin (172), alpha-enolase (173), and anti-endothelial antibodies. Anti-endothelial antibodies are particularly interesting as these are seen in other disorders, such as SLE and renal allograft rejection (174). Other vasculitides have also been associated with anti-endothelial antibodies. These have been shown to cause upregulation of E-selectin, VCAM-1, ICAM-1, and NFκB (175). Responses to these antibodies include upregulation of inflammatory cytokines and apoptosis of the endothelial cells.

In KD subjects, a polyclonal response against endothelial cells has been described (176); however, not universally (177). Particularly during generalized inflammation, cytokines such as IFN-γ, IL-1, and TNF can reveal this IgG and IgM anti-endothelial response (178, 179). In cell lysis assays, pathogenesis was eliminated by clearing the serum through anti-IgG and anti-IgM sepharose columns arguing against a role of peripheral anti-IgA responses. This does not eliminate the potential role of intra-tissue IgA+ plasma cell development in pathogenesis as has been postulated (180, 181). Other studies support significant IgM mediated cytotoxicity against endothelial cells in KD patients (182). Prevalent IgM anti-endothelial responses in KD have also been shown without cytokine stimulation (182, 183). In a mouse model system, anti-endothelial antibody responses were replicated, but these did not demonstrate cardiac vascular involvement (184).

Recently, the autoimmune considerations in KD have been reviewed (170). The case report of anti-B cell monoclonal antibody success was proposed by the authors to be due to the downregulation of such an anti-endothelial invasive effect (140).

Although intriguing, it remains unknown if these anti-endothelial responses actually contribute to the vasculitis in KD and other vasculitides (175).

Human Pathologic Studies

A small number of studies, due to the necessary reliance on autopsy specimens, support limited B cell infiltration into the coronary arteries (185). These limited studies have shown that coronary infiltrates develop over time with late fibrosis occurring in the intima and adventitial layers and can be divided into an acute, subacute and chronic state formation (90). In the acute phase, neutrophils are the predominant initial cell infiltrate (186). This can result in necrotizing arteritis that destroys the adventitia leading to aneurysm formation (90).

A number of studies have noted lymphocytic infiltrates in samples from later timepoints. In a study of eight specimens, two of which were within the first 2 weeks of illness, showed predominant monocytes on day 6 and no CD3+ (T cell) nor CD20+ (B cells) cells. T and B cells were shown in the one sample from day 10 but both monocytes and neutrophils were more predominant (186). B cell responses were highest on day 10 and 17 overall, but one of the two samples from day 17 had very few B cells. Another small study of seven subjects, all from over 13 days of illness, showed IgA+ plasma cell infiltrates. These were seemingly specific to KD; however, the fourteen control specimens were from autopsies that succumbed generally from non-inflammatory and non-cardiac syndromes. Notably, mature memory and immature B cells (CD20+ cells) were lacking (180). If the previous day 10 B cell infiltrates became plasma cells as has been postulated (187), these studies would be consistent. Also consistent, in a series of six KD specimens who were not diagnosed with aneurysms compared to 21 non-inflamed controls, neutrophil infiltration in adventia and intima layers was quickly followed by lymphocyte infiltrates, then mixed lymphocyte, eosinophils, and plasma cell infiltrates were demonstrated later, near day 19 of illness (186, 188). Other reports support monocyte infiltration with more significant CD8 T cell responses, however there were few early samples here as well (187). Overall, innate immune cells are the predominant in early infiltrates.

Prominent nodular infiltrates, similar to atherosclerotic plaque formation, have also been described, but these appear to occur at later timepoints (>3 weeks). These infiltrates consisted of T cells, macrophages, B cells and prevalent IgM+ plasma cells, with less frequent IgA+ plasma cells. The authors compare these to similar B cell rich lesions driven by both superantigens and specific infectious antigens (189).

The largest study, relying on electron microscopic studies, suggests that there is an early necrotizing arteritis suggestive

of an acute viral infection, followed by a vasculitis, then luminal myofibroblast proliferation (90). There were a number of differences from previous reported pathological specimens, including lack of granulomatous inflammation, lack of small vessel pathology, minimal medial hyperplasia or scarring, and lack of atherosclerosis. Overall most studies are consistent with an early phase with neutrophil infiltration when severe is termed necrotizing arteritis, with later lymphocyte and plasma cell infiltration still in the background of significant monocytes.

Only few studies on long-term sequelae have been published. There seems to be an increased risk of cardiac death in survivors of KD. Limited human pathology specimens show no long-term inflammatory infiltrates (186, 188). The limited data on adult follow-up cases of KD implies there is a greater lifetime risk of cardiac issues and early mortality (15–18). Even those who had KD without noticeable aneurysms may have endothelial dysfunction and increased arterial stiffness (158). A clinical trial on long-term consequences is actively recruiting (NCT03750123-CAVASAKI trial). As established clinical cohorts age, the lifetime risk of childhood KD should be revealed.

Unfortunately, disparity of reports, lack of early timepoints, and lack of control tissue sample from cases experiencing ongoing inflammation make firm conclusions difficult. Collection and study of these types rare samples should continue.

Studies on Circulating Immune Cells

In the few published studies on peripheral cell subsets during acute KD, circulating B cells are generally elevated (6, 9, 45, 71, 190). Lack of changes in acute and convalescent B cells subgroups and increases in CD69+ natural killer and $\gamma\delta$ T cells supported a role for the innate immune system (71). B cells did seem to be in an "activated" phenotype, being positive for CD86 (190). After stimulation of the TLR-9 receptor there was a global increase in the ability of B cells to secrete IgM, IgG, and IgA with a notable expansion in IgA+ B cell numbers (190). One study showed a paucity of IgA + peripheral B cells from acute KD samples compared to controls continuing through convalescence (8) that was not replicated in other studies. Reports do show increased IgA immune complexes and levels (13), although immune complexes do not necessarily portend worse prognosis (191). Overall, in the small number of studies relating to the peripheral blood B cell compartment, overall B cells numbers are increased and B cells are more reactive.

Although, total numbers of cells do not show consistent results, clonal expansion within the B cell compartment can be studied. A specific immune response to an agent typically has an initial inherent immune component that leads to antigen presentation to effector cells. Receptors on the effector cell surface (T-cell receptors in T cells and Immunoglobulin, or antibody, in B cells) bind specific targeted areas of the agent, termed epitopes. Specific recognition by T and B lymphocytes leads to stimulation, lymphocyte replication and clonal expansion; what is termed an oligoclonal response. Oligoclonal expansion is shown in peripheral IgM+ B cells in KD (9). Oligoclonal plasma cell infiltrates, predominantly IgA+, have been shown in KD arterial specimens (192). Heavy and light chain sequences were obtained and cloned into full length expression vectors from these cardiac vessel samples. These chimeric antibodies identified intracellular inclusions (ICI) in bronchial epithelium samples from children with KD (46, 104). However, similarly cloned antibodies revealed self-antigen targeting (181). Additionally, 26% of the control group, composed primarily of adult patients, had similar inclusion bodies, and next generation sequencing from these ICIs did not reveal an etiology (193). Although plasma cell infiltration outlined above is intriguing, a similar pathological response is seen in a number of inflammatory conditions such as NMDAR encephalitis (194), primary sclerosing cholangitis, (195) multiple sclerosis, (196) and responses to tumors (197). ICI in cells can be any number of structures (aggresomes, stress granules, p-bodies, prion-aggregates, aggresome-like induced structures (ALIS) and autophagosomes) and this has been recently reviewed (164). Currently, it is unclear of the significance of this work.

Similar Plasmablast (PB) Responses in KD Compared to Infections

Plasmablasts (PBs), derived from naïve and memory responses, are B cells transitioning to plasma cells that circulate in the peripheral blood cell compartment. They are characterized by surface expression of CD19, with CD20 downregulation, and high levels of CD27 and CD38. After antigenic challenge (vaccination and natural infections), CD19+, CD20lo, CD27+ and CD38 + PBs can be seen in the peripheral blood (8, 198–200). Immunization studies in adults, with pathogens such as tetanus, influenza and rabies, show PBs are enriched for specific antibodies against the challenge antigen, temporally peak 5–10 days after immunization, and are predictive of later sero-immunity (198, 201–203). In comparison to the general circulating B cell population, PBs are enriched for B cells that produce infection-specific antibodies (204–209) Although certain infections, such as dengue virus, may set off exceedingly high PB levels (210–212), excessive PB responses are usually an indicator of autoimmune flares (213). This excessive circulating PB response seen specifically correlates with CRP level in studies on ulcerative colitis (212, 214) and IGG4 related disease (215, 216). Besides correlation of an inflammatory state consistent with infection and inflammation, little is known regarding regulatory or pathologic consequences of PB elevation.

We postulated if KD is caused by an infection, we should see a predictable rise of PBs in the peripheral blood. On single timepoint collection, we showed 15 of 18 KD samples had elevation of their PBs, and overall this response was similar to the range of data shown in our 69 infected controls (45). Results of this study are consistent with the majority of the literature that show B cell stimulation and increasing peripheral B cell numbers during KD (6, 9, 71, 190). Importantly, the levels were not consistent with a pure autoimmune response as they did not correlate with CRPs and were not overly excessive. Unfortunately, only five children had repeat samples, but from these it did not appear that IVIG has an effect on PB numbers. As PBs rise and fall over time, we have ongoing studies collecting samples over time to confirm a dynamic PB response similar to infections occurs in KD. Other groups have recently shown

similar PB elevation during KD, but this was compared to healthy controls (217).

Ongoing studies are exploring heavy and light chain usage in B cells and PBs during KD with next generation sequencing techniques. From our initial evaluation, a number of these clones have markers of affinity maturation (multiple clonal members, isotype switching, increased nucleotide substitutions from predicted germlines, and increases in the subgroup replacement to silent nucleotide mutation (R/S) ratios) (218). Our group and other are expressing cloned sequences as monoclonal antibodies in the attempt to find their antigenic target.

Because of reported oligoclonal responses and characteristics suggesting response to infection seen in PBs and antibodies during KD, we hypothesize the antibodies derived from PBs during KD are specific against the etiology that led to KD within that child.

DISCUSSION

As reviewed, a number of studies support a roll for B cells, plasma cells, and antibodies in the pathogenesis of KD. Although B cell and plasma cell infiltration in pathology specimens is intriguing, whether they are bystanders activated by a superantigen effect, are responding to a self-antigen revealed by inflammation, or specific against an infectious etiology is currently unknown. An autoimmune component to this disease has long been postulated, and overlapping genomic risk associations with lupus and rheumatoid arthritis suggest this to play a role. Genomic and proteomic approaches strongly suggest a role for the innate immune system in pathogenesis, but associations with BLK, and CD40 also support a potential role for B cells. The increasingly appreciated role of B cells as immune system modulators may explain these associations and align the disparate data.

Humoral immune responses continue to be worth exploration in children with KD. Like the mouse models and attempts at developing new therapeutics, it is hard to be confident in any one approach without knowledge of the etiology. Compelling recent data suggests that exploration of the specific B cell responses is an encouraging path to discovering improved diagnostics and potentially the pathogen that sets off this immune cascade.

This is a rich opportunity for clinical investigators. Rigorous studies are needed on those children who present with KD. If any pulmonary findings are found, bronchial washings should be obtained and stored for potential molecular diagnostics. Other samples, such as PBMCs and serum, should be taken and banked for future studies. Thorough autopsy evaluation should be pursued on any subjects who succumb during the acute or convalescent phases of KD. Improved reporting and national registries would go a long way in establishing a representative pool of patients. Studies currently ongoing on peripheral cytokine profiles, B cells and PBs may show a consistent marker to help define who has KD. A correlative diagnostic marker, possibly even antibody derived, would be a highly desirable first step in future studies.

As outlined herein, evidence from genomics, transcriptomics, and proteomics support a role for B cells in the pathogenesis of KD, and continued studies on B cell responses may assist in identifying the etiology of KD.

AUTHOR CONTRIBUTIONS

MH conceived and was the sole contributor to this manuscript.

FUNDING

Relative funding includes a generous grant from the Wildermuth Foundation provided through the Variety Club of Buffalo.

REFERENCES

1. Kawasaki T. Kawasaki disease. *Acta Paediatr.* (1995) 84:713–5. doi: 10.1111/j.1651-2227.1995.tb13742.x
2. McCrindle BW, Rowley AH, Newburger JW, Burns JC, Bolger AF, Gewitz M, et al. Diagnosis, treatment, and long-term management of kawasaki disease: a scientific statement for health professionals from the American Heart Association. *Circulation.* (2017) 135:e927–99. doi: 10.1161/CIR.0000000000000484
3. Newburger JW, Takahashi M, Gerber MA, Gewitz MH, Tani LY, Burns JC, et al. Diagnosis, treatment, and long-term management of Kawasaki disease: a statement for health professionals from the committee on rheumatic fever, endocarditis and kawasaki disease, council on cardiovascular disease in the young, American Heart Association. *Circulation.* (2004) 110:2747–71. doi: 10.1161/01.CIR.0000145143.19711.78
4. Yorifuji T, Tsukahara H, Doi H. Breastfeeding and risk of kawasaki disease: a nationwide longitudinal survey in Japan. *Pediatrics.* (2016) 137:e20153919. doi: 10.1542/peds.2015-3919
5. Lee YC, Kuo HC, Chang JS, Chang LY, Huang LM, Chen MR, et al. Two new susceptibility loci for Kawasaki disease identified through genome-wide association analysis. *Nat Genet.* (2012) 44:522–5. doi: 10.1038/ng.2227
6. Chang CJ, Kuo HC, Chang JS, Lee JK, Tsai FJ, Khor CC, et al. Replication and meta-analysis of GWAS identified susceptibility loci in Kawasaki disease confirm the importance of B lymphoid tyrosine kinase (BLK) in disease susceptibility. *PLoS ONE.* (2013) 8:e72037. doi: 10.1371/journal.pone.0072037
7. Kuo HC, Lo MH, Hsieh KS, Guo MM, Huang YH. High-dose aspirin is associated with anemia and does not confer benefit to disease outcomes in Kawasaki disease. *PLoS ONE.* (2015) 10:e0144603. doi: 10.1371/journal.pone.0144603
8. Shingadia D, O'Gorman M, Rowley AH, Shulman ST. Surface and cytoplasmic immunoglobulin expression in circulating B-lymphocytes in acute Kawasaki disease. *Pediatr Res.* (2001) 50:538–43. doi: 10.1203/00006450-200110000-00019
9. Lee HH, Park IH, Shin JS, Kim DS. Immunoglobulin V(H) chain gene analysis of peripheral blood IgM-producing B cells in patients with Kawasaki disease. *Yonsei Med J.* (2009) 50:493–504. doi: 10.3349/ymj.2009.50.4.493
10. Newburger JW, Takahashi M, Gerber MA, Gewitz MH, Tani LY, Burns JC, et al. Diagnosis, treatment, and long-term management of Kawasaki disease: a statement for health professionals from the committee on rheumatic fever, endocarditis, and Kawasaki disease, council on cardiovascular disease in the young, American Heart Association. *Pediatrics.* (2004) 114:1708–33. doi: 10.1542/peds.2004-2182
11. Terai M, Honda T, Yasukawa K, Higashi K, Hamada H, Kohno Y. Prognostic impact of vascular leakage in acute Kawasaki disease. *Circulation.* (2003) 108:325–30. doi: 10.1161/01.CIR.0000079166.93475.5F
12. Jun HO, Yu JJ, Kang SY, Seo CD, Baek JS, Kim YH, et al. Diagnostic characteristics of supplemental laboratory criteria for incomplete Kawasaki

disease in children with complete Kawasaki disease. *Korean J Pediatr.* (2015) 58:369–73. doi: 10.3345/kjp.2015.58.10.369
13. Ohshio G, Furukawa F, Khine M, Yoshioka H, Kudo H, Hamashima Y. High levels of IgA-containing circulating immune complex and secretory IgA in Kawasaki disease. *Microbiol Immunol.* (1987) 31:891–8. doi: 10.1111/j.1348-0421.1987.tb03150.x
14. Yanagawa H, Yashiro M, Nakamura Y, Sakata K, Kawasaki T. Iv gamma globulin treatment of Kawasaki disease in Japan: results of a nationwide survey. *Acta Paediatr.* (1995) 84:765–8. doi: 10.1111/j.1651-2227.1995.tb13752.x
15. Pinna GS, Kafetzis DA, Tselkas OI, Skevaki CL. Kawasaki disease: an overview. *Curr Opin Infect Dis.* (2008) 21:263–70. doi: 10.1097/QCO.0b013e3282fbf9cd
16. Nakamura Y, Yanagawa H, Harada K, Kato H, Kawasaki T. Mortality among persons with a history of Kawasaki disease in Japan: the fifth look. *Arch Pediatr Adolesc Med.* (2002) 156:162–5. doi: 10.1001/archpedi.156.2.162
17. Nakamura Y, Aso E, Yashiro M, Uehara R, Watanabe M, Tajimi M, et al. Mortality among persons with a history of Kawasaki disease in Japan: can paediatricians safely discontinue follow-up of children with a history of the disease but without cardiac sequelae? *Acta Paediatr.* (2005) 94:429–34. doi: 10.1111/j.1651-2227.2005.tb01913.x
18. Gordon JB, Kahn AM, Burns JC. When children with Kawasaki disease grow up: myocardial and vascular complications in adulthood. *J Am Coll Cardiol.* (2009) 54:1911–20. doi: 10.1016/j.jacc.2009.04.102
19. Chrissoheris MP, Donohue TJ, Young RS, Ghantous A. Coronary artery aneurysms. *Cardiol Rev.* (2008) 16:116–23. doi: 10.1097/CRD.0b013e31815d0573
20. Burgner D, Harnden A. Kawasaki disease: what is the epidemiology telling us about the etiology? *Int J Infect Dis.* (2005) 9:185–94. doi: 10.1016/j.ijid.2005.03.002
21. Abuhammour WM, Hasan RA, Eljamal A, Asmar B. Kawasaki disease hospitalizations in a predominantly African-American population. *Clin Pediatr.* (2005) 44:721–5. doi: 10.1177/000992280504400812
22. Clark DE, Denby KJ, Kaufman LM, Fill MA, Piya B, Krishnaswami S, et al. Predictors of intravenous immunoglobulin non-response and racial disparities in Kawasaki disease. *Pediatr Infect Dis J.* (2018) 37:1227–34. doi: 10.1097/INF.0000000000002019
23. Porcalla AR, Sable CA, Patel KM, Martin GR, Singh N. The epidemiology of Kawasaki disease in an urban hospital: does African American race protect against coronary artery aneurysms? *Pediatr Cardiol.* (2005) 26:775–81. doi: 10.1007/s00246-005-0916-5
24. Scuccimarri R. Kawasaki disease. *Pediatr Clin North Am.* (2012) 59:425–45. doi: 10.1016/j.pcl.2012.03.009
25. Fujita Y, Nakamura Y, Sakata K, Hara N, Kobayashi M, Nagai M, et al. Kawasaki disease in families. *Pediatrics.* (1989) 84:666–9.
26. Rodo X, Ballester J, Cayan D, Melish ME, Nakamura Y, Uehara R, et al. Association of Kawasaki disease with tropospheric wind patterns. *Sci Rep.* (2011) 1:152. doi: 10.1038/srep00152
27. Burns JC, Cayan DR, Tong G, Bainto EV, Turner CL, Shike H, et al. Seasonality and temporal clustering of Kawasaki syndrome. *Epidemiology.* (2005) 16:220–5. doi: 10.1097/01.ede.0000152901.06689.d4
28. Kao AS, Getis A, Brodine S, Burns JC. Spatial and temporal clustering of Kawasaki syndrome cases. *Pediatr Infect Dis J.* (2008) 27:981–5. doi: 10.1097/INF.0b013e31817acf4f
29. Makino N, Nakamura Y, Yashiro M, Ae R, Tsuboi S, Aoyama Y, et al. Descriptive epidemiology of Kawasaki disease in Japan, 2011–2012: from the results of the 22nd nationwide survey. *J Epidemiol.* (2015) 25:239–45. doi: 10.2188/jea.JE20140089
30. Mauro A, Fabi M, Da Fre M, Guastaroba P, Corinaldesi E, Calabri GB, et al. Kawasaki disease: an epidemiological study in central Italy. *Pediatr Rheumatol Online J.* (2016) 14:22. doi: 10.1186/s12969-016-0084-6
31. Chen JJ, Ma XJ, Liu F, Yan WL, Huang MR, Huang M, et al. Epidemiologic features of Kawasaki disease in shanghai from 2008 through 2012. *Pediatr Infect Dis J.* (2016) 35:7–12. doi: 10.1097/INF.0000000000000914
32. Chang A, Delmerico AM, Hicar MD. Spatiotemporal analysis and epidemiology of Kawasaki disease in Western New York: a sixteen year review of cases presenting to a single tertiary care center. *Pediatr Infect Dis J.* (2018) 38:582–8. doi: 10.1097/INF.0000000000002239
33. Burns JC, Herzog L, Fabri O, Tremoulet AH, Rodo X, Uehara R, et al. Seasonality of Kawasaki disease: a global perspective. *PLoS ONE.* (2013) 8:e74529. doi: 10.1371/journal.pone.0074529
34. Manlhiot C, O'Shea S, Bernknopf B, LaBelle M, Chahal N, Dillenburg RF, et al. Epidemiology of Kawasaki disease in Canada 2004 to 2014: comparison of surveillance using administrative data vs periodic medical record review. *Can J Cardiol.* (2018) 34:303–9. doi: 10.1016/j.cjca.2017.12.009
35. Dergun M, Kao A, Hauger SB, Newburger JW, Burns JC. Familial occurrence of Kawasaki syndrome in North America. *Arch Pediatr Adolesc Med.* (2005) 159:876–81. doi: 10.1001/archpedi.159.9.876
36. Newburger JW, Taubert KA, Shulman ST, Rowley AH, Gewitz MH, Takahashi M, et al. Summary and abstracts of the seventh international Kawasaki disease symposium: december 4–7, 2001, Hakone, Japan. *Pediatr Res.* (2003) 53:153–7. doi: 10.1203/00006450-200301000-00026
37. Rowley AH, Shulman ST. The Epidemiology and pathogenesis of Kawasaki disease. *Front Pediatr.* (2018) 6:374. doi: 10.3389/fped.2018.00374
38. Nakagawa A, Ito M, Iwaki T, Yatabe Y, Asai J, Hayashi K. Chronic active Epstein-Barr virus infection with giant coronary aneurysms. *Am J Clin Pathol.* (1996) 105:733–6. doi: 10.1093/ajcp/105.6.733
39. Rodo X, Curcoll R, Robinson M, Ballester J, Burns JC, Cayan DR, et al. Tropospheric winds from northeastern China carry the etiologic agent of Kawasaki disease from its source to Japan. *Proc Natl Acad Sci USA.* (2014) 111:7952–7. doi: 10.1073/pnas.1400380111
40. Manlhiot C, Mueller B, O'Shea S, Majeed H, Bernknopf B, Labelle M, et al. Environmental epidemiology of Kawasaki disease: linking disease etiology, pathogenesis and global distribution. *PLoS ONE.* (2018) 13:e0191087. doi: 10.1371/journal.pone.0191087
41. Bell DM, Brink EW, Nitzkin JL, Hall CB, Wulff H, Berkowitz ID, et al. Kawasaki syndrome: description of two outbreaks in the United States. *N Engl J Med.* (1981) 304:1568–75. doi: 10.1056/NEJM198106253042603
42. Baker AL, Lu M, Minich LL, Atz AM, Klein GL, Korsin R, et al. Associated symptoms in the ten days before diagnosis of Kawasaki disease. *J Pediatr.* (2009) 154:592–5.e2. doi: 10.1016/j.jpeds.2008.10.006
43. Freeman AF, Crawford SE, Finn LS, Lopez-Andreu JA, Ferrando-Monleon S, Perez-Tamarit D, et al. Inflammatory pulmonary nodules in Kawasaki disease. *Pediatr Pulmonol.* (2003) 36:102–6. doi: 10.1002/ppul.10333
44. Jordan-Villegas A, Chang ML, Ramilo O, Mejias A. Concomitant respiratory viral infections in children with Kawasaki disease. *Pediatr Infect Dis J.* (2010) 29:770–2. doi: 10.1097/INF.0b013e3181dba70b
45. Martin M, Wrotniak BH, Hicar M. Suppressed plasmablast responses in febrile infants, including children with Kawasaki disease. *PLoS ONE.* (2018) 13:e0193539. doi: 10.1371/journal.pone.0193539
46. Rowley AH, Baker SC, Orenstein JM, Shulman ST. Searching for the cause of Kawasaki disease–cytoplasmic inclusion bodies provide new insight. *Nat Rev Microbiol.* (2008) 6:394–401. doi: 10.1038/nrmicro1853
47. Geme JW Jr. A biological perspective of slow virus infection and chronic disease. *West J Med.* (1978) 128:382–9.
48. Shimizu C, Shike H, Baker SC, Garcia F, van der Hoek L, Kuijpers TW, et al. Human coronavirus NL63 is not detected in the respiratory tracts of children with acute Kawasaki disease. *J Infect Dis.* (2005) 192:1767–71. doi: 10.1086/497170
49. Lee KY, Han JW, Lee JS. Kawasaki disease may be a hyperimmune reaction of genetically susceptible children to variants of normal environmental flora. *Med Hypotheses.* (2007) 69:642–51. doi: 10.1016/j.mehy.2006.12.051
50. Rhim JW, Kang HM, Han JW, Lee KY. A Presumed etiology of Kawasaki disease based on epidemiological comparison with infectious or immune-mediated diseases. *Front Pediatr.* (2019) 7:202. doi: 10.3389/fped.2019.00202
51. Esposito S, Polinori I, Rigante D. The gut microbiota-host partnership as a potential driver of Kawasaki syndrome. *Front Pediatr.* (2019) 7:124. doi: 10.3389/fped.2019.00124
52. Sleeper LA, Minich LL, McCrindle BM, Li JS, Mason W, Colan SD, et al. Evaluation of Kawasaki disease risk-scoring systems for intravenous immunoglobulin resistance. *J Pediatr.* (2011) 158:831–5.e3. doi: 10.1016/j.jpeds.2010.10.031

53. Dominguez SR, Anderson MS. Advances in the treatment of Kawasaki disease. *Curr Opin Pediatr.* (2013) 25:103–9. doi: 10.1097/MOP.0b013e32835c1122
54. Parthasarathy P, Agarwal A, Chawla K, Tofighi T, Mondal TK. Upcoming biomarkers for the diagnosis of Kawasaki disease: a review. *Clin Biochem.* (2015) 48:1188–94. doi: 10.1016/j.clinbiochem.2015.02.013
55. Kimura Y, Yanagimachi M, Ino Y, Aketagawa M, Matsuo M, Okayama A, et al. Identification of candidate diagnostic serum biomarkers for Kawasaki disease using proteomic analysis. *Sci Rep.* (2017) 7:43732. doi: 10.1038/srep43732
56. Okuma Y, Suda K, Nakaoka H, Katsube Y, Mitani Y, Yoshikane Y, et al. Serum Tenascin-C as a novel predictor for risk of coronary artery lesion and resistance to intravenous immunoglobulin in Kawasaki disease- a multicenter retrospective study. *Circ J.* (2016) 80:2376–81. doi: 10.1253/circj.CJ-16-0563
57. Yokouchi Y, Oharaseki T, Enomoto Y, Sato W, Imanaka-Yoshida K, Takahashi K. Expression of tenascin C in cardiovascular lesions of Kawasaki disease. *Cardiovasc Pathol.* (2019) 38:25–30. doi: 10.1016/j.carpath.2018.10.005
58. Kim DS, Lee HK, Noh GW, Lee SI, Lee KY. Increased serum interleukin-10 level in Kawasaki disease. *Yonsei Med J.* (1996) 37:125–30. doi: 10.3349/ymj.1996.37.2.125
59. Hirao J, Hibi S, Andoh T, Ichimura T. High levels of circulating interleukin-4 and interleukin-10 in Kawasaki disease. *Int Arch Allergy Immunol.* (1997) 112:152–6. doi: 10.1159/000237447
60. Nakamura J, Watanabe S, Kimura H, Kobayashi M, Karasawa T, Kamata R, et al. Adeno-associated virus vector-mediated interleukin-10 induction prevents vascular inflammation in a murine model of Kawasaki disease. *Sci Rep.* (2018) 8:7601. doi: 10.1038/s41598-018-25856-0
61. Heine G, Drozdenko G, Grun JR, Chang HD, Radbruch A, Worm M. Autocrine IL-10 promotes human B-cell differentiation into IgM- or IgG-secreting plasmablasts. *Eur J Immunol.* (2014) 44:1615–21. doi: 10.1002/eji.201343822
62. Ko TM, Kuo HC, Chang JS, Chen SP, Liu YM, Chen HW, et al. CXCL10/IP-10 is a biomarker and mediator for Kawasaki disease. *Circ Res.* (2015) 116:876–83. doi: 10.1161/CIRCRESAHA.116.305834
63. Kasaian MT, Whitters MJ, Carter LL, Lowe LD, Jussif JM, Deng B, et al. IL-21 limits NK cell responses and promotes antigen-specific T cell activation: a mediator of the transition from innate to adaptive immunity. *Immunity.* (2002) 16:559–69. doi: 10.1016/S1074-7613(02)00295-9
64. Spolski R, Leonard WJ. Interleukin-21: a double-edged sword with therapeutic potential. *Nature reviews Drug discovery.* (2014) 13:379–95. doi: 10.1038/nrd4296
65. Bae YJ, Kim MH, Lee HY, Uh Y, Namgoong MK, Cha BH, et al. Elevated serum levels of IL-21 in Kawasaki disease. *Allergy Asthma Immunol Res.* (2012) 4:351–6. doi: 10.4168/aair.2012.4.6.351
66. Ettinger R, Sims GP, Fairhurst AM, Robbins R, da Silva YS, Spolski R, et al. IL-21 induces differentiation of human naive and memory B cells into antibody-secreting plasma cells. *J Immunol.* (2005) 175:7867–79. doi: 10.4049/jimmunol.175.12.7867
67. Engelberg R, Martin M, Wrotniak BH, Hicar MD. Observational study of Interleukin-21 (IL-21) does not distinguish Kawasaki disease from other causes of fever in children. *Pediatr Rheumatol Online J.* (2017) 15:32. doi: 10.1186/s12969-017-0163-3
68. Abe J, Jibiki T, Noma S, Nakajima T, Saito H, Terai M. Gene expression profiling of the effect of high-dose intravenous Ig in patients with Kawasaki disease. *J Immunol.* (2005) 174:5837–45. doi: 10.4049/jimmunol.174.9.5837
69. Nomura I, Abe J, Noma S, Saito H, Gao B, Wheeler G, et al. Adrenomedullin is highly expressed in blood monocytes associated with acute Kawasaki disease: a microarray gene expression study. *Pediatr Res.* (2005) 57:49–55. doi: 10.1203/01.PDR.0000147745.52711.DD
70. Nishida K, Watanabe K, Echigo S, Mayumi M, Nishikimi T. Increased plasma adrenomedullin levels in Kawasaki disease with coronary artery involvement. *Am J Med.* (2001) 111:165–6. doi: 10.1016/S0002-9343(01)00781-1
71. Ikeda K, Yamaguchi K, Tanaka T, Mizuno Y, Hijikata A, Ohara O, et al. Unique activation status of peripheral blood mononuclear cells at acute phase of Kawasaki disease. *Clin Exp Immunol.* (2010) 160:246–55. doi: 10.1111/j.1365-2249.2009.04073.x
72. Ling XB, Lau K, Kanegaye JT, Pan Z, Peng S, Ji J, et al. A diagnostic algorithm combining clinical and molecular data distinguishes Kawasaki disease from other febrile illnesses. *BMC Med.* (2011) 9:130. doi: 10.1186/1741-7015-9-130
73. Hoang LT, Shimizu C, Ling L, Naim AN, Khor CC, Tremoulet AH, et al. Global gene expression profiling identifies new therapeutic targets in acute Kawasaki disease. *Genome Med.* (2014) 6:541. doi: 10.1186/s13073-014-0102-6
74. Jaggi P, Mejias A, Xu Z, Yin H, Moore-Clingenpeel M, Smith B, et al. Whole blood transcriptional profiles as a prognostic tool in complete and incomplete Kawasaki Disease. *PLoS ONE.* (2018) 13:e0197858. doi: 10.1371/journal.pone.0197858
75. Murata H. Experimental candida-induced arteritis in mice. Relation to arteritis in the mucocutaneous lymph node syndrome. *Microbiol Immunol.* (1979) 23:825–31. doi: 10.1111/j.1348-0421.1979.tb02815.x
76. Hashimoto Y, Fukazawa R, Nagi-Miura N, Ohno N, Suzuki N, Katsube Y, et al. Interleukin-1beta Inhibition Attenuates Vasculitis in a Mouse Model of Kawasaki Disease. *J Nippon Med Sch.* (2019) 86:108–16. doi: 10.1272/jnms.JNMS.2019_86-206
77. Takahashi K, Oharaseki T, Yokouchi Y, Miura NN, Ohno N, Okawara AI, et al. Administration of human immunoglobulin suppresses development of murine systemic vasculitis induced with Candida albicans water-soluble fraction: an animal model of Kawasaki disease. *Mod Rheumatol.* (2010) 20:160–7. doi: 10.3109/s10165-009-0250-5
78. Lehman TJ, Walker SM, Mahnovski V, McCurdy D. Coronary arteritis in mice following the systemic injection of group B Lactobacillus casei cell walls in aqueous suspension. *Arthritis Rheum.* (1985) 28:652–9. doi: 10.1002/art.1780280609
79. Duong TT, Silverman ED, Bissessar MV, Yeung RS. Superantigenic activity is responsible for induction of coronary arteritis in mice: an animal model of Kawasaki disease. *Int Immunol.* (2003) 15:79–89. doi: 10.1093/intimm/dxg007
80. Schulte DJ, Yilmaz A, Shimada K, Fishbein MC, Lowe EL, Chen S, et al. Involvement of innate and adaptive immunity in a murine model of coronary arteritis mimicking Kawasaki disease. *J Immunol.* (2009) 183:5311–8. doi: 10.4049/jimmunol.0901395
81. Chan WC, Duong TT, Yeung RS. Presence of IFN-gamma does not indicate its necessity for induction of coronary arteritis in an animal model of Kawasaki disease. *J Immunol.* (2004) 173:3492–503. doi: 10.4049/jimmunol.173.5.3492
82. Yeung RS. Kawasaki disease: update on pathogenesis. *Curr Opin Rheumatol.* (2010) 22:551–60. doi: 10.1097/BOR.0b013e32833cf051
83. Hui-Yuen JS, Duong TT, Yeung RS. TNF-alpha is necessary for induction of coronary artery inflammation and aneurysm formation in an animal model of Kawasaki disease. *J Immunol.* (2006) 176:6294–301. doi: 10.4049/jimmunol.176.10.6294
84. Chen S, Lee Y, Crother TR, Fishbein M, Zhang W, Yilmaz A, et al. Marked acceleration of atherosclerosis after Lactobacillus casei-induced coronary arteritis in a mouse model of Kawasaki disease. *Arterioscler Thromb Vasc Biol.* (2012) 32:e60–71. doi: 10.1161/ATVBAHA.112.249417
85. Wakita D, Kurashima Y, Crother TR, Noval Rivas M, Lee Y, Chen S, et al. Role of Interleukin-1 signaling in a mouse model of kawasaki disease-associated abdominal aortic aneurysm. *Arterioscler Thromb Vasc Biol.* (2016) 36:886–97. doi: 10.1161/ATVBAHA.115.307072
86. Lau AC, Duong TT, Ito S, Wilson GJ, Yeung RS. Inhibition of matrix metalloproteinase-9 activity improves coronary outcome in an animal model of Kawasaki disease. *Clin Exp Immunol.* (2009) 157:300–9. doi: 10.1111/j.1365-2249.2009.03949.x
87. Bratincsak A, Limm-Chan BN, Nerurkar VR, Ching LL, Reddy VD, Lim E, et al. Study design and rationale to assess Doxycycline Efficacy in preventing coronary Artery Lesions in children with Kawasaki disease (DEAL trial) - A phase II clinical trial. *Contemp Clin Trials.* (2018) 65:33–8. doi: 10.1016/j.cct.2017.11.014
88. Matundan HH, Sin J, Rivas MN, Fishbein MC, Lehman TJ, Chen S, et al. Myocardial fibrosis after adrenergic stimulation as a long-term sequela in a mouse model of Kawasaki disease vasculitis. *JCI Insight.* (2019) 4:e126279. doi: 10.1172/jci.insight.126279

89. Kim M, Kim K. Elevation of cardiac troponin I in the acute stage of Kawasaki disease. *Pediatr Cardiol.* (1999) 20:184–8. doi: 10.1007/s002469900437
90. Orenstein JM, Shulman ST, Fox LM, Baker SC, Takahashi M, Bhatti TR, et al. Three linked vasculopathic processes characterize Kawasaki disease: a light and transmission electron microscopic study. *PLoS ONE.* (2012) 7:e38998. doi: 10.1371/journal.pone.0038998
91. Takahashi K, Oharaseki T, Yokouchi Y. Pathogenesis of Kawasaki disease. *Clin Exp Immunol.* (2011) 164(Suppl. 1):20–2. doi: 10.1111/j.1365-2249.2011.04361.x
92. Dou J, Li H, Sun L, Yan W, Lv H, Ding Y. Histopathological and ultrastructural examinations of rabbit coronary artery vasculitis caused by bovine serum albumin: an animal model of Kawasaki disease. *Ultrastruct Pathol.* (2013) 37:139–45. doi: 10.3109/01913123.2012.750409
93. Orenstein JM, Rowley AH. An evaluation of the validity of the animal models of Kawasaki disease vasculopathy. *Ultrastruct Pathol.* (2014) 38:245–7. doi: 10.3109/01913123.2014.932314
94. De Inocencio J, Hirsch R. Evidence for superantigen mediated process in Kawasaki disease. *Arch Dis Child.* (1995) 73:275–6. doi: 10.1136/adc.73.3.275-b
95. Curtis N. Kawasaki disease and toxic shock syndrome–at last the etiology is clear? *Adv Exp Med Biol.* (2004) 549:191–200. doi: 10.1007/978-1-4419-8993-2_26
96. Leung DY, Meissner HC, Fulton DR, Murray DL, Kotzin BL, Schlievert PM. Toxic shock syndrome toxin-secreting *Staphylococcus aureus* in Kawasaki syndrome. *Lancet.* (1993) 342:1385–8. doi: 10.1016/0140-6736(93)92752-F
97. Leung DY, Sullivan KE, Brown-Whitehorn TF, Fehringer AP, Allen S, Finkel TH, et al. Association of toxic shock syndrome toxin-secreting and exfoliative toxin-secreting *Staphylococcus aureus* with Kawasaki syndrome complicated by coronary artery disease. *Pediatr Res.* (1997) 42:268–72. doi: 10.1203/00006450-199709000-00004
98. Matsubara K, Fukaya T. The role of superantigens of group A Streptococcus and *Staphylococcus aureus* in Kawasaki disease. *Curr Opin Infect Dis.* (2007) 20:298–303. doi: 10.1097/QCO.0b013e3280964d8c
99. Uchiyama T, Kato H. The pathogenesis of Kawasaki disease and superantigens. *Jpn J Infect Dis.* (1999) 52:141–5.
100. Abe J, Kotzin BL, Jujo K, Melish ME, Glode MP, Kohsaka T, et al. Selective expansion of T cells expressing T-cell receptor variable regions V beta 2 and V beta 8 in Kawasaki disease. *Proc Natl Acad Sci USA.* (1992) 89:4066–70. doi: 10.1073/pnas.89.9.4066
101. Abe J, Kotzin BL, Meissner C, Melish ME, Takahashi M, Fulton D, et al. Characterization of T cell repertoire changes in acute Kawasaki disease. *J Exp Med.* (1993) 177:791–6. doi: 10.1084/jem.177.3.791
102. Yoshioka T, Matsutani T, Iwagami S, Toyosaki-Maeda T, Yutsudo T, Tsuruta Y, et al. Polyclonal expansion of TCRBV2- and TCRBV6-bearing T cells in patients with Kawasaki disease. *Immunology.* (1999) 96:465–72. doi: 10.1046/j.1365-2567.1999.00695.x
103. Choi IH, Chwae YJ, Shim WS, Kim DS, Kwon DH, Kim JD, et al. Clonal expansion of CD8+ T cells in Kawasaki disease. *J Immunol.* (1997) 159:481–6.
104. Rowley AH, Baker SC, Shulman ST, Fox LM, Takahashi K, Garcia FL, et al. Cytoplasmic inclusion bodies are detected by synthetic antibody in ciliated bronchial epithelium during acute Kawasaki disease. *J Infect Dis.* (2005) 192:1757–66. doi: 10.1086/497171
105. Pietra BA, De Inocencio J, Giannini EH, Hirsch R. TCR V beta family repertoire and T cell activation markers in Kawasaki disease. *J Immunol.* (1994) 153:1881–8.
106. Sakaguchi M, Kato H, Nishiyori A, Sagawa K, Itoh K. Characterization of CD4+ T helper cells in patients with Kawasaki disease (KD): preferential production of tumour necrosis factor-alpha (TNF-alpha) by V beta 2- or V beta 8- CD4+ T helper cells. *Clin Exp Immunol.* (1995) 99:276–82. doi: 10.1111/j.1365-2249.1995.tb05545.x
107. Lv YW, Wang J, Sun L, Zhang JM, Cao L, Ding YY, et al. Understanding the pathogenesis of Kawasaki disease by network and pathway analysis. *Comput Math Methods Med.* (2013) 2013:989307. doi: 10.1155/2013/989307
108. Ozen S, Batu ED. Vasculitis pathogenesis: can we talk about precision medicine? *Front Immunol.* (2018) 9:1892. doi: 10.3389/fimmu.2018.01892
109. Xie X, Shi X, Liu M. The Roles of Genetic factors in Kawasaki disease: a systematic review and meta-analysis of genetic association studies. *Pediatr Cardiol.* (2018) 39:207–25. doi: 10.1007/s00246-017-1760-0
110. Onouchi Y. The genetics of Kawasaki disease. *Int J Rheum Dis.* (2018) 21:26–30. doi: 10.1111/1756-185X.13218
111. Onouchi Y, Gunji T, Burns JC, Shimizu C, Newburger JW, Yashiro M, et al. ITPKC functional polymorphism associated with Kawasaki disease susceptibility and formation of coronary artery aneurysms. *Nat Genet.* (2008) 40:35–42. doi: 10.1038/ng.2007.59
112. Chi H, Huang FY, Chen MR, Chiu NC, Lee HC, Lin SP, et al. ITPKC gene SNP rs28493229 and Kawasaki disease in Taiwanese children. *Hum Mol Genet.* (2010) 19:1147–51. doi: 10.1093/hmg/ddp586
113. Lin MT, Wang JK, Yeh JI, Sun LC, Chen PL, Wu JF, et al. Clinical Implication of the C Allele of the ITPKC Gene SNP rs28493229 in Kawasaki disease: association with disease susceptibility and BCG scar reactivation. *Pediatr Infect Dis J.* (2011) 30:148–52. doi: 10.1097/INF.0b013e3181f43a4e
114. Peng Q, Chen C, Zhang Y, He H, Wu Q, Liao J, et al. Single-nucleotide polymorphism rs2290692 in the 3'UTR of ITPKC associated with susceptibility to Kawasaki disease in a Han Chinese population. *Pediatr Cardiol.* (2012) 33:1046–53. doi: 10.1007/s00246-012-0223-x
115. Lou J, Xu S, Zou L, Zhong R, Zhang T, Sun Y, et al. A functional polymorphism, rs28493229, in ITPKC and risk of Kawasaki disease: an integrated meta-analysis. *Mol Biol Rep.* (2012) 39:11137–44. doi: 10.1007/s11033-012-2022-0
116. Khor CC, Davila S, Breunis WB, Lee YC, Shimizu C, Wright VJ, et al. Genome-wide association study identifies FCGR2A as a susceptibility locus for Kawasaki disease. *Nat Genet.* (2011) 43:1241–6. doi: 10.1038/ng.981
117. Kuo HC, Yu HR, Juo SH, Yang KD, Wang YS, Liang CD, et al. CASP3 gene single-nucleotide polymorphism (rs72689236) and Kawasaki disease in Taiwanese children. *J Hum Genet.* (2011) 56:161–5. doi: 10.1038/jhg.2010.154
118. Onouchi Y, Ozaki K, Buns JC, Shimizu C, Hamada H, Honda T, et al. Common variants in CASP3 confer susceptibility to Kawasaki disease. *Hum Mol Genet.* (2010) 19:2898–906. doi: 10.1093/hmg/ddq176
119. Kuo HC, Hsu YW, Wu CM, Chen SH, Hung KS, Chang WP, et al. A replication study for association of ITPKC and CASP3 two-locus analysis in IVIG unresponsiveness and coronary artery lesion in Kawasaki disease. *PLoS ONE.* (2013) 8:e69685. doi: 10.1371/journal.pone.0069685
120. Onouchi Y, Suzuki Y, Suzuki H, Terai M, Yasukawa K, Hamada H, et al. ITPKC and CASP3 polymorphisms and risks for IVIG unresponsiveness and coronary artery lesion formation in Kawasaki disease. *Pharmacogenomics J.* (2013) 13:52–9. doi: 10.1038/tpj.2011.45
121. Alphonse MP, Duong TT, Shumitzu C, Hoang TL, McCrindle BW, Franco A, et al. Inositol-Triphosphate 3-Kinase C mediates inflammasome activation and treatment response in Kawasaki disease. *J Immunol.* (2016) 197:3481–9. doi: 10.4049/jimmunol.1600388
122. Burgner D, Davila S, Breunis WB, Ng SB, Li Y, Bonnard C, et al. A genome-wide association study identifies novel and functionally related susceptibility Loci for Kawasaki disease. *PLoS Genet.* (2009) 5:e1000319. doi: 10.1371/journal.pgen.1000319
123. Onouchi Y, Ozaki K, Burns JC, Shimizu C, Terai M, Hamada H, et al. A genome-wide association study identifies three new risk loci for Kawasaki disease. *Nat Genet.* (2012) 44:517–21. doi: 10.1038/ng.2220
124. Kwon YC, Kim JJ, Yun SW, Yu JJ, Yoon KL, Lee KY, et al. Male-specific association of the FCGR2A His167Arg polymorphism with Kawasaki disease. *PLoS ONE.* (2017) 12:e0184248. doi: 10.1371/journal.pone.0184248
125. Onouchi Y, Onoue S, Tamari M, Wakui K, Fukushima Y, Yashiro M, et al. CD40 ligand gene and Kawasaki disease. *Eur J Hum Genet.* (2004) 12:1062–8. doi: 10.1038/sj.ejhg.5201266
126. Orozco G, Eyre S, Hinks A, Bowes J, Morgan AW, Wilson AG, et al. Study of the common genetic background for rheumatoid arthritis and systemic lupus erythematosus. *Ann Rheum Dis.* (2011) 70:463–8. doi: 10.1136/ard.2010.137174
127. Laird RM, Laky K, Hayes SM. Unexpected role for the B cell-specific Src family kinase B lymphoid kinase in the development of IL-17-producing gammadelta T cells. *J Immunol.* (2010) 185:6518–27. doi: 10.4049/jimmunol.1002766

128. Samuelson EM, Laird RM, Maue AC, Rochford R, Hayes SM. Blk haploinsufficiency impairs the development, but enhances the functional responses, of MZ B cells. *Immunol Cell Biol.* (2012) 90:620–9. doi: 10.1038/icb.2011.76
129. Sim BK, Park H, Kim JJ, Yun SW, Yu JJ, Yoon KL, et al. Assessment of the clinical heterogeneity of Kawasaki disease using genetic variants of BLK and FCGR2A. *Korean Circ J.* (2019) 49:99–108. doi: 10.4070/kcj.2018.0224
130. Lou J, Zhong R, Shen N, Lu XZ, Ke JT, Duan JY, et al. Systematic confirmation study of GWAS-identified genetic variants for Kawasaki disease in a Chinese population. *Sci Rep.* (2015) 5:8194. doi: 10.1038/srep08194
131. Kuo HC, Li SC, Guo MM, Huang YH, Yu HR, Huang FC, et al. Genome-Wide association study identifies novel susceptibility genes associated with coronary artery aneurysm formation in Kawasaki disease. *PLoS ONE.* (2016) 11:e0154943. doi: 10.1371/journal.pone.0154943
132. Tremoulet AH, Jain S, Jaggi P, Jimenez-Fernandez S, Pancheri JM, Sun X, et al. Infliximab for intensification of primary therapy for Kawasaki disease: a phase 3 randomised, double-blind, placebo-controlled trial. *Lancet.* (2014) 383:1731–8. doi: 10.1016/S0140-6736(13)62298-9
133. Mori M, Hara T, Kikuchi M, Shimizu H, Miyamoto T, Iwashima S, et al. Infliximab versus intravenous immunoglobulin for refractory Kawasaki disease: a phase 3, randomized, open-label, active-controlled, parallel-group, multicenter trial. *Sci Rep.* (2018) 8:1994. doi: 10.1038/s41598-017-18387-7
134. Hamada H, Suzuki H, Onouchi Y, Ebata R, Terai M, Fuse S, et al. Efficacy of primary treatment with immunoglobulin plus ciclosporin for prevention of coronary artery abnormalities in patients with Kawasaki disease predicted to be at increased risk of non-response to intravenous immunoglobulin (KAICA): a randomised controlled, open-label, blinded-endpoints, phase 3 trial. *Lancet.* (2019) 393:1128–37. doi: 10.1016/S0140-6736(18)32003-8
135. Aoyagi R, Hamada H, Sato Y, Suzuki H, Onouchi Y, Ebata R, et al. Study protocol for a phase III multicentre, randomised, open-label, blinded-end point trial to evaluate the efficacy and safety of immunoglobulin plus cyclosporin A in patients with severe Kawasaki disease (KAICA Trial). *BMJ Open.* (2015) 5:e009562. doi: 10.1136/bmjopen-2015-009562
136. Newburger JW, Takahashi M, Beiser AS, Burns JC, Bastian J, Chung KJ, et al. A single intravenous infusion of gamma globulin as compared with four infusions in the treatment of acute Kawasaki syndrome. *N Engl J Med.* (1991) 324:1633–9. doi: 10.1056/NEJM199106063242305
137. Newburger JW, Sleeper LA, McCrindle BW, Minich LL, Gersony W, Vetter VL, et al. Randomized trial of pulsed corticosteroid therapy for primary treatment of Kawasaki disease. *N Engl J Med.* (2007) 356:663–75. doi: 10.1056/NEJMoa061235
138. Kobayashi T, Kobayashi T, Morikawa A, Ikeda K, Seki M, Shimoyama S, et al. Efficacy of intravenous immunoglobulin combined with prednisolone following resistance to initial intravenous immunoglobulin treatment of acute Kawasaki disease. *J Pediatr.* (2013) 163:521–6. doi: 10.1016/j.jpeds.2013.01.022
139. Kuo HC, Guo MM, Lo MH, Hsieh KS, Huang YH. Effectiveness of intravenous immunoglobulin alone and intravenous immunoglobulin combined with high-dose aspirin in the acute stage of Kawasaki disease: study protocol for a randomized controlled trial. *BMC Pediatr.* (2018) 18:200. doi: 10.1186/s12887-018-1180-1
140. Sauvaget E, Bonello B, David M, Chabrol B, Dubus JC, Bosdure E. Resistant Kawasaki disease treated with anti-CD20. *J Pediatr.* (2012) 160:875–6. doi: 10.1016/j.jpeds.2012.01.018
141. Koizumi K, Hoshiai M, Moriguchi T, Katsumata N, Toda T, Kise H, et al. Plasma exchange downregulates activated monocytes and restores regulatory T cells in Kawasaki disease. *Ther Apher Dial.* (2019) 23:92–8. doi: 10.1111/1744-9987.12754
142. Lo MS, Newburger JW. Role of intravenous immunoglobulin in the treatment of Kawasaki disease. *Int J Rheum Dis.* (2018) 21:64–9. doi: 10.1111/1756-185X.13220
143. Galeotti C, Kaveri SV, Bayry J. IVIG-mediated effector functions in autoimmune and inflammatory diseases. *Int Immunol.* (2017) 29:491–8. doi: 10.1093/intimm/dxx039
144. Burns JC, Franco A. The immunomodulatory effects of intravenous immunoglobulin therapy in Kawasaki disease. *Expert Rev Clin Immunol.* (2015) 11:819–25. doi: 10.1586/1744666X.2015.1044980
145. Burns JC, Kone-Paut I, Kuijpers T, Shimizu C, Tremoulet A, Arditi M. Review: found in translation: international initiatives pursuing interleukin-1 blockade for treatment of acute Kawasaki disease. *Arthritis Rheumatol.* (2017) 69:268–76. doi: 10.1002/art.39975
146. Katz U, Shoenfeld Y, Zandman-Goddard G. Update on intravenous immunoglobulins (IVIg) mechanisms of action and off- label use in autoimmune diseases. *Curr Pharm Des.* (2011) 17:3166–75. doi: 10.2174/138161211798157540
147. Chaigne B, Mouthon L. Mechanisms of action of intravenous immunoglobulin. *Transfus Apher Sci.* (2017) 56:45–9. doi: 10.1016/j.transci.2016.12.017
148. Samuelsson A, Towers TL, Ravetch JV. Anti-inflammatory activity of IVIG mediated through the inhibitory Fc receptor. *Science.* (2001) 291:484–6. doi: 10.1126/science.291.5503.484
149. Ballow M. Mechanisms of immune regulation by IVIG. *Curr Opin Allergy Clin Immunol.* (2014) 14:509–15. doi: 10.1097/ACI.0000000000000116
150. Guo MM, Tseng WN, Ko CH, Pan HM, Hsieh KS, Kuo HC. Th17- and Treg-related cytokine and mRNA expression are associated with acute and resolving Kawasaki disease. *Allergy.* (2015) 70:310–8. doi: 10.1111/all.12558
151. Rasouli M, Heidari B, Kalani M. Downregulation of Th17 cells and the related cytokines with treatment in Kawasaki disease. *Immunol Lett.* (2014) 162(1 Pt A):269–75. doi: 10.1016/j.imlet.2014.09.017
152. Olivito B, Taddio A, Simonini G, Massai C, Ciullini S, Gambineri E, et al. Defective FOXP3 expression in patients with acute Kawasaki disease and restoration by intravenous immunoglobulin therapy. *Clin Exp Rheumatol.* (2010) 28(1 Suppl. 57):93–7.
153. Lee HK, Kim DS, Noh GW, Lee KY. Effects of intravenous immune globulin on the peripheral lymphocyte phenotypes in Kawasaki disease. *Yonsei Med J.* (1996) 37:357–63. doi: 10.3349/ymj.1996.37.5.357
154. Ehara H, Kiyohara K, Izumisawa Y, Ito T. Early activation does not translate into effector differentiation of peripheral CD8T cells during the acute phase of Kawasaki disease. *Cell Immunol.* (2010) 265:57–64. doi: 10.1016/j.cellimm.2010.07.003
155. Doi M, Takeda T, Sakurai Y, Kato J, Hayashi T, Fukuda K, et al. Altered immunoglobulin A and M levels associated with changes in BAFF and APRIL after administration of intravenous immunoglobulin to treat Kawasaki disease. *J Investig Allergol Clin Immunol.* (2010) 20:413–8.
156. Seite JF, Goutsmedt C, Youinou P, Pers JO, Hillion S. Intravenous immunoglobulin induces a functional silencing program similar to anergy in human B cells. *J Allergy Clin Immunol.* (2014) 133:181–8.e1–9. doi: 10.1016/j.jaci.2013.08.042
157. Kobayashi T, Saji T, Otani T, Takeuchi K, Nakamura T, Arakawa H, et al. Efficacy of immunoglobulin plus prednisolone for prevention of coronary artery abnormalities in severe Kawasaki disease (RAISE study): a randomised, open-label, blinded-endpoints trial. *Lancet.* (2012) 379:1613–20. doi: 10.1016/S0140-6736(11)61930-2
158. Chen KY, Curtis N, Dahdah N, Kowalski R, Cheung M, Burgner DP. Kawasaki disease and cardiovascular risk: a comprehensive review of subclinical vascular changes in the longer term. *Acta Paediatr.* (2016) 105:752–61. doi: 10.1111/apa.13367
159. Kato H, Koike S, Yokoyama T. Kawasaki disease: effect of treatment on coronary artery involvement. *Pediatrics.* (1979) 63:175–9.
160. Research Committee of the Japanese Society of Pediatric C, Cardiac Surgery Committee for Development of Guidelines for Medical Treatment of Acute Kawasaki Disease. Guidelines for medical treatment of acute Kawasaki disease: report of the Research Committee of the Japanese Society of Pediatric Cardiology and Cardiac Surgery (2012 revised version). *Pediatr Int.* (2014) 56:135–58. doi: 10.1111/ped.12317
161. Tacke CE, Burgner D, Kuipers IM, Kuijpers TW. Management of acute and refractory Kawasaki disease. *Expert Rev Anti Infect Ther.* (2012) 10:1203–15. doi: 10.1586/eri.12.101
162. Mpofu S, Fatima F, Moots RJ. Anti-TNF-alpha therapies: they are all the same (aren't they?). *Rheumatology.* (2005) 44:271–3. doi: 10.1093/rheumatology/keh483
163. Tay C, Liu YH, Hosseini H, Kanellakis P, Cao A, Peter K, et al. B-cell-specific depletion of tumour necrosis factor alpha inhibits atherosclerosis

development and plaque vulnerability to rupture by reducing cell death and inflammation. *Cardiovasc Res.* (2016) 111:385–97. doi: 10.1093/cvr/cvw186
164. Lindquist ME, Hicar MD. B Cells and antibodies in Kawasaki disease. *Int J Mol Sci.* (2019) 20:1834. doi: 10.3390/ijms20081834
165. Chan H, Chi H, You H, Wang M, Zhang G, Yang H, et al. Indirect-comparison meta-analysis of treatment options for patients with refractory Kawasaki disease. *BMC Pediatr.* (2019) 19:158. doi: 10.1186/s12887-019-1504-9
166. Lipsky PE, Thompson PA, Rosenwasser LJ, Dinarello CA. The role of interleukin 1 in human B cell activation: inhibition of B cell proliferation and the generation of immunoglobulin-secreting cells by an antibody against human leukocytic pyrogen. *J Immunol.* (1983) 130:2708–14.
167. Lee Y, Schulte DJ, Shimada K, Chen S, Crother TR, Chiba N, et al. Interleukin-1beta is crucial for the induction of coronary artery inflammation in a mouse model of Kawasaki disease. *Circulation.* (2012) 125:1542–50. doi: 10.1161/CIRCULATIONAHA.111.072769
168. Tremoulet AH, Pancoast P, Franco A, Bujold M, Shimizu C, Onouchi Y, et al. Calcineurin inhibitor treatment of intravenous immunoglobulin-resistant Kawasaki disease. *J Pediatr.* (2012) 161:506–12.e1. doi: 10.1016/j.jpeds.2012.02.048
169. Heidt S, Roelen DL, Eijsink C, Eikmans M, van Kooten C, Claas FH, et al. Calcineurin inhibitors affect B cell antibody responses indirectly by interfering with T cell help. *Clin Exp Immunol.* (2010) 159:199–207. doi: 10.1111/j.1365-2249.2009.04051.x
170. Sakurai Y. Autoimmune aspects of Kawasaki disease. *J Investig Allergol Clin Immunol.* (2019) 29:251–61. doi: 10.18176/jiaci.0300
171. Cunningham MW, Meissner HC, Heuser JS, Pietra BA, Kurahara DK, Leung DY. Anti-human cardiac myosin autoantibodies in Kawasaki syndrome. *J Immunol.* (1999) 163:1060–5.
172. Gupta M, Johann-Liang R, Bussel JB, Gersony WM, Lehman TJ. Elevated IgA and IgM anticardiolipin antibodies in acute Kawasaki disease. *Cardiology.* (2002) 97:180–2. doi: 10.1159/000063118
173. Chun JK, Lee TJ, Choi KM, Lee KH, Kim DS. Elevated anti-alpha-enolase antibody levels in Kawasaki disease. *Scand J Rheumatol.* (2008) 37:48–52. doi: 10.1080/03009740701607075
174. Cines DB, Lyss AP, Reeber M, Bina M, DeHoratius RJ. Presence of complement-fixing anti-endothelial cell antibodies in systemic lupus erythematosus. *J Clin Invest.* (1984) 73:611–25. doi: 10.1172/JCI111251
175. Savage CO, Williams JM. Anti endothelial cell antibodies in vasculitis. *J Am Soc Nephrol.* (2007) 18:2424–6. doi: 10.1681/ASN.2007070767
176. Barron KS. Kawasaki disease in children. *Curr Opin Rheumatol.* (1998) 10:29–37. doi: 10.1097/00002281-199801000-00005
177. Nash MC, Shah V, Reader JA, Dillon MJ. Anti-neutrophil cytoplasmic antibodies and anti-endothelial cell antibodies are not increased in Kawasaki disease. *Br J Rheumatol.* (1995) 34:882–7. doi: 10.1093/rheumatology/34.9.882
178. Leung DY, Collins T, Lapierre LA, Geha RS, Pober JS. Immunoglobulin M antibodies present in the acute phase of Kawasaki syndrome lyse cultured vascular endothelial cells stimulated by gamma interferon. *J Clin Invest.* (1986) 77:1428–35. doi: 10.1172/JCI112454
179. Leung DY, Geha RS, Newburger JW, Burns JC, Fiers W, Lapierre LA, et al. Two monokines, interleukin 1 and tumor necrosis factor, render cultured vascular endothelial cells susceptible to lysis by antibodies circulating during Kawasaki syndrome. *J Exp Med.* (1986) 164:1958–72. doi: 10.1084/jem.164.6.1958
180. Rowley AH, Eckerley CA, Jack HM, Shulman ST, Baker SC. IgA plasma cells in vascular tissue of patients with Kawasaki syndrome. *J Immunol.* (1997) 159:5946–55.
181. Rowley AH, Baker SC, Shulman ST, Garcia FL, Guzman-Cottrill JA, Chou P, et al. Detection of antigen in bronchial epithelium and macrophages in acute Kawasaki disease by use of synthetic antibody. *J Infect Dis.* (2004) 190:856–65. doi: 10.1086/422648
182. Fujieda M, Oishi N, Kurashige T. Antibodies to endothelial cells in Kawasaki disease lyse endothelial cells without cytokine pretreatment. *Clin Exp Immunol.* (1997) 107:120–6. doi: 10.1046/j.1365-2249.1997.d01-894.x
183. Kaneko K, Savage CO, Pottinger BE, Shah V, Pearson JD, Dillon MJ. Antiendothelial cell antibodies can be cytotoxic to endothelial cells without cytokine pre-stimulation and correlate with ELISA antibody measurement in Kawasaki disease. *Clin Exp Immunol.* (1994) 98:264–9. doi: 10.1111/j.1365-2249.1994.tb06136.x
184. Grunebaum E, Blank M, Cohen S, Afek A, Kopolovic J, Meroni PL, et al. The role of anti-endothelial cell antibodies in Kawasaki disease - *in vitro* and *in vivo* studies. *Clin Exp Immunol.* (2002) 130:233–40. doi: 10.1046/j.1365-2249.2002.02000.x
185. Landing BH, Larson EJ. Are infantile periarteritis nodosa with coronary artery involvement and fatal mucocutaneous lymph node syndrome the same? Comparison of 20 patients from North America with patients from Hawaii and Japan. *Pediatrics.* (1977) 59:651–62.
186. Takahashi K, Oharaseki T, Naoe S, Wakayama M, Yokouchi Y. Neutrophilic involvement in the damage to coronary arteries in acute stage of Kawasaki disease. *Pediatr Int.* (2005) 47:305–10. doi: 10.1111/j.1442-200x.2005.02049.x
187. Brown TJ, Crawford SE, Cornwall ML, Garcia F, Shulman ST, Rowley AH. CD8 T lymphocytes and macrophages infiltrate coronary artery aneurysms in acute Kawasaki disease. *J Infect Dis.* (2001) 184:940–3. doi: 10.1086/323155
188. Fujiwara T, Fujiwara H, Nakano H. Pathological features of coronary arteries in children with Kawasaki disease in which coronary arterial aneurysm was absent at autopsy. Quantitative analysis. *Circulation.* (1988) 78:345–50. doi: 10.1161/01.CIR.78.2.345
189. Kuijpers TW, Biezeveld M, Achterhuis A, Kuipers I, Lam J, Hack CE, et al. Longstanding obliterative panarteritis in Kawasaki disease: lack of cyclosporin A effect. *Pediatrics.* (2003) 112:986–92. doi: 10.1542/peds.112.4.986
190. Giordani L, Quaranta MG, Marchesi A, Straface E, Pietraforte D, Villani A, et al. Increased frequency of immunoglobulin (Ig)A-secreting cells following Toll-like receptor (TLR)-9 engagement in patients with Kawasaki disease. *Clin Exp Immunol.* (2011) 163:346–53. doi: 10.1111/j.1365-2249.2010.04297.x
191. Mason WH, Jordan SC, Sakai R, Takahashi M, Bernstein B. Circulating immune complexes in Kawasaki syndrome. *Pediatr Infect Dis.* (1985) 4:48–51. doi: 10.1097/00006454-198501000-00012
192. Rowley AH, Shulman ST, Spike BT, Mask CA, Baker SC. Oligoclonal IgA response in the vascular wall in acute Kawasaki disease. *J Immunol.* (2001) 166:1334–43. doi: 10.4049/jimmunol.166.2.1334
193. Rowley AH, Baker SC, Shulman ST, Garcia FL, Fox LM, Kos IM, et al. RNA-containing cytoplasmic inclusion bodies in ciliated bronchial epithelium months to years after acute Kawasaki disease. *PLoS ONE.* (2008) 3:e1582. doi: 10.1371/journal.pone.0001582
194. Martinez-Hernandez E, Horvath J, Shiloh-Malawsky Y, Sangha N, Martinez-Lage M, Dalmau J. Analysis of complement and plasma cells in the brain of patients with anti-NMDAR encephalitis. *Neurology.* (2011) 77:589–93. doi: 10.1212/WNL.0b013e318228c136
195. Takuma K, Kamisawa T, Igarashi Y. Autoimmune pancreatitis and IgG4-related sclerosing cholangitis. *Curr Opin Rheumatol.* (2011) 23:80–7. doi: 10.1097/BOR.0b013e3283412f60
196. Krumbholz M, Derfuss T, Hohlfeld R, Meinl E. B cells and antibodies in multiple sclerosis pathogenesis and therapy. *Nat Rev Neurol.* (2012) 8:613–23. doi: 10.1038/nrneurol.2012.203
197. Wouters MCA, Nelson BH. Prognostic significance of tumor-infiltrating B cells and plasma cells in human cancer. *Clin Cancer Res.* (2018) 24:6125–35. doi: 10.1158/1078-0432.CCR-18-1481
198. Wrammert J, Smith K, Miller J, Langley WA, Kokko K, Larsen C, et al. Rapid cloning of high-affinity human monoclonal antibodies against influenza virus. *Nature.* (2008) 453:667–71. doi: 10.1038/nature06890
199. van Zelm MC, van der Burg M, van Dongen JJ. Homeostatic and maturation-associated proliferation in the peripheral B-cell compartment. *Cell Cycle.* (2007) 6:2890–5. doi: 10.4161/cc.6.23.4952
200. Nutt SL, Hodgkin PD, Tarlinton DM, Corcoran LM. The generation of antibody-secreting plasma cells. *Nat Rev Immunol.* (2015) 15:160–71. doi: 10.1038/nri3795
201. Fink K. Origin and function of circulating plasmablasts during acute viral infections. *Front Immunol.* (2012) 3:78. doi: 10.3389/fimmu.2012.00078
202. Odendahl M, Mei H, Hoyer BF, Jacobi AM, Hansen A, Muehlinghaus G, et al. Generation of migratory antigen-specific plasma blasts and mobilization of resident plasma cells in a secondary immune response. *Blood.* (2005) 105:1614–21. doi: 10.1182/blood-2004-07-2507

203. Blanchard-Rohner G, Pulickal AS, Jol-van der Zijde CM, Snape MD, Pollard AJ. Appearance of peripheral blood plasma cells and memory B cells in a primary and secondary immune response in humans. *Blood.* (2009) 114:4998–5002. doi: 10.1182/blood-2009-03-211052
204. Balakrishnan T, Bela-Ong DB, Toh YX, Flamand M, Devi S, Koh MB, et al. Dengue virus activates polyreactive, natural IgG B cells after primary and secondary infection. *PLoS ONE.* (2011) 6:e29430. doi: 10.1371/journal.pone.0029430
205. Lee FE, Falsey AR, Halliley JL, Sanz I, Walsh EE. Circulating antibody-secreting cells during acute respiratory syncytial virus infection in adults. *J Infect Dis.* (2010) 202:1659–66. doi: 10.1086/657158
206. Di Niro R, Lee SJ, Vander Heiden JA, Elsner RA, Trivedi N, Bannock JM, et al. Salmonella infection drives promiscuous B cell activation followed by extrafollicular affinity maturation. *Immunity.* (2015) 43:120–31. doi: 10.1016/j.immuni.2015.06.013
207. Kauffman RC, Bhuiyan TR, Nakajima R, Mayo-Smith LM, Rashu R, Hoq MR, et al. Single-cell analysis of the plasmablast response to vibrio cholerae demonstrates expansion of cross-reactive memory B cells. *MBio.* (2016) 7:e02021–16. doi: 10.1128/mBio.02021-16
208. Liao HX, Chen X, Munshaw S, Zhang R, Marshall DJ, Vandergrift N, et al. Initial antibodies binding to HIV-1 gp41 in acutely infected subjects are polyreactive and highly mutated. *J Exp Med.* (2011) 208:2237–49. doi: 10.1084/jem.20110363
209. Liao H, Yu Y, Li S, Yue Y, Tao C, Su K, et al. Circulating plasmablasts from chronically human immunodeficiency virus-infected individuals predominantly produce polyreactive/autoreactive antibodies. *Front Immunol.* (2017) 8:1691. doi: 10.3389/fimmu.2017.01691
210. Garcia M, Iglesias A, Landoni VI, Bellomo C, Bruno A, Cordoba MT, et al. Massive plasmablast response elicited in the acute phase of hantavirus pulmonary syndrome. *Immunology.* (2017) 151:122–35. doi: 10.1111/imm.12713
211. Wrammert J, Onlamoon N, Akondy RS, Perng GC, Polsrila K, Chandele A, et al. Rapid and massive virus-specific plasmablast responses during acute dengue virus infection in humans. *J Virol.* (2012) 86:2911–8. doi: 10.1128/JVI.06075-11
212. Tarlton NJ, Green CM, Lazarus NH, Rott L, Wong AP, Abramson ON, et al. Plasmablast frequency and trafficking receptor expression are altered in pediatric ulcerative colitis. *Inflamm Bowel Dis.* (2012) 18:2381–91. doi: 10.1002/ibd.22962
213. Rivas JR, Ireland SJ, Chkheidze R, Rounds WH, Lim J, Johnson J, et al. Peripheral VH4+ plasmablasts demonstrate autoreactive B cell expansion toward brain antigens in early multiple sclerosis patients. *Acta Neuropathol.* (2017) 133:43–60. doi: 10.1007/s00401-016-1627-0
214. Hosomi S, Oshitani N, Kamata N, Sogawa M, Okazaki H, Tanigawa T, et al. Increased numbers of immature plasma cells in peripheral blood specifically overexpress chemokine receptor CXCR3 and CXCR4 in patients with ulcerative colitis. *Clin Exp Immunol.* (2011) 163:215–24. doi: 10.1111/j.1365-2249.2010.04290.x
215. Mattoo H, Mahajan VS, Della-Torre E, Sekigami Y, Carruthers M, Wallace ZS, et al. *De novo* oligoclonal expansions of circulating plasmablasts in active and relapsing IgG4-related disease. *J Allergy Clin Immunol.* (2014) 134:679–87. doi: 10.1016/j.jaci.2014.03.034
216. Wallace ZS, Mattoo H, Carruthers M, Mahajan VS, Della Torre E, Lee H, et al. Plasmablasts as a biomarker for IgG4-related disease, independent of serum IgG4 concentrations. *Ann Rheum Dis.* (2015) 74:190–5. doi: 10.1136/annrheumdis-2014-205233
217. Xu M, Jiang Y, Wang J, Liu J, Liu C, Liu D, et al. Distinct variations of antibody secreting cells and memory B cells during the course of Kawasaki disease. *BMC Immunol.* (2019) 20:16. doi: 10.1186/s12865-019-0299-7
218. Shlomchik MJ, Marshak-Rothstein A, Wolfowicz CB, Rothstein TL, Weigert MG. The role of clonal selection and somatic mutation in autoimmunity. *Nature.* (1987) 328:805–11. doi: 10.1038/328805a0

Conflict of Interest: The author declares that the research was conducted in the absence of any commercial or financial relationships that could be construed as a potential conflict of interest.

frontiers in Pediatrics

CASE REPORT
published: 19 June 2020
doi: 10.3389/fped.2020.00316

Ventricular Septal Rupture After Blunt Chest Trauma in an Infant: A Case Report and Mini-Review

Xu Zhu[1,2], *Xiaojuan Ji*[2,3*], *Chun Wu*[2,4], *Harvey Ho*[5], *Kunfeng Jiang*[1,2], *Yanqin Wang*[1,2] *and Ke Bai*[2,6]

[1] *Department of Cardiology, Children's Hospital of Chongqing Medical University, Chongqing, China,* [2] *Ministry of Education Key Laboratory of Child Development and Disorders, Chongqing Key Laboratory of Child Infection and Immunity, National Clinical Research Center for Child Health and Disorders, China International Science and Technology Cooperation Base of Child Development and Critical Disorder, Chongqing, China,* [3] *Department of Ultrasound, Children's Hospital of Chongqing Medical University, Chongqing, China,* [4] *Department of Cardiothoracic Surgery, Children's Hospital of Chongqing Medical University, Chongqing, China,* [5] *Auckland Bioengineering Institute, The University of Auckland, Auckland, New Zealand,* [6] *Department of Intensive Care Unit, Children's Hospital of Chongqing Medical University, Chongqing, China*

OPEN ACCESS

Edited by:
Xupei Huang,
Florida Atlantic University,
United States

Reviewed by:
Ziyad M. Hijazi,
Rush University, United States
Runmei Zou,
Central South University, China

****Correspondence:***
Xiaojuan Ji
jixiaojuan@hospital.cqmu.edu.cn

Specialty section:
This article was submitted to Pediatric Cardiology, a section of the journal Frontiers in Pediatrics

Received: *25 February 2020*
Accepted: *15 May 2020*
Published: *19 June 2020*

Citation:
Zhu X, Ji X, Wu C, Ho H, Jiang K, Wang Y and Bai K (2020) Ventricular Septal Rupture After Blunt Chest Trauma in an Infant: A Case Report and Mini-Review. Front. Pediatr. 8:316. doi: 10.3389/fped.2020.00316

Ventricular septal rupture (VSR) due to blunt chest trauma (BCT) is rare in infants. Traumatic VSR should be considered in infants with acute congestive cardiac failure following blunt trauma to the chest. Echocardiography is the method of choice for diagnosis and guiding the management of VSR. In this case report, we present a case of VSR caused by BCT in a 1-year and 9-month-old infant, who was diagnosed by emergency bedside echocardiography. We also provide a mini-review of literatures on BCT-induced VSR in children.

Keywords: ventricular septal rupture, blunt chest trauma, echocardiography, infant, therapy

INTRODUCTION

Ventricular septal defect (VSD) is the most common congenital heart disease (1). Acquired VSD is very rare, and is mainly due to trauma, myocardial infarction, or complications of cardiac surgery such as valve replacements or closure of VSD, endocarditis (2). Ventricular septal rupture (VSR), also called traumatic VSD, is a rare complication of blunt chest trauma (BCT) in children (3–5). The formation mechanism of VSD after BCT has been suggested as the ischemic myocardial rupture associated with initial trauma, and/or the reopening of spontaneously closed congenital VSD (6, 7). In addition, during ventricular isovolumic contraction, chest trauma may produce sufficient ventricular force to cause myocardial rupture (6, 7).

Non-invasive imaging of the intra-cardiac structure with high spatial and temporal resolutions can be obtained by echocardiography in children. Therefore, echocardiography is the modality of choice for the diagnosis and management of VSR (4, 8). Bedside echocardiography is the most rapid and feasible modality to diagnose and follow-up acute and severe VSR cases. In this study, we report a case of VSR in an infant following BCT, whereby bedside echocardiography revealed a muscular ventricular septal defect and a ventricular aneurysm on the left ventricular posterior wall opposite the muscular ventricular defect.

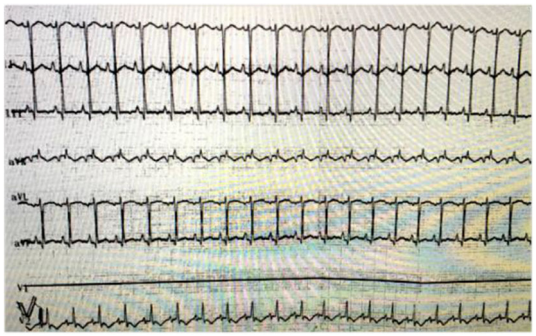

FIGURE 1 | Bedside electrocardiogram revealed ST segment elevation.

CASE

A1-year and 9-month-old male infant was presented with a history of being involved in a motor vehicle accident 5 h earlier in which he sustained blunt force chest trauma. From the time of admission to the 7th day, he was not on a ventilator, and the ECG monitor showed that his vital signs were stable. His breath was in a regular rhythm, and a Grade 2–3/6 systolic murmur was detected at the left lower sternal border. On the 7th day after admission, the vital signs of the infant were unstable: he was in respiratory distress (respiratory rate 70/min), and his heart rate was 145–155 times per minute. His blood oxygen saturation decreased to 78%. Scratches can be seen on the skin of the occipital scalp and the left forearm.

Myocardial zymogram evaluations revealed that hypersensitive troponin 1 was increased to 10.281 μg/L, and the creatine kinase MB isoenzyme was increased to 7.29 μg/L. The bedside electrocardiogram showed pathological Q wave and ST segment elevation (**Figure 1**). Chest computed tomography showed double lung contusion.

Emergency bedside echocardiography demonstrated funnel-shaped muscular ventricular septal defect (M-VSD). The diameters of the left and right ventricular shunt orifice were 10 and 5 mm, respectively (**Figures 2A,B**). Color Doppler flow imaging showed a bidirectional shunt between the left and right ventricles (**Figures 2A,B**), and also revealed severe mitral regurgitation (**Figure 3A**), and mild pulmonary hypertension (**Figure 3B**). Opposite of the muscular ventricular defect, it was noted that a ventricular aneurysm on the left ventricular posterior wall had formed (**Figure 3C**). The thickness of the myocardium appeared irregular with the thinnest region measuring 3.0 mm.

The infant underwent cardio-surgery to occlude the M-VSD with an occluder (SQFDQ-II i, 10 mm, LEPU Medical, China) under direct vision, which was monitored by trans-esophageal echocardiogram. After occlusion of the M-VSD, the ventricular aneurysm on the left ventricular posterior wall was repaired surgically by intermittent pad stitching. The mitral valvuloplasty and foramen ovale suture closure were performed under cardiopulmonary bypass. The intraoperative findings were consistent with those of echocardiography. Both immediate trans-esophageal and trans-thoracic echocardiogram showed no residual shunt after operation (**Figure 4**).

From post-operation day 1–16 the infant had been in a stable condition (T 36.8°C, R 30/min, HR 131 times per minute, BP 90/54 mmHg, SPO_2 96–99%). The cardiac functions of the infant were normal (EF 57% FS 29% E/A 1.4 IRT 42 ms). On post-operation day 13, he was weaned off the ventilator and was extubated. On the 16th day after operation, the blood oxygen saturation rate was decreased (the lowest level reached 27%). The infant was in a critical condition, and tracheal intubation was performed on the patient. His parents decided to give up treatment.

DISCUSSION

Traumatic VSDs present in 2–10% of BCT cases from motor vehicle accidents, and children are more prone to VSR due to the pliability of the immature chest wall (6, 9, 10). The increased intraventricular pressure after atrioventricular valve closure and the sudden elevation of pressure caused by the impact of BCT make the ventricular septum susceptible to rupture (10–12). The contused myocardium can become necrotic and subsequently perforate because of the two postulated mechanisms of VSR (6, 7). VSR may occur several hours to months after blunt trauma (13). In the case of our infant patient, rupture occurred on the seventh day post-BCT injury.

Congenital VSD usually occurs adjacent to the membranous septum (14). The most common localization of traumatic VSD is in the muscular portion of the interventricular septum near the cardiac apex (12). In this specific case there was no previous history of congenital heart disease. Bedside echocardiography showed M-VSD and a ventricular aneurysm on the left ventricular posterior wall. Electrocardiogram revealed myocardial ischemia, with myocardial zymogram (troponin 1 and creatine kinase MB) further hinting myocardial damage. VSR was diagnosed as a complication of BCT, which was confirmed in the cardiac operation. It is evident in this case study that bedside echocardiography is an effective tool for rapid and accurate assessment of cardiac injury, providing anatomical, and hemodynamic information (8, 15).

The case described herein is similar to the acquired VSR cases due to BCT previously reported in children (4–7, 10). Specifically, Ogunkunle et al. reported BCT induced VSR in a 7-year-old child (4). Behrle et al. reported a case of 6-year-old girl run over by a van, and emergency echocardiograms

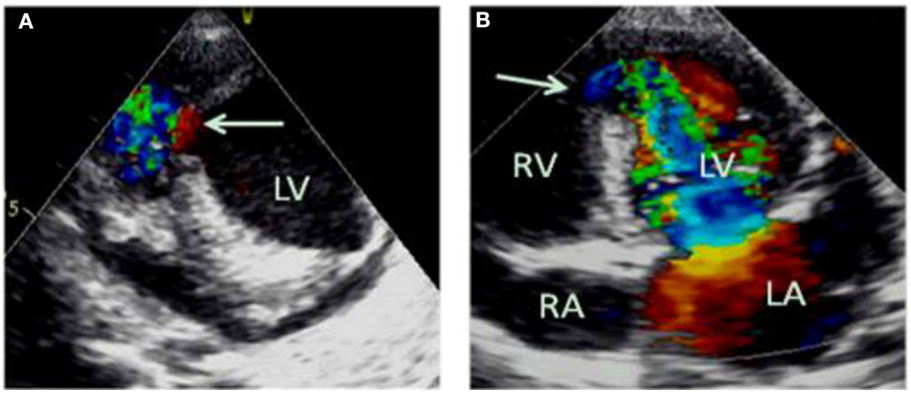

FIGURE 2 | Emergency bedside transthoracic echocardiography revealed funnel shaped M-VSD **(A)**. The white arrows indicate the left and right ventricular shunt orifice **(A,B)**. Color Doppler flow imaging show a bidirectional shunt between the left and right ventricles **(A,B)**. LA, left atrium; RA, right atrium; LV, left ventricle; RV, right ventricle.

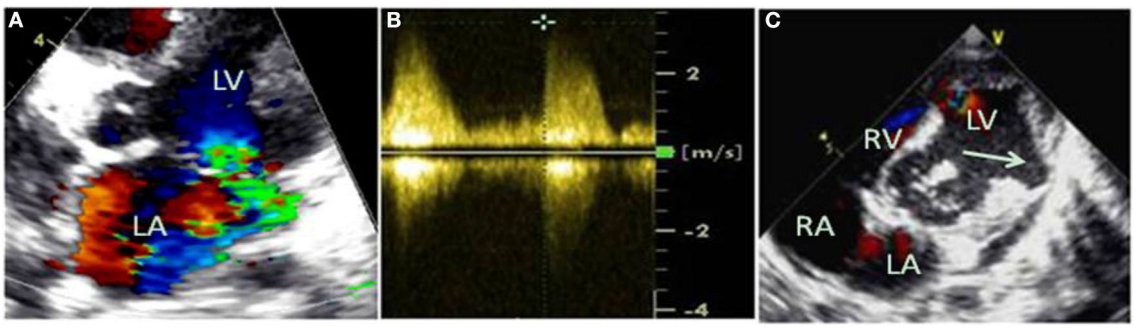

FIGURE 3 | Color Doppler flow imaging revealed severe mitral regurgitation **(A)**, and mild pulmonary hypertension was estimated by continuous-wave doppler **(B)**. Opposite the muscular ventricular defect, a ventricular aneurysm on the left ventricular posterior wall was formed **(C)**, indicated by the arrow.

demonstrated a ventricular septal pseudo-aneurysm (12 × 15 mm) in her superior muscular septum (7). The pseudo-aneurysm was left untreated and remained stable during the patient's 3-month hospitalization. Steed et al. reported a septal avulsion case in a 15-year-old child caused by motor vehicle accident (6), and the aorta of the child was opened in surgery and a septal avulsion was excised through the aortic valve. In another car accident, an anterior M-VSD and a left ventricular aneurysm (28 × 25 mm) were detected in a 13-year-old boy 1 day after the accident (10). The aneurysm was incised during ventricular fibrillation. According to the current literature, our patient (1-year and 9-month old) represents the youngest child whose VSR and septal aneurysm were caused by the complication of BCT after a car accident. A muscular septal occluded device was utilized in a minimally invasive closure, and the aneurysm was also treated in cardiac surgery. Recently, Wu et al. reported a traumatic VSD case in a 1-year-old boy caused by chest compression after a slippery accident by an adult (16). The authors suggest that the appearance of new heart murmur after chest trauma as the clinical clue of traumatic VSD.

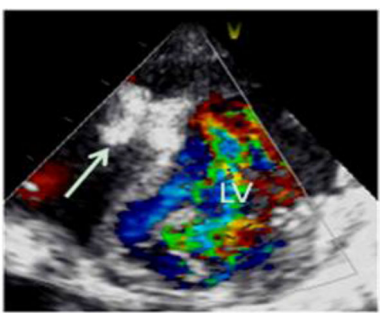

FIGURE 4 | Transthoracic echocardiogram showed no residual shunt after operation, and the arrow indicates the occluding device.

CONCLUSION

We present the case of a child with VSR following blunt chest trauma due to a motor vehicle accident. The M-VSD was occluded with invasive closure, and

ventricular aneurysm was surgically repaired. To our knowledge, similar co-occurrence of these features has never been reported.

DATA AVAILABILITY STATEMENT

The raw data supporting the conclusions of this article will be made available by the authors, without undue reservation.

ETHICS STATEMENT

Informed consent was obtained from the child' legal guardian for the publication of any potentially identifiable images or data included in this article.

AUTHOR CONTRIBUTIONS

XJ, CW, KJ, KB, and YW participated in the diagnosis and treatment of the case. XZ collected clinic data. XZ and HH prepared the manuscript. All authors read and approved the manuscript as submitted.

FUNDING

This work was funded by National Natural Science Foundation of China (Grant No. 81301300); Chongqing Science and Technology Commission (cstc2016shmszx 130009); China Postdoctoral Science Foundation funded project (2018T110949); and Project of Chongqing Municipal Human Resources and Social Security Bureau (cx2019065).

REFERENCES

1. Hoffman JIE, Kaplan S. The incidence of congenital heart disease. *J Am Coll Cardiol.* (2002) 39:1890–900. doi: 10.1016/S0735-1097(02)01886-7
2. Sinisalo JP, Sreeram N, Jokinen E, Qureshi SA. Acquiredleft ventricular-right atrium shunts. *Eur J CardiothoracSurg.* (2011) 39:500–6. doi: 10.1016/j.ejcts.2010.04.027
3. Hamdan-Challe M, Godin M, Bouchart F, Doguet F. Isolated ventricular septal rupture secondary to blunt trauma. *Interact CardioVasc Thorac Surg.* (2010) 11:667–9. doi: 10.1510/icvts.2010.242602
4. Ogunkunle OO, Duru CO, Omokhodion SI, Adebayo BE. Acquired ventricular septal defect: a rare sequel of blunt chest trauma in a 7-year-old boy. *Nigerian J Clin Pract.* (2015) 18:297–9. doi: 10.4103/1119-3077.151072
5. Saxena A, Ramasamy S, Devagourou V, Math R. Ventricular septal rupture in a 4-year-old child following blunt chest injury. *Pediatr Cardiol.* (2009) 30:1188–9. doi: 10.1007/s00246-009-9529-8
6. Steed M, Guerra V, Recto MR, Yang S-G, Frieberg E, Fox C, et al. Ventricular septal avulsion and ventricular septal defect after blunt trauma. *Ann Thoracic Surg.* (2012) 94:1714–6. doi: 10.1016/j.athoracsur.2012.03.014
7. Behrle N, Dyke P, Dalabih A. Interventricular septal pseudoaneurysm after blunt chest trauma in a 6 year old: an illustrative case and review. *Pediatr Emerg Care.* (2018) 34:e39–40. doi: 10.1097/PEC.0000000000000821
8. Jeon K, Lim W-H, Kang S-H, Cho I, Kim K-H, Kim H-K, et al. Delayed Diagnosis of traumatic ventricular septal defect in penetrating chest injury: small evidence on echocardiography makes big difference. *J Cardiovasc Ultrasound.* (2010) 18:28–30. doi: 10.4250/jcu.2010.18.1.28
9. Ozay B, Ozer N, Ketenci B, Demirtas M. Unsuspected location of a ventricular septal defect after blunt chest trauma. *Thorac cardiovasc Surg.* (2008) 56:110–1. doi: 10.1055/s-2006-924704
10. Stamm C, Feit LR, Geva T, del Nido PJ. Repair of ventricular septal defect and left ventricular aneurysm following blunt chest trauma. *Eur J Cardiothorac Surg.* (2002) 22:154–6. doi: 10.1016/S1010-7940(02)00197-5
11. Dowd MD, Krug S. Pediatric blunt cardiac injury: epidemiology, clinical features, and diagnosis. *J Trauma Acute Care Surg.* (1996) 40:61–7. doi: 10.1097/00005373-199601000-00012
12. Kotrec M, Jassal DS, Zieroth S, Freed DH, Tam JW. Ventricular septal defect as a result of direct trauma from mechanical mitral valve prosthesis. *Can J Cardiol.* (2011) 27:263.e21–3. doi: 10.1016/j.cjca.2010.12.022
13. Dehghani P, Ibrahim R, Collins N, Latter D, Cheema AN, Chisholm RJ. Post-traumatic ventricular septal defects–review of the literature and a novel technique for percutaneous closure. *J Invasive Cardiol.* (2009) 21:483–7.
14. Cleland WP, Ellman TLP, Goodwin J, Hollman A. Repair of ventricular septal defect following indirect trauma. *Br J Dis Chest.* (1961) 55:17–22. doi: 10.1016/S0007-0971(61)80019-3
15. Bromberg BI, Mazziotti MV, Canter CE, Spray TL, Strauss AW, Foglia RP. Recognition and management of nonpenetrating cardiac trauma in children. *J Pediatrics.* (1996) 128:536–41. doi: 10.1016/S0022-3476(96)70366-9
16. Wu H-W, Chien J-H, Weng K-P, Lin C-C, Chen B-H, Huang S-M, et al. Traumatic ventricular septal defect in a 1-year-old boy after accidental chest compression by an adult. *Pediatr Emerg Care.* (2019) 35:e90. doi: 10.1097/PEC.0000000000001077

Conflict of Interest: The authors declare that the research was conducted in the absence of any commercial or financial relationships that could be construed as a potential conflict of interest.

frontiers in Pediatrics

ORIGINAL RESEARCH
published: 12 August 2020
doi: 10.3389/fped.2020.00451

The Anti-inflammatory Effect of Soluble Epoxide Hydrolase Inhibitor and 14, 15-EET in Kawasaki Disease Through PPARγ/STAT1 Signaling Pathway

*Na Dai[1,2†], Chunyan Yang[1,3†], Qing Fan[2], Minmin Wang[1], Xiaoyue Liu[1], Haizhao Zhao[1] and Cuifen Zhao[1]**

[1] Department of Pediatrics, Qilu Hospital, Shandong University, Jinan, China, [2] Department of Pediatrics, Jinan Maternity and Child Care Hospital, Jinan, China, [3] Department of Pediatrics, Liaocheng People's Hospital, Liaocheng, China

OPEN ACCESS

Edited by:
Fu Lijun,
Shanghai Children's Medical Center, China

Reviewed by:
Tiewei Lv,
Children's Hospital of Chongqing Medical University, China
Maoping Chu,
The Second Affiliated Hospital and Yuying Children's Hospital of Wenzhou Medical University, China

***Correspondence:**
Cuifen Zhao
zhaocuifen@sdu.edu.cn

†These authors have contributed equally to this work

Specialty section:
This article was submitted to Pediatric Cardiology, a section of the journal Frontiers in Pediatrics

Received: 15 February 2020
Accepted: 29 June 2020
Published: 12 August 2020

Citation:
Dai N, Yang C, Fan Q, Wang M, Liu X, Zhao H and Zhao C (2020) The Anti-inflammatory Effect of Soluble Epoxide Hydrolase Inhibitor and 14, 15-EET in Kawasaki Disease Through PPARγ/STAT1 Signaling Pathway. Front. Pediatr. 8:451. doi: 10.3389/fped.2020.00451

Soluble epoxide hydrolase (sEH) is responsible for rapid degradation of 14, 15-EET, which is one of the isomers of EETs and plays an important role in cardiovascular diseases. In this study, we investigated the mechanism by which sEH inhibitor AUDA played an anti-inflammatory effect in HCAECs. Our results indicated that AUDA treatment promoted PPARγ expression, while knockdown of PPARγ blocked the cell growth and STAT1 expression inhibition induced by 100 μmol/L AUDA in HCAECs. AUDA also inhibited the overexpression of TNF-α, IL-1 β, and MMP-9 induced by KD sera in HCAECs. Moreover, 30 blood samples from children with Kawasaki disease (KD) were collected with 30 healthy children as the control group. QPCR and ELISA assays were used to detect the level of 14, 15-EET, TNF-α, IL-1β, and MMP-9. We found that the level of 14, 15-EET was higher in peripheral blood of children with KD compared with healthy controls ($P < 0.05$). In comparison to KD children with non-coronary artery lesion (nCAL), the level of 14, 15-EET was higher in peripheral blood of KD children with coronary artery lesion (CAL) ($P < 0.05$). Compared with healthy control group, the expression levels of TNF-α, IL-1β, and MMP-9 in patients with KD were significantly up-regulated. Compared with nCAL KD children, the expression levels of TNF-α, IL-1β, and MMP-9 in CAL children were abnormally high ($P < 0.05$). Our study indicated that AUDA played an anti-inflammatory effect in HCAECs through PPARγ/STAT1 signaling pathway, and 14, 15-EET is up-regulated in children with KD, suggesting that 14, 15-EET involved in the progression of KD.

Keywords: Kawasaki disease, 14, 15-EET, coronary injury, AUDA, PPARγ

INTRODUCTION

Studies have shown that arachidonic acid (ARA) is converted to endogenous lipid EETs by P450 arachidonic acid cyclooxygenase (ARA cyclooxygenase), while EETs are converted to inactive DHET by sEH *in vivo* (1, 2). Cytochrome P450 2J2 (CYP2J2) is a major human ARA cyclooxygenase that produces all four EETs isomers: 5, 6-EET, 8, 9-EET, 11, 12-EET, and 14, 15-EET (3). 14, 15-EET plays an important role in cardiovascular diseases (4, 5). A number of studies have shown that 14, 15-EET promotes PDGF-induced proliferation of porcine aortic smooth muscle cells by inhibiting

COX-mediated PGE2 synthesis, and has extensive cardioprotective functions, involving in a variety of cardiovascular diseases (6).

In previous studies, we found that AUDA, a sEH inhibitor, could inhibit the expression of MMP-9, IL-1β, and TNF-α *in vitro* and *in vivo*, thus protecting and repairing myocardial injury (7). In this study, we explored the specific mechanism of AUDA in the process of myocardial protection. We also collected peripheral blood samples from patients with Kawasaki disease (KD) to investigate 14, 15-EET level and its significance in coronary artery lesion (CAL). This study provides evidence for the clinical treatment of KD targeted by EETs.

MATERIALS AND METHODS

Cell Culture and Transfection

HCAECs were obtained from the Wuhan Culture Collection. The culture and treatment with AUDA of HCAECs was performed as mentioned in our previous study (7). Cells were cultured in medium with 10% KD sera to establish KD cell model. PPARγ specific siRNA and over-expression plasmid were all purchased from Shanghai Genechem Co., Ltd. and transfected into HCAECs using Lipofectamine 2000 (Thermo Fisher Scientific, San Jose, CA, USA) following the manufacturer's instruction.

CCK8

Cell proliferation was detected using cell counting kit-8 (CCK-8) assay (Beyotime Institute of Biotechnology, Haimen, China), which was performed according to the description in our previous study (7).

Sample Inclusion Criteria

This study included 30 children with KD hospitalized in Qilu Hospital from June 2018 to January 2019, all of which met the fourth revised diagnostic criteria of Kawasaki Disease Research Committee of Japan (8). All children were not treated with aspirin or gamma globulin before admission. KD complicated with CAL diagnosed with Z-value >2.5 by the same echocardiologist (8). There was significant difference in Z-value between CAL and nCAL groups.

Sample Collection

The venous blood of the normal control group and KD patients was collected 3 ml each, and centrifuged at 3,000 rpm for 10 min, and the prepared plasma was stored in a refrigerator at −80°C. Parental informed consent was obtained. The clinical data of KD and normal control were collected and compiled. The present study was approved by the ethics committee of Qilu Hospital, Shandong University and informed consents were obtained from all patients and healthy control.

Quantitative Real-Time PCR (qPCR)

Total RNA was extracted, and then reverse transcribed to cDNA. The expression of PPARγ, STAT1, MMP-9, IL-1β, and TNF-α was detected by qPCR using SYBR Premix Ex Taq II. The relative quantification was identified by the $2^{-\Delta\Delta Ct}$ method after standardization to the GAPDH level. Following primers were used in this research: PPARγ-F 5′-GGCCCTGGCAAAACATTTGT-3′, PPARγ-R 5′-GATGGCCACCTCTTTGCTCT-3′, STAT1-F 5′-GGCACGCACACAAAAGTGAT-3′, STAT1-R 5′-AGAGGTCGTCTCGAGGTCAA-3′, TNF-α-F 5′-ACCGCAGTCCAGAAAGTCTC-3′, TNF-α-R 5′-TGCAGGCCTCAGGATCAAAG-3′, IL-1β-F 5′-TGGGCCTCCTCTCCTACT-3′, IL-1β-R 5′-CTTCCCCCATTCATCCCAGG-3′, MMP-9-F 5′-GACTGAGTACCTGAACCGGC-3′, MMP-9-R 5′-AGTTCCACAAAGGCATCCCAG-3′, GAPDH-F 5′-TCTCTGCTCCTCCCTGTTCT-3′, and GAPDH-R 5′-ATCCGTTCACACCGACCTTC-3′.

ELISA

The levels of 14, 15-EET (cat. no.ab175812, Abcam), MMP-9 (cat. no.ab246539, Abcam), IL-1β (cat. no.ab100562, Abcam), and TNF-α (cat. no.ab181421, Abcam) were examined using ELISA kits.

Statistical Analysis

Prism 5.0 (GraphPad Software, Inc., La Jolla, CA, USA) was used for data analysis. Data are expressed as the mean ± standard error. The significance of differences among several groups was determined using one-way analysis of variance and Bonferroni posttest. $P < 0.05$ was considered to indicate a statistically significant difference. All experiments in this research were performed in triplicate.

RESULTS

AUDA Promotes the Proliferation of Human Coronary Arterial Endothelial Cells (HCAECs) by Up-Regulating PPARγ

To investigate the mechanism by which AUDA played an anti-inflammatory effect, we detected the mRNA level of PPARγ in HCAECs using qPCR. As shown in **Figure 1A**, the mRNA level of PPARγ increased significantly after the treatment of 100 μ mol/L AUDA, suggesting that PPARγ might be the target of AUDA in HCAECs. Then, we transfected PPARγ specific siRNA or PPARγ over-expression plasmid into HCAECs to further verify the effect of AUDA on PPARγ. From qPCR results, PPARγ expression was significantly inhibited by PPARγ siRNA and promoted by PPARγ over-expression plasmid (**Figure 1A**). CCK-8 assay was performed to confirm the proliferation of HCAECs. As shown in **Figure 1B**, the OD value of the PPARγ knockdown group (si-PPARγ) decreased significantly, while the OD value of the PPARγ over-expression group increased significantly. In addition, after the treatment of PPARγ knockdown cells with 100 μmol/L AUDA, the OD value decreased markedly compared with 100 μmol/L AUDA group (**Figure 1B**). Moreover, in order to investigate whether the overexpression of PPARγ formed a feedback inhibition on the proliferative effect of AUDA, we overexpressed PPARγ at the same time as AUDA treatment (AUDA+PPARγ group). The results show that the overexpression of PPARγ did not affect the effect of AUDA compared with the AUDA group ($P < 0.05$, **Figure 1**). These data indicated that PPARγ knockdown blocked the cell growth induced by 100 μmol/L AUDA in HCAECs.

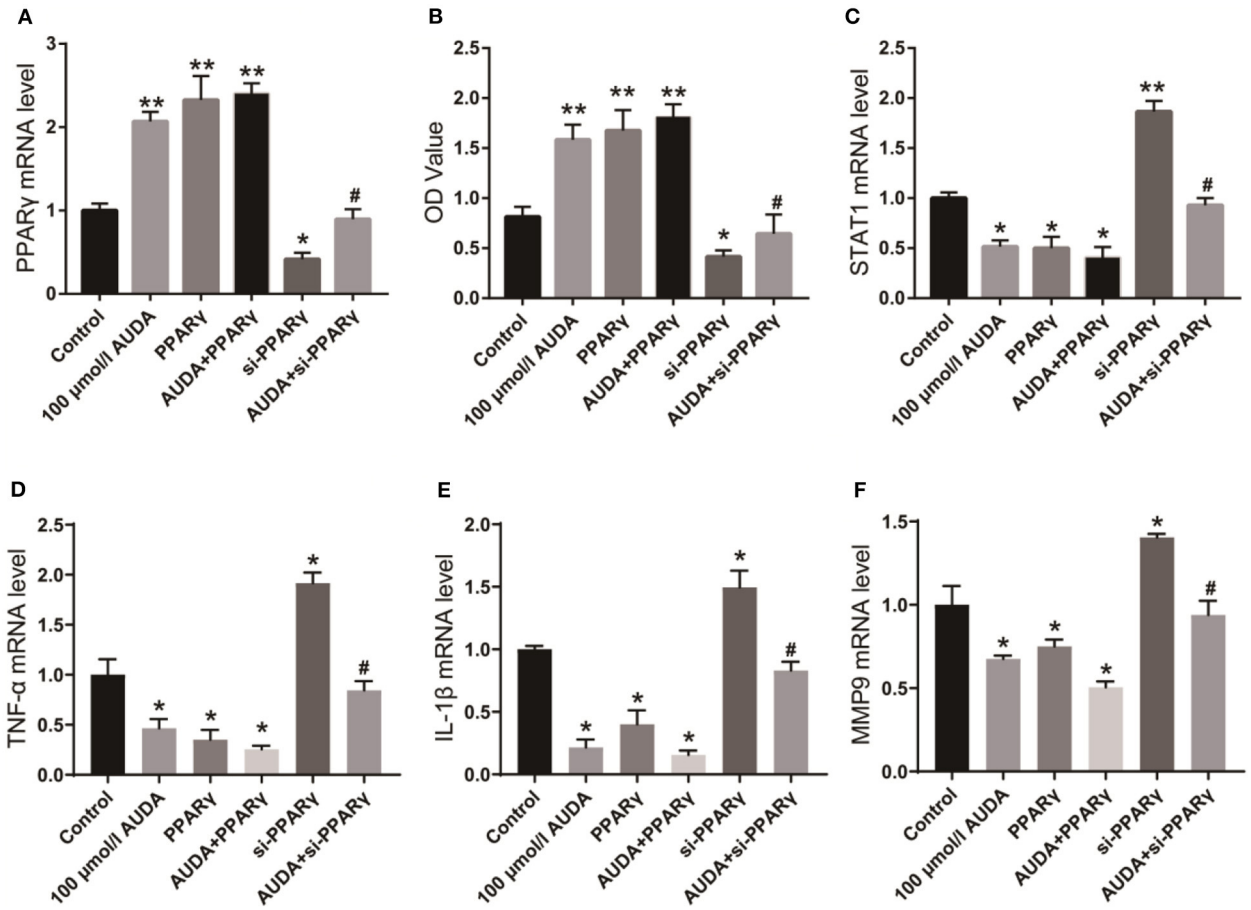

FIGURE 1 | AUDA inhibited JAK/STAT1 signaling pathway by upregulating PPARγ. **(A)** The expression of PPARγ in human coronary artery endothelial cells was detected by qPCR; **(B)** The proliferation of coronary artery endothelial cells in each group was determined by CCK-8; **(C)** The expression of STAT1, a key protein in the downstream pathway of PPARγ was detected by qPCR. The mRNA levels of TNF-α **(D),** IL-1β **(E)**, and MMP-9 **(F)** in each group were detected using qPCR. $^{*}P < 0.05$, $^{**}P < 0.05$ vs. control group, $^{\#}P < 0.05$ vs. 100 μmol/L AUDA group.

AUDA Inhibits JAK/STAT1 Signaling Pathway and Inflammatory Factors by Up-Regulating PPARγ

STAT1 is a critical protein of JAK/STAT1 signaling pathway, as well as a key factor in the pathogenesis and progression of inflammation (9, 10). Its downstream inflammatory factors such as TNF-α, IL-1β, and MMP-9 play crucial roles in the progression of KD (11, 12). Therefore, we investigated the effect of AUDA on STAT1 and inflammatory factors using qPCR. As shown in **Figure 1C**, STAT1 mRNA level decreased significantly after treatment with 100 μmol/LAUDA or overexpression of PPARγ, but increased significantly after knocking down PPARγ. After the treatment of PPARγ knockdown cells with 100 μmol/L AUDA, STAT1 expression increased to the level of control group, which was significantly higher than that of 100 μmol/L AUDA group. The expression levels of TNF-α, IL-1β, and MMP-9 were also significantly inhibited by 00 μmol/L AUDA and PPARγ, and significantly increased after PPARγ knockdown (**Figures 1D,E**). Moreover, PPARγ knockdown rescued the inhibition of TNF-α, IL-1β, and MMP-9 expression induced by the treatment of 100 μmol/L AUDA (**Figures 1D,E**). These results suggested that AUDA played an anti-inflammatory role by upregulating PPARγ and inhibiting JAK/STAT1 signaling pathway in HCAECs.

AUDA Blocks the Inflammatory Response Induced by KD Sera in HCAECs

Next, we treated the 10% KD sera cultured HCAECs with 100 μmol/ L AUDA to further investigate the effect of AUDA on KD. As shown in **Figure 2A**, KD sera inhibited the proliferation in HCAECs compared with the control group. 100 μmol/L AUDA treatment rescued the inhibition of proliferation induced by KD sera. Moreover, the mRNA level of TNF-α, IL-1β, and MMP-9 increased in KD sera cultured HCAECs compared with the control, and decreased by the treatment of 100 μmol/L AUDA (**Figures 2B–D**). These results indicated that AUDA could block the inflammatory response induced by KD sera, suggesting an anti-inflammation effects of AUDA in KD sera cultured HCAECs.

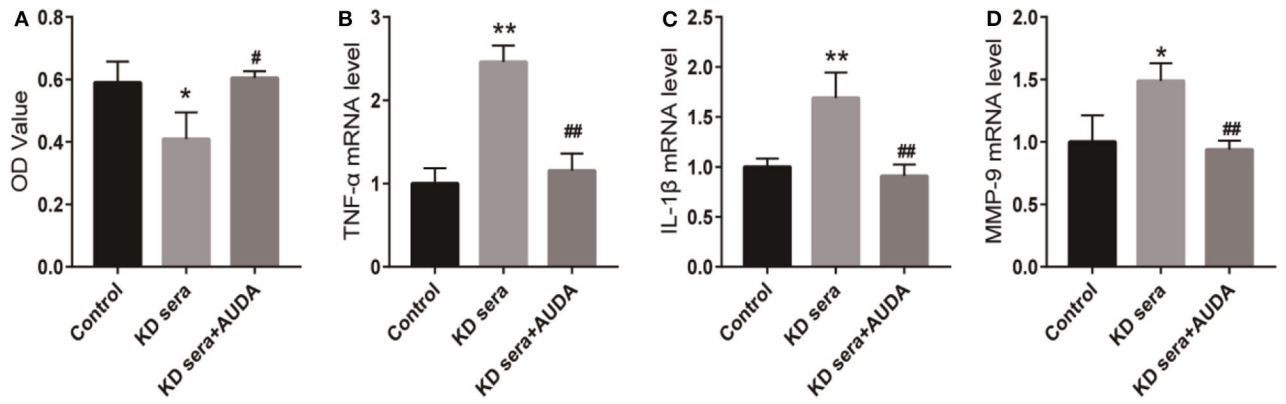

FIGURE 2 | AUDA blocked the inflammatory response induced by KD sera in HCAECs. HCAECs were cultured with 10% KD sera (KD sera group) with cells in conventional culture as the control group. KD sera group cells were treated with 100 μmol/L AUDA to generate the KD sera + AUDA group. **(A)** The proliferation of HCAECs in each group was detected by CCK-8. The mRNA levels of TNF-α **(B)**, IL-1β **(C)**, and MMP-9 **(D)** in each group were detected using qPCR. $^{*}P < 0.05$ vs. control; $^{**}P < 0.01$ vs. control; $^{\#}P < 0.05$ vs. KD sera; $^{\#\#}P < 0.01$ vs. KD sera.

Clinical Data of Samples

A total of 30 patients with KD and 30 healthy children were enrolled in the study to detect 14, 15-EET level in peripheral blood. The average age of 30 patients with KD was 25 ± 6 m. Among them, 18 patients with CAL had an average age of 23 ± 9 m, while 12 patients without CAL had an average age of 26 ± 6 m. Compared with the normal control, the content of leukocytes, platelet, monocytes, and C-reactive protein in peripheral blood of patients with KD were significantly increased ($P < 0.05$), while the levels of leukocytes, neutrophils and C-reactive protein in peripheral blood of patients with CAL were significantly higher than those of patients without CAL ($P < 0.05$, **Table 1**).

14, 15-EET Level in Peripheral Blood of Patients With KD and Its Relationship With CAL

The level of 14, 15-EET in peripheral blood samples of 30 patients with KD and 30 healthy children was detected using ELISA. As shown in **Figure 3A**, the level of 14, 15-EET in peripheral blood of KD patients was significantly higher than that of control group, which was statistically significant ($P < 0.01$). Thirty KD patients were divided into two groups: CAL group (12 cases) and nCAL group (18 cases). The level of 14, 15-EET in the CAL group was significantly higher than that in the nCAL group via comparing 14, 15-EET level in the two groups (**Figure 3B**). These results suggest that 14, 15-EET is closely related to the progression of KD and plays a role in the process of CAL in patients with KD. It is a potential target for clinical intervention.

Expression of TNF-α, IL-1β, and MMP-9 in Peripheral Blood of Patients With KD

The mRNA levels of TNF-α, IL-1β, and MMP-9 in peripheral blood of KD patients and control children were detected using qPCR. As shown in **Figure 4**, the mRNA levels of TNF-α, IL-1β, and MMP-9 in peripheral blood of KD patients were significantly up-regulated compared with the control group. Results detected though ELISA showed that protein levels of TNF-α, IL-1β, and MMP-9 in peripheral blood of KD patients were also significantly up-regulated (**Figure 5**). These results suggest that TNF-α, IL-1β, and MMP-9 are involved in the progression of KD.

The Relationship Between the Expression of TNF-α, IL-1β, and MMP-9 in Peripheral Blood and CAL in KD Patients

Further analysis of the expression levels of inflammatory factors in KD patients with CAL or nCAL showed that levels of TNF-α, IL-1β, and MMP-9 in patients with CAL were significantly higher than those in patients with nCAL (**Figure 6**). The protein levels of TNF-α, IL-1β, and MMP-9 in the CAL group were also significantly higher than those in the nCAL group (**Figure 7**). These results confirm that TNF-α, IL-1β, and MMP-9 are involved in the progress of inflammation and play roles in the development of CAL in KD patient.

DISCUSSION

In previous studies, we found that the proliferation, migration, adhesion, and angiogenesis were enhanced after the treatment of 100 μmol/L AUDA in HCAECs (7). PPARγ antagonist GW9662 could block the growth induced by AUDA in HCAECs, indicating that AUDA promoted the migration, adhesion, proliferation, and angiogenesis of HCAECs through the EETs-PPARγ signaling pathway (7). In this study, we knocked down/overexpressed PPARγ in HCAECs to further confirm our hypothesis. Our results proved that knockdown of PPARγ blocked the proliferation induced by AUDA, while PPARγ overexpression promoted the proliferation of HCAECs. Moreover, AUDA treatment activated STAT1 signaling

TABLE 1 | Blood routine test results of selected patients and normal controls.

Groups		Cases (*n*)	Age (m)	Leukocyte (× 10^9/L)	Platelet (× 10^9/L)	Monocyte (× 10^9/L)	C-reactive protein (mg/L)
Control		30	25 ± 7	4.8 ± 0.6	220 ± 20	0.8 ± 0.3	3.5 ± 1.1
KD	nCAL	12	26 ± 6	14.5 ± 4.2*	320 ± 30*	1.7 ± 0.7*	49.6 ± 29.9*
	CAL	18	23 ± 9	19.6 ± 3.9*#	350 ± 30	2.0 ± 0.7*	96.9 ± 67.2*#

*$P < 0.05$ vs. Control; #$P < 0.05$ vs. nCAL.

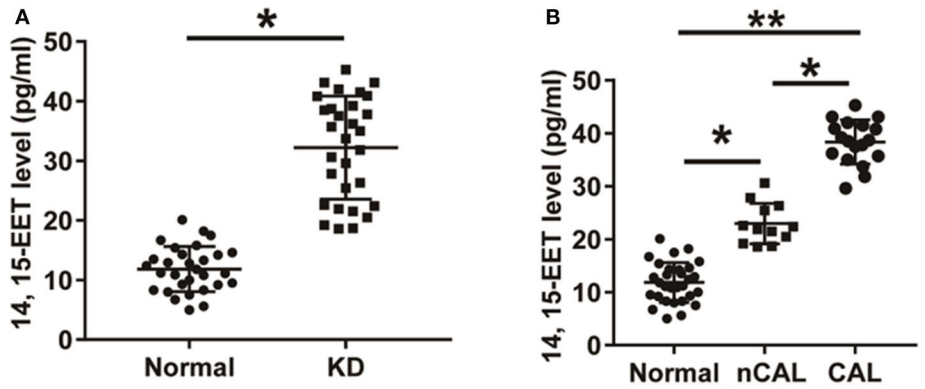

FIGURE 3 | The level of 14, 15-EET in KD patients and control children. **(A)** ELISA was performed to detect 14, 15-EET level in patients with KD and normal control group. **(B)** The level of 14, 15-EET in KD patients with CAL or nCAL. *$P < 0.05$; **$P < 0.01$.

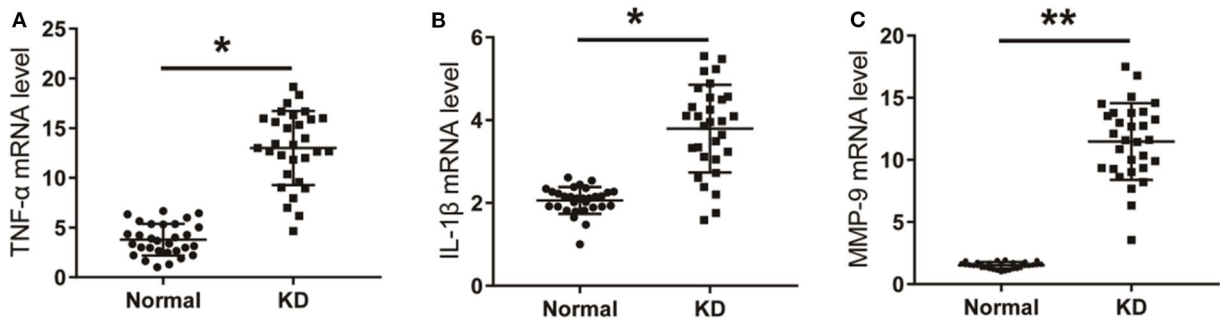

FIGURE 4 | The level of inflammatory factors in KD patients. **(A)** TNF-α in KD patients and control children. **(B)** IL-1β in KD patients and control children. **(C)** MMP-9 in KD patients and control children. *$P < 0.05$; **$P < 0.01$.

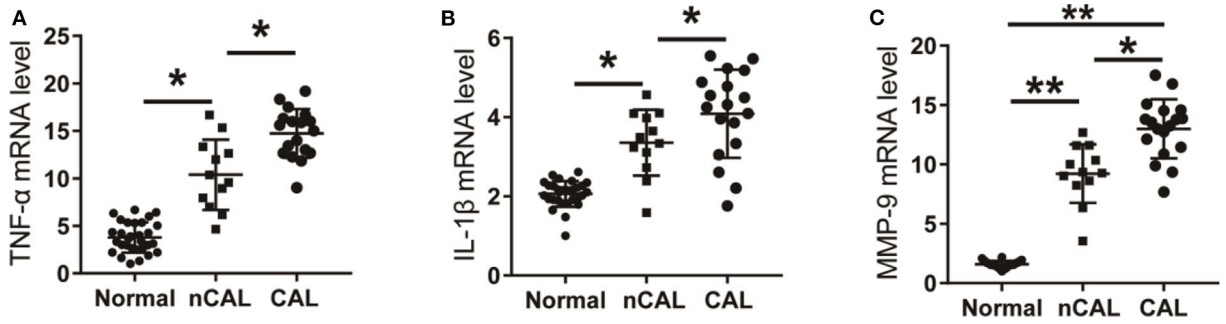

FIGURE 5 | The levels of inflammatory factors in KD patients with CAL or nCAL. **(A)** TNF-α level in patients with KD. **(B)** IL-1β level in patients with KD. **(C)** MMP-9 level in patients with KD. *$P < 0.05$; **$P < 0.01$.

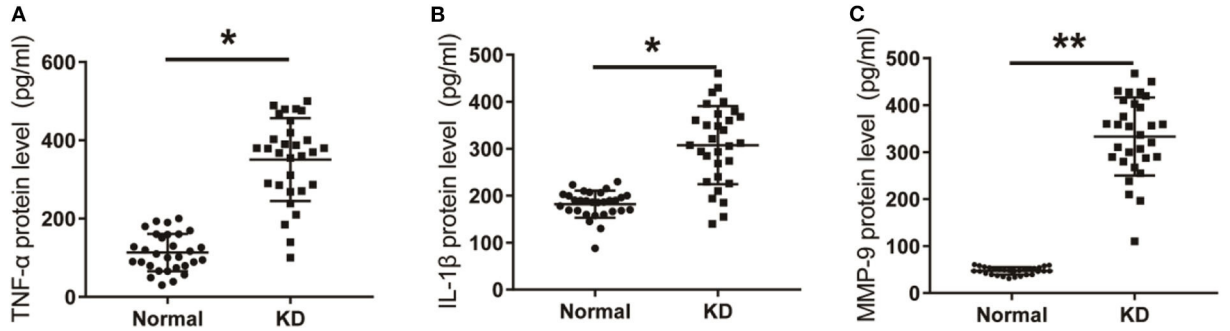

FIGURE 6 | Expression of inflammatory factors in KD patients and control group. **(A)** TNF-α protein level in KD patients was detected by Elisa. **(B)** IL-1β protein level in KD patients. **(C)** MMP-9 protein level in KD patients. *$P < 0.05$; **$P < 0.01$.

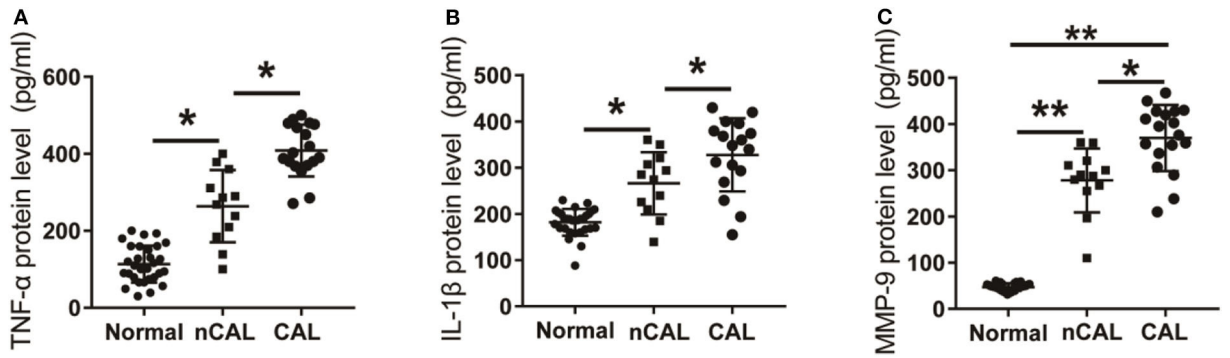

FIGURE 7 | Expression of inflammatory factors in peripheral blood of KD patients and control children with CAL or nCAL. **(A)** TNF-α protein level in peripheral blood of patients with or without CAL; **(B)** IL-1β protein level in peripheral blood of patients with CAL or nCAL; **(C)** MMP-9 protein level in peripheral blood of patients with CAL or nCAL. *$P < 0.05$; **$P < 0.01$.

pathway by upregulating PPARγ expression, suggesting an anti-inflammatory role of AUDA in HCAECs. Interestingly, AUDA could also rescue the inhibition of proliferation and increased expression of TNF-α, IL-1β, MMP-9 induced by KD sera. Thus, we hypothesized that AUDA could block the inflammatory response in KD, which needs further verification *in vitro* and *in vivo*.

EETs have significant anti-inflammatory effects and also play important roles in promoting angiogenesis and cardiovascular protection (13–15). As an important subtype of the family, 14, 15-EET plays an anti-inflammatory role in many organs (16, 17). In human endothelial cells, hypoxia can increase the level of 14, 15-EET, and CYP2C, and then inhibit the up-regulation of vascular cell adhesion molecule-1 (VCAM-1). Another study reports that 11, 12-EET and 14, 15-EET promotes the release of heparin-binding EGF-like growth factor (HB-EGF) from cell surface by up-regulating the activity of multiple MMPs family proteins (18, 19). The treatment of myocardial ischemia/reperfusion rat model with low concentration of 14, 15-EET can alleviate the arrhythmia and cardiac function changes of ischemia/reperfusion and reduce the scope of myocardial infarction. However, the role of 14, 15-EET in vascular endothelial cells remains unclear.

In the present study, the level of 14, 15-EET in peripheral blood of 30 patients with KD was detected through ELISA test. The results showed that 14, 15-EET level in peripheral blood of patients with KD was significantly higher than that of healthy controls. Further analysis showed that the level of 14, 15-EET in peripheral blood of KD patients with CAL was significantly higher than that of KD patients with nCAL. The expression of inflammatory factors TNF-α, IL-1β, and MMP-9 in peripheral blood of KD patients was significantly higher than that of normal group, and the level of inflammatory factors TNF-α, IL-1β, and MMP-9 in KD patients with CAL was significantly higher than that in patients with nCAL. The dysfunction and injury of vascular endothelial cells is the initial link of vasculitis in KD (20). Overexpression of pro-inflammatory cytokines such as TNF-α and interleukins (IL) in sera of patients with KD stimulates increased expression of vascular endothelial cell adhesion molecules including MMP-9, which in turn promotes the adhesion of neutrophils, monocytes and lymphocytes to vascular endothelium and lead to vascular endothelial cell injury (20). These results indicate that EETs are involved in anti-inflammatory regulation in the process of CAL through regulating the expression of inflammatory factors. Studies have shown that EETs are up-regulated in many diseases. In the diabetic model of mice, the increased expression of EETs significantly inhibits the apoptosis of pancreatic-β cells, and then improves the function of pancreatic-β cells (21). Some scholars have found that the level of EETs in the plasma of patients with acute heart failure increases significantly, while

the level of EETs in the plasma of patients with chronic heart failure decreases. Because of the initiation of anti-inflammatory mechanism, EETs are up-regulated in the early stage of KD to play a cardioprotective role. Chronic heart failure may lead to abnormal synthesis of endogenous EETs, resulting in a decrease in EETs levels.

The high level of EETs in peripheral blood of KD patients induces cascade reactions of downstream targets and signaling pathways. Research shows that EETs are negatively correlated with MMP-9 in endothelial cells. The expression of MMP-9 in peripheral blood of KD patients was positively correlated with inflammatory factors TNF-α and L-1β. Some scholars have found that P450 cyclooxygenase or EETs can effectively inhibit homocysteine (Hcy), thereby inhibiting the binding level of transcription factor NF-kappa B to DNA, and ultimately inhibiting the level of MMP-9, through overexpression of P450 cyclooxygenase or exogenous supplementation of EETs in mouse aortic endothelial cells (MAECs) (22). 14, 15-EET has delayed cardioprotective effect, which is related to the activity of ERK and the expression of phosphorylated ERK1/ERK2 (23). In addition, EETs can also exert analgesic and anti-inflammatory effects through MAPK and cAMP/PKA signaling pathways (24–26). At present, the specific downstream targets for EETs to participate in anti-inflammation are not very clear. Several studies have shown that there are high affinity EETs binding sites in both cell membranes and cells (14). The male rats treated with exogenous EETs (100–300 mg/kg) showed a series of unique behaviors, including transient activity, exploratory behavior, and chewing. EETs binding screening of 47 potential receptors reveals that high affinity radioligands of peripheral benzodiazepine receptor (PBR), cannabinoid receptor 2 (CB2), neurokinin-2 (NK2) receptor, and dopamine D3 receptor (DRD3) are replaced by EETs with low micromolar concentration (15). In these receptors, PBR has been shown to be involved in inflammation. PBR density increases significantly after ischemic brain injury, but its specific mechanism remains unclear (27).

In conclusion, AUDA promotes the proliferation of HCAECs by upregulating the expression of PPARγ and inhibiting the JAK/STAT1 signaling pathway. 14, 15-EET is significantly up-regulated in peripheral blood of KD patients and participates in the anti-inflammatory effect of KD patients with CAL. However, the exploration of AUDA and 14, 15-EETs in this study is limited, and the related mechanisms, pharmacokinetics, and pharmacology need to be studied urgently, which will also be the focus of our future research.

DATA AVAILABILITY STATEMENT

All datasets generated for this study are included in the article/supplementary material.

ETHICS STATEMENT

The studies involving human participants were reviewed and approved by Jinan Maternity and Child Care Hospital. Written informed consent to participate in this study was provided by the participants' legal guardian/next of kin.

AUTHOR CONTRIBUTIONS

ND and CY mainly performed the experiments. ND and QF analyzed the data and wrote the paper. ND, CY, MW, XL, and HZ helped with the experiments. MW helped analyzed the data. CY and CZ helped modify the paper. All authors had edited and approved the final manuscript.

FUNDING

This work was supported by Shandong key research and development plan (2019GSF108186 and 2014GSF118066), Shandong, China.

REFERENCES

1. Wang Q, Shi G, Teng Y, Li X, Xie J, Shen Q, et al. Successful reduction of inflammatory responses and arachidonic acid–cyclooxygenase 2 pathway in human pulmonary artery endothelial cells by silencing adipocyte fatty acid-binding protein. *J Inflamm*. (2017) 14:8. doi: 10.1186/s12950-017-0155-6
2. Maayah ZH, Abdelhamid G, Elshenawy OH, Elsherbeni AA, Althurwi HN, Mcginn E, et al. The role of soluble epoxide hydrolase enzyme on daunorubicin-mediated cardiotoxicity. *Cardiovasc Toxicol*. (2017) 18:268–83. doi: 10.1007/s12012-017-9437-8
3. Park SK, Herrnreiter A, Pfister SL, Gauthier KM, Falck BA, Falck JR, et al. GPR40 is a low affinity epoxyeicosatrienoic acid receptor in vascular cells. *J Biol Chem*. (2018) 293:e20170231. doi: 10.1074/jbc.RA117.001297
4. Huang H, Gao J, Liu P, Zhang S, Shi G, He W, et al. A0996 downregulated serum 14, 15-EET is associated with abdominal aortic calcification in patients with primary aldosteronism. *J Hypertens*. (2018) 36:e112. doi: 10.1097/01.hjh.0000548448.82989.7e
5. Falck JR, Kodela R, Manne R, Atcha KR, Puli N, Dubasi N, et al. 14,15-epoxyeicosa-5,8,11-trienoic acid (14,15-EET) surrogates containing epoxide bioisosteres: influence upon vascular relaxation and soluble epoxide hydrolase inhibition. *J Med Chem*. (2009) 52:5069–75. doi: 10.1021/jm900634w
6. Yang T, Peng R, Guo Y, Shen L, Zhao S, Xu D. The role of 14,15-dihydroxyeicosatrienoic acid levels in inflammation and its relationship to lipoproteins. *Lipids Health Dis*. (2013) 12:151. doi: 10.1186/1476-511X-12-151
7. Dai N, Zhao C, Kong Q, Li D, Cai Z, Wang M. Vascular repair and anti-inflammatory effects of soluble epoxide hydrolase inhibitor. *Exp Ther Med*. (2019) 17:3580–8. doi: 10.3892/etm.2019.7396
8. Lin Y, Xiao-Hui LI, Shi L. Interpretation of the 2017 edition of diagnosis, treatment, and long-term management of Kawasaki disease:a scientific statement for health professionals from the american heart association. *Chin J Pract Pediatr*. (2017) 135:e927–99.
9. Ballegeer M, Looveren KV, Timmermans S, Eggermont M, Libert C. Glucocorticoid receptor dimers control intestinal STAT1 and TNF-induced inflammation in mice. *J Clin Invest*. (2018) 128:3265–79. doi: 10.1172/JCI96636
10. Dai J, Xu LJ, Han GD, Sun HL, Zhu GT, Jiang HT, et al. MicroRNA-125b promotes the regeneration and repair of spinal cord injury through regulation of JAK/STAT pathway. *Eur Rev Med Pharmacol Sci*. (2018) 22:582–9. doi: 10.26355/eurrev_201802_14271
11. Lee Y, Wakita D, Dagvadorj J, Shimada K, Arditi M. IL-1 signaling is critically required in stromal cells in Kawasaki disease vasculitis mouse model: role

of both IL-1α and IL-1β. *Arterioscler Thromb Vasc Biol*. (2015) 35:2605–16. doi: 10.1161/ATVBAHA.115.306475
12. Aeschlimann FA, Yeung RSM. TNF and IL-1 targeted treatment in Kawasaki disease. *Curr Treat Options Rheumatol*. (2016) 2:283–95. doi: 10.1007/s40674-016-0053-8
13. Kandhi S, Zhang B, Froogh G, Qin J, Alruwali N, Le Y, et al. EETs promote hypoxic pulmonary vasoconstriction via constrictor prostanoids. *AJP Lung Cell Mol Physiol*. (2017) 313:L350–9. doi: 10.1152/ajplung.00038.2017
14. Spector AA, Fang X, Snyder GD, Weintraub NL. Epoxyeicosatrienoic acids (EETs): metabolism and biochemical function. *Prog Lipid Res*. (2004) 43:55–90. doi: 10.1016/S0163-7827(03)00049-3
15. Inceoglu B, Schmelzer KR, Morisseau C, Jinks SL, Hammock BD. Soluble epoxide hydrolase inhibition reveals novel biological functions of epoxyeicosatrienoic acids (EETs). *Prostaglandins Other Lipid Mediat*. (2007) 82:42–9. doi: 10.1016/j.prostaglandins.2006.05.004
16. Cheranov SY, Karpurapu M, Wang D, Zhang B, Venema RC, Rao GN. An essential role for SRC-activated STAT-3 in 14,15-EET-induced VEGF expression and angiogenesis. *Blood*. (2008) 111:5581–91. doi: 10.1182/blood-2007-11-126680
17. Luo J, Yao JF, Deng XF, Zheng XD, Jia M, Wang YQ, et al. 14, 15-EET induces breast cancer cell EMT and cisplatin resistance by up-regulating integrin αvβ3 and activating FAK/PI3K/AKT signaling. *J Exp Clin Cancer Res*. (2018) 37:23. doi: 10.1186/s13046-018-0694-6
18. Michaelis UR, Fisslthaler B, Barbosa-Sicard E, Falck JR, Fleming I, Busse R. Cytochrome P450 epoxygenases 2C8 and 2C9 are implicated in hypoxia-induced endothelial cell migration and angiogenesis. *J Cell Sci*. (2005) 118:5489–98. doi: 10.1242/jcs.02674
19. Chen JK, Capdevila J, Harris RC. Heparin-binding EGF-like growth factor mediates the biological effects of P450 arachidonate epoxygenase metabolites in epithelial cells. *Proc Natl Acad Sci USA*. (2002) 99:6029–34. doi: 10.1073/pnas.092671899
20. Nonoyama S. Immunological abnormalities and endothelial cell injury in Kawasaki disease. *Acta Paediatr Jpn*. (2007) 33:752–5. doi: 10.1111/j.1442-200X.1991.tb02604.x
21. Luo P, Wang MH. Eicosanoids, β-cell function, and diabetes. *Prostaglandins Other Lipid Mediat*. (2011) 95:1–10. doi: 10.1016/j.prostaglandins.2011.06.001
22. Moshal KS, Zeldin DC, Sithu SD, Utpal S, Neetu T, Munish K, et al. Cytochrome P450 (CYP) 2J2 gene transfection attenuates MMP-9 via inhibition of NF-kappabeta in hyperhomocysteinemia. *J Cell Physiol*. (2010) 215:771–81. doi: 10.1002/jcp.21356
23. Wang HX, Zeng XJ, Jiang Y, Ling-Qiao LU, Hao G, Zhu YF, et al. Relationship between delayed cardioprotection effect of 11,12-EET and phosphorylated ERK during ischemia and reperfusion in the rat myocardium. *Chin J Pathophysiol*. (2006) 22:2328–31. doi: 10.3321/j.issn:1000-4718.2006.12.008
24. Jiang JX, Zhang SJ, Xiong YK, Jia YL, Sun YH, Lin XX, et al. EETs attenuate Ox-LDL-induced LTB4 production and activity by inhibiting p38 MAPK phosphorylation and 5-LO/BLT1 receptor expression in rat pulmonary arterial endothelial cells. *PLoS ONE*. (2015) 10:e0128278. doi: 10.1371/journal.pone.0128278
25. Yang C, Kwan YW, Au AL, Poon CC, Zhang Q, Chan SW, et al. 14,15-Epoxyeicosatrienoic acid induces vasorelaxation through the prostaglandin EP(2) receptors in rat mesenteric artery. *Prostaglandins Other Lipid Mediat*. (2010) 93:44–51. doi: 10.1016/j.prostaglandins.2010.06.004
26. Carroll MA, Doumad AB, Li J, Cheng MK, Falck JR, Mcgiff JC. Adenosine2A receptor vasodilation of rat preglomerular microvessels is mediated by EETs that activate the cAMP/PKA pathway. *Am J Physiol*. (2006) 291:155–61. doi: 10.1152/ajprenal.00231.2005
27. Rojas S, Martín A, Arranz MJ, Pareto D, Purroy J, Verdaguer E, et al. Imaging brain inflammation with [(11)C]PK11195 by PET and induction of the peripheral-type benzodiazepine receptor after transient focal ischemia in rats. *J Cereb Blood Flow Metab*. (2007) 27:1975–86. doi: 10.1038/sj.jcbfm.9600500.

Conflict of Interest: The authors declare that the research was conducted in the absence of any commercial or financial relationships that could be construed as a potential conflict of interest.

frontiers in Pediatrics

REVIEW
published: 25 August 2020
doi: 10.3389/fped.2020.00493

Insights Into Coronary Artery Lesions in Kawasaki Disease

Danfeng Zhang[1,2], *Lingjuan Liu*[1,2], *Xupei Huang*[3]* *and Jie Tian*[1,2]*

[1] *Ministry of Education Key Laboratory of Child Development and Disorders, Department of Cardiology, National Clinical Research Center for Child Health and Disorders, China International Science and Technology Cooperation Base of Child Development and Critical Disorders, Children's Hospital of Chongqing Medical University, Chongqing, China,* [2] *Chongqing Key Laboratory of Pediatrics, Chongqing, China,* [3] *Department of Biomedical Science, Charles E. Schmidt College of Medicine, Florida Atlantic University, Boca Raton, FL, United States*

This review summarizes recent advances in understanding the development of coronary arteritis in Kawasaki disease. Kawasaki disease is the most common cause of acquired heart disease among children characterized with coronary artery abnormalities, which can cause myocardial ischemia, infarction, and even death. The pathogenic factors of Kawasaki disease and the pathological process of coronary artery disease are not clear at present, which brings challenges to the prevention and treatment of the disease. The treatment of Kawasaki disease focuses mainly on timely administration of intravenous high doses of immunoglobulin and aspirin. However, there are still some patients who do not respond well to this standard treatment, and its management remains a challenge. As a result, coronary artery lesions still occur in patients and affect their quality of life. In this review, we discuss updated research data of Kawasaki disease coronary artery lesions.

Keywords: Kawasaki disease, coronary artery lesions, genetic susceptibility, biomarker, long-term outcomes

OPEN ACCESS

Edited by:
Oswin Grollmuss,
Université Paris-Sud, France

Reviewed by:
Mamoru Ayusawa,
Nihon University Itabashi Hospital, Japan
Hiromichi Hamada,
Tokyo Women's Medical University Yachiyo Medical Center, Japan

***Correspondence:**
Xupei Huang
xhuang@health.fau.edu
Jie Tian
jietian@cqmu.edu.cn

Specialty section:
This article was submitted to Pediatric Cardiology, a section of the journal Frontiers in Pediatrics

Received: *21 November 2019*
Accepted: *14 July 2020*
Published: *25 August 2020*

Citation:
Zhang D, Liu L, Huang X and Tian J (2020) Insights Into Coronary Artery Lesions in Kawasaki Disease. Front. Pediatr. 8:493. doi: 10.3389/fped.2020.00493

INTRODUCTION

The first case of Kawasaki disease (KD) was described in the 1960s, by Tomisaku Kawasaki (he termed it mucocutaneous lymph node syndrome then, and now it is called Kawasaki disease), which is an acute febrile illness, self-limited of unknown etiology, which mainly affects children under 5 years of age, especially those under 3 years of age (1). Coronary artery lesions in Kawasaki disease patients are not initially detected until cardiac complications have been observed in 1–2% of patients. Most of the sudden deaths result from coronary artery occlusion and rupture in patients (6/37) (2–4). A long-term prognosis is measured by the severity of coronary artery lesions. Some patients have a risk of coronary thrombosis and stenosis, leading to ischemia and even sudden death. As a result, Kawasaki disease is now the leading cause of acquired heart disease in developed countries, not rheumatic heart disease (5, 6). Coronary artery lesions have been reduced from 25 to 5% after treatment with intravenous immunoglobulin (IVIG) plus aspirin (7). However, due to different levels of diagnosis and treatment in different regions, treatment delay (i.e., longer than 10 days after fever) may occur, and some patients fail to respond to conventional treatment regimens. These patients have an increased chance of severe coronary artery damage that causes death or requires a heart transplant. Fortunately, randomized controlled clinical trials of IVIG plus steroid or infliximab in primary treatment have shown a significant reduction of this risk (8, 9). Coronary artery is the most frequently involved site in Kawasaki disease (10). The main manifestations include destruction of vessel wall structure, dilation, rupture, stenosis, and even obstruction of the vessels. This review focuses on recent progress related to the understanding of CAL in Kawasaki disease.

EPIDEMIOLOGY OF CAL

The degree of CAL varies from simple dilation to different size and number of aneurysms during the acute phase and even to stenosis or occlusion of the lumen most likely involving the left main coronary artery followed by the right coronary artery in a Chinese study (11).

When intravenous immunoglobulin (IVIG) combined with aspirin is used in the treatment of Kawasaki disease, the incidence rate of CAL decreases significantly. Currently, after initial therapy with IVIG combined with aspirin, coronary artery lesions mainly occur in patients who do not respond to IVIG therapy and are in complete Kawasaki disease (may be due to the delay of treatment) (12, 13).

However, there are regional differences in CAL incidence rates. From 2004 to 2014 in Canada, CAL affected 3.5% of all patients (14). In the United States, 2.25–3.20% of patients with Kawasaki disease suffered from coronary artery aneurysms, but higher in the West (27.1%) (*Z* score) (15, 16). In the United Kingdom, a study shows, from 2013 to 2015, the CAL rate was 19% in all patients (*Z* score) (17). In Australia, a recent study shows the incidence of coronary artery (CA) dilatation is 16.7%, and 6.8% had CA aneurysms based on absolute diameter measurements of coronary arteries (18).

Several studies show a highest incidence among Asian and Pacific islanders (19). In Taiwan, from 1976 to 2007, CAL (based on absolute diameter measurements) were about 20.2–31.5% in Kawasaki patients (20). In Korea, 12.66% of Kawasaki patients showed CAL based on absolute diameter measurements (21). In Shanghai from 2008 through 2012, 15.9% of Kawasaki cases developed CAL defined as dilation or aneurysm (based on absolute diameter measurements) (11). In Japan, a nationwide survey showed about 9.7% of Kawasaki patients experienced acute-phase CAL (based on absolute diameter measurements), and 2.8% experienced CAL in the follow-up procedure (1 month after onset) (coronary dilatation, 1.8%; giant aneurysms, 0.18%; coronary stenosis, 0.02%, and myocardial infarction, 0.004%). Coronary artery lesion varies with gender and age. Men and infants are more prone to coronary artery lesion (22).

In general, the rate of coronary artery lesion in Kawasaki disease varies with different regions and races even in the same region at different times (20), which is probably related to local environment, different diagnostic criteria, and other pathological factors. However, the pathological agents are not identified so far.

PATHOPHYSIOLOGY OF CAL

A sequential model of Kawasaki disease vascular lesions was proposed in the early autopsy results of children who died of Kawasaki disease. This model suggests that neutrophils infiltrate the coronary arteries during the first 1–2 weeks of the disease, and then the neutrophils are replaced by monocytes, and the inflammation subsides automatically within 2 months after fever onset (23). The inflammatory process is manifested as endothelial dysfunction, the destruction of collagen and elastic fibers, and the loss of the structural and functional integrity of damaged coronary arteries, leading to a thickening of the intima, the interruption of laminar flow and blood flow, and thrombosis. However, this does not explain the presence of chronic vascular inflammation in a small number of patients who die months after the onset and subsequent endothelial dysfunction and thickening of the intima (24–26). In 2012, Rowley research group performed a large-sample pathology study that identified necrotizing arteritis, subacute chronic arteritis, and luminal myofibroblast proliferation—three interrelated rather than progressive pathologic processes in Kawasaki disease CAL pathological changes (27). Necrotizing arteritis occurs within 2 weeks of onset and is usually a self-limiting process characterized by infiltration of neutrophils in the vascular wall that begins when endothelial cells are stimulated by inflammatory factors in serum and express adhesion molecules and receptors on the surface of endothelial cells that leads to progressive necrosis of endothelial cells, mediators, and the outer membrane of medium arteries, especially coronary arteries. Subacute chronic arteritis is the infiltration of lymphocytes/macrophages, plasma cells, and eosinophils and can be found in all cases. Takahashi also describes that the inflammatory cells that appear in the coronary arterial lesions are mainly composed of macrophages in all patients. In addition, numerous neutrophils are also identified in the coronary arterial lesions of the patients who died 10 days after the onset of KD (28). However, in some cases (small number), the earliest time is 6 days after the onset, indicating a lack of time continuity. The earliest infiltrating cells cannot be identified. Inflammatory activation of the coronary artery depends on multiple inflammatory pathways, especially pathways associated with activated T lymphocyte function and type I interferon-induced pathways (29). The MMPS family, especially mmp-2 and mmp-9, can cause the destruction of middle structures of the arteries resulting from the degradation associated with CAL (30–32). Subacute chronic vasculitis also occurs in the first 2 weeks and is accompanied by infiltration of other inflammatory cells, involving blood vessels throughout the body, but mainly involving medium-sized arteries, especially coronary arteries. Myofibroblast proliferation is closely related to subacute chronic vasculitis and is a unique process involving the proliferation of myofibroblasts and the accumulation of matrix degradation products that gradually block the arterial lumen. The origin of these myofibroblast-like cells is unknown; one research finds endothelial-mesenchymal transition (EndoMT) can be activated by sera from KD patients, but there is no further study on whether this is related to myofibroblast-like cells (33). Current research in other models suggest that they may originate from multiple sources, including vascular smooth muscle cells by losing differentiation marker smoothelin, perivascular progenitor cells via proliferation, vascular endothelial cells (ECs) through EndoMT, and circulating or adventitial fibroblasts via epithelial-mesenchymal transition (EMT) (34–38). Whether these mechanisms are the same in Kawasaki disease needs further study. The failure to restore normal coronary artery lesions may be due to the persistence of vessel wall inflammation and coronary artery endothelial dysfunction.

These pathological processes are based on autopsy of dead patients or heart transplant patients, which are the most severe

cases and do not fully reflect the whole process of Kawasaki disease coronary artery lesions.

BIOMARKERS FOR DIAGNOSIS OF CAL

At the beginning, echocardiography was not widely used to evaluate coronary artery lesions in patients. Clinicians proposed different scoring systems to evaluate coronary artery lesions in patients with Kawasaki disease according to their characteristics, blood test results, and clinical course. Asai and Kusakawa's scoring system was widely used in the 1970s and 1980s, followed by Harada's in the 1990s. However, the sensitivity and specificity of this score vary from region to region. Currently, the evaluation of coronary artery lesions in Kawasaki disease mainly relies on color Doppler ultrasound, but ultrasound cannot accurately reflect the specific situation of coronary artery damage (39). It is reported that patients with normal ultrasound can still have coronary artery endothelial dysfunction, intima, and media change (40). Accurate diagnosis of coronary artery lesions is the focus of our attention. Biomarkers are necessary to assist in the determination of coronary artery lesions. There are some potential biomarkers of CAL formation (**Table 1**). Plasma clusterin level, NT-proBNP, CRP, and IL-6 are highly suggestive of coronary artery lesions (41, 43, 44). Increased expression of nitric oxide synthase (iNOS) in neutrophils suggests the occurrence of coronary artery lesions in KD patients (42). Kenichi et al. report higher serum sLR11 level may be the biomarker of CAL at the convalescent phase (45). Pi et al. find that 11-DH-TXB2, sP-selectin, IPF, and sCD40L levels are related to the degree of CAL (48). MicroRNA (miRNA) is considered to be one of the most promising biomarker resources in various types of nucleic acid research, including KD (49, 50). Xing et al. and Li et al. show that high levels of mir-92a-3p and miR-182-5p are a high risk factor for the occurrence of CAL (46, 47).

Other studies show that matrix metalloproteinases degrade the extracellular matrix, leading to matrix remodeling. The imbalance of the MMP family is also one of the markers of CAL, especially MMP-9 and MMP-9:MMP-2 (32, 51). Liu et al., using a protein general analysis, found five significantly differentially expressed proteins in patients with CAL, including kininogen 1 (KNG1), complement factor H (CFH), fibronectin 1 (FN1), mannose binding lectin 2 (MBL2), and serpin family C member 1 (SERPINC1). However, these are not specific markers for CAL (52).

A take-home message is that, although variety of biological markers have emerged, no specific biological markers so far are confirmed for the diagnosis and prognosis of the disease because of the lack of multicenter and multispecies clinical data. Although the detection of NT-proBNP and CRP is highly feasible compared to other clinical assays, the sensitivity and specificity are limited.

GENETIC BACKGROUND OF CAL

Kawasaki disease is a disease closely related to genetic susceptibility. However, it is not clear whether there

TABLE 1 | Biomarkers associated with CAL formation.

Biomarker	Clusterin	iNOS	Il-6	CRP	NT-proBNP	sLR11	mir-92a-3p	miR-182-5p	11-DH-TXB2, sP-selectin, IPF, sCD40L
No. of cases	14	24	22	22	197	23	12	11	21
No. of control	33	31	50	50	664	20	18	50	23
Ethnicity	Taiwanese	Japaneses	Indian	Indian	Asian	Japanese	Chinese	Chinese	Chinese
Sensitivity (%)	69.7	NA	81.8	72.7	0.82	NA	81.8	NA	NA
Specificity (%)	64.3	NA	82	74	0.72	NA	66.7	NA	NA
Diagnostic criteria	Absolute diameter	Absolute diameter	Z score	Z score	Absolute diameter and Z score	Absolute diameter	Absolute diameter	Z score	Absolute diameter
Level of evidence	3B	3B	3B	3B	3A	3B	3B	3B	3B
References	Yu et al. (41)	Yu et al. (42)	Nandi and Pal (43)	Nandi and Pal (43)	Zheng et al. (44)	Watanabe et al. (45)	Rong et al. (46)	Li et al. (47)	Pi et al. (48)

TABLE 2 | Genes associated with CAL formation.

Gene	Chromosome Location	Method	Populations	References	Potential mechanism
HLA-B HLA-E	6p21.3	Genotyping Meta-analysis	Chinese, Taiwanese	Lin et al. (53) Xie and Shi (54) Hsieh et al. (55)	Antigen-presentation
ITPKC	19q13.2	Genotyping	Japanese, Taiwanese	Onouchi et al. (56) Kuo et al. (57)	C calcineurin/NFAT pathway
CD40	20q13	Genotyping	Taiwanese	Kuo et al. (58)	Immune activation
HMGB1	13q12.3	Genotyping	Koreans	Ahn et al. (59)	Gene transcription
MICB	6p21.3	TaqMan Allelic Discrimination assay	Taiwanese	Hsieh et al. (60)	Antigen-presentation
CASP3	4q34-35	Genotyping, Two-locus gene model	Japanese, Taiwanese	Onouchi et al. (61) Kuo et al. (57)	Gene transcription
KCNN2	5q22.3	GWAS	Koreans	Kim et al. (62)	Potassium mediators/small conductance calcium activation channels
FCGR2A	1q23.3	Genotyping	Japanese	Taniuchi et al. (63)	Signal transmission
Il-10	1q32.1	Genotyping	Han Chinese, Taiwanese, Koreans	Lin et al. (64)	NA
ITPR3	6p21.3	Genotyping	Taiwanese	Huang et al. (65)	innate immune responses
MMP	11q22.2	Genotyping	Japanese, Euro-Americans, Koreans	Ikeda et al. (66) Shimizu et al. (67) Park and Shin (68)	Inflammation and Tissue remodeling
TGF-βR2	3p24.1	Direct sequencing	Koreans	Choi et al. (69)	TGF-β pathway
PELI1	2p13.3	GWAS	Koreans, Taiwanese	Kim et al., (62)	TLR signaling

is a correlation between coronary artery lesions and genetic polymorphism.

Based on several genome-wide association studies (GWAS) and other gene polymorphism studies, the data suggest that CAL formation in KD is related to various genetic factors, such as HLA-E, HLA-B, CD40, FCGR2A, HMGB1, MICB, PELI1, ITPKC, CASP3, MMP (MMP-3, MMP-13), IL-10, ITPR3, and so on (**Table 2**) (53–59, 61, 63–68). Onouchi et al. identify a functional SNP (rs28493229) in the ITPKC gene on chromosome 19q13.2 that may be significantly correlated with the progression of CAL through the Ca2+/NFAT signaling pathway as a negative regulator of T-cell activation but only in Japanese and Caucasian populations. CD40 can activate both humoral and cellular immunity by stimulating antigen-presenting cells and vascular endothelial cells. Kuo et al. indicate that the genetic polymorphisms of CD40 (rs4810485) are involved in CAL of KD in a Taiwanese population. A Korean GWAS study showed that the functional SNP (rs17136627) of a KCNN2 gene that plays a role in potassium mediators/small conductance calcium activation channels in KD patients without CAL and in patients with medium or giant aneurysms is closely related to the development of severe CAL (70). Kuo et al. find that gene combinations [LOC100133214 (rs2517892) and IL2RA(rs3118470)] influence CAL in 384 SNPs (71). The TGF-βsignaling pathway may play an important role in EMT and pro-inflammatory cell infiltration in CAL formation (72). Shimizu et al., using a candidate gene approach, find variants in genes in the transforming growth factor (TGF)-β signaling pathway (TGFβ2, TGFβR2, and SMAD3) are associated with the *Z* scores of CAL in patients of Euro-Americans and Koreans (69, 73).

Although there are lots of genomic-based studies, the limitation of these studies is obvious because these studies receive data based on local population, small sample size, and different definitions of CAL. Furthermore, how to relate these genomic data with phenotype analyses is still a challenge. More studies with different populations are needed in the future.

IMMUNE MECHANISMS OF CAL

Kawasaki disease is an inflammation of blood vessels throughout the body. Abnormal activation of the immune system is an important link in the development of coronary artery lesions.

The innate immune system (cellular and humoral) is involved in the disease in an early stage characterized by the production of numerous neutrophils, majority γδT cells, pathogen-associated molecular patterns (PAMPs), the elevated levels of damage-associated molecular patterns (DAMPs), and circulating inflammatory cytokines, such as interleukin (IL) 1, IL-6, and tumor necrosis factor -α (TNF-α) in the acute stage (74–76). Meanwhile, the intestinal mucosal permeability and sIgA are closely related to vasculitis in a KD animal model (77). A CAWS-induced model indicates that NLRP3 in BMDCs are important for vasculitis formation (78). The markers associated with antigen presentation (CD74, CD1c, CD20, TLR7) and activated myeloid dendritic cells are significantly elevated in coronary tissue (79, 80).

TABLE 3 | Drugs that can reduce the occurrence or severity of CAL plus with immunoglobulin.

Drug	Study design	Populations	Sample size	References	*P*-value
Cyclosporine	Randomized controlled trial	Japanese	175	Hamada et al. (89)	$p = 0.010$
Avastatin	Prospective	Americans	NA	Tremoulet et al. (9)	Under way
Infliximab	Randomized controlled trial	Americans	196	Tremoulet et al. (9)	$P = 0.045$
Prednisolone	Randomized controlled trial	Japanese	248	Kobayashi et al. (8)	$P < 0.0001$

The activation of the adaptive immune system appears in the later stage of the disease, mainly as the increase of regulatory T-cells, and memory T- and memory B-cells. The self-limited nature of the disease coupled with a low rate of recurrence and the presence of oligo-clonal IgA implies that Kawasaki disease is associated with a super-antigen rather than with a conventional antigen. In the animal model of Kawasaki disease, vasculitis induced by LCWE, CD8+ T-cells, rather than CD4+ T-cells, NK T-cells, or TReg cells, is an important factor in the production of CAL (81). Interestingly, in patients with CAL, CD40L was highly expressed in CD4+ T-cells and platelets although there was no significant difference between CD8+ T-cells and serum (82). As a distinct subset of CD4+ T-cells, Tfh 1 (follicular T helper) cells in the CALs+ group were significantly lower. In contrast, cTfh2 cells in the CALs+ group significantly increased (83).

The immunological responses vary with different pathological conditions. It is understandable that the different studies mentioned above produced different results, which are probably due to the different animal models used and the different disease stages applied in the studies. As for why the immune response is focused on the vascular wall in KD, no studies have been proposed so far, which may be related to the vascularity of related antigens.

DIAGNOSIS AND TREATMENT OF CAL

The American Heart Association scientific statement in 2004 and Japanese guidelines in 2008 classify abnormality using *Z* score ($\geq$2.5) but aneurysms by absolute dimensions (6, 84). AHA classified aneurysms based on *Z* scores until 2017 (CAl: *Z* score $>$ 2 or a decrease in *Z* score $\geq$ 1 during follow-up) (85). There are seven systems to calculate *Z* score; these systems differ by age range, race, the formula used to calculate BSA, and the regression method used for analysis. Canadian subjects by Dallaire and Japanese subjects by Kobayashi are more rigorous than others (86, 87). The *Z*-score is better than the absolute dimensions in assessing the severity of coronary artery dilatation in proximal segments (88), but the left circumflex branch is not available. Because of the limitation of ultrasound, computed-tomographic angiography, cardiac magnetic resonance imaging, and invasive angiography can be used when necessary.

Currently, the main method of KD therapy is intravenous immunoglobulin (IVIG) combined with aspirin, which can effectively reduce systemic inflammatory response but has no direct effect on endothelial cells. Based on the understanding of genetic influences on CAL susceptibility, A clinical trial in Japan has found cyclosporine, which can block the calcineurin-NFAT pathway, can significantly reduce the incidence of CAL (12/86 patients vs. 27/87 patients) at higher risk for IVIG resistance (89). Avastatin can inhibit regular T-cell function, endothelial/epithelial mesenchymal transformation, and the abnormal expression of MMPS, and now, a Phase I/IIa clinical trial is currently underway (90). In addition, low-density lipoprotein can lower cholesterol, and the pleiotropic effects of statins in endothelial cells can improve endothelial cellular function, decreasing oxidative stress and alleviating inflammation (91). Infliximab (a TNFα receptor blocker) cannot reduce the incidence of CAL; however, it can effectively alleviate the progression of CAL during the follow-up (9, 92). In one study, prednisolone reduces the incidence of CAL in patients who are not responding to IVIG (3% vs. 23%) (8).

Although there have been some positive results (**Table 3**), existing experiments have been limited to a specific population, and further studies are needed to determine whether they are effective in other populations. In addition, how to accurately predict the occurrence of IVIG resistance and CAL is the premise of the use of these protocols since the use of additional treatment is unnecessary in low-risk patients.

LONG-TERM OUTCOMES

Kato et al. followed up 598 patients for 10 to 21 years. Most of the patients (55%) with small or medium-sized coronary artery aneurysms returned to normal luminal dimension 6 to 18 months later, but some patients developed stenosis and MI. Those without CAL did not show abnormalities in the ultrasound follow-up (93). A follow-up of more than 10 years of coronary angiography revealed that, although some small and medium aneurysms returned to normal size, there was still morphological and vascular dysfunction, and there was no vascular dysfunction during follow-up in patients without CAL in the acute phase (94). After the death from KD (with or without CAL in the acute phase), chronic inflammation can be found in coronary artery pathological sections. It has been reported that, in Kawasaki disease patients, long-term isotope nuclear imaging can show high metabolism in the coronary site (95). Non-invasive assessment of arterial structure and function in 60 patients at least 2 years after KD, 60 patients with or without CAL, presented a high risk of cardiovascular disease, including increased aortic IMT and carotid distensibility (96, 97). Other studies have shown that the segmental thickening of the intima can be found in the degraded coronary aneurysm after IVUS check, and even no CAL in the acute phase (98). Recent

studies have reported new aneurysm onset or further expansion in the late period, and one patient without CAL died 3 years after the onset, probably due to coronary artery disease (99, 100). The prognosis of CAL mainly depends on the degree of stenosis of the lumen, but due to the limitations of coronary angiography and autopsy, the incidence of it in follow-up data is insufficient. In patients, intimal thickening with calcification in coronary aneurysm segment detected by intravascular ultrasound in Kawasaki disease outbreak a few years later are similar to adult coronary atherosclerosis change (101).

Coronary artery lesions are a chronic process, and it is necessary to have a careful follow-up study to observe patients because some vascular dysfunction can occur later even when coronary aneurysm disappears. In some cases, no CAL was found in the acute phase, which suggests, in general, a good prognosis. However, a long-term cardiovascular risk is still possible. It is difficult to make it clear because the follow-up data so far are limited to monitoring the middle age and aging patients with a high incidence of cardiovascular disease.

CONCLUSION

Kawasaki disease was considered to be a self-limited disease in the past. However, according to the abovementioned information, we can find that coronary artery lesions in Kawasaki disease are a chronic process, and there are still abnormalities in the coronary artery structure or function during convalescence. For the treatment of Kawasaki disease, especially for the treatment of coronary artery lesions, more studies are needed on the mechanisms underlying the occurrence of coronary artery lesions, which can provide us with information regarding precise molecular targets of intervention. Follow-up is an important part of the CAL long-term outcome, which mainly relies on the echocardiogram. However, echocardiograph examination has its limitations that cannot accurately assess CAL. Thus, more specific and sensitive coronary artery lesion biomarkers and advanced imaging technology should be useful and helpful. So far, the long-term follow-up data are still scarce. Therefore, performing long-term follow-up observation of Kawasaki disease and collecting data from follow-up in the future is crucial for us to have a deeper understanding of this disease.

AUTHOR CONTRIBUTIONS

DZ contributed to conception and wrote the first draft of the manuscript. All authors contributed to manuscript revision, read, and approved the submitted version.

REFERENCES

1. Kawasaki T. Acute febrile mucocutaneous syndrome with lymphoid involvement with specific desquamation of the fingers and toes in children (in Japanese). *Arerugi.* (1967) 16:178–222.
2. Yanagisawa M, Kobayashi N. Myocardial infarction due to coronary thromboarteritis, following acute febrile mucocutaneous lymph node syndrome (MLNS) in an infant. *Pediatrics.* (1974) 54:277–80.
3. Amano S, Hazama F. Pathology of Kawasaki disease: I pathology and morphogenesis of the vascular changes. *Jap Circul J.* (1979) 43:633–43. doi: 10.1253/jcj.43.633
4. Amano S, Hazama F. Pathology of Kawasaki disease: II distribution and incidence of the vascular lesions. *Jap Circul J.* (1979) 43:741–8. doi: 10.1253/jcj.43.741
5. Akagi T, Rose V, Benson LN, Newman A, Freedom RM. Outcome of coronary artery aneurysms after Kawasaki disease. *J Pediatr.* (1992) 121(Pt. 1):689–94. doi: 10.1016/S0022-3476(05)81894-3
6. Newburger JW, Takahashi M, Gerber MA, Gewitz MH, Tani LY, Burns JC, et al. Diagnosis, treatment, and long-term management of Kawasaki disease: a statement for health professionals from the Committee on Rheumatic Fever, Endocarditis and Kawasaki Disease, Council on Cardiovascular Disease in the Young, American Heart Association. *Circulation.* (2004) 110:2747–71. doi: 10.1161/01.CIR.0000145143.19711.78
7. Furusho K, Kamiya T, Nakano H, Kiyosawa N, Shinomiya K, Hayashidera T, et al. High-dose intravenous gammaglobulin for Kawasaki disease. *Lancet.* (1984) 2:1055–8. doi: 10.1016/S0140-6736(84)91504-6
8. Kobayashi T, Saji T, Otani T, Takeuchi K, Nakamura T, Arakawa H, et al. Efficacy of immunoglobulin plus prednisolone for prevention of coronary artery abnormalities in severe Kawasaki disease (RAISE study): a randomised, open-label, blinded-endpoints trial. *Lancet.* (2012) 379:1613–20. doi: 10.1016/S0140-6736(11)61930-2
9. Tremoulet AH, Jain S, Jaggi P, Jimenez-Fernandez S, Pancheri JM, Sun X, et al. Infliximab for intensification of primary therapy for Kawasaki disease: a phase 3 randomised, double-blind, placebo-controlled trial. *Lancet.* (2014) 383:1731–8. doi: 10.1016/S0140-6736(13)62298-9
10. Yonesaka S, Takahashi T, Eto S, Sato T, Otani K, Ueda T, et al. Biopsy-proven myocardial sequels in Kawasaki disease with giant coronary aneurysms. *Cardiol Young.* (2010) 20:602–9. doi: 10.1017/S1047951109991132
11. Chen JJ, Ma XJ, Liu F, Yan WL, Huang MR, Huang M, et al. Epidemiologic features of Kawasaki disease in Shanghai from 2008. through 2012. *Pediatr Infect Dis J.* (2016) 35:7–12. doi: 10.1097/INF.0000000000000914
12. Türkuçar S, Yildiz K, Acari C, Dundar HA, Kir M, Ünsal E. Risk factors of intravenous immunoglobulin resistance and coronary arterial lesions in Turkish children with Kawasaki disease. *Turkish J Pediatr.* (2020) 62:1–9. doi: 10.24953/turkjped.2020.01.001
13. Xie T, Wang Y, Fu S, Wang W, Xie C, Zhang Y, et al. Predictors for intravenous immunoglobulin resistance and coronary artery lesions in Kawasaki disease. *Pediatr Rheumatol Online J.* (2017) 15:17. doi: 10.1186/s12969-017-0149-1
14. Manlhiot C, O'Shea S, Bernknopf B, LaBelle M, Chahal N, Dillenburg RF, et al. Epidemiology of Kawasaki Disease in Canada 2004 to 2014: comparison of surveillance using administrative data vs periodic medical record review. *Can J Cardiol.* (2018) 34:303–9. doi: 10.1016/j.cjca.2017.12.009
15. Okubo Y, Nochioka K, Sakakibara H, Testa M, Sundel RP. National survey of pediatric hospitalizations due to Kawasaki disease coronary artery aneurysms in the USA. *Clinical Rheumatol.* (2017) 36:413–19. doi: 10.1007/s10067-016-3512-6
16. Dominguez SR, Anderson MS, El-Adawy M, Glodé MP. Preventing coronary artery abnormalities: a need for earlier diagnosis and treatment of Kawasaki disease. *Pediatr Infect Dis J.* (2012) 31:1217–20. doi: 10.1097/INF.0b013e318266bcf9
17. Tulloh RMR, Mayon-White R, Harnden A, Ramanan AV, Tizard EJ, Shingadia D, et al. Kawasaki disease: a prospective population survey in the UK and Ireland from 2013 to (2015). *Arch Dis Child.* (2019) 104:640–46. doi: 10.1136/archdischild-2018-315087
18. Saundankar J, Yim D, Itotoh B, Payne R, Maslin K, Jape G, et al. The epidemiology and clinical features of Kawasaki disease in Australia. *Pediatrics.* (2014) 133:e1009–14. doi: 10.1542/peds.2013-2936
19. Skochko SM, Jain S, Sun X. Kawasaki disease outcomes and response to therapy in a multiethnic community: a 10-year experience. *J Pediatr.* (2018) 203:408–15. doi: 10.1016/j.jpeds.2018.07.090

20. Lue HC, Chen LR, Lin MT, Chang LY, Wang JK, Lee CY, et al. Epidemiological features of Kawasaki disease in Taiwan, 1976-2007: results of five nationwide questionnaire hospital surveys. *Pediatr Neonatol.* (2014) 55:92–6. doi: 10.1016/j.pedneo.2013.07.010
21. Kim GB, Park S, Eun LY, Han JW, Lee SY, Yoon KL, et al. Epidemiology and clinical features of Kawasaki disease in South Korea, 2012-2014. *Pediatr Infect Dis J.* (2017) 36:482–5. doi: 10.1097/INF.0000000000001474
22. Makino N, Nakamura Y, Yashiro M, Ae R, Tsuboi S, Aoyama Y, et al. Descriptive epidemiology of Kawasaki disease in Japan,2011–2012: From the results of the 22nd nationwide survey. *J Epidemiol.* (2015) 25:239–45. doi: 10.2188/jea.JE20140089
23. Amano S, Hazama F, Kubagawa H, Tasaka K, Haebara H, Hamashima Y. General pathology of Kawasaki disease on the morphological alterations corresponding to the clinical manifestations. *Acta Pathol Japonica.* (1980) 30:681–94. doi: 10.1111/j.1440-1827.1980.tb00966.x
24. Tacke CE, Kuipers IM, Groenink M, Spijkerboer AM, Kuijpers TW. Cardiac magnetic resonance imaging for noninvasive assessment of cardiovascular disease during the follow-up of patients with Kawasaki disease. *Circ Cardiovasc Imaging.* (2011) 4:712–20. doi: 10.1161/CIRCIMAGING.111.965996
25. Cicala S, Pellegrino T, Storto G, Caprio MG, Paladini R, Mainolfi C, et al. Noninvasive quantification of coronary endothelial function by SPECT imaging in children with a history of Kawasaki disease. *Eur J Nucl Med Mol Imaging.* (2010) 37:2249–55. doi: 10.1007/s00259-010-1575-1
26. Dhillon R, Clarkson P, Donald AE, Powe AJ, Nash M, Novelli V, et al. Endothelial dysfunction late after Kawasaki disease. *Circulation.* (1996) 94:2103–06. doi: 10.1161/01.CIR.94.9.2103
27. Takahashi K, Oharaseki T, Naoe S, Wakayama M, Yokouchi Y. Neutrophilic involvement in the damage to coronary arteries in acute stage of Kawasaki disease. *Pediatr Int.* (2005) 47:305–10. doi: 10.1111/j.1442-200x.2005.02049.x
28. Orenstein JM, Shulman ST, Fox LM, Baker SC, Takahashi M, Bhatti TR, et al. Three linked vasculopathic processes characterize Kawasaki disease: a light and transmission electron microscopic study. *PloS ONE.* (2012) 7:e38998. doi: 10.1371/journal.pone.0038998
29. Rowley AH, Wylie KM, Kim KY, Pink AJ, Yang A, Reindel R, et al. The transcriptional profile of coronary arteritis in Kawasaki disease. *BMC Genomics.* (2015) 16:1076. doi: 10.1186/s12864-015-2323-5
30. Korematsu S, Ohta Y, Tamai N, Takeguchi M, Goto C, Miyahara H, et al. Cell distribution differences of matrix metalloproteinase-9 and tissue inhibitor of matrix metalloproteinase-1 in patients with Kawasaki disease. *Pediatr Infect Dis J.* (2012) 31:973–4. doi: 10.1097/INF.0b013e31825ba6b3
31. Gavin PJ, Crawford SE, Shulman ST, Garcia FL, Rowley AH. Systemic arterial expression of matrix metalloproteinases 2 and 9 in acute Kawasaki disease. *Arterioscler Thromb Vasc Biol.* (2003) 23:576–81. doi: 10.1161/01.ATV.0000065385.47152.FD
32. Kuo HC, Li SC, Huang LH, Huang YH. Epigenetic hypomethylation and upregulation of matrix metalloproteinase 9 in Kawasaki disease. *Oncotarget.* (2017) 8:60875–91. doi: 10.18632/oncotarget.19650
33. He M, Chen Z, Martin M, Zhang J, Sangwung P, Woo B, et al. miR-483 targeting of CTGF suppresses endothelial-to-mesenchymal transition: therapeutic implications in Kawasaki disease. *Circ. Res.* (2017) 120:354–65. doi: 10.1161/CIRCRESAHA.116.310233
34. Sartore S, Chiavegato A, Faggin E, Franch R, Puato M, et al. Contribution of adventitial fibroblasts to neointima formation and vascular remodeling: from innocent bystander to active participant. *Circul Res.* (2001) 89:1111–21. doi: 10.1161/hh2401.100844
35. Kramann R, Schneider RK, DiRocco DP, Machado F, Fleig S, Bondzie PA, et al. Perivascular Gli1+ progenitors are key contributors to injury-induced organ fibrosis. *Cell Stem Cell.* (2015) 16:51–66. doi: 10.1016/j.stem.2014.11.004
36. Mack M. Origin of myofibroblasts and cellular events triggering fibrosis. *Kidney Int.* (2015) 87:297–307. doi: 10.1038/ki.2014.287
37. Meng XM, Wang S, Huang XR, Yang C, Xiao J, Zhang Y, et al. Inflammatory macrophages can transdifferentiate into myofibroblasts during renal fibrosis. *Cell Death Dis.* (2016) 7:e2495. doi: 10.1038/cddis.2016.402
38. Christen T, Verin V, Bochaton-Piallat M, Popowski Y, Ramaekers F, Debruyne P, et al. Mechanisms of neointima formation and remodeling in the porcine coronary artery. *Circulation.* (2001) 103:882–8. doi: 10.1161/01.CIR.103.6.882
39. Tsuda E. Role of imaging studies in Kawasaki disease. *Int J Rheum Dis.* (2018) 21:56–63. doi: 10.1111/1756-185X.13210
40. Chen KY, Curtis N, Dahdah N, Kowalski R, Cheung M, Burgner DP. Kawasaki disease and cardiovascular risk: a comprehensive review of subclinical vascular changes in the longer term. *Acta Paediatr.* (2016) 105:752–61. doi: 10.1111/apa.13367
41. Yu HR, Kuo HC, Huang EY, Liang CD, Hwang KP, Lin IC, et al. Plasma clusterin levels in predicting the occurrence of coronary artery lesions in patients with Kawasaki disease. *Pediatr Cardiol.* (2010) 31:1151–56. doi: 10.1007/s00246-010-9769-7
42. Yu X, Hirono KI, Ichida F, Uese K, Rui C, Watanabe S, et al. Enhanced iNOS expression in leukocytes and circulating endothelial cells is associated with the progression of coronary artery lesions in acute Kawasaki disease. *Pediatr Res.* (2004) 55:688–94. doi: 10.1203/01.PDR.0000113464.93042.A4
43. Nandi A, Pal P. A comparison of serum IL6 and CRP levels with respect to coronary changes and treatment response in Kawasaki disease patients: a prospective study. *Rheumatol Int.* (2019) 39:1797–801. doi: 10.1007/s00296-019-04375-9
44. Zheng X, Zhang Y, Liu L, Yue P, Wang C, Zhou K, et al. N-terminal pro-brain natriuretic peptide as a biomarker for predicting coronary artery lesion of Kawasaki disease. *Sci Rep.* (2020) 10:5130. doi: 10.1038/s41598-020-62043-6
45. Watanabe K, Suzuki H, Jiang M, Haniu H, Numano F, Hoshina S, et al. Soluble LR11 is a novel biomarker for vascular lesions late after Kawasaki disease. *Atherosclerosis.* (2016) 246:94–7. doi: 10.1016/j.atherosclerosis.2015.12.035
46. Rong X, Jia L, Hong L, Pan L, Xue X, Zhang C, et al. Serum miR-92a-3p as a new potential biomarker for diagnosis of Kawasaki disease with coronary artery lesions. *J Cardiovasc Transl Res.* (2017) 10:1–8. doi: 10.1007/s12265-016-9717-x
47. Li SC, Huang LH, Chien KJ, Pan CY, Lin PH, Lin Y, et al. MiR-182-5p enhances *in vitro* neutrophil infiltration in Kawasaki disease. *Mol Genet Genom Med.* (2019) 7:e990. doi: 10.1002/mgg3.990
48. Pi L, Che D, Long H, Fang Z, Li J, Lin S, et al. Immature platelets and antiplatelet therapy response to aspirin in Kawasaki disease. *Drug Design Dev Ther.* (2018) 12:1353–62. doi: 10.2147/DDDT.S163705
49. Kuo HC, Hsieh KS, Ming-Huey Guo M, Weng KP, Ger LP, Chan WC, et al. Next-generation sequencing identifies micro-RNA-based biomarker panel for Kawasaki disease. *J Allergy Clin Immunol.* (2016) 138:1227–30. doi: 10.1016/j.jaci.2016.04.050
50. Su YJ, Lin IC, Wang L, Lu CH, Huang YL, Kuo HC. Next generation sequencing identifies miRNA-based biomarker panel for lupus nephritis. *Oncotarget.* (2018) 9:27911–19. doi: 10.18632/oncotarget.25575
51. Sakata K, Hamaoka K, Ozawa S, Niboshi A, Yahata T, Fujii M, et al. Matrix metalloproteinase-9 in vascular lesions and endothelial regulation in Kawasaki disease. *Circ J.* (2010) 74:1670–75. doi: 10.1253/circj.CJ-09-0980
52. Liu W, Liu C, Zhang L, Xie X, Gu X, Sang C, et al. Molecular basis of coronary artery dilation and aneurysms in patients with Kawasaki disease based on differential protein expression. *Mol Med Rep.* (2018) 17:2402–14. doi: 10.3892/mmr.2017.8111
53. Lin YJ, Wan L, Wu JY, Sheu JJ, Lin CW, Lan YC, et al. HLA-E gene polymorphism associated with susceptibility to Kawasaki disease and formation of coronary artery aneurysms. *Arthritis Rheumat.* (2009) 60:604–10. doi: 10.1002/art.24261
54. Xie X, Shi X. The roles of genetic factors in Kawasaki disease: a systematic review and meta-analysis of genetic association studies. *Pediatr Cardiol.* (2018) 39:207–25. doi: 10.1007/s00246-017-1760-0
55. Hsieh YY, Lin YJ, Chang CC, Chen DY, Hsu CM, Wang YK, et al. Human lymphocyte antigen B-associated transcript 2, 3, and 5 polymorphisms and haplotypes are associated with susceptibility of Kawasaki disease and coronary artery aneurysm. *J Clin Lab Anal.* (2010) 24:262–8. doi: 10.1002/jcla.20409
56. Onouchi Y, Gunji T, Burns JC, Shimizu C, Newburger JW, Yashiro M, et al. ITPKC functional polymorphism associated with Kawasaki disease susceptibility and formation of coronary artery aneurysms. *Nat Genet.* (2008) 40:35–42. doi: 10.1038/ng.2007.59

57. Kuo HC, Hsu YW, Wu CM, Chen SH, Hung KS, Chang WP, et al. A replication study for association of ITPKC and CASP3 two-locus analysis in IVIG unresponsiveness and coronary artery lesion in Kawasaki disease. *PloS ONE.* (2013) 8:e69685. doi: 10.1371/journal.pone.0069685
58. Kuo HC, Chao MC, Hsu YW, Lin YC, Huang YH, Yu HR, et al. CD40 Gene polymorphisms associated with susceptibility and coronary artery lesions of Kawasaki disease in the Taiwanese population. *Sci World J.* (2012) 2012:520865. doi: 10.1100/2012/520865
59. Ahn JG, Bae Y, Shin D, Nam J, Kim KY, Kim DS. HMGB1 gene polymorphism is associated with coronary artery lesions and intravenous immunoglobulin resistance in Kawasaki disease. *Rheumatology.* (2019) 58:770–5. doi: 10.1093/rheumatology/key356
60. Hsieh YY, Chang CC, Hsu CM, Chen SY, Lin WH, Tsai FJ. Major histocompatibility complex class I chain-related gene polymorphisms: associated with susceptibility to Kawasaki disease and coronary artery aneurysms. *Genet Test Mol Biomark.* (2011) 15:755–63. doi: 10.1089/gtmb.2011.0001
61. Onouchi Y, Suzuki Y, Suzuki H, Terai M, Yasukawa K, Hamada H, et al. ITPKC and CASP3 polymorphisms and risks for IVIG unresponsiveness and coronary artery lesion formation in Kawasaki disease. *Pharmacogenomics J.* (2013) 13:52–9. doi: 10.1038/tpj.2011.45
62. Kim JJ, Hong YM, Sohn S, Jang GY, Ha KS, Yun SW, et al. A genome-wide association analysis reveals 1p31 and 2p13.3 as susceptibility loci for Kawasaki disease. *Hum Genet.* (2011) 129:487–95. doi: 10.1007/s00439-010-0937-x
63. Taniuchi S, Masuda M, Teraguchi M, Ikemoto Y, Komiyama Y, Takahashi H, et al. Polymorphism of Fc gamma RIIa may affect the efficacy of gamma-globulin therapy in Kawasaki disease. *J Clin Immunol.* (2005) 25:309–13. doi: 10.1007/s10875-005-4697-7
64. Lin YJ, Lan YC, Lai CH, Lin TH, Huang SM, Liao CC, et al. Association of promoter genetic variants in interleukin-10 and Kawasaki disease with coronary artery aneurysms. *J Clin Lab Anal.* (2014) 28:461–4. doi: 10.1002/jcla.21710
65. Huang YC, Lin YJ, Chang JS, Chen SY, Wan L, Sheu JJ, et al. Single nucleotide polymorphism rs2229634 in the ITPR3 gene is associated with the risk of developing coronary artery aneurysm in children with Kawasaki disease. *Int J Immunogenet.* (2010) 37:439–43. doi: 10.1111/j.1744-313X.2010.00943.x
66. Ikeda K, Ihara K, Yamaguchi K, Muneuchi J, Ohno T, Mizuno Y, et al. Genetic analysis of MMP gene polymorphisms in patients with Kawasaki disease. *Pediatr Res.* (2008) 63:182–5. doi: 10.1203/PDR.0b013e31815ef224
67. Shimizu C, Matsubara T, Onouchi Y, Jain S, Sun S, Nievergelt CM, et al. Matrix metalloproteinase haplotypes associated with coronary artery aneurysm formation in patients with Kawasaki disease. *J Hum Genet.* (2010) 55:779–84. doi: 10.1038/jhg.2010.109
68. Park JA, Shin KS. Polymorphism of matrix metalloproteinase-3 promoter gene as a risk factor for coronary artery lesions in Kawasaki disease. *J Korean Med Sci.* (2005) 20:607–11. doi: 10.3346/jkms.2005.20.4.607
69. Choi YM, Shim KS, Yoon KL, Han MY, Cha SH, Kim SK, et al. Transforming growth factor beta receptor II polymorphisms are associated with Kawasaki disease. *Korean J Pediatr.* (2012) 55:18–23. doi: 10.3345/kjp.2012.55.1.18
70. Kim JJ, Park YM, Yoon D, Lee KY, Seob Song M, Doo Lee H, et al. Identification of KCNN2 as a susceptibility locus for coronary artery aneurysms in Kawasaki disease using genome-wide association analysis. *J Hum Genet.* (2013) 58:521–5. doi: 10.1038/jhg.2013.43
71. Kuo HC, Chang JC, Guo MM, Hsieh KS, Yeter D, Li SC, et al. Gene-gene associations with the susceptibility of Kawasaki disease and coronary artery lesions. *PloS ONE.* (2015) 10:e0143056. doi: 10.1371/journal.pone.0143056
72. Shimizu C, Oharaseki T, Takahashi K, Kottek A, Franco A, Burns JC. The role of TGF-β and myofibroblasts in the arteritis of Kawasaki disease. *Hum Pathol.* (2013) 44:189–98. doi: 10.1016/j.humpath.2012.05.004
73. Shimizu C, Jain S, Davila S, Hibberd ML, Lin KO, Molkara D, et al. Transforming growth factor-beta signaling pathway in patients with Kawasaki disease. *Circ Cardiovasc Genet.* (2011) 4:16–25. doi: 10.1161/CIRCGENETICS.110.940858
74. Furukawa S, Matsubara T. Mononuclear cell subsets and coronary artery lesions in Kawasaki disease. *Arch Dis Child.* (1992) 67:706–8. doi: 10.1136/adc.67.6.706
75. Armaroli G, Verweyen E, Pretzer C, Kessel K, Hirono K, Ichida F, et al. Monocyte-derived interleukin-1β as the driver of S100A12-induced sterile inflammatory activation of human coronary artery endothelial cells: implications for the pathogenesis of Kawasaki disease. *Arthritis Rheumatol.* (2019) 71:792–804. doi: 10.1002/art.40784
76. Hara T, Nakashima Y, Sakai Y, Nishio H, Motomura Y, Yamasaki S. Kawasaki disease: a matter of innate immunity. *Clin Exp Immunol.* (2016) 186:134–43. doi: 10.1111/cei.12832
77. Noval Rivas M, Wakita D, Franklin MK, Carvalho TT, Abolhesn A, Gomez AC, et al. Intestinal permeability and IgA provoke immune vasculitis linked to cardiovascular inflammation. *Immunity.* (2019) 51:508–21.e6. doi: 10.1016/j.immuni.2019.05.021
78. Anzai F, Watanabe S, Kimura H, Kamata R, Karasawa T, Komada T, et al. Crucial role of NLRP3 inflammasome in a murine model of Kawasaki disease. *J Mol Cell Cardiol.* (2020) 138:185–96. doi: 10.1016/j.yjmcc.2019.11.158
79. Cameron SA, White SM, Arrollo D, Shulman ST, Rowley AH. Arterial immune protein expression demonstrates the complexity of immune responses in Kawasaki disease arteritis. *Clin Exp Immunol.* (2017) 190:244–50. doi: 10.1111/cei.13010
80. Yilmaz A, Rowley A, Schulte DJ, Doherty TM, Schröder NW, Fishbein MC, et al. Activated myeloid dendritic cells accumulate and co-localize with CD3+ T cells in coronary artery lesions in patients with Kawasaki disease. *Exp Mol Pathol.* (2007) 83:93–103. doi: 10.1016/j.yexmp.2007.01.007
81. Noval Rivas M, Lee Y, Wakita D, Chiba N, Dagvadorj J, Shimada K, et al. CD8+ T cells contribute to the development of coronary arteritis in the lactobacillus casei cell wall extract-induced murine model of Kawasaki disease. *Arthritis Rheumatol.* (2017) 69:410–21. doi: 10.1002/art.39939
82. Wang CL, Wu YT, Liu CA, Lin MW, Lee CJ, Huang LT, et al. Expression of CD40 ligand on CD4+ T-cells and platelets correlated to the coronary artery lesion and disease progress in Kawasaki disease. *Pediatrics.* (2003) 111:E140–7. doi: 10.1542/peds.111.2.e140
83. Xu M, Jiang Y, Wang J, Liu D, Wang S, Yi H, et al. Distribution of distinct subsets of circulating T follicular helper cells in Kawasaki disease. *BMC Pediatr.* (2019) 19:43. doi: 10.1186/s12887-019-1412-z
84. JCS Joint Working Group. Guidelines for diagnosis and management of cardiovascular sequelae in Kawasaki disease (JCS 2008): digest version. *Circ J.* (2010) 74:1989–2020. doi: 10.1253/circj.CJ-10-74-0903
85. McCrindle BW, Rowley AH, Newburger JW, Burns JC, Bolger AF, Gewitz M, et al. Diagnosis, treatment, and long-term management of Kawasaki disease: a scientific statement for health professionals from the American Heart Association. *Circulation.* (2017). 135:e927–99. doi: 10.1161/CIR.0000000000000484
86. Kobayashi T, Fuse S, Sakamoto N, Mikami M, Ogawa S, Hamaoka K, et al. Z Score project investigators. A new Z score curve of the coronary arterial internal diameter using the lambda mu sigma method in a pediatric population. *J Am Soc Echocardiogr.* (2016) 29:794–801. doi: 10.1016/j.echo.2016.03.017
87. Dallaire F, Dahdah N. New equations and a critical appraisal of coronary artery Z scores in healthy children. *J Am Soc Echocardiogr.* (2011) 24:60–74. doi: 10.1016/j.echo.2010.10.004
88. Burns JC, Franco A. The immunomodulatory effects of intravenous immunoglobulin therapy in Kawasaki disease. *Expert Rev Clin Immunol.* (2015) 11:819–25. doi: 10.1586/1744666X.2015.1044980
89. Hamada H, Suzuki H, Onouchi Y, Ebata R, Terai M, Fuse S, et al. Efficacy of primary treatment with immunoglobulin plus ciclosporin for prevention of coronary artery abnormalities in patients with Kawasaki disease predicted to be at increased risk of non-response to intravenous immunoglobulin (KAICA): a randomised controlled, open-label, blinded-endpoints, phase 3 trial. *Lancet.* (2019) 393:1128–37. doi: 10.1093/rheumatology/kez063.031
90. Tremoulet AH, Jain S, Burns JC. Evaluating a novel treatment for coronary artery inflammation in acute Kawasaki disease: a phase I/IIa trial of atorvastatin. *Expert Opin Orphan Drugs.* (2015) 3:967–70. doi: 10.1517/21678707.2015.1066246
91. Liao JK, Laufs U. Pleiotropic effects of statins. *Annu Rev Pharmacol Toxicol.* (2005) 45:89–118. doi: 10.1146/annurev.pharmtox.45.120403.095748

92. Dionne A, Burns JC, Dahdah N, Tremoulet AH, Gauvreau K, de Ferranti SD, et al. Treatment intensification in patients with Kawasaki disease and coronary aneurysm at diagnosis. *Pediatrics.* (2019) 143:e20183341. doi: 10.1542/peds.2018-3341
93. Kato H, Sugimura T, Akagi T, Sato N, Hashino K, Maeno Y, et al. Long-term consequences of Kawasaki disease A 10- to 21-year follow-up study of 594 patients. *Circulation.* (1996) 94:1379–85. doi: 10.1161/01.CIR.94.6.1379
94. Iemura M, Ishii M, Sugimura T, Akagi T, Kato H. Long term consequences of regressed coronary aneurysms after Kawasaki disease: vascular wall morphology and function. *Heart.* (2000) 83:307–11. doi: 10.1136/heart.83.3.307
95. Kakimoto N, Suzuki H, Kubo T, Suenaga T, Takeuchi T, Shibuta S, et al. Evaluation of coronary arterial lesions due to Kawasaki disease using optical coherence tomography. *Can J Cardiol.* (2014) 30:956.e7-9. doi: 10.1016/j.cjca.2014.04.028
96. Chen KY, Zannino D, Curtis N, Cheung M, Burgner D. Increased aortic intima-media thickness following Kawasaki disease. *Atherosclerosis.* (2017) 260:75–80. doi: 10.1016/j.atherosclerosis.2017.03.022
97. Gopalan K, Singh S, Vignesh P, Gupta A, Rohit M, Attri SV. Carotid intima-media thickness and lipid profile in children with Kawasaki disease: a single-center follow-up study after a mean duration of 69 years. *J Clin Rheumatol.* (2018) 24:385–9. doi: 10.1097/RHU.0000000000000754
98. Hamaoka A, Niboshi A, Ozawa S, Tamiya H, Ito H, Shiraishi I, et al. Linear shadows inside coronary arterial lesions on two-dimensional echocardiograhpy in Kawasaki disease patients. *J Cardiol.* (2009) 53:349–54. doi: 10.1016/j.jjcc.2008.12.011
99. Ozawa J, Suzuki H, Hasegawa S, Numano F, Haniu H, Watanabe K, et al. Two cases of new coronary aneurysms that developed in the late period after Kawasaki disease. *Pediatr Cardiol.* (2013) 34:1992–5. doi: 10.1007/s00246-012-0543-x
100. Holve TJ, Patel A, Chau Q, Marks AR, Meadows A, Zaroff JG. Long-term cardiovascular outcomes in survivors of Kawasaki disease. *Pediatrics.* (2014) 133:e305–11. doi: 10.1542/peds.2013-1638
101. Mitani Y, Ohashi H, Sawada H, Ikeyama Y, Hayakawa H, Takabayashi S, et al. *In vivo* plaque composition and morphology in coronary artery lesions in adolescents and young adults long after Kawasaki disease: a virtual histology-intravascular ultrasound study. *Circulation.* (2009) 119:2829–2836. doi: 10.1161/CIRCULATIONAHA.108.818609

Conflict of Interest: The authors declare that the research was conducted in the absence of any commercial or financial relationships that could be construed as a potential conflict of interest.

frontiers in Pediatrics

MINI REVIEW
published: 24 September 2020
doi: 10.3389/fped.2020.526969

Cardiovascular Involvement in Kawasaki Disease Is Much More Than Mere Coronary Arteritis

Rakesh Kumar Pilania[1], *Ankur Kumar Jindal*[1], *Dharmagat Bhattarai*[1], *Sanjeev Hanumantacharya Naganur*[2] *and Surjit Singh*[1]*

[1] *Allergy Immunology Unit, Department of Paediatrics, Advances Paediatrics Centre, Post Graduate Institute of Medical Education and Research, Chandigarh, India,* [2] *Department of Cardiology, Advances Cardiac Centre, Post Graduate Institute of Medical Education and Research, Chandigarh, India*

Kawasaki disease (KD) is now a common cause of acquired heart disease in children. Coronary artery involvement is the most serious complication in children with KD. Several non-coronary complications have now been identified in this condition but these are often overlooked. Myocarditis is an integral component of KD and may be more common than coronary artery abnormalities. Pericardial involvement and valvular abnormalities have also been observed in patients with KD. KD shock syndrome is now being increasingly recognized and may be difficult to differentiate clinically from toxic shock syndrome. Endothelial dysfunction has been reported both during acute stage and also on follow-up. This may be a potentially modifiable cardiovascular risk factor.

Keywords: cardiac biomarkers, echocardiography, Kawasaki disease, Kawasaki disease shock syndrome, myocarditis, pericarditis

OPEN ACCESS

Edited by:
Xupei Huang,
Florida Atlantic University,
United States

Reviewed by:
Hiromichi Hamada,
Tokyo Women's Medical University
Yachiyo Medical Center, Japan
Moshe Arditi,
Cedars Sinai Medical Center,
United States
Chisato Shimizu,
University of California, San Diego,
United States

***Correspondence:**
Surjit Singh
surjitsinghpgi@rediffmail.com

Specialty section:
This article was submitted to Pediatric Cardiology, a section of the journal Frontiers in Pediatrics

Received: *15 January 2020*
Accepted: *25 August 2020*
Published: *24 September 2020*

Citation:
Pilania RK, Jindal AK, Bhattarai D, Naganur SH and Singh S (2020) Cardiovascular Involvement in Kawasaki Disease Is Much More Than Mere Coronary Arteritis. Front. Pediatr. 8:526969. doi: 10.3389/fped.2020.526969

INTRODUCTION

Kawasaki disease (KD) is one of the commonest vasculitides in children (1, 2). At time of its first recognition in 1967 by Dr. Tomisaku Kawasaki, it was described as "*mucocutaneous lymph node syndrome*" and was considered as a benign disease with self-limiting course (3). However, autopsy studies later revealed the coronary artery complications associated with KD (4). Over time, it has now been realized that KD may cause several other cardiac complications as well (5, 6) (**Table 1**). It has been shown that myocarditis in KD is, in fact, more common than coronary artery involvement and may be almost universal (7). In this review, we have discussed various non-coronary cardiac complications in patients with KD.

MYOCARDITIS

Myocarditis appears to be an integral part of KD and may be seen in all patients (7, 8). Fujiwara et al. in 1978 have reported autopsy studies on 20 patients with KD (4). The authors classified pathology of KD into four clinico-pathological stages and noted pancarditis on histology. In the first 9 days of illness, predominant finding was carditis associated with edema and inflammatory cell infiltrate in all three layers of heart (4). Yutani et al. have performed right ventricular biopsy in 201 patients with KD after periods ranging from 1 month to 11 years of diagnosis of KD (9). They showed that myocarditis and fibrotic changes were seen in all patients. Sequelae of myocarditis were evident even during follow-up (9). Similarly, Yonesaka et al. have performed subendocardial myocardial biopsies and showed that findings of myocyte disarray, interstitial

TABLE 1 | Cardiovascular complications of Kawasaki disease (KD).

S. no	Complication
1.	Coronary artery abnormalities (dilatation, aneurysm)
2.	Coronary artery aneurysms and thrombosis
3.	Coronary stenosis
4.	Coronary calcification
5.	Myocarditis
6.	Myocardial infarction
7.	Kawasaki disease shock syndrome
8.	Pericarditis, pericardial effusion and cardiac tamponade
9.	Cardiac fibrosis
10.	Cardiomyopathy
11.	Endothelial dysfunction
12.	Systemic artery aneurysms

fibrosis and myocardial cell degeneration persist in patients with KD on follow-up (10). Necropsies have shown that patients with KD developed diffuse myocardial fibrosis and increased expression of transforming growth factor (TGF)-β in wall of coronary artery aneurysm (11). These studies help explain the pathogenesis of myocardial fibrosis/cardiomyopathy in children with KD on follow-up (9–12).

In 1995, Anderson et al. had published the long term effects of KD on cardiac function in 67 patients. Authors performed serial M-mode echocardiograms at baseline, 1–3, 3–12 months, and after 1 year of diagnosis. This study showed that left atrial and left ventricular dimensions continued to be abnormal in more than 50% of patients even 1 year after KD. Fractional shortening was abnormal initially but normalized at 3 months of follow-up. Left ventricular emptying was significantly reduced. Moreover, almost a third of patients evaluated beyond 1 year had diastolic dysfunction. This was amongst the first few studies showing that patients with KD had abnormalities in cardiac functions even in absence of CAAs (13).

Nakaoka et al. have recently reported on cardiac function in patients with KD having asymptomatic coronary artery disease by cardiac magnetic resonance (CMR) imaging. It was found that transmural extent of late gadolinium enhancement in this subgroup was ≤50% and these patients had subendocardial infarction with normal left ventricular function (14).

Pathophysiology

KD myocarditis often develops as a result of acute or subacute inflammation of interstitial tissue of myocardium and is usually concentrated around the coronaries. Myocardial inflammation peaks by day 10 of illness and gradually subsides by end of 3 weeks. During this stage, there is inflammation of small arteries of the myocardium including perivasculitis. Inflammation in interstitial tissue of the myocardium develops as a result of spill of inflammatory cells from perivasculitis. This explains prompt recovery of myocardial function following administration of intravenous immunoglobulin (IVIg) in these patients. Pathophysiology of KD myocarditis, therefore, differs in several aspects from viral myocarditis. While viral myocarditis is characterized by predominant lymphocytic interstitial cell infiltrates, edema and myocyte or myocardial fiber bundle necrosis, KD myocarditis on other hands is characterized by myocardial interstitial edema, vasodilatation and inflammatory cell infiltration. Severe myocarditis in patents with KD can manifest independent of coronary artery involvement. Rarely, patents with KD and severe inflammatory myocardial inflammation can have degenerative changes resulting in cardiomyopathy (8, 15, 16).

Clinical Characteristics

Myocarditis, which is one of the earliest presentations of KD, usually presents within first 10 days of illness in contrast to coronary artery vasculitis and coronary artery abnormalities (CAAs) that usually develop after day 10 of illness (8, 15). Audible gallop, tachycardia and hyperdynamic precordium are the subtle clinical correlates of KD myocarditis. Strain abnormalities and evidence of systolic and diastolic dysfunction are correlates of KD myocarditis on echocardiography (8).

Asymptomatic Myocarditis

Myocarditis in patients with KD is often asymptomatic and can easily be missed (6, 8).

Symptomatic Myocarditis

Myocarditis in KD can present clinically as unexplained tachycardia, congestive cardiac failure, hemodynamic instability, requirement of inotropic support and arrhythmias (17–23). Symptomatic myocarditis remains a significant cause of morbidity and mortality during the initial phase of the KD (15, 24–26).

Viral Myocarditis vs. KD Associated Myocarditis

Myocarditis of KD needs to be differentiated from viral myocarditis:

- Viral myocarditis generally follows a prodrome and at time of clinical presentation patients are usually afebrile. Myocarditis in KD develops in the early phase of disease and is usually accompanied by high grade fever (8).
- Myocardial dysfunction in KD is usually transient and responds dramatically to anti-inflammatory therapy with intravenous immunoglobulin (IVIg) (8, 15). Response to IVIg in viral myocarditis is, at best, modest (27, 28).
- The pathological changes in KD largely consist of interstitial edema and inflammatory cell infiltrate, while in viral myocarditis cell necrosis is the predominant finding (15).

Biomarkers for Myocarditis

Several biomarkers have been proposed in patients with KD to evaluate myocardial dysfunction and injury. The biomarker that has shown clinical promise is N-terminal pro B-type natriuretic peptide (NT-proBNP) (8, 29, 30).

NT-proBNP

In response to volume and pressure cardiac overload, pre-pro-BNP is synthesized and processed to pro-BNP. Pro-BNP is then

processed to biologically active BNP fragment, and NT-pro-BNP which is inert. NT-ProBNP is preferred to BNP as a biomarker for laboratory assays as it has a longer half-life. Synthesis of pro-BNP from cardiac myocytes is controlled by many factors including mechanical factors like dilatation and strain of cardiac chambers, various neurohormonal factors and cytokines (e.g., interleukin-1 β or tumor necrosis factor α). Interpretation of pro-BNP levels is difficult as it can be affected by several factors other than myocardial damage. Pro-BNP levels are age dependent and are highest in infancy and early childhood (31). Presence of acute kidney injury and decreased glomerular filtration is also associated with falsely elevated pro-BNP levels (30). Several studies have found NT-ProBNP to be a useful marker for diagnosis as well as for assessment of disease severity in KD (29, 32, 33). Age specific cut-off values have been calculated and Z scores are also available for assessment of elevated levels of pro-BNP (29, 31). Reddy et al. have assayed levels of pro-BNP during the acute stage of KD. The authors reported that levels above 1025 pg/ml have a specificity of 96% and sensitivity of 88% for diagnosis of KD (33).

Studies have shown a positive correlation of NT-pro-BNP with C-reactive protein and hypoalbuminemia in children with KD during initial phase of disease. NT-pro-BNP levels are significantly raised during the acute phase of KD when compared to controls (32, 34). Levels of NT-pro-BNP showed negative correlation with left ventricular (LV) ejection fraction, fractional shortening, cardiac index values, diastolic function and positive correlation with impairment in ventricular relaxation (32, 34).

NT-pro-BNP is a valuable assessment tool in clinical evaluation of patients with incomplete forms of KD (29, 35, 36). Dionne et al. have proposed a diagnostic algorithm based on NT-pro-BNP. This is very useful in patients with incomplete forms of KD (29).

Cardiac Troponins

Serum cardiac troponins are superior to creatine kinase (CK)-MB for detection of myocardial damage in myocarditis (37). Kim et al. have compared cardiac troponin I and CK-MB levels in 45 patients with KD. Authors showed that levels of cardiac troponin I were elevated in 18 (40%) patients, while CK-MB levels were elevated in 11 (24%) patients (38).

Sato et al. have measured cardiac troponin by a highly sensitive assay and shown that cardiac troponin levels are elevated in 1/3rd of children with KD during the acute phase. These levels may continue to remain elevated during the convalescent phase as well (34). However, levels of cardiac troponin have very weak correlation with NT-pro-BNP and there was no significant correlation with systolic or diastolic function or CAAs in patients with KD (34). Checchia et al. have shown that elevation of cardiac troponin I in patients with KD was not significant and there was no significant correlation with development of CAAs (39).

Other Cardiac Biomarkers

Soluble suppression of tumorigenicity-2 (ST2) belongs to the IL-1 receptor family. It is released by cardiomyocytes and fibroblasts during stress phase of KD myocarditis. It has been reported to be positively correlated with impairment of ventricular relaxation in patients with KD (27). Gamma-glutamyl transferase and alanine transferase, however, have not been found to be useful in establishing a clinical diagnosis of KD (40).

Imaging in Myocarditis

Echocardiographic Features

2D-echocardiography remains the mainstay of imaging for cardiovascular assessment in KD both during acute phase and long-term follow-up (1, 2, 36, 41, 42). It cannot be overemphasized that cardiac assessment in patients with KD is just not limited to coronary artery assessment and detailed cardiac assessment for ventricular functions, wall motion abnormalities, valvular functions, and pericardial effusion need to be performed as well (**Figure 1**). Traditional echocardiographic evaluation of KD myocarditis by M mode includes parameters for left ventricular systolic dysfunction and left ventricular dilatation. The diastolic function of the heart is assessed by inflow parameters across both atrio-ventricular valves by pulse wave doppler and tissue doppler.

Myocarditis is universal in almost all patients with KD during the acute phase of disease. Transient left ventricular dysfunction can occur in more than 50% patients (43). Newburger et al. showed that left ventricular dysfunction in patients with KD appears unrelated to development of CAAs (44). Normal systolic function is restored after recovery from acute illness in most of the patients with KD. However, diastolic dysfunction has also been found in many studies. Therefore, ventricular function assessment should be an integral part of echocardiographic evaluation in children with KD. This should include assessment of regional wall motion abnormalities that are often a surrogate marker for coronary artery involvement (1, 41).

Speckle tracking echocardiography (STE) is a sensitive tool that can accurately detect myocardial strain and can quantify myocardial function with high reproducibility. More sensitive measures of myocardial deformation, such as *global longitudinal strain*, *circumferential strain*, and *strain rate* have been reported to be decreased in KD (45). Strain abnormalities in patients with KD have been seen even in absence of apparent systolic function abnormalities.

Xu et al. have shown that left ventricular systolic strain decreased significantly in children with KD during acute phase of disease. However, it improved rapidly after IVIg therapy and normalized by 6–8 weeks (46). Regional left ventricular strain was found to be impaired in basal infero-septal, basal anterolateral, apical septal, and apical inferior segments in patients with KD during midterm follow up when compared with controls (47). Left atrial strain is a well-recognized surrogate marker for raised left ventricular end diastolic pressure and left ventricular diastolic dysfunction. Lower values of left atrial strain have been reported during the acute stage in KD and this may improve during follow-up (48). Studies have reported correlation between depressed strain and disease severity (49, 50). Strain imaging may also be useful during follow-up of these patients (51). Newburger et al. showed that velocity of circumferential fiber shortening corrected for wall stress, was reduced in patients with KD during and up to 3 months after acute illness and improved spontaneously by 1 year (44).

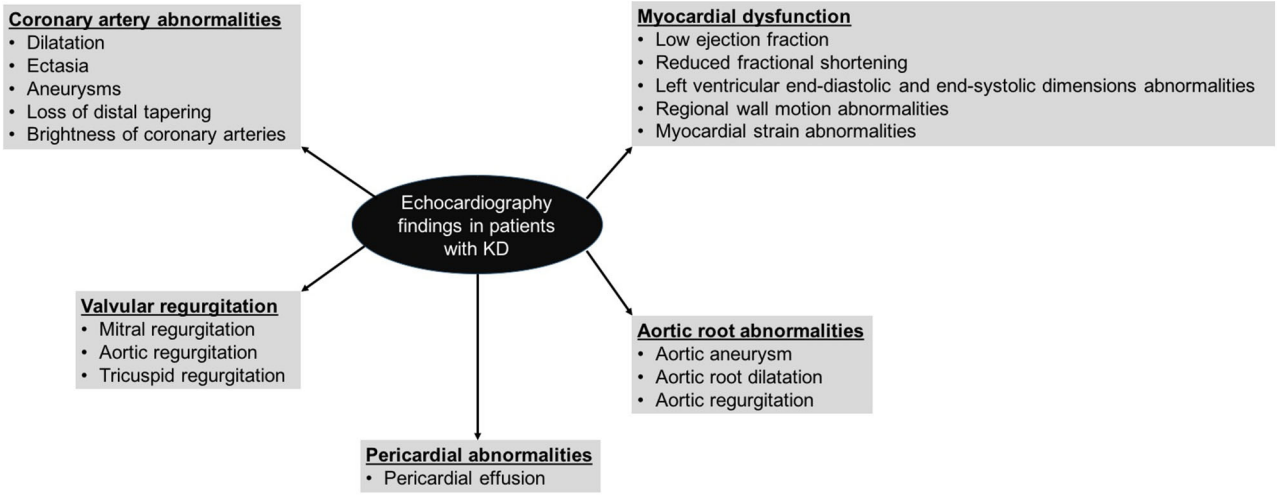

FIGURE 1 | Echocardiography findings in patients with Kawasaki disease.

Dedeoglu et al. have evaluated myocardial deformation at 6 months follow-up and measured global as well as regional myocardial strain by STE and showed impaired left ventricular strain in patients with KD in basal and apical segments. However, there was no association between LV dysfunction and CAAs (47). Wang et al. compared STE findings in patients with IVIg resistant KD and IVIg responsive patients with KD. It was found that the former had more severe ventricular dysfunction (52).

To conclude, mere assessment of "Z" scores of coronary arteries in children with KD is not enough. Attempts should be made to look for abnormalities of myocardial function. It is also apparent that myocardial dysfunction in KD can occur independent of coronary artery involvement.

Other Imaging Modalities

There are several inherent limitations associated with 2D-echocardiography. It is highly observer dependent and the results are not always reproducible (36, 41). Studies using nuclear scans have shown that myocardial inflammation can be seen in more than 50% of patients. We have published our experience on exercise myocardial perfusion scintigraphy on 84 patients with KD at least 1 month after onset of illness (53). In this study, 12 (14.3%) patients showed reversible perfusion defects and these can be seen even in patients with no demonstrable CAAs on echocardiography (53).

Tacke et al. have evaluated cardiac function in children with KD at follow-up and showed that there was no significant difference in cardiac function and fibrosis in patients with KD compared to controls while using CMR at long-term follow-up (54). In a more recent study, Bratis et al. have reported LV myocardial deformation indices using CMR and found that there was reduced myocardial strain values during the convalescent phase and this was irrespective of coronary artery involvement (55). Clearly, we need more studies to fully comprehend the residual effects of KD on the myocardium.

ECG Features

Several conduction and repolarization abnormalities have been reported in patients with KD. These include non-specific ST and T-wave changes, PR interval prolongation, QT dispersion abnormalities and arrhythmias. In presence of severe myocarditis/pericarditis, low voltage complexes, and symptomatic arrhythmias may be seen (56–58). Bifid T-wave in limb leads have also been noted during the acute phase of KD (59). QT dispersion abnormalities may persist for several months (56, 57). Persistence of repolarization abnormalities in follow-up may indicate higher risk of ventricular arrhythmia during follow-up of patients with KD even in absence of obvious echocardiographic abnormalities (60).

Long Term Complications of Myocarditis

In conclusion, while it is likely that most children with KD myocarditis would remain well on follow-up and attain normal systolic function, a few patients may go on to develop myocardial dysfunction, fibrosis, myocardial infarction later in life. Further, these manifestations may occur even in patients who have had no obvious CAAs (7, 8, 11).

KD SHOCK SYNDROME (KDSS)

KDSS is said to be occur when a patient with clinical diagnosis of KD develops systolic hypotension or shock. Although shock during acute stage of KD was recognized more than two decades ago (61–63), Kanegaye et al. defined KDSS for the first time in 2009 (64). In this study, hemodynamic instability was observed in 13/187 (7%) patients with KD (64). Since then, this entity has been reported from several centers across the world (65–67). These patients are often misdiagnosed as toxic shock syndrome (TSS) and this led to delays in institution of appropriate therapy (66, 67). KDSS is usually seen in older children and is more commonly reported in boys (66, 68, 69), although some studies

have also noted a female predominance (70). Some authorities believe that KDSS may, in fact, be a unique subtype of KD (65). KDSS still remains an under-recognized complication (71).

The etiopathogenesis of KDSS remains poorly understood. It involves a combination of myocardial dysfunction (secondary to myocarditis) and distributive shock (caused by increased vascular permeability which is secondary to dysregulated cytokine storm) (8, 66, 72).

Patients with KDSS have been reported to have increased incidence of gastrointestinal manifestations, hyponatremia, anemia, thrombocytopenia, hypoalbuminemia, elevated inflammatory markers (e.g., neutrophila, high CRP, ESR), IVIg resistance, CAAs (up to 65%), morbidity and mortality (up to 6.8%) (65, 68, 69, 73). In addition, levels of several cytokines (e.g., TNF-α, interferon-γ) are found to be elevated in patients with KDSS (74). Whether these biomarkers can be considered for early diagnosis of KDSS remains conjectural.

How Does One Differentiate Between TSS and KDSS?

The clinical presentation of KDSS and TSS may appear similar and it may be very difficult to differentiate the two conditions at bedside. Lin et al. retrospectively analyzed 16 patients with KDSS and 17 patients with TSS (69). It was found that patients with KDSS were usually younger and had less prominent gastrointestinal symptoms. While anemia and thrombocytosis were more commonly seen in patients with KD, lymphopenia was characteristic of TSS. Further, CAAs and valvular abnormalities were seen only in KDSS (69, 75).

Hyper-Inflammatory Syndrome Associated With COVID-19—A Novel Syndrome

Severe acute respiratory syndrome coronavirus 2 (SARS-CoV-2) infection has rapidly spread worldwide since it was first identified in Wuhan, China in November 2019. Initial reports suggested that SARS-CoV-2 causes milder disease in children. However, by late April 2019 a hyper-inflammatory syndrome had been identified (76). This was characterized by high grade persistent fever and multisystemic clinical manifestations suggesting a delayed hyperimmune response to SARS-CoV-2 infection. This novel syndrome has been variably termed as "multisystem inflammatory disorder in children and adolescents," "multisystem inflammatory syndrome in children (MIS-C)," "pediatric inflammatory multisystem syndrome temporally associated with SARS-CoV-2 (PIMS-TS)" (77). Clinical features of this syndrome include cardiovascular collapse (e.g., hypotension, myocarditis, and myocardial dysfunction), predominant gastrointestinal symptoms (e.g., diarrhea, vomiting, and pain abdomen), features similar to KD (e.g., rash, conjunctival injection, and extremity changes), and neurological manifestations (e.g., headache, irritability, and encephalopathy). Reported data suggest that patients with MIS-C are usually older, have predominant gastrointestinal manifestations (some may present with acute surgical abdomen) and have myocardial dysfunction. Clinical findings in this syndrome may mimic those of KDSS and TSS (77–79). MIS-C and KD are probably two distinct entities as they have differences in demographic, laboratory and clinical findings (80, 81). Whittaker et al. have compared patients with PIMS-TS with KD, KDSS and TSS (82). Authors reported that patients with PIMS-TS are older than the ones in latter three categories. Further, patients with PIMS-TS were found to have higher inflammatory markers, more pronounced lymphopenia, and higher levels of troponins and NT-pro-BNP (82).

PERICARDITIS

Pericarditis is a common but an under-reported manifestation in patients with KD. Gowin et al. (83) reported pericarditis in 6/30 (20%) patients while Hamza et al. (84) found pericardial involvement in 7.8% of patients with KD.

Pericardial involvement is usually mild and not clinically significant. Septate pericarditis (85) and tamponade (86–88) that may occasionally be fatal has also been reported. Cardiac tamponade may be a component of polyserositis syndrome in patients with KD or may follow rupture of one of the coronary artery aneurysms in the pericardial cavity (89). While polyserositis leading to tamponade would manifest during the acute stage, tamponade caused by rupture of aneurysm may appear at any time (90, 91) and may even manifest several years after acute KD (92). Printz et al. reported transient pericardial effusion in 3% patients of KD and it resolved by 5 weeks (93).

Mild pericarditis may resolve with IVIg and aspirin. Patients with more severe forms of pericarditis may require additional immunomodulatory therapy (94). Cardiac tamponade from coronary artery aneurysmal rupture may require urgent pericardial window and emergency coronary artery bypass grafting (89, 90).

VALVULAR ABNORMALITIES

Valvular regurgitation in acute phase has been ascribed to pancarditis, while patients having persistent valvular abnormalities are likely to have valvular dysfunction and papillary muscle dysfunction due to coronary ischemia (95). Myocardial inflammation can lead to valvular regurgitation. The most common abnormality is mitral regurgitation (MR) during acute phase of KD—this usually resolves on follow-up. It is seen commonly in patients with KD who have wall motion abnormalities or reduced ejection fraction (1, 8, 41, 93, 96). Some patients can go on to develop severe MR due to rupture of chorda tendinae. This complication may result in rapid clinical deterioration and even fatalities if not recognized and treated in time (97–99) Cardiac auscultation is, therefore, very important in patients with KD especially during the convalescent phase. Aortic regurgitation (AR) has also been reported (100, 101).

de La Harpe et al. have recently published 30 years of experience in KD and showed that 20% of patients in their cohort had valvular involvement and of these 88% had mitral valve dysfunction (96). Printz et al. have prospectively performed 2D-echocardiogtaphy on 198 patients with KD at baseline, 1 and 5 weeks of onset of illness (93). They showed that

27% of patients with KD had mild mitral regurgitation at baseline echocardiography during acute phase. Although MR had resolved significantly on follow-up at 5 weeks, 9% patients continued to have residual valvular dysfunction (93). It has, therefore, been suggested that Doppler evaluation should be a part of echocardiography evaluation in children with KD for assessment of valvular regurgitation abnormalities.

AORTIC ROOT INVOLVEMENT

KD is a systemic vasculitis and affects several non-coronary arteries in the body. Aortic root dilatation during acute stage of KD has been reported in up to 10% patients with KD (93). Ravekes et al. assessed aortic root abnormalities in patients with KD (102). Aortic root diameters were assessed during mid-systole and at four different time points (i.e., within first 10 days, at 2, 6 weeks, and 1 year). It was observed that aortic root diameters were significantly higher as compared to controls. A significant increase in aortic root diameter was noted at 2 weeks of follow-up. Subsequently, no significant increase in aortic root diameter was noted at 6 weeks and at 1 year follow-up but the aortic root continued to remain dilated (102). Printz et al. reported aortic root dilatation at baseline, at 1 week and at 5 weeks in patients with KD (93). These authors did not report any significant change in aortic root diameters when assessed at different time intervals. Size of aortic root was found to correlate with coronary artery diameters but not with inflammatory parameters. Both studies used body surface area adjusted Z scores for assessment of aortic root diameter. AR was reported in 1–4% patients and was more common at 1 year of follow-up. Patients with AR may require valve replacement later in life (62, 103).

Increase in stiffness of aorta and decrease in elasticity has also been reported by several authors leading to functional impairment of aorta. This has been observed both during the acute stage and several years after the diagnosis of KD (104–106).

SYSTEMIC ARTERY INVOLVEMENT

Kato et al. first time performed angiography studies in patients with KD and revealed that 13/594 (2.2%) patients had systemic artery aneurysm (SAAs) in addition to CAAs (107). It was reported that SAAs were present only in patients who had multiple giant CAAs. Since than there have been reports of SAAs involving large arteries (e.g., iliac, femoral, subclavian, axillary). Recently Zhao et al. have reported full-body magnetic resonance angiography (MRA) or peripheral angiography in patients with KD for identification of SAAs (108). MRA ($n = 110$) was performed in patients with KD who had presumed risk factors for SAAs (e.g., patients having giant coronary aneurysm, increasing size aneurysm during acute phase or IVIg resistant KD). Peripheral angiography ($n = 52$) was performed along with CT coronary angiography in patients with giant or medium sized coronary aneurysms. Authors reported that 23/162 (14.2%) patients with KD having CAAs had SAAs, while overall prevalence was 23/1148 (2%). Most commonly affected arteries were axillary and common iliac. Risk factors for development of SAAs were young age and pronged fever (108). It appears that KD may also have a component of systemic vasculitis but this needs more detailed evaluation (107–109).

ENDOTHELIAL DYSFUNCTION IN PATIENTS WITH KD

Endothelial dysfunction in KD often goes unrecognized. It is attributed to release of pro-inflammatory mediators that lead to production of reactive oxygen species. Brachial artery flow mediated dilatation (FMD) evaluation is a reliable marker for endothelial dysfunction. FMD depicts the capacity of brachial artery to increase its diameter in response to increase in blood flow. Studies have shown endothelial dysfunction of brachial artery in patients with KD that may persist even a decade after the acute stage (105, 110–115). Dietz et al. has observed the increased stiffness index patients with KD and CAAs (116). These abnormalities have also been reported in patients who have no obvious CAAs detected during acute stage of KD (117). Pulse wave velocity (PWV) is also a simple and non-invasive tool for assessment of arterial stiffness. Studies have shown that PWV is higher in patients with history of KD as compared to controls (118). Carotid intima-media thickness (cIMT), well-recognized as a surrogate marker for atherosclerosis, has been found to be significantly higher in children with KD on follow-up. These studies emphasize the need for long-term follow-up of children with KD even in situations wherein there have been no CAAs (116, 119–122).

It is conjectural whether endothelial dysfunction correlates with occurrence of CAAs (123–126). Patients with KD and CAAs have been reported to have an increased risk of myocardial infarction and early deaths (11, 116, 127–130). Recent literature has, however, suggested that long term cardiovascular morbidity in patients with KD may not only be restricted to patients who have been detected to have CAAs (11, 131). Autopsy studies have demonstrated luminal myofibroplastic proliferation in both aneurysmal as well as non-aneurysmal coronary arteries (16). Therefore, it is prudent to counsel patients with KD with regard to modifiable cardiovascular risk factors.

To conclude, it is clear that KD is associated with several cardiovascular sequelae. While CAAs are the most well-recognized complications of this condition, other affectations like myocarditis, KDSS, valvular abnormalities, and endothelial dysfunction are now being increasingly recognized. Early identification and appropriate treatment of these complications is of paramount importance.

AUTHOR CONTRIBUTIONS

RP and AJ: writing of initial draft of manuscript, editing and revision of manuscript at all stages of its production, and review of literature. DB and SN: contributed to editing of manuscript and review of literature. SS: inception of idea, critically revision of the manuscript at all stages of its production, final approval of manuscript, and review of literature. All authors contributed to the article and approved the submitted version.

REFERENCES

1. McCrindle BW, Rowley AH, Newburger JW, Burns JC, Bolger AF, Gewitz M, et al. Diagnosis, treatment, and long-term management of Kawasaki disease: a scientific statement for health professionals from the American Heart Association. *Circulation.* (2017) 135:e927–9. doi: 10.1161/CIR.0000000000000484
2. Singh S, Jindal AK, Pilania RK. Diagnosis of Kawasaki disease. *Int J Rheum Dis.* (2018) 21:36–44. doi: 10.1111/1756-185X.13224
3. Kawasaki T. Acute febrile mucocutaneous syndrome with lymphoid involvement with specific desquamation of the fingers and toes in children. *Arerugi Allergy.* (1967) 16:178–222.
4. Fujiwara H, Hamashima Y. Pathology of the heart in Kawasaki disease. *Pediatrics.* (1978) 61:100–7.
5. Kato H. Cardiovascular complications in Kawasaki disease: coronary artery lumen and long-term consequences. *Prog Pediatr Cardiol.* (2004) 19:137–45. doi: 10.1016/j.ppedcard.2004.08.007
6. Jindal AK, Pilania RK, Prithvi A, Guleria S, Singh S. Kawasaki disease: characteristics, diagnosis and unusual presentations. *Expert Rev Clin Immunol.* (2019) 15:1089–104. doi: 10.1080/1744666X.2019.1659726
7. Dahdah N. Not just coronary arteritis, Kawasaki disease is a myocarditis, too. *J Am Coll Cardiol.* (2010) 55:1507–8. doi: 10.1016/j.jacc.2009.11.067
8. Dionne A, Dahdah N. Myocarditis and Kawasaki disease. *Int J Rheum Dis.* (2018) 21:45–9. doi: 10.1111/1756-185X.13219
9. Yutani C, Go S, Kamiya T, Hirose O, Misawa H, Maeda H, et al. Cardiac biopsy of Kawasaki disease. *Arch Pathol Lab Med.* (1981) 105:470–3.
10. Yonesaka S, Nakada T, Sunagawa Y, Tomimoto K, Naka S, Takahashi T, et al. Endomyocardial biopsy in children with Kawasaki disease. *Acta Paediatr Jpn Overseas Ed.* (1989) 31:706–11. doi: 10.1111/j.1442-200X.1989.tb01384.x
11. Gordon JB, Kahn AM, Burns JC. When children with Kawasaki disease grow up. *J Am Coll Cardiol.* (2009) 54:1911–20. doi: 10.1016/j.jacc.2009.04.102
12. Yonesaka S, Takahashi T, Eto S, Sato T, Otani K, Ueda T, et al. Biopsy-proven myocardial sequels in Kawasaki disease with giant coronary aneurysms. *Cardiol Young.* (2010) 20:602–9. doi: 10.1017/S1047951109991132
13. Anderson TM, Meyer RA, Kaplan S. Long-term echocardiographic evaluation of cardiac size and function in patients with Kawasaki disease. *Am Heart J.* (1985) 110(1 Pt 1):107–15. doi: 10.1016/0002-8703(85)90523-X
14. Nakaoka H, Tsuda E, Morita Y, Kurosaki K. Cardiac function by magnetic resonance imaging in coronary artery occlusions after Kawasaki disease. *Circ J.* (2020) 84:792–8. doi: 10.1253/circj.CJ-19-0511
15. Harada M, Yokouchi Y, Oharaseki T, Matsui K, Tobayama H, Tanaka N, et al. Histopathological characteristics of myocarditis in acute-phase Kawasaki disease. *Histopathology.* (2012) 61:1156–67. doi: 10.1111/j.1365-2559.2012.04332.x
16. Orenstein JM, Shulman ST, Fox LM, Baker SC, Takahashi M, Bhatti TR, et al. Three linked vasculopathic processes characterize Kawasaki disease: a light and transmission electron microscopic study. *PLoS ONE.* (2012) 7:e38998. doi: 10.1371/journal.pone.0038998
17. Yoshikawa H, Nomura Y, Masuda K, Hazeki D, Yotsumoto K, Arata M, et al. Four cases of Kawasaki syndrome complicated with myocarditis. *Circ J.* (2006) 70:202–5. doi: 10.1253/circj.70.202
18. Peduzzi TL, Pitetti RD. Myocardial infarction and atypical Kawasaki disease in a 3-month-old infant. *Pediatr Emerg Care.* (2002) 18:E16–9. doi: 10.1097/00006565-200210000-00008
19. Aggarwal P, Suri D, Narula N, Manojkumar R, Singh S. Symptomatic myocarditis in Kawasaki disease. *Indian J Pediatr.* (2012) 79:813–4. doi: 10.1007/s12098-011-0552-4
20. De Rosa G, Andreozzi L, Piastra M, Castelli B, Rigante D. Acute myocarditis as a revealing clue of complete Kawasaki disease. *Reumatismo.* (2018) 70:115–6. doi: 10.4081/reumatismo.2018.1101
21. Madhusudan S, Singh S, Rohit M, Gupta A, Suri D, Rawat A. Late symptomatic myocarditis in Kawasaki disease: an unusual manifestation. *Indian J Pediatr.* (2014) 81:404–5. doi: 10.1007/s12098-014-1339-1
22. Haney I, Beghetti M, McCrindle BW, Gow RM. Ventricular arrhythmia complicating Kawasaki disease. *Can J Cardiol.* (1995) 11:931–3.
23. Fujino M, Hata T, Kuriki M, Horio K, Uchida H, Eryu Y, et al. Inflammation aggravates heterogeneity of ventricular repolarization in children with Kawasaki disease. *Pediatr Cardiol.* (2014) 35:1268–72. doi: 10.1007/s00246-014-0926-2
24. Singh S, Bhattad S, Gupta A, Suri D, Rawat A, Rohit M. Mortality in children with Kawasaki disease: 20 years of experience from a tertiary care centre in North India. *Clin Exp Rheumatol.* (2016) 34:S129–33.
25. Gupta K, Rohit M, Sharma A, Nada R, Jain S, Varma S. An adolescent with kawasaki disease. *Indian Pediatr.* (2016) 53:51–6. doi: 10.1007/s13312-016-0791-6
26. Pucci A, Martino S, Tibaldi M, Bartoloni G. Incomplete and atypical kawasaki disease: a clinicopathologic paradox at high risk of sudden and unexpected infant death. *Pediatr Cardiol.* (2012) 33:802–5. doi: 10.1007/s00246-012-0186-y
27. Robinson J, Hartling L, Vandermeer B, Klassen TP. Intravenous immunoglobulin for presumed viral myocarditis in children and adults. *Cochrane Database Syst Rev.* (2015) CD004370. doi: 10.1002/14651858.CD004370.pub3
28. Jensen LD, Marchant DJ. Emerging pharmacologic targets and treatments for myocarditis. *Pharmacol Ther.* (2016) 161:40–51. doi: 10.1016/j.pharmthera.2016.03.006
29. Dionne A, Meloche-Dumas L, Desjardins L, Turgeon J, Saint-Cyr C, Autmizguine J, et al. N-terminal pro-B-type natriuretic peptide diagnostic algorithm versus American Heart Association algorithm for Kawasaki disease. *Pediatr Int.* (2017) 59:265–70. doi: 10.1111/ped.13154
30. Dionne A, Dahdah N. A decade of NT-proBNP in acute kawasaki disease, from physiological response to clinical relevance. *Children (Basel).* (2018) 5:141. doi: 10.3390/children5100141
31. Jun H, Ko KO, Lim JW, Yoon JM, Lee GM, Cheon EJ. Age-adjusted plasma N-terminal pro-brain natriuretic peptide level in Kawasaki disease. *Korean J Pediatr.* (2016) 59:298–302. doi: 10.3345/kjp.2016.59.7.298
32. Sun Y, Wei C, Wang W, Zheng X, Wang Y, Ma S, et al. Serum brain natriuretic peptide in children with Kawasaki disease. *World J Emerg Med.* (2010) 1:114–7.
33. Reddy M, Singh S, Rawat A, Sharma A, Suri D, Rohit MK. Pro-brain natriuretic peptide (ProBNP) levels in North Indian children with Kawasaki disease. *Rheumatol Int.* (2016) 36:551–9. doi: 10.1007/s00296-016-3430-6
34. Sato YZ, Molkara DP, Daniels LB, Tremoulet AH, Shimizu C, Kanegaye JT, et al. Cardiovascular biomarkers in acute Kawasaki disease. *Int J Cardiol.* (2013) 164:58–63. doi: 10.1016/j.ijcard.2011.06.065
35. Rawat A, Singh S. Biomarkers for diagnosis of Kawasaki Disease. *Indian Pediatr.* (2015) 52:473–4. doi: 10.1007/s13312-015-0658-2
36. Pilania RK, Bhattarai D, Singh S. Controversies in diagnosis and management of Kawasaki disease. *World J Clin Pediatr.* (2018) 7:27–35. doi: 10.5409/wjcp.v7.i1.27
37. Bachmaier K, Mair J, Offner F, Pummerer C, Neu N. Serum cardiac troponin T and creatine kinase–MB elevations in murine autoimmune myocarditis. *Circulation.* (1995) 92:1927–32. doi: 10.1161/01.CIR.92.7.1927
38. Kim M, Kim K. Elevation of cardiac troponin i in the acute stage of Kawasaki disease. *Pediatr Cardiol.* (1999) 20:184–8. doi: 10.1007/s002469900437
39. Checchia PA, Borensztajn J, Shulman ST. Circulating cardiac troponin I levels in Kawasaki disease. *Pediatr Cardiol.* (2001) 22:102–6. doi: 10.1007/s002460010170
40. Chaudhary H, Nameirakpam J, Kumrah R, Pandiarajan V, Suri D, Rawat A, et al. Biomarkers for Kawasaki disease: clinical utility and the challenges ahead. *Front Pediatr.* (2019) 7:242. doi: 10.3389/fped.2019.00242
41. McCrindle BW, Cifra B. The role of echocardiography in Kawasaki disease. *Int J Rheum Dis.* (2018) 21:50–5. doi: 10.1111/1756-185X.13216
42. Pilania RK, Jindal AK, Guleria S, Singh S. An update on treatment of Kawasaki disease. *Curr Treat Options Rheumatol.* (2019) 5:36–55. doi: 10.1007/s40674-019-00115-z
43. Ajami G, Borzouee M, Amoozgar H, Ashnaee F, Kashef S, Nesar MS, et al. Evaluation of myocardial function using the Tei index in patients with Kawasaki disease. *Cardiol Young.* (2010) 20:44–8. doi: 10.1017/S1047951109991910
44. Newburger JW, Sanders SP, Burns JC, Parness IA, Beiser AS, Colan SD. Left ventricular contractility and function in Kawasaki syndrome. Effect of intravenous gamma-globulin. *Circulation.* (1989) 79:1237–46. doi: 10.1161/01.CIR.79.6.1237

45. McCandless RT, Minich LL, Wilkinson SE, McFadden ML, Tani LY, Menon SC. Myocardial strain and strain rate in Kawasaki disease. *Eur Heart J Cardiovasc Imaging.* (2013) 14:1061–8. doi: 10.1093/ehjci/jet041
46. Xu Q-Q, Ding Y-Y, Lv H-T, Zhou W-P, Sun L, Huang J, et al. Evaluation of left ventricular systolic strain in children with Kawasaki disease. *Pediatr Cardiol.* (2014) 35:1191–7. doi: 10.1007/s00246-014-0915-5
47. Dedeoglu R, Barut K, Oztunc F, Atik S, Adrovic A, Sahin S, et al. Evaluation of myocardial deformation in patients with Kawasaki disease using speckle-tracking echocardiography during mid-term follow-up. *Cardiol Young.* (2017) 27:1377–85. doi: 10.1017/S1047951117000580
48. Wang H, Ruan L, Shang J, Song Y, Tong M, Wu T. Left atrial subclinical dysfunction in children with Kawasaki disease: a two-dimensional speckle tracking echocardiograpy study. *Minerva Pediatr.* (2019). doi: 10.23736/S0026-4946. [Epub ahead of print].
49. Gaur L, Waloff K, Schiller O, Sable CA, Frank LH. Noncoronary inflammation in Kawasaki disease is associated with abnormal myocardial deformation in the acute phase. *J Am Soc Echocardiogr.* (2014) 27:1329–35. doi: 10.1016/j.echo.2014.09.014
50. Frank B, Davidson J. Myocardial strain and strain rate in Kawasaki disease: range, recovery, and relationship to systemic inflammation/coronary artery dilation. *J Clin Exp Cardiolog.* (2016) 7:432. doi: 10.4172/2155-9880.1000432
51. Azak E, Cetin II, Gursu HA, Kibar AE, Surucu M, Orgun A, et al. Recovery of myocardial mechanics in Kawasaki disease demonstrated by speckle tracking and tissue Doppler methods. *Echocardiography.* (2018) 35:380–7. doi: 10.1111/echo.13773
52. Wang H, Shang J, Tong M, Song Y, Ruan L. Evaluation of left ventricular function in immunoglobulin-resistant children with Kawasaki disease: a two-dimensional speckle tracking echocardiography study. *Clin Cardiol.* (2019) 42:753–9. doi: 10.1002/clc.23213
53. Kashyap R, Mittal BR, Bhattacharya A, Manojkumar R, Singh S. Exercise myocardial perfusion imaging to evaluate inducible ischaemia in children with Kawasaki disease. *Nucl Med Commun.* (2011) 32:137–41. doi: 10.1097/MNM.0b013e3283411c67
54. Tacke CE, Romeih S, Kuipers IM, Spijkerboer AM, Groenink M, Kuijpers TW. Evaluation of cardiac function by magnetic resonance imaging during the follow-up of patients with Kawasaki disease. *Circ Cardiovasc Imaging.* (2013) 6:67–73. doi: 10.1161/CIRCIMAGING.112.976969
55. Bratis K, Hachmann P, Child N, Krasemann T, Hussain T, Mavrogeni S, et al. Cardiac magnetic resonance feature tracking in Kawasaki disease convalescence. *Ann Pediatr Cardiol.* (2017) 10:18–25. doi: 10.4103/0974-2069.197046
56. Ghelani SJ, Singh S, Manojkumar R. QT interval dispersion in North Indian children with Kawasaki disease without overt coronary artery abnormalities. *Rheumatol Int.* (2011) 31:301–5. doi: 10.1007/s00296-009-1252-5
57. Reddy S, Rai M, Singh Chouhan RR, Rao S, Kamath N. Electrocardiographic analysis of repolarization changes in south Indian children with kawasaki disease after the acute phase of illness. *Int J Pediatr.* (2018) 2018:1062154. doi: 10.1155/2018/1062154
58. Parihar M, Singh S, Vignesh P, Gupta A, Rohit M. Mid-term risk for subclinical atherosclerosis and chronic myocarditis in children with kawasaki disease and transient coronary abnormalities. *Pediatr Cardiol.* (2017) 38:1123–32. doi: 10.1007/s00246-017-1626-5
59. Oyamada J, Shimizu C, Kim J, Williams MR, Png E, Hibberd ML, et al. Bifid T waves on the ECG and genetic variation in calcium channel voltage-dependent beta 2 subunit gene (CACNB2) in acute Kawasaki disease. *Congenit Heart Dis.* (2019) 14:213–20. doi: 10.1111/chd.12696
60. Dahdah N, Jaeggi E, Fournier A. Long-term changes in depolarization and repolarization after kawasaki disease. *Pediatr Res.* (2003) 53:162. doi: 10.1203/00006450-200301000-00049
61. Gamillscheg A, Zobel G, Karpf EF, Dacar D, Beitzke A, Stein JI, et al. Atypical presentation of Kawasaki disease in an infant. *Pediatr Cardiol.* (1993) 14:223–6. doi: 10.1007/BF00795375
62. Fuse S, Tomita H, Ohara T, Iida K, Takamuro M. Severely damaged aortic valve and cardiogenic shock in an infant with Kawasaki disease. *Pediatr Int.* (2003) 45:110–3. doi: 10.1046/j.1442-200X.2003.01666.x
63. Dominguez SR, Friedman K, Seewald R, Anderson MS, Willis L, Glodé MP. Kawasaki disease in a pediatric intensive care unit: a case-control study. *Pediatrics.* (2008) 122:e786–90. doi: 10.1542/peds.2008-1275
64. Kanegaye JT, Wilder MS, Molkara D, Frazer JR, Pancheri J, Tremoulet AH, et al. Recognition of a Kawasaki disease shock syndrome. *Pediatrics.* (2009) 123:e783–9. doi: 10.1542/peds.2008-1871
65. Gamez-Gonzalez LB, Moribe-Quintero I, Cisneros-Castolo M, Varela-Ortiz J, Muñoz-Ramírez M, Garrido-García M, et al. Kawasaki disease shock syndrome; a unique and severe subtype of kawasaki disease. *Pediatr Int.* (2018) 60:781–90. doi: 10.1111/ped.13614
66. Taddio A, Rossi ED, Monasta L, Pastore S, Tommasini A, Lepore L, et al. Describing Kawasaki shock syndrome: results from a retrospective study and literature review. *Clin Rheumatol.* (2017) 36:223–8. doi: 10.1007/s10067-016-3316-8
67. Pilania RK, Jindal AK, Srikrishna VV, Samprathi M, Singhal M, Singh S. Hypotension in a febrile child-beware of Kawasaki disease shock syndrome. *J Clin Rheumatol.* (2020) 26:e130–1. doi: 10.1097/RHU.0000000000001002
68. Gámez-González LB, Murata C, Muñoz-Ramírez M, Yamazaki-Nakashimada M. Clinical manifestations associated with Kawasaki disease shock syndrome in Mexican children. *Eur J Pediatr.* (2013) 172:337–42. doi: 10.1007/s00431-012-1879-1
69. Lin Y-J, Cheng M-C, Lo M-H, Chien S-J. Early differentiation of Kawasaki disease shock syndrome and toxic shock syndrome in a pediatric intensive care unit. *Pediatr Infect Dis J.* (2015) 34:1163–7. doi: 10.1097/INF.0000000000000852
70. Zhang Q, Liao Y, Du J. Kawasaki disease shock syndrome: a report of two cases and literature review. *Pediatr Investig.* (2019) 3:81–5. doi: 10.1002/ped4.12127
71. Derespina KR, Kaushik S, Medar SS. Pediatric shock: an uncommon and underrecognized etiology. *J Pediatr Intensive Care.* (2020) 9:210–2. doi: 10.1055/s-0039-1700964
72. Gatterre P, Oualha M, Dupic L, Iserin F, Bodemer C, Lesage F, et al. Kawasaki disease: an unexpected etiology of shock and multiple organ dysfunction syndrome. *Intensive Care Med.* (2012) 38:872–8. doi: 10.1007/s00134-012-2473-8
73. Schuster JE, Palac HL, Innocentini N, Rowley AH, Young LT, Shulman ST. Hyponatremia is a feature of kawasaki disease shock syndrome: a case-control study. *J Pediatr Infect Dis Soc.* (2017) 6:386–8. doi: 10.1093/jpids/piw081
74. Li Y, Zheng Q, Zou L, Wu J, Guo L, Teng L, et al. Kawasaki disease shock syndrome: clinical characteristics and possible use of IL-6, IL-10 and IFN-γ as biomarkers for early recognition. *Pediatr Rheumatol.* (2019) 17:1. doi: 10.1186/s12969-018-0303-4
75. Brain AN, Frame JD, Eve MD. Early lymphopenia in burned children with and without the toxic shock syndrome. *Burns.* (1988) 14:120–4. doi: 10.1016/0305-4179(88)90216-1
76. Verdoni L, Mazza A, Gervasoni A, Martelli L, Ruggeri M, Ciuffreda M, et al. An outbreak of severe Kawasaki-like disease at the Italian epicentre of the SARS-CoV-2 epidemic: an observational cohort study. *Lancet.* (2020) 395:1771–8. doi: 10.1016/S0140-6736(20)31103-X
77. Bhat CS, Gupta L, Balasubramanian S, Singh S, Ramanan AV. Hyperinflammatory syndrome in children associated with COVID-19: need for awareness. *Indian Pediatr.* (2020). [Epub ahead of print].
78. Pouletty M, Borocco C, Ouldali N, Caseris M, Basmaci R, Lachaume N, et al. Paediatric multisystem inflammatory syndrome temporally associated with SARS-CoV-2 mimicking Kawasaki disease (Kawa-COVID-19): a multicentre cohort. *Ann Rheum Dis.* (2020) 79:999–1006. doi: 10.1136/annrheumdis-2020-217960
79. Koné-Paut I, Cimaz R. Is it Kawasaki shock syndrome, Kawasaki-like disease or pediatric inflammatory multisystem disease? The importance of semantic in the era of COVID-19 pandemic. *RMD Open.* (2020) 6:e001333. doi: 10.1136/rmdopen-2020-001333
80. Rowley AH. Understanding SARS-CoV-2-related multisystem inflammatory syndrome in children. *Nat Rev Immunol.* (2020) 20:453–4. doi: 10.1038/s41577-020-0367-5
81. Rowley AH. Diagnosing SARS-CoV-2 related multisystem inflammatory syndrome in children (MIS-C): focus on the gastrointestinal tract and the myocardium. *Clin Infect Dis.* (2020). doi: 10.1093/cid/ciaa1080. [Epub ahead of print].
82. Whittaker E, Bamford A, Kenny J, Kaforou M, Jones CE, Shah P, et al. Clinical characteristics of 58 children with a pediatric inflammatory

multisystem syndrome temporally associated with SARS-CoV-2. *JAMA*. (2020) 324:259–69. doi: 10.1001/jama.2020.10369
83. Gowin E, Małecka I, Stryczyńska-Kazubska J, Michalak M, Wysocki J, Górzna-Kamińska H. Cardiac complications in children with Kawasaki disease in our own experience. *Kardiol Pol.* (2015) 74:75–82. doi: 10.5603/KP.a2015.0136
84. Hamza HS, Raouf WA, Zaher AZ, Agha HM. Acute Kawasaki disease with emphasis on the echocardiographic profile: a single center experience. *Glob Cardiol Sci Pract.* (2017) 2017:e201727. doi: 10.21542/gcsp.2017.27
85. Sonçagi A, Devrim I, Karagöz T, Dilber E, Celiker A, Ozen S, et al. Septated pericarditis associated with Kawasaki disease: a brief case report. *Turk J Pediatr.* (2007) 49:312–4.
86. Ozdogu H, Boga C. Fatal cardiac tamponade in a patient with Kawasaki disease. *Heart Lung.* (2005) 34:257–9. doi: 10.1016/j.hrtlng.2004.12.003
87. Kuppuswamy M, Gukop P, Sutherland G, Venkatachalam C. Kawasaki disease presenting as cardiac tamponade with ruptured giant aneurysm of the right coronary artery. *Interact Cardiovasc Thorac Surg.* (2010) 10:317–8. doi: 10.1510/icvts.2009.215731
88. Dahlem PG, von Rosenstiel IA, Lam J, Kuijpers TW. Pulse methylprednisolone therapy for impending cardiac tamponade in immunoglobulin-resistant Kawasaki disease. *Intensive Care Med.* (1999) 25:1137–9. doi: 10.1007/s001340051025
89. Miyamoto T, Ikeda K, Ishii Y, Kobayashi T. Rupture of a coronary artery aneurysm in Kawasaki disease: a rare case and review of the literature for the past 15 years. *J Thorac Cardiovasc Surg.* (2014) 147:e67–9. doi: 10.1016/j.jtcvs.2014.02.035
90. Mok GC, Sung RY, Yam MC, Arifi AA, Lam WW, Fok TF. A child with Kawasaki disease who survived after rupture of a coronary artery aneurysm. *Eur J Pediatr.* (2003) 162:634–6. doi: 10.1007/s00431-003-1265-0
91. Hwong TM., Arifi AA, Wan IY., Thung K., Wan S, Sung RY., et al. Rupture of a giant coronary artery aneurysm due to Kawasaki disease. *Ann Thorac Surg.* (2004) 78:693–5. doi: 10.1016/j.athoracsur.2003.06.015
92. Koike R, Oku T, Satoh H, Sawada Y, Suma H, Takeuchi A, et al. Right ventricular myocardial infarction and late cardiac tamponade due to right coronary artery aneurysm–a case report. *JPN J Surg.* (1990) 20:463–7. doi: 10.1007/BF02470833
93. Printz BF, Sleeper LA, Newburger JW, Minich LL, Bradley T, Cohen MS, et al. Noncoronary cardiac abnormalities are associated with coronary artery dilation and with laboratory inflammatory markers in acute Kawasaki disease. *J Am Coll Cardiol.* (2011) 57:86–92. doi: 10.1016/j.jacc.2010.08.619
94. Okada S, Hasegawa S, Suzuki Y, Matsubara T, Shimomura M, Okuda M, et al. Acute pericardial effusion representing the TNF-α-mediated severe inflammation but not the coronary artery outcome of Kawasaki disease. *Scand J Rheumatol.* (2015) 44:247–52. doi: 10.3109/03009742.2014.956140
95. Akagi T, Kato H, Inoue O, Sato N, Imamura K. Valvular heart disease in Kawasaki syndrome: incidence and natural history. *Am Heart J.* (1990) 120:366–72. doi: 10.1016/0002-8703(90)90081-8
96. de La Harpe M, di Bernardo S, Hofer M, Sekarski N. Thirty years of Kawasaki disease: a single-center study at the University Hospital of Lausanne. *Front Pediatr.* (2019) 7:11. doi: 10.3389/fped.2019.00011
97. Kitamura S, Kawashima Y, Kawachi K, Harima R, Ihara K, Nakano S, et al. Severe mitral regurgitation due to coronary arteritis of mucocutaneous lymph node syndrome. a new surgical entity. *J Thorac Cardiovasc Surg.* (1980) 80:629–36. doi: 10.1016/S0022-5223(19)37751-7
98. Akagi T, Kato H, Inoue O, Sato N. Valvular heart disease in Kawasaki syndrome. Incidence and natural history. *Kurume Med J.* (1989) 36:137–49. doi: 10.2739/kurumemedj.36.137
99. Shiraishi I, Nishimura K, Sakaguchi H, Abe T, Kitano M, Kurosaki K, et al. Acute rupture of chordae tendineae of the mitral valve in infants: a nationwide survey in japan exploring a new syndrome. *Circulation.* (2014) 130:1053–61. doi: 10.1161/CIRCULATIONAHA.114.008592
100. Nakano H, Nojima K, Saito A, Ueda K. High incidence of aortic regurgitation following Kawasaki disease. *J Pediatr.* (1985) 107:59–63. doi: 10.1016/S0022-3476(85)80615-6
101. Liu FF, Liu HH, Qiu Z, Wang JJ, Samadli S, Wu Y, et al. Clinical observation of noncoronary cardiac abnormalities in Chinese children with Kawasaki disease. *Eur J Clin Invest.* (2020) 50:e13210. doi: 10.1111/eci.13210
102. Ravekes WJ, Colan SD, Gauvreau K, Baker AL, Sundel RP, van der Velde ME, et al. Aortic root dilation in Kawasaki disease. *Am J Cardiol.* (2001) 87:919–22. doi: 10.1016/S0002-9149(00)01541-1
103. Fukunaga S, Egashira A, Arinaga K, Akasu I, Kai E, Higashi T, et al. Aortic valve replacement for aortic regurgitation due to Kawasaki disease. Report of two cases. *J Heart Valve Dis.* (1996) 5:231–4.
104. Gupta A, Singh S, Gupta A, Suri D, Rohit M. Aortic stiffness studies in children with Kawasaki disease: preliminary results from a follow-up study from North India. *Rheumatol Int.* (2014) 34:1427–32. doi: 10.1007/s00296-014-3000-8
105. Pinto FF, Gomes I, Loureiro P, Laranjo S, Timóteo AT, Carmo MM. Vascular function long term after Kawasaki disease: another piece of the puzzle? *Cardiol Young.* (2017) 27:488–97. doi: 10.1017/S1047951116000780
106. Schäfer M, Truong U, Ivy DD, Fonseca B, Malone L, DiMaria M, et al. Children with Kawasaki disease present elevated stiffness of great arteries: phase-contrast MRI study: elevated stiffness of great arteries in KD. *J Magn Reson Imaging.* (2018) 48:1228–36. doi: 10.1002/jmri.26167
107. Kato H, Sugimura T, Akagi T, Sato N, Hashino K, Maeno Y, et al. Long-term consequences of Kawasaki disease. a 10- to 21-year follow-up study of 594 patients. *Circulation.* (1996) 94:1379–85. doi: 10.1161/01.CIR.94.6.1379
108. Zhao Q, Chu C, Wu L, Liang X, Sun S, He L, et al. Systemic artery aneurysms and Kawasaki disease. *Pediatrics.* (2019) 144:e20192254. doi: 10.1542/peds.2019-2254
109. Bray M, Ramirez A, Muscal E, De Guzman M. Systemic vascular involvement in Kawasaki disease: a single center cohort. In: *2019 ACR/ARP Annual Meeting* (2019). p. 71.
110. Deng Y-B, Li T-L, Xiang H-J, Chang Q, Li C-L. Impaired endothelial function in the brachial artery after Kawasaki disease and the effects of intravenous administration of vitamin C. *Pediatr Infect Dis J.* (2003) 22:34–9. doi: 10.1097/00006454-200301000-00011
111. Dhillon R, Clarkson P, Donald AE, Powe AJ, Nash M, Novelli V, et al. Endothelial dysfunction late after kawasaki disease. *Circulation.* (1996) 94:2103–6. doi: 10.1161/01.CIR.94.9.2103
112. Ikemoto Y, Ogino H, Teraguchi M, Kobayashi Y. Evaluation of preclinical atherosclerosis by flow-mediated dilatation of the brachial artery and carotid artery analysis in patients with a history of Kawasaki disease. *Pediatr Cardiol.* (2005) 26:782–6. doi: 10.1007/s00246-005-0921-8
113. Noto N, Okada T, Karasawa K, Ayusawa M, Sumitomo N, Harada K, et al. Age-related acceleration of endothelial dysfunction and subclinical atherosclerosis in subjects with coronary artery lesions after Kawasaki disease. *Pediatr Cardiol.* (2009) 30:262–8. doi: 10.1007/s00246-008-9329-6
114. Ghelani SJ, Singh S, Manojkumar R. Endothelial dysfunction in a cohort of North Indian children with Kawasaki disease without overt coronary artery involvement. *J Cardiol.* (2009) 53:226–31. doi: 10.1016/j.jjcc.2008.11.006
115. Liu X, Huang G, Liang X, Ma X. Endothelial progenitor cells and arterial functions in the late convalescence period of Kawasaki disease. *Acta Paediatr.* (2009) 98:1355–9. doi: 10.1111/j.1651-2227.2009.01334.x
116. Dietz SM, Tacke CEA, Hutten BA, Kuijpers TW. Peripheral endothelial (dys)function, arterial stiffness and carotid intima-media thickness in patients after Kawasaki disease: a systematic review and meta-analyses. *PLoS ONE.* (2015) 10:e0130913. doi: 10.1371/journal.pone.0130913
117. Routhu SK, Singhal M, Jindal AK, Kumar V, Yadav AK, Singh S. Assessment of endothelial dysfunction in acute and convalescent phases of Kawasaki disease using automated edge detection software: a preliminary study From North India. *J Clin Rheumatol.* (2019). doi: 10.1097/RHU.0000000000001233. [Epub ahead of print].
118. Iwazu Y, Minami T, Kotani K. Pulse wave velocity in Kawasaki disease. *Angiology.* (2017) 68:189–95. doi: 10.1177/0003319716651789
119. Meena RS, Rohit M, Gupta A, Singh S. Carotid intima-media thickness in children with Kawasaki disease. *Rheumatol Int.* (2014) 34:1117–21. doi: 10.1007/s00296-013-2820-2
120. Gopalan K, Singh S, Vignesh P, Gupta A, Rohit M, Attri SV. Carotid intima-media thickness and lipid profile in children with Kawasaki disease: a single-center follow-up study after a mean duration of 6.9 years. *J Clin Rheumatol.* (2018) 24:385–9. doi: 10.1097/RHU.0000000000000754
121. Chen KYH, Curtis N, Dahdah N, Kowalski R, Cheung M, Burgner DP. Kawasaki disease and cardiovascular risk: a comprehensive review of

subclinical vascular changes in the longer term. *Acta Paediatr.* (2016) 105:752–61. doi: 10.1111/apa.13367
122. Dusad S, Singhal M, Pilania RK, Suri D, Singh S. CT coronary angiography studies after a mean follow-up of 3.8 years in children with Kawasaki disease and spontaneous defervescence. *Front Pediatr.* (2020) 8:274. doi: 10.3389/fped.2020.00274
123. Ishikawa T, Iwashima S. Endothelial dysfunction in children within 5 years after onset of Kawasaki disease. *J Pediatr.* (2013) 163:1117–21. doi: 10.1016/j.jpeds.2013.04.046
124. Niboshi A, Hamaoka K, Sakata K, Yamaguchi N. Endothelial dysfunction in adult patients with a history of Kawasaki disease. *Eur J Pediatr.* (2008) 167:189–96. doi: 10.1007/s00431-007-0452-9
125. Mori Y, Katayama H, Kishi K, Ozaki N, Shimizu T, Tamai H. Persistent high fever for more than 10 days during acute phase is a risk factor for endothelial dysfunction in children with a history of Kawasaki disease. *J Cardiol.* (2016) 68:71–5. doi: 10.1016/j.jjcc.2015.08.008
126. Ding Y-Y, Ren Y, Feng X, Xu Q-Q, Sun L, Zhang J-M, et al. Correlation between brachial artery flow-mediated dilation and endothelial microparticle levels for identifying endothelial dysfunction in children with Kawasaki disease. *Pediatr Res.* (2014) 75:453–8. doi: 10.1038/pr.2013.240
127. Brogan P, Burns JC, Cornish J, Diwakar V, Eleftheriou D, Gordon JB, et al. Lifetime cardiovascular management of patients with previous Kawasaki disease. *Heart Br Card Soc.* (2020) 106:411–20. doi: 10.1136/heartjnl-2019-315925
128. Tsuda E, Hirata T, Matsuo O, Abe T, Sugiyama H, Yamada O. The 30-year outcome for patients after myocardial infarction due to coronary artery lesions caused by Kawasaki disease. *Pediatr Cardiol.* (2011) 32:176–82. doi: 10.1007/s00246-010-9838-y
129. Tsuda E, Hamaoka K, Suzuki H, Sakazaki H, Murakami Y, Nakagawa M, et al. A survey of the 3-decade outcome for patients with giant aneurysms caused by Kawasaki disease. *Am Heart J.* (2014) 167:249–58. doi: 10.1016/j.ahj.2013.10.025
130. Fukazawa R, Kobayashi T, Mikami M, Saji T, Hamaoka K, Kato H, et al. nationwide survey of patients with giant coronary aneurysm secondary to Kawasaki disease 1999–2010 in Japan. *Circ J.* (2017) 82:239–46. doi: 10.1253/circj.CJ-17-0433
131. Shimizu C, Sood A, Lau HD, Oharaseki T, Takahashi K, Krous HF, et al. Cardiovascular pathology in 2 young adults with sudden, unexpected death due to coronary aneurysms from Kawasaki disease in childhood. *Cardiovasc Pathol.* (2015) 24:310–6. doi: 10.1016/j.carpath.2015.02.006

Conflict of Interest: The authors declare that the research was conducted in the absence of any commercial or financial relationships that could be construed as a potential conflict of interest.

frontiers in Pediatrics

ORIGINAL RESEARCH
published: 12 November 2020
doi: 10.3389/fped.2020.533759

A New Diagnostic Model to Distinguish Kawasaki Disease From Other Febrile Illnesses in Chongqing: A Retrospective Study on 10,367 Patients

*Zhilin Huang[1], Xu-Hai Tan[2], Haolin Wang[3], Bo Pan[1], Tie-Wei Lv[1] and Jie Tian[1]**

[1] Department of Heart, Ministry of Education Key Laboratory of Child Development and Disorders, National Clinical Research Center for Child Health and Disorders, China International Science and Technology Cooperation Base of Child Development and Critical Disorders, Chongqing Key Laboratory of Pediatrics, Children's Hospital of Chongqing Medical University, Chongqing, China, [2] Department of Pediatric, People's Hospital of Hongan, Hubei, China, [3] College of Medical Informatics, Chongqing Medical University, Chongqing, China

OPEN ACCESS

Edited by:
Xupei Huang, Florida Atlantic University, United States

Reviewed by:
Wen Shen, Florida Atlantic University, United States
Yuejin Li, Morgan State University, United States

***Correspondence:**
Jie Tian
jietian@cqmu.edu.cn

Specialty section:
This article was submitted to Pediatric Cardiology, a section of the journal Frontiers in Pediatrics

Received: *10 February 2020*
Accepted: *17 September 2020*
Published: *12 November 2020*

Citation:
Huang Z, Tan X-H, Wang H, Pan B, Lv T-W and Tian J (2020) A New Diagnostic Model to Distinguish Kawasaki Disease From Other Febrile Illnesses in Chongqing: A Retrospective Study on 10,367 Patients. Front. Pediatr. 8:533759. doi: 10.3389/fped.2020.533759

Objective: Kawasaki disease (KD) is one of the most prevailing vasculitis among infants and young children, and has become the leading cause of acquired heart disease in childhood. Delayed diagnosis of KD can lead to serious cardiovascular complications. We sought to create a diagnostic model to help distinguish children with KD from children with other febrile illnesses [febrile controls (FCs)] to allow prompt treatment.

Methods: Significant independent predictors were identified by applying multivariate logistic regression analyses. A new diagnostic model was constructed and compared with that from diagnostic tests created by other scholars.

Results: Data from 10,367 patients were collected. Twelve independent predictors were determined: a lower percentage of monocytes (%MON), phosphorus, uric acid (UA), percentage of lymphocyte (%LYM), prealbumin, serum chloride, lactic dehydrogenase (LDH), aspartate aminotransferase: alanine transaminase (AST: ALT) ratio, higher level of globulin, gamma-glutamyl transpeptidase (GGT), platelet count (PLT), and younger age. The AUC, sensitivity, and specificity of the new model for cross-validation of the KD diagnosis was 0.906 ± 0.006, 86.0 ± 0.9%, and 80.5 ± 1.5%, respectively. An equation was presented to assess the risk of KD, which was further validated using KD (n = 5,642) and incomplete KD (n = 809) cohorts.

Conclusions: Children with KD could be distinguished effectively from children with other febrile illnesses by documenting the age and measuring the level of %MON, phosphorus, UA, globulin, %LYM, prealbumin, GGT, AST:ALT ratio, serum chloride, LDH, and PLT. This new diagnostic model could be employed for the accurate diagnosis of KD.

Keywords: kawasaki disease, children, febrile illnesses, diagnostic model, independent predictors

INTRODUCTION

Kawasaki disease (KD) is a vasculitis of unknown etiology that, in general, occurs in childhood and is the most common cause of acquired heart disease (1). The incidence of KD is highest in children who live in East Asia or who are of Asian ancestry living in other parts of the world (2–5). KD incidence in underdeveloped regions and countries is not known as few cases are reported (e.g., in Southeast Asia), which may be related to the lower level of diagnosis.

KD can cause cardiovascular complications. In particular, coronary-artery aneurysms (CAAs) develop in about 15–25% of children who have not been treated for KD (6). These CAAs are associated mainly with occlusion of coronary arteries and cardiac ischemia, which can result in increased morbidity and even mortality.

The prevalence of CAA development in KD and related morbidity and mortality has decreased significantly as a result of treatment with high-dose intravenous immunoglobulin (IVIG) (7, 8). Early diagnosis is the most vital factor in achieving optimal treatment outcomes.

However, rapid discrimination of KD from other febrile illnesses is difficult, which leads to delays in the diagnosis of KD and treatment with IVIG. Diagnosis beyond 10 days of fever has been suggested to result in an increased prevalence of CAAs by 2.8- to 7.1-fold (9, 10). Patients who fail to meet the principal clinical findings for a diagnosis of KD (referred to as "incomplete KD") may develop CAAs.

Diagnosis of KD in the earliest phase after symptom onset is crucial and it is important to initiate treatment to lower the risk of CAAs (11). However, timely identification is challenging because diagnosis is based on clinical findings and nonspecific laboratory testing (12, 13). A specific diagnostic approach for patients with KD is lacking. The diagnosis of KD according to the criteria established by Tomisaku Kawasaki in 1967 is based on a constellation of clinical features (14). The clinical features of KD overlap with those of many other common childhood illnesses, such as infection by echoviruses, adenoviruses (15), Epstein–Barr virus (EBV), and measles. These viral illnesses share many of the signs of mucocutaneous inflammation and closely mimic KD. There is, therefore, an urgent need for sensitive and specific diagnostic tests to discriminate KD from other conditions that also cause prolonged fever in children.

Numerous studies have reported some discrimination between KD and other febrile illnesses based on certain laboratory parameters, but none have been validated (16–18). The major issue with those studies has been the selection of febrile controls (FCs), which might not represent the population of patients who could be confused with KD patients. Another issue has been the use of different models for prediction from different populations, which may not be sufficiently accurate and sensitive in Chinese populations (19). In addition, a common limitation of those reports was a small study cohort.

This retrospective study aimed to identify significant predictors and establish a new diagnostic model to differentiate children with KD from FCs. We reviewed the data from 10,367 patients from Chongqing City in China. We compared our data with results from studies by Falcini et al. (16), Barone et al. (19), Okada et al. (18), Song et al. (20), and Ling et al. (21) with regard to predictive ability, sensitivity, and specificity.

MATERIALS AND METHODS

Ethical Approval of the Study Protocol

The study protocol were approved by the Ethics Committee of the Children's Hospital Affiliated to Chongqing Medical University (Chongqing, China). Written informed consent from the parents of children was not required. The study was undertaken in accordance with the Declaration of Helsinki 1964 and its later amendments.

Study Design

We evaluated (retrospectively) the clinical findings of consecutive KD patients and FCs (who shared some features of KD) treated from October 2007 to December 2017 in Chongqing Children's Hospital (Chongqing, China). These patients were divided into two groups: KD and FCs.

The diagnostic criteria for KD in our hospital are in accordance with those set by the American Heart Association (22). These diagnostic criteria include $\geq$5 days of fever accompanied by four or five of the following clinical findings: (i) bilateral conjunctival injection; (ii) changes in the oral mucous membranes; (iii) changes in the peripheral extremities; (iv) polymorphous rash; (v) cervical lymphadenopathy. The inclusion criterion was KD as the main diagnosis upon hospital discharge. Patients who received IVIG treatment in other medical institutions before hospital admission were excluded from our study.

FCs had a documented fever ($\geq$38.0°C) accompanied by at least one of the following clinical signs of KD: (i) skin rash; (ii) conjunctival injection; (iii) enlargement of cervical lymph nodes; (iv) changes in the peripheral extremities; (v) pharyngeal abnormalities (21). We also compared incomplete KD and FCs to further validate our model. "Incomplete KD" were said to occur if there were $\leq$3 of the clinical findings of KD.

Data Collection

A total of 10,367 people met the inclusion criteria and were enrolled in our study to develop the model. There were 5,642 cases in the KD group (54.42%) and 4,725 casesin the FCs group (45.58%). The data of 809 cases with incomplete KD were collected to further validate the performance of the developed model.

Data before initial IVIG treatment were collected: age (months); sex; white blood cell count (WBC); platelet distribution width (PDW); platelet count (PLT); mean platelet volume (MPV); red blood cell count (RBC); hemoglobin (HB); packed cell volume (PCV); red blood cell distribution width (RDW); total red blood cell distribution width (RDWa); erythrocyte morphology; mean corpuscular hemoglobin (MCH); mean corpuscular volume (MCV); platelet-large-cell ratio (P-LCR); total number of lymphocytes; total number of monocytes; total number of neutrophils; percentage of lymphocytes (%LYM); thrombocytosis; percentage of neutrophils (%NEU); leucocyte

morphology; percentage of monocytes (%MON); hematuria; urinary vitamin C; urinary sugar; urinary protein; urinary bilirubin; urine transparency; ovum (stool); phagocytes in stool; red blood cells in stool; gamma-glutamyl transpeptidase (GGT); alkaline phosphatase (ALP); lactic dehydrogenase (LDH); aspartate aminotransferase (AST); alanine transaminase (ALT); AST:ALT ratio; direct bilirubin (DBIL); albumin; prealbumin; total protein (TP); total bilirubin (TBIL); globulin; ketone body (KET); creatinine; bile acid (BA); blood urea nitrogen (BUN); uric acid (UA); C-reactive protein (CRP); phosphorus; and serum levels of sodium, potassium, magnesium, chloride, and calcium upon hospital admission.

If there were more than two laboratory reports before the initial IVIG treatment with regard to routine blood analyses, kidney function, routine urinalyses, liver function, routine stool analyses, CRP level, and electrolytes, we used the reports with the highest values of WBC, %NEU, ALT, AST, BUN, CRP and lowest levels of TP, serum chloride, and albumin (23).

Statistical Analyses

De-identified clinical laboratory findings were extracted from electronic medical records (EMRs) for comparison between the KD group and the FCs group. For variables with a missing detection rate <25%, we undertook multiple imputations by chained equations (MICE) (24). MICE is the principal method to address the problem of missing data and was employed to reduce bias in our study. The adopted method for MICE was linear regression, and the number of multiple imputations and the number of iterations were 5 and 10, respectively. Data are the mean ± standard deviation (SD) for continuous data or as a percentage for categorical data (**Table 1**).

One of our challenges was that KD assessment is not very sensitive to individual predictors. To identify significant predictors effectively, data were standardized (rescaled) to have a mean of 0 and an SD of 1. The Mann–Whitney *U*-test was carried out for comparison of continuous data. Categorical data were assessed using the chi-square test for comparison between the two groups. For all analyses, $P < 0.05$ was considered significant. Selected data that were significantly different between the two groups were entered into multivariate analyses. To develop a reliable prediction model for the KD diagnosis, we divided the dataset into five subgroups randomly. One of the five subgroups was used as the test set and the remaining four subgroups were used to form the training set each time, and the experiments were repeated five times (known as 5-fold cross-validation). The least absolute shrinkage and selection operator (LASSO) regression model were applied for further feature selection using the significantly different indicators obtained by the univariate analysis. Finally, we developed the diagnostic model based on multivariate logistic regression analysis. The odds ratio (OR) with a 95% confidence interval (CI) was calculated to determine the score of an independent predictor and establish a new prediction model. We did not carry out the Hosmer–Lemeshow test because it can lead to misleadingly significant values with large sample sizes. The predictive performance of the proposed model was evaluated using the receiver operating characteristic (ROC) curve and the area under the ROC curve (AUC). We constructed an equation to increase the usefulness of the individual risk probability of KD diagnosis that could be applied in clinical practice. Statistical analyses were conducted using Python for Statistical Computing.

RESULTS

Comparison Between the KD Group and FCs Group by Univariate Analysis

Table 1 shows the clinical/laboratory findings in the two groups using univariate analysis. The level of 24 variables of the KD group was significantly higher than that of the FCs group: thrombocytosis; PLT; WBC; total number of neutrophils; %NEU; total number of monocytes; hematuria; vitamin C in urine; sugar in urine; protein in urine; bilirubin in urine; urine transparency; phagocytes in stool; red blood cells in stools; GGT; ALT; DBIL; TBIL; globulin; KET; BA; CRP; serum calcium.

The level of 32 variables was significantly lower in the KD group than that in the FCs group: RDWa; RDW; PCV; abnormal erythrocyte morphology; MPV; RBCs; PDW; MCH; MCV; total number of lymphocytes; abnormal leukocyte morphology; %LYM; %MON; P-LCR; HB; ovum in stools; AST; AST:ALT ratio; LDH; ALP; TP; albumin; prealbumin; creatinine; BUN; UA; phosphorus; age; serum levels of sodium, chloride, potassium, and magnesium.

Patients in the KD group were predominantly male and younger than those in the FCs group.

Independent Predictors and Diagnostic Model for KD

For multivariate logistic regression analyses, we selected significant variables derived from the univariate analysis through LASSO constraints to balance accuracy and simplicity. Fifteen variables (one demographic variable and 14 laboratory variables) were identified by "tuning" of the hyper-parameter lambda. Among the 15 variables, however, 12 variables were significant and were applied to multivariate logistic regression analyses. No significant difference was observed for the level of CRP, albumin, or HB (**Table 2**). Multivariate logistic regression analysis identified significant independent predictors for the KD group to be: lower levels of %MON, phosphorus, UA, %LYM, prealbumin, AST:ALT ratio, serum chloride, and LDH; higher levels of globulin, GGT, and PLT; younger age. **Table 3** shows the OR (95%CI) values of those predictors.

We obtained a model as shown in Equation (1):

$$\begin{aligned}\ln(\mathrm{P}/(1-\mathrm{P})) = {} & 0.211 + (-0.471) \times \%\mathrm{MON} + (-0.414) \\ & \times \mathrm{phosphorus} + (-0.325) \times \mathrm{UA} + (0.416) \\ & \times \mathrm{globulin} + (-0.751) \times \%\mathrm{LYM} + (-1.121) \\ & \times \mathrm{prealbumin} + (0.283) \times \mathrm{GGT} + (-0.562) \\ & \times \mathrm{AST:ALTratio} + (-0.285) \times \mathrm{chloride} \\ & + (-1.009) \times \mathrm{LDH} + (0.461) \times \mathrm{PLT} \\ & + (-0.817) \times \mathrm{age(inmonths)} \end{aligned} \quad (1)$$

where P is the expected probability that the diagnosis is KD.

TABLE 1 | Univariate analysis comparison of the KD group and FCs group.

Variable	KD group		FCs group		*P*-value
	N	Mean ± SD/Counts (%)	*N*	Mean ± SD/Counts (%)	
Blood test					
Red blood cell count, 1,012/L	4,593	3.97 ± 0.45	4,379	4.26 ± 0.54	<0.001
Absolute value of Red blood cell Distribution, fL	4,244	40.49 ± 4.52	4,174	41.56 ± 5.92	<0.001
Red blood cell distribution width, %	4,559	13.95 ± 1.78	4,368	14.24 ± 2.00	0.001
Packed cell volume, %	4,592	31.98 ± 3.54	4,379	34.61 ± 4.06	<0.001
Erythrocyte morphology (abnormal)*	4,405	291 (0.066)	4,346	322 (0.074)	<0.001
Mean platelet volume, fL	4,358	9.91 ± 1.06	4,161	10.19 ± 1.11	<0.001
Platelet distribution width, fL	4,430	11.48 ± 2.23	4,159	11.84 ± 2.41	<0.001
Thrombocytocrit, %	4,222	0.44 ± 0.50	3,923	0.39 ± 0.54	<0.001
Platelet count, 109/L	4,593	384.53 ± 163.33	4,379	308.46 ± 146.99	<0.001
White blood cell, 109/L	4,592	15.11 ± 6.31	4,379	10.87 ± 6.91	<0.001
Mean Corpuscular Hemoglobin, pg	4,440	26.29 ± 2.11	4,378	26.62 ± 2.61	<0.001
Mean corpuscular volume	4,593	80.79 ± 6.28	4,379	81.70 ± 2.29	<0.001
Absolute value of lymphocyte	4,329	3.63 ± 2.02	4,257	4.09 ± 2.77	0.016
Leucocyte morphology (abnormal)*	4,522	55 (0.012)	4,180	86 (0.021)	<0.001
Percentage of lymphocyte	4,592	0.26 ± 0.14	4,379	0.42 ± 0.20	<0.001
Absolute value of neutrophil	4,481	10.73 ± 5.71	4,260	6.14 ± 5.93	<0.001
Percentage of neutrophil	4,593	0.69 ± 0.16	4,379	0.52 ± 0.22	<0.001
Absolute value of monocyte	4,196	0.42 ± 0.65	4,082	0.39 ± 0.29	<0.001
Percentage of monocyte	4,399	0.03 ± 0.02	4,314	0.04 ± 0.02	<0.001
Platelet-large-cell ratio, %	4,174	24.24 ± 8.20	3,870	26.24 ± 8.80	0.001
Hemoglobin, g/l	4,593	104.14 ± 11.61	4,379	112.81 ± 14.32	<0.001
Urine test					
Blood urine (positive)*	4,932	302 (0.061)	4,230	223 (0.053)	<0.001
Vitamin C (positive)*	4,932	2,870 (0.582)	4,256	1,951 (0.458)	<0.001
Urine sugar (positive)*	5,092	737 (0.145)	4,236	286 (0.068)	<0.001
Urine protein (positive)*	5,094	575 (0.113)	4,256	168 (0.039)	<0.001
Urobilirubin (positive)*	5,094	132 (0.026)	4,256	21 (0.005)	0.001
The transparency of the urine (positive)*	4,931	570 (0.116)	4,252	243 (0.057)	<0.001
Stool test					
Ovum (positive)*	4,990	0	4,276	1 (<0.001)	<0.001
Red blood cell (positive)*	4,990	66 (0.013)	4,276	43 (0.010)	<0.001
Phagocyte (positive)*	4,990	2 (<0.001) (0.00)	4,276	0	<0.001
Biochemical test					
Gamma- glutamyl transpeptidase, U/L	5,043	86.14 ± 111.70	4,286	34.43 ± 72.89	<0.001
Alanine transaminase, IU/L	5,043	69.32 ± 100.90	4,285	43.54 ± 120.35	<0.001
Aspartate aminotransferase, IU/L	5,271	50.53 ± 90.22	4,286	63.02 ± 205.80	<0.001
Lactic dehydrogenase, IU/L	5,272	300.45 ± 151.70	4,286	398.71 ± 534.56	<0.001
Alkaline phosphatase, IU/L	5,043	182.00 ± 121.16	4,286	184.31 ± 101.62	0.007
AST:ALT ratio	5,042	1.17 ± 0.83	4,284	1.05 ± 0.78	<0.001
Direct bilirubin, umol/L	4,678	5.55 ± 10.79	3,844	3.02 ± 5.67	<0.001
Total bilirubin, umol/L	5,037	10.77 ± 14.25	4,284	9.69 ± 18.51	<0.001
Total Protein, g/L	5,043	60.01 ± 7.40	4,289	62.95 ± 7.63	<0.001
Albumin, g/L	5,043	36.76 ± 4.96	4,289	41.38 ± 5.67	<0.001
Prealbumin, mg/L	4209	65.50 ± 41.73	3,694	124.88 ± 54.58	<0.001
Globulin, g/L	5,043	23.25 ± 5.98	4,289	21.57 ± 6.02	<0.001
Creatinine, umol/L	4,894	26.27 ± 16.43	4075	29.39 ± 21.49	<0.001
Blood urea nitrogen, mmol/L	4,892	2.90 ± 1.52	4,075	3.46 ± 2.38	<0.001
Ketone body*	5,094	0.49 ± 0.97	4,256	0.39 ± 0.88	<0.001

(Continued)

TABLE 1 | Continued

Variable	KD group		FCs group		*P*-value
	N	Mean ± SD/Counts (%)	*N*	Mean ± SD/Counts (%)	
Bile acid	4,226	22.15 ± 43.60	3,790	12.40 ± 23.76	<0.001
Uric acid, umol	4,885	210.20 ± 83.58	4,074	259.66 ± 115.96	<0.001
Inflammatory factor					
C-reactive protein, mg/L	4,421	60.08 ± 52.85	4,256	23.03 ± 43.19	<0.001
Ion					
Serum phosphorus, mmol/L	4,858	1.30 ± 0.30	4,131	1.50 ± 0.35	<0.001
Serum sodium, mmol/L	4,861	137.19 ± 3.26	4,151	138.34 ± 3.54	<0.001
Serum potassium, mmol/L	4,861	4.22 ± 0.68	4,149	4.40 ± 0.65	<0.001
Serum magnesium, mmol/L	4,859	0.92 ± 0.11	4,131	0.93 ± 0.11	<0.001
Serum chloride, mmol/L	4,859	101.20 ± 3.76	4,132	103.28 ± 4.37	<0.001
Serum calcium, mmol/L	4,499	2.29 ± 0.16	4,016	2.26 ± 0.20	<0.001
Demographics					
Age, month	5,642	31.75 ± 25.11	4,725	42.35 ± 42.34	<0.001
Sex (male)*	5,641	3,943 (0.70)	4,725	2,785 (0.59)	<0.001

*ALT, Alanine transaminase; AST, Aspartate aminotransferase; *for categorical variables; N, number of samples; SD, standard deviation; W value for Wilcoxon-Mann-Whitney test; $\chi 2$ value for chi-square test.*

TABLE 2 | The OR (95%CI) values of the independent predictors for the KD diagnosis.

	Multiple logistic regression analysis after LASSO (5-fold cross validation)									
Predictors	**Group 1**		**Group 2**		**Group 3**		**Group 4**		**Group 5**	
	OR value (95%CI)	***P*-value**	**OR value (95%CI)**	***P*-value**	**OR value (95%CI)**	***P*-value**	**OR value (95%CI)**	***P*-value**	**OR value (95%CI)**	***P*-value**
%MON	0.620 (0.575–0.669)	<0.001	0.616 (0.571–0.665)	<0.001	0.621 (0.576–0.670)	<0.001	0.648 (0.601–0.700)	<0.001	0.657 (0.610–0.708)	<0.001
CRP	1.085 (0.996–1.182)	0.062	1.070 (0.985–1.163)	0.11	1.099 (1.008–1.198)	0.032	1.108 (1.018–1.207)	0.018	1.015 (0.933–1.103)	0.731
Phosphorus	0.659 (0.608–0.714)	<0.001	0.662 (0.612–0.717)	<0.001	0.686 (0.634–0.743)	<0.001	0.689 (0.636–0.746)	<0.001	0.651 (0.601–0.706)	<0.001
UA	0.748 (0.690–0.811)	<0.001	0.728 (0.672–0.787)	<0.001	0.729 (0.673–0.789)	<0.001	0.704 (0.650–0.762)	<0.001	0.728 (0.672–0.788)	<0.001
Globulin	1.484 (1.373–1.605)	<0.001	1.492 (1.382–1.611)	<0.001	1.479 (1.368–1.598)	<0.001	1.488 (1.377–1.609)	<0.001	1.509 (1.395–1.632)	<0.001
Albumin	0.956 (0.873–1.047)	0.332	0.939 (0.860–1.026)	0.164	0.995 (0.910–1.088)	0.906	0.938 (0.857–1.027)	0.165	0.915 (0.836–1.002)	0.054
%LYM	0.499 (0.458–0.544)	<0.001	0.496 (0.455–0.541)	<0.001	0.491 (0.451–0.535)	<0.001	0.485 (0.445–0.529)	<0.001	0.478 (0.439–0.522)	<0.001
Prealbumin	0.323 (0.290–0.360)	<0.001	0.364 (0.329–0.404)	<0.001	0.335 (0.301–0.373)	<0.001	0.357 (0.322–0.397)	<0.001	0.361 (0.325–0.401)	<0.001
HB	0.934 (0.863–1.010)	0.088	0.911 (0.843–0.985)	0.019	0.932 (0.862–1.009)	0.083	0.923 (0.853–0.998)	0.045	0.918 (0.848–0.994)	0.036
GGT	1.245 (1.142–1.358)	<0.001	1.296 (1.186–1.416)	<0.001	1.317 (1.199–1.446)	<0.001	1.293 (1.182–1.415)	<0.001	1.366 (1.238–1.508)	<0.001
AST:ALT ratio	0.579 (0.530–0.633)	<0.001	0.581 (0.532–0.634)	<0.001	0.589 (0.538–0.645)	<0.001	0.566 (0.518–0.619)	<0.001	0.571 (0.523–0.624)	<0.001
Chloride	0.757 (0.700–0.819)	<0.001	0.790 (0.736–0.849)	<0.001	0.765 (0.713–0.821)	<0.001	0.735 (0.684–0.790)	<0.001	0.737 (0.686–0.792)	<0.001
LDH	0.309 (0.254–0.374)	<0.001	0.368 (0.306–0.443)	<0.001	0.358 (0.297–0.431)	<0.001	0.409 (0.341–0.490)	<0.001	0.353 (0.292–0.425)	<0.001
PLT	1.567 (1.448–1.696)	<0.001	1.532 (1.417–1.657)	<0.001	1.547 (1.430–1.673)	<0.001	1.582 (1.462–1.712)	<0.001	1.526 (1.408–1.653)	<0.001
AGE	0.435 (0.401–0.472)	<0.001	0.446 (0.412–0.484)	<0.001	0.449 (0.415–0.487)	<0.001	0.455 (0.419–0.493)	<0.001	0.441 (0.406–0.478)	<0.001

OR, odds ratio; CI, confidence interval; LASSO, least absolute shrinkage, and selection operator; %MON, percentage of monocyte; CRP, C-reactive protein; UA, uric acid; %LYM, percentage of lymphocyte; HB, hemoglobin; GGT, gamma-glutamyl transpeptidase; AST, aspartate aminotransferase; ALT, alanine transaminase; LDH, lactic dehydrogenase; PLT, platelet count.

Hence, we could determine the individual-risk probability of the KD diagnosis. The coefficients represent the contribution of the variables in Equation (1). Taking the GGT level as an example and assuming that the other items are unchanged, the OR of having the KD diagnosis increases by 26.6% (OR − 1 = 1.266 − 1 = 0.266) with an increase of one SD (one rescaled unit) in the GGT level. The greater the positive coefficient of the level of globulin, the GGT level, and PLT level would increase the possibility of KD diagnosis. The greater the negative coefficient in the level of %MON, phosphorus, UA, %LYM, prealbumin, AST:ALT ratio, chloride, LDH and age would decrease the OR of the KD diagnosis. Taking a patient with confirmed KD as an example, the indicators would be: PLT = 801 × 10^9/L (normal range, 100–380); %LYM = 0.11 (0.3–0.6); %MON = 0.06 (0.02–0.08); GGT = 150 U/L (0–25); globulin = 20.2 g/L (15.3–35); phosphorus = 0.74 mmol/L

TABLE 3 | The OR (95%CI) values of the independent predictors for the KD diagnosis.

Multiple logistic regression analysis using the 12 indicators with statistical significance (5-fold cross validation)										
Predictors	**Group 1**		**Group 2**		**Group 3**		**Group 4**		**Group 5**	
	OR value (95%CI)	***P*-value**	**OR value (95%CI)**	***P*-value**	**OR value (95%CI)**	***P*-value**	**OR value (95%CI)**	***P*-value**	**OR value (95%CI)**	***P*-value**
%MON	0.614 (0.569–0.662)	<0.001	0.608 (0.563–0.655)	<0.001	0.614 (0.569–0.662)	<0.001	0.639 (0.592–0.689)	<0.001	0.649 (0.603–0.699)	<0.001
Phosphorus	0.650 (0.600–0.705)	<0.001	0.654 (0.604–0.708)	<0.001	0.682 (0.630–0.738)	<0.001	0.680 (0.628–0.736)	<0.001	0.641 (0.592–0.695)	<0.001
UA	0.743 (0.686–0.806)	<0.001	0.722 (0.667–0.781)	<0.001	0.727 (0.672–0.787)	<0.001	0.699 (0.646–0.757)	<0.001	0.722 (0.666–0.781)	<0.001
Globulin	1.509 (1.397–1.629)	<0.001	1.521 (1.410–1.641)	<0.001	1.499 (1.388–1.619)	<0.001	1.520 (1.407–1.641)	<0.001	1.535 (1.420–1.658)	<0.001
%LYM	0.480 (0.442–0.520)	<0.001	0.477 (0.440–0.518)	<0.001	0.472 (0.436–0.512)	<0.001	0.461 (0.425–0.501)	<0.001	0.468 (0.431–0.508)	<0.001
Prealbumin	0.304 (0.275–0.335)	<0.001	0.340 (0.309–0.373)	<0.001	0.320 (0.290–0.353)	<0.001	0.331 (0.300–0.364)	<0.001	0.337 (0.306–0.371)	<0.001
GGT	1.266 (1.161–1.380)	<0.001	1.323 (1.211–1.445)	<0.001	1.329 (1.211–1.459)	<0.001	1.322 (1.208–1.446)	<0.001	1.401 (1.270–1.545)	<0.001
AST:ALT ratio	0.574 (0.526–0.626)	<0.001	0.573 (0.525–0.625)	<0.001	0.583 (0.533–0.638)	<0.001	0.557 (0.510–0.609)	<0.001	0.564 (0.517–0.616)	<0.001
Chloride	0.752 (0.696–0.813)	<0.001	0.784 (0.730–0.843)	<0.001	0.762 (0.710–0.818)	<0.001	0.729 (0.679–0.783)	<0.001	0.735 (0.684–0.789)	<0.001
LDH	0.315 (0.260–0.382)	<0.001	0.378 (0.314–0.454)	<0.001	0.361 (0.300–0.435)	<0.001	0.417 (0.348–0.499)	<0.001	0.359 (0.298–0.433)	<0.001
PLT	1.599 (1.481–1.728)	<0.001	1.569 (1.453–1.695)	<0.001	1.577 (1.460–1.703)	<0.001	1.621 (1.501–1.751)	<0.001	1.559 (1.442–1.686)	<0.001
AGE	0.433 (0.399–0.469)	<0.001	0.443 (0.409–0.479)	<0.001	0.447 (0.413–0.483)	<0.001	0.452 (0.417–0.489)	<0.001	0.436 (0.403–0.472)	<0.001

OR, odds ratio; CI, confidence interval; LASSO, least absolute shrinkage, and selection operator; %MON, percentage of monocyte; UA, uric acid; %LYM, percentage of lymphocyte; GGT, gamma-glutamyl transpeptidase; AST, aspartate aminotransferase; ALT, alanine transaminase; LDH, lactic dehydrogenase; PLT, platelet count.

TABLE 4 | The diagnostic capabilities of the new model and the previous studies.

	AUC	**Sensitivity**	**Specificity**
The new model	0.906 ± 0.006	0.860 ± 0.009	0.805 ± 0.015
Falcini et al.	0.791 ± 0.012	0.784 ± 0.012	0.686 ± 0.018
Okada et al.	0.785 ± 0.014	0.779 ± 0.013	0.702 ± 0.022
Barone et al.	0.798 ± 0.017	0.787 ± 0.022	0.700 ± 0.012
Xiu-Yu et al.	0.793 ± 0.014	0.780 ± 0.011	0.704 ± 0.018
Ling et al.	0.724 ± 0.013	0.758 ± 0.010	0.594 ± 0.019

AUC, area under the curve.

(1.29–2.26); UA = 128 μmol/L (100–410), prealbumin = 60 mg/L (100–300); AST:ALT ratio = 0.36 (0.23–2.47); chloride = 95.9 mmol/L (98–107); LDH = 300 U/L (110–330); age = 25 months.

McFadden's R^2 was 0.431 ± 0.005 for our model. The sensitivity, specificity, and AUC values of the 5-fold cross-validation are shown in **Table 4**. The AUC, sensitivity, and specificity of our diagnostic model for the KD diagnosis was 0.906 ± 0.006, 86.0 ± 0.9%, and 80.5 ± 1.5%, respectively.

The logistic model for the identified variables without standardization used to support further investigations is shown in Equation (2).

$$\begin{aligned}\mathrm{Ln}(\mathrm{P}/(1-\mathrm{P})) = {} & 13.534 + (-26.224) \times \%\mathrm{MON} + (-1.227) \\ & \times \mathrm{phosphorus} + (-0.003) \times \mathrm{UA} + (0.069) \\ & \times \mathrm{globulin} + (-3.905) \times \%\mathrm{LYM}\% + (-0.020) \\ & \times \mathrm{prealbumin} + (0.003) \times \mathrm{GGT} + (-0.552) \\ & \times \mathrm{AST:ALTratio} + (-0.068) \times \mathrm{chloride} \\ & + (-0.003) \times \mathrm{LDH} + (0.003) \times \mathrm{PLT} \\ & + (-0.024) \times \mathrm{age(months)} \end{aligned} \quad (2)$$

We validated the proposed model (Equation 2) using the collected dataset (cohort of 10,367 patients): a consistent performance was obtained. The ROC curve is shown in **Figure 1**, and the AUC, sensitivity, and specificity were 0.906 ± 0.006, 86.0 ± 0.9%, and 80.5 ± 1.5%, respectively.

Comparison Between the New Diagnostic Model and Models Used in Previous Diagnostic Studies

Compared with previous studies in which the KD diagnosis was tested, **Figure 1** shows that our model had an AUC (0.906 ± 0.006) that was higher than that obtained in the studies of Falcini et al. (0.791 ± 0.012), Barone et al. (0.798 ± 0.017), Okada et al. (0.785 ± 0.014), Song et al. (0.793 ± 0.014), and Ling et al. (0.724 ± 0.013).

We compared the model for the KD diagnosis in those previous studies with the KD diagnosis in our cohort: the sensitivity and specificity in our new model were better (**Table 4**). In addition, a validation dataset (809 patients with incomplete KD) was used to further assess the effectiveness of our new diagnostic model: the AUC was 0.816 (**Figure 2**). The sensitivity and specificity of this regression model were 70.6 and 80.7%, respectively.

DISCUSSION

We discovered that a high level of GGT, PLT, and globulin, a low level of %MON, phosphorus, UA, %LYM, prealbumin, AST:ALT ratio, chloride, LDH, and age were independent predictors for the diagnosis of KD. We developed a new model to diagnose KD accurately, with high sensitivity and specificity for the early diagnosis of KD that could be used as the basis of a diagnostic test.

Importantly, we reviewed (retrospectively) 10,367 patients from Chongqing (one of the biggest cities in western China)

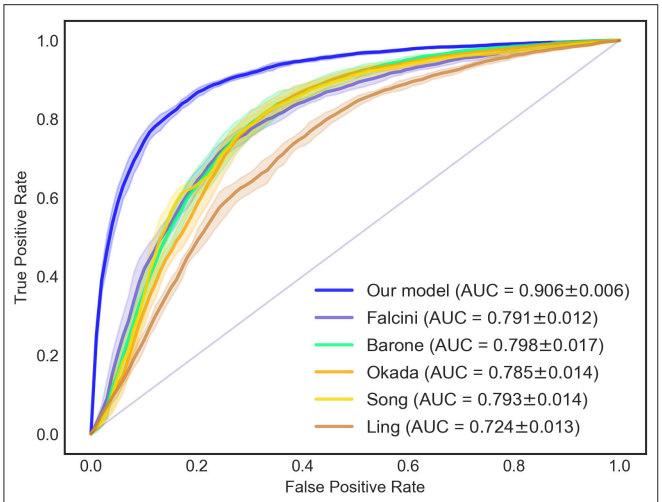

FIGURE 1 | ROC and AUC of the diagnostic models for KD diagnosis. The AUC of the new KD diagnostic prediction model was 0.906 ± 0.006. Compared with previous KD diagnosis studies, the AUC value of the new model was higher than the methods of Falcini (0.791 ± 0.012), Barone (0.798 ± 0.017), Okada (0.785 ± 0.014), Song (0.793 ± 0.014), and Ling (0.724 ± 0.013). ROC, receiver-operator characteristic curves; AUC, area under the curve.

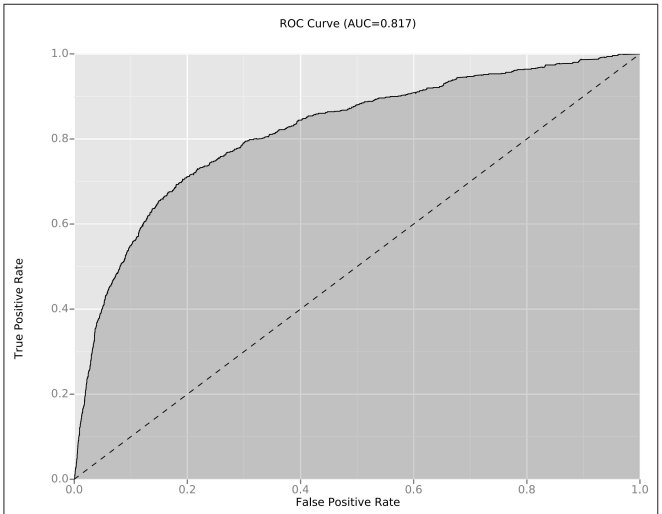

FIGURE 2 | ROC and AUC of the diagnostic models for incomplete KD diagnosis. The AUC value of the new diagnostic model for incomplete KD diagnosis was 0.816. ROC, receiver-operator characteristic curves; AUC, area under the curve.

and built a new model that can be used in the early diagnosis of KD in underdeveloped countries where a poor standard of living, literacy rate, and other socio-economic conditions can be a great challenge.

The KD diagnosis is based mainly on clinical findings and non-specific laboratory indicators. However, several febrile illnesses and KD have similar clinical manifestations: scarlet fever, EBV infection, juvenile idiopathic arthritis, measles, and adenovirus infection. In addition, 15–36.2% of children with KD do not have all the clinical manifestations of KD (incomplete KD), which can lead to misdiagnosis or delayed diagnosis of KD (25). Therefore, our new algorithm for KD diagnosis was validated in patients with incomplete KD (who display atypical findings and constitute a major concern in the diagnosis of a child with a fever of >5-day duration). The AUC of our predictive model was 0.816, which suggests that it is useful and reliable.

For fever patients with the assertive KD diagnosis, the timely initiation of treatment with IVIG can reduce the risk of CAAs significantly. Patients with incomplete KD who do not have the principal clinical features of KD but have a prolonged unexplained fever and inflammation carry an increased risk of CAAs (26). One reason for the increased risk of developing CAAs in atypical KD is a late diagnosis, which usually occurs in patients that do not exhibit all the clinical signs of KD. Given the overlap in clinical presentation with other conditions that also cause a prolonged fever in children (27), initial treatment with a single, high dose of IVIG is likely to be delayed while awaiting exclusion of other febrile illnesses. Furusho et al. (28) and Newburger et al. (7) reported that initial treatment with IVIG within the first 10 days of illness reduced the prevalence of CAAs 5-fold compared with that in children not treated with IVIG. Thus, a specific and sensitive diagnostic test that distinguishes KD from other febrile illnesses accurately would be a huge advance in KD management, reducing needless examinations and inappropriate treatments, and enabling prompt administration of IVIG.

In establishing the FCs group, our aim was to include several illnesses with symptoms that overlap with KD: lymphangitis, exanthema subitum, measles, and other viral illnesses (e.g., adenovirus infection), and childhood inflammatory disorders. The features that we recognized enabled discrimination of KD from other febrile illnesses of childhood and overlapping inflammatory symptoms. Some patients with non-KD disease but with semblable signs could be treated with IVIG. In the absence of pathognomonic features, the diagnosis of KD is reliant on the identification of principal clinical findings and exclusion of other similar diseases with known causes, which leads to a high missed detection rate for the first visit/preliminary diagnosis. Therefore, we used routinely collected electronic medical records (EMRs) data that are available at the early stage of hospitalization to distinguish KD from other febrile illnesses. We did not refer to the recommendation of "at least 5 days of fever" and enable diagnosis earlier than medical experts using current KD diagnosis guidelines to suggest timely intervention. We developed a highly sensitive and specific algorithm for the diagnosis of KD. A prospective study of the laboratory variables in our model will be essential to determine its potential applications.

Several tests to diagnose KD have been developed. Ling et al. (29) reported one method, which involves combining clinical and molecular methods to distinguish KD from other febrile illnesses. That is the future research direction, but our diagnostic model did not include molecular methods. Such advanced technology must be validated in terms of its clinical value and if it is validated and practical, we will consider modifying our diagnostic algorithm by adding more sensitive and specific indicators.

Maki et al. (30) reported a diagnostic scoring system using contrast-enhanced computed tomography (CT) findings for differentiating KD patients from children with other unexplained febrile illnesses and cervical lymphadenopathy. The sensitivity, specificity, and accuracy of their scoring system was 86%, 86%, and 86%, respectively, for diagnosing KD. The outstanding advantages of CT are high-density resolution, clear cross-section anatomy, and details of lesions, but it involves radiation exposure and is expensive. Ultrasound is non-invasive, does not involve radiation exposure, and is inexpensive. Therefore, from the perspective of safety and expense, our diagnostic model is more practical for clinicians and patients. In addition, enlargement of cervical lymph nodes is the least common feature of KD.

Independent predictors, such as the level of WBC, CRP, HB, %NEU, AST, ALT, TBL, albumin, and serum sodium, shown in previous diagnostic studies (17, 20, 21, 31) had a significant difference in the KD group and FCs group in our study. However, these predictors were not included in the final multivariate logistic regression model. In addition, the results of the univariate analysis may be different in various populations from different regions between the KD group and the FCs group. For example, the WBC level was significantly different between the KD group and FCs group in studies by Stemberger et al. (31), and Ling et al. (21), but not so in the study by Huang et al. (17). The CRP level was significantly different between the KD group and FCs group in our study and that of Song et al. (20), but not in the studies of Ling et al. or Stemberger et al. The serum level of chloride was significantly different between the two groups in our study, but not so in the studies of Stemberger et al. and Huang et al. This might be attributed to the fact that KD pathology is associated with genetic polymorphisms, and the genetic determinants of KD are different in various regions and populations, as reported elsewhere (32, 33). This difference might be related to the unknown etiology and genetic polymorphisms of KD, which can lead to different predictors for the KD diagnosis in different populations. Another possible reason for these discrepancies is the small number of patients studied and limited laboratory data. These differences might affect the difference between studies.

In our study, some new factors were significantly different between the KD group and FCs group: level of RBCs, RDWa, RDW, PCV, MPV, PDW, MCH, MCV, protein in urine, hematuria, AST, ALT, ALB, as well as serum levels of calcium, sodium, magnesium, and potassium. However, none of those factors were independent predictors. The urinary protein level in KD patients was much higher than that in FCs, which suggested that the function of glomerular vessels in KD patients was impaired. Muta et al. (34) reported that KD patients had a reduction in the serum level of sodium and phosphorus. We observed a significantly lower serum level of chlorine, phosphorus, potassium, magnesium, calcium, and sodium in the KD group, which suggested that kidney vasculitis might lead to adverse effects on tubular reabsorption and renal function. In addition, the increase in the level of GGT, ALT, DBIL, and TBIL, lower level of albumin and prealbumin, and the higher urinary level of bilirubin in the KD group might imply a more severe inflammatory reaction in the liver of KD patients (35).

We showed that age and the level of GGT, PLT, globulin, %MON, phosphorus, UA, %LYM, prealbumin, AST:ALT ratio, chloride, LDH were independent predictors for the diagnosis of KD. Among those predictors, studies have reported levels of PLT, P-LYM, GGT, and P-MON to be different (17, 21). An increased PLT is a characteristic feature of KD. In some studies, the degree of thrombocytosis was correlated with the risk of CAAs in KD. Durongpisitkul et al. (36) and Wang et al. (37) reported a reduction of %LYM in patients with KD, thereby suggesting a stronger inflammatory response. In this context, the GGT level in the KD group was much higher than that in the FCs group, a result which is in accordance with the data from a study by Tremoulet et al. (38) and Ting et al. (39). Tremoulet et al. (40) reported that the increased level of GGT was used to predict resistance to treatment with IVIG and an increased risk for CAAs. Age also plays a very important part in the clinical manifestations of KD. Stemberger et al. (31) have reported that age-related differences were present in the initial presentation of KD in a pediatric emergency department. Based on the individual predictors mentioned above, we established a new model for KD diagnosis with a sensitivity of 86%, a specificity of 81%, and an AUC of 0.907.

One of the strengths of our study was the use of routinely collected EMRs from a large dataset of KD patients and FCs over one decade. This sample size and number of items are much larger than those used in previous models for KD diagnosis. Another strength of the study was the use of FCs. For some febrile patients with a diagnosis of KD upon hospital admission, the diagnosis upon hospital discharge was febrile illness for which KD had been included in the differential diagnosis and who had a fever and at least one of the clinical features of KD. Our diagnostic algorithm for diagnosis in patients with KD may be used to help guide clinicians, especially in underdeveloped countries, in initial decisions about the stage of therapy.

Our study had four main limitations. First, a selection bias may have been present because our study was retrospective and from a single center. Second, some variables were not available, which might have led to a bias in statistical analyses. For data items with a missing detection rate $<25\%$, we undertook MICE to reduce the risk of bias. Third, the treatment and assessment of patients were done by multiple clinical teams. Fourth, although all FCs had a standardized set of clinical laboratory tests for KD as recommended by pediatricians, very few FCs underwent echocardiography.

CONCLUSIONS

This is the first study with large sample sizes to discriminate KD from other febrile illnesses in China. The diagnosis of KD could be predicted using age as well as the level of %MON, phosphorus, UA, globulin, %LYM, prealbumin, GGT, AST:ALT ratio, serum chloride, LDH, and PLT. Future prospective studies must be done to validate the utility of this new model and improve KD diagnosis.

DATA AVAILABILITY STATEMENT

The datasets generated for this study will not be made publicly available According to the Ethics Committee of the Children's Hospital Affiliated to Chongqing Medical University, we have been approved to use this part of clinical data for clinical research, but no permission has been granted for public inquiry and sharing.

ETHICS STATEMENT

This study was approved by the Ethics Committee of the Children's Hospital Affiliated to Chongqing Medical University.

AUTHOR CONTRIBUTIONS

ZH designed the study, collected and analyzed the data, and drafted the initial manuscript. X-HT collected and analyzed the data. HW built the model and prepared all figures. BP edited the manuscript. T-WL and JT designed the study, reviewed, and edited the manuscript. All authors contributed to the article and approved the submitted version.

FUNDING

The present study was supported by research grants from the National Natural Science Foundation of China (81974030) and the Science and Technology Innovation of Social Undertakings and People's Livelihood Security of Chongqing (cstc 2015shms-ztzx0031).

SUPPLEMENTARY MATERIAL

The Supplementary Material for this article can be found online at: https://www.frontiersin.org/articles/10.3389/fped.2020.533759/full#supplementary-material

REFERENCES

1. Burns JC, Glodé MP. Kawasaki syndrome. *Lancet.* (2004) 364:533–44. doi: 10.1016/S0140-6736(04)16814-1
2. Kim GB, Park S, Eun LY, Han JW, Lee SY, Yoon KL, et al. Epidemiology and clinical features of Kawasaki Disease in South Korea, 2012-2014. *Pediatr Infect Dis J.* (2017) 36:482–5. doi: 10.1097/INF.0000000000001474
3. Makino N, Nakamura Y, Yashiro M, Ae R, Tsuboi S, Aoyama Y, et al. Descriptive epidemiology of Kawasaki disease in Japan, 2011-2012: from the results of the 22nd nationwide survey. *J Epidemiol.* (2015) 25:239–45. doi: 10.2188/jea.JE20140089
4. Lue HC, Chen LR, Lin MT, Chang LY, Wang JK, Lee CY, et al. Estimation of the incidence of Kawasaki disease in Taiwan. A comparison of two data sources: nationwide hospital survey and national health insurance claims. *Pediatr Neonatol.* (2014) 55:97–100. doi: 10.1016/j.pedneo.2013.05.011
5. Kao AS, Getis A, Brodine S, Burns JC. Spatial and temporal clustering of Kawasaki syndrome cases. *Pediatr Infect Dis J.* (2008) 27:981–5. doi: 10.1097/INF.0b013e31817acf4f
6. Kato H, Sugimura T, Akagi T, Sato N, Hashino K, Maeno Y, et al. Long-term consequences of Kawasaki disease. A 10- to 21-year follow-up study of 594 patients. *Circulation.* (1996) 94:1379–85. doi: 10.1161/01.CIR.94.6.1379
7. Newburger JW, Takahashi M, Burns JC, Beiser AS, Chung KJ, Duffy CE, et al. The treatment of Kawasaki syndrome with intravenous gamma globulin. *New Engl J Med.* (1986) 315:341–7. doi: 10.1056/NEJM198608073150601
8. Newburger JW, Takahashi M, Beiser AS, Burns JC, Bastian J, Chung KJ, et al. A single intravenous infusion of gamma globulin as compared with four infusions in the treatment of acute Kawasaki syndrome. *New Engl J Med.* (1991) 324:1633–9. doi: 10.1056/NEJM199106063242305
9. Wilder MS, Palinkas LA, Kao AS, Bastian JF, Turner CL, Burns JC. Delayed diagnosis by physicians contributes to the development of coronary artery aneurysms in children with Kawasaki syndrome. *Pediatr Infect Dis J.* (2007) 26:256–60. doi: 10.1097/01.inf.0000256783.57041.66
10. Anderson MS, Todd JK, Glode MP. Delayed diagnosis of Kawasaki syndrome: an analysis of the problem. *Pediatrics.* (2005) 115:e428–33. doi: 10.1542/peds.2004-1824
11. Newburger JW, Takahashi M, Gerber MA, Gewitz MH, Tani LY, Burns JC, et al. Diagnosis, treatment, and long-term management of Kawasaki disease: a statement for health professionals from the Committee on Rheumatic Fever, Endocarditis, and Kawasaki Disease, Council on Cardiovascular Disease in the Young, American Heart Association. *Pediatrics.* (2004) 114:1708–33. doi: 10.1542/peds.2004-2182
12. Kawasaki T, Kosaki F, Okawa S, Shigematsu I, Yanagawa H. A new infantile acute febrile mucocutaneous lymph node syndrome (MLNS) prevailing in Japan. *Pediatrics.* (1974) 54:271–6.
13. Morens DM, Nahmias AJ. Kawasaki disease: a 'new' pediatric enigma. *Hosp Pract.* (1978) 13:109–12, 119–20. doi: 10.1080/21548331.1978.11707402
14. Kawasaki T. [Acute febrile mucocutaneous syndrome with lymphoid involvement with specific desquamation of the fingers and toes in children]. *Arerugi.* (1967) 16:178–222.
15. Jaggi P, Kajon AE, Mejias A, Ramilo O, Leber A. Human adenovirus infection in Kawasaki disease: a confounding bystander? *Clin Infect Dis.* (2013) 56:58–64. doi: 10.1093/cid/cis807
16. Falcini F, Ozen S, Magni-Manzoni S, Candelli M, Ricci L, Martini G, et al. Discrimination between incomplete and atypical Kawasaki syndrome versus other febrile diseases in childhood: results from an international registry-based study. *Clin Exp Rheumatol.* (2012) 30:799–804.
17. Huang MY, Gupta-Malhotra M, Huang JJ, Syu FK, Huang TY. Acute-phase reactants and a supplemental diagnostic aid for Kawasaki disease. *Pediatr Cardiol.* (2010) 31:1209–13. doi: 10.1007/s00246-010-9801-y
18. Okada Y, Minakami H, Tomomasa T, Kato M, Inoue Y, Kozawa K, et al. Serum procalcitonin concentration in patients with Kawasaki disease. *J Infect.* (2004) 48:199–205. doi: 10.1016/j.jinf.2003.08.002
19. Barone SR, Pontrelli LR, Krilov LR. The differentiation of classic Kawasaki disease, atypical Kawasaki disease, and acute adenoviral infection: use of clinical features and a rapid direct fluorescent antigen test. *Arch Pediatr Adolesc Med.* (2000) 154:453–6. doi: 10.1001/archpedi.154.5.453
20. Xiu-Yu S, Jia-Yu H, Qiang H, Shu-Hui D. Platelet count and erythrocyte sedimentation rate are good predictors of Kawasaki disease: ROC analysis. *J Clin Lab Anal.* (2010) 24:385–8. doi: 10.1002/jcla.20414
21. Ling XB, Kanegaye JT, Ji J, Peng S, Sato Y, Tremoulet A, et al. Point-of-care differentiation of Kawasaki disease from other febrile illnesses. *J Pediatr.* (2013) 162:183–8.e3. doi: 10.1016/j.jpeds.2012.06.012
22. McCrindle BW, Rowley AH, Newburger JW, Burns JC, Bolger AF, Gewitz M, et al. Diagnosis, treatment, and long-term management of Kawasaki Disease: a scientific statement for health professionals from the American Heart Association. *Circulation.* (2017) 135:e927–99. doi: 10.1161/CIR.0000000000000484
23. Tan XH, Zhang XW, Wang XY, He XQ, Fan C, Lyu TW, et al. A new model for predicting intravenous immunoglobin-resistant Kawasaki disease in Chongqing: a retrospective study on 5277 patients. *Sci Rep.* (2019) 9:1722. doi: 10.1038/s41598-019-39330-y
24. Azur MJ, Stuart EA, Frangakis C, Leaf PJ. Multiple imputation by chained equations: what is it and how does it work? *Int J Methods Psychiatr Res.* (2011) 20:40–9. doi: 10.1002/mpr.329

25. Yu JJ. Diagnosis of incomplete Kawasaki disease. *Kor J Pediatr.* (2012) 55:83–7. doi: 10.3345/kjp.2012.55.3.83
26. Minich LL, Sleeper LA, Atz AM, McCrindle BW, Lu M, Colan SD, et al. Delayed diagnosis of Kawasaki disease: what are the risk factors? *Pediatrics.* (2007) 120:e1434–40. doi: 10.1542/peds.2007-0815
27. Newburger JW, Takahashi M, Gerber MA, Gewitz MH, Tani LY, Burns JC, et al. Diagnosis, treatment, and long-term management of Kawasaki disease: a statement for health professionals from the Committee on Rheumatic Fever, Endocarditis and Kawasaki Disease, Council on Cardiovascular Disease in the Young, American Heart Association. *Circulation.* (2004) 110:2747–71. doi: 10.1161/01.CIR.0000145143.19711.78
28. Furusho K, Kamiya T, Nakano H, Kiyosawa N, Shinomiya K, Hayashidera T, et al. High-dose intravenous gammaglobulin for Kawasaki disease. *Lancet.* (1984) 2:1055–8. doi: 10.1016/S0140-6736(84)91504-6
29. Ling XB, Lau K, Kanegaye JT, Pan Z, Peng S, Ji J, et al. A diagnostic algorithm combining clinical and molecular data distinguishes Kawasaki disease from other febrile illnesses. *BMC Med.* (2011) 9:130. doi: 10.1186/1741-7015-9-130
30. Maki H, Maki Y, Shimamura Y, Fukaya N, Ozawa Y, Shibamoto Y. Differentiation of Kawasaki Disease from other causes of fever and cervical lymphadenopathy: a diagnostic scoring system using contrast-enhanced CT. *Am J Roentgenol.* (2019) 212:665–71. doi: 10.2214/AJR.18.20262
31. Stemberger Maric L, Papic N, Sestan M, Knezovic I, Tesovic G. Challenges in early diagnosis of Kawasaki disease in the pediatric emergency department: differentiation from adenoviral and invasive pneumococcal disease. *Wiener klinische Wochenschrift.* (2018) 130:264–72. doi: 10.1007/s00508-018-1324-1
32. Del Principe D, Pietraforte D, Gambardella L, Marchesi A, Tarissi de Jacobis I, Villani A, et al. Pathogenetic determinants in Kawasaki disease: the haematological point of view. *J Cell Mol Med.* (2017) 21:632–9. doi: 10.1111/jcmm.12992
33. Lin MT, Wang JK, Yeh JI, Sun LC, Chen PL, Wu JF, et al. Clinical implication of the C allele of the ITPKC Gene SNP rs28493229 in Kawasaki Disease: association with disease susceptibility and BCG scar reactivation. *Pediatr Infect Dis J.* (2011) 30:148–52. doi: 10.1097/INF.0b013e3181f43a4e
34. Muta H, Ishii M, Egami K, Hayasaka S, Nakamura Y, Yanagawa H, et al. Serum sodium levels in patients with Kawasaki disease. *Pediatr Cardiol.* (2005) 26:404–7. doi: 10.1007/s00246-004-0789-z
35. Sano T, Kurotobi S, Matsuzaki K, Yamamoto T, Maki I, Miki K, et al. Prediction of non-responsiveness to standard high-dose gamma-globulin therapy in patients with acute Kawasaki disease before starting initial treatment. *Eur J Pediatr.* (2007) 166:131–7. doi: 10.1007/s00431-006-0223-z
36. Durongpisitkul K, Soongswang J, Laohaprasitiporn D, Nana A, Prachuabmoh C, Kangkagate C. Immunoglobulin failure and retreatment in Kawasaki disease. *Pediatr Cardiol.* (2003) 24:145–8. doi: 10.1007/s00246-002-0216-2
37. Hua W, Sun Y, Wang Y, Fu S, Wang W, Xie C, et al. A new model to predict intravenous immunoglobin-resistant Kawasaki disease. *Oncotarget.* (2017) 8:80722–9. doi: 10.18632/oncotarget.21083
38. Tremoulet AH, Jain S, Chandrasekar D, Sun X, Sato Y, Burns JC. Evolution of laboratory values in patients with Kawasaki disease. *Pediatr Infect Dis J.* (2011) 30:1022–6. doi: 10.1097/INF.0b013e31822d4f56
39. Ting EC, Capparelli EV, Billman GF, Lavine JE, Matsubara T, Burns JC. Elevated gamma-glutamyltransferase concentrations in patients with acute Kawasaki disease. *Pediatr Infect Dis J.* (1998) 17:431–2. doi: 10.1097/00006454-199805000-00020
40. Tremoulet AH, Best BM, Song S, Wang S, Corinaldesi E, Eichenfield JR, et al. Resistance to intravenous immunoglobulin in children with Kawasaki disease. *J Pediatr.* (2008) 153:117–21. doi: 10.1016/j.jpeds.2007.12.021

Conflict of Interest: The authors declare that the research was conducted in the absence of any commercial or financial relationships that could be construed as a potential conflict of interest.

frontiers in Pediatrics

ORIGINAL RESEARCH
published: 02 December 2020
doi: 10.3389/fped.2020.521936

Medical Image-Based Hemodynamic Analyses in a Study of the Pulmonary Artery in Children With Pulmonary Hypertension Related to Congenital Heart Disease

Liping Wang[1], *Jinlong Liu*[1,2,3]*, *Yumin Zhong*[4], *Mingjie Zhang*[1], *Jiwen Xiong*[1], *Juanya Shen*[1,2,3], *Zhirong Tong*[1,2,3] and *Zhuoming Xu*[1]*

[1] Department of Thoracic and Cardiovascular Surgery, Shanghai Children's Medical Center, Shanghai Jiao Tong University School of Medicine, Shanghai, China, [2] Pediatric Translational Medicine Institute, Shanghai Jiao Tong University School of Medicine, Shanghai, China, [3] Shanghai Engineering Research Center of Virtual Reality of Structural Heart Disease, Shanghai Children's Medical Center, Shanghai Jiao Tong University School of Medicine, Shanghai, China, [4] Department of Radiology, Shanghai Children's Medical Center, Shanghai Jiao Tong University School of Medicine, Shanghai, China

OPEN ACCESS

Edited by:
Hongfang Jin,
Peking University First Hospital, China

Reviewed by:
Ju Liu,
Shandong University, China
Tiewei Lv,
Children's Hospital of Chongqing Medical University, China

***Correspondence:**
Jinlong Liu
jinlong_liu_man@163.com
Zhuoming Xu
zmxcicu@163.com

Specialty section:
This article was submitted to Pediatric Cardiology, a section of the journal Frontiers in Pediatrics

Received: *20 December 2019*
Accepted: *13 October 2020*
Published: *02 December 2020*

Citation:
Wang L, Liu J, Zhong Y, Zhang M, Xiong J, Shen J, Tong Z and Xu Z (2020) Medical Image-Based Hemodynamic Analyses in a Study of the Pulmonary Artery in Children With Pulmonary Hypertension Related to Congenital Heart Disease. Front. Pediatr. 8:521936. doi: 10.3389/fped.2020.521936

Objective: Pulmonary hypertension related to congenital heart disease (PH-CHD) is a devastating disease caused by hemodynamic disorders. Previous hemodynamic research in PH-CHD mainly focused on wall shear stress (WSS). However, energy loss (EL) is a vital parameter in evaluation of hemodynamic status. We investigated if EL of the pulmonary artery (PA) is a potential biomechanical marker for comprehensive assessment of PH-CHD.

Materials and Methods: Ten PH-CHD patients and 10 age-matched controls were enrolled. Subject-specific 3-D PA models were reconstructed based on computed tomography. Transient flow, WSS, and EL in the PA were calculated using non-invasive computational fluid dynamics. The relationship between body surface area (BSA)-normalized EL ($\dot{E}$) and PA morphology and PA flow were analyzed.

Results: Morphologic analysis indicated that the BSA-normalized main PA (MPA) diameter ($D_{MPAnorm}$), MPA/aorta diameter ratio (D_{MPA}/D_{AO}), and MPA/(left PA + right PA) [$D_{MPA}/D_{(LPA+RPA)}$] diameter ratio were significantly larger in PH-CHD patients. Hemodynamic results showed that the velocity of the PA branches was higher in PH-CHD patients, in whom PA flow rate usually increased. WSS in the MPA was lower and $\dot{E}$ was higher in PH-CHD patients. $\dot{E}$ was positively correlated with $D_{MPAnorm}$, D_{MPA}/D_{AO}, and $D_{MPA}/D_{(LPA+RPA)}$ ratios and the flow rate in the PA. $\dot{E}$ was a sensitive index for the diagnosis of PH-CHD.

Conclusion: $\dot{E}$ is a potential biomechanical marker for PH-CHD assessment. This hemodynamic parameter may lead to new directions for revealing the potential pathophysiologic mechanism of PH-CHD.

Keywords: pulmonary hypertension, energy loss, congenital heart disease, computational fluid dynamics, wall shear stress

INTRODUCTION

Congenital heart disease (CHD) is an anatomic defect associated with abnormal cardiovascular development *in utero*. Medical research shows that CHD prevalence at birth has increased from 0.6 to 0.9% in recent years, and that Asia has the highest prevalence of all regions evaluated (1).

In recent years, although advances in cardiac surgical skills and perioperative management have reduced CHD-related mortality dramatically, CHD remains the leading cause of death due to birth defects in the first year of life (2). The mortality increases if it is accompanied by severe complications.

Pulmonary hypertension (PH) is a common complication of CHD that can start at any age. Timely and accurate diagnosis reduces the severity of pulmonary vascular remodeling and the risk of heart failure, thereby giving patients a chance to receive the best course of treatment and long-term outcomes.

However, the diagnosis and prognosis of PH have not improved much in recent years (3). The main reason is a lack of understanding of its pathophysiology. PH is a response to abnormal hemodynamics in CHD patients (4–6), which appear before morphologic remodeling (7). Therefore, knowing the hemodynamic characteristics of the pulmonary artery (PA) may benefit comprehension of pathophysiologic mechanisms and yield more detailed information for the diagnosis and treatment of PH in CHD (PH-CHD).

Right-heart catheterization and transthoracic echocardiography (TTE) are used commonly for PH-CHD evaluation. However, neither the invasive catheterization nor the non-invasive TTE can be used to provide detailed information on hemodynamics.

Thanks to the development of computer and medical imaging technologies, computational fluid dynamics (CFD) has been employed to obtain local hemodynamics of the measured site and display them in a visual and stereoscopic way, which enables the study of the relationship between hemodynamics and CHD development. In recent years, CFD has been used to illustrate hemodynamic characteristics in patients with PH (8, 9). Many of those studies have concentrated mainly on assessment of shear stress (9, 10). Nevertheless, it has been shown that increased energy loss (EL) is closely related to the long-term outcome of patients (11–13).

EL is closely related to vascular morphology and flow patterns, and it is a crucial parameter in evaluation of hemodynamic disorders. Lee and colleagues (14) studied EL in the PA in different pathophysiologic scenarios and concluded that EL increased in patients with abnormal pulmonary vascular morphology. A recent study in adult patients with chronic thromboembolic pulmonary hypertension (CTEPH) demonstrated that alteration of energy dissipation in the PA has substantial effects on disease development (15).

In children with PH-CHD, abnormal morphology of the PA and flow status may influence EL. Few studies have investigated this biomechanical factor and its potential effect on this population.

We used CFD to explore subject-specific hemodynamics, including wall shear stress (WSS) and EL, which are expected to assist better understanding of PH-CHD pathophysiology and clinical decision making. For controlling intergroup variation caused by age, body surface area (BSA) was used to normalize quantitative indices.

MATERIALS AND METHODS

Ethical Approval of the Study Protocol

The study protocol was approved by the Health Research Ethics Board of Shanghai Children's Medical Center within Shanghai Jiao Tong University School of Medicine (Shanghai, China). Written informed consent was obtained from the parent/legal guardian of participants.

Patient Selection

We enrolled 10 PH-CHD patients with a velocity of tricuspid regurgitation (TR) $\geq$4.0 m/s and/or a predominantly right-to-left shunt of the ventricular septum, which was measured by TTE. Meanwhile, a control group of 10 age-matched CHD patients without PH were recruited to exclude confounders and control intergroup variation for better single-factor analysis. The diagnosis of the control group was established when TTE showed a velocity of TR $\leq$ 2.9 m/s and/or left-to-right shunt of the ventricular septum $\geq$4.0 m/s. The enrollment criteria followed the guideline of PH, which was the general consent achieved at the 6th World Symposium on Pulmonary Hypertension (16, 17). Detailed clinical information on these patients is shown in **Table 1**.

All the clinical data of patients were collected: sex, age, weight, height, BSA, body mass index (BMI), left ventricular ejection fraction (LVEF), and contrast-enhanced computed tomography (CT) of the chest.

We excluded individuals with stenosis of the right ventricular outflow tract, pulmonary disease, or other diseases that could be an underlying cause of PH.

Model Reconstruction

Sixty-four-row contrast-enhanced volumetric CT (Discovery CT750 HD; General Electric, Boston, MA, USA) data were used for reconstruction of 3-D subject-specific PA models in Mimics 20.0 (Materialize, Leuven, Belgium) and surface smoothing in 3-Matic 11.0 (Materialize, Leuven, Belgium). **Figure 1** shows the lateral and anterior views of the 3-D-reconstructed PA geometries of these 20 patients.

The maximum diameter of the main PA (D_{MPA}), left PA (D_{LPA}), and right PA (D_{RPA}) was measured. Subject-specific aorta models were reconstructed to obtain the maximum diameter of the aorta (D_{AO}). These vascular parameters were normalized by BSA to control for age-related deviation. The D_{MPA}/D_{AO} and $D_{MPA}/D_{(LPA+RPA)}$ ratios were calculated to compare morphologic differences among different vessel segments.

Governing Equations

We assumed that the PA flow was that of an incompressible Newtonian fluid. The Navier–Stoke (N-S) equations (1) were used to describe the 3-D blood flow in the PA, which has a

TABLE 1 | Patient-specific clinical data.

	Patients	Diagnosis	Shunt size (cm)	Shunt velocity (m/s)	TR (m/s)	PI (m/s)
Non-PH	1	VSD	0.75	4.00 (left to right)	Mild	Mild
	2	CoA	/	/	Mild	2.06
	3	VSD	0.66	4.19 (left to right)	Mild	Mild
	4	VSD	0.70	4.80 (left to right)	Mild	Mild
	5	VSD	0.87	4.76 (left to right)	Mild	Mild
	6	VSD/ASD	1.05 (VSD)	4.95 (left to right, VSD)	Mild	Mild
	7	VSD	1.25	4.03 (left to right)	Mild	Mild
	8	VSD/ASD	0.77 (VSD)	5.00 (left to right, VSD)	Mild	Mild
	9	PAPVC/ASD	0.66 (II ASD)	/	2.70	Mild
	10	PAPVC/ASD	1.52 (II ASD)	/	2.80	1.85
PH-CHD	1	Cor (obstructed)/PDA	0.1 (PDA)	2.09 (right to left)	5.00	Mild
	2	Supracardiac TAPVC (obstructed)/ASD	1.38	right to left	4.10	Mild
	3	VSD	1.1	Bi-directional	4.28	3.67
	4	VSD	0.89	Bi-directional	4.68	4.59
	5	VSD/ASD/PDA	0.97/0.15 (VSD/PDA)	Bi-directional	5.62	Mild
	6	CAVC/PDA	0.96/0.21 (VSD/PDA)	Bi-directional	/	Mild
	7	VSD/ASD	0.70 (VSD)	Bi-directional	4.66	Mild
	8	Supracardiac TAPVC (obstructed)/VSD/ASD	0.40 (VSD)	Bi-directional	4.79	4.04
	9	CAVC/PDA	2.00/0.28 (VSD/PDA)	Bi-directional	/	3.00
	10	VSD	1.93	Bi-directional	/	4.01

VSD, ventricular septal defect; CoA, coarctation; ASD, atrial septal defect;PDA, patent ductus arteriosus;CAVC, atrioventricular septal defect;BSA, body surface area; PAPVC, partial anomalous pulmonary venous drainage; Cor, cor triatriatum; TAPVC, total anomalous pulmonary venous drainage; TR, tricuspid regurgitation; PI, pulmonary insufficiency.

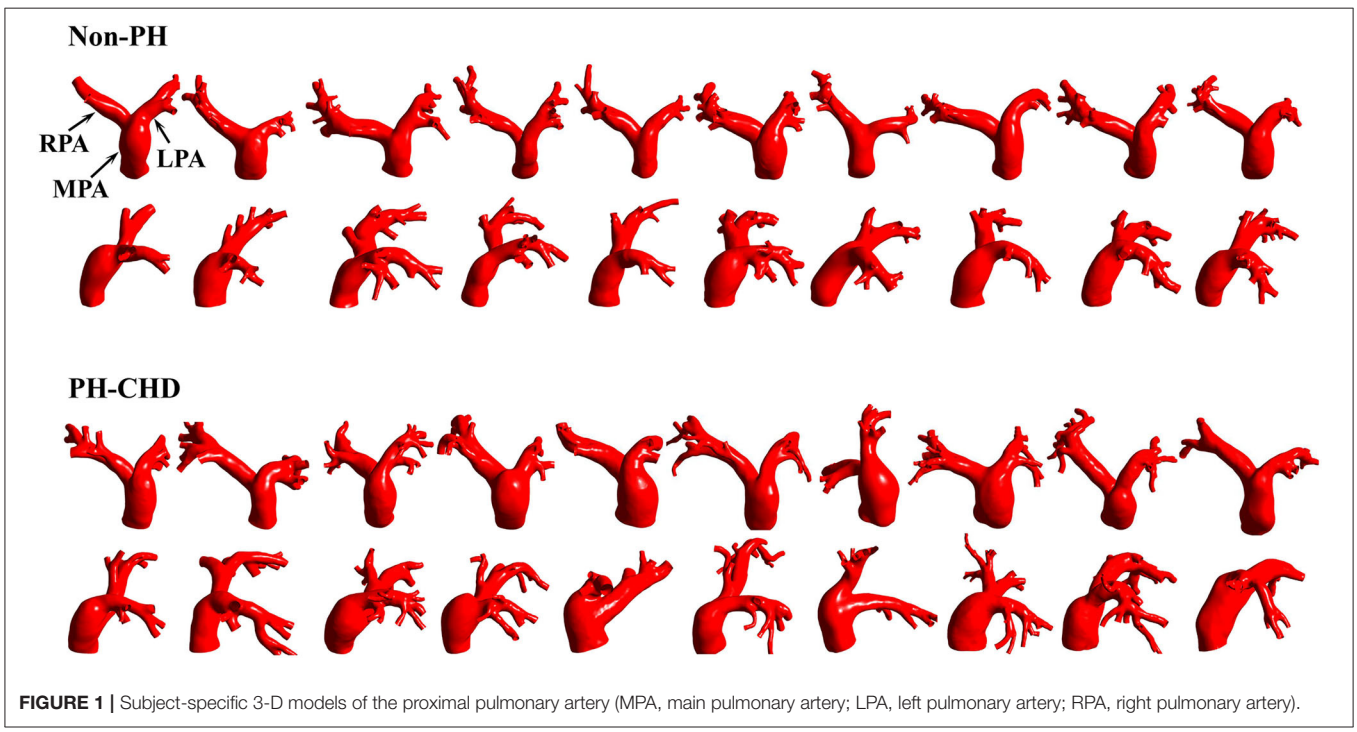

FIGURE 1 | Subject-specific 3-D models of the proximal pulmonary artery (MPA, main pulmonary artery; LPA, left pulmonary artery; RPA, right pulmonary artery).

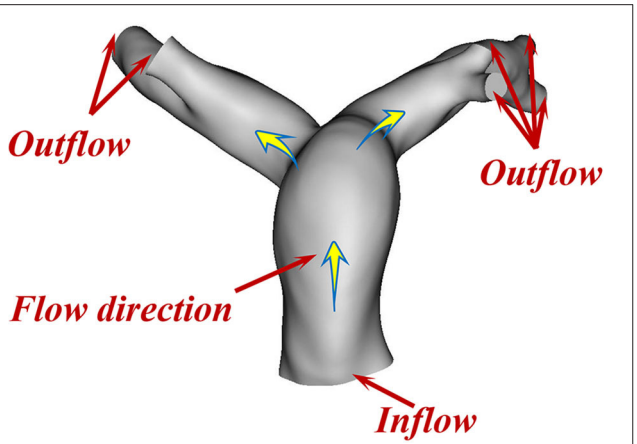

FIGURE 2 | Inflow and outflow in the PA (schematic).

constant density ($\rho = 1{,}060\ kg/m^3$) and viscosity ($\mu = 4.0 \times 10^{-3}$ Pa s).

$$\begin{cases} \frac{\partial}{\partial t}(\rho u_i) + \frac{\partial}{\partial x_j}(\rho u_i u_j) = \frac{\partial p}{\partial x_i} + \frac{\partial}{\partial x_j}\left[\mu\left(\frac{\partial u_i}{\partial x_j} + \frac{\partial u_j}{\partial x_i}\right)\right] + f_i \\ \frac{\partial \rho}{\partial t} + \frac{\partial}{\partial x_j}(\rho u_j) = 0 \end{cases} \quad (1)$$

where $i, j = 1, 2, 3$; x_1, x_2, x_3, represents the coordinate axes; u_i, u_j are velocity vectors; p is pressure; t is time; and f_i indicates the action of body forces and was omitted in the practical calculation. The average Reynolds number among all models ranged from 2,700 to 5,500. The maximum Reynolds number ranged from 5,700 to 13,000. Thus, we assumed the flow in the PA was turbulent, and we used a standard k-ε model to solve complex pulsatile flow.

Mesh Generation

Mesh generation was undertaken to discretize the computational domain and solve the governing equations using commercial software (ANSYS®-ICEM CFD 2019; Canonsburg, PA, USA). We used tetrahedral grids to discretize the volume layers of the fluid domain. Three body-fitted prism layers were used to improve the accuracy of calculation of the boundary layer of WSS. Grid independence was carried out to find the optimized mesh for CFD simulation, and the results were stable with a grid number reaching 0.9 million. The meshes of PH-CHD patients and controls were ∼1.5 and ∼1 million elements, respectively.

Boundary Conditions and Calculation

We used the pulsatile velocity of the MPA obtained by TTE as the inlet boundary condition. In addition, we assumed relative pressure as the outlet boundary condition and rigid with no-slip boundary conditions for the vessel wall. **Figure 2** shows the inflow and outflow in the PA schematically.

We used ANAYS®-CFX 2019 (Canonsburg, PA, USA) to solve the blood flow in the PA. The convergence criteria were set to 10^{-5} for each time step. More detailed information of the method has been reported in our previous work (13, 18–20).

Hemodynamic Evaluation

Transient PA streamlines, WSS, and EL were calculated to evaluate the biomechanical differences of patients with and without PH-CHD.

To better display the flow pattern during a cardiac period, we calculated the velocity and flow pattern at six time points (a–f) in a cardiac cycle.

WSS demonstrates the frictional force between blood flow and the vessel wall and was determined using Equation (2, 21, 22):

$$\tau wall = -\mu \left.\frac{\partial ux}{\partial n}\right|_{n=0} \quad (2)$$

where u_x is the velocity of the fluid near the vessel wall and n is the height above the vessel wall.

EL is the energy difference between the inlet and outlet of the calculated domain and was calculated by Equation (3):

$$EL = E_{inlet} - E_{outlet} \quad (3)$$

$$= \sum_{inlet}\left(P_i + \frac{1}{2}\rho u_i^2\right)Q_i - \sum_{outlet}\left(P_0 + \frac{1}{2}\rho u_0^2\right)Q_0 \quad (4)$$

where P is the static pressure, Q is the flow rate, and i, j are the inlet and outlet of PA, respectively. To control for age-related variation among patients, the BSA normalized EL ($\dot{E}$) was determined using Equation (4):

$$\dot{E} = \frac{EL}{S} \quad (5)$$

where S represents the BSA.

Statistical Analysis

Statistical analyses were carried out using SPSS 23.0 (IBM, Armonk, NY, USA). The Shapiro–Wilk test was used to check the normality of all parameters. Data with a normal distribution were analyzed using Student's t-test. Associations between variables were analyzed by Pearson's correlation coefficient (r) with two-tailed probability (p). A receiver operating characteristic (ROC) curve was used to measure the sensitivity and specificity of the calculated parameters. A threshold $p < 0.05$ was considered significant.

RESULTS

Demographic and Morphologic Analyses

Table 2 shows the demographic and morphologic measurements obtained in the two groups. The baseline data of sex, age, weight, height, BSA, BMI, and LVEF were similar in the two groups. The morphologic parameters of normalized D_{LPA} ($D_{LPAnorm}$), normalized D_{RPA} ($D_{RPAnorm}$), and normalized D_{AO} (D_{AOnorm}) were not significantly different between the groups. However, the normalized D_{MPA} ($D_{MPAnorm}$), D_{MPA}/D_{AO}, and $D_{MPA}/D_{(LPA+RPA)}$ ratios were, in general, larger in PH-CHD patients. These data indicate that the MPA was dilated markedly and there was relative stenosis in the LPA and RPA in PH-CHD patients.

Streamlines

The subject-specific streamlines of the PA were computed to investigate differences in flow patterns. Statistical analyses revealed that the flow rate in the PA [in L/(min·m^2)] was significantly higher at the normalized mean ($V_{meannorm}$) and maximum ($V_{maxnorm}$) velocity in PH-CHD patients than in controls (19.63 ± 6.223 vs. 11.94 ± 3.651, $p = 0.004$; 50.05 ± 13.882 vs. 29.98 ± 8.031, $p = 0.001$).

Figure 3 shows an example of the plots of PA flow rate in a cardiac cycle and the streamlines generated at six specific time points in two patients. One was a PH-CHD patient, and the other was a matched control subject. The velocity at the MPA was not significantly different between the two groups. However, at the PA branches, especially the bifurcation of the MPA into the LPA and RPA, the velocity was visibly higher in the PH-CHD patient than in the control subject. The velocity decreased faster in the non-PH patient than in the control subject during slow ejection and diastole (**Figures 3C–F**). Meanwhile, turbulent flow was observed at the same time point. Conversely, blood flow was relatively steady in the PH-CHD patient.

TABLE 2 | Subject-specific clinical data for the two groups.

	PH-CHD group	Control group	*p*-value
Sex (male/ female)	6/4	3/7	0.370
Age (month)	35.1 ± 31.239	40.20 ± 25.961	0.696
Height (cm)	84.40 ± 22.965	97.00 ± 24.585	0.252
Weight (kg)	11.05 ± 5.459	14.77 ± 6.441	0.180
BSA (m^2)	0.50 ± 0.209	0.60 ±0.229	0.221
BMI (kg/m^2)	14.76 ± 1.106	15.39 ± 2.678	0.501
LVEF (%)	69.75 ± 11.306	66.55 ± 2.448	0.403
Normalized D_{MPA} (cm)	4.93 ± 1.568	3.29 ± 0.913	0.010*
Normalized D_{LPA} (cm)	2.63 ± 0.871	1.99 ± 0.454	0.058
Normalized D_{RPA} (cm)	2.88 ± 0.993	2.15 ± 0.500	0.058
Normalized D_{AO} (cm)	3.33 ± 1.089	2.89 ± 0.870	0.336
D_{MPA}/D_{AO}	1.50 ± 0.235	1.17 ± 0.240	0.006*
$D_{MPA}/D_{(LPA+RPA)}$	0.91 ± 0.115	0.79 ± 0.084	0.019*

*BSA, body surface area; BMI, body mass index; LVEF, left ventricular ejection fraction; D, diameter; MPA, main pulmonary artery; AO, aorta; LPA, left pulmonary artery; RPA, right pulmonary artery; * $p < 0.05$.*

Wall Shear Stress

Figure 4 shows the results of detailed examination of the subject-specific WSS obtained in six patients of different ages. Simulated results demonstrated that the WSS of the MPA was visibly lower in PH-CHD patients than in control subjects. However, the spatially averaged WSS and time-averaged WSS were not significantly different between the two groups (7.35 ± 2.780 vs. 6.37 ± 3.978 Pa, $p = 0.525$; 2.41 ± 0.945 vs. 1.90 ± 0.983 Pa, $p = 0.249$). These average values could not reflect the local variation of WSS at the MPA, LPA, and RPA.

Energy Loss

EL of the PA was significantly higher in the PH group than in the control group (60.41 ± 46.551 vs. 26.34 ± 18.175 mW, $p = 0.031$). **Figure 5** shows the relationship between EL and the flow rate and morphology of the PA. There's a positive correlation of EL and the flow rate of PA (Vmean: $r = 0.843$, $p = 0.000$; Vmax: $r = 0.867$, $p = 0.000$) but a weakened relationship with D_{MAP} ($r = 0.483$, $p = 0.031$) and no relationship with D_{LPA} (0.413, 0.071) and D_{RPA} (0.374, 0.104). $\dot{E}$ was calculated to control the intergroup variation caused by age.$\dot{E}$ was increased predominantly in the PH

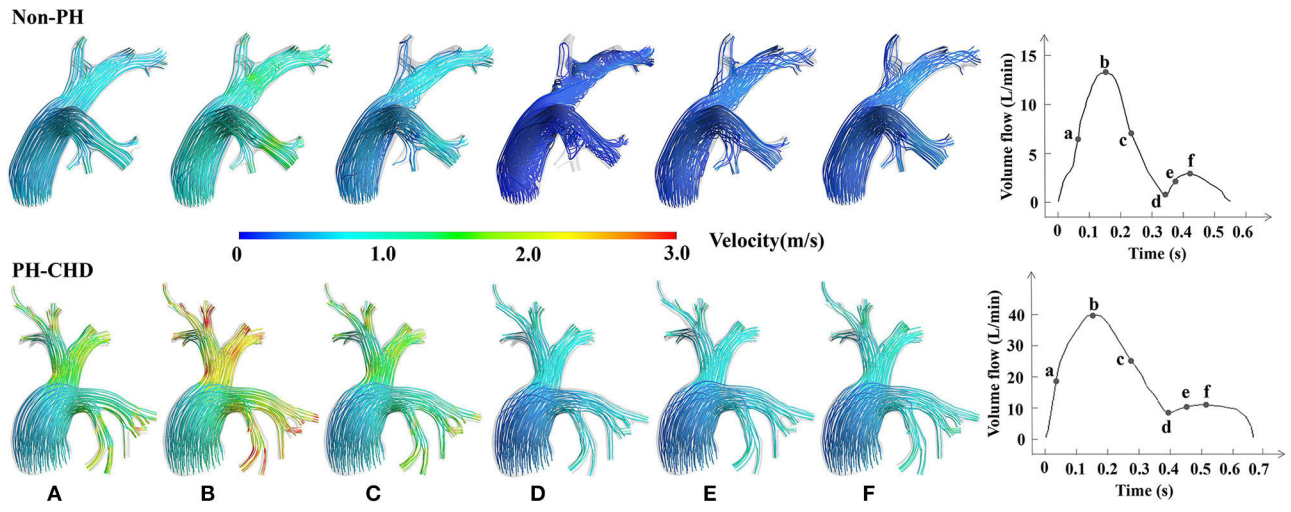

FIGURE 3 | Subject-specific streamlines at six time points in one cardiac period. **(A)** The midpoint of the period from the beginning of the cardiac cycle to the highest velocity reached in the rapid ejection phase, which is assumed to show rapid variation in the velocity. **(B)** The time point at the highest velocity of blood flow in one cardiac cycle. **(C)** The midpoint of the period when the velocity of blood flow decreased from the highest to the lowest, which is assumed to show rapid variation in the velocity during the slow ejection phase. **(D)** The time point at the lowest velocity of blood flow in one cardiac cycle. **(E)** The midpoint of the period between point **d** and the time point at the highest velocity in diastole with rapid variation in the velocity observed in diastole. And **(F),** The time at the highest velocity of diastole.

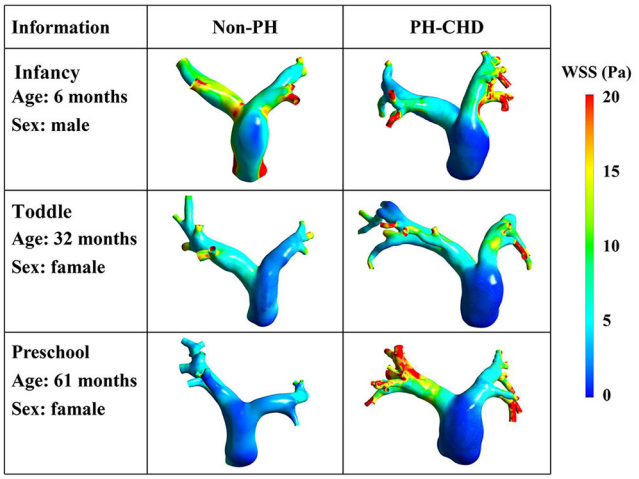

FIGURE 4 | Distribution of wall shear stress at maximum velocity.

group (121.60 ± 64.820 vs. 45.15 ± 25.302 mW/m^2, $p = 0.007$). **Figure 6** shows the $\dot{E}$ was positively correlated with $D_{MPAnorm}$ ($r = 0.501$, $p = 0.025$), $D_{LPAnorm}$ (0.483, 0.031), $D_{RPAnorm}$ (0.491, 0.028), $V_{meannorm}$ (0.861, 0.000), and $V_{maxnorm}$ (0.839, 0.000).

ROC curve analysis was performed to evaluate the diagnostic value of $\dot{E}$ in PH-CHD patients (**Figure 7**). It shows that $\dot{E}$ has a high AUC, sensitivity, and specificity.

DISCUSSION

PH is one of the most complex and devastating complications of CHD. Various studies (4–6) have demonstrated that the biomechanical mechanism underlying this disease has a major role in PH-CHD development.

Early studies on hemodynamics in PH focused mainly on the metric of WSS, its action on vascular morphology/function, and disease progression. However, several other hemodynamics studies have shown that EL is a key factor in evaluation of hemodynamic disorders (23–25).

Here, we provided new clues to explore more deeply the multiple pathologies of PH-CHD using non-invasive CFD. In the present study, we hypothesized that the hemodynamic parameter of EL could be used to explain the role of abnormal flow dynamics on PH-CHD. To control age-related variation, BSA was used to normalize subject-specific EL ($\dot{E}$).

Based on CFD calculations, the flow-dynamic features were significantly different between PH-CHD patients and control subjects. A high flow rate and velocity [in L/(min·m^2)] in PA branches were observed only in PH-CHD patients ($V_{meannorm}$: 19.63 ± 6.223 vs. 11.94 ± 3.651, $p = 0.004$; $V_{maxnorm}$: 50.05 ± 13.882 vs. 29.98 ± 8.031, $p = 0.001$) (**Figure 3**). Expansion of the MPA is one reason for this finding because it causes relative narrowing of the LPA and RPA. This conclusion (**Table 2**) was supported by a statistical comparison of the two groups with regard to $D_{MPAnorm}$ as well as D_{MPA}/D_{AO} and $D_{MPA}/D_{(LPA+RPA)}$ ratios. Vortex flow, which occurred during diastole, was observed only in control subjects. The streamlines were relatively steady in PH-CHD patients.

Sanz et al. (10) showed that velocity was a sensitive index for PH evaluation and was closely correlated to pressure and resistance in pulmonary circulation. Tang et al. (4) compared flow patterns between people with and without PH. They found that obvious turbulent flow occurred in a model of a normal PA, a finding that is in accordance with the present study. However, they demonstrated that the flow rate in the PA was higher than in normal subjects: This is exactly the opposite of what we discovered. The difference may have been because of the types of PH explored in these two studies. PH-CHD is a flow-induced disease. Pulmonary blood flow is increased in these patients due to congenital cardiovascular malformations. Abnormal blood flow in pulmonary circulation alters expression of flow-sensitive vascular regulatory factors and is the essential trigger for the development and progression of PH (26–28).

WSS denotes the force generated by the friction between blood flow and the endothelium. It is considered to be a vital biomechanical parameter for evaluation of blood flow–related diseases (29, 30). In healthy people, pulmonary endothelial cells can adapt to a normal range of shear stress. Prolonged abnormal WSS damages the function of pulmonary vessels by destroying endothelial structure and interfering with signal conduction. This process is closely related to PH-CHD development.

WSS has become a "hot topic" in the study of PH-CHD in recent years. Several studies have shown that WSS is a sensitive parameter for evaluating the function of endothelial cells (31, 32). Kheyfets et al. (33) found that WSS was closely related to the elasticity and resistance of the pulmonary artery. Tang et al. (4) explored the WSS of the PA in five PH patients and five control subjects. They showed that the WSS of the MPA was decreased significantly in patients with PH, which was about 20% that of the control group. **Figure 4** shows that lower WSS was found in the MPA of PH-CHD patients than in the control subjects. These results are in accordance with those reported previously (4, 9).

In healthy individuals, blood flow is arranged so that EL is low and normal cardiovascular circulation is maintained (34, 35). However, complex cardiovascular malformations in patients with PH-CHD can promote inefficient interactions between pulmonary blood flow and pulmonary structure, which increase EL. The cumulative effect of EL places an extra burden on the heart and may contribute to pulmonary vascular remodeling. Thus, understanding the influence of interrupted flow patterns and altered morphology on EL and the role of increased EL in PH-CHD may benefit clinical diagnosis and treatment.

Nagao et al. (15) explored energy dissipation in healthy people and patients with CTEPH before and after balloon pulmonary angioplasty (BPA) using phase-contrast magnetic resonance imaging. They found that EL was significantly higher in CTEPH patients than in healthy people and that BPA decreased EL. Preoperative EL was an independent and sensitive indicator that predicted patient outcomes.

We showed that EL and $\dot{E}$ were significantly higher in patients with PH-CHD than in non-PH patients (60.41 ± 46.551 vs. 26.34 ± 18.175 mW, $p = 0.031$; 121.60 ± 64.820 vs. 45.15 ± 25.302

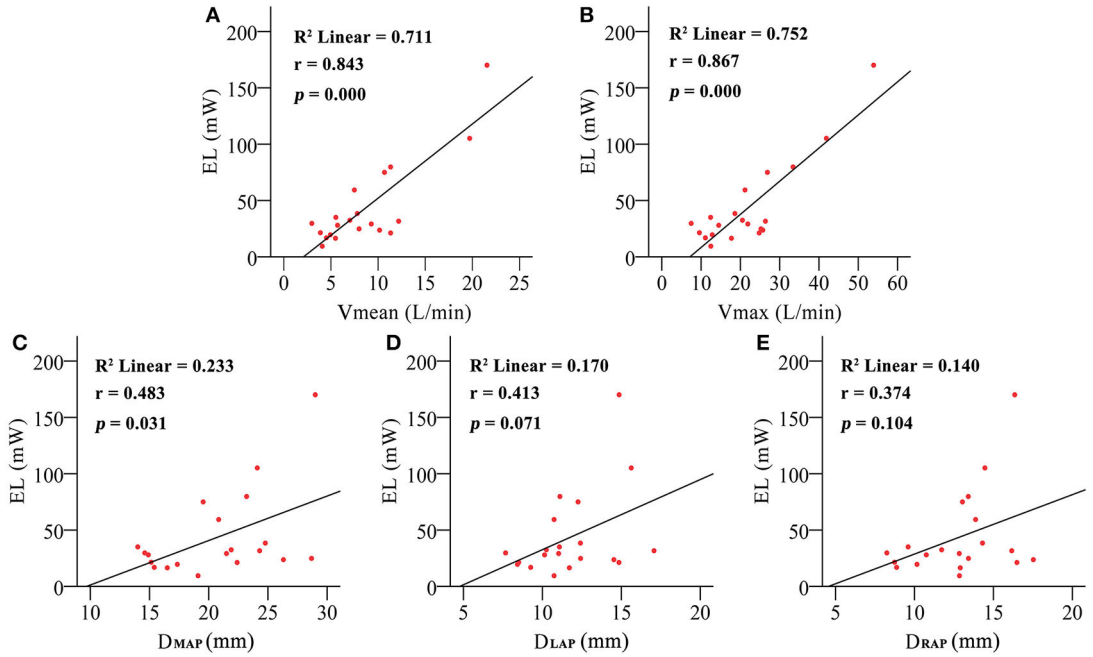

FIGURE 5 | The correlation between energy loss (EL) and mean pulmonary artery inflow (V_{mean}) **(A)**, maximum pulmonary artery inflow (V_{max}) **(B)**, mean pulmonary artery diameter (D_{MPA}) **(C)**, left pulmonary artery diameter (D_{LPA}) **(D),** and right pulmonary artery diameter (D_{RPA}) **(E)**.

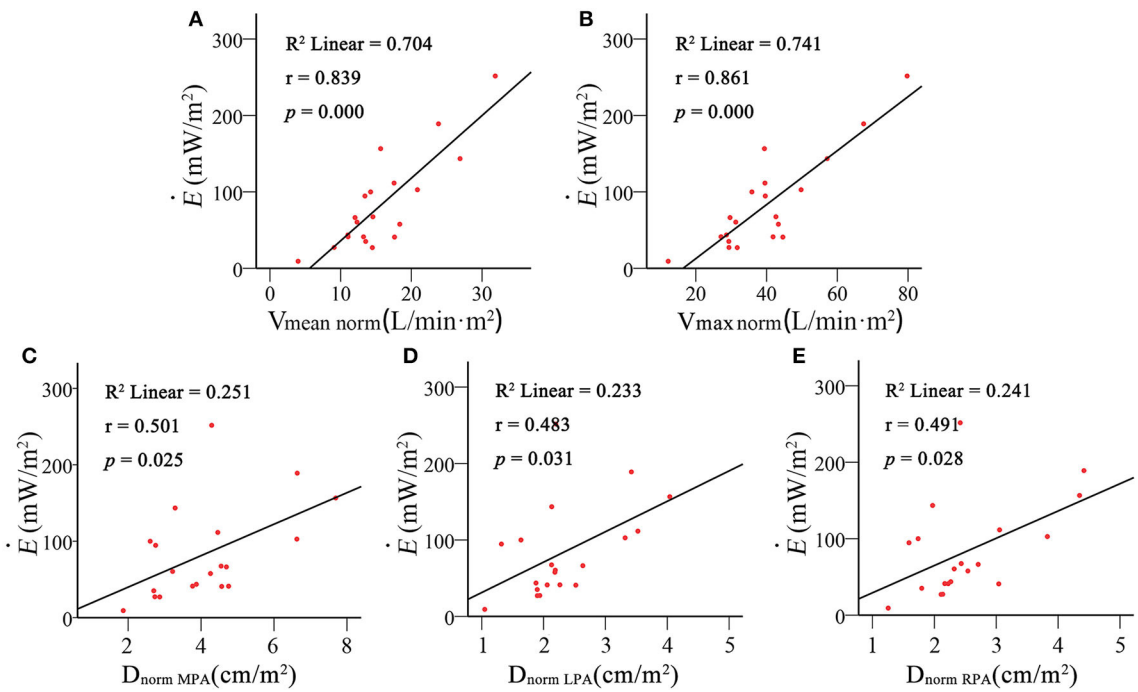

FIGURE 6 | Correlation analysis of body surface area (BSA)-normalized energy loss ($\dot{E}$) with BSA-normalized mean pulmonary artery inflow ($V_{meannorm}$) **(A)**, maximum pulmonary artery inflow ($V_{maxmean}$) **(B)**, mean pulmonary artery diameter ($D_{MPAnorm}$) **(C)**, left pulmonary artery diameter ($D_{LPAnorm}$) **(D)** and right pulmonary artery diameter ($D_{RPAnorm}$) **(E)**.

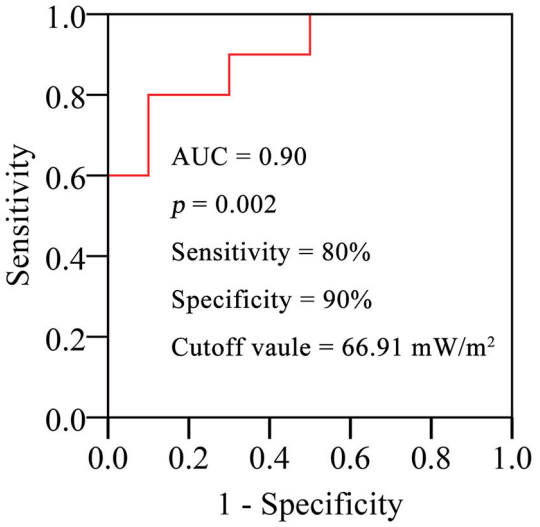

FIGURE 7 | ROC curves analysis of $\dot{E}$ in the pulmonary artery for diagnosing PH-CHD.

mW/m^2, $p = 0.007$, respectively). In fact, PH-CHD is a right ventricular–pulmonary artery (RV-PA) coupling disease (14). Increased pulmonary arterial pressure and pulmonary arterial resistance gradually damage the structure and function of the right ventricle. EL indicates the compensation of ventricular work. Higher EL indicates that the ventricle must do more work to maintain the stability of the circulatory system. Hence, in patients with PH-CHD, excessively high EL increases the burden on the right ventricle and the risk of right-heart failure. Thus, we provide a theoretical basis for future CFD research of the RV-PA coupling of PH-CHD.

On the other hand, studies have examined EL in patients with CHD extensively. Those studies show that abnormal vessel morphology has a significant effect on EL and the long-term prognoses of patients (36, 37). In the present study, there is a positive relationship between EL and the flow rate of PA but a poor relationship with the morphology of PA (**Figure 5**). Considering that the development of cardiovascular morphology and function are different in children of different age groups, we use BAS to normalize EL. $\dot{E}$ was positively correlated with the morphology and flow rate in the PA (**Figure 6**). It implies that age is a strong confounding factor, and normalized EL is a better predictive parameter. Changes in PA morphology, relatively stenosed PA branches, and increased PA flow rate are the main factors of $\dot{E}$. ROC curve analysis revealed that the $\dot{E}$ was sensitive diagnostic characteristics in PH-CHD (**Figure 7**). All these results imply that EL is an important factor in PH-CHD evaluation. However, it is worth noting that the cutoff values are just for reference due to the limited cases.

LIMIT OF THE STUDY

Our study had limitations. Ten PH-CHD patients and 10 age-matched controls were enrolled. Due to the relatively small sample size, only two patients were diagnosed as having irreversible PH-CHD based on postoperative follow-up data. Thus, we cannot offer a clear cutoff for operable and inoperable patients. However, we did identify hemodynamic parameters that were significantly different between the two groups. These results lay a foundation for further study on the reversibility of PH-CHD in a large population of patients. Our simulation assumed that the vessel wall was rigid, and the influence of vascular elasticity on hemodynamics was ignored. However, we aimed to reveal the relationship between hemodynamic indices and PH-CHD by comparing the hemodynamics of the two groups. Therefore, the properties of the vessel wall were simplified in this simulation. Each case was simulated under the same vessel condition, so the rigid-wall hypothesis had little effect on the results.

CONCLUSION

$\dot{E}$ is a potential biomechanical parameter for PH-CHD evaluation. The alteration of $\dot{E}$ is closely related to the morphology and flow rate of the PA. This study may offer a new clue for exploring the potential physiopathologic mechanism of PH-CHD and provide more intuitive information for clinicians to make appropriate clinical decisions.

DATA AVAILABILITY STATEMENT

All datasets generated for this study are included in the article/supplementary material.

ETHICS STATEMENT

This study was approved by the Institutional Health Research Ethics Board of the Shanghai Children's Medical Center, Shanghai Jiao Tong University School of Medicine, and written informed consent was obtained from parent/legal guardian of participants.

AUTHOR CONTRIBUTIONS

LW undertook CFD calculations, statistical analyses, and manuscript preparation. JL and ZX contributed to the study design, data collection, and manuscript preparation. YZ and MZ organized the clinical data. JX, JS, and ZT participated in model reconstruction. All authors contributed to the article and approved the submitted version.

FUNDING

The authors express gratitude for the support of the National Nature Science Foundation of China (81771934 to ZX; 81970439 and 81501558 to JL), Shanghai International Science and Technology Cooperation Projects (18410721400 to JL), Shanghai Jiao Tong University Medical and Engineering Intersection Fund (YG2019ZDA03 to ZX), and Fund of Shanghai Science and Technology Committee (17441903300 to JL; 17DZ2253100 to JL).

REFERENCES

1. van der Linde D, Konings EE, Slager MA, Witsenburg M, Helbing WA, Takkenberg JJ, et al. Birth prevalence of congenital heart disease worldwide: a systematic review and meta-analysis. *J Am Coll Cardiol.* (2011) 58:2241–7. doi: 10.1016/j.jacc.2011.08.025
2. Benjamin EJ, Blaha MJ, Chiuve SE, Cushman M, Das SR, Deo R, et al. Heart Disease and Stroke Statistics-2017 Update: A Report from the American heart association. *Circulation.* (2017) 135:e146–e603. doi: 10.1161/CIR.0000000000000485
3. Humbert M, Gerry Coghlan J, Khanna D. Early detection and management of pulmonary arterial hypertension. *Eur Respir Rev.* (2012) 21:306–12. doi: 10.1183/09059180.00005112
4. Tang BT, Pickard SS, Chan FP, Tsao PS, Taylor CA, Feinstein JA. Wall shear stress is decreased in the pulmonary arteries of patients with pulmonary arterial hypertension: an image-based, computational fluid dynamics study. *Pulm Circ.* (2012) 2:470–6. doi: 10.4103/2045-8932.105035
5. van der Feen DE, Bartelds B, de Boer RA, Berger RMF. Assessment of reversibility in pulmonary arterial hypertension and congenital heart disease. *Heart.* (2019) 105:276–82. doi: 10.1136/heartjnl-2018-314025
6. Dolan JM, Kolega J, Meng H. High wall shear stress and spatial gradients in vascular pathology: a review. *Ann Biomed Eng.* (2013) 41:1411–27. doi: 10.1007/s10439-012-0695-0
7. Kheyfets VO, Rios L, Smith T, Schroeder T, Mueller J, Murali S, et al. Patient-specific computational modeling of blood flow in the pulmonary arterial circulation. *Comput Methods Programs Biomed.* (2015) 120:88–101. doi: 10.1371/journal.pone.0205829
8. Schafer M, Ivy DD, Barker AJ, Kheyfets V, Shandas R, Abman SH, et al. Characterization of CMR-derived haemodynamic data in children with pulmonary arterial hypertension. *Eur Heart J Cardiovasc Imaging.* (2017) 18:424–31. doi: 10.1093/ehjci/jew152
9. Yang W, Dong M, Rabinovitch M, Chan FP, Marsden AL, Feinstein JA. Evolution of hemodynamic forces in the pulmonary tree with progressively worsening pulmonary arterial hypertension in pediatric patients. *Biomech Model Mechanobiol.* (2019) 18:779–96. doi: 10.1007/s10237-018-01114-0
10. Wang HH, Tseng WI, Yu HY, Chang MC, Peng HH. Phase-contrast magnetic resonance imaging for analyzing hemodynamic parameters and wall shear stress of pulmonary arteries in patients with pulmonary arterial hypertension. *Magma (New York, N.Y.).* (2019) 32:617–27. doi: 10.1007/s10334-019-00767-x
11. Honda T, Itatani K, Takanashi M, Mineo E, Kitagawa A, Ando H, et al. Quantitative evaluation of hemodynamics in the Fontan circulation: a cross-sectional study measuring energy loss in vivo. *Pediatr Cardiol.* (2014) 35:361–7. doi: 10.1007/s00246-013-0783-4
12. Khiabani RH, Whitehead KK, Han D, Restrepo M, Tang E, Bethel J, et al. Exercise capacity in single-ventricle patients after Fontan correlates with haemodynamic energy loss in TCPC. *Heart.* (2015) 101:139–43. doi: 10.1136/heartjnl-2014-306337
13. Zhang WM, Liu JL, Yan Q, Liu JF, Hong HF, Mao L. Computational haemodynamic analysis of left pulmonary artery angulation effects on pulmonary blood flow. *Interact Cardiovasc Thorac Surg.* (2016) 23:519–25. doi: 10.1093/icvts/ivw179
14. Lee N, Taylor MD, Hor KN, Banerjee RK. Non-invasive evaluation of energy loss in the pulmonary arteries using 4D phase contrast MR measurement: a proof of concept. *Biomed Eng Online.* (2013) 23:12. doi: 10.1186/1475-925X-12-93
15. Nagao M, Yamasaki Y, Abe K, Hosokawa K, Kawanami S, Kamitani T, et al. Energy efficiency and pulmonary artery flow after balloon pulmonary angioplasty for inoperable chronic thromboembolic pulmonary hypertension: analysis by phase-contrast MRI. *Eur J Radiol.* (2017) 87:99–104. doi: 10.1016/j.ejrad.2016.12.015
16. Simonneau G, Montani D, Celermajer DS, Denton CP, Gatzoulis MA, et al. Haemodynamic definitions and updated clinical classification of pulmonary hypertension. *Eur Respir J.* (2019) 53:1801913. doi: 10.1183/13993003.01913-2018
17. Rosenzweig EB, Abman SH, Adatia I, Beghetti M, Bonnet D, et al. Paediatric pulmonary arterial hypertension: updates on definition, classification, diagnostics and management. *Eur Respir J.* (2019) 53:1801916. doi: 10.1183/13993003.01916-2018
18. Sun Q, Liu JL, Qian Y, Zhang H, Wang Q, Sun Y, et al. Computational haemodynamic analysis of patient-specific virtual operations for total cavopulmonary connection with dual superior venae cavae. *Eur J Cardiothorac Surg.* (2014) 45:564–9. doi: 10.1093/ejcts/ezt394
19. Liu JL, Sun Q, Qian Y, Hong HF, Liu JF. Numerical simulation and hemodynamic analysis of the modified Blalock-Taussig shunt. *Conf Proc IEEE Eng Med Biol Soc.* (2013) 707–10. doi: 10.1109/EMBC.2013.6609598
20. Wang LP, Zhang MJ, Chen X, Hong HF, Liu JL, Xu ZM, et al. Hemodynamic analysis of pulmonary arterial hypertension associated with congenital heart disease: a numerical study of patient-specific models. 2018 11th international congress on image and signal processing. *BioMed Eng Informat.* (2018). doi: 10.1109/cisp-bmei.2018.8633167. [Epub ahead of print].
21. Ali D, Sen S. Finite element analysis of mechanical behavior, permeability and fluid induced wall shear stress of high porosity scaffolds with gyroid and lattice-based architectures[J]. *J Mech Behav Biomed Mater.* (2017) 75:262–70. doi: 10.1016/j.jmbbm.2017.07.035
22. Bossers SS, Cibis M, Kapusta L, Potters WV, Snoeren MM, Wentzel JJ, et al. Long-term serial follow-up of pulmonary artery size and wall shear stress in Fontan patients[J]. *Pediatr Cardiol.* (2016) 37:637–45. doi: 10.1007/s00246-015-1326-y
23. Akins CW, Travis B, Yoganathan AP. Energy loss for evaluating heart valve performance. *J Thorac Cardiovasc Surg.* (2008) 136:820–33. doi: 10.1016/j.jtcvs.2007.12.059
24. D'Souza GA, Banerjee RK, Taylor MD. Evaluation of pulmonary artery stenosis in congenital heart disease patients using functional diagnostic parameters: An in vitro study. *J Biomech.* (2018) 81:58–67. doi: 10.1016/j.jbiomech.2018.09.014
25. Rijnberg FM, Hazekamp MG, Wentzel JJ, de Koning PJH, Westenberg JJM, Jongbloed MRM, et al. Energetics of blood flow in cardiovascular disease: concept and clinical implications of adverse energetics in patients with a Fontan circulation. *Circulation.* (2018) 137:2393–407. doi: 10.1161/CIRCULATIONAHA.117.033359
26. Dickinson MG, Bartelds B, Borgdorff MA, Berger RM. The role of disturbed blood flow in the development of pulmonary arterial hypertension: lessons from preclinical animal models. *Am J Physiol Lung Cell Mol Physiol.* (2013) 305:L1–14. doi: 10.1152/ajplung.00031.2013
27. van der Feen DE, Dickinson MG, Bartelds B, Borgdorff MA, Sietsma H, Levy M, et al. Egr-1 identifies neointimal remodeling and relates to progression in human pulmonary arterial hypertension. *J Heart Lung Transplant.* (2016) 35:481–90. doi: 10.1016/j.healun.2015.12.004
28. Warboys CM, de Luca A, Amini N, Luong L, Duckles H, Hsiao S, et al. Disturbed flow promotes endothelial senescence via a p53-dependent pathway. *Arterioscler Thromb Vasc Biol.* (2014) 34:985–95. doi: 10.1161/ATVBAHA.114.303415
29. Tang E, Wei ZA, Whitehead KK, Khiabani RH, Restrepo M, Mirabella L, et al. Effect of Fontan geometry on exercise haemodynamics and its potential implications. *Heart.* (2017) 103(22). 1806–1812. doi: 10.1136/heartjnl-2016-310855
30. Liang L, Steinman DA, Brina O, hnafa C, Cancelliere NM, Pereira VM. Towards the clinical utility of CFD for assessment of intracranial aneurysm rupture - a systematic review and novel parameter-ranking tool. *J Neurointerv Surg.* (2019) 11:153–158. doi: 10.1136/neurintsurg-2018-014246
31. Song S, Yamamura A, Yamamura H, Ayon RJ, Smith KA, Tang H, et al. Flow shear stress enhances intracellular Ca2+ signaling in pulmonary artery smooth muscle cells from patients with pulmonary arterial hypertension. *Am J Physiol Cell Physiol.* (2014) 307:C373–83. doi: 10.1152/ajpcell.00115.2014
32. Park SK, La Salle DT, Cerbie J, Cho JM, Bledsoe A, Nelson A, et al. Elevated arterial shear rate increases indexes of endothelial cell autophagy and nitric oxide synthase activation in humans. *Am J Physiol Heart Circ Physiol.* (2019) 316:H106–h12. doi: 10.1152/ajpheart.00561.2018
33. Kheyfets V, Thirugnanasambandam M, Rios L, Evans D, Smith T, Schroeder T, et al. The role of wall shear stress in the assessment of right ventricle hydraulic workload. *Pulm Circ.* (2015) 5:90–100. doi: 10.1086/679703
34. Pedrizzetti G, Domenichini F. Nature optimizes the swirling flow in the human left ventricle. *Phys Rev Lett.* (2005) 95:108101. doi: 10.1103/PhysRevLett.95.108101

35. Kilner PJ, Yang GZ, Wilkes AJ, Mohiaddin RH, Firmin DN, Yacoub MH. Asymmetric redirection of flow through the heart. *Nature.* (2000) 404:759–61. doi: 10.1038/35008075
36. Bahlmann E, Gerdts E, Cramariuc D, Gohlke-Baerwolf C, Nienaber CA, Wachtell K, et al. Prognostic value of energy loss index in asymptomatic aortic stenosis. *Circulation.* (2013) 127:1149–56. doi: 10.1161/CIRCULATIONAHA.112.078857
37. Kamphuis VP, Elbaz MSM, van den Boogaard PJ, Kroft LJM, van der Geest RJ, de Roos A, et al. Disproportionate intraventricular viscous energy loss in Fontan patients: analysis by 4D flow MRI. *Eur Heart J Cardiovasc Imaging.* (2019) 20:323–33. doi: 10.1093/ehjci/jey096

Conflict of Interest: The authors declare that the research was conducted in the absence of any commercial or financial relationships that could be construed as a potential conflict of interest.

frontiers in Pediatrics

ORIGINAL RESEARCH
published: 04 December 2020
doi: 10.3389/fped.2020.462367

Prediction for Intravenous Immunoglobulin Resistance Combining Genetic Risk Loci Identified From Next Generation Sequencing and Laboratory Data in Kawasaki Disease

*Liqin Chen[1], Sirui Song[1], Qianqian Ning[2], Danying Zhu[1], Jia Jia[2], Han Zhang[1], Jian Zhao[1], Shiying Hao[3,4], Fang Liu[5], Chen Chu[5], Meirong Huang[6], Sun Chen[7], Lijian Xie[1], Tingting Xiao[1] and Min Huang[1]**

[1] Department of Cardiology, Shanghai Children's Hospital, Shanghai Jiao Tong University, Shanghai, China, [2] Shanghai Center for Bioinformation Technology, Shanghai, China, [3] Department of Cardiothoracic Surgery, Stanford University School of Medicine, Stanford, CA, United States, [4] Clinical and Translational Research Program, Betty Irene Moore Children's Heart Center, Lucile Packard Children's Hospital, Palo Alto, CA, United States, [5] Heart Center, Children's Hospital of Fudan University, Shanghai, China, [6] Department of Cardiology, Shanghai Children's Medical Center Affiliated to Shanghai Jiao Tong University, Shanghai, China, [7] Department of Pediatric Cardiology, Xinhua Hospital, Affiliated to Shanghai Jiao Tong University School of Medicine, Shanghai, China

OPEN ACCESS

Edited by:
Hongfang Jin,
Peking University First Hospital, China

Reviewed by:
Xiaoqiong Gu,
Guangzhou Medical University, China
Yanfei Wang,
Guangzhou Medical University, China

***Correspondence:**
Min Huang
huangmin@sjtu.edu.cn

Specialty section:
This article was submitted to Pediatric Cardiology, a section of the journal Frontiers in Pediatrics

Received: 27 March 2019
Accepted: 11 November 2020
Published: 04 December 2020

Citation:
Chen L, Song S, Ning Q, Zhu D, Jia J, Zhang H, Zhao J, Hao S, Liu F, Chu C, Huang M, Chen S, Xie L, Xiao T and Huang M (2020) Prediction for Intravenous Immunoglobulin Resistance Combining Genetic Risk Loci Identified From Next Generation Sequencing and Laboratory Data in Kawasaki Disease. Front. Pediatr. 8:462367. doi: 10.3389/fped.2020.462367

Background: Kawasaki disease (KD) is the most common cause of acquired heart disease. A proportion of patients were resistant to intravenous immunoglobulin (IVIG), the primary treatment of KD, and the mechanism of IVIG resistance remains unclear. The accuracy of current models predictive of IVIG resistance is insufficient and doesn't meet the clinical expectations.

Objectives: To develop a scoring model predicting IVIG resistance of patients with KD.

Methods: We recruited 330 KD patients (50 IVIG non-responders, 280 IVIG responders) and 105 healthy children to explore the susceptibility loci of IVIG resistance in Kawasaki disease. A next generation sequencing technology that focused on 4 immune-related pathways and 472 single nucleotide polymorphisms (SNPs) was performed. An R package SNPassoc was used to identify the risk loci, and student's *t*-test was used to identify risk factors associated with IVIG resistance. A random forest-based scoring model of IVIG resistance was built based on the identified specific SNP loci with the laboratory data.

Results: A total of 544 significant risk loci were found associated with IVIG resistance, including 27 previous published SNPs. Laboratory test variables, including erythrocyte sedimentation rate (ESR), platelet (PLT), and C reactive protein, were found significantly different between IVIG responders and non-responders. A scoring model was built using the top 9 SNPs and clinical features achieving an area under the ROC curve of 0.974.

Conclusions: It is the first study that focused on immune system in KD using high-throughput sequencing technology. Our findings provided a prediction of the IVIG resistance by integrating the genotype and clinical variables. It also suggested a new perspective on the pathogenesis of IVIG resistance.

Keywords: Kawasaki disease, intravenous immunoglobulin resistance, gene, laboratory data, predictive model

INTRODUCTION

Kawasaki disease (KD) is an acute systemic vasculitis of unknown origin, and has been the leading cause of pediatric acquired heart disease. The diagnosis of KD is based on the presence of fever for at least 5 days and 5 clinical criteria including rash, bilateral bulbar conjunctival injection, erythema of oral and pharyngeal mucosa, erythema and edema of the hands and feet, and cervical lymphadenopathy (1). The primary treatment for Kawasaki disease is intravenous immunoglobulin (IVIG). However, there were 10–20% of patients who were resistant to IVIG, causing an increased risk of coronary artery lesions (CALs) (2).

A few scoring systems were developed to predict IVIG resistance in patients with KD. Kobayashi scoring model was constructed, including day of illness at initial treatment, age in months, percentage of white blood cells representing neutrophils, platelet count, and serum aspartate aminotransferase, sodium, and C-reactive protein, which yielded a sensitivity of 86% and specificity of 68% for a cut-off point four or more (3). The sensitivity of the Kobayashi scoring model, however, was low (31.4–57.1%) when validated on patients in Korea, North America, and China (3–5). One potential reason is the variations of genes and environments in different population, indicating the necessity of including the genetic factors into the IVIG resistance prediction. A variety of genetic markers associated with IVIG unresponsiveness and CAL formation in KD patients were found by Genome-wide association studies (GWAS), including *inositol 1,4,5-trisphosphate 3-kinase C* (*ITPKC*), *caspase-3* (*CASP3*), *FCGR2A, CD40*, and *interleukin1 beta* (*IL-1B*) (6–9).

Our study aims to develop a model to provide a prediction of the IVIG resistance for patients with KD in China. A low-cost, high-accuracy targeted capture sequencing technology was used to identify genes and SNP loci associated with immune system in KD. The initial targeted capture goal area included 560 genes and 472 SNPs susceptibility loci reported in previous KD studies. The identified genes were involved in T cell receptors signaling pathways, transforming growth factor-beta (TGF-β) signal pathway, toll-like receptors signaling pathways and cytokine receptors. Using the identified genes, SNPs, as well as clinical variables, a scoring model was built to evaluate the risk of IVIG resistance of KD patients.

METHODS

Study Population

Patients who were diagnosed as KD and received IVIG treatment at Shanghai Children's Hospital from 2015 to 2018 were recruited. The diagnosis criteria of KD were based on the guidelines proposed by the American Heart Association in 2017 (1). Children were diagnosed as KD who had the presence of fever for at least 5 days and fulfilled four of following clinical features:erythema of mucosa with strawberry tongue and cracking lips, bilateral non-purulent conjunctivitis, dysmorphic skin rashes, erythema, and edema of the hands and feet in acute phase or periungual desquamation in subacute phase and unilateral cervical lymphadenopathy. All the patients were treated with high dose IVIG (2 g/kg) within 10 days of the onset of the disease. Aspirin (3–5 mg/kg/day) was given until inflammation was resolved or no evidence of coronary changes existed under 2-dimensional echocardiography test. CAL was defined by the increment of internal diameter of 3 mm ($\leq$5 years old) or 4 mm (>5 years old), or 1.5 times larger of internal diameter than the adjacent segment, according to the guidelines of Japanese Ministry of Health (10). KD patients who had recurrent or persistent fever within 36 h after the end of IVIG treatment were defined as IVIG non-responders. This study has been reviewed and approved by the ethics committee of children's hospital affiliated to Shanghai Jiao Tong University (2017R034-E02). The informed consent was obtained by the parents or their guardians.

Clinical Data Capturing

Clinical data of patients who visited the Shanghai Children's Hospital were entered into a database called Clinical Information System (CIS) on a daily basis. In this study, electronic medical records of KD patients were identified and extracted from the CIS using Doctor Research Information Management (DRIM) system, and a structured database was built to support the following analyses (11).

DNA Extraction and Targeted Enrichment of Genomic Region Technology

Blood samples of each KD patient were collected by the EDTA anticoagulation tube. DNA was extracted using Genomic DNA Extraction Kit (Cat. No.DP329, TIANGEN Bioscience Beijing), and the library was constructed using KAPA HTP Library preparation kit (Cat. No. KK8234, Roche, USA). Illumina HiSeq X10 (Illumina USA) was used as the sequencing platform for libraries target enriched by custom capture array. The hybridization probes of the custom capture array consisted of previous published 472 GWAS hotspots related to KD and 560 candidate genes among 4 KEGG pathways including Toll-like receptor signaling pathway, Cytokine receptor interaction, TGF-β signaling pathway and T cell receptor signaling pathway. The

targeted capture chips were designed by SeqCap EZ Choice (Roche, Switzerland).

Statistical Analysis

The raw data were mapped to the human reference genome (hg19) using the Burrows-Wheeler alignment (BWA v0.7.15) tool (12) and Picard tool (v1.135) was used to process for PCR duplicates (http://broadinstitute.github.io/picard/). Candidate SNPs were detected using GATK (v3.7) HaplotypeCaller algorithm (13), and filtered with following parameters "QD <2.0 || FS >60.0 || MQ <40.0 || MQRankSum <-12.5 || ReadPosRankSum <-8.0." Variants annotation was performed using ANNOVAR (14), and genetic risk-alleles associated IVIG resistance were analyzed using R package SNPassoc (15). All statistical analyses were performed in R. Student's *t*-test was used to compare the differences of clinical features between the IVIG non-responders and IVIG responders. $P < 0.05$ was considered statistically significant. The scoring model of IVIG resistance was developed based on the identified specific SNP loci as well as the laboratory data. R package ipred was used to train the model (16).

Weighted Genetic Risk Scoring System

The cumulative effects of candidate SNPs were calculated though wGRS system designed by De Jager et al. (17). The wGRS was calculated by multiplying the weight by the risk allele number (0, 1, or 2), and taking the sum across SNPs:

$$wGRS = \sum_{k=1}^{n} w^k G^k$$

where n is the number of SNP, k is SNP, w^k is the corresponding weight of SNP [ln(OR)], and G^k is the number of the risk allele (0, 1, or 2). wGRS was compared between the IVIG responders and non-responders using the Wilcoxon rank-sum test with continuity correction. The performance of the model was evaluated by the area under the receiver operating characteristic (ROC) curve.

RESULTS

Clinical Characteristics of IVIG Non-responders

A total of 330 KD patients were enrolled in this study, with 50 (15.2%) IVIG non-responders and 280 (84.8%) IVIG responders. The male to female ratio was 1.77:1.0 (211:119). All the patients received IVIG treatment (2 g/kg) and aspirin with 3–5 mg/kg/day. Treatment was repeated on 50 patients due to the IVIG resistance. Forty-eight patients were ultimately found with CAL, and 15 of the 48 patients showed IVIG resistance.

There was no significant difference in gender and age distribution between IVIG responders and non-responders (**Table 1**). Consistent with previous studies of the epidemiology and presentation of KD, the majority of patients were male [76% (38 of 50) in IVIG non-responders and 62% (173 of 280) in IVIG responders]. Though IVIG non-responders were younger (30.5 ± 24.5 months) than IVIG responders (34.3 ± 27.3 months), the difference was not significant ($P > 0.05$).

TABLE 1 | Patients diagnose and characteristics.

	No. of patients	No. of male	No. of female	Age, month, mean ± SD
IVIG-non-response	50	38	12	30.5 ± 24.5
IVIG-response	280	173	107	34.3 ± 27.3

The differences of clinical features that may be related to IVIG resistance between two groups were calculated (**Figure 1**). As shown in **Table 2**, 6 clinical variables met the condition of $P < 0.05$ and percentage of patients with adequate data <30% were found. Compared with the subjects who were responsive to the IVIG therapy, IVIG non-responders were more likely to have higher C-reactive protein level, higher percentage of neutrophils, lower platelet count, lower serum albumin concentration, lower erythrocyte sedimentation rate, and lower hemoglobin level. Patients with IVIG resistance had longer fever duration (**Table 2**).

Risk Loci Affecting IVIG Unresponsiveness

To identify the gene variants associated with IVIG resistance, 330 patients diagnosed as KD and 105 healthy children were recruited in this phase. A second-generation sequencing focusing on the exon regions of 560 genes in four immune related pathways and 472 KD-associated SNPs reported in previous GWAS studies were conducted. The average sequencing depth of KD samples and normal samples were 477X and 445X, respectively. A total of 15,677 SNP sites were found in all samples. Genotypes of 544 SNPs in targeted regions were significantly different ($P < 0.05$) between IVIG responders and non-responders. The common variants were identified that the minor allele frequency (MAF) of the gene or SNP was more than 1%.

There were 14 SNPs (MAF >1%) that showed significant difference between IVIG non-responders and IVIG responders ($P < 0.001$; **Table 3**). Among all identified risk loci, SNP rs840016 that located at the region of *CD247* showed the largest correlation ($P = 5.4 \times 10^{-4}$). An increasing risk of IVIG resistance was observed (odd ratio = 3.77) by comparing the risk allele (T allele) to the non-risk allele (C allele). Another SNP rs2463260 A/G ($P = 4.2 \times 10^{-4}$) located in chromosome 1 was filtered out with an odd ratio 3.35, which risk allele was G. rs56401579G/A and rs56193546C/T located at *FLT4* gene region were also related with IVIG unresponsiveness, which odd ratios were 3.33 when risk alleles compared with non-risk alleles. The minor alleles of rs10271133C/T and rs2007404T/C that located in *CUL1* gene region showed high incidence of IVIG resistance. Moreover, transformation of rs77317995T/A located in *ACVR2B* gene region from major allele to minor allele was associated with protection from IVIG resistance. rs6530599A/G, rs6530600A/G, and rs1136210A/G located on chromosome Y (*CD24*) were found to be protective gene associated with IVIG unresponsiveness ($P = 7.0 \times 10^{-4}$, odds ratio, 0.55). The frequencies of AA, AG, and GG genotypes were 17.1, 82.5, and 0.5% in males, while that were 16.0%, 0.8%, and 83.2% in females. Besides, rs2232595C/T, rs16949924G/C, rs12358961T/A, and rs742185A/G were found association with IVIG unresponsiveness.

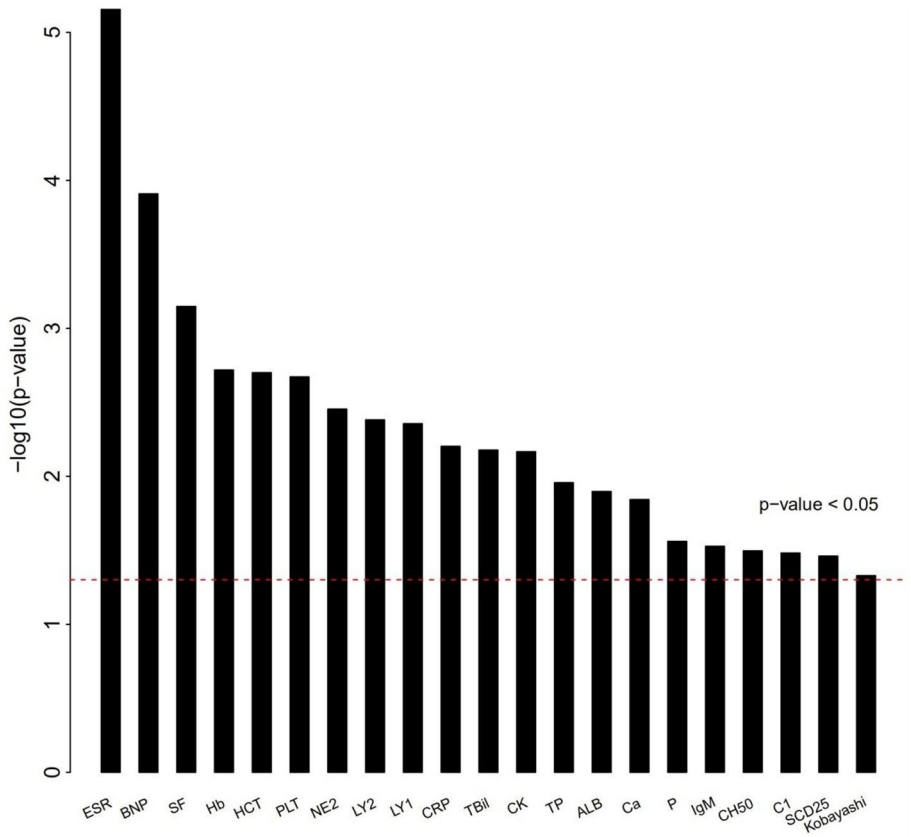

FIGURE 1 | Differences of clinical characteristics between IVIG unresponders and responders. Clinical variables as *x* axis and *P*-value of clinical variables with *y* axis. The clinical variables were different significantly between IVIG unresponders and responders ($P < 0.05$).

wGRS Analysis and ROC Curve Analysis

To detect the diagnostic accuracy of clinical evaluations of IVIG treatment for KD patients using candidate SNPs, a wGRS system was applied (17). Four hundred and forty eight SNPs (MAF >1%) that reached suggestive significance were identified between IVIG non-responders and IVIG responders ($P < 0.05$). To identify more effective predictors, the risk loci between IVIG resistant group and healthy control group were evaluated, where 198 SNPs (MAF >1%) were found significantly different. Nine SNPs were identified to be rick loci associated with IVIG resistance by comparing 488 SNPs and 198 SNPs, and were used to build a scoring model (**Supplementary Table 1**).

Nine SNPs (**Supplementary Table 1**) with $P < 3\times 10^{-3}$ were included in the wGRS algorithm. None of two SNPs out of 9 showed strong linkage disequilibrium. The difference of wGRS scores between the two groups was significant (Wilcoxon rank-sum test, $P = 2.0 \times 10^{-7}$) (**Figure 2**). The scoring model which based on wGRS score of 9 SNPs yielded a sensitivity of 76% and specificity of 70.7% for a cutoff point of 0.141 (**Figure 3**). C-reactive protein level, percentage of neutrophils, platelet count, serum albumin concentration, erythrocyte sedimentation rate, and hemoglobin level were identified with highest risk for IVIG unresponsiveness. The six clinical variables and wGRS score of 9 SNPs were used to generate a composite scoring model which revealed better sensitivity (96.8%) and specificity (91.2%) for a cutoff point of 0.207 (**Figure 4**).

We also tested Kobayashi scoring system to predict KD patients who resistant to IVIG. The sensitivity and specificity were 34.5 and 88% in the Kobayashi scoring system.

DISCUSSION

In this study, we established a novel scoring model to predict IVIG resistance in KD. Patients with 6 abnormal clinical variables (C-reactive protein level, percentage of neutrophil, platelet count, serum albumin concentration, erythrocyte sedimentation rate, and hemoglobin level) were more likely to be resistant to IVIG therapy. The wGRS score of SNPs were effective in identifying IVIG resistance.

T-cell receptor zeta chain (CD3ζ) encoded by *CD247* is a component of the T-cell receptor (TCR) complex. CD3ζ chain can alter TCR signaling and participate in T cell activation (18). Previous studies found that CD247 were associated with Systemic lupus erythematosus (SLE) and other autoimmune

TABLE 2 | Clinical indicators of IVIG non-responders and IVIG responders.

Clinical indicators	IVIG non-responders	Patients with adequate data, %	IVIG responders	Patient with inadequate data, %	*P*-value
Fever days	11.91 ± 2.96	10	7.79 ± 2.96	2.86	2.0×10^{-5}
PLT ($\times 10^9$/L)	315.46 ± 121.27	12	361.38 ± 121.27	3.93	3.19×10^{-2}
CRP (mg/L)	103.78 ± 46.04	14	65.59 ± 46.04	3.57	2.0×10^{-5}
ALB (g/L)	33.62 ± 3.86	16	36.22 ± 3.86	6.07	2.1×10^{-3}
ESR (mm/h)	71.15 ± 29.13	18	88.24 ± 29.13	7.86	6.6×10^{-3}
Hb (g/L)	105.81 ± 10.59	20	109.55 ± 10.59	13.21	2.75×10^{-2}
NE (%)	72.96 ± 15.69	28	64.82 ± 15.69	3.93	4.1×10^{-3}
HCT (%)	31.36 ± 2.86	30	32.51 ± 2.86	4.29	1.43×10^{-2}
LY (%)	19.85 ± 13.06	30	26.17 ± 13.06	3.93	1.27×10^{-2}
LYM ($\times 10^9$/L)	2.62 ± 2.05	30	3.52 ± 2.05	4.64	3.5×10^{-3}
TP (g/L)	59.00 ± 6.29	32	63.37 ± 6.29	6.43	1.9×10^{-3}
TBil (μmol/L)	18.56 ± 12.61	40	9.80 ± 12.61	16.07	3.30×10^{-2}
CK (U/L)	34.59 ± 66.16	42	56.73 ± 66.16	17.86	1.0×10^{-4}
Kobayashi	2.59 ± 1.58	42	1.54 ± 1.58	17.14	6.3×10^{-3}
Ca (mmol/L)	2.22 ± 0.12	50	2.29 ± 0.12	25.00	2.97×10^{-2}
P (mmol/L)	1.07 ± 0.28	50	1.30 ± 0.28	25.36	2.0×10^{-3}
SF (ng/ml)	218.00 ± 90.26	56	149.99 ± 90.26	34.29	3.46×10^{-2}
BNP (pg/ml)	2975.17 ± 1210.82	60	782.36 ± 1210.82	36.79	1.1×10^{-2}
IL-2R (pg/ml)	84383.11 ± 48547.54	72	43036.82 ± 48547.54	48.93	4.69×10^{-2}
IgM (g/L)	0.84 ± 0.49	74	1.12 ± 0.49	63.57	4.4×10^{-3}
CH50 (μ/ml)	50.19 ± 9.37	78	58.98 ± 9.37	63.93	7.0×10^{-4}
C1 (mg/L)	173.67 ± 53.43	80	207.37 ± 53.43	2.86	6.8×10^{-3}

PLT, platelet count; CRP, C-reactive protein; ALB, albumin; ESR, erythrocyte sedimentation rate; Hb, Hemoglobin; NE%, percentage of neutrophils; HCT, Hematocrit; LY%, percentage of lymphocyte; LYM, lymphocyte absolute value; TP, total protein; TBIL, total bilirubin; CK, creatine kinase; Ca, serum calcium; P, serum phosphorus; SF, serum ferritin; BNP, brain natriuretic peptide; IL-2R, interleukin-2 receptor; IgM, Immunoglobulin M; CH50, 50% of complement hemolytic activity; C1, complement 1.
P-value for continuous variables from t-test.

TABLE 3 | 14 SNP associated with IVIG unresponsive in KD.

CHR	Position	SNP	Nearby Gene(s)	Region	Ref/ Alt	Freq	OR	*P*-value	Adjusted by gender	Adjusted by age	*P*-value adjusted by age and gender
1	40,229,368	rs2463260	*PPIE*	Exonic	A/G	0.06	3.35	4.2×10^{-4}	$4.6 \times 10–^{4}$	1.6×10^{-2}	1.5×10^{-2}
1	167,408,670	rs840016	*CD247*	Intronic	C/T	0.02	3.77	5.4×10^{-4}	5.4×10^{-3}	1.0×10^{-1}	1.33×10^{-1}
3	38,534,142	rs77317995	*ACVR2B*	UTR3	T/A	0.36	0.46	4.4×10^{-4}	4.2×10^{-4}	1.3×10^{-2}	1.2×10^{-2}
5	180,053,090	rs56401579	*FLT4*	Intronic	G/A	0.04	3.33	3.6×10^{-4}	5.4×10^{-4}	3.2×10^{-3}	4×10^{-3}
5	180,053,097	rs56193546	*FLT4*	Intronic	C/T	0.04	3.33	3.6×10^{-4}	5.4×10^{-4}	3.2×10^{-3}	4×10^{-3}
7	148,480,990	rs10271133	*CUL1*	Intronic	C/T	0.05	3.58	8×10^{-5}	8.2×10^{-5}	6.5×10^{-3}	5×10^{-3}
7	148,487,395	rs2007404	*CUL1*	Intronic	T/C	0.11	2.62	8.8×10^{-4}	9.2×10^{-4}	1.4×10^{-1}	1.4×10^{-1}
10	6,066,195	rs12358961	*IL2RA*	Intronic	T/A	0.07	2.94	4.7×10^{-4}	5.5×10^{-4}	1.2×10^{-1}	1.4×10^{-1}
15	66,727,597	rs16949924	*MAP2K1*	Intronic	G/C	0.05	2.97	8.8×10^{-4}	9.7×10^{-4}	2.2×10^{-1}	2.21×10^{-1}
20	36,989,335	rs2232595	*LBP*	Intronic	C/T	0.02	3.74	9.6×10^{-4}	6.6×10^{-4}	2.1×10^{-3}	2×10^{-3}
22	50,705,059	rs742185	*MAPK11*	Intronic	A/G	0.09	2.87	5.1×10^{-4}	5.1×10^{-4}	3.0×10^{-1}	3.02×10^{-1}
Y	21,153,275	rs6530599	*CD24*	ncRNA_intronic	A/G	0.57	0.55	7×10^{-4}	8.4×10^{-4}	3.6×10^{-1}	3.66×10^{-1}
Y	21,153,459	rs6530600	*CD24*	ncRNA_intronic	A/G	0.57	0.55	7×10^{-4}	8.4×10^{-4}	3.6×10^{-1}	3.66×10^{-1}
Y	21,153,474	rs1136210	*CD24*	ncRNA_intronic	A/G	0.57	0.55	7×10^{-4}	8.4×10^{-4}	3.6×10^{-1}	3.66×10^{-1}

Ref/Alt, reference allele and alternative allele; OR, indicates odds ratio; and UTR, untranslated region.

disorders by T cell-mediated mechanism (19, 20). Interleukin-2 receptor subunit alpha encoded by *IL2RA* gene is a hallmark antigen of regulatory T cells, and functions in the suppression of immune responses and maintenance of immune homeostasis (21, 22). Kuo et al. (23) reported that *IL2RA* (rs3118470) was significantly associated with CAL formation in KD patients. We

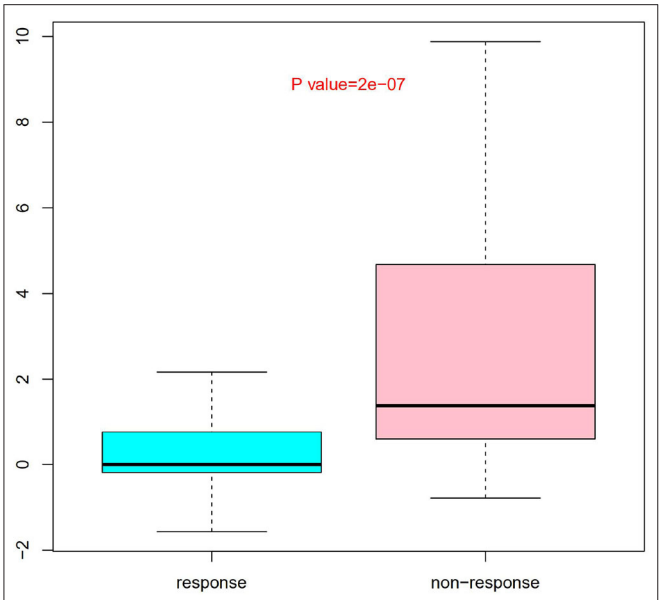

FIGURE 2 | Evaluation difference of weighted genetic risk score (wGRS) of 9 SNPs between IVIG non-responders and responders. Group as *x* axis and wGRS scores of 9 SNPs with *y* axis. The difference of wGRS scores between the two groups was significant (Wilcoxon rank-sum test, $P = 2.0 \times 10^{-7}$).

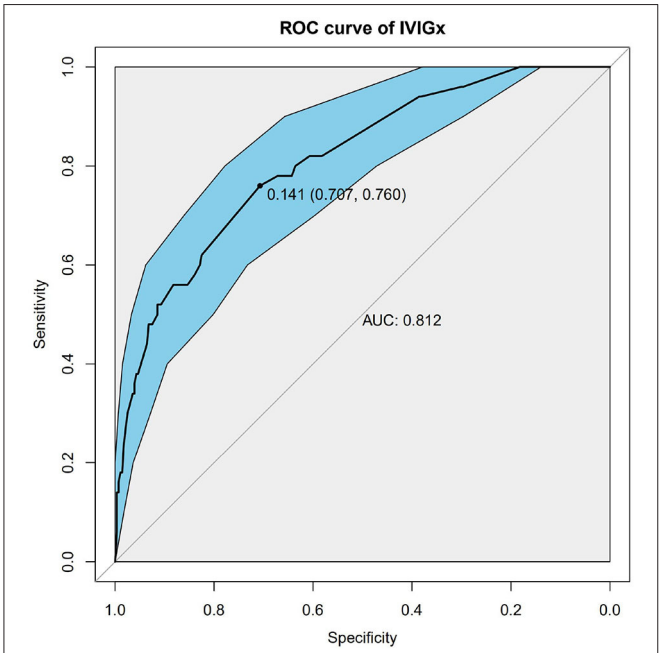

FIGURE 3 | Receiver operating characteristic (ROC) curve analysis of the model using weighted genetic risk score (wGRS) of 9 SNPs to predict IVIG resistance in KD. ROC of wGRS with Specificity as *x* axis and sensitivity with *y* axis. The most predictive wGRS value (0.141) and the corresponding specificity and sensitivity (76 and 70.7%) were shown.

found that SNP rs840016 C/T located at *CD247* and rs12358961 T/A located at *ILR2A* have association with the increasing risk of IVIG resistance.

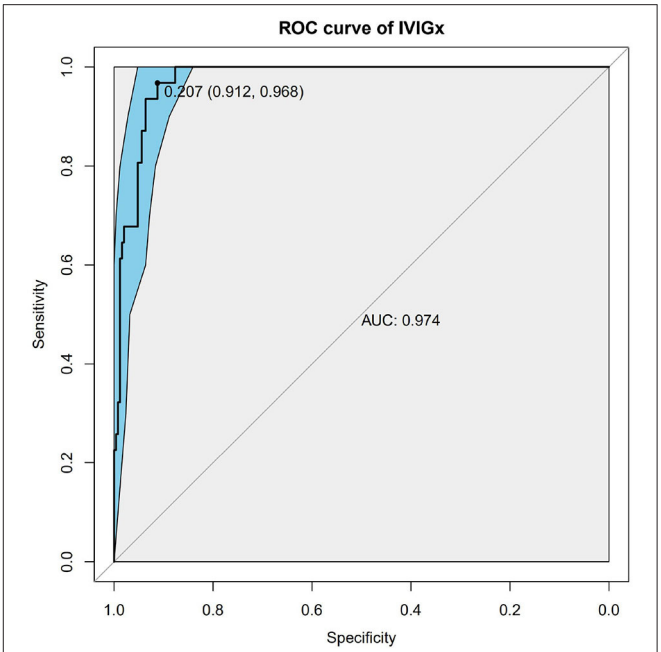

FIGURE 4 | Receiver operating characteristic (ROC) curve analysis of the combinatory model based on weighted genetic risk score (wGRS) of 9 SNPs and clinical variables. ROC of wGRS with Specificity as *x* axis and sensitivity with *y* axis. The most predictive wGRS value (0.207) and the corresponding specificity and sensitivity (91.2 and 96.8%) were shown.

Lipopolysaccharide binding protein (LBP) is a phase protein that is synthesized mainly in the liver and binds lipopolysaccharide (LPS) to initiate the immune response. LPS is presented to cluster of differentiation (CD) 14, which interacts with toll-like receptor to activate the immune (24). A study about postoperative patients with sepsis, LBP plasma concentration showed similar course with CRP in predicting outcome (25). The fms related tyrosine kinase (FLT4) is known as the vascular endothelial growth factor receptor (VEGFR) 3, which is a protein kinase and regulates endothelial cell growth and angiogenesis (26). Some study reported that the increased serum level of VEGF had associated with serum levels of CRP in acute phase of KD (27). The level of CRP was higher in IVIG un-responders than IVIG responders in our study. We also found *LBP* and *FLT4* gene variants were positively correlated with IVIG treatments.

The MAPK pathway is a signal transduction pathway and regulates fundamental cell activities including proliferation, transcriptional regulation, differentiation and survival. Mitogen-activated protein kinases (MAPK) is activated by TGF-β1 that induces endothelial cell apoptosis. MAPK 11 (p38β) is the predominant form of MAPK (28). He et al. (29) reported that MAPK11 mediated p38 activity was associated with osteolytic bone destruction in breast cancer cells. Zhang et al. (30) reported the oncogenic mutations within the β3-αC loop of *MAP2K1* have profound effect on drug response and can be critical for targeted therapies. Activin A receptor type 2B (ACVR2B) is activated by the activin family of ligands of TGF-β superfamily and activate SMAD2/3 signaling pathway (31). Genetic variants

in TGF-β/SMAD3 signaling pathway were consistently associated with KD susceptibility, CAL and IVIG therapy response (32). We found that patients with genetic variants of *MAPK11* and *MAP2K1* had higher risk of IVIG unresponsiveness. The mechanism of *MAPK11 and MAP2K1* associated with IVIG resistance may participate in the TGF-β/SMAD3 signaling pathway. It is interesting that rs77317995T/A located in gene *ACVR2B* may be the protective factor of IVIG treatment in our study.

CD24 is a phosphatidylinositol (GPI)-linked protein expressed on the cell surface that have been implicated in the stimulation of T cell and differentiation of B cells. *CD24* gene is a member of multigene family and have homologous sequences on chromosome 6 and chromosome. Lee et al. (33) reported that high expression of CD24 can reduce inflammatory response by regulating NFκB in juvenile human chondrocytes. KD was found affects males 1.5 times more than female (34). We reported that three SNPs located at *CD24* on chromosome Y were associated with IVIG resistance. The frequency of risk allele A may explain the predominance of males in IVIG resistant group.

Cullin1 (CUL1) is the first and most extensively characterized member of the cullin family and an essential component of SCF E3 ubiquitin ligase complex. A study has reported that the expression of CUL1 in colorectal cancer (CRC) can be valuable molecular markers to predict the prognosis of the CRC patients (35). Huang et al. (36) proposed that CUL1 is associated with the disease-specific survival of the breast cancer and may serve as a therapeutic target for breast cancer metastasis. In our study, there are two SNPs located at *CUL1* which associated with KD and can predict IVIG resistance.

Kuo et al. (37) first applied wGRS analysis to KD patients for IVIG responsiveness evaluation based on 11 single-nucleotide polymorphisms. The specificity and sensitivity of the scoring model were 81.7 and 79.2% after adjusted for sex effects. We then aggregated laboratory characteristics and genetic variations to build a scoring system for IVIG resistance prediction. We found that high C-reactive protein, high percentage of neutrophils, and low albumin were independent risk factors for IVIG resistance. Compared with the Kobayashi score, a predictor of IVIG resistance and CAL development based on Japanese patients, the sensitivity of our proposed model was higher (sensitivity 76–96.8%). Our findings were consistent with a study from UK that reported a failure of Kobayashi score in identifying IVIG resistance (38). Berdej-Szczot et al. (39) also found a reduced accuracy of Kobayashi score in predicting IVIG resistance in Poland. When Lin et al. (40) applied the Kobayashi score to predict the effect of IVIG therapy for KD patients in China Taiwan, they found that the sensitivity and specificity of the model were only 62 and 71%. Gene indicators can improve the accuracy of score system to predict IVIG unresponsive for KD patients, and these genetic variations together with the clinical indicators might suggest the development of disease and outcome of the therapy.

The study had several limitations. (1) We could not evaluate the new scoring model in other cohort of KD patients because the measurement of gene were not routine at other medical institution. (2) This was a single medical center, selection bias might occur such as the lack of adequate data of KD patients.

CONCLUSIONS

We developed a predicting scoring system based on both clinical variables and gene variants. Using target enrichment of genomic region technology, several SNPs were found significantly different between IVIG responders and non-responders. The proposed model based on the wGRS score of SNPs and clinical features showed a high sensitivity, and can be implemented to predict IVIG resistance for KD patients.

DATA AVAILABILITY STATEMENT

This article contains previously unpublished data. The name of the repository and accession number are not available.

ETHICS STATEMENT

This study was carried out in accordance with the ethics committee of children's hospital affiliated to Shanghai Jiao Tong University of guidelines, ethics committee of children's hospital affiliated to Shanghai Jiao Tong University with written informed consent from all subjects. All subjects gave written informed consent in accordance with the Declaration of Helsinki. The protocol was approved by the ethics committee of children's hospital affiliated to Shanghai Jiao Tong University.

AUTHOR CONTRIBUTIONS

MiH and TT contributed to conception and design of the study. LX, CC, FL, MeH, and SC contributed to the manuscript revision. SS, JJ, JZ, and SH performed data analysis. LC, QN, and HZ wrote the draft of manuscript. All authors contributed to the article and approved the submitted version.

FUNDING

This study was supported by Clinical Science and Technology Innovation funding of Shanghai Hospital Development Center (grant number: SHDC12016119); Shanghai Science and Technology Committee research funding (grant number: 17411954300); Shanghai Jiao Tong University medical engineering cooperation youth funding (grant number: YG2016QN41); and Shanghai Municipality Health Commission research funding (grant number: 2019SY025).

ACKNOWLEDGMENTS

We would like to thank Guoying Huang (Children's Hospital of Fudan University).

SUPPLEMENTARY MATERIAL

The Supplementary Material for this article can be found online at: https://www.frontiersin.org/articles/10.3389/fped.2020.462367/full#supplementary-material

REFERENCES

1. McCrindle BW, Rowley AH, Newburger JW, Burns JC, Bolger AF, Gewitz M, et al. Diagnosis, treatment, and long-term management of kawasaki disease: a scientific statement for health professionals from the American Heart Association. *Circulation.* (2017) 135:e927–99. doi: 10.1161/CIR.0000000000000484
2. Makino N, Nakamura Y, Yashiro M, Ae R, Tsuboi S, Aoyama Y, et al. Descriptive epidemiology of Kawasaki disease in Japan, 2011-2012: from the results of the 22nd nationwide survey. *J Epidemiol.* (2015) 25:239–45. doi: 10.2188/jea.JE20140089
3. Park HM, Lee DW, Hyun MC, Lee SB. Predictors of nonresponse to intravenous immunoglobulin therapy in Kawasaki disease. *Korean J Pediatr.* (2013) 56:75–9. doi: 10.3345/kjp.2013.56.2.75
4. Sleeper LA, Minich LL, McCrindle BM, Li JS, Mason W, Colan SD, et al. Evaluation of Kawasaki disease risk-scoring systems for intravenous immunoglobulin resistance. *J Pediatr.* (2011) 158:831–5 e3. doi: 10.1016/j.jpeds.2010.10.031
5. Song R, Yao W, Li X. Efficacy of four scoring systems in predicting intravenous immunoglobulin resistance in children with Kawasaki disease in a children's hospital in Beijing, North China. *J Pediatr.* (2017) 184:120–4. doi: 10.1016/j.jpeds.2016.12.018
6. Khor CC, Davila S, Breunis WB, Lee YC, Shimizu C, Wright VJ, et al. Genome-wide association study identifies FCGR2A as a susceptibility locus for Kawasaki disease. *Nat Genet.* (2011) 43:1241–6. doi: 10.1038/ng.981
7. Lee YC, Kuo HC, Chang JS, Chang LY, Huang LM, Chen MR, et al. Two new susceptibility loci for Kawasaki disease identified through genome-wide association analysis. *Nat Genet.* (2012) 44:522–5. doi: 10.1038/ng.2227
8. Onouchi Y, Suzuki Y, Suzuki H, Terai M, Yasukawa K, Hamada H, et al. ITPKC and CASP3 polymorphisms and risks for IVIG unresponsiveness and coronary artery lesion formation in Kawasaki disease. *Pharmacogenomics J.* (2013) 13:52–9. doi: 10.1038/tpj.2011.45
9. Huang YH, Hsu YW, Lu HF, Wong HS, Yu HR, Kuo HC, et al. Interferon-gamma genetic polymorphism and expression in Kawasaki disease. *Medicine.* (2016) 95:e3501. doi: 10.1097/MD.0000000000003501
10. JCS Joint Working Group. Guidelines for diagnosis and management of cardiovascular sequelae in Kawasaki disease (JCS 2013). *Circ J.* (2014) 78:2521–62. doi: 10.1253/circj.CJ-66-0096
11. Zhu DY, Song SR, Zhang H, Zhao J, Jiang B, Xie LJ, et al. Establishment of a new scoring model for IVIG non-response of Kawasaki disease. *Int J Pediatr.* (2018) 45:532–642. doi: 10.3760/cma.j.issn.1673-4408.2018.07.010
12. Li H, Durbin R. Fast and accurate short read alignment with Burrows-Wheeler transform. *Bioinformatics.* (2009) 25:1754–60. doi: 10.1093/bioinformatics/btp324
13. McKenna A, Hanna M, Banks E, Sivachenko A, Cibulskis K, Kernytsky A, et al. The genome analysis toolkit: a mapreduce framework for analyzing next-generation DNA sequencing data. *Genome Res.* (2010) 20:1297–303. doi: 10.1101/gr.107524.110
14. Wang K, Li M, Hakonarson H. ANNOVAR: functional annotation of genetic variants from high-throughput sequencing data. *Nucl Acids Res.* (2010) 38:e164. doi: 10.1093/nar/gkq603
15. Gonzalez JR, Armengol L, Sole X, Guino E, Mercader JM, Estivill X, et al. SNPassoc: an R package to perform whole genome association studies. *Bioinformatics.* (2007) 23:644–5. doi: 10.1093/bioinformatics/btm025
16. Mardin CY, Hothorn T, Peters A, Junemann AG, Nguyen NX, Lausen B. New glaucoma classification method based on standard Heidelberg retina tomograph parameters by bagging classification trees. *J Glaucoma.* (2003) 12:340–6. doi: 10.1097/00061198-200308000-00008
17. De Jager PL, Chibnik LB, Cui J, Reischl J, Lehr S, Simon KC, et al. Integration of genetic risk factors into a clinical algorithm for multiple sclerosis susceptibility: a weighted genetic risk score. *Lancet Neurol.* (2009) 8:1111–9. doi: 10.1016/S1474-4422(09)70275-3
18. Christopoulos P, Dopfer EP, Malkovsky M, Esser PR, Schaefer HE, Marx A, et al. A novel thymoma-associated immunodeficiency with increased naive T cells and reduced CD247 expression. *J Immunol.* (2015) 194:3045–53. doi: 10.4049/jimmunol.1402805
19. Martins M, Williams AH, Comeau M, Marion M, Ziegler JT, Freedman BI, et al. Genetic association of CD247 (CD3zeta) with SLE in a large-scale multiethnic study. *Genes Immun.* (2015) 16:142–50. doi: 10.1038/gene.2014.73
20. Blazquez-Moreno A, Perez-Portilla A, Agundez-Llaca M, Dukovska D, Vales-Gomez M, Aydogmus C, et al. Analysis of the recovery of CD247 expression in a PID patient: insights into the spontaneous repair of defective genes. *Blood.* (2017) 130:1205–8. doi: 10.1182/blood-2017-01-762864
21. Hinks A, Ke X, Barton A, Eyre S, Bowes J, Worthington J, et al. Association of the IL2RA/CD25 gene with juvenile idiopathic arthritis. *Arthritis Rheum.* (2009) 60:251–7. doi: 10.1002/art.24187
22. Xia ZL, Qin QM, Zhao QY. A genetic link between CXCR5 and IL2RA gene polymorphisms and susceptibility to multiple sclerosis. *Neurol Res.* (2018) 40:1040–7. doi: 10.1080/01616412.2018.1517110
23. Kuo HC, Chang JC, Guo MM, Hsieh KS, Yeter D, Li SC, et al. Gene-gene associations with the susceptibility of Kawasaki disease and coronary artery lesions. *PLoS ONE.* (2015) 10:e0143056. doi: 10.1371/journal.pone.0143056
24. Kim D, Mun S, Lee J, Park A, Seok A, Chun YT, et al. Proteomics analysis reveals differential pattern of widespread protein expression and novel role of histidine-rich glycoprotein and lipopolysaccharide-binding protein in rheumatoid arthritis. *Int J Biol Macromol.* (2018) 109:704–10. doi: 10.1016/j.ijbiomac.2017.12.075
25. Tschaikowsky K, Hedwig-Geissing M, Schmidt J, Braun GG. Lipopolysaccharide-binding protein for monitoring of postoperative sepsis: complemental to C-reactive protein or redundant? *PLoS ONE.* (2011) 6:e23615. doi: 10.1371/journal.pone.0023615
26. Cornejo KM, Deng A, Wu H, Cosar EF, Khan A, St Cyr M, et al. The utility of MYC and FLT4 in the diagnosis and treatment of postradiation atypical vascular lesion and angiosarcoma of the breast. *Hum Pathol.* (2015) 46:868–75. doi: 10.1016/j.humpath.2015.02.014
27. Thornton S. Contribution of angiogenic genes to the complex genetic trait underlying Kawasaki disease. *Arthritis Rheum.* (2006) 54:1361–5. doi: 10.1002/art.21810
28. Ferrari G, Terushkin V, Wolff MJ, Zhang X, Valacca C, Poggio P, et al. TGF-beta1 induces endothelial cell apoptosis by shifting VEGF activation of p38(MAPK) from the prosurvival p38beta to proapoptotic p38alpha. *Mol Cancer Res.* (2012) 10:605–14. doi: 10.1158/1541-7786.MCR-11-0507
29. He Z, He J, Liu Z, Xu J, Yi SF, Liu H, et al. MAPK11 in breast cancer cells enhances osteoclastogenesis and bone resorption. *Biochimie.* (2014) 106:24–32. doi: 10.1016/j.biochi.2014.07.017
30. Zhang B, Chen Y, Dai P, Yu H, Ma J, Chen C, et al. Oncogenic mutations within the β3-αC loop of *EGFR/ERBB2/BRAF/MAP2K1* predict response to therapies. *Mol Genet Genomic Med.* (2020) 8:e1395. doi: 10.1002/mgg3.1395
31. Liu M, Hammers DW, Barton ER, Sweeney HL. Activin receptor type IIB inhibition improves muscle phenotype and function in a mouse model of spinal muscular atrophy. *PLoS ONE.* (2016) 11:e0166803. doi: 10.1371/journal.pone.0166803
32. Shimizu C, Jain S, Davila S, Hibberd ML, Lin KO, Molkara D, et al. Transforming growth factor-beta signaling pathway in patients with Kawasaki disease. *Circ Cardiovasc Genet.* (2011) 4:16–25. doi: 10.1161/CIRCGENETICS.110.940858
33. Lee J, Smeriglio P, Dragoo J, Maloney WJ, Bhutani N. CD24 enrichment protects while its loss increases susceptibility of juvenile chondrocytes towards inflammation. *Arthritis Res Ther.* (2016) 18:292. doi: 10.1186/s13075-016-1183-y
34. Huang WC, Huang LM, Chang IS, Chang LY, Chiang BL, Chen PJ, et al. Epidemiologic features of Kawasaki disease in Taiwan, 2003-2006. *Pediatrics.* (2009) 123:e401–5. doi: 10.1542/peds.2008-2187
35. Wang W, Deng J, Wang Q, Yao Q, Chen W, Tan Y, et al. Synergistic role of Cul1 and c-Myc: prognostic and predictive biomarkers in colorectal cancer. *Oncol Rep.* (2017) 38:245–52. doi: 10.3892/or.2017.5671
36. Huang YF, Zhang Z, Zhang M, Chen YS, Song J, Hou PF, et al. CUL1 promotes breast cancer metastasis through regulating EZH2-induced the autocrine expression of the cytokines CXCL8 and IL11. *Cell Death Dis.* (2018) 10:2. doi: 10.1038/s41419-018-1258-6
37. Kuo HC, Wong HS, Chang WP, Chen BK, Wu MS, Yang KD, et al. Prediction for intravenous immunoglobulin resistance by using weighted genetic risk score identified from genome-wide association study in Kawasaki disease. *Circ Cardiovasc Genet.* (2017) 10:e001625. doi: 10.1161/CIRCGENETICS.116.001625

38. Davies S, Sutton N, Blackstock S, Gormley S, Hoggart CJ, Levin M, et al. Predicting IVIG resistance in UK Kawasaki disease. *Arch Dis Child.* (2015) 100:366–8. doi: 10.1136/archdischild-2014-307397
39. Berdej-Szczot E, Malecka-Tendera E, Gawlik T, Firek-Pedras M, Szydlowski L, Gawlik A. Risk factors of immunoglobulin resistance and coronary complications in children with Kawasaki disease. *Kardiol Pol.* (2017) 75:261–6. doi: 10.5603/KP.a2016.0179
40. Lin MT, Chang CH, Sun LC, Liu HM, Chang HW, Chen CA, et al. Risk factors and derived formosa score for intravenous immunoglobulin unresponsiveness in Taiwanese children with Kawasaki disease. *J Formos Med Assoc.* (2016) 115:350–5. doi: 10.1016/j.jfma.2015.03.012

Conflict of Interest: The authors declare that the research was conducted in the absence of any commercial or financial relationships that could be construed as a potential conflict of interest.

Advantages of publishing in Frontiers

OPEN ACCESS
Articles are free to read for greatest visibility and readership

FAST PUBLICATION
Around 90 days from submission to decision

HIGH QUALITY PEER-REVIEW
Rigorous, collaborative, and constructive peer-review

TRANSPARENT PEER-REVIEW
Editors and reviewers acknowledged by name on published articles

Frontiers
Avenue du Tribunal-Fédéral 34
1005 Lausanne | Switzerland

Visit us: www.frontiersin.org
Contact us: frontiersin.org/about/contact

REPRODUCIBILITY OF RESEARCH
Support open data and methods to enhance research reproducibility

DIGITAL PUBLISHING
Articles designed for optimal readership across devices

FOLLOW US
@frontiersin

IMPACT METRICS
Advanced article metrics track visibility across digital media

EXTENSIVE PROMOTION
Marketing and promotion of impactful research

LOOP RESEARCH NETWORK
Our network increases your article's readership